METHODS IN MOLECULAR MEDICINE™

Aging

Methods and Protocols

Edited by

Yvonne A. Barnett

Christopher R. Barnett

Humana Press

1

Understanding Aging

Bernard L. Strehler

1. Background

Enormous advances in our understanding of human aging have occurred during the last 50 yr. From the late 19th to the mid-20th centuries only four comprehensive and important sources of information were available:

1. August Weismann's book entitled *Essays on Heredity and Kindred Biological Problems* (the first of these essays dealt with The Duration of Life; ***1***). Weissmann states (p. 10) "In the first place in regulating the length of life, the advantage to the species, and not to the individual, is alone of any importance. This must be obvious to any one who has once thoroughly thought out the process of natural selection…".
2. A highly systematized second early source of information on aging was the collection of essays edited by Cowdry and published in 1938. This 900+ page volume contains 34 chapters and was appropriately called *Problems of Aging*.
3. At about the same time Raymond Pearl published his book on aging ***(2)***. Pearl believed that aging was the indirect result of cell specialization and that only the germ line was resistant to aging. Unfortunately Pearl died in the late 1930s and is largely remembered now for having been the founding editor of *Quarterly Review of Biology* while he was at the Johns Hopkins University, this author's alma mater.
4. Alexis Carrel wrote a monumental scientific and philosophical book, *Man, the Unknown* ***(3)***. Carrel believed that he had demonstrated that vertebrate cells could be kept in culture and live indefinitely, a conclusion challenged by others (more on this later).

Probably the most useful of all the more recent books published on aging was Alex Comfort's *The Biology of Senescence* ***(4)***, which supplied much of the source information that this author used in writing *Time, Cells and Aging* (***5–7***; I am most grateful to Dr. Christine Gilbert, of Cyprus, for her efforts in

From: *Methods in Molecular Medicine*, Vol. 38: *Aging Methods and Protocols*
Edited by: Y. A. Barnett and C. R. Barnett

the revision of the third edition of *Time, Cells and Aging,* and for the most stimulating discussions we have had over the years). The extremely useful and thoroughly documented book called *Developmental Physiology and Aging* by Paul Timeras ***(8)*** is a fine source of critical appraisals of the science in both areas. Many of the more recent books on aging are cited later. The success of my own journal (*Mechanisms of Ageing and Development*) is largely due to the work of our excellent editorial board and to the careful work and prodding of my dear wife, Theodora Penn Strehler, who passed away on 12 February, 1998. This chapter is dedicated to her living memory and the love she gave to me for 50 years of marriage and joy and sadness — and the kindness she showed to all who knew her. *Requiescat in pacem*.

2. Overview of a Systematic Approach

My own synthesis and analysis of the nature and causes of aging were presented in a book called *Time, Cells and Aging*. To use terms consistently in discussing aging, a set of four properties that all aging processes must meet are defined in that book:

1. Aging is a *process*; i.e., it does not occur suddenly, but rather is the result of very many individual events.
2. The results of aging are *deleterious* in the sense that they decrease the ability of an individual to survive as he or she ages.
3. Aging is *universal within a species*. However, aging may not occur in every species. Thus, certain "accidents" such as those that result from a specific infection are not part of the aging process.
4. Aging is *intrinsic* to the living system in which it occurs (i.e., it reflects the qualities of DNA, RNA, and other structures or organelles that were inherited from the parental generation).

The central thesis presented in *Time, Cells and Aging* is that the possible causes of aging can be divided into:

1. Those that are built into the system as specific DNA or RNA coding (or catalytic) sequences, and
2. Those that are the result of controllable or uncontrollable environmental factors including radiation, nutrition, and lifestyle.

Two key phenomena are shown by aging animals:

1. The probability of a human dying *doubles* about every 8 yr, a fact that was first discovered by an English Insurance Actuary by the name of Benjamin Gompertz about 165 yr ago ***(9)***. Thus, the following equation, derived from Gompertz's work, accurately describes the probability of dying as a function of age in a particular environment: $R = k + R0e^{at}$ where, R(ate) of death at any age equals the probability of dying at age 0 multiplied by an age-dependent factor that is equal

to e raised to the a times t power, where a is a function of the doubling time and t is the age attained. A better fit to observed mortality rates is given by adding a constant (k) (which largely reflects environmental factors).

If one plots log R against t(age) one obtains a remarkably precise straight line, usually between ages 30 and 90. A Gompertz curve is obtained for the mortality rate vs age for a variety of animals—humans, horses, rats, mice, and even *Drosophila melanogaster*, a much studied insect.

2. A second general fact or law is provided by my own summary and analysis of the pioneering quantitative work of Nathan Shock on maximum functional ability of various body systems' ability to do work as humans age. Shock's studies (on humans) implied to me that after maturity is reached the following equation describes a multitude of maximum work capacity of various body parts: $W_{max} = W_{max}(30)\ (1 - Bt)$ where B varies from about 0.003 per yr to almost 0.01 per yr—depending on the system whose maximal function is being measured. For example, maximum nerve conduction velocity declines by about 0.003 per yr ***(10)*** and vital capacity as well as maximum breathing capacity declines by about 1% per yr ***(11)***.

The Gompertz and Shock equations pose the following puzzling and key question: "How can a linearly declining ability in various functions cause a logarithmic increase in our chances of dying as we age ?" A probable answer to this question was provided by this author in collaboration with Prof. Albert Mildvan ***(12–14)***. Our theory made two assumptions. The first of these is that the equation derived from Shock's work (that the maximum work capacity of a variety of body systems declines linearly after maturity is reached) is valid. This, as shown earlier, is the very simple equation: $W_{max} = W_{max}(30)\ (1 - Bt)$, where W_{max} is the maximum ability to do work at age t, $W_{max}(30)$ is the maximum ability to do work at age 30, where B is the fraction of function lost per yr, and t is the age in years. Of course B varies from species to species and the t term is some small fraction of the maximum longevity of a species.

The second assumption is that the energy distribution of challenges to survival is very similar to the kinetic energy distribution of atoms and molecules as defined in the Maxwell–Boltzmann equation. This equation or law defines how kinetic energy is distributed in a collection of atoms or molecules at a specific temperature (where temperature is defined as the average kinetic energy and is equal to $KE = 0.5\ mv^2$). This distribution has a maximum value near the average kinetic energy of the particles in the system. But higher and higher energies are generated through random successive multiple collisions between particles. The reason that this is possible is easily understood through an analogy in which the particles are seen as billiard balls. Consider the case when one of two spherical billiard balls can absorb momentum from another such sphere. This happens in billiards when one ball strikes the second ball squarely. In that case, the moving billiard ball stops and the formerly stationary

one moves off at about 45° from the direction in which the first one was moving. The law of conservation of momentum is $mv = K$ for any two colliding structures. Because the balls are not perfectly elastic some heat will be generated during the collision, but this is a very small fraction of the total momentum and kinetic energy of the two particles. This is evident from the fact that one cannot feel a warming of either of the billiard balls after such a collision and the fact that the ball that is struck moves at about the same velocity that the first ball had before the two balls collided. Now consider the special case where two such billiard balls are traveling at right angles to each other when they collide and that the collision between them is "on center" so that one of the balls stops dead in its tracks and the other ball moves off at a 45° angle at a speed that conserves total momentum. (That is, the moving ball is now moving along the line that defined the center of gravity of the two balls as they were moving before they collided.) If momentum the two balls is conserved (the momenta are added) then the speed of the struck moving ball should be twice that which both of the balls had before they collided. There is no obvious reason why momentum is not conserved in this manner. But the kinetic energy $(1/2)mv^2$ of the moving ball will be much greater than the sum of the kinetic energies they had before collision. (In fact the total kinetic energy of the two balls moving at the same velocity before they collided is *two times as great after they collide than it was before this special kind of collision happened*!) This is a most surprising seeming "violation" of the Law of Conservation of Energy. It would seem to follow from this that certain kinds of very improbable collisions result in an increase in the kinetic energy of the pair of balls. This seems almost obvious from the fact that the kinetic energies of atoms or molecules is not equal among atoms or molecules in a closed system. Instead, it follows the Maxwell–Boltzmann distribution. Where does this energy come from? Perhaps from the Einsteinian conversion of mass to energy. Thus it appears that if one constructs a device in which collisions of the non-random kind described previously took place one should be able to get more energy out of the system than one puts in—essentially because the structure of such a machine minimizes the entropy of collisions by causing only certain very rare collisions to take place. I have spent many months testing this revolutionary theory, but the results produced from my "Perpetual Motion Machine" have failed to demonstrate any such gain in kinetic energy. There appears to be no other explanation for the distribution of kinetic energy among atoms and molecules than the kind of collisions discussed here! It's unfortunate that it doesn't work at the macro level. In any event, if a small probability exists that improbable collisions, such as discussed previously, are rare and cause an increase in momentum of one of the balls or atoms then the probability that a series of similar collisions that increase momentum of particular atom or molecule will give that atom or molecule greater and

greater energy will decrease very rapidly as the number of such improbable events increases. In fact, the number of such combined events will decrease logarithmically as the energy possessed by such an atom or molecule increases linearly. Such a decreasing exponential is part of the classical form of the Maxwell–Boltzmann equation—and defines the number of atoms with momenta greater than some particular high value. In fact, the distribution of momentum is described by a symmetrical bell-shaped curve (a Maxwellian curve) whereas the distribution of energy follows the Maxwell–Boltzmann curve.

To return to the Gompertz equation as it applies to the probability of dying vs age, Mildvan and I postulated that the energy distribution of challenges to living systems is very similar to the Maxwell–Boltzmann distribution. For example. obviously one knows that small challenges such as cutting a finger or tripping or stumbling are very frequent compared to the chance of falling down the stairs, being hit by a speeding automobile, or experiencing an airplane crash. Similarly, the frequency of coming down with a very serious diseases (infections by a new influenza virus, blood clots in the coronary arteries or key arteries in the brain, aortic aneurysms, cancer) is much rarer than is coming down with a minor infection (e.g., a cold or acne) or bumping one's shin against a coffee table. It may have been that the "Sidney" flu somehow was exported from Hong Kong to Australia by a "carrier" passenger in an airplane and thence to the Uunited States via another carrier who gave it to someone who infected my great grandson, who in turn infected our entire family at Christmas time, 1997 and led to my sadness at losing the person, Theodora (my wife), I had deeply loved and enjoyed for 50 years. The separate events leading to this personal tragedy were each improbable, but they resulted in a very large challenge that one of us was unable to overcome! This illustrates the principle that it takes many unlikely events to lead to a major challenge to humans—or to molecules.

The theory of absolute reaction rates states that $R = C(kt/h)e^{-(F^*/RT)}$, where F^* is the free energy of activation of a reaction. The free energy of activation is in turn defined as the amount of energy needed to break a bond that must be broken in order for a chemical reaction to occur. Of course the free energy needed is derived from multiple collisions and the number of particles that possess a given excess energy equal to that required for a given reaction to occur increases as a function of the absolute temperature. Note that the RT (gas constant times absolute temperature) leads to an exponentially decreasing rate of reaction as T (absolute temperature) is lowered linearly because the T term is in the dividend of the negative exponential term $e^{-(F^*/RT)}$. If one plots the log of the rate against $1/T$ one obtains a straight line whose slope is a measure of the minimum amount of energy (T^*) required to cause a reaction to happen. Such a plot is called an Arrhenius plot. Therefore, if one defines the events that

lead to possible death similarly and takes into account the linear decline in the body's ability to resist challenges (through the expenditure of the right kind of energy in a particular system or systems) decreases linearly as we age, one obtains the Gompertz equation. Thus, the Gompertz equation results from the logarithmic distribution of size of challenges we encounter interacting with linear loss of functions of various kinds during aging observed by Shock.

3. Ten Key Experimental Questions—Plus Some Answers

Although several hundred specific questions or theories regarding the source(s) of aging in humans and other nucleated species (eukaryotes) are possible, only 10 of the most carefully examined "theories" are highlighted here. Space does not permit a complete discussion of each of these questions.

1. How does the temperature of the body affect the rate of aging?

The activation energy of a particular chemical reaction is the amount of energy that is derived from accidental collisions among atoms or molecules to *break the bonds needed for the reaction to occur*. If the reaction is a catalyzed one then the activation energy is about 10–20 kcal/mol. By contrast, if the reaction is not catalyzed the energy required is that which will break a bond in a reacting substance. Covalent bonds require between 75 and 130 kcal to be broken, whereas in the presence of an appropriate catalyst the bond is weakened by its combination with the catalyst so that it only takes 6–20 kcal to break it. If one plots the log of the rate of a reaction against the reciprocal of the absolute temperature one often obtains a remarkably straight line. Such a plot is called an Arrhenius plot (after the man who discovered it). The slope of the straight line obtained in such a plot will generally be high (50–200 kcal for uncatalysed reactions and 6–19 kcal for catalyzed ones. In order to calculate the activation energy of aging I plotted my own results on the effects of temperature in *Drosophila* life-spans ***(15,16)*** together with those of Loeb and Northrup ***(17,18)*** and others and found the activation energy to be between 15 and 19 kcal. Thus, in the cold-blooded animal, *Drosophila* (a fruit fly), the rate of aging appears to be determined by a catalyzed reaction or possibly by the effects of temperature on the rates of production and destruction of harmful substances such as $^{\bullet}OH$ radicals that attack DNA and other cell parts. It is known that trout live much longer in cold lakes than in warmer ones but no quantitative studies of their longevities at a variety of temperatures have, to my knowledge, been made. Because mammals operate at essentially constant body temperatures, it is not an easy matter to study the effect of body temperatures on humans or similar mammals. One might find a correlation between the body temperatures of the descendants of centenarians and the descendants of shorter lived persons, but such a study is unlikely to be funded (as I know from personal experience!).

2. Are changes in connective tissue a key cause of aging?

There is no doubt the age-related alterations to the structure and therefore biological properties of connective tissues can lead to cosmetic through to pathological changes in vivo. The onset of such pathologies may in some instances increase the chances of death.

It is widely recognized that changes in the elasticity of skin (less elasticity) as we grow older occurs in humans. If one pinches the skin on the back of the hand and pulls up on it, it returns to its original shape (flat) in a short time, about 1 s for young persons and about 3 s or more for older skin. This change is primarily due to the attrition of the elastic fibers that are present in the dermis. If the skin is exposed during early life to large amounts of ultraviolet radiation such as that in sunlight, some of the collagen is converted into a fiber that resembles elastin. This transformation leads to the uneven contraction of the skin, that is, wrinkles are formed. The collagen in the skin and elsewhere in the body becomes less plastic as it matures (for a discussion of the chemical processes underlying these maturity changes please *see **19–23***). Alteration in the physical properties of the elastic tissue found in blood vessels can lead to changes in blood pressure in vivo.

There are many examples of pathologies that result from age-related alterations to connective tissues. Particularly in fair-skinned persons, exposure to ultraviolet light can lead to damage of skin cells and may lead to basal cell and squamous cell cancers (both of which are relatively easily treated) and even melanomas (difficult to treat successfully if not diagnosed at very early stages). Alterations to the structure of bone can lead to osteoporosis. Physical changes to the cartilage in joints can lead to the onset of osteoarthritis.

3. Does a significant fraction of the mitochondria of old mammals suffer from defects, either in DNA or in other key components?

The mitochondria we possess are all derived from our mother's egg, as are various other materials such as particular RNA molecules. Mitochondria are the cell factories in which the energy provided when food is oxidized is converted into the unstable molecule called ATP. ATP is used to contract muscles, to pump ions across neural membranes, and is used to manufacture proteins and RNAs.

The production of ATP can be assayed (***24–26***; John Totter and I (at the Oak Ridge National Laboratory in 1951) developed an assay for ATP using McElroy's reaction ***(24)*** that is able to measure a billionth of a gram of ATP (1 millionth of a milligram). This method has been widely used in various biological and biomedical studies but the description of the method was published so many years ago (1951–52) that it is no longer associated with our names. In my laboratory we used this assay to study the production of ATP by mitochon-

dria obtained from animals of different ages. We found no differences between mitochondria from 8-mo-old rat hearts and 24-mo-old rat hearts, using α-ketoglutaric acid as substrate. Later it was reported that some mitochondria from old animals oxidize different substrates such as succinate less efficiently than do mitochondria derived from young animals. Later in this book Miquel et al. summarize the literature, including much of their own work, on various morphological and functional changes that accumulate with age in mitochondria. These changes are thought to result from an accumulation of various types of mutations in the mitochondrial genome (much of which codes for polypeptides involved in Complex I and II of the respiratory redox chain) that result from primarily reactive oxygen species damage to the mitochondrial genome that is poorly, if at all, repaired. Turnbull et al. present two chapters later in this book on the analysis of mitochondrial DNA mutations. Such an age-related decrease in mitochondrial function has been proposed to lead to the bioenergetic decline of cells and tissues and so contribute to the aging process ***(27)***.

4. Is a limitation in the number of divisions a body cell can undergo (in cell culture) a significant cause of aging?

Alexis Carrel reported ***(3)*** that he was able to keep an embryonic chicken heart alive for more than 22 yr. This is, of course, much longer than chickens usually live and Carrel concluded that regular supplements of the growth medium with embryo extracts would keep these cultures alive for very long times, perhaps indefinitely. To quote from p. 173 of the Carrel book, "If by an appropriate technique, their volume is prevented from increasing, they never grow old." Colonies obtained from a heart fragment removed in January 1912, from a chick embryo, are growing as actively today as 23 yr ago. In fact, are they immortal? Maybe so. For many individuals, including myself at about 13 yr of age, these findings were very exciting. Perhaps man would eventually be able to conquer his oldest enemy, aging. It was at about that time that I decided on a career in aging research.

In 1965 my good friend Leonard Hayflick reported some research he and a colleague (Moorhouse) had carried out that appeared to be contrary to what the renaissance man, Carrel, had concluded ***(28)***. Hayflick found that human fibroblasts in a culture medium could go through only about 50 doublings, after which the cells died or stopped dividing (now known as replicative senescence) or both. Hayflick's data have been confirmed by many persons, including this author, who with Robert Hay ***(29)*** carried out similar experiments on chicken fibroblasts that were only capable of about 20 doublings. However, because a new layer of skin cells is produced about every 4 d (about 90 doublings per yr and 9000 doublings in a 100-yr lifetime), and because red blood cells are produced by the millions every 120 d and because the crypt cells in the lining of

the intestine give rise to the entire lining of the cleft in which the crypt cells lie, it seemed to me unreasonable that the Hayflick limit applies to normal cells in the body. In the case of skin cells Hayflick countered with the idea that if each of the progenitor cells in the skin could divide only 50 times, then the reason might be that cells moved out of the dividing cell structure (the one cell thick, basal cell layer) that gives rise to the epidermis after they had gone through 40 or 50 doublings. This seemed a reasonable and possibly correct theory, so (with the help of my late wife), we showed that the cells did not leave the basal layer two or four or eight cells at a time, but rather the daughter cells of cells labeled with tritiated thymine moved out of the basal layer randomly (the reader is encouraged to read pp. 37–55 of the third edition of *Time, Cells and Aging* for further discussion in this regard). Such a finding may cast strong doubt on the relevance of in vitro clonal "aging" to the debilities of old age.

I offer one possibility that may account for the apparent contradiction between the findings of Carrel on one hand and of Hayflick on the other. The antibiotics routinely used during the "fibroblast cloning" experiments (and other experiments performed since on the phenomenon of replicative senescence) might in themselves cause a decrease in the number of divisions possible. Carrel was unable to use antibiotics in his studies because they were not yet discovered or manufactured when he carried out his 22-yr experiment on chick heart viability. Hayflick states in his recent book that he has evidence that Carrel's embryo extract supplements contained living cells and that this is why the tissues Carrel studied remained alive for times greater than the lifetime of a chicken. Carrel had to use very careful means to replace his media every so often over a period of 20 yr. Besides, Carrel did not allow his organ cultures to grow, so cell division was either absent or cells possibly present in the embryo extracts he added were able to differentiate into replacement cells for heart tissues. Because the heart is a syncytium of cells, it is difficult to imagine how a steady state of replacement of old cells by cells possibly present in the embryo extract could take place, particularly within the center of the organ culture! This logic argues for the validity of Carrel's reports. Moreover, fibroblasts are quite different from myoblasts and do not form syncytia.

In very recent times a popular proposal has been that telomeres, the sequences of noncoding DNA located at the end of chromosomes, shorten each time a normal cell divides and that in some way this shortening "counts" the number of cell divisions that a cell population has experienced, perhaps owing to the loss of essential genes that have critical functions for cell viability ***(30,31)***. What is not clear is how the documented process of replicative senescence in vivo leads to the development of physiological malfunction and the onset of age-related pathologies in vivo. Changes in the expression of a number of gene functions, including increases in the expression of genes coding for

growth factors and extracellular matrix components, have been found by studying cells in replicative senescence in vitro. Researchers have been able to detect relatively small numbers of senescent fibroblasts and epithelial cells in older animals and human tissues in vivo using β-galactosidase staining (pH > 6). They have postulated that even such small numbers of cells, exuding various entities because of activated genes etc., might be sufficient to alter tissue homeostasis and so lead to physiological effects. This suggestion has yet to be proven and the role of replicative senescence in aging remains an area of intense research activity.

5. Are errors in the transcription and/or translation of DNA a key source of aging? Or, alternatively, are changes in the rate of transcription or translation of the information in DNA a key cause?

Medvedev ***(32)*** was the first to propose that the stability of DNA was responsible for the length of life of different species. Orgel then proposed his "error theory of aging" in which he proposed that errors in DNA replication, transcription of RNA, and translation on the products might be responsible for the deterioration of function during aging ***(33)***. Over a number of years a major effort was made in this author's laboratory to test the idea that development and aging were caused by changes in the specific codons different kinds of cells were able to translate. Initial studies showed that the aminoacylated tRNA's for a variety of amino acids differed from one kind of cell to another and a theory called the "Codon Restriction Theory of Development and Aging" was published in *Journal of Theoretical Biology* ***(34)***. The theory was then tested against the actual codon usage of about 100 different messenger RNAs and it was indeed found that certain kinds of gene products (e.g., the globin parts of hemoglobins) do in fact have very similar patterns of codon usages and codon dis-usages in messages ranging from birds (chickens) to mice and rats to humans! On these bases, the inability to translate specific codons in specific kinds of tissues may indeed turn out to be important in the control of gene expression (at least in some tissues).

6. Are changes in RNA qualities responsible for aging?

Whether the kinds of RNA present in cells is important in controlling differentiation and aging is an issue that has arisen when it was discovered that certain RNA molecules possess catalytic activity, e.g., are able to generate themselves by catalytically transforming their precursors ***(35)***. I have recently read evidence that even the transfer of growing polypeptide chains to the amino acid on the a tRNA to the "next" position is catalyzed in the ribosomes by a particular kind of RNA. Whether changes in catalytic RNA populations cause certain disabilities during aging has not yet been tested, to my knowledge.

7. Do long-lived cells selectively fail in humans?

The answer to this question is certainly yes. The main sites in which clear age changes take place are in cells that cannot be replenished without a disruption in their functions in the body. Key cell types are neurons, heart muscle, skeletal muscle, and certain hormone producing cells. The important precursor of both androgens and estrogens, DHAE, declines linearly with age in men and women and may well be a product of cells that are not replenishable. But even more obvious is the postmitotic nature of cells in the nervous system and other nonreplenishing tissues such as skeletal and heart muscle. Thus, damage to the cells making up these organs generally cannot be repaired through replacement because such postmitotic cells cannot be made to divide. In the case of the brain, continual replacement of old cells by new ones might preserve reflex brain function, but most such newly incorporated nerve cells would replace neurons in whose facilitated synapses useful memories had been stored. Thus, paradoxically, higher animals, particularly humans, age because some key kinds of cells they possess have long, but not indefinitely long, lifetimes. (Although it is fairly obvious I would like it to be called "The Strehler Paradox," so that way I might be remembered for something unless a different version of the perpetual motion machine I proved unworkable actually generated useful energy!)

8. What are the underlying causes of the age-related decline in the immune system?

The immune system consists of two major forms: innate and acquired. Innate immunity comprises polymorphonuclear leukocytes, natural killer cells, and mononuclear phagocytes and utilizes the complement cascade as the main soluble protein effector mechanism. This type of immunity recognizes carbohydrate structures that do not exist on eukaryotic cells; thus foreign pathogens can be detected and acted against. Lymphocytes are the major cells involved in the system of acquired immunity, with antibodies being the effector proteins. The T-cell receptor (TCR) and antibodies recognize specific antigenic structures.

Deterioration of the immune system with aging ("immunosenescence") is believed to contribute to morbidity and mortality in man due to the greater incidence of infection, as well as possibly autoimmune phenomena and cancer in the aged. T lymphocytes are the major effector cells in controlling pathogenic infections, but it is precisely these cells that seem to be most susceptible to dysregulated function in association with aging.

Decreases in cell-mediated immunity are commonly measured in elderly subjects. By most parameters measured, T-cell function is decreased in elderly compared to young individuals. Moreover, prospective studies over the years have suggested a positive association between good T-cell function in vitro and

individual longevity. The numbers and/or function of other immune cells are also altered with age: antigen-presenting cells are less capable of presenting antigen in older age; the number of natural killer cells increases in older age, and these cells are functionally active; there is some evidence that granulocyte function may be altered with age; B lymphocyte responses also alter with age, as responses against foreign antigens decline whereas responses against self-antigens increase ***(36,37)***. Currently much effort is being directed toward elucidating the processes leading to the phenomenon of immunosenescence. The reader is encouraged to read a special issue of *Mechanisms of Ageing and Development* that was dedicated to publishing the proceedings of a recent international meeting on immunosenescence ***(38)***.

One positive aspect of immunosenescence, however, is that the risk of transplant rejection is reduced with age.

9. Are ordinary mutations a major cause of aging? Or, alternatively, is the instability of tandemly repeated DNA sequences a major cause of aging?

In 1995 a Special issue of *Mutation Research* entitled "Somatic Mutations and Ageing: Cause or Effect?" was published, with an overview from this author highlighting the history of this field of science ***(39)***.

Much of the early results from the experiments on the effects of ionizing radiation and chemical mutagens on the life-span of *Drosophila* and other animals were inconsistent with a simple mutation theory of aging. However, the research papers presented in the special issue of *Mutation Research*, and elsewhere, do suggest an involvement of somatic and mitochondrial mutation in the physiological and pathological decline associated with the aging process. I also believe that some other kind of DNA change, the occurrence of which was not accelerated by radiation proportionally to dose (as are ordinary mutations), could be responsible for aging. This kind of postulated change in DNA might well occur sufficiently frequently, even in unirradiated animals, to cause aging!

In humans the nucleolar organizing regions (NORs), which can be detected by silver staining, are regions containing rDNA which is the template on which rRNA is formed. There are about five or six pairs of chromosomes that possess such NOR regions. It has been shown that the number of NORs decreases with time in a variety of human cells. Perhaps, I thought, losses of such tandemly duplicated regions takes place at a relatively high rate in nondividing human cells during aging, but is not appreciably increased by exposure to moderate amounts of radiation. After all, radiation affects all kinds of DNA and the rDNA genes may well be able to repair most of the damage they receive either during aging or as a result of chemical or electromagnetic radiation such as UV light and X-rays or by neutrons. I postulated that mutations that cause the loss of rDNA might be responsible for human aging because the more severe such loss

is, the greater should be the loss of function of any cell in manufacturing proteins. Such mutations could be the kind that cause the linear decrease in function of various parts of the body observed by Shock. Although I thought this unlikely to occur, particularly in postmitotic cells, we were eager to disprove it, because loss of important genetic material would be very difficult to reverse (e.g., through the use of a "clever" virus), whereas a defect in the regulation of gene expression which had been the focus of our research should require simpler, but presently unknown, treatments to modify the rate of aging—which at that time seemed to be on the horizon.

To test the possibility that rDNA loss is a major cause of aging, I asked a very talented postdoctoral trainee, the late Roger Johnson, to work to study the rDNA content of various mammalian tissues. He owned a small airplane that made it possible for him to fly to Davis, California to obtain a variety of tissues of control beagle dogs of different ages that were killed as part of an ongoing study by the Atomic Energy Commission to determine the pathological effects of radiation. We obtained fresh samples from the following organs: brain, heart, skeletal muscle, kidney, spleen, and liver. When we compared the rDNA content of the brains of beagles of various ages we found that the results were not what we had hoped for and expected—namely, that no difference would be found between young and old animals. Instead, the findings were that the rDNA content decreased by about 30% in brains of dogs from approx 0–10 yr of age ***(40)***. We then proceeded to compare the effect of age on the DNA of heart, skeletal muscle, kidneys, spleen, and liver. Decreases in rDNA of about the same magnitude were found in the other two postmitotic tissues, heart and skeletal muscle, but were not detected in liver DNA or kidney DNA. A small, probably insignificant, loss of these gene sequences was detected in dog spleens ***(41,42)***. After the work on dogs was completed, we began to study human heart and found a substantial loss of rDNA of aged humans ***(43)***. We later studied two different areas of the human brain, the somatosensory cortex and the hippocampus. The fresh autopsy samples were kindly supplied by the Los Angeles coroner. We discovered that the rate of loss of rDNA from human brain and heart was about 70% per 100 yr. This rate is only about 1/7th of the rate observed in dogs and thus is inversely proportional to the maximum longevity of these two species (approx 120 yr and approx 16 yr). The ratio of these two life-spans is very close to 7:1 and the ratio of loss of rDNA/yr is about 1:7. The two parts of the human brain measured were almost identical in their rDNA content, although the loss was of course greater in old tissues than in young ones. This indicates that the measurements are reliable or at least that, if errors were made, the errors must be very small. Over a period of about 10 yr we continued to publish studies on humans. Most of these studies were reported in *Mechanisms of Aging and Development*.

A very interesting class of mutants in *Drosophila* are called the *minute* mutants. My former dear friend Kimball Atwood (who has departed to the great genetics lab in the sky) noted that there are many different *minute* mutants and that they are found in various places on essentially all of the four chromosomes this animal possesses. He suggested that the mutants might reflect the loss of at least part of the tRNA coding regions for specific tRNAs. I don't know whether this hypothesis has been critically tested—if it hasn't it certainly should be. Deficiency (but not total absence of specific tDNAs that decode specific amino acids) would be expected to interfere with the normal growth rate of all parts of the developing fly embryo—hence the name, *minute*.

10. What causes Alzheimer's disease and cancers—and what means are now available to control these tragic diseases of the elderly (and of certain younger persons as well)?

I spent considerable time and effort recently studying another major scientific question: Is a specific temporal code used in transmitting, decoding, and storing information (memories) in the mammalian brain? I had published a theory on this concept in *Perspectives in Biology and Medicine* in 1969 ***(44)***. Knowledge of such a coding system could be quite interesting and probably useful in understanding the familial forms of Alzheimer's disease. I studied the patterns in time of nerve discharges in response to specific stimuli to the eyes of monkey brains. In the meantime I had constructed an electronic memory system I thought might mimic the brain. I made some progress and wrote a program that serially mimicked how I thought the brain might store and recognize patterns. I also constructed an electronic analogue that worked quite well. But, I made little progress in obtaining a clear answer regarding the validity of my hypothesis until a brilliant French scientist, Dr. Remy Lestienne, wrote to ask whether he could spend a year working with my "group" (at that time only me!). After we had worked together for only a month we discovered that the brain really did produce extremely precise copies of doublets, triplets, quadruplets, and even sextuplets of pulses. Then we analyzed various parameters, including the decay time for the occurrence of repeating patterns. The patterns we used were precisely repeated with variances between copies of the same pattern of less than 1/7th of a millisecond for each of the three intervals that make up a pattern. This was most surprising, because the duration of a nerve impulse is about 1 ms. Perhaps the most important discovery we made was that each repeating triplet was surrounded by about seven doublets that were part of the repeating pattern and equally precisely replicated. Thus, we had not disproved my theory, but rather found evidence that it was probably correct, at least for short-term memories.

While this research was going on I also developed an electronic simulation of the basic concepts and obtained a U.S. Patent on this device in 1993. I also received a second patent that proposed a means to recognize different vowels on the basis of the differences in logarithms of frequencies generated within the mouth and nasopharyngeal cavities. Because the absolute frequencies that children and women and men use to produce vowels are quite different a puzzle existed as to how different vowels are understood despite the fact that the absolute frequencies generated are much different from person to person. A large-scale implementation of the content addressable temporal coding has not been implemented although a very simple version was constructed by me and an improved version was created by a most ingenious Japanese engineer named Yuki Nakayama (sponsored by my friend H. Ochi, who has a consuming interest in aging research and is quite wealthy.) Perhaps the very new CD recorder that Sony has recently marketed may be modified to construct a new and inexpensive way to implement a device able to store the 10^{14} bits the human brain evidently can store and retrieve upon proper cueing.

Alzheimer's disease is manifested by the loss of memory, initially that involving the recent past. One can remember minuscule details of the more distant past, but sometimes forgets what day of the week it is and what one wanted to get from the kitchen when one gets there. This realization of defects in remembering recent events can be quite disconcerting to those of us who have enjoyed the use of memory, logic, and analogy in solving scientific problems and important problems generated by the process of getting older. Alzheimer's is also called presenile dementia, which means that it can occur as early as the late 40s or 50s, long before other signs of senility manifest themselves. As the disease progresses victims may even lose the ability to recognize family members or even their spouses or their own names. When the brains of persons who die of various diseases are autopsied, it is possible to recognize those who have advanced stages of Alzheimer's degeneration by looking for the many "plaques" characteristic of Alzheimer's. Similar plaques are found in the brains of essentially all very elderly persons, but they are markedly more numerous in the brains of true inheritors of the acute form of this age change in brain anatomy—persons with Alzheimer's. The plaques are visible on the surface of the brain and consist of localized patches of changed brain tissue visible to the naked eye. When the plaques are examined microscopically at least three characteristics are obvious: (1) the plaques contain many dead or dying cells; (2) most of the cells that are still alive in a plaque possess long tangles of fibers that are not found in profusion in "normal" neurons elsewhere in the same individual's brain biopsy; and (3) the cells are surrounded by very large accretions of antibody-like substances called amyloid. These deposits often encase the entire cell body of a neuron. It is important to note that these amyloid

deposits are evidently different from most other kinds of amyloid found in the brain and elsewhere. The key difference appears to be that a cleavage product of the amyloid characteristic of Alzheimer's causes cell death by opening Ca^{2+} channels in the neural membranes' neuroreceptor regions. This causes a permanent depolarization of the cells and evidently is the cause of their death and the loss of memories the cells or cell groups store. The most exciting research on this subject of which I am aware is that the drug Flupirtine now used in Europe for the treatment of Alzheimer's, reportedly with some success, prevents the influx of Ca^{2+} into cells that are pretreated with this substance when Alzheimer's amyloid is presented to them. This work, recently published in *Mechanisms of Ageing and Development*, was carried out by my good friend, Werner Mueller, who will become Editor-in-Chief of the journal when I cease my editorial responsibilities at the end of this year ***(45)***. I believe this is the most significant finding to be published on possible treatment of a very sad disease of the elderly.

Cancer is a common cause of morbidity and mortality in the elderly. The spectrum of the major types of cancers occurring in the early years of life (leukemias and sarcomas) is different from that occurring in later life (carcinomas and lymphomas). The most frequent cancers in women in Western societies are breast, ovarian, and colorectal, and in men prostate, lung, and colorectal. The multistep theory of carcinogenesis ***(46)*** predicts the age-related increased risk (5th power of age in both short-lived species such as rats and long-lived species such as humans) for the development of a wide range of different types of cancer (with the exception of the familial forms of the disease). The underlying molecular cause of cancer is the accumulation of mutations within a number of genes associated with the control of cell growth, division, and cell death. Despite the great variety of cells that can give rise to cancer there are now somewhat effective treatments for many of them (surgery, radiotherapy, and/or chemotherapy). Optimal treatment for many cancers is more likely the earlier the diagnosis is made. Among the most promising of new treatments for some cancers is the use of radioactively labeled antibodies to the surface antigens present on some cancer cells but not on normal cells. The labeled antibody seeks out the surface of the cancer cell and the radioactivity attached to it selectively radiates and destroys the tumor cells. Another recent treatment that appears to have at least some success is the use of substances that prevent angiogenesis, thereby effectively "asphyxiating" the dangerous tumor.

References

1. Weissmann, A. (1891) *Essays on Heredity and Kindred Biological Problems*, Oxford University Press, Clarendon, London, and New York.

2. Pearl, R. (1921) The biology of natural death, public policy and the population problem. *Sci. Month.* 193–212.
3. Carrel, A. (1935) *Man the Unknown*, Harper, New York.
4. Comfort, A. (1956) *The Biology of Senescence*, Rinehart, New York.
5. Strehler, B. L. (1962) *Time, Cells and Aging*, 1st ed., Academic Press, New York.
6. Strehler, B. L. (1977) *Time, Cells and Aging*, 2nd ed., Academic Press New York.
7. Strehler, B. L. (1999) *Time, Cells and Aging*, 3rd ed., Master Print Demetriades Bros., Cyprus.
8. Timeras, P. (1972) Decline in homeostatic regulation, in *Developmental Physiology and Aging* (Timeras, P. S., ed.), MacMillan Press, New York, pp. 542–563.
9. Gompertz, B. (1825) On the nature of the function expressive of the law of human mortality. On a new mode for determining life contingencies. *Philos. Trans. R. Soc. Lond.* **115,** 513–585.
10. Norris, A., Shock, N., and Wagman, I. (1953) Age changes in the maximum conduction velocity of motor fibers of human ulnar nerve. *J. Physiol.* **5,** 589–593.
11. Shock, N. and Yiengst, M. (1955) Age changes in basal respiratory measurement and metabolism in males. *J. Gerontol.* **10,** 31–40.
12. Mildvan, A. S. and Strehler, B. L. (1960) A critique of theories of mortality, in *The Biology of Aging* (Strehler, B. L., et al., eds.), Publ. No. 6, Am. Inst. Biol. Sci., Washington, D.C., pp. 399–415.
13. Strehler, B. L. (1960) Fluctuating energy demands as determinants of the death pricess (a parsimonious theory of the Gompertz function in (Strehler, B. L., et al., eds.), Publ. No. 6, Am. Inst. Biol. Sci., pp. 309–314.
14. Strehler, B. L. and Mildvan, A. (1960) A general theory of mortality and aging. *Science* **132,** 14–21.
15. Strehler, B. L. (1961) Studies on the comparative physiology of aging. II. On the mechanism of temperature life-shortening in *Drosophila* melanogaster. *J. Gerontol.* **16,** 2–12.
16. Strehler, B. L. (1962) Further studies on the thermally induced aging of *Drosophila* melanogaster. *J. Gerontol.* **17,** 347–352.
17. Loeb, J. and Northrop, J. H. (1916) Is there a temperature coefficient for the duration of life? *Proc. Natl. Acad. Sci. USA* **2,** 456.
18. Loeb, J. and Northrop, J. H. (1917) On the influence of food and temperature on the duration of life. *J. Biol. Chem.* **32,** 103–121.
19. Sinex, F. M. (1964) Cross linkage and aging. *Adv. Gerontol. Res.* **1,** 167–178.
20. Houuck, G. Dehesse, C., and Jacob, R. (1967) The effect of aging upon collagen catabolism. *Symp. Soc. Exp. Biol.* **21,** 403–426.
21. Franzblau, C. and Lent, R. (1968) Studies on the chemistry of elastin. *Brookhaven Symp. Biol.* **21,** 358–377.
22. Gallop, P., Blumenfeld, O., Henson, E., and Schneider, A. (1968) Isolation and identification of alpha amino aldehyde and collagen. *Biochemistry* **7,** 2409–2430.
23. Franzblau, C. Fariz, P., and Papaioannou, R. (1969) Lysenonorleucine. A new amino acid from hydrolysate of elastin. *Biochemistry* **8,** 2833–2837.

24. McElroy, W. (1947) The energy stored for bioluminescence in an isolated system. *Proc. Natl. Acad. Sci. USA* **33,** 342–345.
25. McElroy, W. and Strehler, B. L. (1949) Factors influencing the response of the bioluminescent reaction to ATP. *Arch. Biochem.* **22,** 420–433.
26. Strehler, B. L. and Totter, J. R. (1962) Firefly luminescence in the study of energy transfer mechanisms. 1. Substrate and enzyme determination. *Arch. Biochem. Biophys.* **40,** 28–41.
27. Fleming, J. E., Miquel, J., Cottrell, S. F., Yenguyan, L. S., and Economas, A. S. (1982) Is cell aging caused by respiration dependent injury to the mitochondrial genome? *Gerontology* **28,** 44–53.
28. Hayflick, L. (1965) The limited *in vitro* lifetime of human diploid strains. *Exp. Cell Res.* **37,** 614–638.
29. Hay, R. L., Menzies, R. A., Morgan, H. P., and Strehler, B. L. (1967) The division potential of cells in continuous growth as compared to cells subcultured after maintenance in stationary phase. *Exp. Gerontol.* **35,** 44.
30. Chang, E. and Harley, C. B. (1995) Telomere length and replicative aging in human vascular tissues. *Proc. Natl. Acad. Sci. USA* **92,** 11,190–11,194.
31. Bodnar, A. G., Ouellette, M., and Frolnis, M. (1998) Extension of lifespan by introduction of telomerase into normal human cells. *Science* **279,** 349–352.
32. Medvedev, Sh. A. (1961) *Aktual. Vopr. Sour. Biol.* **51,** 299.
33. Orgel, L. E. (1970) The maintenance of the accuracy of protein synthesis and its relevance to aging: a correction. *Proc. Natl. Acad. Sci. USA* **67,** 1426–1429.
34. Strehler, B. L., Hirsch, G., Gusseck, D., Johnson, R., and Bick, M. (1971) The codon restriction theory of aging and development. *J. Theor. Biol.* **33,** 429–474.
35. Andron, L. and Strehler, B. L. (1973) Recent evidence on tRNA and tRNA acylase-mediated cellular control mechanisms. A review. *Mech. Ageing Dev.* **2,** 97–116.
36. Pawelec, G. and Solana, R. (1997) Immunosenescence. *Immunol. Today* **18,** 514–516.
37. Pawelec, G., Remarque, E., Barnett, Y., and Solana, R. (1998) T cells and aging. *FIBS* **3,** 59–99.
38. Special edition of *Mechanisms of Aging and Development* (1998), **102**.
39. Special issue of *Mutation Research* (1995) Somatic Mutations and Aging: Cause or Effect? **338,** 1–234.
40. Johnson, R. and Strehler, B. L. (1972) Loss of genes coding for ribosomal RNA in aging brain cells. *Nature (Lond.)* **240,** 412–414.
41. Johnson, R., Chrisp, C., and Strehler, B. L. (1972) Selective loss of ribosomal RNA genes during the aging of post-mitotic tissues. *Mech. Ageing Dev.* **1,** 183–198.
42. Johnson, L. K., Johnson, R. W., and Strehler, B. L. (1975) Cardiac hypertrophy, aging and changes in cardiac ribosomal RNA gene dosage in man. *J. Mol. Cell. Cardiol.* **7,** 125–133.
43. Strehler, B. L., Johnson, L. K., and Chang, M. P. (1979) Loss of hybridizable ribosomal DNA from human postmitotic tissues during aging: I Age-dependent loss in human myocardium. Mech. Age. *Dev.* **11,** 371–378.
44. Strehler, B. L. (1969) Information handling in the nervous system: an analogy to molecular genetic coder-decoder mechanisms. *Perspect. Biol. Med.* **12,** 548–612.

45. Perovic, S., Böhm, M., Meesters, E., Meinhardt, A., Pergande, G., and Müller, W. F. G. (1998) Pharmacological intervention in age-associated brain disorders by Flupirtine: Alzheimer's and Prion diseases. *Mech. Age. Dev.* **101,** 1–19.
46. Vogelstein, B. and Kinzler, N. W. (1993) The multistep nature of cancer. *TIG* 9, 138–141.

2

Use of the Fibroblast Model in the Study of Cellular Senescence

Vincent J. Cristofalo, Craig Volker, and Robert G. Allen

1. Introduction

In this chapter, we present standard procedures for the culture of human cells that exhibit a finite proliferative capacity (replicative life-span). The use of a cell culture model has the advantage of providing a controlled environment to study a wide variety of cellular phenomena. It also has the inherent limitation of isolating cells from the regulatory elements that might be provided by other types of cells in vivo. Nevertheless, cell culture models have been crucial to our current understanding of mechanisms of growth, differentiation, development, and neoplasia and numerous other disease states. In this chapter we present procedures for human fibroblast culture including serum-free cultivation of cells, which is necessary when the cellular environment must be fully defined. In addition, we present procedures for the determination of replicative life-span, saturation density, and assessment of replicative capacity from labeled thymidine incorporation in fibroblasts. The methods described here have been well tested and provide highly reproducible results ***(1,2)***.

1.1. Cellular Senescence

Phenotypically and karyotypically normal human cells exhibit a limited capacity to proliferate in culture ***(3,4)***. This finite proliferative potential of normal cells in culture is thought to result from multiple changes ***(5)*** and has frequently been used as one model of human aging. Although most replicative life-span data are derived from fibroblasts, other types of cells such as glial cells ***(6)***, keratinocytes ***(7)***, vascular smooth muscle cells ***(8)***, lens cells ***(9)***, endothelial cells ***(10)***, lymphocytes ***(11)***, liver ***(12)***, and melanocytes ***(13)*** are also known to exhibit a limited replicative life-span in culture. Both environ-

From: *Methods in Molecular Medicine*, Vol. 38: *Aging Methods and Protocols*
Edited by: Y. A. Barnett and C. R. Barnett

mental and genetic factors appear to influence the proliferative life-span of fibroblasts from normal individuals ***(5,14,15)***. Not all of the determinants of proliferative capacity are known; however, a variety of changes are associated with the decline of proliferative capacity including changes in gene expression, telomere shortening, and signal transduction. These are all thought to be important factors that influence replicative life-span ***(15–20)***.

1.1.1. Telomere-Shortening

Loss of telomeric repeats is tightly linked to the cessation of mitotic activity associated with cellular senescence ***(16,17,21,22)***. The telomeres of human chromosomes are composed of several kilobases of simple repeats $(TTAGGG)_n$. Telomeres protect chromosomes from degradation, rearrangements, end-to-end fusions, and chromosome loss ***(23)***. During replication DNA polymerases synthesize DNA in a 5' to 3' direction; they also require an RNA primer for initiation. The terminal RNA primer required for DNA replication cannot be replaced with DNA, which results in a loss of telomeric sequences with each mitotic cycle ***(21,23)***. Cells expressing T antigen are postulated to exhibit an increase in their proliferative life-span because they are able to continue proliferating beyond the usual limit imposed by telomere length ***(24)***. Immortalized and transformed cells exhibit telomerase activity that compensates for telomere loss by adding repetitive units to the telomeres of chromosomes after mitosis ***(23,25–27)***. Cultures derived from individuals with Hutchinson–Gilford syndrome ***(28)*** often exhibit decreased proliferative potential, albeit results with these cell lines are variable ***(29)***. Fibroblast cultures established from individuals with Hutchinson–Gilford progeria syndrome that exhibit a lower proliferative capacity than cells from normal individuals also exhibit shorter telomeres; however, the rate of telomere shortening per cell division appears to be similar in progeria fibroblasts and normal cells ***(16)***. It has recently been demonstrated that proliferative senescence can be delayed and possibly eliminated by transfection of normal cells with telomerase to prevent telomere loss ***(30)***. It is also interesting to note that other repetitive DNA sequences become shorter during proliferative senescence ***(31,32)***

1.1.2. Mitogenic Responses and Signal Transduction

As a result of senescence-associated changes, cells assume a flattened morphology and ultimately cease to proliferate in the presence of serum ***(5)***. Numerous factors may contribute to the senescent phenotype; however, the principal characteristic of cellular senescence in culture is the inability of the cells to replicate DNA. Paradoxically, the machinery for DNA replication appears to remain intact, as indicated by the fact that infection with SV-40 initiates a round of semiconservative DNA replication in senescent cells ***(33)***.

Nevertheless, senescent cells fail to express the proliferating cell nuclear antigen (PCNA), a cofactor of DNA polymerase δ, apparently as a result of a post-transcriptional block ***(34)***. Furthermore, senescent fibroblasts fail to complement a temperature-sensitive DNA polymerase α mutant ***(35,36)***. This may contribute to the failure of senescent cells to progress through the cell cycle because it is known that a direct relationship exists between the concentration of DNA polymerase α and the rate of entry into S phase ***(37)***. It has also been observed that replication-dependent histones are also repressed in senescent cells and that a variant histone is uniquely expressed ***(18)***.

It might also be noted that the senescence-dependent cessation of growth is not identical to G_0 growth arrest that occurs in early passage cells that exhibit contact inhibited growth or that are serum starved. Several lines of evidence suggest that senescent cells are blocked in a phase of the cell cycle with many characteristics of late G_1. For example, thymidine kinase is cell cycle regulated; it appears at the G_1/S boundary. Thymidine kinase activity is similar in cultures of proliferating young and senescent WI-38 cells ***(38,39)***. It should also be noted that thymidine triphosphate synthesis, which normally occurs in late G_1, is not impaired in senescent cells ***(39)***. Furthermore, the nuclear fluorescence pattern of senescent cells stained with quinacrine dihydrochloride is also typical of cells blocked in late G_1 or at the G_1/S boundary ***(33,40)***. In addition, Rittling et al. ***(41)*** demonstrated that 11 genes expressed between early G_1 and the G_1/S boundary are mitogen inducible in both young and senescent cells. On the other hand, growth-regulated genes such as *cdc2*, *cycA*, and *cycB*, which are expressed in G_1, are repressed in senescent cells ***(42)***. These observations suggest the possibility that senescent cells are irreversibly arrested in a unique state different from the normal cell cycle stages.

As cells approach the end of their proliferative potential in culture they become increasingly refractory to mitogenic signals ***(15,43,44)***. The signal transduction pathways that convey these mitogenic signals play significant roles in the regulation of cell proliferation and adaptive responses; hence, decline in the activity of elements in these pathways may contribute significantly to the senescent phenotype. For example, there is a senescence-associated loss in the capacity of cells to activate protein kinase C ***(45)*** or to increase interleukin-6 (IL-6) mRNA abundance ***(46)*** following stimulation with phorbol esters. Furthermore, transcriptional activation of c-*fos* following stimulation of cultures with serum is also diminished in senescent cells ***(18,47)***. Other genes such as *Id1* and *Id2*, which encode negative regulators of basic helix–loop–helix transcription factors, fail to respond to mitogens in senescent cells ***(48)***

Although signal transduction efficiency declines with replicative age, the members of affected pathways are seldom influenced uniformly by senescence. For example, both the number of receptors (per unit cell surface area) and

receptor affinities for epidermal growth factor (EGF), platelet-derived growth factor (PDGF), and insulin-like growth factor-one (IGF-one) remain constant throughout the proliferative life of fetal lung WI-38 fibroblasts ***(49–51)***; however, senescent WI-38 cells produce neither the mRNA nor the protein for IGF-I ***(52)***. Similarly, young and senescent WI-38 fibroblasts have similar baseline levels of intracellular Ca^{2+} and exhibit similar changes in cytosolic Ca^{2+} fluxes following growth factor stimulation ***(53)***; however, the expression of calmodulin protein is uncoupled from the cell cycle and exists in variable amounts in senescent WI-38 cells ***(53)***. The calmodulin-associated phosphodiesterase activity also appears to be diminished in late-passage cells (Cristofalo et al., unpublished results). At least some of the changes in signal transduction associated with senescence may also stem from alterations in the cellular redox environment, because the rate of oxidant generation increases during senescence ***(54)*** and some steps in various signal transduction pathways are highly sensitive to changes in redox balance. The protein abundances of protein kinase A (PKA) and various isoforms of protein kinase C (PKC) are unchanged or slightly increased by senescence ***(20,55)***; however, PKC translocation from the cytoplasm to the plasma membrane is impaired in senescent fibroblasts ***(45,56)***.

Changes in signal transduction efficiency associated with senescence are not necessarily the result of any decrease or loss of components of signaling pathways. Experiments performed in various types or immortal and normal cells reveal that increases in signal transduction components can also impede signaling pathways. This is most clearly seen in the case of the extracellular signal-regulated kinase (ERK) pathway where the correct sequence and duration of activation and inactivation of ERKs at the G_1/S boundary ***(57–59)*** is required for entry into S phase. Indeed, constitutive ERK activation has an inhibitory effect on cell cycle progression, both in NIH 3T3 fibroblasts ***(58)*** and in Xenopus oocytes ***(60)***. Furthermore, overexpression of oncogenic *ras* in human fibroblasts leads to a senescent-like state rather than to an immortal phenotype ***(61)***. Thus, increases as well as decreases in individual components of pathways may contribute to senescence-associated changes in signal transduction. Taken together, senescence-associated changes in mitogenic signaling pathways occur for a variety of reasons that may include any imbalances in or dysregulation of controlling pathways. Interestingly, these effects are largely confined to proliferation and noncritical functions because, if maintained, subpopulations of cells can survive indefinitely in a senescent state.

1.2. Relevance to Aging

Before beginning our discussion of methods for the propagation of human fibroblasts and determination of replicative life-span, we digress briefly to discuss interpretation of this type of data. We shall also consider the relationship

between changes observed during senescence in vitro and aging in vivo. Finally, we will examine a second hypothesis that suggests that senescence in vitro recapitulates at least some aspects of developmental changes associated with differentiation.

The finite replicative life-span for normal cells in culture is thought to result from multiple environmental and genetic mechanisms ***(5)*** and has frequently been used as a model of human aging. Historically the use of replicative life-span of cell cultures as a model for aging has been accepted because (1) fibroblast replicative life-span in vitro has been reported to correlate directly with species maximum life-span potential ***(62)***, and most importantly (2) cultures of normal human cells have been reported to exhibit a negative correlation between proliferative life-span and the age of the donor from whom the culture was established ***(8,16,63–68)***. Other types of evidence also appear to support the strength of the model. For example, the colony-forming capacity of individual cells has also been reported to decline as a function of donor age ***(69,70)***. Various disease states of cell donors have been found to significantly influence the proliferative life-spans of cells in culture. For example, cell strains established from diabetic ***(68,71)*** and Werner's patients exhibit diminished proliferative potential ***(19,28,65,72,73)***. Cultures derived from individuals with Hutchinson–Gilford syndrome ***(28)*** and Down's syndrome ***(28,74)*** may also exhibit decreased proliferative potential, albeit results with these cell lines are more variable ***(29)***. Collectively, these observations have been interpreted to suggest that the proliferative life-span of cells in culture reflects the physiological age as well as any pathological state of the donor from which the cells were originally obtained.

It must be noted that interpretation of replicative life-span data is often difficult owing to large individual variations and relatively low correlations. For example, one large study ***(75)*** determined replicative life-span in more than 100 cell lines, yet obtained a correlation coefficient of only–0.33. Hence, it is difficult to assess whether the reported negative correlations between donor age and replicative life-span indicate any compromise of physiology or proliferative homeostasis in vivo ***(75,76)***. A major factor that has influenced the results of most studies is the health status of donors when tissue biopsies were taken to establish the cell cultures ***(68,75)***. Most studies include cell lines established from donors who were not screened thoroughly for disease, as well as cell lines derived from cadavers to determine the effects of donor age on proliferative potential. Variations in the biopsy site have also been a factor that probably influenced the results of many studies ***(68,75)***.

Studies of rodent skin fibroblasts appear to support the existence of a small, but significant, inverse correlation between donor age and replicative life-span ***(67,77,78)***. Furthermore, it has also been observed that treatment of hamster

skin fibroblasts with growth promoters can extend the proliferative life of cultures established from young donors but has negligible effects on cultures established from older donors ***(79)***. Aside from inherent species differences and the effects of inbreeding that may influence these results, it is also apparent that rodent skin is better protected from some types of environmental injury such as light exposure. However, even in rodents, the relationship between donor age and proliferative potential is not entirely clear. For example, an examination of hamster skin fibroblast cultures established from the same donors at different ages reveals no age-associated changes in proliferative potential in animals older than 12 mo ***(78)***.

To address these issues, we recently examined the proliferative potential of 124 human fibroblast cell lines from the Baltimore Longitudinal Study of Aging (BLSA) ***(80)***. All of these cell lines were established from donors described as healthy, at the time the biopsy was taken, using the criteria of the BLSA. This study revealed no significant change in proliferative potential of cell lines with donor age, nor did we observe a significant difference between fetal and postnatally derived cultures ***(80)***. Goldstein et al. ***(68)*** also reported that no relationship between proliferative life-span and donor age could be found in healthy donors but did observe a relationship in diabetic donors. In addition, we performed a longitudinal study by determining the replicative life-span of cell lines established from individuals sampled sequentially at different ages. As in the case of the cross-sectional analysis, no relationship between donor age and replicative potential was found in this longitudinal study. Indeed, cell lines established from individuals at older ages frequently exhibited a slightly greater proliferative potential than the cell lines established from the same individuals at younger ages ***(80)***.

1.2.1. Relationship of In Vitro and In Vivo Models

One of the underlying assumptions of in vitro aging models is that the changes observed during proliferative senescence bear at least some homology to those observed during aging in vivo. In fact, both similar (concordant) and dissimilar (discordant) changes have been observed between aging-associated changes observed in vivo and in vitro; these are summarized in **Table 1**.

Although the results presented in **Table 1** clearly demonstrate that some similarities do exist between aging in vivo and replicative senescence, it remains unclear whether these changes arise through a common mechanism or via distinct pathways. As seen in **Table 1**, senescence in tissue culture and aging in the intact organism are not homologous. Others have noted that progressive morphological changes begin to develop in diploid cell cultures shortly after they are established regardless of the donor age; no cells are found in vivo

Table 1
Aging in Cell Culture Replicative Senescence vs Donor Age

Concordant features			Discordant features		
Collagenase	(↑)[a]	***(81,82)***	c-*fos* induction	(↓)	***(20,83,84)***
Stromelysin	(↑)	***(85)***	*EPC-1* mRNA	(↓)	***(86,87)***
PAI-1	(↑)	***(88,89)***	*H-twist* mRNA	(↓)	(***90***; *unpublished*)
IGF-BP3	(↓)	***(91)***	*G-6-PDH* mRNA	(=)[b]	***(54,92)***
TIMP-1	(↓)	***(85)***	Fibronectin	(↑)	***(93)***
HSP 70	(↓)	***(94,95)***	*ND-4* mRNA	(↑)	***(96,97)***
Response to Ca^{2+}	(↓)	***(98,99)***	*p21* mRNA	(↑)	***(100,101)***
			MnSOD mRNA	(↑?)	***(102,103)***
			β-Galactosidase	(↑)	(Cristofalo, *unpublished*)
			Chemiluminescence	(↑)	***(54,96)***
			H_2O_2 Generation	(↑)	***(54,96)***
			Collagen a(1)I mRNA	(↓)	***(100,104,105)***
			Proliferative capacity	(↓)	***(80)***
			Saturation density	(↓)	***(80)***

[a]Arrow indicates direction of change in replicative senescence.
[b]Indicates no change.
G-6-PDH, glucose-6-phosphate dehydrogenase; HSP 70, heat shock protein 70; IGF-BP3, insulin-like growth factor binding protein-3; PAI-1, plasmogen activator inhibitor-1; SOD, superoxide dismutase; TIMP-1, tissue inhibitor of metalloproteinase-1.

at any age that exhibit the morphological phenotype of cells, in vitro, at the end of their replicative life-span ***(106)***.

Rubin ***(76)*** suggests that the limited replicative life-span in vitro may be an artifact that reflects the failure of diploid cells to adapt to the trauma of dissociation and the radically foreign environment of cell culture. However, that hypothesis ignores factors such as telomere shortening that appear to influence proliferative life and that are not dependent on the culture environment. Presently, it is possible to state that the loss of proliferative potential in vitro does not directly reflect changes in replicative capacity that occur in vivo during aging and that changes in gene expression associated with replicative senescence are not completely homologous with changes observed during aging in vivo.

1.2.2. Relationship Between Senescence and Development

One view of the limited proliferative capacity of cells in culture is that it stems from the effects of the culture environment on the state of differentiation of the cells ***(107–113)***. Although the state of differentiation may change in

Table 2
Comparison of Replicative Senescence of Fetal Cells In Vitro with Differences Between Fetal and Adult Cells?

Concordant			Discordant		
ND-4 mRNA	(↑)	***(96,97)***	c-*fos* induction	(=)[b]	***(84)***
MnSOD activity	(↑)	***(103,114)***	*EPC-1* mRNA	(↑)	***(86,87,97)***
Catalase activity	(↑)	***(92)***	*Cu/Zn SOD* mRNA	(↑)	***(102)***[c]
IL-1α	(↑)	***(103,115)***	*MnSOD* mRNA	(↑)	***(102,114)***[c]
IL-1β	(↑)	***(103,115)***	Cu/Zn SOD activity	(↑)	***(102)***[c]
Response to PDGF-BB	(↑)	***(116)***	*COX-1* mRNA	(↑)	***(96)***[c]
			SD[d] mRNA	(↑)	***(96)***[c]
			COX activity	(↑)	***(96)***[c]
			ND[d] activity	(↑)	***(96)***[c]
			SD activity	(↑)	***(96)***[c]
			G-6-PDH mRNA	(↑)	***(92)***
			PDGF requirement	(↑)	***(117)***
			Collagen a(1)I mRNA	(Ø)	***(100,118)***
			β-Actin	(Ø)	(***100***; *unpublished*)

[a]Arrow indicates direction of difference between proliferatively young fetal and adult cells.
[b]Indicates no change.
[c]Based on observations of changes during proliferative senescence, made in this laboratory that will be presented elsewhere ***(54)***.
[d]ND=NADH dehydrogenase; SD=succinate dehydrogenase.

cells that senesce in vitro, there is, in fact, no evidence that the changes in gene expression observed in fetal cells as they senesce in vitro, are tantamount to differentiation, in vivo. While some analogous changes can be found they are greatly outnumbered by the discordant differences that characterize these two distinct phenomena. Hence, a comparison of senescence-associated changes and differences that exist between fetal and postnatal cells reveals little similarity (**Table 2**).

At least some analogous similarities exist between senescence in fetal fibroblasts and developmental changes that occur in vivo. For example, it has been observed that addition of PDGF-BB stimulated an increased mRNA abundance of the transcript encoding the PDGF-A chain in fetal and newborns; however, the response was greatly decreased in adult cells. Senescence in vitro of newborn fibroblasts appears to result in the acquisition of the adult phenotype ***(116)***. In contrast, there are a number of differences reported between fetal- and adult-derived cell lines related to growth factor requirements for proliferation and migration ***(117,119–121)*** that remain disparate even as these cultures become

senescent. For example, Wharton ***(119)*** has shown that fetal dermal fibroblasts will proliferate in plasma or serum while adult dermal fibroblasts require serum. It is also noteworthy that the expression of some genes, such as *SOD-2*, increases during proliferative senescence but only in some types of fibroblasts ***(114)***; in other types of fibroblasts no change is observed ***(54,114)***. It might be expected that cells placed in culture will be deprived of those signals that direct the normal sequence of developmental pathways and that differentiation, if it occurs, is to an aberrant state. Alternatively, fetal cell lines may arise from different precursor cells than do adult fibroblasts and thus merely differentiate to a different fibroblast type.

1.2.3. Limitations and Strengths of the System

Although the loss of proliferative potential in vitro may not directly reflect changes in replicative capacity that occur in vivo during aging, cell cultures remain a powerful tool for a variety of aging-related studies. These include studies of heritable damage to cell populations that simulate the effects of aging in vivo ***(76)***, a variety of chemical and molecular manipulations used to induce a senescence phenotype, the effects of stress ***(61,76,122–125)***, and as a system to study abnormal growth or quiescence ***(5)***. The model may also help to further elucidate the effects of diseases that alter proliferative life-span ***(19,28,65,68,71–73,126)***. Loss of capacity for senescence is a necessary step for immortalization and transformation to a malignant phenotype. The model may also prove useful in studies of the relationship between differentiation and replicative aging ***(117,119–121)***.

2. Materials

The serum-supplemented and serum-free, growth factor-supplemented formulations presented each give optimal growth of human diploid fibroblast-like cells. We also present methods for growth of cells in a defined medium using a defined growth factor cocktail ***(2,127)***. All reagents and materials for cell culture must be sterile, and all manipulations should be performed in a laminar flow hood. Serial propagation is generally performed in serum-supplemented media, yet serum is a complex fluid with numerous known and unknown bioactive components. For many studies, it is often desirable if not crucial to use a serum-free growth medium of defined composition.

2.1. Serum-Supplemented Medium

Suppliers and more detailed information on the items required for the preparation of serum-supplemented media are listed in **Table 3**.

1. Incomplete Eagle's modified minimum essential medium: Cells are grown in Eagle's modified minimum essential medium (MEM). Although the medium can

Table 3
Components of Standard Growth Medium

Component	Amount/L	Supplier	Cat. no.
Auto-Pow™, autoclavable powder Eagle MEM with Earle's salts without glutamine and without sodium bicarbonate	1 pkg	ICN	11-100-22
100× Basal medium Eagle vitamins	10 mL	ICN	16-004-49
200 m*M* L-Glutamine	10 mL	Sigma	G3126
Sodium bicarbonate (7.5% solution)	26 mL	Sigma	S5761
FBS[a]	100 mL	Various	

[a]FBS is from a variety of suppliers and tested on a lot-by-lot basis. *See* **Note 1**.

be purchased in liquid form, it is considerably less expensive to prepare the medium from a commercially available mix. In our laboratory incomplete MEM is prepared by dissolving Auto-Pow™ powder (9.4 g) and 100× basal medium Eagle vitamins (10 mL) in 854 mL of deionized, distilled water. After the incomplete medium has been mixed and dissolved, it should be divided into two equal portions (432 mL each) and placed in 1-L bottles (*see* **Note 2**). The caps are screwed on loosely, autoclave tape is applied, and the bottles are autoclaved for 15 min at 121°C (*see* **Note 3**). As soon as the sterilization cycle is finished, the pressure is quickly released and the bottles are quickly removed from the autoclave. The bottles are allowed to cool to room temperature in a laminar flow hood. When the bottles have cooled, the caps are tightened. Incomplete medium is stored at 4°C in the dark.

2. 100× Basal medium Eagle vitamins: Filter-sterilized 100× basal medium Eagle vitamins are purchased in 100-mL bottles and stored at –20°C. When first thawed, using sterile procedures, the vitamin solution is divided into 10-mL portions and stored in sterile 15-mL centrifuge tubes at –20°C until use.
3. L-Glutamine (200 m*M*): L-Glutamine (14.6 g) is dissolved in 500 mL of deionized, distilled water without heating. This solution is then sterilized in a laminar flow hood using a 0.2 µm pore size bottletop filter. Aliquots (50 mL) are added to sterile 100-mL bottles that are then capped and stored at –20°C until use. When thawed for use, the glutamine solution is divided into 5-mL portions and stored at –20°C in sterile 15-mL centrifuge tubes until use.
4. Sodium bicarbonate (7.5% w/v): Sodium bicarbonate (37.5 g) is dissolved in 500 mL of deionized, distilled water. This solution is then filter sterilized using a 0.2-µm pore size bottletop filter. The sterile solution is stored at 4°C.
5. Fetal bovine serum (FBS): Prior to purchase, various lots of fetal bovine serum (FBS) are tested for 3 consecutive weeks to determine their effects on the rate of cell proliferation and saturation density. The serum lot that gives the best growth response is chosen, and quantities that will last about 1 yr are purchased. The serum is stored at –20°C until use. Once thawed, serum is stored at 4°C for subsequent use; it should not be refrozen.

Table 4
Components of Serum-Free Growth Medium

Component	Amount	Supplier	Cat. no.
MCDB-104, a modified basal medium with L-glutamine, without $CaCl_2$, without Na_2HPO_4, without $NaHCO_3$, and without HEPES, and with sodium pantothenate substituted for calcium pantothenate	1 pkg/L	Gibco-BRL	82-5006EA
Sodium phosphate, dibasic	0.426 g/L	Sigma	S5136
Sodium chloride	1.754 g/L	Sigma	S5886
Calcium chloride dihydrate	1 m*M*	Sigma	C7902
Sodium bicarbonate	1.176 g/L	Sigma	S5761
HEPES[a]	11.9 g/L	Sigma	H9136
1 *M* Sodium hydroxide[a]	25 mL/L	Sigma	S2770
EGF), human recombinant	25 ng/mL	Gibco-BRL	13247-010
IGF-I, human recombinant	100 ng/mL	Gibco-BRL	13245-014
Insulin	5 µg/mL	Sigma	I6634
Ferrous sulfate heptahydrate	5 µ*M*	Sigma	F8633
1 *M* Hydrochloric acid	Trace	Sigma	H9892
Dexamethasone	55 ng/mL	Sigma	D4902
95% Ethanol (not denatured)	Trace	Pharmco	111000-190CSGL

[a]Not used in growth medium. *See* **Note 1**.

6. Standard serum-supplemented growth medium (complete medium with 10% v/v FBS): To prepare the standard serum-supplemented growth medium (complete medium with 10% v/v FBS), add 13 mL of filter-sterilized 7.5% (w/v) sodium bicarbonate to 432 mL of sterile, incomplete Eagle's MEM. The sodium bicarbonate must be added first because low pH can affect glutamine and serum components. After addition of the sodium bicarbonate add 50 mL of sterile FBS. Just before use the medium is prewarmed to 37°C in a warm water bath, then transferred to a laminar flow hood where 5 mL of a 200 m*M* solution of filter-sterilized L-glutamine is added. Complete medium is generally prepared fresh for each use. If this medium must be stored for periods exceeding 1 wk, additional filter-sterilized L-glutamine (1 mL/100 mL of complete medium) is added just before use.

2.2. Serum-Free Medium

Suppliers and more detailed information on the items required for the preparation of serum-free media are listed in **Table 4**.

1. Serum-free growth medium: This medium is prepared by dissolving a packet of powdered MCDB-104 medium (with L-glutamine, without $CaCl_2$, without

Na_2HPO_4, without $NaHCO_3$, and without *N*-[2-hydroxyethyl]piperazine-*N*'-[2-ethanesulfonic acid] (HEPES), with sodium pantothenate substituted for calcium pantothenate) in 700 mL of deionized, distilled water. The packet is also rinsed several times to dissolve any medium powder that may have adhered to it. The following additional components are then added in the order listed: 0.426 g of Na_2HPO_4, 1.754 g of NaCl, 1.0 mL of a 1 *M* $CaCl_2$ solution, and 1.176 g of $NaHCO_3$. For most studies HEPES is not used. The final volume is brought to 1 L with deionized, distilled water. Incomplete medium is sterilized by filtration through a 0.2-µm bottletop filter into sterile glass bottles. Using sterile procedures in a laminar flow hood, a 5% CO_2/95% air mixture is passed through a sterile, cotton-filled $CaCl_2$ drying tube, through a sterile pipet, and bubbled into the medium (*see* **Note 4**). As the medium becomes saturated with the gas mixture, its color changes from pink to a salmon color. The final pH is 7.3–7.5. Incomplete medium is generally prepared fresh for each use, but it may be stored for up to 3 wk at 4°C. If unused complete medium is stored longer than 1 wk, additional L-glutamine (1 mL/100 mL of complete medium) should be added before use.

2. HEPES-buffered incomplete medium for stock solutions: The pH of carbon dioxide/bicarbonate-buffered MCDB-104 solutions rises during thawing, resulting in Ca_2PO_4 precipitate formation. Thus, growth factor and soybean trypsin inhibitor solutions that are stored frozen are prepared in HEPES-buffered solutions. To prepare 1 L of HEPES-buffered incomplete medium, mix medium as described previously except 11.9 g of HEPES free acid and 25.0 mL of 1 *M* NaOH are added instead of sodium bicarbonate. The pH of the medium is adjusted to 7.5 by titration with additional 1 *M* NaOH and the volume is brought to a final volume of 1 L with deionized, distilled water. The medium is sterilized by filtration through a 0.2-µm bottletop filter into sterile glass bottles. The HEPES-buffered incomplete medium may be stored at –20°C until needed.
3. Concentrated growth factor stock solutions: For these procedures, use sterile plastic pipets and perform all manipulations in a laminar flow hood. Stock solutions of growth factors (100×) are prepared in HEPES-buffered incomplete medium at the following concentrations: EGF (2.5 µg/mL) and either IGF-I (10 µg/mL) or insulin (500 µg/mL) (*see* **Note 5**). All stock solutions are dispensed with sterile plastic pipets into sterile 1.0-mL cryogenic vials. The stock solutions may be stored at –20°C for short periods (up to 4 wk) or at –70°C for longer periods (3–4 mo). Dexamethasone (5 mg/mL) is prepared in 95% nondenatured ethanol. This solution is then diluted into HEPES-buffered incomplete medium to give a 100× stock solution (5.5 µg/mL). Stock dexamethasone is stored in sterile, siliconized test tubes. Ferrous sulfate is prepared fresh, just prior use. After preparation 5 µL of 1 *M* hydrochloric acid is added to each 10 mL of the ferrous sulfate 100× stock (0.5 m*M*). This solution is sterilized by filtration through a 0.2-µm filter.
4. Complete serum-free growth medium: For 100 mL of complete serum-free growth medium, 1 mL of each of the 100× stock solutions are added to 96 mL of

Table 5
Components of Trypsinization Solution

Component	Final amount	Supplier	Cat. no.
Sodium chloride	6.8 g/L	Sigma	S5886
Potassium chloride	0.4g/L	Sigma	P5405
Sodium phosphate monohydrate, monobasic 0.14g/L	Sigma	S5655	
Glucose	1 g/L	Sigma	G6152
50× MEM amino acids, without glutamine	20 mL/L	Gibco-BRL	11130-051
100× basal medium Eagle vitamins	10 mL/L	ICN	16-004-49
0.5% Phenol red	10 mL/L	ICN	16-900-49
Sodium bicarbonate (7.5% solution)	5 mL/50 mL	Sigma	S5761
Trypsin, 2.5% in Hanks' balanced salt solution	5 mL/50 mL	Sigma	T4674
Soybean trypsin inhibitor, type I-S	1 mg/mL	Sigma	T6522

incomplete medium (MCDB-104). The resultant concentrations in the serum-free medium are: 25 ng/mL of EGF, 100 ng/mL of IGF-I, or 5 µg/mL of insulin (*see* **Note 5**); 55 ng/mL of dexamethasone; and 5 µ*M* of ferrous sulfate.

5. Soybean trypsin inhibitor solution for serum-free propagation: Soybean trypsin inhibitor (100 mg) is added to 100 mL of HEPES-buffered incomplete medium. This solution is sterilized by filtration through a 0.2-µm bottletop filter into a sterile bottle. The sterile solution is then dispensed into sterile 15-mL centrifuge tubes in 7-mL portions and stored at –20°C. When needed, the solution is thawed and diluted 1:1 with bicarbonate-buffered incomplete medium.

2.3. Trypsinization

Suppliers and more detailed information on the items required for the preparation of trypsinization solution are listed in **Table 5**.

1. Ca^{2+}/Mg^{2+}-free medium: Cells tend to aggregate in media containing calcium; it is thus desirable to use a medium that is low in Ca^{2+} and Mg^{2+} for mixing trypsin solution. To prepare Ca^{2+}/Mg^{2+}-free medium, the following ingredients are added to 900 mL of deionized, distilled water with magnetic stirring: 6.8 g of NaCl, 0.4 g of KCl, 0.14 g of $NaH_2PO_4 \cdot H_2O$, 1 g of glucose, 20 mL of 50× MEM amino acids without glutamine, 10 mL of 100× basal medium Eagle vitamins, and 10 mL of a 0.5% (w/v) solution of phenol red. The solution is then diluted to 1 L with deionized, distilled water and sterilized by filtration. The Ca^{2+}/Mg^{2+}-free medium is stored at 4°C until use.
2. Trypsin stock solution (2.5%): Filter-sterilized trypsin (2.5%) in Hanks' buffered salts solution is purchased in 100-mL bottles and stored at –20°C. Repeated

Table 6
Items for Thymidine Incorporation

Item	Supplier	Cat. no.
[^{3}H-methyl]-Thymidine, 2 Ci/mmol; 1 mCi/mL	Dupont NEN	NET-027A
Coverslip, No. 1, 22 mm × 22 mm	Thomas	6662-F55
Coverslip rack, ceramic	Thomas	8542-E30
Coverslip rack, glass	Fisher	08-812
Chloroform	Sigma	C5312
95% Ethanol, not denatured	Pharmco	111000190CSGL
95% Sulfuric acid	Sigma	S1526
70% Nitric acid	Sigma	25,811-3
Sodium hydroxide	Sigma	S5881
Petri dish, glass, 100 mm	Thomas	3483-K33
NTB-2 Emulsion	Eastman Kodak	165 4433
D-19 Developer	Eastman Kodak	146 4593
Acid fixer	Eastman Kodak	197 1746
Hematoxylin, Harris Modified	Fisher	SH30-500D
Permount	Fisher	SP15-100
Microscope slide, 3 in × 1 in	Thomas	6684-H61
Lab-Tek® Chamberslide™, two-chamber	Nalge Nunc	177380
Lab-Tek® Chamberslide™, four-chamber	Nalge Nunc	177437
Lab-Tek® Chamberslide™, eight-chamber	Nalge Nunc	177445
Sodium phosphate, dibasic	Sigma	S5136
Potassium phosphate, monobasic	Sigma	P5655
Methanol	Fisher	A408-1
Slide mailer, polypropylene	Thomas	6707-M27
Slide box, polypropylene	Thomas	6708-G08

freeze–thaw will very rapidly decrease activity. The bulk trypsin solution should be thawed only once, dispensed in 5-mL portions in sterile 15-mL centrifuge tubes and then stored at –20°C until use.

3. Trypsin solution (0.25%): Five milliliters of sterile sodium bicarbonate (7.5%) is added to 40 mL of ice-cold Ca^{2+}/Mg^{2+}-free medium. Subsequently, 5 mL of freshly thawed 2.5% trypsin stock is added to the solution. This solution should be prepared just before the cells are treated and should be kept on ice.

2.4. Thymidine Incorporation

Suppliers and more detailed information on the items required for measurement of thymidine incorporation are listed in **Table 6**.

1. [^{3}H-*methyl*]-thymidine stock solution: Under sterile conditions, [^{3}H-*methyl*]-thymidine (2 Ci/mmol, 1 mCi/mL) is diluted to a concentration of 5 µCi/mL in ster-

ile medium. This stock solution is aliquoted (5-mL portions) in a laminar flow hood using sterile procedures into sterile, 15-mL centrifuge tubes and stored at –20°C until use.

2. Phosphate-buffered saline (PBS) solution: dissolve 8 g of NaCl, 0.2 g of KCl, 1.44 g of Na_2HPO_4, and 0.24 g of KH_2PO_4 in 900 mL of H_2O with magnetic stirring. The pH is adjusted to 7.4 with HCl, the volume adjusted to 1 L, and the solution is autoclaved for 20 min at 121°C.
3. Emulsion: Kodak NTB-2 emulsion is purchased in a lightproof container. The emulsion is stored at 4°C (*see* **Note 6**).
4. Developer and Fixer
   a. Kodak D-19 developer is purchased in packets that make 1 gal when reconstituted. The entire packet is used at one time and the solution is stored in a brown bottle in the dark. The developer remains useable for 1–3 mo. When the developer turns yellow, it is discarded.
   b. Acid fixer is made and stored in the same manner as the D-19 developer.

3. Methods

3.1. Cell Propagation in Serum-Supplemented Medium

Cells may be grown in a variety of culture vessels (*see* **Note 7**). Amounts described in the following procedure are for a T-75 flask. Proportional amounts are used for other size vessels; i.e., for a T-25 flask, one third of all of the amounts given is used. Trypsinization and seeding of flasks should be performed in a sterile environment (*see* **Note 8**).

To propagate adherent cells:

1. Prepare fresh trypsin solution (0.25%) and place it on ice; prepare fresh growth medium and warm it to 37°C.
2. Using sterile procedures in a laminar flow hood, remove spent growth medium from the culture vessel. For flasks and bottles, the medium should be removed by aspiration or decanting from the side opposite the cell growth surface. For cell culture plates and dishes, the medium should be removed by aspiration from the edge of the growth surface.
3. Gently wash the monolayers of adherent cells twice with 0.25% trypsin solution (4 mL).
4. Remove residual trypsin solution by aspiration from the side opposite the cell growth surface (flasks) or from the edge of the growth surface (plates, dishes, and slides) as appropriate.
5. Add enough trypsin solution (0.25%) to wet the entire cell sheet (2 mL/T-75).
6. The culture vessel should be tightly capped to maintain sterility and placed at 37°C.
7. The cells will assume a rounded morphology as they are released from the growth surface. Detachment of the cells should be monitored using a microscope. As a general rule, detachment will be complete within 15 min. The trypsinization process may be speeded up by gently tapping the sides of the flask. Care should be

taken to not splash cell suspension against the top and sides of the flask, because this will lead to errors in the determination of the number of cells in the flask.

8. When all of the cells have detached from the growth surface, as determined by inspection with a microscope, the flask is returned to the laminar flow hood. Complete medium with 10% v/v FBS is carefully pipeted down the growth surface of the vessel to neutralize the trypsin and to aid in pooling the cells. For a T-75 flask, 8 mL of complete medium is used. The final harvest volume is 10 mL.
9. Cell clumps should be dispersed by drawing the entire suspension into a 10-mL pipet and then allowing it to flow out gently against the wall of the vessel. The process is repeated at least three times. The procedure is then repeated with a 5-mL pipet. Until the procedure becomes routine, a sample is withdrawn and examined under the microscope to ensure that a suspension of single cells has been achieved. During this process, the cells should be kept on ice to inhibit cell aggregation and reattachment.
10. Using sterile procedures, remove an aliquot from the cell suspension, then dilute it into Isoton II in a counting vial. Typically, 0.5 mL of the cell suspension is diluted into 19.5 mL of Isoton II.
11. Count the sample with a Coulter Counter.
12. Calculate the number of cells in the harvest. Calculate the volumes of cell suspension and complete medium needed for new cell culture growth vessels. In most cases, cells are seeded at a density of 1×10^4 cells/cm^2 of cell growth surface, and the total volume of cell suspension plus complete medium added to the culture vessels is maintained at 0.53 mL/cm^2 of cell growth surface.
13. In the laminar flow hood, add the calculated amounts of complete medium to new culture vessels.
14. Dissolved CO_2 in equilibrium with HCO_3^- is the principal buffer system of the medium, although serum also has some buffering capacity. Because CO_2 is volatile, the gas phases in the flasks are adjusted to the proper pCO_2 to maintain the pH of the medium at 7.4. Using sterile procedures in a laminar flow hood, a 5% CO_2/95% air mixture is passed through a sterile, cotton-filled $CaCl_2$ drying tube, through a sterile pipet, and into the gas phase of the cell culture flask with the growth surface down. As the gas mixture is flushed over the medium surface, the color of the medium will change from a dark red toward a red-orange. The flask is flushed until the medium no longer changes color. At this point, the gas above the medium is 5% CO_2 and the pH of the medium is 7.4 (*see* **Note 4**). The flask is then tightly capped to prevent gas exchange with the outside environment. Cells grown in culture plates, dishes, and Lab-Tek® slides, which are not gas-tight, are not equilibrated with the gas mixture in this manner; instead they must be grown in incubators that provide a humidified, 5% CO_2 atmosphere.
15. The cell harvest is resuspended with 10-mL and 5-mL pipets, as before. Inoculate each culture vessel to a final density of 1×10^4 cells/cm^2 of growth surface.
16. Briefly flush the culture vessel a second time with the 5% CO_2/95% air mixture to replace the CO_2 lost when the vessel was opened. Cap the flask tightly and

incubate at 37°C. Periodically, examine the color of the medium to ensure that the seal is gas tight.

17. The cumulative population doubling level (cPDL) at each subcultivation is calculated directly from the cell count (*see* **Note 7**).

Example:

One week after seeding a T-75 flask with the standard inoculum of 7.5×10^5 cells at a cPDL of 37.2, the cells are harvested. One doubling would yield $2 \times 7.5 \times 10^5 = 1.5 \times 10^6$ cells; two doublings would result in $4 \times 7.5 \times 10^5 = 3.0 \times 10^6$ cells; three doublings would yield $8 \times 7.5 \times 10^5 = 6.0 \times 10^6$ cells, etc. Thus, the population doubling increase is calculated by the formula:

$$N_H/N_I = 2^X$$

or

$$[\log_{10}(N_H) - \log_{10}(N_I)]/\mathrm{Log}_{10}(2) = X$$

where N_I = inoculum number, N_H = cell harvest number, and X = population doublings. The population doubling increase that is calculated is then added to the previous population doubling level to yield the cPDL. For example, if 9.1×10^6 cells were harvested, then the population doubling increase can be calculated from the expression:

$$9.1 \times 10^6 \text{ cells} = 2\,(X) \times 7.5 \times 10^5 \text{ cells}$$

$$X \log_{10} 2 = \log_{10}(9.1 \times 10^6) - \log_{10}(7.5 \times 10^5)$$

$$X = 3.6$$

The population doubling increase is added to the previous cPDL to give the new cPDL of the cell population. For this example, the new cPDL is 37.2 + 3.6 = 40.8. The end of the replicative life-span was defined by failure of the population to double after 4 wk in culture with 3 wk of consecutive refeeding.

3.2. Cell Propagation in Serum-Free Medium

1. Because undefined mitogens and inhibitors present in serum complicate the interpretation of cell growth response results, soybean trypsin inhibition solution should be used to stop trypsin instead of complete medium with 10% v/v FBS to wash and collect the cells from the growth surfaces of flasks. Otherwise, cells are released from the surface of their culture vessel exactly as described previously for propagation of cells in serum-supplemented medium (**Subheading 3.1., steps 1–12**).
2. Wash the cells to remove residual mitogens and trypsin inhibitor, rather than using them directly to inoculate the culture flasks:
   a. Under sterile conditions, the cells are pelleted by centrifugation at 75*g* for 5 min at 4°C.

b. The centrifuge tubes are placed in ice, transferred to a laminar flow hood, the supernatant is removed, and the cells are resuspended in 10 mL of incomplete serum-free growth medium (**Subheading 2.1.**).
c. Under sterile conditions, the cells are again pelleted by centrifugation, and after removal of the supernatant, the cells are resuspended in 10 mL of complete serum-free growth medium (**Subheading 2.2.**).

3. Determine the cell number with the Coulter Counter as before, using an aliquot of the cell suspension (0.5 mL)
4. Cells are then seeded exactly as described in **Subheading 3.1.**, **steps 13–17**, except that serum-free cell growth medium is used.

3.3. Replicative Life-Span

As noted previously, cells in culture exhibit a finite number of replications. At the end of their in vitro life-span substantial cell death occurs; however, a stable population emerges that can exist in a viable, though nondividing, state indefinitely ***(128)***. Furthermore, small subpopulations of cells may retain some growth capacity even after the vast majority of cells in a culture are no longer able to divide. As a practical matter, cultures of cells may be considered to have reached the end of their proliferative life-span when the cell number fails to double after 4 wk of maintenance in growth medium with weekly refeedings. The maximum proliferative capacity of the cells is determined as follows:

When cell cultures are near the end of their proliferative life-span, at least four identical sister flasks are prepared. One flask is harvested each week. If the number of cells harvested is at least double the number inoculated, cells are subcultivated as usual. One of the sister flasks may also need to be harvested to provide enough cells for subcultivation into four flasks. If the number of cells harvested is not at least double the number inoculated, all of the sister flasks are refed by replacement of the spent medium with fresh complete medium and equilibration with 5% CO_2/95% air mixture. This process is repeated three times. When cultures fail to double during this period, the culture may be considered to have reached the end of proliferative life or to be "phased out."

3.4. Saturation Density

Cultures are grown until the cells are densely packed and no mitotic figures are apparent. This usually requires from 7 to 10 d after seeding for early passage cells, and more than 9 d for later passage cells. To estimate the saturation density, these confluent and quiescent cells are then harvested and counted as described previously.

3.5. Microscopic Estimate of Cell Density

It is often desirable to obtain an estimate of cell density without harvesting the cells. A stage micrometer is used to calibrate the eyepiece micrometer and

determine the diameter of the field of view for each objective and ocular lens used. The area of the field of view is calculated as Area = πr^2, where r is the radius of the field of view.

Scan the sample to ensure that the cells are uniformly distributed. Then count at least 400 cells using random fields. Since the standard deviation of a Poisson distribution is the square root of the number, 400 cells are counted. The square root of 400 ***(20)*** is 5%, which is the limit of statistical reliability for most biological work. Record the number of cells and the number of fields counted. The cell density is then calculated as follows:

cell density = (no. of cells counted)/([no. of fields counted] · [area per field])

3.6. Thymidine Incorporation

3.6.1. Coverslips

1. Place coverslips in a clean, glass rack using forceps.
2. Lower the rack containing the coverslips into a solution of chloroform/95% ethanol (1:1) and allow to soak for 30 min.
3. Rinse the coverslips with deionized water.
4. Submerge the coverslips in a 95:5 solution of concentrated sulfuric acid (95%)/concentrated nitric acid (70%), previously prepared in a fume hood and allowed to cool to room temperature. Soak the coverslips in this solution for 30 min.
5. Rinse the coverslips thoroughly in deionized water.
6. The rack containing the coverslips should then be lowered into a solution 0.2 *M* NaOH and allowed to soak for 30 min.
7. Remove the coverslips from the NaOH solution and rinsed at least three times in deionized water.
8. Remove the coverslips from the rack and allow to air-dry on lint-free disposable wipes.
9. When completely dry, bake the coverslips for 3 h at 180°C for sterilization.

3.6.2. Cell Slides

1. In a laminar flow hood, under sterile conditions, cells are harvested and counted in the usual manner.
2. Cells are seeded at a density of 1×10^4 cells/cm^2 on Lab-Tek® slides or in cell culture dishes that contain coverslips (**Subheading 3.6.1.**). If using coverslips use sterile forceps to arrange them in the dish so that they do not overlap one another.
3. Immediately after seeding, the slides and dishes are placed in an incubator at 37°C in an atmosphere of 5% CO_2/95% air.
4. Twenty-four hours later, add the stock solution of [^{3}H-*methyl*]-thymidine (specific activity 2 Ci/mmol; **Subheading 2.4.**) to the cultures to a final concentration of 0.1 µCi/mL.
5. After 30 h ***(129)***, the labeling medium is removed, and cells are immediately washed twice with PBS (**Subheading 2.4.**), fixed in 100% methanol for 15 min,

and air-dried. If cells are grown on coverslips, remove the coverslips from the dishes and place in a clean ceramic or glass rack using forceps prior to washing and fixing. If a Lab-Tek® slide is used, the plastic container and gasket must be removed prior to washing and fixing. These procedures should be done rapidly to limit damage to the cells. The cells must not be permitted to dry before they are fixed.

6. Mount coverslips with the cell surface up using mounting resin. Allow the resin to dry overnight.

3.6.3. Autoradiography

1. Remove the Kodak NTB-2 emulsion from storage at 4°C and place it in a warm room at 37°C. The emulsion will liquefy in 3–4 h. The emulsion may also be melted by placing it in a 40°C water bath in the dark for about 1–1.5 h. Do not shake the bottle because the resultant bubbles may cause irregularities in the final emulsion thickness.
2. In a dark room, the desired amount of emulsion is gently, but thoroughly mixed in a 1:1 ratio with deionized, distilled water.
3. Add 15–20 mL of the 1:1 emulsion/water solution to a container (a slide mailer works well for this) previously set up in a 40°C water bath in the dark.
4. Dip each slide individually into the slide mailer. One dip is sufficient to coat the slide.
5. Place each dipped slide in a standing (vertical) position in a wire test tube rack to drain off excess emulsion. The slides are allowed to dry for 30 min in the dark.
6. The dipped slides are placed into a slide box with a desiccant. The box is covered and sealed with black electrical tape. The box is placed inside a second light-tight container that also contains a desiccant and this is also sealed with electrical tape.
7. The container is placed at 4°C for 4 d.

Development of Cell Slides

1. Pour Kodak D-19 developer and acid fixer into large glass dishes.
2. Open the slide containers in a dark room (photo-safe light can be used), and remove the slides and place them in racks.
3. Place the slides in developer for 5 min.
4. Transfer the slides fixer for 5 min.
5. At this point, the room light may be turned on, if desired. Gently rinse the slides for 15 min in cold running water. The slides should next be lightly stained with Harris" modified hematoxylin stain to enhance nuclear visualization.

3.6.5. Staining Slides

1. Place the developed slides in staining dishes containing Harris" modified hematoxylin stain for 5–10 min. This amount of time is sufficient to produce light staining.
2. Drain slides in slide racks on paper towels.

3. Rinse the slides continuously with deionized, distilled water until the excess stain is removed and then drain them on paper towels.
4. Excess emulsion should be wiped from the back of slides while they are still damp
5. Air-dry the slides.

3.6.6. Counting Labeled Nuclei

1. For ease in identifying the limits of individual chambers under the microscope, if Lab-Tek® slides are used, the stain between the individual chambers can be removed with the end of a paper clip or push pin.
2. Silver grains over nuclei where [^{3}H-*methyl*]-thymidine has been incorporated into the DNA will be readily visible at 400× magnification. Nuclei with five or more grains are considered labeled.
3. To determine the percentage of labeled nuclei, at least 400 cells are counted per coverslip or chamber using random fields. Typically, determinations are done in duplicate.

4. Notes

1. It is important that the highest quality deionized, distilled water is used to prepare growth medium and all other reagents used for cell culture.
2. It is important that the bottles not be filled to more than one half volume to prevent overflow during sterilization.
3. Prolonged heat destroys some medium components.
4. Cells in a culture environment require carbon dioxide for growth and survival, and we have found that well controlled CO_2/bicarbonate buffered media gives superior growth when compared with media containing synthetic buffers, such as HEPES.
5. Insulin and IGF-I both stimulate growth through the IGF-I receptor, although insulin has lower affinity for the IGF-I receptor and 50-fold higher concentrations are required to achieve comparable growth. Insulin is less expensive than IGF-I, and despite the reduced specificity, insulin is satisfactory for most experiments.
6. Emulsion should never be stored near high-energy sources of radioactivity.
7. Cell cultures are typically subcultivated weekly. Multiple identical sister flasks are prepared at subcultivation, as a hedge against potential contamination or other anomalies. Because a substantial fraction (25–60%) of the cells do not survive subcultivation ***(130)***, the number of cells does not generally increase above the seeded cell number until approx 24 h after subcultivation.
8. Cultures should routinely examined microscopically for contamination, and tested for mycoplasma at 5-wk intervals ***(131)***.

Acknowledgments

This work was supported by the National Institutes of Health Grants AG00378 and AG00532.

References

1. Cristofalo, V. J. and Charpentier, R. (1980) A standard procedure for cultivating human diploid fibroblastlike cells to study cellular aging. *J. Tissue Cult. Methods* **6,** 117–121.
2. Phillips, P. D. and Cristofalo, V. J. (1989) Cell culture of human diploid fibroblasts in serum-containing and serum-free media, in *Cell Growth and Division: A Practical Approach* (Baserga, R., ed.), IRL, Washington, DC, pp. 121–132.
3. Swim, H. E. and Parker, R. F. (1957) Culture characteristics of human fibroblasts propagated serially. *Am. J. Hyg.* **66,** 235–243.
4. Hayflick, L. and Moorhead, P. S. (1961) The serial cultivation of human diploid cell strains. *Exp. Cell Res.* **25,** 585–621.
5. Cristofalo, V. J. and Pignolo, R. J. (1993) Replicative senesence of human fibroblast-like cells in culture. *Physiol. Rev.* **73,** 617–638.
6. Ponten, J. (1973) Aging properties of glia, in *INSERM* (Bourliere, F., Courtois, Y., Macieira-Coelho, A., and Robert, L., eds.), INSERM, Paris, pp. 53–64.
7. Rheinwald, J. G. and Green, H. (1975) Serial cultivation of strains of human epidermal keratinocytes: the formation of keratinizing colonies from single cells. *Cell* **6,** 331–343.
8. Bierman, E. L. (1978) The effects of donor age on the *in vitro* life span of cultured human arterial smooth-muscle cells. *In Vitro* **14,** 951–955.
9. Tassin, J., Malaise, E., and Courtois, Y. (1979) Human lens cells have an *in vitro* proliferative capacity inversely proportional to the donor age. *Exp. Cell Res.* **123,** 388–392.
10. Mueller, S. N., Rosen, E. M., and Levine, E. M. (1980) Cellular senescence in a cloned strain of bovine fetal aortic endothelial cells. *Science* **207,** 889–891.
11. Tice, R. R., Schneider, E. L., Kram, D., and Thorne, P. (1979) Cytokinetic analysis of impaired proliferative response of peripheral lymphocytes from aged humans to phytohemagglutinin. *J. Exp. Med.* **149,** 1029–1041.
12. Le Guilly, Y., Simon, M., Lenoir, P., and Bourel, M. (1973) Long-term culture of human adult liver cells: morphological changes related to *in vitro* senescence and effect of donor's age on growth potential. *Gerontologia* **19,** 303–313.
13. Medrano, E. E., Yang, F., Boissy, R., Farooqui, J., Shah, V., Matsumoto, K., Nordlund, J. J., and Park, H. Y. (1994) Terminal differentiation and senescence in the human melanocyte: repression of tyrosine-phosphorylation of the extracellular signal-regulated kinase 2 selectively defines the two phenotypes. *Mol. Biol. Cell* **5,** 497–509.
14. Cristofalo, V. J., Palazzo, R., and Charpentier, R. (1980) Limited lifespan of human diploid fibroblasts *in vitro*: metabolic time or replications?, in *Neural Regulatory Mechanisms During Aging* (Adelman, R. C., Roberts, J., Baker, G. T., Baskin, S. I. and Cristofalo, V. J., eds.), Alan R. Liss, New York, pp. 203–206.
15. Cristofalo, V. J., Phillips, P. D., Sorger, T., and Gerhard, G. (1989) Alterations in the responsiveness of senescent cells to growth factors. *J. Gerontol.* **44,** 55–62.
16. Allsopp, R. C., Vaziri, H., Patterson, C., Goldstein, S., Younglai, E. V., Futcher, A. B., Greider, C. W., and Harley, C. B. (1992) Telomere length predicts replicative capacity of human fibroblasts. *Proc. Natl. Acad. Sci. USA* **89,** 10,114–10,118.

17. Wright, W. E. and Shay, J. W. (1992) Telomere positional effects and the regulation of cellular senescence. *TIG* **8,** 193–197.
18. Seshadri, T. and Campisi, J. (1990) Repression of c-*fos* transcription and an altered gentic program in senescent human fibroblasts. *Science* **247,** 205–209.
19. Oshima, J., Campisi, J., Tannock, C. A., and Martin, G. M. (1995) Regulation of c-*fos* expression in senescing Werner syndrome fibroblasts differs from that observed in senescing fibroblasts from normal donors. *J. Cell. Physiol.* **162,** 277–283.
20. Keogh, B. P., Tresini, M., Cristofalo, V. J., and Allen, R. G. (1995) Effects of cellular aging on the induction of c-*fos* by antioxidant treatments. *Mech. Ageing Dev.* **86,** 151–160.
21. Levy, M. Z., Allsopp, R. C., Futcher, A. B., Greider, C. W., and Harley, C. B. (1992) Telomere end-replication problem and cell aging. *J. Mol. Biol.* **225,** 951–960.
22. von Zglinicki, T., Saretzki, G., Döcke, W., and Lotze, C. (1995) Mild hyperoxia shortens telomeres and inhibits proliferation of fibroblasts: a model for senescence? *Exp. Cell Res.* **220,** 186–192.
23. Feng, J., Funk, W. D., Wang, S.-S., Weinrich, S. L., Avilion, A. A., Chiu, C.-C., Adams, R. R., Chang, E., Allsopp, R. C., Yu, J., Le, S., West, M. D., Harley, C. B., Andrews, W. H., Greider, C. W., and Villeponteau, B. (1995) The RNA component of human telomerase. *Science* **269,** 1236–1241.
24. Counter, C. M., Avilion, A. A., LeFeuvre, C. E., Stewart, N. G., Greider, C. W., Harley, C. B., and Bacchetti, S. (1992) Telomere shortening associated with chromosome instability is arrested in immortal cells which express telomerase activity. *EMBO J.* **11,** 1921–1929.
25. Blasco, M. A., Funk, W., Villeponteau, B., and Greider, C. W. (1995) Functional characterization and developmental regulation of mouse telomerase RNA. *Science* **269,** 1267–1270.
26. Wainwright, L. J., Middleton, P. G., and Rees, J. L. (1995) Changes in mean telomere length in basal cell carcinomas of the skin. *Genes Chromosomes Cancer* **12,** 45–49.
27. Hiyama, K., Ishioka, S., Shirotani, Y., Inai, K., Hiyama, E., Murakami, I., Isobe, T., Inamizu, T., and Yamakido, M. (1995) Alterations in telomeric repeat length in lung cancer are associated with loss of heterozygosity in p53 and Rb. *Oncogene* **10,** 937–944.
28. Goldstein, S. and Harley, C. B. (1979) *In vitro* studies of age-associated diseases. *Fed. Proc.* **38,** 1862–1867.
29. Brown, W. T. (1990) Genetic diseases of premature aging as models of senescence, in *Annual Review of Gerontology and Geriatrics*, vol. 10 (Cristofalo, V. J. and Lawton, M. P., eds.), Springer, New York, pp. 23–52.
30. Bodnar, A. G., Ouellette, M., Frolkis, M., Holt, S. E., Chiu, C.-P., Morin, G. B., Harley, C. B., Shay, J. W., Lichtsteiner, S., and Wright, W. E. (1998) Extension of life-span by introduction of telomerase into normal human cells. *Science* **279,** 349–352.
31. Harley, C. B., Shmookler Reis, R. J., and Goldstein, S. (1982) Loss of repetitious DNA in proliferating somatic cells may be due to unequal recombination. *J. Theor. Biol.* **94,** 1–12.
32. Shmookler Reis, R. J. and Goldstein, S. (1980) Loss of reiterated DNA sequences during serial passage of human diploid fibroblasts. *Cell* **21,** 739–749.

33. Gorman, S. D. and Cristofalo, V. J. (1985) Reinitiation of cellular DNA synthesis in BrdU-selected nondividing senescent WI-38 cells by simian virus 40 infection. *J. Cell. Physiol.* **125,** 122–126.
34. Chang, C.-D., Phillips, P., Lipson, K. E., Cristofalo, V. J., and Baserga, R. (1991) Senescent human fibroblasts have a post-transcriptional block in the expression of the proliferating cell nuclear antigen gene. *J. Biol. Chem.* **266,** 8663–8666.
35. Pendergrass, W. R., Saulewicz, A. C., Hanaoka, F., and Norwood, T. H. (1994) Murine temperature-sensitive DNA polymerase alpha mutant displays a diminished capacity to stimulate DNA synthesis in senescent human fibroblast nuclei in heterokaryons at the nonpermissive condition. *J. Cell. Physiol.* **158,** 270–276.
36. Pendergrass, W. R., Angello, J. C., Saulewicz, A. C., and Norwood, T. H. (1991) DNA polymerase alpha and the regulation of entry into S phase in heterokaryons. *Exp. Cell Res.* **192,** 426–432.
37. Pendergrass, W. R., Angello, J. C., Kirschner, M. D., and Norwood, T. H. (1991) The relationship between the rate of entry into S phase, concentration of DNA polymerase alpha, and cell volume in human diploid fibroblast-like monokaryon cells. *Exp. Cell Res.* **192,** 418–425.
38. Cristofalo, V. J. (1973) Cellular senescence, factors modulating cell proliferation *in vitro*, in *INSERM* (Bourliere, F., Courtois, Y., Maciera-Coelho, A., and Robert, L., eds.), INSERM, Paris, pp. 65–92.
39. Olashaw, N. E., Kress, E. D., and Cristofalo, V. J. (1983) Thymidine triphosphate synthesis in senescent WI38 cells. Relationship to loss of replicative capacity. *Exp. Cell Res.* **149,** 547–554.
40. Pignolo, R. J., Martin, B. G., Horton, J. H., Kalbach, A. N., and Cristofalo, V. J. (1998) The pathway of cell senescence: WI-38 cells arrest in late G_1 and are unable to traverse the cell cycle from a true G_0 state. *Exp. Gerontol.* **33,** 67–80.
41. Rittling, S. R., Brooks, K. M., Cristofalo, V. J., and Baserga, R. (1986) Expression of cell cycle-dependent genes in young and senescent WI-38 fibroblasts. *Proc. Natl. Acad. Sci. USA* **83,** 3316–3320.
42. Stein, G. H., Drullinger, L. F., Robetorye, R. S., Pereira-Smith, O. M., and Smith, J. R. (1991) Senescent cells fail to express *cdc2*, *cycA*, and *cycB* in response to mitogen stimulation. *Proc. Natl. Acad. Sci. USA* **88,** 11,012–11,016.
43. Cristofalo, V. J., Doggett, D. L., Brooks-Frederich, K. M., and Phillips, P. D. (1989) Growth factors as probes of cell aging. *Exp. Gerontol.* **24,** 367–374.
44. Hosokawa, M., Phillips, P. D., and Cristofalo, V. J. (1986) The effect of dexamethasone on epidermal growth factor binding and stimulation of proliferation in young and senescent WI38 cells. *Exp. Cell Res.* **164,** 408–414.
45. De Tata, V., Ptasznik, A., and Cristofalo, V. J. (1993) Effect of the tumor promotor phorbol 12-myristate 13-acetate (PMA) on proliferation of young and senescent WI-38 human diploid fibroblasts. *Exp. Cell Res.* **205,** 261–269.
46. Goodman, L. and Stein, G. H. (1994) Basal and induced amounts of interleukin 6 mRNA decline progressively with age in human fibroblasts. *J. Biol. Chem.* **269,** 19250–19255.

47. Wheaton, K., Atadja, P., and Riabowol, K. (1996) Regulation of transcription factor activity during cellular aging. *Biochem. Cell Biol.* **74,** 523–534.
48. Hara, E., Uzman, J. A., Dimri, G. P., Nehlin, J. O., Testori, A., and Campisi, J. (1996) The helix–loop–helix protein Id-1 and a retinoblastoma protein binding mutant of SV40 T antigen synergize to reactivate DNA synthesis in senescent human fibroblasts. *Dev. Genet.* **18,** 161–172.
49. Gerhard, G. S., Phillips, P. D., and Cristofalo, V. J. (1991) EGF- and PDGF-stimulated phosphorylation in young and senescent WI-38 cells. *Exp. Cell Res.* **193,** 87–92.
50. Phillips, P. D., Kuhnle, E., and Cristofalo, V. J. (1983) ^{125}I-EGF binding activity is stable throughout the replicative life-span of WI-38 cells. *J. Cell. Physiol.* **114,** 311–316.
51. Phillips, P. D., Pignolo, R. J., and Cristofalo, V. J. (1987) Insulin-like growth factor-I: specific binding to high and low affinity sites and mitogenic action throughout the life span of WI-38 cells. *J. Cell. Physiol.* **133,** 135–143.
52. Ferber, A., Chang, C., Sell, C., Ptasznik, A., Cristofalo, V. J., Hubbard, K., Ozer, H. L., Adamo, M., Roberts, C. T., Jr., LeRoith, D. (1993) Failure of senescent human fibroblasts to express the insulin-like growth factor-1 gene. *J. Biol. Chem.* **268,** 17,883–17,888.
53. Brooks-Frederich, K. M., Cianciarulo, F. L., Rittling, S. R., and Cristofalo, V. J. (1993) Cell cycle-dependent regulation of Ca^{2+} in young and senescent WI-38 cells. *Exp. Cell Res.* **205,** 412–415.
54. Allen, R. G., Tresini, M., Keogh, B. P., Doggett, D. L., and Cristofalo, V. J. (1999) Differences in electron transport potential antioxidant defenses and oxidant generation in young and senescent fetal lung fibroblasts (WI-38). *J. Cell. Physiol.* **180,** 114–122.
55. Blumenthal, E. J., Miller, A. C., Stein, G. H., and Malkinson, A. M. (1993) Serine/threonine protein kinases and calcium-dependent protease in senescent IMR-90 fibroblasts. *Mech. Ageing Dev.* **72,** 13–24.
56. Venable, M. E., Blobe, G. C., and Obeid, L. M. (1994) Identification of a defect in the phospholipase D/diacylglycerol pathway in cellular senescence. *J. Biol. Chem.* **269,** 26,040–26,044.
57. Cook, S. J. and McCormick, F. (1996) Kinetic and biochemical correlation between sustained p44ERK1 (44 kDa extracellular signal-regulated kinase 1) activation and lysophosphatidic acid-stimulated DNA synthesis in Rat-1 cells. *Biochem. J.* **320,** 237–245.
58. Lavoie, J. N., G, L. A., Brunet, A., Muller, R., and Pouyssegur, J. (1996) Cyclin D1 expression is regulated positively by the p42/p44MAPK and negatively by the p38/HOGMAPK pathway. *J. Biol. Chem.* **271,** 20608–20616.
59. Meloche, S. (1995) Cell cycle reentry of mammalian fibroblasts is accompanied by the sustained activation of $p44^{mapk}$ and $p42^{mapk}$ isoforms in the G_1 phase and their inactivation at the G_1/S transition. *J. Cell. Physiol.* **163,** 577–588.
60. Walter, S. A., Guadagno, T. M., and Ferrell, J. E., Jr. (1997) Induction of a G_2-phase arrest in *Xenopus* egg extracts by activation of p42 mitogen-activated protein kinase. *Mol. Biol. Cell* **8,** 2157–2169.

61. Serrano, M., Lin, A. W., McCurrach, M. E., Beach, D., and Lowe, S. W. (1997) Oncogenic *ras* provokes premature cell senescence associated with accumulation of p53 and p16^{ink4a}. *Cell* **88,** 593–602.
62. Rohme, D. (1981) Evidence for a relationship between longevity of mammalian species and life spans of normal fibroblasts *in vitro* and erythrocytes *in vivo*. *Proc. Natl. Acad. Sci. USA* **78,** 5009–5013.
63. Hayflick, L. (1965) The limited *in vitro* lifetime of human diploid strains. *Exp. Cell Res.* **37,** 614–636.
64. Schneider, E. L. and Mitsui, Y. (1976) The relationship between *in vitro* cellular aging and *in vivo* human age. *Proc. Natl. Acad. Sci. USA* **73,** 3584–3588.
65. Martin, G. M., Sprague, C. A., and Epstein, C. J. (1970) Replicative life-span of cultivated human cells. *Lab. Invest.* **23,** 86–92.
66. Guilly, Y. L., Simon, M., Lenoir, P., and Bourel, M. (1973) Long-term culture of human adult liver cells: morphological changes related to *in vitro* senescence and effect of donor's age on growth potential. *Gerontoglia (Basel)* **19,** 303–313.
67. Bruce, S. A., Deamond, S. F., and Ts'o, P. O. P. (1986) *In vitro* senescence of syrian hamster mesenchymal cells of fetal to aged adult origin, inverse relationship between *in vivo* donor age and *in vitro* proliferative capacity. *Mech. Ageing Dev.* **34,** 151–173.
68. Goldstein, S., Moerman, E. J., Soeldner, J. S., Gleason, R. E., and Barnett, D. M. (1978) Chronologic and physiologic age affect replicative life-span of fibroblasts from diabetic, prediabetic, and normal donors. *Science* **199,** 781–782.
69. Schneider, E. L. (1979) Cell replication and aging: *in vitro* and *in vivo* studies. *Fed. Proc.* **38,** 1857–1861.
70. Smith, J. R., Pereira-Smith, O. M., and Schneider, E. L. (1978) Colony size distribution as a measure of *in vivo* and *in vitro* aging. *Proc. Natl. Acad. Sci. USA* **75,** 1353–1356.
71. Goldstein, S., Littlefield, J. W., and Soeldner, J. S. (1969) Diabetes mellitus and aging: diminished plating efficiency of cultured human fibroblasts. *Proc. Natl. Acad. Sci. USA* **64,** 155–160.
72. Martin, G. M. (1978) Genetic syndromes in man with potential relevance to pathobiology of aging, in *Genetic Effects on Aging* (Bergsma, D. and Harrison, D. E., eds.), Alan Liss, New York, pp. 5–39.
73. Danes, B. S. (1971) Progeria: a cell culture study on aging. *J. Clin. Invest.* **50,** 2000–2003.
74. Schneider, E. L. and Epstein, C. J. (1972) Replication rate and lifespan of cultured fibroblasts in Down's syndrome. *Proc. Soc. Exp. Biol. Med.* **141,** 1092–1094.
75. Martin, G. M., Ogburn, C. E., and Sprague, C. A. (1981) Effects of age on cell division capacity, in *Aging: A Challenge to Science and Society*, vol. 1 (Danon, D., Shock, N. W., and Marios, M., eds.), Oxford University Press, Oxford, England, pp. 124–135.
76. Rubin, H. (1997) Cell aging *in vivo* and *in vitro*. *Mech. Ageing Dev.* **98,** 1–35.
77. Pignolo, R. J., Masoro, E. J., Nichols, W. W., Brandt, C. I., and Cristofalo, V. J. (1992) Skin fibroblasts from aged Fischer 344 rats undergo similar changes in replicative life span but not immortalization with caloric restriction of donors. *Exp. Cell Res.* **201,** 16–22.

78. Bruce, S. A. and Deamond, S. F. (1991) Longitudinal study of *in vivo* wound repair and *in vitro* cellular senescence of dermal fibroblasts. *Exp. Gerontol.* **26,** 17–27.
79. Deamond, S. F. and Bruce, S. A. (1991) Age-related differences in the promoter-induced extension of *in vitro* proliferative life span of syrian hamster fibroblasts. *Mech. Ageing Dev.* **60,** 143–152.
80. Cristofalo, V. J., Allen, R. G., Pignolo, R. P., Martin, B. M., and Beck, J. C. (1998) Relationship between donor age and the replicative life spans of human cells in culture: a re-evaluation. *Proc. Natl. Acad. Sci. USA* **95,** 10614–10619.
81. Millis, A. J. T., Sottile, J., Hoyle, M., Mann, D. M., and Diemer, V. (1989) Collagenase production by early and late passage cultures of human fibroblasts. *Exp. Gerontol.* **24,** 559–575.
82. Sottile, J., Mann, D. M., Diemer, V., and Millis, A. J. (1989) Regulation of collagenase and collagenase mRNA production in early- and late-passage human diploid fibroblasts. *J. Cell. Physiol.* **138,** 281–290.
83. Seshadri, T. and Campisi, J. (1989) Growth-factor-inducible gene expression in senescent human fibroblasts. *Exp. Gerontol.* **24,** 515–522.
84. Grassilli, E., Bellesia, E., Salomoni, P., Croce, M. A., Sikora, E., Radziszewska, E., Tesco, G., Vergelli, M., Latorraca, S., Babieri, D., Fagiolo, U., Santacaterina, S., Amaducci, L., Tiozzo, R., Sorbi, S., and Franceschi, C. (1996) C-Fos/C-Jun expression and AP-1 activation in skin fibroblasts from centenarians. *Biochem. Biophys. Res. Commun.* **226,** 517–523.
85. Millis, A. J., Hoyle, M., McCue, H. M., and Martini, H. (1992) Differential expression of metalloproteinase and tissue inhibitor of metalloproteinase genes in aged human fibroblasts. *Exp. Cell Res.* **201,** 373–379.
86. Pignolo, R. J., Cristofalo, V. J., and Rotenberg, M. O. (1993) Senescent WI-38 cells fail to express EPC-1, a gene induced by young cells upon entry into the G_0 state. *J. Biol. Chem.* **268,** 8949–8957.
87. Tresini, M., Pignolo, R., Allen, R. G., Rottenberg, M. O., and Cristofalo, V. J. (1999) Expression of EPC-1 in human skin fibroblasts derived from donors of different ages. *J. Cell Physiol.* **179,** 11–17.
88. West, M. D., Shay, J. W., Wright, W. E., and Linskens, M. H. K. (1996) Altered expression of plasmogen activator and plasmogen activator inhibitor during cellular senescence. *Exp. Gerontol.* **31,** 175–193.
89. Ranby, M., Bergsdorf, N., Nisson, T., Mellbring, G., Winblad, B., and Bucht, G. (1986) Age dependence of tissue plasminogen activator concentrations in plasma, as studied by an improved enzyme-linked immunosorbent assay. *Clin. Chem.* **32,** 2160–2165.
90. Wang, S. M., Phillips, P. D., Sierra, F., and Cristofalo, V. J. (1996) Altered expression of the *twist* gene in young versus senescent human diploid fibroblasts. *Exp. Cell Res.* **228,** 138–145.
91. Goldstein, S., Moerman, E. J., and Baxter, R. C. (1993) Accumulation of insulin-like growth factor binding protein-3 in conditioned medium of human fibroblasts increases with chronological age of donor and senescence *in vitro*. *J. Cell. Physiol.* **156,** 294–302.
92. Keogh, B. P., Allen, R. G., Pignolo, R., Horton, J., Tresini, M., and Cristofalo, V. J. (1996) Expression of hydrogen peroxide and glutathione metabolizing enzymes in

human skin fibroblasts derived from donors of different ages. *J. Cell. Physiol.* **167,** 512–522.
93. Takeda, K., Gosiewska, A., and Peterkofsky, B. (1992) Similar, but not identical, modulation of expression of extracellular matrix components during *in vitro* and *in vivo* aging of human skin fibroblasts. *J. Cell. Physiol.* **153,** 450–459.
94. Deguchi, Y., Negoro, S., and Kishimoto, S. (1988) Age-related changes of heat shock protein gene transcription in human peripheral blood mononuclear cells. *Biochem. Biophys. Res. Commun.* **157,** 580–584.
95. Kumazaki, T., Wadhwa, R., Kaul, S. C., and Mitsui, Y. (1997) Expression of endothelin, fibronectin, and mortalin as aging and mortality markers. *Exp. Gerontol.* **32,** 95–103.
96. Allen, R. G., Keogh, B. P., Tresini, M., Gerhard, G. S., Volker, C., Pignolo, R. J., Horton, J., and Cristofalo, V. J. (1997) Development and age-associated differences in electron transport potential and consequences for oxidant generation. *J. Biol. Chem.* **272,** 24,805–24,812.
97. Doggett, D. L., Rotenberg, M. O., Pignolo, R. J., Phillips, P. D., and Cristofalo, V. J. (1992) Differential gene expression between young and senescent, quiescent WI-38 cells. *Mech. Ageing Dev.* **65,** 239–255.
98. Praeger, F. C. and Gilchrest, B. A. (1986) Influence of increased extracellular calcium and donor age on density-dependent growth inhibition of human fibroblasts (42345) *Proc. Soc. Exp. Biol. Med.* **182,** 315–321.
99. Praeger, F. C. and Cristofalo, V. J. (1986) The growth of WI-38 in a serum-free, growth factor-free, medium with elevated calcium concentrations. *In Vitro* **22,** 355–359.
100. Furth, J. J., Allen, R. G., Tresini, M., Keogh, B., and Cristofalo, V. J. (1997) Abundance of α1(I) and α1(III) procollagen and p21 mRNAs in fibroblasts cultured from fetal and postnatal donors. *Mech. Ageing Dev.* **97,** 131–142.
101. Nakanishi, M., Robertorye, R. S., Adami, G. R., Pereira-Smith, O. M., and Smith, J. R. (1995) Identification of the active region of the DNA synthesis inhibitory gene $p21^{Sdi1/CIP1/WAF1}$. *EMBO J.* **14,** 555–563.
102. Allen, R. G., Keogh, B. P., Gerhard, G., Pignolo, R., Horton, J., and Cristofalo, V. J. (1995) Expression and regulation of SOD activity in human skin fibroblasts from donors of different ages. *J. Cell. Physiol.* **165,** 576–587.
103. Kumar, S., Millis, A. J. T., and Baglioni, C. (1992) Expression of interleukin 1-inducible genes and production of interleukin 1 by aging human fibroblasts. *Proc. Natl. Acad. Sci. USA* **89,** 4683–4687.
104. Lapiere, C. M. (1988) Aging of fibroblasts, collagen and the dermis, in *Cutaneous Aging* (Kligman, A. M. and Takase, Y., eds.), University of Tokyo Press, Tokyo, 47–60.
105. Choi, A. M. K., Olsen, D. R., Cook, K. G., Deamond, S. F., Uitto, J., and Bruce, S. A. (1992) Differential extracellular matrix gene expression by fibroblasts during their proliferative life span *in vitro* and senescence. *J. Cell. Physiol.* **151,** 147–155.
106. Robbins, E., Levine, E. M., and Eagle, H. (1970) Morphologic changes accompanying senescence of cultured human diploid cells. *J. Exp. Med.* **131,** 1211–1222.
107. Bell, E., Marek, L. F., Levinstone, D. S., Merril, C., Sher, S., and Eden, M. (1978) Loss of division potential *in vitro*: aging or differentiation? *Science* **202,** 1158–1163.

108. Bell, E., Marek, L., Sher, S., Merrill, C., Levinstone, D., and Young, I. (1979) Do diploid fibroblasts in culture age? *Int. Rev. Cytol.* (Suppl. 10), 1–9.
109. Bayreuther, K., Francz, P. I., Gogol, J., Maier, M., and Meinrath, G. (1991) Differentiation of primary and secondary fibroblasts in cell culture systems. *Mutat. Res.* **256,** 233–242.
110. Kontermann, K. and Bayreuther, K. (1979) The cellular aging of rat fibroblasts *in vitro* is a differentiation process. *Gerontology* **25,** 261–274.
111. Bayreuther, K., Rodemann, H. P., Hommel, R., Dittamann, K., Albiez, M., and Francz, P. I. (1988) Human skin fibroblasts *in vitro* differentiate along a terminal cell lineage. *Proc. Natl. Acad. Sci. USA* **85,** 5112–5116.
112. Campisi, J. (1997) Aging and cancer: the double-edged sword of replicative senescence. *J. Am. Geriatr. Soc.* **45,** 482–488.
113. Livinstone, D., Eden, M., and Bell, E. (1983) Similarity of sister-cell trajectories in fibroblast clones. *J. Cell Sci.* **59,** 105–119.
114. Linskens, M. H. K., Fseng, J., Andrews, W. H., Enlow, B. E., Saati, S. M., Tonkin, L. A., Funk, W. D., and Villeponteau, B. (1995) Cataloging altered gene expression in yong and senescent cells using enhanced differential display. *Nucleic Acids Res.* **23,** 3244–3251.
115. Kumar, S., Vinci, J. M., Millis, A. J. T., and Baglioni, C. (1993) Expression of interleukin-1α and β in early passage fibroblasts from aging individuals. *Exp. Gerontol.* **28,** 505–513.
116. Karlsson, C. and Paulsson, Y. (1994) Age-related induction of platelet-derived growth factor A-chain mRNA in normal human fibroblasts. *J. Cell. Physiol.* **158,** 256–262.
117. Slayback, J. R., Cheung, L. W., and Geyer, R. P. (1977) Comparative effects of human platelet growth factor on the growth and morphology of human fetal and adult diploid fibroblasts. *Exp. Cell Res.* **110,** 462–466.
118. Furth, J. J. (1991) The steady state levels of type I collagen mRNA are reduced in senescent fibroblasts. *J. Gerontol.* **46,** B122-B124.
119. Wharton, W. (1984) Newborn human skin fibroblasts senesce *in vitro* without acquiring adult growth factor requirements. *Exp. Cell Res.* **154,** 310–314.
120. Clemmons, D. R. (1983) Age-dependent production of a competent factor by human fibroblasts. *J. Cell. Physiol.* **114,** 61–67.
121. Kondo, H. and Yonezawa, Y. (1995) Fetal-adult phenotype transition, in terms of the serum dependency and growth factor requirements, of human skin fibroblast migration. *Exp. Cell Res.* **220,** 501–504.
122. Chen, Q., Fisher, A., Reagan, J. D., Yan, L. J., and Ames, B. N. (1995) Oxidative DNA damage and senescence of human diploid fibroblasts. *Proc. Natl. Acad. Sci. USA* **92,** 4337–4341.
123. Venable, M. E., Lee, J. Y., Smyth, M. J., Bielawska, A., and Obeid, L. M. (1995) Role of ceramide in cellular senescence. *J. Biol. Chem.* **270,** 30701–30708.
124. Tresini, M., Mawaldewan, M., Cristofalo, V. J., and Sell, C. (1998) A phosphatidylinositol 3-kinase inhibitor induces a senescent-like growth arrest in human diploid fibroblasts. *Cancer Res.* **58,** 1–4.

125. Ogryzko, V. V., Hirai, T. H., Russanova, V. R., Barbie, D. A., and Howard, B. H. (1996) Human fibroblast commitment to a senescence-like state in response to histone deacetylase inhibitors is cell cycle dependent. *Mol. Cell. Biol.* **16,** 5210–5218.
126. Goldstein, S., Moerman, E. J., Soeldner, J. S., Gleason, R. E., and Barnett, D. M. (1979) Diabetes mellitus and genetic prediabetes. Decreased replicative capacity of cultured skin fibroblasts. *J. Clin. Invest.* **63,** 358–370.
127. Phillips, P. D. and Cristofalo, V. J. (1988) Classification system based on the functional equivalency of mitogens that regulate WI-38 cell proliferation. *Exp. Cell Res.* **175,** 396–403.
128. Matsumura, T., Zerrudo, Z., and Hayflick, L. (1979) Senescent human diploid cells in culture: suvival, DNA synthesis and morphology. *J. Gerontol.* **34,** 328–334.
129. Cristofalo, V. J. and Sharf, B. B. (1973) Cellular senescence and DNA synthesis: thymidine incorporation as a measure of population age in human diploid cells. *Exp. Cell Res.* **76,** 419–427.
130. Cristofalo, V. J. and Kritchevsky, D. (1965) Growth and glycolysis in the human diploid cell strain WI-38. *Proc. Soc. Exp. Biol. Med.* **118,** 1109–1113.
131. Levine, E. M. (1972) Mycoplasma contamination of animal cell cultures: a simple, rapid detection method. *Exp. Cell Res.* **74,** 99–109.

3

Human T-Cell Clones

Graham Pawelec

1. Introduction

Techniques for generating human T-cell clones (TCCs) were first described nearly two decades ago ***(1,2)***. This was a direct consequence of the discovery of T-cell growth factor and the subsequent ability to propagate T-cells over extended periods ***(3)***. Early on, numerous publications in immunology indicated an apparently unlimited growth potential of normal mammalian T lymphocyte cultures; however, even at this time, other investigators challenged this conclusion ***(4,5)***. Nonetheless, the possibility remained that at least some TCCs represented an exception to the rule of the Hayflick Limit for growth of normal somatic cells. If this were the case, the real relevance of replicative senescence as a universal phenomenon would be highly questionable. On the other hand, if those T-cells surviving apparently indefinitely were endowed with the properties of stem cells rather than differentiated cells, this quandary would be resolved. However, as far as could be judged, the apparently immortal TCCs described in the literature seemed to possess all the attributes of normal T-cells, not stem cells. Several explanations for this apparent paradox have been proposed, the most likely of which may be that such immortal lines are in fact abnormal. Few clones were tested for karyotypic or other abnormalities. Such analyses, when performed, often revealed genetic aberrations in human as well as murine clones ***(6,7)***. In the case of murine cells, continuous cultures often transform spontaneously in culture, but in humans this is rare or absent.

We and others have systematically approached the question of longevity of normal human TCCs using variations of the original interleukin-2 (IL-2)-dependent cloning and propagation protocol ***(1,2)***. This procedure involves limiting dilution of the cell suspension to be cloned, and microwell culture of the

From: *Methods in Molecular Medicine*, Vol. 38: *Aging Methods and Protocols*
Edited by: Y. A. Barnett and C. R. Barnett

diluted cells on an irradiated feeder cell layer in the presence of chemically defined media supplemented with growth factors (e.g., IL-2). We wished to establish whether culture aging of TCCs did occur, how it could be characterized, and whether it depended on the source and nature of the T-cells studied. The first question approached was to what extent culture conditions affected cloning efficiencies and longevity of the TCC ***(8)***; most of our early data were then obtained using a standard culture system employing medium supplemented with human serum (HS) and natural IL-2 ***(9)*** and using feeder cells consisting of a pool of peripheral blood mononuclear cells (PBMCs) from >20 random healthy donors. The T-cells to be cloned were derived from young adult donors and were mostly prestimulated with alloantigens. Under these conditions, the type of T-cell predominantly derived was $CD4^+$ and carried the α/β T-cell receptor (TCR2). This chapter therefore focuses on this type of TCC, and not on CD8 or TCR1 cells, which seem to behave somewhat differently in culture, but which we have not studied so extensively.

For meaningful studies of T-cell aging in vitro, it is essential to know the in vivo age of the starting T-cell population. This is impossible in a mixture of T-cells from an adult individual, as separation of subsets according to naive cell and memory cell markers is a crude and inaccurate method. Assessing age by measuring telomere lengths, even of individual cells, is also not satisfactory, as it cannot take into account whether telomerase has been activated at some point in these cells ***(10)***. The only way to be sure that all T-cells being studied are of the same age at the beginning of the experiment is to isolate precursors and cause them to differentiate into T-cells in vitro ***(11,12)***. Longevity comparisons between these pre-T-cell-derived precursors and TCCs from mature T-cells of the same donors suggested that the latter have a shorter life expectancy corresponding to the time required for the precursors to develop into T-cells in vitro ***(13)***. We therefore hypothesized that the T-cell "clock" was first set at the time when fully mature T-cells were generated and not at some time beforehand at the precursor or stem cell level ***(14)***. Going further back in the T-cell differentiation pathway, $CD34^+$ stem cells have the potential to develop into T-cells in in vitro culture systems ***(15)***, and this property could be exploited to study T-cell aging. Thus far, cumbersome thymic organ culture or thymic stromal cell culture systems have been required for this; here we present a variant TCC culture protocol that allows the generation of mature T-cells from isolated $CD34^+$ stem cells in liquid culture in the absence of thymic components.

2. Materials

1. T-cell growth factors (TCGFs): The quality and purity of the T-cell growth factors employed is critical. The main and most commonly used TCGF is IL-2 in the form of purified recombinant protein. Nowadays, many companies offer high-

quality IL-2; the investigator should pretest a batch for suitability for the cells being cultured. Mixtures of TCGFs may be useful in some circumstances, especially IL-2 + IL-4 or IL-2 + IL-7 (*see* **Subheading 3.**). Major suppliers are Genzyme, Endogen, PeproTech, R and D Systems, Boehringer-Mannheim, and so on.

2. Monoclonal antibodies (MAbs): Again, there are many suppliers of different antibodies, and companies favored will be different in different parts of the world. Major suppliers are Becton-Dickinson, Coulter-Immunotech, DAKO, and so on. However, for certain purposes, such as cell isolation with magnetic beads (*see* **Subheading 2.3.1.**), it may be economically desirable to obtain hybridoma cells and produce MAb oneself. The hybridoma cells are easy to grow, and for the purposes of cell separation, culture supernatants do contain enough MAbs. Obtaining hybridomas may be a problem, but cell banks such as the American Type Culture Collection (ATCC) can provide hybridomas secreting MAbs against common antigens sufficient for most cell separation purposes.
3. Magnetic beads:
   a. Dynabeads (Dynal, Oslo, Norway): In this method, the T-cell population is negatively selected after the cells are labeled with cocktails of MAbs against B cells (e.g., CD19), natural killer (NK) cells (CD16), monocytes (CD14), major histocompatibility class (MHC) II, etc. Because of the amount of MAbs required it is recommended that hybridoma supernatants are used. Dynabeads M450 coated with sheep anti-mouse IgG can be employed for most negative cell separations.
   b. Miltenyi CD34 Progenitor Kit (Miltenyi Biotec, Bergisch-Gladbach, Germany) is supplied with the necessary reagents for CD34 cell isolation by positive selection. The magnetic particles are precoated with CD34 MAbs directed against a particular exposed epitope of CD34 (class II epitope); purity of the derived population can then be checked with a MAb directed at a different epitope (e.g., anti-class I MAb My10 from Coulter-Immunotech).
4. Culture medium: Human serum for supplementing media such as RPMI 1640 or IDMEM to support long-term growth of T-cells cannot be reliably obtained commercially. It is necessary to prepare and screen the serum on T-cells in the laboratory. Serum can be obtained or purchased from blood banks, but it is difficult to obtain enough male nontransfused AB donors for regular use. It may be satisfactory to use male nontransfused donors of any blood type, as we do. Serum is separated from coagulated blood by centrifugation and one aliquot from each of at least 20 sera prepared at the same time is heat inactivated (30 min at 56°C). The bulk of the sera are frozen separately. The test samples are then separately tested for their ability to support T-cell proliferation. Those that are judged satisfactory are then thawed and pooled. Culture medium must be supplemented with 10–20% of such serum pools to support long-term T-cell growth.

   Alternatively, use X-Vivo 10 or X-Vivo 15 serum-free medium (BioWhittacker), formula unknown.

3. Method

3.1. Source of Cells to Be Cloned

3.1.1. Purification of T Cells (see **Note 1**)

1. Selectively deplete non-T-cells from PBMC using a cocktail of antibodies for CD14 (expressed by monocytic cells, macrophages, dendritic cells), CD16 (on NK cells), CD19 (B cells and B-cell precursors), and HLA-DR (monocytes, B cells, activated T-cells, and dendritic cells).
2. Incubate 10^7 cells/mL at 4°C for 30 min with approx 10 µg/mL of each antibody, centrifuge, wash twice, and resuspend in 1.5 mL of phosphate-buffered saline (PBS) with 0.1% bovine serum albumin (BSA).
3. Add approx 10^8 washed Dynabeads in 0.5 mL and incubate at room temperature for 1 h. Gently shake occasionally. Add 2 mL of PBS and put the tube into the magnetic field for 1–2 min. Gently aspirate the supernatant. This contains the negatively selected cells not held by the magnet. Wash twice and control purity with anti-T-cell antibody by immunofluorescence.
4. Remove any possible remaining functional accessory cells by treating the population with L-leucyl-L-leucine methyl esther (LME). Incubate at 2.5×10^6/mL in 10 m*M* LME for 45 min at room temperature in culture medium without serum.
5. Wash twice and then check absence of functional accessory cells. This can be done by stimulating with T-cell mitogens such as phytohemagglutinin in the absence of added cells. There should be no response. After reconstitution of accessory function with B-lymphoblastoid cell lines (B-LCLs) the response should be measurable. A typical protocol is to incubate 2.5×10^4 T-cells per round-bottom microtiter plate well in culture medium together with 1% phytohemagglutinin (PHA, *M* form; Gibco-BRL) in triplicate. A duplicate set of wells receives in addition 2.5×10^4 B-LCL cells (irradiated at 80 Gy). Proliferation can be assessed 3 d later, for example, by addition of 37 kBq/well of tritiated thymidine and assessing incorporated nuclear radioactivity after 8–16 h.

3.1.2. Purification of $CD34^+$ Cells

1. Separate low-density mononuclear cells (MNCs, <1.077 g/mL) from buffy coats from healthy adult donors by isopycnic centrifugation (e.g., 25 min, 400*g* over Lymphoprep). Wash twice and centrifuge through a cushion of 10% BSA in PBS to remove platelets.
2. Separate cells using the MiniMACS Multisort system (Miltenyi Biotec, Bergisch-Gladbach): incubate 5×10^8 MNCs for 5 min at 12°C in 500 µL of FcR-blocking reagent (Miltenyi Biotec) and then with the same volume of CD34 Multisort microbeads without washing. Then incubate at 4°C for 45 min, centrifuge, and resuspend in PBS–EDTA.
3. Rinse MS+ separation columns (Miltenyi Biotec) and place in the magnetic field. Load 10^8 cells onto each column in 500 µL. Wash thrice and discard eluate. Remove column from the magnetic field and elute $CD34^+$ cells with 1.5 mL of

buffer. Load this eluate onto a second column and isolate the $CD34^+$ cells isolated by repeating the above procedure.

4. Incubate the microbead-labeled $CD34^+$ cell population with Multisort Release Reagent (Miltenyi Biotec) for 10 min at 12°C to release beads from the cells.
5. Then load the suspension onto a third MS column in a magnetic field. Centrifuge the eluate containing bead-free $CD34^+$ cells through a cushion of 10% BSA in PBS for 10 min at 600*g*. Resuspend pellet by adding 30 µL of stop reagent and 10 µL of streptavidin-conjugated microbeads (Miltenyi Biotec) and then incubate at 6°C for 30 min.
6. Resuspend cells in 500 µL of buffer and load onto freshly prepared MS columns in a magnetic field. Collect eluate containing the $CD34^+$ cells and check purity. For this, incubate the cells for 30 min at 4°C with phycoerythrin (PE)-conjugated CD34 MAb directed against an epitope other than that used for bead separation. Greater than 98% of the cell population must be $CD34^+$.

3.2. LD Cloning, Propagation, and Longevity Assessment

1. Resuspend cells for cloning in culture medium (*see* **Note 2**) and adjust the concentrations so that 10 µL contain 45, 4.5, or 0.45 cells. Pipet 10 µL of the 0.45 suspension to 60 × 1 mm diameter wells of culture trays ("Terasaki plates") and leave in a vibration-free area for 1 h. Check distribution of cells in the wells visually using an inverted microscope (being careful to look around the edges of the wells). Only 37% of the wells should contain cells according to the Poisson distribution. Readjust dilutions if necessary, replate, and check again.
2. Plate multiple trays (at least five) with the 0.45 cells/10 µL suspension, one with 4.5 and one with 45. Add feeder cells to each well. Irradiated (30 Gy) pooled PBMCs can most flexibly be used as feeder cells at 1×10^4/well (*see* **Note 3**).
3. Stack plates wrapped in aluminum foil for ease of handling and as a precaution against contamination. Incubate at 37°C in 5% CO_2 in air in a humidified incubator for up to a week and then examine the plates using an inverted microscope.
4. Transfer contents of wells containing viable growing cells (> one third full) to 7 mm diameter flat-bottom microtiter plate wells with fresh medium and 1×10^5 feeder cells. Retain Terasaki plates for up to 2–3 wk and examine again at intervals to identify any late positive wells. Transfer these to microtiter plates as well.
5. Examine microtiter plates every few days. Split those becoming overcrowded with growing cells 1:1 into new culture wells and re-feed with medium (but not feeder cells). After about a week in microtiter plates, transfer contents of wells with growing cells into 16 mm diameter cluster plate wells with $2–5 \times 10^5$ feeder cells, and fresh medium (*see* **Note 4**).
6. Observe after 3–4 d. Divide wells that are full or nearly full into four, the others into two, with fresh media, but no more feeder cells. After a total of about a week in cluster plates, count the number of cells in each clone and subculture to 2×10^5/well, again with $2–5 \times 10^5$ feeders/well and fresh medium. Supplement with fresh medium after 3–4 d and subculture again if necessary. Continue to propagate by

weekly or fortnightly subculture with new feeder cells and fresh medium (*see* **Note 5**).

7. Estimate longevity in terms of population doublings (PDs). Score initial limiting dilution cloning wells as positive if at least one third full of growing cells. One third of the surface of a Terasaki well is equivalent to about 1000 cells (= 10 PDs). Use the number of clones derived at this stage to calculate the average life-span of all clones derived, that is, do not include clones achieving less than this number of PD in the analysis. The number of cells per microtiter plate well prior to cluster plate transfer is approx 1×10^5 (= approx 17 PDs). Assume that clones dying between the Terasaki and microtiter plate stages have undergone 17 PDs, and use this figure in calculations of average longevity. After clones are transferred to 16 mm diameter cluster wells, the number of PDs undergone can be estimated for each clone from the exact number of cells counted at each subculture. Cryopreserve cells at any point of their life-spans. Continue calculations of PDs undergone on the basis of the number of viable cells replated after thawing, not the number of cells originally present. Take maximum life-span of cells in each cloning experiment to be the PDs corresponding to the time point of the death of the longest living clone in each case (*see* **Note 6**).

4. Notes

1. For many applications where mature T-cells are to be cloned, it is not necessary to purify them beforehand. PBMCs as the starting population can be so stimulated that only T-cells can grow (e.g., with T-cell mitogens or antigens). When using $CD34^+$ cells, purity is, however, critical, because contaminating non-CD34 cells most likely have a growth advantage over the $CD34^+$ cells.
2. Clearly the culture medium employed is a critical aspect of the technique. For many years, we and others found that although T-cells could be grown for limited periods in completely chemically defined serum-free media, cloning and long-term propagation in such media was not possible. We and others were forced to use a serum supplement, most commonly FCS or HS. In our experience, very few batches of FCS prove suitable for human T-cell cloning and extensive propagation. Unfortunately, the same was true for commercially available HS. We have therefore always obtained material from blood banks and prepared the serum ourselves. Because of paucity of AB blood donors, we have always used nontransfused male blood. Each serum is separately heat inactivated (56°C, 30 min) and individually tested for its ability to support lymphocyte proliferation. Sera supporting acceptable levels of proliferation (usually around 80% of tested samples) are pooled and used at 10–20% v/v with culture medium (RPMI 1640 or IMDMEM). However, note that $CD34^+$ cells cannot be grown in either FCS- or HS-containing medium. Two factors recently enabled us successfully to grow these cells and facilitate their differentiation into mature T-cells. The first was to use the serum-free medium X-Vivo 10 without adding any other serum supplement. This medium is also suitable for the cloning and long-term propagation of TCC derived

from mature T-cells. The second factor was to use a suitable cytokine cocktail that supported the viability of the stem cells and also allowed T-cell growth to take place. This consisted of stem cell factor (SCF), flt3-L, and IL-3, together with IL-2 and either oncostatin M (OM) or IL-7.

3. Use autologous PBMCs, a mixture of autologous PBMCs and autologous B-lymphoblastoid line cells, or other appropriate antigen-presenting cells (APC), in the presence of specific antigen. Alternatively, use an antigen-non-specific stimulus such as 50 ng/mL of the anti-CD3 monoclonal antibody OKT3 or 2 μg/mL of purified or 1% crude PHA, together with the same number of allogeneic or autologous PBMCs, or pooled PBMCs (irradiated at 30 Gy).
4. Clones successfully propagated in cluster plate wells for 2 wk can be taken to be established. They can at this point be cryopreserved, although it is advisable to retain some of each clone in culture to test different conditions to establish optimal parameters for each particular clone. Human TCCs can be readily cryopreserved using the same protocols as are suitable for freezing resting T-cells. Having a frozen stock enables the different culture conditions to be tested to optimize growth, without risking the loss of the whole clone. Restimulation parameters should be established for each clone. T-cells require periodic reactivation through the T-cell antigen receptor to retain responsiveness to growth factors. This can be accomplished either specifically or nonspecifically. All clones can be propagated with weekly restimulation; some but not all can be propagated with restimulation only every 2 wk. It should be established whether each clone can be propagated with the most convenient feeder cells (80 Gy-irradiated B-LCL) instead of PBMC feeders. Most TCCs flourish on B-LCLs alone, but some need the presence of PBMCs as well (this is especially true during cloning). Propagation of the TCCs on PBMC feeders can also be continued, but for practical reasons it may often be more convenient and easier to grow large amounts of B-LCLs than to isolate the PBMCs.
5. For convenience, it is also easier to grow TCCs in scaled-up culture vessels than in 16 mm-diameter culture wells. However, not all clones can be adapted to growth in flasks. This has to be tested for each clone, using between 1×10^5 and 5×10^{5}/mL of TCCs with an equal number of feeders in tissue culture flasks. Clones not growing under these conditions can rarely be adapted to growth in flasks by altering the amounts or concentrations of TCCs or feeders or by increasing or decreasing the frequency of stimulation and/or feeding.
6. Longevity estimation in PD is an extremely conservative measurement indicating the absolute minimum number of cell divisions achievable by each cell. This is because it simply assumes that all daughter cells at each cell division are viable and themselves capable of dividing and generating two viable progeny. In reality, it is highly likely that this is not the case.

Acknowledgments

Work in the author's laboratory is supported by the Deutsche Forschungsgemeinschaft, the Dr. Mildred Scheel Foundation, the Dieter Schlag Founda-

tion, the VERUM Foundation, the Novartis Foundation for Gerontological Research, the *f*ortüne Program of University of Tübingen Medical Faculty, and the European Commission (*see* http://www.medizin.uni-tuebingen.de/eucambis/).

References

1. Bach, F. H., Inouye, H., Hank, J. A., and Alter, B. J. (1979) Human T-lymphocyte clones reactive in primed lymphocyte typing and cytotoxicity. *Nature* **281,** 307–309.
2. Pawelec, G. and Wernet, P. (1980) Restimulation properties of human alloreactive cloned T cell lines. Dissection of HLA-D-region alleles in population studies and in family segregation analysis. *Immunogenetics* **11,** 507–519.
3. Morgan, D. A., Ruscetti, F. W., and Gallo, R. C. (1976) Selective *in vitro* growth of T-lymphocytes from normal human bone marrows. *Science* **193,** 1007–1008.
4. Effros, R. B. and Walford, R. L. (1984) T cell cultures and the Hayflick limit. *Hum. Immunol.* **9,** 49–65.
5. Pawelec, G. (1985) Functions and changing activities of interleukin 2-dependent human T lymphocyte clones derived from sensitization in mixed leukocyte cultures, in *T Cell Clones* (von Boehmer, H. and Haas, W., eds.), Elsevier, Amsterdam, Holland, pp. 311–322.
6. Johnson, J. P., Cianfriglia, M., Glasebrook, A. L. and Nabholz, M. (1982) Karyotype evolution of cytolytic T cell lines, in *Isolation, Characterisation, and Utilisation of T Lymphocyte Clones* (Fathman, C. G., Fitch, F. W., eds.), Academic Press, New York, pp. 183–191.
7. Kaltoft, K., Pedersen, C. B., Hansen, B. H., and Thestrup-Pedersen, K. (1995) Appearance of isochromosome 18q can be associated with *in vitro* immortalization of human T lymphocytes. *Cancer Genet. Cytogenet.* **81,** 13–16.
8. Kahle, P., Wernet, P., Rehbein, A., Kumbier, I., and Pawelec, G. (1981) Cloning of functional human T lymphocytes by limiting dilution: impact of feeder cells and interleukin 2 sources on cloning efficiencies. *Scand. J. Immunol.* **4,** 493–502.
9. Pawelec, G., Schwuléra, U., Blaurock, M., Busch, F. W., Rehbein, A., Balko, I., and Wernet, P. (1987) Relative cloning efficiencies and long-term propagation capacity for T cell clones of highly purified natural interleukin 2 compared to recombinant interleukin 2 in man. *Immunobiology* **174,** 67–75.
10. Effros, R. B. and Pawelec, G. (1997) Replicative senescence of T lymphocytes: does the Hayflick Limit lead to immune exhaustion? *Immunol. Today* **18,** 450–454.
11. Pohla, H., Adibzadeh, M., Buhring, H. J., Siegels-Hubenthal, P., Deikeler, T., Owsianowsky, M., Schenk, A., Rehbein, A., Schlotz, E., Schaudt, K., and Pawelec, G. (1993) Evolution of a $CD3^+CD4^+$ alpha/beta T-cell receptor$^+$ mature T-cell clone from $CD3^-CD7^+$ sorted human bone marrow cells. *Dev. Immunol.* **3,** 197–210.
12. Preffer, F. I., Kim, C. W., Fischer, K. H., Sabga, E. M., Kradin, R. L., and Colvin, R. B. (1989) Identification of pre-T cells in human blood. Extrathymic differentiation of $CD7^+CD3^-$ cells into $CD3^+$ gamma/delta or alpha/beta + T cells. *J. Exp. Med.* **170,** 177–190.

13. Adibzadeh, M., Pohla, H., Rehbein, A., and Pawelec, G. (1995) Long-term culture of monoclonal human T lymphocytes: models for immunosenescence? *Mech. Ageing. Dev.* **83,** 171–183.
14. Pawelec, G., Rehbein, A., Haehnel, K., Merl, A., and Adibzadeh, M. (1997) Human T cell clones as a model for immunosenescence. *Immunol. Rev.* **160,** 31–43.
15. Freedman, A. R., Zhu, H. H., Levine, J. D., Kalams, S., and Scadden, D. T. (1996) Generation of human T lymphocytes from bone marrow $CD34^+$ cells *in vitro*. *Nat. Med.* **2,** 46–51.

4

Telomeres and Replicative Senescence

Hector F. Valenzuela and Rita B. Effros

1. Introduction

Telomere length measurement can be used both to monitor the proliferation of long-term cultures of somatic cells as well as to determine the replicative history of in vivo-derived cells. The most frequently used technique for telomere length measurement is Southern hybridization ***(1,2)***. The method consists of isolating total genomic DNA, digesting the DNA with restriction enzymes so as to isolate the undigested telomere restriction fragments (TRFs), and separating these fragments by gel electrophoresis. The DNA is denatured and transferred from the gel to a membrane or filter, and the DNA samples are then hybridized to radiolabeled complementary probe. However, when blotting TRF DNA to the membrane, differential transfer may occur owing to inefficient transfer of larger fragments of DNA (>10 kb) to a membrane. As the mean length of the TRF is based on the assumption that the amount of telomeric DNA (TTAGGG repeats) in a given TRF is proportional to the length ***(3,4)***, this would lead to possible error in calculating the mean length of the telomeres. The method that we present here avoids these potential problems by eliminating the membrane blot step altogether and probing the gel directly.

The following protocol has been refined for measuring telomeric DNA length from human cells. Similar protocols can be adapted to measure telomere lengths in cells from other species. However, researchers should adjust the probe sequence for hybridization (not all species have the same telomere sequence) and optimize the restriction enzymes to obtain TRF within the resolvable molecular weight range of the gel because some species may have extremely long telomeres. For more information regarding telomeres, we suggest reading Kipling's *The Telomeres* ***(5)***.

From: *Methods in Molecular Medicine*, Vol. 38: *Aging Methods and Protocols*
Edited by: Y. A. Barnett and C. R. Barnett

The TRF assay method that we present here can be divided into three stages: (1) isolation and digestion of genomic DNA; (2) gel electrophoresis, drying, and hybridization; and (3) analysis of TRF length. We will emphasize in this protocol the measurements of the TRF after the DNA isolation. As mentioned previously, the protocol improves on the standard Southern blot procedure by eliminating the DNA transfer from gel to membrane, thereby reducing the time and labor involved. After digestion, the DNA fragments are separated in an agarose gel, which is then dried. The gel is then denatured, neutralized, and hybridized in a manner similar to the membrane in the usual Southern blot method. Once the gel is washed, it can be analyzed directly by densitometry of an autoradiograph or by using a phosphorimager ***(3)***.

2. Materials

1. Denaturing buffer solution: 1.5 *M* NaCl, 0.5 *M* NaOH. Dissolve 43.83 g of NaCl and 10 g of NaOH in 400 mL of distilled water, then raise volume to 500 mL. Store at room temperature.
2. Neutralization buffer solution (1.5 *M* NaCl, 0.5 *M* Tris-Cl): Dissolve 43.83 g of NaCl and 39.4 g of Tris-Cl in 450 mL of distilled water. Adjust pH to 8.0 (with approx 2 g of NaOH). Raise volume to 500 mL. Store at room temperature.
3. Hybridization buffer solution: Mix 64 mL of distilled water, 25 mL 20× saline sodium citrate (SSC), 10 mL of Denhardt's reagent (50×), and 1 mL of sodium pyrophosphate (stock 1 *M*). Sterile filter with 0.22 µm filter. Store at 4°C. The 50× Denhardt's reagent (Sigma Chemical, St. Louis, MO, USA) can be prepared using 5 g of bovine serum albumin, 5 g of Ficoll, and 5 g of polyvinylpyrrolidine.
4. 20× SSC washing solution (3 *M* NaCl, 0.3 *M* sodium citrate): Dissolve 175.3 g of NaCl and 88.2 g of sodium citrate in 800 mL of H_2O. Adjust pH to 7 with a few drops of NaOH. Raise volume to 1 L with distilled water. Prepare 1.5L of 0.5× SSC for washes. Sterilize by autoclaving, and store at room temperature. The solution is stable for several months.
5. Probe: The probe sequence can be either $(TTAGGG)_3$ or $(CCCTAA)_3$. Prepare an aliquot concentration of 40 pmol/µL. Store at –20°C (*see* **Subheading 3.**, **step 4**).
6. Ladders: A ladder that ranges from 1 to 20 kb is required. Alternatively, we advise mixing two ladders, a 1 kb ladder at 1 µg/µL (Gibco-BRL) and λDNA *Hin*dIII digest at 1 µg/µL (New England BioLabs). Store at –20°C.
7. Enzymes: Restriction enzymes *Hin*fI and *Rsa*I (New England BioLabs). Use appropriate buffer to ensure maximum activity. Klenow polymerase (Gibco-BRL) and T4 polynucleotide kinase (Gibco-BRL) are used for labeling ladder and probe, respectively.
8. Quick Spin Columns Sephadex G25 Fine (Boehringer Mannhein cat. no. 1273949).
9. Polyethylene bags for hybridization step. (Fisher bags cat. no. 01-812-10E; Fisher International Headquarters, 50 Fadem Rd, Springfield, NJ 07081-3193, USA: Tel: 201-467-6400; Fax: 201-379-7415).

10. Isotopes: require [α-^{32}P]ATP and [γ-^{32}P]ATP for labeling ladder and probe, respectively. Alternatively one can use ^{33}P isotopes, but do not mix these different isotopes in the same gel. ^{33}P is safer to handle but requires twice the exposure time of ^{32}P.
11. Gel apparatus: Gel cast of 15–20 cm long and thin combs (2 mm).
12. Whatman 3MM paper cut out to 2.5 cm longer than gel in both length and width.

3. Methods

1. Isolation of genomic DNA: The isolation of the genomic DNA can be performed by any number of standard protocols in the literature. We recommend "DNAzol" DNA Isolation reagent (Molecular Research Center, Inc., 5645 Montgomery Road, Cincinnati, OH 45212, USA; Tel: 513-841-0900; Fax: 513-841-0080). The main consideration in selecting a protocol should be to choose a method that yields DNA fragments larger than 60 kb; otherwise results may be skewed (*see* **Note 1**).
2. Digestion of genomic DNA: For the digestion of 10 µg of high molecular weight DNA use the following recipe:

   10 µg of Genomic DNA
   10 µL of 10× reaction buffer
   2 µL of *Hin*fI
   2 µL of *Rsa*I
   X µL dH_2O
   100 mL (final volume). Incubate at 37°C for 2–3 h.

   Run 2 mL of digested DNA with undigested DNA on a mini-gel to test for completion of digestions. Digestion is incomplete if there are fragments larger than 50 kb. The amount of DNA loaded per lane must be at least 1–2 µg; a larger amount of DNA increases the sensitivity of detection, especially for short telomeres.
3. Agarose gel: Pour a 0.5% agarose/0.5× TBE gel. The gel must be at least 10 cm long (we recommend 15–20 cm) and must be approx 3/4 cm thick. The longer gel allows good separation of large fragments of DNA and the thin combs prevent the DNA from diffusing. Run gel for a total of 750 V/h. Do not run gel faster than 50 V, as this prevents good resolution of long telomere fragments. We recomend 30 V, which should then be run for 25 h (for a total of 750 V/h).
4. Loading DNA onto gel: Load at least 1–2 µg of DNA per lane. Labeling of 1 kb and λDNA *Hin*dIII digest ladders is performed as follows in a 1.5-mL Eppendorf tube. Ladders should be loaded last onto the gel to minimize exposure to radiation.

   0.5 µL of 1 kb ladder
   0.5 µL of λDNA *Hin*dIII digest ladder
   4 µL of 10× Klenow buffer
   3 µL of [α-^{32}P]ATP
   31 µL dH_2O (or add dH_2O to 40 µL final volume)
   1 µL Klenow fragment
   40 µL (final volume)

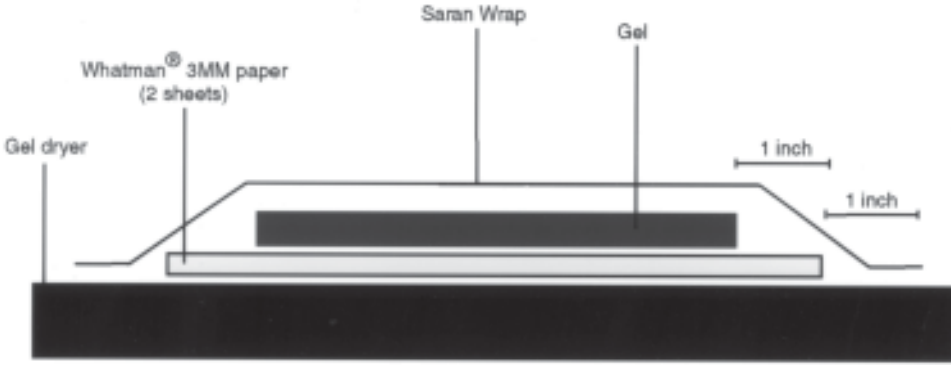

Fig. 1. Setup for drying the agarose gel in a gel dryer.

Incubate 2 min at 37°C, and put on ice while you prepare the quick spin column to remove the unincorporated [α-^{32}P]ATP. For a freshly prepared ladder use 0.5 µL/lane (*see* **Notes 2** and **3**).

5. Gel drying: Place two sheets of 3MM Whatman chromatography paper in gel drier, then place gel on top leaving 2.5 cm around the margins of the gel. Finally, place Saran wrap over gel and Whatman paper (**Fig. 1**). Dry gel under vacuum at 60°C for 45–75 min.

   Note: Start preparing the probe (**step 7**) and prewarm hybridization buffer (**step 8**) (*see* **Note 4**)
6. Gel washes: Remove gel from vacuum dryer by holding gel at the opposite end from the wells. Gels occasionally tear during this step, and by handling the end furthest from the wells, the chance of tearing the gel in the area near the DNA is reduced. One should keep in mind that at this point the gel is radioactive from the labeled ladder, so all proper precautions should be maintained. If Whatman paper sticks to gel, use water to peel them apart. Place the gel in a Pyrex dish container and add enough denaturing reagent (500 mL) to completely submerge gel. Let sit at room temperature for 10 min with gentle shaking. Dispose of buffer by pouring into proper radioactive waste. Repeat washing with neutralization buffer (500 mL) in the same Pyrex container for 10 min at room temperature with gentle shaking. Upon completion of this wash, dispose of buffer in the same manner.
7. Probe labeling reaction can be prepared the following way in a 1.5-mL Eppendorf tube:

   1 µL of 40 pmol/µL of $(TTAGGG)_3$ oligo
   5.3 µL of 10× T4 polynucleotide kinase buffer
   6.5 µL of [γ-^{32}P]ATP
   1.5 µL of T4 polynucleotide kinase
   38.7 µL of dH2O
   53 µL (final volume)

Incubate reaction at 37°C for 30 min, then use a quick spin column to separate unincorporated [γ-^{32}P]ATP.

8. Hybridization of gel: Prewarm the hybridization buffer (15 mL) to 37°C. For a gel 10–20 cm in length use 15 mL (but no more than 20 mL) of hybridization buffer. Add 1 µL of label probe for every 1 mL of hybridization buffer. Keep at 37°C while you prepare the gel.

   Prepare the gel for hybridization by placing the gel in a hybridization bag. Perform this by cutting open two sides of the bag, so that it opens up like a book. This method will prevent the gel from sticking to plastic that may lead to tearing of the gel. Place gel inside and seal ends of plastic bag once again with an Impulse Sealer so that there is only one opening. (There should be 1–2 cm of margin space between the gel and the plastic bag.) Through this opening add the prewarmed hybridization buffer with the added probe. Check the seals for leaks over the Pyrex container before proceeding. **Caution:** The hybridization solution will be highly radioactive.

   Before sealing the open end of the bag, remove any bubbles that may be in the bag. (Remember to do this over a Pyrex container in case of leaks.) It may be helpful in removing the final bubbles to seal the bag at the very edge, then squeeze the remaining bubbles to one edge, sealing them off with a second seal. You must remove most of the bubbles before the second seal for this double sealing to work.
9. Incubate the gel at 37°C for at least 6 h (although we recommend overnight). For very weak probes, 2–3 d may be necessary.
10. Washing with SSC: Cut open plastic bag, remove the hybridization solution, and dispose in a proper radioactive waste receptacle. Carefully place gel in a Pyrex container and add 500 mL of 0.5× SSC (prewarmed at 37°C) for 6–7 min. Repeat the same wash two more times. Remove all SSC, then enclose the gel in Saran Wrap before exposing to imaging film (*see* **Note 5**).
11. Analysis: Analysis of the TRF length can be done either by densitometric scanning of the autoradiogram or by using a phosphoimager (*see* **Note 6**)

4. Notes

1. For the isolation of genomic DNA, we recommend using a guanidium based method, such as DNAzol® (Molecular Research Center). This method is fast (30 min) and reliable; however, we emphasize the importance of using wide-mouth tips to prevent DNA shearing during the isolation steps.
2. Along with the samples, we recommend including two control DNA fragments, one from cells with long telomeres and the other from cells with short telomeres. For the long telomere source, one can use a subline of the 293 tumor, which has stable TRF length of approx 10.5 kb. As source of short telomeres, Daudi cells, with a mean TRF length of approx 3.9 kb, can be used. Prepare a large batch of genomic DNA from the control cell lines, aliquot into small amounts, and use these as standards to compare gel-to-gel variations in the sizes of TRF that may occur between experiments. It may be necessary to add more than 2 µg of DNA

for cells that have short telomeres. Longer telomeres, because they have more TTAGGG repeats, give a stronger signal than short telomeres.

The term "TRF length" is not synonymous with "telomere length." The TRF includes both the telomere repeats and the adjacent subtelomeric region that contains both repetitive and nonrepetitive sequences .

3. We suggest using ladders at both ends of the gel. Use 0.5 µL/lane of ladder labeling reaction mix when using freshly prepared material. If the ladder was prepared at an earlier time, add up to 1 µL/lane, but beware of adding too much lest the signal be overexposed, making it impossible to quantitate TRF length. If this problem occurs, one may either add more (>2 µg/lane) genomic DNA, or a smaller quantity of labeled DNA ladder per lane (but not less than 5 µg/lane).

   Gel orientation can be marked in a number of ways, such as by cutting away a corner of the gel, loading two lanes with the ladder on one side of gel, or loading control TRF DNA on one side of gel.
4. Note that a 0.5% agarose gel is extremely fragile, and we suggest using a spatula or the back of a Pyrex dish during all transfers. Gels can be stored for up to 2 d at this stage, for example, if the probe is not ready. This can be done by placing the gel in a sealed plastic bag with 2 mL of 2× SSC at 4°C, as described in **Subheading 3**.
5. If the background radiation is too high, place gel once for 1 h (or twice for 30 min each) at 48°C in 0.1× SSC. Shortening exposure time may also reduce background. If the problem continues, one should increase the amount of DNA, which reduces the noise by reducing the background. Adding lower concentrations of probe will also help reduce the background.

   If there is no signal, lengthen exposure time. Verify that probe was properly labeled. Verify that hybridization solution has no precipitates. If precipitate is seen, it is necessary to prepare fresh hybridization solution.
6. The mean TRF length is calculated by integrating signal intensity over TRF distribution on gel as a function of mol wt. Divide a scanned TRF image into a grid in which columns cover the entire length of TRF sample analyzed and there are at least 30 boxes dividing each column (**Fig. 2**). The following equation can then be used to calculate the mean TRF length:

$$\text{Mean TRF length} = \Sigma(OD_i \cdot L_i) / \Sigma(OD_i)$$

where OD_i is the intensity signal and L_i is the mol wt at a particular (i) box in the grid as compared to a size marker from a ladder. Before using above equation for TRF length analysis, background must be subtracted from OD_i. For each sample the background can be calculated by averaging the OD from the top two boxes and bottom two boxes adjacent to the smear. The average background OD is then subtracted from each box in the grid for that particular sample. Alternatively, some phosphorimagers (Packard, Instant Imager) come included with software that can quantitate the intensities of signals to obtain mean values that are plotted to preassigned values from a ladder.

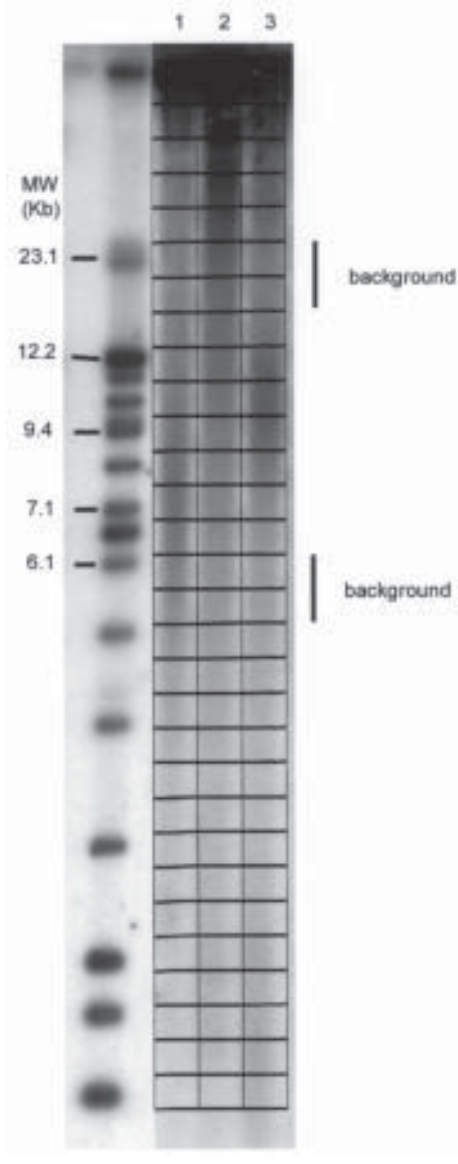

Fig. 2. Calculation of mean TRF length. Exposed image has been divided into columns and rows where OD and *L* values can be measured. For column 3, the boxes used for calculating the background are indicated.

Acknowledgments

The authors wish to thank Dr. Choy-Pik Chiu (Geron Corporation, Menlo Park, CA) for providing comments on the manuscript, and the Geron Corpora-

tion for their generous help in establishing the telomere assays in our laboratory. This work was supported by the National Institute on Aging (AG10415), the UCLA AIDS Institute, and the Seigel Life Project/UCLA Center on Aging.

References

1. Southern, E. M. (1975) Detection of specific sequences among DNA fragments separated by gel electrophoresis. *J. Mol. Biol.* **98,** 503.
2. Sambrook, J., Fritsch, E. F., and Maniatis, T. (1989) Molecular Cloning A Laboratory Manual, Cold Spring Harbor Laboratory Press, Cold Spring Harbor, NY, pp. 9.31–9.58.
3. Allsopp, R. C., Vaziri, H., Patterson, C., Goldstein, S., Younglai, E. V., Futcher, A. B., Greider, C. W., and Harley, C. B. (1992) Telomere length predicts replicative capacity of human fibroblasts. *Proc. Natl. Acad. Sci. USA* **89,** 10,114–10,118.
4. Harley, C. B., Futcher, A. B., Greider, C. W. (1990) Telomere shorten during ageing of human fibroblasts. *Nature* **345,** 458–469.
5. Kipling, D. (1995) *The Telomere*, Oxford University Press, pp. 1–12, 78–96, 130–142, 146–163.

5

Detection of Molecular Events During Apoptosis by Flow Cytometry

Ruaidhri J. Carmody,* Ana P. Costa-Pereira,* Sharon L. McKenna, and Tom G. Cotter

1. Introduction

Apoptosis describes an intrinsic cell suicide program that may be activated by both endogenous and exogenous stimuli. This method of cell death is characterized by specific morphological features including chromatin condensation, nuclear fragmentation, cell shrinkage, membrane blebbing, and the formation of membrane-bound vesicles termed apoptotic bodies ***(1)***. Apoptosis has come to be referred to as the physiological mode of cell death, as it allows cellular destruction in the absence of an associated inflammatory response. In contrast, necrosis is a pathological mode of cell death that occurs under circumstances of severe cellular injury/trauma. Necrotic cell death involves cell swelling and organelle disruption, followed by lysis and release of cellular debris. This form of cell death may cause damage to surrounding tissue due to the inappropriate triggering of an inflammatory response ***(2)***.

Apoptosis occurs during normal mammalian development and also plays an important role in subsequent tissue homeostasis by balancing cell division with cell death ***(3)***. Apoptosis has also been ascribed a role in several disease states including malignancy and neurodegenerative disorders, in which deregulation or inappropriate activation of the apoptotic program contributes to the observed pathology. The physiological importance of apoptosis in the maintenance of tissue homeostasis, and the observation of apoptotic cell death in age-related degenerative disorders such as Alzheimer's disease and Parkinson's disease (reviewed in **ref. *4***), suggests that the regulation of apoptosis may be a critical parameter for consideration in studies of aging.

*These authors have contributed equally to this work.

From: *Methods in Molecular Medicine*, Vol. 38: *Aging Methods and Protocols*
Edited by: Y. A. Barnett and C. R. Barnett

This chapter outlines some current procedures for the detection of apoptosis and the analysis of intracellular molecular events important in apoptotic pathways. Biochemical events include the generation of reactive oxygen species (ROS) and disruption of mitochondrial transmembrane potential ($\Delta\psi_m$). The methods described in this chapter all utilize a flow cytometer for quantitative analysis of data. Several techniques (e.g., propidium iodide [PI] or terminal deoxyuridine triphosphate [dUTP] nick end labeling [TUNEL]) assay may, however, be adapted for use with a fluorescent microscope. Flow cytometric analysis has the advantage of a rapid assessment of large numbers of cells in a highly quantitative, nonsubjective manner. In addition, flow cytometry enables the parallel assessment of two and possibly three parameters in the same cell. Cell sorting may also be an option for some users (*see* also subsequent sections).

1.1. Translocation of Phosphatidylserine

Several studies have shown that phosphatidylserine (PS) is asymmetrically distributed and is preferentially located in the inner leaflet of the plasma membrane (P*M*) ***(5)***. In the early stages of apoptosis in virtually all cell types, redistribution of membrane phospholipids results in the exposure of PS on the outer membrane ***(6)***. PS exposure has been shown to be tightly coupled to other apoptosis-associated changes ***(7)***, and seems to be stimulus independent ***(6)***. Externalization of PS, following the induction of apoptosis, can be readily detected using recombinant Annexin V, a protein that binds with high affinity to PS in a Ca^{2+}-dependent manner ***(8)***. Because necrotic cells have lost their membrane integrity, they may also stain positive with Annexin V. However, dual staining with PI enables membrane-disrupted cells to be readily distinguished. Secondary necrotic cells are apoptotic cells which have subsequently lost membrane integrity (*see* **Subheading 4.1.1.**), and therefore cannot be distinguised from primary necrotic cells using this method.

As Annexin V detects a cell surface marker, no fixation or permeabilization is required for the procedure. The cells are therefore analyzed "alive" and may be recovered by fluorescence-activated cell sorter (FACS) sorting for further analytical purposes. This method also facilitates dual labeling for surface antigens that recognize native antigen conformations.

1.2. DNA Fragmentation

The degradation of DNA into oligonucleosomal sized fragments of 180–200 basepairs by specific endonuclease activity is a major biochemical event during apoptosis in most cell types ***(9)***. This DNA fragmentation was originally observed as a ladder pattern using agarose gel electrophoresis. However, this method of detection is essentially qualitative and does not allow for the identification of subpopulations of apoptotic cells. Several flow cytometric methods

have been described that allow the quantitative analysis of DNA fragmentation as well as the parallel measurement of other parameters such as cell cycle and antigen expression ***(10,11)***. The most commonly used of these methods is the TUNEL assay.

The TUNEL assay is based on the addition of biotinylated dUTP nucleotide to 3' hydroxyl termini at DNA strand breaks. This reaction is catalyzed by the enzyme terminal deoxynucleotidyl transferase that repetitively adds deoxyribonucleotide to the 3' hydroxyl termini of DNA. Fluoresceinated avidin is then employed in a second step reaction to fluorescently label the DNA strand breaks, thus allowing the detection of DNA strand breaks by flow cytometry.

1.3. Reactive Oxygen Species

The generation of ROS and alterations in the cellular redox state have been reported to be a common biochemical event in apoptosis ***(12)***. Moreover, ROS have been proposed to be putative second messengers in the initiation of apoptosis. The production of ROS during cytotoxic drug induced apoptosis and inhibition of apoptosis by antioxidants supports this view ***(12)***. Oxidative stress is also believed to play a role in Parkinson's disease and amylotrophic lateral sclerosis disease states, the latter of which has been linked to genetic lesions in a cellular antioxidant pathway ***(4)***. Possible sources of intracellular ROS include the depletion of cellular antioxidants such as glutathione, disruption of mitochondrial respiration, and the activation of oxidant-producing enzymes such as NADPH oxidase.

The fluorescent probes 2',7'-dichlorofluorescein diacetate (DCFH/DA) and dihydorethidium (DHE) may be used for the measurement of intracellular peroxide and superoxide anion levels, respectively. DCFH/DA is cell permeant and is nonfluorescent until the acetate groups are removed by cellular esterase activity and a peroxide group is subsequently encountered. Hydrolyzed, oxidized DFCH/DA fluoresces at 529 nm (FL-1, log scale; *see* **Subheading 3.** and **Table 1**) (**Fig. 1A**,**B**) and is unable to leave the cell, thus allowing the measurement of intracellular peroxides by flow cytometry.

DHE is also cell permeant and is oxidised to ethidium by superoxide anion. Once oxidised, ethidium is free to intercalate with DNA in the nucleus whereupon it emits fluorescence at 605 nm (FL-2) (*see* **Fig. 1A**,**C**).

1.4. Mitochondrial Transmembrane Potential Alterations

Emerging evidence suggests a central role for mitochondria during apoptosis induced by a diverse range of stimuli in a number of cell types. Indeed, several groups have proposed mitochondria as the central executors of apoptosis (reviewed in **ref.** ***13***). Mitochondrial events during apoptosis include release of cytochrome-c and disruption of the transmembrane potential ($\Delta\psi_m$) ***(13)***. Dis-

Table 1
Summary of Assays and Probes Described in this Chapter[a]

Probe/Assay	Parameter measured	Emission (nm)	Channel
Annexin-V	PS translocation	515	FL-1
TUNEL	DNA fragmentation	515	FL-1
Antigen analysis	Antigen expression	580	FL-2
PI	DNA content	620	FL-2
DHE	Superoxide anion	605	FL-2
DCFH/DA	Peroxide	529	FL-1
JC-1	Mitochondrial membrane potential	590	FL-2

[a]The table includes the emission peak of probes and the channel through which data should be collected and analyzed.

ruption of $\Delta\psi_m$ is believed to occur through permeability transition (PT), a process that involves the opening of the mitochondrial PT pore, allowing release of solutes 1.5 kDa and smaller and subsequent disruption of $\Delta\psi_m$. Importantly, inhibitors of PT also inhibit apoptosis in several models of apoptosis, supporting the view that disruption of mitochondrial function is central to the apoptotic process.

The cell permeant fluorescent probe JC-1 can be employed to monitor changes in $\Delta\psi_m$ in intact cells. In the presence of a high $\Delta\psi_m$ JC-1 forms what are termed J-aggregates that fluoresce strongly at 590 nm (FL-2). Reduced $\Delta\psi_m$ results in a reduced FL-2 signal in JC-1-stained cells (**Fig. 2A**,**B**). This method has been demonstrated to be quantitative in addition to qualitative and allows subpopulations of cells with different mitochondrial properties to be identified ***(14)***.

2. Materials

2.1. Annexin V Assay

1. Fluoresceinated Annexin V (Annexin V-FITC) (e.g., Bender MedSystems, Heidelberg, Germany). Protect from light and store at –20°C.
2. Binding buffer: 10 m*M* *N*-[2-hydroxyethyl]piperazine-*N*'-[2-ethanesulfonic acid] (HEPES)/NaOH, pH 7.4, 140 m*M* NaCl, 2.5 m*M* $CaCl_2$. Store at 4°C.
3. PI. Protect from light and store at 4°C.
4. Phosphate-buffered saline (PBS): 8.06 m*M* Na_2HPO_4, 1.47 m*M* KH_2PO_4, pH 7.4; 2.27 m*M* KCl, and 137 m*M* NaCl.

2.2. Terminal dUTP Nick End Labelling (TUNEL) Assay

1. Fixation buffer: 2% (w/v) *p*-Formaldehyde in PBS, pH 7.4 (*see* **Subheading 2.1.** for PBS formulation).

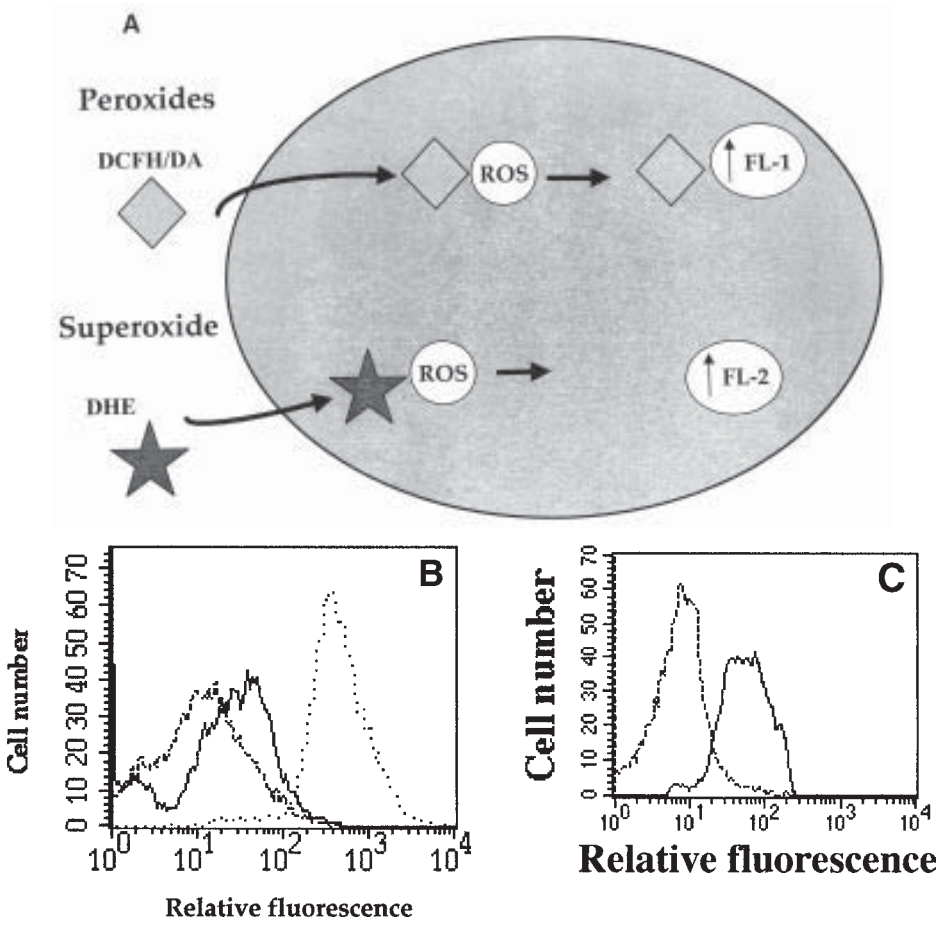

Fig. 1. **(A)** Schematic diagram illustrating the analysis of intracellular peroxides and superoxide using the fluorescent probes DCFH/DA and DHE. Hydrolysis and oxidation of DCFH/DA causes it to fluoresce in FL-1, while the oxidation of DHE to ethidium results in an increase in fluorescence in FL-2 owing to the intercalation of ethidium with cellular DNA. **(B)** Production of peroxides in DU145 prostate cancer cells treated with camptothecin. Peroxide levels were assessed in untreated DU145 prostate cells (*dashed line*) treated with 10 µg/mL of camptothecin (solid line) and in cells treated with 1 m*M* H_2O_2 (*dotted line*) for 1 h, as described in **Subheading 2.3**. After 1 h of treatment with 10 µg/mL of camptothecin, there is an increase in peroxide production that can be seen as a shift to the right in relative fluorescence. **(C)** Measurment of superoxide anion in retinal cell primary cultures after 24 h. Retinal cells cultures display high levels of apoptosis after 24 h in culture (*see* **Fig. 4-2**). Staining cells with DHE reveals a significant increase in superoxide levels at 24 h (*solid line*) relative to immediately isolated cells (*dashed line*).

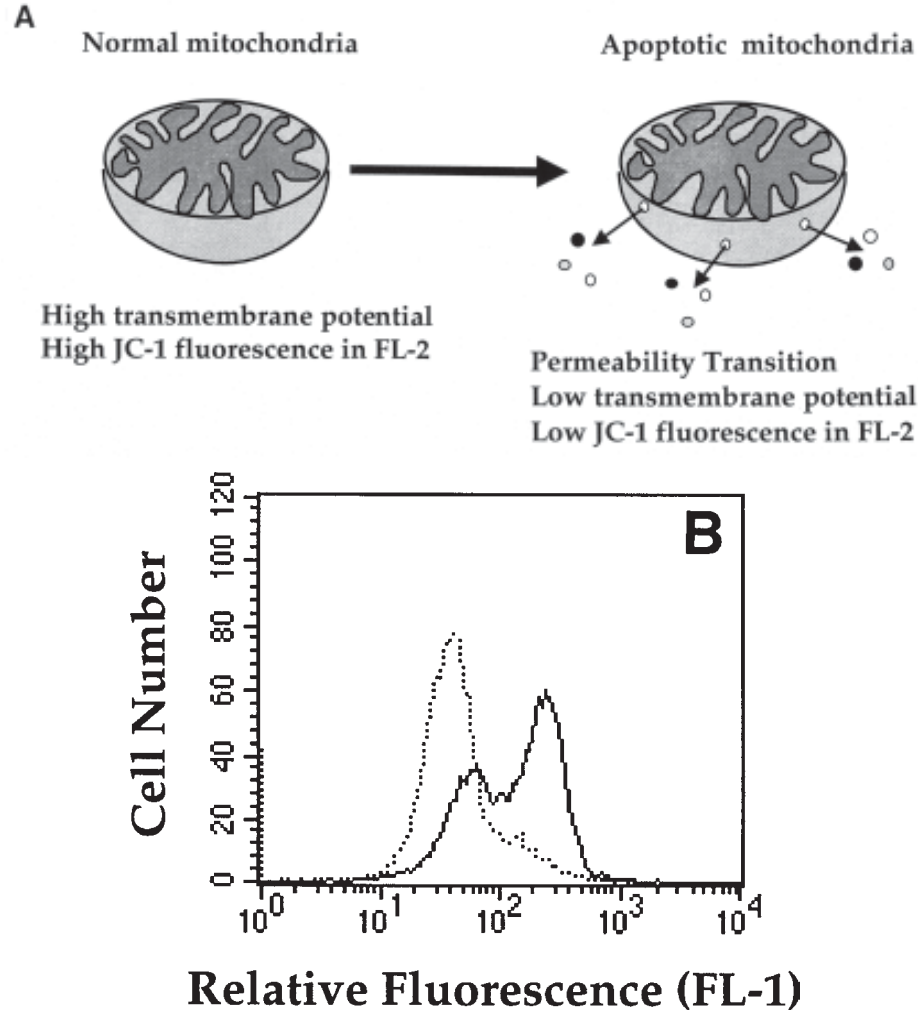

Fig. 2. **(A)** Schematic diagram of mitochondrial events during apoptosis. Intact mitochondria display high transmembrane potential ($\Delta\psi_m$) and fluoresce strongly in FL-2 when stained with JC-1. Apoptotic mitochondria undergo permeability transition resulting in a release of solutes 1.5 KDa and smaller and a loss transmembrane potential, consequently displaying reduced fluorescence in FL-2 when stained with JC-1. **(B)** Alterations in $\Delta\psi_m$ in NSO myeloma cells upon camptothecin treatment. NSO myeloma cells were treated with 30 m*M* ammonia for 18 h. Depolarization in $\Delta\psi_m$ was assessed as described in **Subheading 2.3.**, using JC-1. $\Delta\psi_m$ depolarization can be monitored by measuring the fluorescence in FL-1. Membrane depolarization results in an increase in FL-1 flourescence. Treated cells (*solid line*) show an increase in FL-1 fluorescence relative to untreated cells (*dashed line*).

2. Elongation buffer: 0.2 *M* Potassium cacodylate; 25 m*M* Tris-HCl, pH 6.6; 2.5 m*M* cobalt chloride; 0.25 mg/mL of bovine serum albumin (BSA); 100 U/mL of terminal deoxynucleotidyl transferase (TdT) (e.g., Boehringer Mannheim, East Sussex, UK); 0.5 n*M* biotin-16-dUTP (e.g., Boehringer Mannheim). Make fresh as required.
3. Staining buffer: Dilute 20× saline citrate buffer (0.3 *M* sodium citrate; 3 *M* NaCl, pH 7.0) to 4×; add 2.5 mg/mL of fluoresceinated avidin, 0.1% (v/v) Triton X-100; 5% (w/v) nonfat dried milk, to give 0.6 *M* NaCl and 0.06 *M* sodium citrate. Staining buffer is freshly made and protected from light.

2.3. Detection of Intracellular ROS

1. DCFH/DA (Molecular Probes, Leiden, The Netherlands) prepared as a 5 m*M* stock in dimethyl sulfoxide (DMSO). Protect from light and store at –20°C.
2. DHE (Molecular Probes) prepared as a 10 m*M* stock in DMSO. Protect from light and store at –20°C.

2.4. Measurement of Mitochondrial Transmembrane Potential

1. JC-1 (Molecular Probes), made as a 5 mg/mL stock in DMSO. Protect from light and store at –20°C.

3. Methods

3.1. Annexin V Assay

1. Harvest 1–2.5 × 10^5 cells and resuspend in 200 µL of binding buffer.
2. Dilute Annexin V–flourescein isothiocyanate (FITC) as recommended by the manufacturer.
3. Add diluted Annexin V–FITC and incubate for 10 min at room temperature, in the dark.
4. After a wash in PBS, resuspend cells in binding buffer and add PI (*see* **Subheading 4.1.2.**) (to a final concentration of 5 µg/mL).
5. Quantitate Annexin V binding and PI staining by flow cytometry (FL-1 and FL-2 respectively) (*see* **Note 3**) (*see* **Subheading 3.** and **Table 1**) (**Fig.3**).

3.2. TUNEL Assay

1. Fixation and permeabilization (*see* **Note 4**): Harvest approx 1 × 10^6 cells and suspend in 1 mL PBS. Add 1 mL of 2% (w/v) p-formaldehyde fixation buffer (*see* **Note 5**). Leave on ice for 15 min. Wash once in PBS and resuspend in 2 mL of –20°C 70% (v/v) ethanol. Leave at –20°C for at least two hours or up to two weeks.
2. Elongation: Wash fixed/permeabilized cells twice in PBS and resuspend in 50 µL of elongation buffer. Incubate at 37°C for 30 min. Wash twice in PBS.
3. Staining: Resuspend cells in 100 µL of staining buffer and incubate in the dark at room temperature for 30 min.

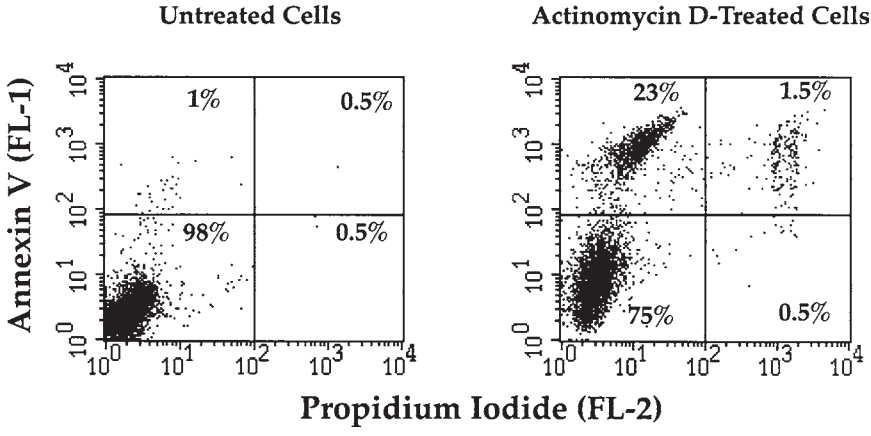

Fig. 3. Annexin V/PI dual staining of human T cells treated with Actinomycin D. Jurkat cells were treated for 4 h with 15 mg/mL of Actinomycin D. Cells were stained with Annexin V-FITC (FL-1, *y*-axis) and PI (FL-2, *x*-axis) as described in **Subheading 2.1**. Normal cells are negative for both Annexin and PI and appear in the *lower left quadrant*. Apoptotic cells with intact membranes stain with Annexin, but not with PI and therefore appear in the *upper left quadrant*. Primary and secondary necrotic cells have disrupted membranes and stain with both Annexin V and PI (*upper right quadrant*).

4. Wash twice in PBS and keep on ice and in the dark until read on a flow cytometer.
5. Measure green fluorescence (labeled DNA strand breaks) following excitation at 488 nm using a 525 nm band pass filter (FL-1, log scale; *see* **Subheading 3.** and **Table 1**).

3.2.1. Analysis of Cell Cycle in Conjunction with TUNEL Assay

After the TUNEL assay procedure has been completed resuspend cells in 1 mL of PBS containing 5 µg/mL of PI, and 0.1% DNase-free RNase A. Cell cycle analysis can then be carried by measuring the red fluorescence of PI at >600 nm (FL-2, linear scale; *see* **Subheading 3.** and **Table 1**) (**Fig. 4-1**).

3.2.2. Analysis of Antigen Expression in Conjunction with TUNEL Assay

The combination of TUNEL staining with immunofluorescence labeling of a cell-specific antigen allows the subsequent analysis of apoptosis in specific subpopulations. Cells may be labeled for antigen expression prior to or following fixation/permeabilization depending on the nature of the epitope. It is recommended that it first be determined whether epitope labeling is affected by the fixation/permeabilization process. The following procedure detects an intra-

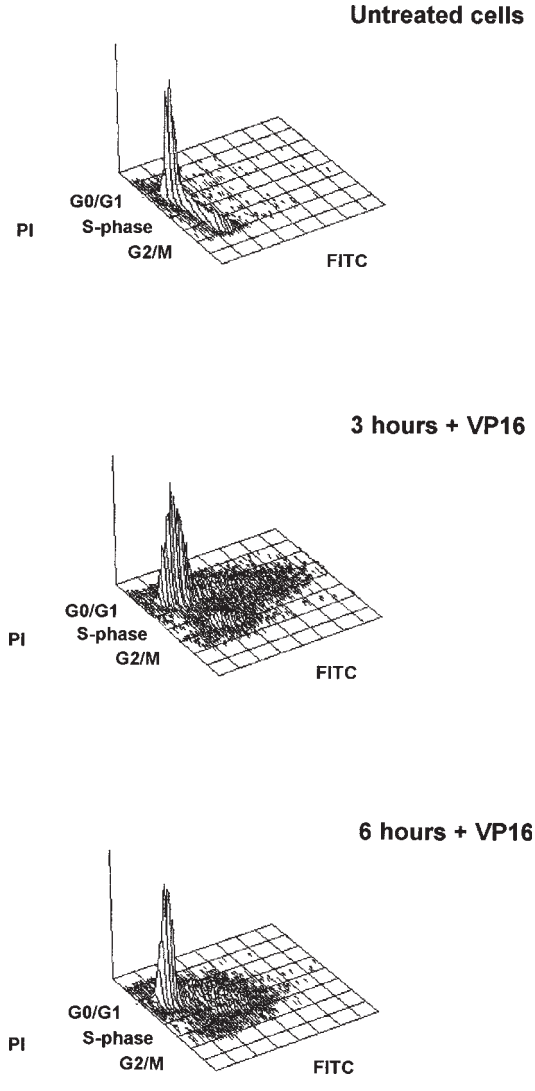

Fig. 4-1. Analysis of apoptosis by TUNEL and cell cycle in human leukemic cells treated with Etoposide. HL-60 cells (myeloid leukemia cell line) were treated for 3 and 6 h with 40 μ*M* Etoposide (VP16). Cells were stained with FITC using the TUNEL procedure as described in **Subheading 2.2**. Dual staining with PI enables cell cycle parameters to be assessed in parallel with apoptosis. This data shows that after a 3-h incubation with VP16 the majority of S-phase cells have initiated endonucleolytic DNA cleavage. Some cleavage is also evident in G_0/G_1 cells, whereas G_2/M cells are relatively resistant. After 6 h, most of the unlabeled G_2/M cells have disappeared. Some of these cells may have labeled with FITC, although most appear to have cycled through to G_0/G_1, where the cell cycle is blocked.

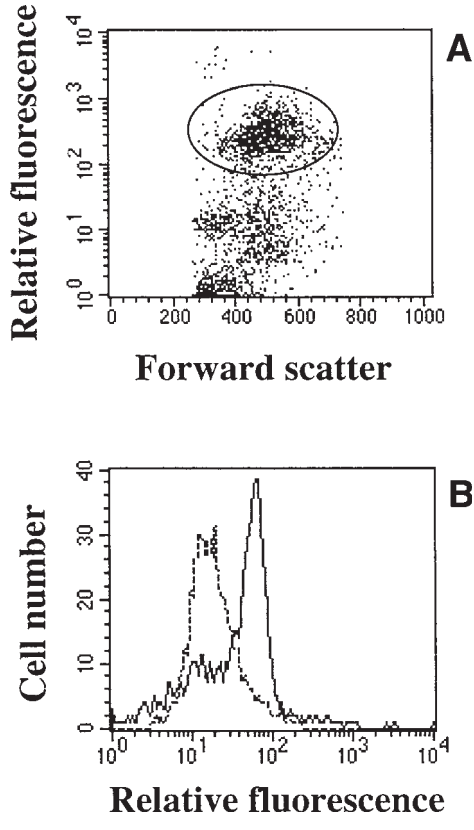

Fig. 4-2. The detection of rod photoreceptor apoptosis in a primary retinal cell culture using dual labeling for rhodopsin expression (rod specific protein) and TUNEL. **(A)** Retinal culture stained with anti-rhodopsin antibody that was subsequently labeled with a phycoerytherin-conjugated secondary antibody. The encircled rhodopsin-positive population (high FL-2, *y*-axis) can be readily distinguished from nonrod cells in the retinal culture. **(B)** TUNEL of rhodopsin-positive cells after 24 h in culture displaying high levels of apoptosis. The *dashed line* represents a negative control of cells stained without the TdT enzyme while the *solid line* represents TUNEL stained rhodopsin-positive cells.

cellular antigen. The cells must therefore be labeled with the specific antibody following fixation.

1. Once the TUNEL assay protocol is completed, incubate cells in appropriately diluted (using PBS/1% BSA, w/v) primary antibody for 60 min.
2. Wash twice in PBS and once in PBS/BSA (0.1%, w/v).
3. Incubate cells in appropriately diluted (using PBS/1% BSA) phycoerythrin-conjugated secondary antibody for 30 min.

4. Antigen expression is analyzed by measuring red fluorescence at >600 nm (FL-2, log scale; *see* **Subheading 3.** and **Table 1**) (**Fig. 4-2**).

3.3. Measurement of ROS

3.3.1. Measurement of Intracellular Peroxide Levels

1. Incubate cells (*see* **Notes 6** and **7**) (5×10^5/mL) with 5 µ*M* DCFH/DA, for 1 h at 37°C, in the dark.
2. Assess peroxide levels using a FACScan flow cytometer with excitation and emission settings of 488 nm and 530 nm, respectively (FL-1, log scale; *see* **Subheading 3.** and **Table 1**) (**Fig. 1B**).

3.3.2. Measurement of Intracellular Superoxide Levels

1. Incubate cells (*see* **Subheadings 4.3.1.** and **4.3.2.**) (5×10^5/mL) with 10 µ*M* hydroethidine, for 15 min at 37°C, in the dark.
2. Superoxide levels are assessed using a FACScan flow cytometer with excitation and emission settings of 488 nm and 600 nm respectively (FL-2) (*see* **Subheading 3.** and **Table 1**; **Fig. 1C**).

3.4. Measurement of Mitochondrial Transmembrane Potential

1. Incubate cells (5×10^5/mL) with 5 µg/mL of JC-1 for 15 min at 37°C, in the dark.
2. Ratiometric measurements are performed using a FACScan flow cytometer, in FL-1 and FL-2 (log scales; *see* **Subheading 3.** and **Table 1**) (**Fig. 2A**).

3.5. Acquisition and Analysis of Flow Cytometric Data

The assays described in this chapter were performed on a FACScan flow cytometer (Beckton Dickinson). An excitation source of 488 nm was obtained using a 15-mW air-cooled argon ion laser. Fluorescence emission was collected through a 530/30 band pass filter (FL-1) on a log scale for TUNEL, DCFH/DA, JC-1, and Annexin-V assays and a 585/42 band pass filter log scale (FL-2) for PI, DHE, JC-1, and antigen labeling assays, while cell cycle analysis (PI) was conducted using a linear scale (FL-2 area). A minimum of 5000 events were collected for each sample. CellQuest™ software version 1.1.1 was used for both acquisition and analysis of data.

4. Notes

4.1. Annexin V Assay

1. Under physiological conditions apoptotic cells are phagocytosed prior to loss of membrane integrity.
2. Following addition of PI, cells should be analyzed with minimal delay, as PI may eventually leak into normal and apoptotic cells.
3. As some cells stain very brightly with FITC, it may be necessary to use FACS compensation (FL-2-FL-1) during data acquisition (*see* **Subheading 3.** and **Table 1**).

4.2. TUNEL Assay

4. If an assessment of necrosis is required in a given population this can be achieved prior to fixation by employing the PI exclusion assay as described in **Subheading 2.1**.
5. This avoids any clumping of cells that may occur if a 1% (w/v) *p*-formaldehyde fixation buffer were added directly to samples.

4.3. Detection of Reactive Oxygen Species

6. Cells can be treated with apoptosis-inducing agents either before, after, or during the incubation period, depending on the time point at which ROS levels are to be measured.
7. As a positive control for peroxide production, cells may be treated with 1 m*M* H_2O_2 for 30–60 min (*see* **Fig. 1B**).

Acknowledgments

This work was supported by the Foundation for Science and Technology (Fundação para a Ciência e a Tecnologia), Lisbon, Portugal, RP Ireland Fighting Blindness, and the EU Biotech Programme.

References

1. Kerr, J. F. R., Wyllie, A. H., and Currie, A. R. (1972) Apoptosis, a basic biological phenomenon with wider implications in tissue kinetics. *Br. J. Cancer* **26,** 239–245.
2. Trump, B. F., Beresky, I. K., and Osornio-Vargas, A. R., eds. (1981) in *Cell Death in Biology and Pathology*, Chapman and Hall, New York.
3. Raff, M. C. (1992) Social controls on cell survival and cell death. *Nature* **365,** 397–400.
4. Gorman, A. M., McGowan, A. J., O'Neill, C., and Cotter, T. G. (1996) Oxidative Stress and apoptosis in neurodegeneration. *J. Neurol. Sci.* **139,** 45–52.
5. Devaux, P. F. (1991) Static and dynamic lipid asymmetry in cell membranes. *Biochemistry* **30,** 1163–1173.
6. Martin, S. J., Reutelingsperger, C. P. M., and Green, D. R. (1996) Annexin V- a specific probe for the detection of phosphatidylserine exposure on the outer plasma membrane leaflet during apoptosis, in *Techniques in Apoptosis: A Users Guide* (Cotter, T. G. and Martin S. M., eds.), Portland Press, London, pp. 107–119.
7. Martin, S. J., Reutelingsperger, C. P. M., McGahon, A. J., Rader, J., van Schie, R. C. A. A., La Face, D. M., and Green, D. R. (1995) Early redistribution of plasma membrane phosphatidylserine is a general feature of apoptosis regardless of the initiating stimulus: Inhibition by overexpression of Bcl-2 and Abl. *J. Exp. Med.* **182,** 1545–1556.
8. Swairjo, M. A., Concha, N. O., Kaetzel, M. A., Dedman, J. R., and Seaton, B. A. (1995) Ca^{2+}-bridging mechanism and phospholipid head group recognition in the membrane-binding protein Annexin V. *Nat. Struct. Biol.* **2,** 968–974.
9. Arends, M. J., Morris, R. G., and Wyllie, A. H. (1990) Apoptosis: the role of the endonuclease. *Am. J. Pathol.* **136,** 593–608.

10. Cotter, T. G. and Martin, S. J., eds. (1996) in *Techniques in Apoptosis*, Portland Press, London.
11. Carmody, R. J., McGowan, A. J., and Cotter, T. G. (1998) Rapid detection of rod photoreceptor apoptosis by flow cytometry. *Cytometry*, **33,** 89–92.
12. McGowan, A. J., Ruiz-Ruiz, M. C., Gorman, A. M., Lopez Rivaz, A., and Cotter, T. G. (1996) Reactive oxygen intermediates (ROI): common mediators of poly(ADP-Ribose)polymerase (PARP) cleavage and apoptosis. *FEBS Lett.* **392,** 299–303.
13. Kroemer, G. (1997) Mitochondrial implication in apoptosis. Towards an endosymbiont hypothesis of apoptosis in evolution. *Cell Death Different*. **4,** 443–456.
14. Salvioli, S., Ardizzoni, A., Franceschi, C., and Cossarizza, A. (1997) JC-1, but not $DiOC_6(3)$ or rhodamine 123, is a reliable fluorescent probe to assess $\Delta\psi m$ change in intact cells: Implications for studies on mitochondrial functionality during apoptosis. *FEBS Lett.* **411,** 77–82.

6

Raf-1 Protein Kinase Activity in T Cells from Aged Mice

Christopher J. Kirk and Richard A. Miller

1. Introduction

Most of our models of signal transduction through the T-cell receptor (TCR) involve components and pathways first described in T-cell clones and T-cell lymphomas such as the Jurkat cell line ***(1)***. These studies, while providing valuable insights, are not always reliable guides to the analogous biochemical events in cells freshly isolated from live donors ***(2)***. Thus, studies of the effects of aging on T-cell activation must frequently begin with a detailed study of the responses of cells from young individuals. Studies of aging effects involve additional challenges, including the difficulty of purifying sufficient numbers of cells from specific subsets, and allowing for the inherent variability among donors of any age.

The mitogen-activated protein kinase (MAPK) pathway involves the sequential activation of three kinases—Raf-1, mitogen-activated protein kinase (MEK), and extracellular-signal-regulated kinase (ERK)—and plays an important role in T-cell activation ***(3)***. Here we describe an in vitro kinase assay for Raf-1, which utilizes Raf-1 specific antibodies and a recombinant substrate, to assess age-related differences in Raf-1 activation in mouse splenic $CD4^+$ T-cells stimulated through the TCR. The problems involved in analyzing Raf-1 activity levels in freshly isolated T-cells are similar to those that are likely to be faced in the study of age-related alterations in the signal transduction of other cell types.

1.1. Isolation of Primary Lymphocytes

T-cell populations are made up of many distinct subsets, each with different activation requirements, some of which change systematically with age. Thus,

From: *Methods in Molecular Medicine*, Vol. 38: *Aging Methods and Protocols*
Edited by: Y. A. Barnett and C. R. Barnett

experiments on unseparated T-cell pools are likely to confound age effects on activation pathways with the effects of subset transitions. Aging leads to an increase in memory cells in both the CD4 and CD8 pools as measured by the increase in $CD44^{hi}$ cells ***(4)***. The naïve and memory pool can be further subdivided based on differences in expression of the membrane glycoprotein, P-glycoprotein, which also shows increased expression with age ***(5)***. It thus seems reasonable to study activation pathways first in separated CD4 and CD8 subsets, and to include studies of separated subsets wherever practical.

Purification of these subsets from spleens begins with the depletion of erythrocytes and B cells by differential centrifugation and panning on anti-IgG-coated plates, respectively ***(6)***. These procedures typically produce $25–35 \times 10^6$ T-cells from a single mouse spleen, among which 85–95% express the CD3 ε-chain characteristic of T-cells. For $CD4^+$ T-cell purification, as is described in this chapter, CD8 cells are depleted by incubation with anti-CD8 antibodies followed by removal with anti-IgG coated magnetic beads. Multiple subsets can be depleted simultaneously; for example, addition of anti-CD44 and anti-CD8 can be used to purify CD4 naïve cells (i.e., $CD4^+CD45RB^{hi}$). Yields of $15–20 \times 10^6$ $CD4^+$ T-cells are usually obtained from a single spleen. The numbers of memory and naïve cells that can be obtained from a single spleen vary depending on the age of the mouse (*see* previous paragraph); experiments involving cell types present only at low frequencies, such as memory cells from young mice, may require pooling spleens of mice of the same age in individual experiments.

1.2. Stimulation of T-Cells with Monoclonal Antibodies to Cell Determinants

Because the number of cells obtained from a single spleen is on the order of $5–20 \times 10^6$ depending on the subset isolated, it is necessary to develop experimental conditions that permit the stimulation and assay of samples as small as $2–5 \times 10^6$ cells. Therefore, choosing appropriate stimuli as well as optimizing stimulation conditions will influence the level of activation of the target enzyme and are important factors in developing reliable assays for aging studies.

Activation of T-cells can be achieved through the use of lectins, such as concanvalin A or phytohemagglutinin, that bind to unknown cell surface determinants. T-cells can also be stimulated using monoclonal antibodies specific for components of the TCR and for other cell surface markers (e.g., CD4 or CD28), or stimulated using pharmacological agents such as phorbol esters and calcium ionophores. We describe here the use of monoclonal antibodies to the ε-chain of the TCR/CD3 complex and CD4 to stimulate $CD4^+$ T-cells isolated from young and old mice. We feel that this provides a physiologically relevant stimulation for a polyclonal population of T-cells. Studies using T-cells from transgenic

mice that express a rearranged antigen-specific TCR will, in future work, provide analogous information about responses to peptides presented by accessory cells, which may more closely mimic the in vivo activation of T-cells.

The T-cells are incubated on ice with the stimulating antibodies followed by crosslinking at 37°C with anti-rat IgG to initiate activation. We use purified ascites fluid as our source of stimulating antibodies, although commercially available monoclonals can also be used. We have found that anti-rat IgG can effectively crosslink anti-CD3ε, even when using hamster clone 145–2C11 as the anti-CD3 reagent. Furthermore, anti-rat IgG has the advantage of being able to crosslink the rat antibodies used as costimulators (such as anti-CD4). The phorbol ester phorbol myristate acetate (PMA) (10 ng/mL) activates Raf-1 in mouse T-cells, and can be used as a positive control. The commonly used human lymphoma cell line Jurkat will also activate Raf-1 in response to either PMA or to anti-CD3 antibodies ***(7)***, although it should be noted that activation of human peripheral blood lymphocytes (PBL) or Jurkat cells with anti-CD3ε does not require the addition of a crosslinking reagent such as anti-rat IgG.

Antibodies to other cell surface markers have been shown either to augment TCR-driven T-cell activation or to activate signaling pathways independently ***(8,9)***. In the case of Raf-1 we have evidence that the costimulatory molecule CD28 plays a role in Raf-1 activation of $CD4^+$ T-cells ***(21)*** while others have shown that CD38 ligation can activate Raf-1 in Jurkat ***(10)***. Little is known about whether aging affects signal transduction from these other cell surface receptors, although our own data suggest that Raf-1 induction by anti-CD28 antibodies in CD4 cells is unaffected by aging in mice.

When stimulating T-cells with antibodies to the TCR or other surface molecules, it is important to determine how time of stimulation and dose of antibodies affect activation of the target enzyme. We found that in splenic $CD4^+$ T-cells, Raf-1 activation occurs within 1 min of crosslinking anti-CD3ε and anti-CD4 (**Fig. 1**). Initial descriptive studies of aging effects should include data on the kinetics of activation in both old and young samples, to see if apparent differences in the level of activation represent merely an alteration in the time course for activation. Furthermore, concentration curves of the antibody or antibodies used must be determined to find the optimal stimulation conditions. We titrated the amounts of anti-CD3ε and anti-CD4, which were purified from ascites fluid, to determine the optimal stimulation conditions for Raf-1 activation in $CD4^+$ T-cells. We found that anti-CD3 concentrations between 0.2 and 7 µg/mL could effectively stimulate Raf-1 in $CD4^+$ T-cells. In our hands, addition of anti-CD4 at concentrations between 2 and 8 µg/mL augments stimulation by anti-CD3, while anti-CD4 costimulation with amounts above or below this range inhibits Raf-1 activation by anti-CD3. Furthermore, anti-CD4 antibodies by themselves could not stimulate Raf-1 ***(21)***.

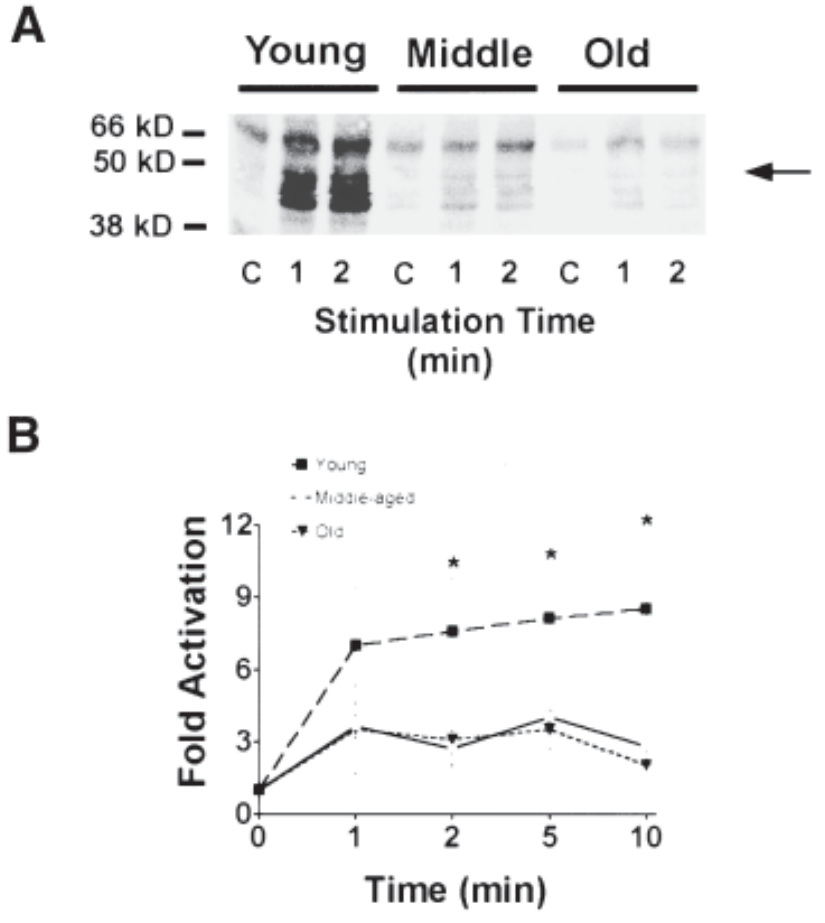

Fig. 1. **(A)** Analyzing Raf-1 kinase activity in $CD4^+$ T cells from young, middle-aged, and old mice. Raf-1 was immunoprecipitated from 3×10^6 $CD4^+$ T cells that were stimulated with crosslinked anti-$CD3^+$ anti-CD4 for the indicated times or crosslinked anti-DNP for 2 min (lanes marked C) and incubated with a KIMEK substrate and [^{32}P]ATP in an in vitro kinase assay. Reaction products were resolved by 10% SDS-PAGE and visualized by a PhosphorImager. *Arrow* indicates the 50-kDa migrating band of KIMEK. **(B)** Data from several experiments ($N = 5$ for 1 and 2 min and $N = 4$ for 5 and 10 min) are presented as -fold increase in Raf-1 kinase activity over anti-DNP-stimulated samples. *$p < 0.05$ for Young vs Old and Young vs Middle-aged by one-way ANOVA followed by a Student–Newman–Keul's *post hoc* test.

1.3. Measurement of Raf-1 Kinase Activity

Raf-1 is a serine/threonine kinase of 74 kDa that is activated by association with activated p21Ras. Besides its association with Ras, Raf-1 activation also

requires either tyrosine or serine/threonine phosphorylation ***(11)***. The importance of Raf-1 activity in T-cell activation and interleukin-2 (IL-2) production has been shown using Jurkat cells transfected with dominant negative forms of Raf-1. In this system, inhibition of Raf-1 blocks IL-2 production through the TCR ***(12,13)***. It has also been shown in Jurkat cells that Raf-1 activation through the TCR involves a protein kinase C dependent step that may be unique to T-cells ***(14)***.

As the first kinase activated in the MAPK pathway, Raf-1 phosphorylates and activates the dual specificity kinases MEK1/2, which, in turn, activate ERK1/2 ***(11)***. Early studies of Raf-1 in vitro kinase activity utilized either nonspecific substrates, such as histone H1, or Raf-1 autophosphorylation ***(11,15)***. Other measures of Raf-1 activity involved analyzing the retardation in mobility of Raf-1 in sodium dodecyl sulfate-polyacrylamide gel electrophoresis (SDS-PAGE), presumably due to activating phosphorylation. However, these assays lack the specificity of analyzing in vitro phosphorylation of a substrate known to be phosphorylated by Raf-1 in vivo. Furthermore, as Raf-1 contains multiple sites of phosphorylation, including those that inhibit kinase function, the slowly migrating form of Raf-1 in SDS-PAGE may contain a collection of differentially phosphorylated species of varying levels of activity ***(11)***.

With the cloning of MEK into plasmids that allow for protein production and purification from *E. coli*, a suitable substrate for in vitro Raf-1 kinase assays is available ***(16)***. We used a plasmid encoding a MEK construct that contains a lysine to methionine substitution at residue 97 in the ATP binding site, and therefore lacks kinase activity ***(16)***. This kinase-inactivated MEK, which we call KIMEK, has been used as a substrate to determine the enzymatic activity of Raf-1 in several cell systems, including Jurkat ***(7)***. In our hands, plasmid-derived KIMEK contains multiple species that migrate closely to the predicted molecular weight for KIMEK of 50 kDa (**Fig. 1**), each of which is phosphorylated by Raf-1 in in vitro kinase assays. These bands are likely to represent degradation products of the KIMEK, and have been noted in other publications using this substrate ***(16,17)***. Another version of KIMEK is commercially available as a GST fusion protein from Upstate Biotechnology (Lake Placid, NY, USA).

Raf-1 function is more difficult to quantify in freshly isolated lymphocytes than in cell lines, in part because Raf-1 protein levels are lower in primary cell isolates. T-cells isolated from spleens are in a quiescent state and contain a small cytosolic compartment as compared to a T-cell clone or Jurkat cell, which are the size of T-cell blasts. In fact, Raf-1 protein levels are approximately tenfold lower per cell in quiescent T-cells than in T-cell blasts ***(18)***, and we have found that Raf-1 protein expression in Jurkat is approximately fivefold greater than in splenic $CD4^+$ T-cells (Kirk and Miller, unpublished results).

Furthermore, limitations in the number of T-cells that can be obtained from each donor make it critical to develop and validate methods to measure kinase activity from the lysates of $2–5 \times 10^6$ cells.

The in vitro kinase assay for Raf-1 involves the immunoprecipitation of Raf-1 from cell lysates followed by incubation with the KIMEK substrate and [^{32}P]ATP. Several precautions in Raf-1 isolation and kinase measurement help to ensure high levels of kinase activity, low levels of background phosphorylation, and maximal difference between age groups. Anti-Raf-1 antibodies can currently be purchased in either mouse monoclonal or rabbit polyclonal forms. Although we have achieved the best results with rabbit polyclonal sera, other forms should be tested in different systems (e.g., using human cells, or different strains of mice or cell types). Increasing the stringency of a lysis buffer will reduce coprecipitation of other kinases, which might otherwise increase the background phosphorylation of bands other than KIMEK. Background phosphorylation can also be reduced by preclearing the lysates with Protein G–Sepharose prior to immunoprecipitation.

2. Materials

1. Mice. We use specific-pathogen free male (BALB/c × C57BL/6)F1 mice purchased from the National Institute on Aging contract colonies at the Charles River Laboratories (Kingston, NJ, USA). Initial work should use animals of several different ages, avoiding the use of animals so old that they are likely to be ill. In our own studies we typically use mice aged approx 3–6 mo, 12–14 mo, and 18–22 mo from strains in which 50% mortality is not reached until 24–26 mo of age. Mice over the age of 15 mo should be examined at necropsy and those with skin lesions, splenomegaly, or macroscopically visible tumors should not be used.
2. Hanks balanced salt solution is supplemented with 0.2% bovine serum albumin (BSA) (HBSS–BSA). It should be used and stored at 4°C unless otherwise noted.
3. Lympholyte-M™ (Cedarlane Laboratory, Ontario, Canada).
4. Antibodies: Antibodies to CD3ε (clone 145-2C11), the dintrophenyl hapten (DNP) (clone UC8), CD4 (clone GK1.5), and CD8 (clone 53.6-7) were produced in our laboratory from cell lines purchased from the American Type Culture Collection (Rockville, MD, USA). Anti-CD62L (clone Mel-14) can be purchased from Pharmingen (San Diego, CA, USA). Anti-rat IgG used in cell stimulation was purchased from Sigma (St. Louis, MO, USA). We find that most lots of goat anti-rat IgG are suitable for crosslinking hamster antibodies (such as anti-CD3ε), and are often superior to anti-hamster antibodies in this system; anti-rat Ig secondary antibodies also have the advantage that they provide crosslinking between hamster anti-CD3 and rat anti-CD4 or anti-CD8 antibodies. Magnetic beads conjugated to anti-rat IgG are obtained from PerSeptive Diagnostics, Cambridge, MA, USA, and polyclonal anti-Raf-1 from Santa Cruz Biotech, Santa Cruz, CA, USA.
5. Preparation of anti-Ig-coated dishes for B-cell depletion. Plates of 150 mm diameter are incubated with 35 mL of phosphate-buffered saline (PBS) containing

1 µg/mL of rabbit anti-mouse IgG (H + L) overnight at 4°C on a level surface. Plates can be stored for 4–7 d at 4°C or kept for long-term storage at –20°C. Prior to use the plates are washed 3× with PBS to remove unbound antibody and incubated for at least 1 h with 30 mL of HBSS–BSA at 4°C. Petri dishes of 100 mm diameter can be prepared in the same way using one-third the volume of rabbit anti-mouse IgG.

6. RPMI supplemented with 10% FCS (RPMI–FCS).
7. Protein G–Sepharose (Pharmacia, Piscataway, NJ, USA)
8. RIPA buffer: 10 m*M* sodium phosphate, pH 7.0; 150 m*M* NaCl, 2 m*M* EDTA, 1% sodium deoxycholate, 1% Nonidet P-40 (NP-40), 0.1% sodium dodecyl sulfate (SDS); 0.1% 2-mercaptoethanol, 50 m*M* NaF, 200 µ*M* Na_3VO_4, 2 µg/mL of aprotinin; 0.5 µg/mL of leupeptin; and 2 µg/mL of pepstatin. Add 0.1 m*M* of phenylmethyl sulfonyl flourite (PMSF) just prior to use.
9. PAN buffer: 10 m*M* PIPES, pH 7.0, 100 m*M* NaCl, 20 µg/mL of aprotinin.
10. Recombinant kinase inactive MEK substrate (KIMEK). We used a plasmid encoding a KIMEK containing a 6 histidine tag (the generous gift of Gary L. Johnson, National Jewish Center for Immunology, Denver, CO, USA), that was expressed and purified as described ***(19)***. Commercially available KIMEK in the form of a glutathione-*S*-transferase (GST) fusion protein is available from Upstate Biotechnology (Lake Placid, NY, USA, cat. no. 14–159).
12. Kinase buffer: 20 m*M* PIPES, pH 7.0, 75 m*M* NaCl, 10 m*M* $MnCl_2$, 20 µg/mL of aprotinin.
13. Nitrocellulose (Schleicher and Shuell, Keene, NH, USA).

3. Methods

3.1. Purification of Splenic CD4+ T-Lymphocytes

3.1.1. T-lymphocyte Purification

1. Kill mice by cervical dislocation or CO_2 asphyxiation. Experiments should be age balanced, with mice of different age groups killed in each experiment.
2. Wet down fur with 70% ethanol and remove spleens to separate Petri dishes (6 mm diameter) containing 6 mL of HBSS–BSA at room temperature.
3. Rub spleens between frosted glass slides to obtain a single cell suspension.
4. Pass suspension through a sheet of nylon mesh to remove cell clumps and connective tissue. Wash plate once with 6 mL of HBSS–BSA and pass through the nylon mesh sheet. Each splenic suspension should be in a volume of 12 mL.
5. Centrifuge splenocytes at ~20°C for 5 min at 500*g*.
6. To remove erythrocytes, resuspend splenocytes in 8 mL of HBSS–BSA warmed to 37°C. Carefully overlay splenocyte suspension on 4 mL of Lympholyte-M™ that has also been warmed to 37°C. Four milliliters of Lympholyte-M™ has the capacity for 100×10^6 lymphocytes (the approximate number of lymphocytes in a single spleen). Centrifuge at room temperature for 15 min at 600*g* with the brake **off**.
7. Remove buffy coat containing lymphocytes and wash with 15 mL of HBSS–BSA. Centrifuge at 4°C for 5 min at 500*g*. If the Lympholyte-M™ has not been

sufficiently diluted there will be incomplete cell pelleting. Dilute further in HBSS–BSA if supernatant shows any turbidity following centrifugation.

8. Resuspend lymphocytes in 15 mL of ice-cold HBSS–BSA and add to anti-Ig-coated dishes. Incubate at 4°C on a level surface for 40 min. Swirl plates once at the end of the first 20 min to redistribute the cells. Dishes of 150 mm diameter should receive approx $120–150 \times 10^6$ erythrocyte-depleted spleen cells; using more cells per dish diminishes cell purity, while using fewer cells diminishes cell yield.
9. Gently separate nonadherent from adherent cells by swirling the plate vigorously and then slowly removing the cell suspension from the tilted dish. It is particularly helpful to remove the last 0.5–1 mL very slowly, allowing the meniscus to collect at the low point of the dish. Wash plate once with 5 mL of ice-cold HBSS–BSA to improve cell yield, again taking care to remove the suspension slowly. Centrifuge cells at 4°C for 5 min at 500*g*.
10. Resuspend cells in ice-cold HBSS–BSA and count. From 25 to 30×10^6 T-cells can be obtained from a single spleen. Remove an aliquot of cells to perform flow cytometry with an antibody to mouse CD3ε to determine the proportion of T-cells in the resulting population (typically 85–90%).

3.1.2. Negative selection of T cell subsets

1. Dilute T-cells, prepared as described in **Subheading 3.1.1.**, into HBSS–BSA to a concentration of approx 5×10^6 cells/mL.
2. Add antibodies to cell markers of subsets to be depleted (i.e., for $CD4^+$ T-cell purification add antibodies to CD8). The amount of antibody needed is based on trial experiments in which CD8 cell contamination of resulting cells is determined by flow cytometric analysis. In our experiments, we use 1 µg of antibody for 10^7 cells at a concentration of 5×10^6 cells/mL.
3. Incubate on ice for 20 min with gentle shaking at 5- to 10-min intervals.
4. Prepare anti-rat IgG-coated beads according to the manufacturer's specifications. Prepare enough for a bead-to-cell ratio of 50:1. Resuspend beads in 0.4 mL of ice-cold HBSS–BSA.
5. Centrifuge cells at 4°C for 5 min at 500*g*. Wash cells once in 10 mL of cold HBSS–BSA.
6. Resuspend cells in 1 mL of cold HBSS–BSA and add 0.4 mL of bead solution.
7. Incubate on ice for 20 min with shaking every 5 min to ensure suspension of beads.
8. Fill tube to 5 mL with cold HBSS–BSA and pass under magnetic field (PerSeptive Diagnostics, Cambridge, MA, USA), which is kept at 4°C.
9. Carefully remove cell suspension without disturbing the beads aligned along the side of tube.
10. Repeat **steps 8** and **9** two to three more times to ensure complete removal of beads.
11. Centrifuge cells at 4°C for 5 min at 500*g*. Resuspend in cold RPMI supplemented with 10% fetal calf serum (FCS) (RPMI–FCS) and count. An aliquot of ~0.5×10^6 cells should be removed at this stage for flow cytometric analysis to assess the purity of selected cells.

3.2. T-lymphocyte Activation

1. Aliquot equal numbers of cells into 1.5-mL tubes in a total volume of 1 mL. A sample from each mouse should be saved for analysis of Raf-1 protein expression levels. In our experience we get usable results from samples as small as 2×10^6 cells/sample, although samples of 5×10^6 cells/sample give stronger signals and are thus preferable when cells are not limiting.
2. Incubate cells with antibodies to the TCR/CD4 complex (anti-CD3ε and anti-CD4) or other cell surface determinants. Some aliquots should also be incubated, as a control, with a nonstimulatory antibody such as monoclonal anti-DNP of the same species and isotype as the antibodies used for cell activation. Incubate the samples on ice for 30 min. Invert the tubes several times during the incubation period.
3. Prepare solutions of RPMI–FCS with 5 µg/mL of anti-rat IgG (crosslinking reagent) and RPMI–FCS with PMA (10 ng/mL). Warm to to 37°C.
4. Centrifuge cells at 1000*g* for 30 s to pellet.
5. Resuspend in 1 mL of warm anti-rat Ig solution or PMA and incubate at 37°C for the desired interval. Raf-1 activation in mouse CD4 T-cells stimulated by anti-CD3 and anti-CD4 is detectable within 1 min and typically reaches a plateau level within 5–10 min before subsiding to lower levels over the next half hour. Stimulation with PMA for 5 min serves as a positive control for Raf-1 activation.
6. Stop reaction by centrifugation at 10,000*g* for 10 s.
7. Wash cells in ice-cold PBS. Centrifuge cells at 10,000*g* for 10 s.
8. Lyse cells in RIPA buffer, using 0.8 mL for immunoprecipitation or 40 µL for protein expression levels.
9. Incubate in RIPA for 15–30 min. Centrifuge cells at 4°C for 10 min at 13,000*g*.
10. Remove pellet or transfer supernatants to a new tube.

3.3. In Vitro Kinase Assay of Raf-1

3.3.1. Raf-1 Immunoprecipitation

1. Preclear samples with 20 µL of Protein G–Sepharose (50% slurry) for 0.5–1 h on a rocker at 4°C. Wash the Protein G–Sepharose several times with lysis buffer before use. Pellet beads and transfer supernatants to new tubes.
2. Add anti-Raf-1 antibodies at 1:100 dilution (i.e., 8 µL for 0.8 mL of lysate) and 25 µL of Protein G–Sepharose. Incubate overnight on a rocker at 4°C.
3. Wash samples twice with ice-cold RIPA using centrifugation at 10,000*g* for 10 s.
4. Wash twice with ice-cold PAN buffer containing 1% NP-40 and once in ice-cold PAN buffer.

3.3.2. Raf-1 Kinase Assay

1. For each sample add 50–100 ng of purified KIMEK and 30 µCi of [γ-^{32}]P-ATP to 30 µL of kinase buffer. The kinase buffer should be prepared for all samples in the same tube to ensure equal loading of KIMEK and [^{32}P]ATP to each sample.
2. Add 30 µL to each sample and incubate for 15 min at 30°C.
3. Stop reaction by addition of 15 µL of 4× reducing sample buffer and boiling.

4. Run samples on 10% SDS-PAGE and transfer to nitrocellulose. Expose blot to X-ray film or an intensifier screen for phosphor storage image analysis.
5. Densitometric values are corrected for background levels and can be expressed as fold activation by expression of the ratio of the densitometric volumes in the stimulated samples to the anti-DNP-stimulated sample.
6. In a separate 10% SDS-PAGE gel transferred to nitrocellulose, the whole cell lysates should be analyzed by Western blot analysis using the anti-Raf-1 antibodies according to the manufacturer's instructions.

4. Notes

1. Because of limitations in the yield of T-cell subsets from mouse spleens, it is important to minimize cell loss during the purification procedures. To that end, careful notice should be paid to the overlay of splenocytes on Lympholyte-M™ and the complete removal of the buffy coat following centrifugation. It is also important to ensure complete removal of nonadherent cells from the T plates. The plates can placed under a microscope to determine if nonadherent cells remain. Further washes of the anti-Ig-coated dishes may be helpful. Lastly, it is important to be sure cells are in a single cell suspension, that is, not clumped, prior to the addition of the anti-rat-Ig-coated magnetic beads to minimize cell loss at that step.
2. The level of Raf-1 kinase activation by antibodies to cell determinants is dependent upon antibody dose and time of stimulation. Dose curves for stimulating antibodies will be necessary, as ascites purification and antibody storage will give varying levels stimulating efficacy.
3. The stringency (i.e., detergent type) of the lysis buffer will determine the amount of nonspecific phosphorylation of bands other than the KIMEK substrate. We use RIPA because it has been shown to bring down Raf-1 in the absence of associated proteins such as 14-3-3 ***(20)***. Because we find the purity of our KIMEK is <75%, we have tried to limit the amount of coprecipitating kinases that may phosphorylate nonspecific proteins in our substrate preparation. However, less stringent buffers can be used if the purity of the KIMEK is high (i.e., commercially produced GST-KIMEK, which is more pure than the 6 histidine tagged KIMEK).
4. It is not necessary to determine protein concentration in cell lysates prior to Raf-1 immunoprecipitation. Assays should be performed using equal cell numbers in each sample. Because contamination by erythrocytes may differ from young and old mice, the total amount of protein is likely to be higher in T-cells from old mice, even though the same number of cells is present in each sample.
5. Because the amount of Raf-1 present in $2–5 \times 10^6$ freshly isolated T-cells is quite low, it is important to reduce the signal-to-noise ratio in the kinase assay. We transfer the kinase samples from the SDS-PAGE to nitrocellulose before autoradiography to remove free [^{32}P]ATP that remains in the gel.

Acknowledgments

This research was supported by Research Grant AG09801 and by training Grants AI-07413 and GM-07315 at the University of Michigan.

References

1. Wange, R. L. and Samelson, L. E. (1996) Complex complexes: signaling at the TCR. *Immunity* **5,** 197–205.
2. Madrenas, J., Wange, R. L., Wang, J. L., Isakov, N., Samelson, L. E., and Germain, R. N. (1995) Zeta phosphorylation without ZAP-70 activation induced by TCR antagonists or partial agonists. *Science* **267,** 515–518.
3. Weiss, A. and Littman, D. R. (1994) Signal transduction by lymphocyte antigen receptors. *Cell* **76,** 263–274.
4. Lerner, A., Yamada, T., and Miller, R. A. (1989) Pgp-1^{hi} T lymphocytes accumulate with age in mice and respond poorly to concanavalin A. *Eur. J. Immunol.* **19,** 977–982.
5. Witkowski, J. M., Li, S. P., Gorgas, G., and Miller, R. A. (1994) Extrusion of the P glycoprotein substrate rhodamine-123 distinguishes CD4 memory T cell subsets that differ in IL-2-driven IL-4 production. *J. Immunol.* **153,** 658–665.
6. Mage, M. G., McHugh, L. L., and Rothstein, T. L. (1977) Mouse lymphocytes with and without surface immunoglobulin: preparative scale separation in polystyrene tissue culture dishes coated with specifically purified anti-immunoglobulin. *J. Immunol. Methods* **15,** 47–56.
7. Franklin, R. A., Tordai, A., Patel, H., Gardner, A. M., Johnson, G. L., and Gelfand, E. W. (1994) Ligation of the T cell receptor complex results in activation of the Ras/Raf-1/MEK/MAPK cascade in human T lymphocytes. *J. Clin. Invest.* **93,** 2134–2140.
8. Rudd, C. E. (1996) Upstream-downstream: CD28 cosignaling pathways and T cell function. *Immunity* **4,** 527–534.
9. Pedraza-Alva, G., Merida, L. B., Burakoff, S. J., and Rosenstein, Y. (1996) CD43-specific activation of T cells induces association of CD43 to Fyn kinase. *J. Biol. Chem.* **271,** 27,564–27,568.
10. Zubiaur, M., Izquierdo, M., Terhorst, C., Malavasi, F., and Sancho, J. (1997) CD38 ligation results in activation of the Raf-1/mitogen-activated protein kinase and the CD3-zeta/zeta-associated protein–70 signaling pathways in Jurkat T lymphocytes. *J. Immunol.* **159,** 193–205.
11. Daum, G., Eisenmann-Tappe, I., Fries, H. W., Troppmair, J., and Rapp, U. R. (1994) The ins and outs of Raf kinases. *Trends Biochem. Sci.* **19,** 474–480.
12. Owaki, H., Varma, R., Gillis, B., Bruder, J. T., Rapp, U. R., Davis, L. S., and Geppert, T. D. (1993) Raf-1 is required for T cell IL2 production. *EMBO J.* **12,** 4367–4373.
13. Izquierdo, M., Bowden, S., and Cantrell, D. (1994) The role of Raf-1 in the regulation of extracellular signal-regulated kinase 2 by the T cell antigen receptor. *J. Exp. Med.* **180,** 401–406.
14. Whitehurst, C. E., Owaki, H., Bruder, J. T., Rapp, U. R., and Geppert, T. D. (1995) The MEK kinase activity of the catalytic domain of RAF–1 is regulated independently of Ras binding in T cells. *J. Biol. Chem.* **270,** 5594–5599.
15. Siegel, J. N., June, C. H., Yamada, H., Rapp, U. R., and Samelson, L. E. (1993) Rapid activation of C-Raf-1 after stimulation of the T-cell receptor or the muscarinic receptor type 1 in resting T cells. *J. Immunol.* **151,** 4116–4127.

16. Lange-Carter, C. A., Pleiman, C. M., Gardner, A. M., Blumer, K. J., and Johnson, G. L. (1993) A divergence in the MAP kinase regulatory network defined by MEK kinase and Raf. *Science* **260,** 315–319.
17. Lange-Carter, C. A. and Johnson, G. L. (1994) Ras-dependent growth factor regulation of MEK kinase in PC12 cells. *Science* **265,** 1458–1461.
18. Zmuidzinas, A., Mamon, H. J., Roberts, T. M., and Smith, K. A. (1991) Interleukin-2-triggered Raf-1 expression, phosphorylation, and associated kinase activity increase through G1 and S in CD3-stimulated primary human T cells. *Mol. Cell Biol.* **11,** 2794–2803.
19. Gardner, A. M., Lange-Carter, C. A., Vaillancourt, R. R., and Johnson, G. L. (1994) Measuring activation of kinases in mitogen-activated protein kinase regulatory network. *Methods Enzymol.* **238,** 258–270.
20. Michaud, N. R., Fabian, J. R., Mathes, K. D., and Morrison, D. K. (1995) 14-3-3 is not essential for Raf-1 function: identification of Raf-1 proteins that are biologically activated in a 14-3-3- and Ras- independent manner. *Mol. Cell Biol.* **15,** 3390–3397.
21. Kirk, C. J. and Miller, R. A. (1998) Analysis of Raf-1 activation in response to TCR activation and costimulation in murine T-lymphocytes: effect of age. *Cellular Immunology* **190,** 33–42.

7

Identification of Differentially Expressed Genes in Young and Senescent T Cells

Andrea Engel, Mahdi Adibzadeh, and Graham Pawelec

1. Introduction

The need to analyze changes in gene expression patterns occuring in senescent cells has stimulated the search for proper methods to identify the actual differences between young and senescent cells. In studies of aging, differential display reverse transcriptase-polymerase chain reaction (DDRT-PCR) has already been applied successfully by several groups. Altered gene expression in young and senescent fibroblast cultures ***(1)***, human mammary epithelial cells ***(2)***, and rat brain cells ***(3,4)*** has been detected with this technique.

In 1992, two different but related strategies were introduced for fingerprinting expressed RNAs as cDNA tags. One was called differential display (DD), ***(5)*** or, according to the PCR nomenclature, DDRT-PCR ***(6,7)***. The other was named RNA arbitrary primed PCR (RAP-PCR) ***(8–10)***. Both variants of RNA fingerprinting are able to detect differences in gene expression of a certain percentage of expressed genes. Under the appropriate conditions, the pattern of fragments derived from one type of cells is reproducible and can be compared with that of another cell type. In both methods, primers of arbitrary sequence are used to generate cDNA tags. This already suggests that in principle any primer could be used to amplify differentially expressed genes.

The first method, DDRT-PCR, uses combinations of 10-mer arbitrary primers with anchored cDNA primers and generates fragments that originate mostly from the poly(A) tail and extend about 50–600 nucleotides upstream ***(5–7,11)***. The original differential display (DDRT-PCR) technique ***(5,6)*** should be able to generate a largely complete pattern of all mRNAs expressed in a particular cell using a reasonable number of primer pairs ***(6)***. In this technique, cDNA is amplified in a PCR with low-stringency annealing (at 42°C) throughout. The

From: *Methods in Molecular Medicine*, Vol. 38: *Aging Methods and Protocols*
Edited by: Y. A. Barnett and C. R. Barnett

PCR primers consist of 10-base arbitrary primer and the same locking primer used in the first strand synthesis (T_{11}VN; V can be A, G, or C; N can be any of the four nucleotides). The process of the DDRT-PCR is the following:

1. During the first strand synthesis, the locking primer samples a sizeable portion of the mRNA (potentially 1/16th) present in the cell.
2. The arbitrary primer permits amplification of reverse-transcribed cDNA species using the locking primer.
3. Repeated PCR cycling with low-stringency results in amplification of products of a size <500 basepairs that can be evaluated on standard acrylamide gels.

The second technology, termed RNA arbitrary primed PCR (RAP-PCR), was developed by M. McClelland and J. Welsh ***(8,10)***. With this technique, an 18-base arbitrary primer is used in both the first and cDNA synthesis reaction and PCR. In the PCR only one primer is used to amplify the cDNA. The PCR consists of a single round of low-stringency amplification (at annealing temperature of 37–42°C) followed by multiple rounds with higher stringency (at annealing temperature of >50°C). By structuring the PCR in this manner, the amplification of genomic DNA (gDNA) should be minimized because there should be a limited chance of incorporating the primer used in the first strand synthesis into both ends of complementary portions of gDNA. In contrast, the 18-base arbitrary primer is incorporated into one end of the cDNA as a result of the reverse transcription of the RNA and into the other end during the single round of low-stringency PCR. Consequently, the authors conclude that the signal should be derived from RNA, not from gDNA. The process of the RAP-PCR is the following:

1. During the first strand synthesis, the arbitrary primer anneals and extends from sites contained within the mRNA.
2. Second strand synthesis proceeds in a similar manner during the single round of low-stringency PCR.
3. PCR amplification at high stringency proceeds strongly, having incorporated the arbitrary primer into both ends of the cDNA.
4. A template-dependent competition exists that determines which potential PCR products will ultimately predominate. PCR products can be analyzed by acrylamide gel electrophoresis.

Any primer of 18 bases can be used in this technique and the PCR products can be larger than 500 basepairs.

Here we present a detailed protocol that uses a poly(T) primer in the reverse transcriptase reaction and only one 18-base primer in the arbitrary amplification of cDNA. The advantage of using the T12AG primer in the reverse transcription is the amplification of mRNA throughout total RNA. Previous experiments have shown that the RAP-PCR principle with one primer in the

random amplification reaction can be used as successfully as if the cDNA were done with the random primer of the following PCR. This method is applicable to any set of two or more eukaryotic cell types and will result in reproducible patterns of PCR products that correspond to expressed genes. Interesting bands are excised from the gel, reamplified, cloned, and sequenced. The differential expression has to be confirmed by Northern blotting, Southern blotting, or nuclear run-on analysis.

2. Materials

2.2 DNA Agarose Gel Electrophoresis

1. 10× TBE: 1 *M* Tris, 0.89 *M* boric acid, 20 m*M* EDTA. Store at room temperature.
2. DNA sample buffer: 0.5% bromophenol blue, 0.5% xylene cyanol, 5% saccharose. Freeze until used in portions of 1 mL, then store at 4°C.

2.2. RNA Gel Electrophoresis

1. 10× 4-morpholine propanesulfonic acid (MOPS): 200 m*M* MOPS, pH 7.0; 50 m*M* sodium acetate, pH 4.8; 10 m*M* EDTA, pH 8.0. Store at room temperature.
2. RNA sample buffer: 17 µL 10× MOPS, 84 µL of formamide, 29 µL of formaldehyde (37%). Prepare fresh prior to use.

2.3. DNA Acrylamide Gel Electrophoresis

1. Sample buffer: 13 mL of double-distilled H_2O (ddH_2O), 13 mL of rehydration buffer (DELECT buffer system), 1% bromophenol blue, 1% xylene cyanol, 250 µL of 0.2 *M* EDTA-Na_2. Store at 4°C.

2.4. Enzymes

1. Alkaline phosphatase (Boehringer Mannheim).
2. AmpliTaq DNA polymerase (Amersham, Braunschweig).
3. Klenow fragment DNA polymerase (Boehringer Mannheim).
4. Reverse transcriptase (Amersham, Braunschweig).
5. RNase (Boehringer, Mannheim).
6. RNasin (RNase inhibitor, Promega, Madison, WI, USA).
7. T4-DNA ligase (Boehringer Mannheim).
8. T4-Oligonucleotide kinase (New England Biolabs, Schwalbach).
9. Taq Long Plus DNA polymerase I (Stratagene, Heidelberg).

2.5. Reaction-Kits, Filters, and Gels

1. CleanGels, 15% (ETC, Kirchentellinsfurt).
2. DELECT Kit for DDRT-PCR electrophoresis (ETC, Kirchentellinsfurt).
3. Hyperbond N^+ Nylon membrane (Amersham, Braunschweig, or any other nylon membrane.
4. Megaprime™ DNA Labeling Kit (Amersham, Braunschweig).

5. QIAquick® Gel Extraction kit (Qiagen, Hilden).
6. Rapid DNA Ligation Kit (Boehringer Mannheim).
7. RAP-PCR Kit (Stratagene, Heidelberg).
8. RNeasy Mini Kit (Qiagen, Hilden).

2.6. Molecular Weight Markers

1. 1 kb DNA Ladder (Gibco-BRL, Eggenstein).
2. 100-basepair DNA Ladder (Gibco-BRL, Eggenstein).

2.7. Silver Staining

1. Fixation solution: 10% acetic acid or 15% EtOH/5% acetic acid. Prepare a fresh solution prior to use.
2. Silver reacting solution: 0.1% $AgNO_3$, 200 µL of formaldehyde (37%). Prepare a fresh solution prior to use.
3. Developing solution: 2.5% Na_2CO_3, 200 µL of formaldehyde (37%), 200 µL of Na-thiosulfate (2%). Prepare a fresh solution prior to use.
4. Stopping/desilver solution: 2.0% (w/v) Glycine. Prepare a fresh solution prior to use.
5. Impregnating solution: 10% Glycerol. Prepare a fresh solution prior to use.

2.8. Cloning of DNA Fragments

1. 50 m*M* $CaCl_2$. Store at 4°C.
2. 10 × Klenow buffer: 500 m*M* Tris-HCl, pH 7.5, 60 m*M* $MgCl_2$, 10 m*M* dithiothreitol (DTT). Freeze until use, then store at 4°C.

2.9. Bacterial Growth Media

1. LB Medium: 10 g/L of bacto-tryptone, 10 g/L of NaCl, 5 g/L of glucose, 5 g/L of yeast extract. Store at 4°C.
2. LB plate agar: LB medium, 15 g/L of agar. Store at 4°C, cover down.

2.10. Plasmid Isolation

1. Resuspension solution: 50 m*M* Tris-HCl, pH 7.5; 10 m*M* EDTA. Store at room temperature.
2. Lysis solution: 0.2 *M* NaOH, 1% sodium dodecyl sulfate (SDS). Store at room temperature.
3. Neutralization solution: 2.55 *M* K-acetate, pH 4.8. Store at room temperature.

2.11. Northern Blotting

1. 20× SSC: 3 *M* NaCl, 0.3 *M* sodium citrate, pH 7.0 (adjust with NaOH). Store at room temperature.
2. Hybridization buffer: 1 m*M* EDTA, pH 8.0, 0.25 *M* Na_2HPO_4, pH 7.2, 7% SDS, 1% BSA. Can be stored at 4°C for a few days.
3. Washing buffer: 1 m*M* EDTA, pH 8.0, 20 m*M* Na_2HPO_4, pH 7.2, 1% SDS. Store at room temperature.

2.12. General Equipment

1. Centrifuge.
2. Centrifuge tubes (15 mL, 50 mL).
3. Electrophoresis tank (for horizontal electrophoresis), gel casting and tray.
4. High-voltage power supply.
5. Incubator at 37°C with a shaker.
6. Centrifuge for microfuge tubes.
7. Multiphor II-chamber (Pharmacia) or any other gel electrophoresis system for horizontal acrylamide gel electrophoresis.
8. PCR Cups Micro Amp
9. Pipet tips (0,1–10 µL, 10–200 µL, 100–1000 µL).
10. Thermocycler
11. Video-Printer Mitsubishi Copy Processor (Software Bioprint Version 5.04, Fröbel, Lindau) or another gel documentation system.
12. Whatman 3MM filter paper.

3. Methods

3.2 RNA Preparation

Basically, RNA can be isolated with any kind of RNA preparation method. We had the best results with the cytoplasmic RNA preparation protocol for the RNeasy-Kit (Qiagen) following the protocols provided. The common $CsCl_2$ isolating method ***(12)***, or total RNA isolation with TRIZOL™ from Biozol or any other RNA isolating-method should also be useful.

The RNA should finally be diluted in RNase-free (diethylpyrocarbonate [DEPC]-treated) water and can be stored at –80°C (*see* also **Note 1**).

3.2. Reverse Transcription of RNA

In this protocol the reverse transcription is done with a T_{12}VN-Primer (T_{12}VN; V can be A, G, or C; N can be any of the four nucleotides) to amplify different "RNA families" with a poly(A) tail, i.e., mRNA. The nucleotides VN should allow the primer to bind at the end of the long poly(A) tail of mRNA (*see also* **Notes 1** and **2**).

1. For the reverse transcriptase reaction, 200 ng of mRNA or 0.5 µg of total RNA should be used. In the first step the RNA is denatured for 5 min at 65°C in a volume of 6 µL. After a short centrifugation (30 s at full speed) the reagents listed in **Table 1** are added.
2. To allow the T_{12}VN primer to find its complementary sequence on the RNA, the probe is incubated for 10 min at room temperature. After that the probe is incubated for 45 min at 42°C in a water bath for the reverse transcriptase reaction. Lastly the enzyme should be denatured by heating the probe for 5 min at 95°C.

Table 1
Components for the Reverse Transcriptase Reaction After Denaturation of the RNA

5 m*M* T_{12}VN-Primer	2 µL
10 m*M* dNTPs	4 µL
5 × RT-buffer	4 µL
0.1 m*M* DTT	2 µL
RNasin	0.5 µL
Reverse transcriptase	1.5 µL

3. After a short centrifugation step the cDNA can be stored for 2–4 wk at –20°C or for a longer period at –80°C.

3.3. Random Amplification of cDNA

In this system, the first step of the amplification reaction is the binding of the random primer at low stringency to one tail of the mRNA. The second cycle, already at higher stringency, forms DNA fragments with primer binding sites on both ends of the fragment. The amplification reaction is then started (*see* also **Note 3**).

1. The PCR is done in a total volume of 50 µL with the components shown in **Table 2**.
2. The PCR-cycles are described in **Table 3**.

With this protocol, oligonucleotides of > 500 basepairs can be amplified. The probes are analyzed by horizontal gel electrophoresis and are detected by silver staining with a nonradioactive method. They also can be stored at –20°C.

3.4. Discontinuous Acrylamide DNA Electrophoresis

For DNA separation, CleanGels and the DELECT-buffer Kit can be used. This system allows a size separation of the DNA in a native, nondenaturing manner. The electrophoresis is done in a horizontal manner in the Multiphor II chamber from Pharmacia. This is an easy and useful method to analyze the PCR products. The gels and buffer systems are available from Pharmacia, Heidelberg or ETC, Kirchentellinsfurt.

Different DNA electrophoresis gels are provided. For these applications 15% gels with 36 slots and a probe volume of 10–15 µL have proven to be useful, but other gel systems can also be used. Here we describe a native electrophoresis in a discontinuous buffer system (DELECT) with 15% gels which are recommended for the separation of small oligonucleotides. The DELECT buffer Kit contains a rehydration buffer for dry gels and a cathode and an anode buffer

Table 2
Mixture for the Random Amplification of cDNA

10× Taq buffer	5 µL
25 m*M* $MgCl_2$	2 µL
10 m*M* dNTPs	10 µL
5 U/mL of Taq Long Plus	0.2 µL
ddH_2O	20.8 µL
Primer (18 n*M*)	2 µL
cDNA (ca. 0.25 ng/µL)	10 µL

Table 3
PCR Conditions for the Random Amplification

Phase	Temperature (°C)	Time	Cycles
	94	5 min	—
Denature	94	30 s	
Anneal	36	30 s	1
Extend	72	1 min	
Denature	94	30 s	
Anneal	50	30 s	35
Extend	72	1 min	
Cool	4	∞	—

for electrophoresis. The following descriptions are always for whole gels of 36 slots. The gels can also be divided according to the number of probes, but the volumes and running conditions then have to be adapted.

3.4.1 Sample Dilution

Four to six microliters of the sample should be diluted 1:1 in loading buffer for acrylamide gel electrophoresis.

3.4.2. Rehydration of the Dry Gel

For rehydration of the gels special chambers are available, but any plain chamber could be used.

1. Pipet 35 mL of rehydration solution in the chamber and lay the gel film — with the gel surface facing down — into the buffer, avoiding air bubbles.
2. Shake the gel slowly for 90 min at room temperature.
3. Remove excess buffer with an absorbant paper (e.g., Whatman paper), dry the sample wells, and wipe buffer off the gel surface with the edge of the filter paper until you can hear a “squeaking.”

Table 4
Running Conditions for a Whole 15% CleanGel

10 min	200 V	20 mA	10 W
60–120 min	375 V	30 mA	20 W
20–60 min	450 V	30 mA	20 W

3.4.3 Application of the Gel and the Electrode Wicks

1. Switch on the thermostatic circulator of the Multiphor II chamber or of a comparable electrophoresis system; adjust to 21°C.
2. Lay two electrode wicks into the compartments of the paper pool, or any comparable chamber.
3. Apply 20 mL of the electrode buffer to each wick (for the anode wick use the anode buffer and for the cathode wick the cathode buffer).
4. Apply a very thin layer of kerosine onto the cooling plate with a tissue paper, to ensure good contact with the gel.
5. Place the gel (surface up) on the center of the cooling plate: the side containing the wells must be oriented toward the cathode.
6. Place the cathodal strip onto the cathodal edge of the gel, and the anodal one onto the other edge. For the DELECT buffer system the strips should be ca. 8 mm away from the edges of the samples. Smooth out any air bubbles.

3.4.4. Sample Application and Gel Electrophoresis

1. Apply 10–15 µL of each sample to the sample wells. To determine the size of the amplifed products it would be worthwhile in addition to apply a molecular weight marker.
2. Clean palladium electrode wires with a wet tissue paper before each electrophoresis run.
3. Move electrodes so that they will rest on the outer edges of the electrode wicks. The running conditions for a whole 36-slot 15% gel are shown in **Table 4**. If gels are divided the voltage should be kept constant and the mA and W should be adjusted according to the gel size (e.g., the half for half-gels).

   Depending on the fragment size, the second step has to be varied in length. The larger the amplified oligonucleotides are, the longer this step has to run. The xylene cyanol runs at a molecular range of ca. 100 basepairs.
4. After running, gels have to be fixed in 10% acetic acid or 15% EtOH/5% acetic acid for at least 30 min. The fixation step can be prolonged overnight.

3.4.5. Silver Staining

1. After fixation, gels are washed 3 × 5 min in ddH_2O. Then the silver staining protocol shown in **Table 5** is performed (*see* also **Note 4**).

Gels can be stored at room temperature after they are shrink-wrapped into a strong cling film.

Table 5
Silver Staining Protocol of a Whole 15% 36-Slot CleanGel

Silver reaction	20–30 min	200 mL	0.1% $AgNO_3$ + 200 µL Formaldehyde (37%)
Washing	Thoroughly wash gel surface with ca. 250 mL of ddH_2O with a squeeze bottle		
Developing	2–5 min (visual control)	200 mL	2.5% Na_2CO_3 + 200 µL of Formaldehyde (37%) + 200 µL of Na thiosulfate (2%)
Stop/desilver	10 min	250 mL	2.0% (g/v) glycine
Impregnate	10 min	250 mL	10% Glycerol

Table 6
PCR Conditions for the Reamplification of Differentially Expressed Oligonucleotides

Phase	Temperature (°C)	Time (min)	No. of cycles
Denature	94	5	—
Denature	94	1	
Anneal	55	2	35
Extent	72	1	
Cool	4	∞	—

3.5. Reamplification of the differentially expressed oligonucleotides

1. The differentially expressed bands can be cut out of the acrylamide gel with a scalpel and then reduced to small pieces with a pipet tip.
2. From 50 to 100 µL of sterile ddH_2O is added and the probes then incubated for 30 min at 65°C and overnight at room temperature to elute the DNA out of the gel.
3. For the reamplification reaction, 10 µL of a 1:10 dilution of the eluted oligonucleotides are used. The PCR mixture is the same as in the amplification reaction. The conditions are shown in **Table 6**.
4. The PCR probes can be analyzed in a regular horizontal DNA electrophoresis with 1.5–2% agarose gels and then detected with an DNA intercalating stain (e.g., ethidium bromide). They also can be stored at –20°C.

The reamplification reaction could amplify multimers of the original oligonucleotide or other bands, which are artefacts from the elution of the acrylamide gel. For further cloning the fragments into a plasmid, only the interesting band should be eluted from an agarose gel by a convenient method. The cloned fragments should further be sequenced, because one eluted band from the random

amplification might contain some fragments of the same size, but with different sequences. This is based on the randomly amplified products in the PCR, which can result in oligonucleotides coincidentally of the same size. The differential expression of the DNA fragments has to be confirmed, i.e., by Northern blotting (*see* also **Note 5**).

3.6. DNA Gel Electrophoresis

1. Agarose gels are prepared with 1× TBE buffer and should have a percentage of 1.5–2.0% agarose.
2. DNA gel electrophoresis is done in a horizontal manner. The gels have to be covered with running buffer (1× TBE). DNA probes are diluted 1:5 (v/v) in sample buffer and loaded into the sample wells of the gels (depending on the concentration and the volume of the gel wells, 10–40 µL of the DNA probe can be taken). To determine the size of the products it would again be useful to apply additionally a molecular weight marker. The orientation of the electrodes has to be chosen so that the DNA can run in the direction of the anode (positively charged electrode), because DNA is negatively charged.

   The voltage should be set to 1–15 V/cm (distance between the electrodes). The tracking dyes incorporated into the sample buffer serve as markers for the progress of the run.
3. At the end, the DNA is stained with ethidium bromide (0.5 µg/mL) for 2–5 min in a staining bath (**Caution:** wear gloves, because ethidium bromide is carcinogenic). After staining, the gels are briefly washed in ddH_2O to remove the surplus ethidium bromide (again wear gloves and collect ethidium bromide waste separately). The DNA bands can be detected in UV light and can be documented with a suitable system (*see also* **Note 7**).

3.7 Purification of Nucleic Acids

3.7.1. Phenol/Chloroform Extraction

Phenol is also a carcinogen, so work under a fume hood. The extraction of aqueous nucleic acids with phenol-chloroform allows the denaturing and removal of proteins (eg., enzymes) from the probes.

1. PCR probes (45–40 µL, *see also* **Notes**) are diluted with ddH_2O to a final volume of 300–500 µL in a microfuge tube.
2. The same volume phenol/chloroform/isoamyl alcohol (25:24:1) is applied and probes are mixed vigorously on a vortex mixer.
3. To separate the aqueous—DNA containing—and the nonaqueous phase the probes are centrifuged at 12,000*g* for 2 min at room temperature.
4. The upper aqueous phase is transferred into a new microfuge tube and the same volume chloroform/isoamyl alcohol (24:1) is added.
5. The probe is mixed and centrifuged again. The upper phase is carried over in a new microfuge tube and the DNA is concentrated with the protocol for ethanol precipitation.

3.7.2 Ethanol precipitation

This protocol can be employed should the sample require concentrating and desalting.

1. To precipitate the DNA, the probe is treated with 1:10 vol 3 *M* NaAc, pH 4.8, and 2–3 vol of cold absolute ethanol. Then it is incubated at least 30 min at –20°C.
2. The precipitated nucleic acids are then centrifuged (12,000*g*, 15 min, 4°C), the supernatant discarded, and the pellet dried at 40–50°C with open cover to remove the surplus alcohol.
3. The DNA pellet can then be diluted in an adequate volume of ddH_2O (to be suitable for the cloning protocol take only 11.7 µL of ddH_2O).

3.5.3 DNA Gel extraction

To elute DNA fragments from the agarose gels many kits are available from several companies. One of the most convenient is the QIAquick Gel Extraction kit (Qiagen, Hilden).

The band of interest can be cut out of the gel under a UV transilluminator with a clean, sharp blade (wear glasses to protect your eyes). The fragment is now transferred into a clean microfuge tube and the extraction can be performed according to the protocol given.

3.8. Quantification by photometry

Absorption at 260 nm is measured in an appropriate photometer to determine the concentration of nucleic acids. An absorption of 1 corresponds to 50 µg/mL double-stranded DNA, 40 µg/mL single-stranded RNA, and 30 µg/mL single-stranded oligonucleotides.

The purity of the probes is determined with the quotient of the OD (optical density) at 260 nm:280 nm. This quotient should not be less than 1.8.

3.9. Cloning of PCR Fragments

3.9.1. Klenow Polymerase Treatment

The 5':3' polymerase activity and the 3':5' exonuclease activity of the Klenow fragment of the polymerase I from *E. coli* is used to blunt the ends of the PCR fragments.

1. The DNA pellet from the ethanol purification is diluted in 11.7 µL of ddH_2O. The following reagents are then added:
   1.5 µL of 10× Klenow-buffer
   1.8 µL of Klenow enzyme (0.8 U/µg of DNA)
   and the probe is incubated for 10 min at 37°C.
2. After that 1.2 µL of dNTPs (1.25 m*M* each nucleotide) are applied and a further incubation step at 37°C for 30–35 min is performed.
3. Heating at 70°C for 10 min denatures the Klenow fragment.

3.9.2. 5'-Phosphorylation of the Fragments

After the blunting of the fragments the 5'-ends have to be phosphorylated before they can be cloned into a plasmid vector. The enzyme T4-polynucleotide kinase (PNK) is employed for this purpose.

1. Add to the probe of 3.9.1:
   2 µL of ATP (10 m*M*)
   1 µL 10 × PNK buffer
   1 µL of PNK
   (final volume: 20 µL)
   An incubation step of 30 min at 37°C is performed.
2. At this stage the PNK can be inactivated for 10 min at 70°C and the probes can be stored at –20°C.
3. Before cloning the probes have to be purified by agarose gel electrophoresis. The fragments of interest can then be separated via the gel from additionally amplified fragments and primer dimers from the reamplification reaction.

3.9.3. Preparation of the Plasmid Vector

1. The plasmid vector (e.g., pUC18, pUC19, Bluescript, or any other vector) is digested with a blunt ending restriction enzyme that cuts the plasmid vector into the multiple cloning site (MCS; i.e., *Sma*I) (*see also* **Note 6**).

   The restriction conditions depend on the enzyme used and should be followed according the product information. The volume should be between 20 and 50 µL and 2 U of the enzyme per microgram DNA should be added. After the incubation the enzyme has to be inactivated. It is mostly possible to heat inactivate the restriction enzymes, but if this should not be the case (see the product information) an agarose gel purification or ethanol precipitation has to be done. The purification of the vector from the restriction enzyme and the buffers is also necessary prior to the following dephosphorylation reaction.
2. To avoid the religation of the vector in the ligation reaction, it has to be dephosphorylated with an alkaline phosphatase. The dephosphorylation reaction is done with 0.04 U alkaline phosphatase/µg DNA in 1× phosphatase buffer (provided by the manufacturer) at 37°C for 60 min. After the incubation the vector has to be purified in an agarose gel and eluted with a suitable method.

3.9.4. Ligation

For the ligation reaction there are many kits provided by several companies. We have had good experience with the Rapid Ligation Kit (Boehringer, Mannheim). This is a method for cloning blunt ended fragments into plasmid vectors. But of course any other ligation method, without using a kit, could be successful (*see* also **Notes 8** and **9**).

A ligation procedure without using a kit requires the following reaction mix:

Dephosphorylated, restricted plasmid (50 ng)/phosphorylated, blunt ended fragment in a ratio 1:3 to 1:5
1× Ligase buffer
1 µL of T4-ligase (5 U/µL)
(total volume 20–40 µL)

The probe can then be incubated at 4°C overnight or at 16–20°C for 3–4 h. The probes can be stored at –20°C.

3.9.5. Preparation of $CaCl_2$ competent cells for transformation

The *E. coli* cells are treated following the $CaCl_2$ procedure from Mandel and Higa ***(13)***.

1. 50 mL of LB medium are inoculated with 5 mL of an overnight preculture of the *E. coli* strain. The culture is then incubated at 37°C to an OD (600 nm) from 0.3 to 0.4.
2. The cells are centrifuged (2500*g*, 10 min, 4°C) and the pellet is resuspended in 100 mL of ice-cold 50 m*M* $CaCl_2$ solution.
3. The cells are centrifuged again (only 1800*g*, 4°C).
4. The pellet is resuspended carefully in 20 mL of $CaCl_2$ and incubated for 20 min on ice.
5. The cells are centrifuged again (1800*g*, 4°C) and the pellet is then carefully resuspended in 10 mL of ice-cold $CaCl_2$ solution. In addition, glycerine is added to a final concentration of 20%. The probes should be divided in aliquots of 200 µL in microfuge tubes and then they can be stored at –80°C for several months.

3.9.6. Transformation

1. Prior to transformation, the ligation reaction mixture is filled with ddH_2O to a final volume of 100 µL.
2. This mixture is added to a 200-µL aliquot of not completely thawed competent bacteria. The probe is then incubated 30 min on ice.
3. After that the bacteria are heat shocked for exactly 45 s at 42°C and 1 mL of 37°C warm LB medium is added at once.
4. The bacteria are incubated for 30–40 min. (They should have the possibility to divide once the plasmid incorporation is stabilized.)
5. Then aliquots of, e.g., 50, 100, and 200 µL are plated onto an LB agar plate with appropriate antibiotics or other selection markers (e.g., β-galactosidase).
6. The plates are incubated at 37°C overnight and can be stored at 4°C for a few days. Positive clones can be inoculated into LB medium with a suitable antibiotic and after an overnight incubation at 37°C (shake) the plasmids can be isolated for further control.

3.9.7. Plasmid Isolation by Alkaline Lysis

For plasmid isolation, many reaction kits are available that can result in extremely pure plasmids. These are required, for example, for sequencing but

for the control of plasmid transformation a simple protocol without using a kit, as described here, is enough.

1. From 1 to 3 mL of an overnight bacteria culture, transformed with a plasmid vector, are pelleted in a microfuge tube by centrifugation (full speed, 3 min).
2. The supernatant is discarded and the pellet is resuspended in 200 µL of cell resuspension solution by pipetting.
3. Next, 200 µL of cell lysis solution are added and mixed by inverting. The solution should clear almost immediately.
4. Then 200 µL of neutralization solution are added and the probes are again mixed by inverting (not by pipetting).
5. Spin down at 12,000*g* for 10 min.
6. Transfer supernatant to new tube. Discard pellet.
7. Add 1/10 of 1 volume of 3 *M* sodium acetate, pH 7.0 and 2.5 volumes of ETOH.
8. The probes are centrifuged at full speed for 5 min and the supernatant is discarded.
9. The pellet should be washed in 300 µL of 70% ethanol and finally dried with open cover at 40–50°C.
10. Then the pellet can be resuspended in 20–30 µL of ddH_2O and stored at –20°C.

The ligation can be checked by a restriction digestion of the plasmid with two enzymes that each cut at one end of the insertion site of the fragment in the multiple cloning site of the plasmid vector. In a common agarose gel electrophoresis the genuine positive plasmids can be detected.

3.10. Verification of the Differentially Amplified Fragments in Northern Blot Analysis

3.10.1. RNA Gel Electrophoresis with a Denaturating Formaldehyde Gel

1. To prepare a 1–1.5% formaldehyde gel add 1–1.5 g of agarose into 73 mL of ddH_2O. The agarose is dissolved by boiling and then cooled in a water bath to 50°C. The volume should be restored with ddH_2O to 73 mL. Then 10 mL of 10× MOPS buffer and 17 mL of formaldehyde (37%) are added and the solution is mixed immediately and placed into a gel track. The fully polymerized gel can be applied into a horizontal gel electrophoresis tray and covered with RNA running buffer (1× MOPS buffer).
2. From 2 to 10 µg RNA is denatured 5 min at 65°C in the following mixture:
   RNA in a final volume of 6 µL (diluted in RNase-free ddH_2O)
   12.5 µL of formamide (deionized)
   2.5 µL of 10× MOPS
   4 µL of formaldehyde (37%)
3. The probe is then chilled on ice and 1:10 sample buffer is added. The probes are applied to the gel. The running conditions can be varied from 100 to 120 V for 3 h or overnight at 20 V.
4. The RNA run can be documented after ethidium bromide staining as for DNA.

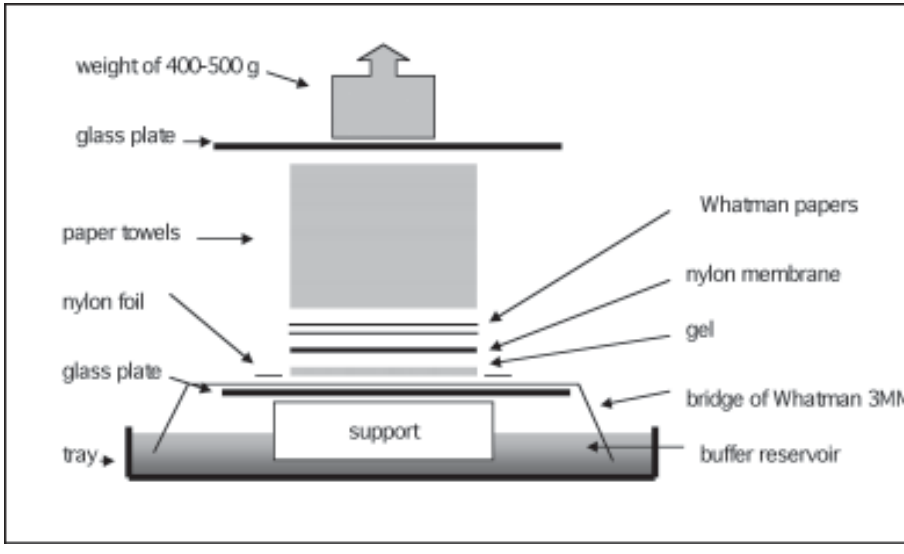

Fig. 1. Northern blotting setup.

3.10.2. Northern Blotting

Here we describe a common method for Northern blotting that is performed with the ordinary capillary flow system. As RNA is electrophoresed in the denaturing system the gel does not need any further denaturation or neutralization.

The RNA is transferred from the gel onto a positively loaded nylon membrane in a chamber construction shown in **Fig. 1**.

The blotting setup is constructed in the following manner:

1. Set up the transfer support into the tray and place a wider glass plate onto the support. Put two pieces of Whatman 3MM paper on the glass plate so that they hang up into the tray. Fill the reservoir with transfer buffer (20× SSC) and wet also the Whatman 3MM paper (avoid air bubbles).
2. Cut a piece of the nylon membrane of the same size as the gel (handle the filter at the edges only!) and wet the filter for 5 min in the transfer buffer. Cut off the lower right corner of the filter (so as not to lose orientation during the procedure).
3. Flood the two Whatman 3MM papers on the glass plate with transfer buffer and place the gel onto the papers. Squeeze out air bubbles by rolling with an RNase-free pipet over the gel. Cut a piece of the size of the gel out of the middle of a piece of common cling film and apply this around the gel. This will ensure that the liquid flow from the reservoir is transferred through the gel.
4. Apply the nylon membrane carefully directly onto the gel and again squeeze out air bubbles as described previously.

5. Wet two or three pieces of Whatman 3MM paper of the same size as the gel and place them onto the membrane. Cut paper towels to the same size and put them onto the Whatman papers to form a stack 7–8 cm high.
6. Apply a glass plate onto the top and a weight of 400–500 g onto it to ensure good contact during the transfer.
7. The RNA is transferred overnight from the gel to the nylon membrane at room temperature.
8. After blotting, the RNA is fixed by incubating the membrane for 5 min onto a Whatman paper that is soaked with 0.05 *M* NaOH (RNA site up). Before storing the filter at 4°C in cling film it should be briefly washed with 2× SSC solution.

3.10.3. Probe Hybridization and Labeling

Here we describe a method which uses the standard megaprime protocol from the Megaprime™ labeling kit (Amersham) (*see also* **Notes 10** and **11**).

1. From 2.5 to 25 ng of the DNA are dissolved in 10 µL of ddH_2O. Twenty-five nanograms of the template DNA are then applied into a microfuge tube and 5 µL of the random primer are added.
2. The DNA is denatured at 95–100°C for 5 min in a boiling water bath.
3. The probe is collected by a short centrifugation step and then kept at room temperature.
4. To label the DNA template the following components are added:
   Unlabeled dNTPs 4 µL each of dCTP, dTTP, dGTP; 2.5 m*M*
   5 µL of reaction buffer
   Radiolabeled dATP
   5 µL of [^{32}P]dATP (specific activity; 3000 Ci/mmol]
   2 µL of DNA polymerase I (at –20°C until needed)
   11 µL of ddH_2O
5. The probe is mixed gently and incubated at 37°C for 10–30 min.
6. The reaction is stopped by heating the probe at 95°C for 5 min. The surplus [^{32}P]ATP can be removed on a Sephadex G50 column.
7. The probe can now be stored at –20°C for 2–3 d. Further storage should be avoided because of the short half-life of ^{32}P.
8. Prior to hybridization, the membrane is incubated for at least 15 min at 65°C or overnight in a prehybridization box with prehybridization solution.
9. For the hybridization, the labeled DNA probe is denatured by heating to 95–100°C for 5 min, and then directly chilled on ice. The labeled DNA probe can now be added into the prehybridization solution at a concentration of 1×10^6 cpm/mL and incubated at 55–65°C for at least 12 h (the higher the hybridization temperature chosen, the higher the stringency of the hybridization).
10. After hybridization, the filters are washed by incubating for 5 min at 65°C. This procedure is repeated if necessary and checked with a hand monitor for radioactive detection (Geiger counter). The membrane is now wrapped in a nylon filter (e.g., Saran Wrap) and the hybridization is detected by autoradiography.

Table 7
Primer Sequence of a β-actin gene that Gives Bands of Different Sizes for cDNA and gDNA

Target	Primer sequence (5' → 3')	Product (bp)
β-Actin sense	GGC GGC ACC ACC ATG TAC CCT	202 (312)
β-Actin antisense	AGG GGC CGG ACT CGT CAT ACT	

4. Notes

1. Working with RNA demands some special precautions, as RNA is rapidly degraded in the presence of the very stable enzyme RNase. The possibility of contamination with RNase should be minimized. Therefore always wear gloves when preparing or handling RNA probes. The laboratory equipment for RNA procedures should be separated if possible or sterilized in an autoclave before use. Equipment that cannot be autoclaved should be treated with 0.5 *M* NaOH or 70% ethanol. RNase can be inactivated with DEPC (**CAUTION:** carcinogen; use a fume hood). DEPC should be added to every solution in a final concentration of 0.1% (but not to solutions that contain Tris) and then incubated overnight in a fume hood with cover open, or if possible autoclaved for 20 min.

   For RNA preparation, a method for isolating cytoplasmic RNA is useful, to avoid amplification of incompletely spliced RNA in the reverse transcription.

   Genomic DNA contamination is one of the major causes of false-positive results. Although most kits guarantee preparation of DNA-free RNA, it would be useful to check samples for possible DNA contaminations. This could be done by an RT-PCR reaction with a primer to genes usually expressed that gives different products with mRNA and gDNA (e.g., **Table 7**).

   In the RNA gel electrophoresis, the formamide that inhibits the RNases can be reduced by half if the additional volume is needed.
2. It is useful to confirm the success of the reverse transcriptase reaction in a simple common PCR reaction with primers to genes usually expressed in the material of interest.
3. The use of too much cDNA in the amplification reaction, or in the reamplification, can have a bad effect on the reaction. In the worst case, there may be no amplification of the DNA at all.

   The various bands of the acrylamide gel should be cut out as small as possible, to avoid contamination with neighboring bands.
4. Silver staining is a very sensitive method for oligonucleotide detection. To be able to differentiate varying bands, the probe dilution in the acrylamide gel electrophoresis has to be optimal. Our experience has shown that 5–8 μL from the amplification reaction are enough to detect clear bands.

   The developing reaction in silver staining can happen very quickly. To avoid the gel becoming too dark it is useful to prepare the stop/desilver solution before-

hand, so that the gel can be transferred rapidly into the stop bath once the reaction has progressed far enough.

5. Before cloning, 5–10 µL of the reamplified fragment should be checked in an agarose gel and the DNA content should be measured. The other 40–45 µL can then be treated with the chloroform phenol extraction protocol.
6. The enzyme content of the restriction probe should not be more than 1:10 of the entire volume, because the enzymes are diluted in a very highly concentrated glycerol solution that inhibits the enzyme activity.
7. Before running an agarose gel, incubate the isolated plasmid vector with 1 U of RNase/20 µL of probe for 10 min at 37°C to remove RNA contamination.
8. Avoid too much pipetting after the ligase is added, because this enzyme is sheared very easily and thereby loses its activity.
9. A satisfactory and very uncomplicated ligation kit is provided by Boehringer Mannheim. The ligation protocol can be followed as described but the incubation time can be extended to 30–45 min instead of the 5 min given in the manufacturer's directions for use.
10. The protocol that is described uses a laboratory equipped for radioactive methods! It would be useful to prepare the radioactively labeled probes in microfuge tubes that have a cover with a screw thread to minimize risk of aerosols upon opening the tubes after heating.

    The polymerase should be added last, because the reaction immediately starts when the enzyme is applied. If one dNTP is missed, every amplification will stop at the complementary nucleotide of the missing nucleotide.
11. The membrane should not be washed for too extended a period, because the labeled probes would be washed away. After that the membrane can be hybridized again with another probe. This process can be repeated up to 4–5 times.

References

1. Linskens, M. H., Feng, J., Andrews, W. H., Enlow, B. E., Saati, S. M., Tonkin, L. A., Funk, W. D., and Villeponteau, B. (1995) Cataloging altered gene expression in young and senescent cells using enhanced differential display. *Nucleic Acids Res.* **25,** 3244–3251.
2. Swisshelm, K., Ryan, K., Tsuchiya, K., and Sager, R. (1995) Enhanced expression of an insulin growth factor-like binding protein (mac 25) in senescent human mammary epithelial cells and induced expression with retinoic acid. *Proc. Natl. Acad. Sci. USA* **92,** 4472–4476.
3. Salehi, M., Hodkins, M. A., Merry, B. J., and Goyns, M. H. (1996) Age-related changes in gene expression in the brain revealed by differential display. *Experientia* **15,** 888–891.
4. Wu, H. C. and Lee, E. H. (1997) Identification of a rat brain gene associated with aging by PCR differential display method. *J. Mol. Neurosci.* **8,** 13–18.
5. Liang, P. and Pardee, A. B. (1992) Differential display of eucaryotic messenger RNA by means of the polymerase chain reaction. *Science* **257,** 967–971.

6. Bauer, D., Müller, H., Reich, J., Riedel, H., Ahrenkiel, V., Warthoe, P., and Strauss, M. (1993) Identification of differentially expressed mRNA species by an improved display technique (DDRT-PCR) *Nucleic Acids Res.* **21,** 4272–4280.
7. Liang, P., Bauer, D., Averboukh, L., Warthoe, P., Rohrwild, M., Müller, H., Strauss, M., and Pardee, A. B. (1995) Analysis of altered gene expression by differential display. *Methods Enzymol.* **254,** 304–321.
8. Welsh, J., Chada, K., Datal, S. S., Cheng, R., Ralph, D., and McClelland, M. (1992) Arbitrary primed PCR fingerprinting of RNA. *Nucleic Acids Res.* **20,** 4965–4970.
9. Welsh, J., Rampino, N., McClelland, M., and Perucho, M. (1995) Nucleic acid fingerprinting by PCR-based methods: applications to problems in aging and mutagenesis. *Mutat. Res.* **338,** 215–229.
10. McClelland, M. and Welsh, J. (1994) RNA fingerprinting by arbitrary primed PCR. *PCR Methods Appl.* **4,** 66–81.
11. Liang, P., Averboukh, L., and Pardee, A. B. (1994) Method of differential display. *Methods Mol. Genet.* **5,** 3–16.
12. Sambrook, F., Fritsch, E. F., and Maniatis, T. (1989) *Molecular Cloning: A Laboratory Manual*, 2nd ed., Cold Spring Harbor Laboratory Press, Cold Spring Harbor, New York.
13. Mandel, M. and Higa, A. (1970) Calcium dependent bacteriophage DNA infection. *J. Mol. Biol.* **53,** 159–162.
14. Wei, Q., Xu, X., Cheng, L., Legerski, R. J., and Ali-Osman, F. (1995) Simultaneous amplification of four DNA repair genes and β-actin in human lymphocytes by multiplex reverse transcriptase PCR. *Cancer Res.* **55,** 5025–5029.

8

Xenobiotic-Metabolizing Enzyme Systems and Aging

Christopher R. Barnett and Costas Ioannides

1. Introduction

The human body is continuously exposed to a wide array of structurally diverse chemicals. Such exposure occurs even at the fetal stage as almost all chemicals that are present in the mother's blood can readily cross the placenta and reach the fetus. Some of these chemicals are ingested voluntarily, for example, medicines and food additives, but the vast majority are taken involuntarily, as environmental contaminants present in the air or in the occupational environment. Undoubtedly, the most important source of such chemicals is the diet, and many dietary constituents have been shown to induce many forms of toxicity including cancer ***(1)***. Exposure to chemicals is thus inevitable and unavoidable. The body cannot exploit these chemicals either to generate energy or transform them to building blocks and consequently its response is to rid itself of their presence. This chapter discusses the role of drug-metabolizing enzyme systems in this process and the effects of age. The measurement of drug-metabolizing activities is of increasing importance in the safety evaluation of drugs in humans. This chapter describes the use of alkylphenoxazone derivatives for investigating selected activities of drug-metabolizing enzymes.

Chemicals that reach the systemic circulation and are distributed throughout the body are generally lipophilic, a property that allows them to traverse the various cellular membranes. Such lipophilic chemicals are also difficult to excrete through the kidney and bile. Consequently, to facilitate their elimination, the body converts them to hydrophilic metabolites, which are much easier to excrete. Furthermore, such metabolism terminates any biological activity that may be manifested by these chemicals, as the products of metabolism are biologically inactive, being unable to interact with the receptors for which the

From: *Methods in Molecular Medicine*, Vol. 38: *Aging Methods and Protocols*
Edited by: Y. A. Barnett and C. R. Barnett

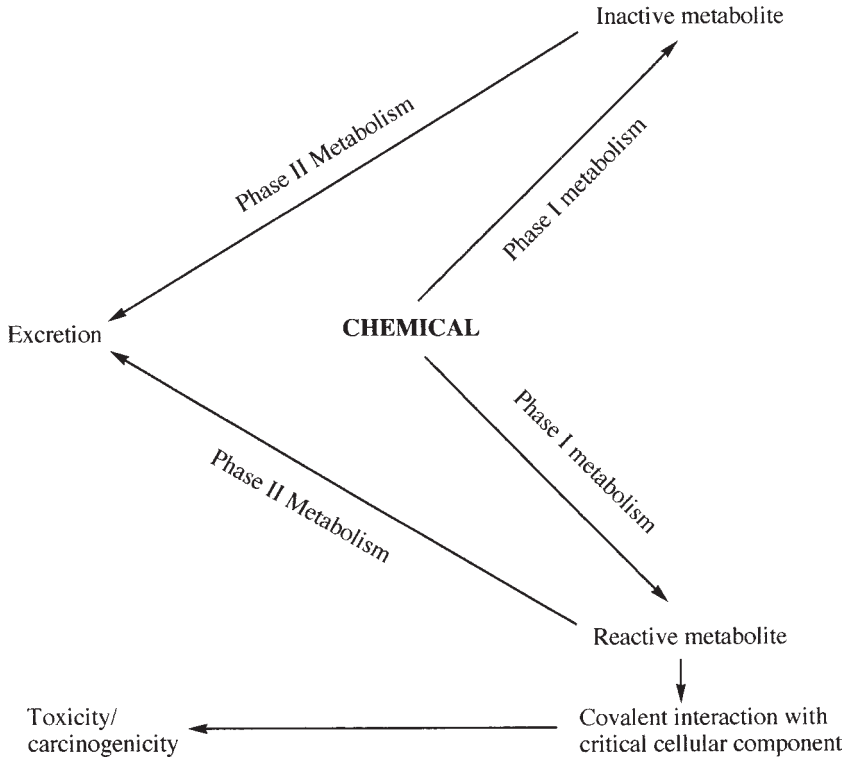

Fig. 1. Metabolic activation of chemicals.

parent compounds often have high affinity. The metabolism of chemicals occurs through an enzymic process that involves a number of enzyme systems present in many tissues, the highest concentration being encountered in the liver. The metabolism of chemicals is generally achieved in two phases. Phase I involves primarily the incorporation of an atom of oxygen to the substrate, producing a more hydrophilic, and in most cases biologically inactive, metabolite that can now participate in Phase II metabolism. During Phase II metabolism, the newly generated metabolite is conjugated with endogenous substrates, such as sulfate and glucuronide, to form highly hydrophilic products that can now be very readily eliminated.

1.1. Metabolic Activation of Chemicals

Although metabolism of chemicals is essentially a deactivation process, with certain chemicals one or more metabolic pathways may lead to the generation of reactive intermediates, a phenomenon known as metabolic activation or bioactivation (**Fig. 1**). Because of their increased chemical reactivity,

these intermediates interact covalently with vital cellular components, leading to the manifestation of toxicity ***(2,3)***. For example, most chemical carcinogens are metabolized to reactive species that interact with DNA to induce mutations that may lead to the formation of tumors. Generally, the activation pathways are usually minor routes of metabolism and the body is well equipped to deal with the limited amounts of reactive intermediates that are produced. This defense mechanism proceeds through conjugation of the reactive intermediates with the endogenous tripeptide glutathione, the glutathione conjugates being excreted in the urine and feces following additional processing that occurs principally in the kidney and intestine. It is therefore not surprising that the cellular concentration of glutathione in the hepatocyte, the major site of the bioactivation of chemicals, is high (about 10 m*M*). Depletion of the tissue stores of glutathione, whether by chemicals or as a consequence of poor nutrition, can potentiate markedly chemical toxicity. The toxicity of the mild analgesic and antipyretic drug paracetamol (acetaminophen) is markedly exacerbated if the animals have been depleted of glutathione as a result of inadequate nutrition ***(4)***.

It is evident that a chemical is subject to metabolism through a number of pathways, most of which will result in deactivation. Certain routes of metabolism, however, will produce deleterious intermediates that are themselves subject to deactivation through metabolism. Clearly, the amount of reactive intermediates available for interaction with cellular components, and hence the degree of toxicity, is largely dependent on the competing pathways of activation and deactivation. If an animal species favors the activation pathways of a chemical it will be susceptible to its toxicity whereas if deactivation is favored it will be resistant. 2-Aceylaminofluorene is a carcinogen that undergoes *N*-hydroxylation to generate the reactive, carcinogenic intermediates. The guinea pig is unable to catalyze this reaction and consequently it is very resistant to the carcinogenicity of this chemical ***(5)***. Clearly, toxicity is not simply a consequence of the intrinsic molecular structure and physicochemical properties of the chemical, but is also largely dependent on the nature and level of the enzymes present in the living organism at the time of exposure. Normally, the activation pathway is a minor route of metabolism, but under certain circumstances it may assume greater importance. Such a situation arises when the deactivation pathways are saturated, as a result of intake of high doses of the chemical or when the activation pathway is selectively induced, for example, as a result of prior exposure to chemicals. Under such circumstances, the production of reactive intermediates is stimulated, overwhelming the deactivation pathways, making an interaction with cellular constituents, and the ensuing toxicity, more likely. Paracetamol is a very safe drug, the activation pathway being a very minor metabolic route. In alcoholics, as a result of alcohol intake,

this pathway is more active so that they may suffer hepatotoxicity even when consuming therapeutic doses of the drug *(6)*.

1.2. The Cytochrome P450-Dependent Mixed-Function Oxidase System

Many enzyme systems participate in the metabolism of chemicals, both Phase I and Phase II. In Phase I metabolism, undoubtedly the most important are the cytochrome P450-dependent mixed-function oxidases, a ubiquitous enzyme system found in almost every tissue, the highest concentration being encountered in the liver *(7)*. It is a very versatile enzyme system, capable of metabolizing structurally very diverse chemicals of markedly different molecular shape and size. There are not many chemicals that find their way in the human body and are not metabolized, at least to a small extent, by the cytochrome P450 system and many are metabolized exclusively by this system. It has evolved to deal with the increasing number of xenobiotics to which humans are exposed. In addition to metabolizing xenobiotics, this enzyme system also makes a major a contribution to the metabolism of endogenous substrates such as steroid hormones, vitamins, fatty acids, and prostaglandins.

The cytochrome P450 system comprises an electron transport chain consisting of the flavoprotein cytochrome P450 reductase and the hemoprotein cytochrome P450, which acts as a terminal oxidase. It catalyzes the incorporation of one atom of molecular oxygen to the substrate while the second atom forms water. Cytochromes P450 achieve their broad substrate specificity by existing as a superfamily of proteins, divided into families on the basis of their structural similarity. Each family may be subdivided into subfamilies that may contain one or more proteins. For example, the cytochrome P450 family one (CYP1) comprises two subfamilies, namely A (CYP1A) and B (CYP1B). The CYP1A subfamily consists of two proteins (isoforms), CYP1A1 and CYP1A2. Only a single protein belongs to the other subfamily (CYP1B1). Of the cytochrome P450 families, the most important contributors to xenobiotic metabolism are CYP1–CYP3, and the major characteristics of these are summarized in **Table 1**. The CYP1 family appears to be the most important in the bioactivation of chemicals *(8,9)*.

1.3. Regulation of Cytochromes P450

It has long been appreciated that humans differ markedly in the way they respond to the same chemical exposure. Dramatic interindividual differences have been noted in the blood levels of drugs following the intake of the same dose, which could account for the fact that they experienced different pharmacological effects, a number developing adverse effects commensurate with overdosage. It has now been recognized that individuals may metabolize the same drug at different rates, reflecting the activity of their drug-metabolizing enzymes,

Table 1
Principal Characteristics of the Xenobiotic-Metabolizing Cytochrome P450 Enzymes

Family	Subfamily	Typical drug substrate	Role in bioactivation	Inducibility by chemicals
CYP1	A	Theophylline	Very extensive	Very high
	B	Theophylline	Very extensive	High
CYP2	A	Propranolol	Limited	Modest
	B	Warfarin	Limited	High
	C	Tolbutamide	Poor	Modest
	D	Debrisoquine	Poor	Not inducible
	E	Chlorzoxazone	Extensive	High
CYP3	A	Erythromycin	Limited	High

particularly the cytochromes P450. Many factors are responsible for the marked interindividual drug-metabolizing activity, including genetic background, nutritional status, presence of disease, and previous exposure to other xenobiotics.

Undoubtedly one of the factors that govern cytochrome P450 activity is genetic makeup. Indeed, it was established some two decades ago that cytochrome P450 isoforms may be polymorphically expressed. This realization followed observations that some persons, about 5–10% of Europeans, displayed exaggerated responses after the intake of therapeutic doses of the antihypertensive drug debrisoquine. This drug is normally deactivated through 4-hydroxylation but the poor metabolizers are unable to carry out this pathway because they lack a functioning CYP2D6, the cytochrome P450 enzyme catalyzing this reaction ***(10)***.

The expression of cytochrome P450 activity is also regulated by the levels of endogenous hormones as well by disease and especially previous exposure to other chemicals, capable of inhibiting or inducing one or more cytochrome P450 proteins. A number of studies established the importance of hormones such as androgens, growth hormone, and thyroid hormone in the regulation of cytochrome P450 enzyme ***(11)***. Changes in the levels and patterns of excretion of hormones may result in selective modulation of cytochrome P450 proteins. For example, hyposecretion of growth hormone has been implicated in the alterations in the hepatic profile of cytochromes P450 observed in animals with insulin-dependent diabetes mellitus ***(12)***.

Exposure to environmental chemicals, as well as many drugs, can up-regulate cytochrome P450 proteins in the liver and other tissues, so that chemicals ingested after induction has occurred will be more extensively metabolized if they rely on the induced enzymes for their metabolism. Human cytochrome P450 proteins have been shown to be induced by alcohol; consumption of cru-

ciferous vegetables or of charcoal-broiled beef; smoking; and intake of drugs such as omeprazole, rifampicin, and phenobarbitone. Cytochrome P450 proteins can also be down-regulated following exposure to exogenous chemicals so that the metabolism of any subsequently ingested chemicals will be suppressed if they rely on the inhibited enzymes for their metabolism. This is very much highlighted in the recently recognized interaction between normal grapefruit juice and a number of drugs including dihydropyridine calcium channel blockers such as felodipine, nisoldipine, and nifedipine as well as of other drugs such as quinidine, midazolam, terfenadine, and cyclosporine ***(13)***. Simultaneous consumption of grapefruit juice with these drugs resulted in higher plasma levels than anticipated, leading to increased adverse effects. These drugs are extensively metabolized in the intestine by CYP3A4, which is effectively inhibited by grapefruit juice. Chemicals can have a differential effect on the expression of individual cytochromes P450. For example, the dietary chemical diallyl sulfide, a naturally occurring chemical in garlic, down-regulates CYP2E1 but up-regulates CYP2B in the liver of rats ***(14)***.

Cytochrome P450 activity is also influenced by the presence of disease. Again the effects are selective, in that only certain isoforms are influenced, with some being depressed whereas others are stimulated. Hepatic disease such as hepatocellular carcinoma has been shown to perturb the profile of cytochromes P450 in patients with cirrhosis and hepatocellular carcinoma ***(15)***. In these situations the disease affects the liver itself, but hepatic cytochrome P450 levels may also be modulated in diseases where the liver is not the primary target of disease such as insulin-dependent diabetes mellitus ***(12)***.

1.4. Drug Metabolism in the Aged

Although in animal studies drug-metabolizing activity has been reported to diminish in the old, the limited studies conducted in humans do not appear to support the view that age is an important determinant of drug metabolism activity. Although a number of drugs are poorly eliminated in the elderly, this does not necessarily reflect reduced metabolic, including cytochrome P450, activity. They may be secondary to the normal physiological changes that accompany old age such as decreased renal capacity to excrete drugs and their metabolites, reduced liver blood flow, decrease in liver mass, and changes in plasma protein levels, one or all of which may account for the impaired drug elimination. Both renal glomerular filtration and tubular function are altered in the aged without any signs of kidney dysfunction. Blood flow in the old may be as little as half of that of the adult, affecting particularly the elimination of drugs having a high extraction ratio, which is defined as the difference in the concentration of drug entering and coming out of the liver divided by the concentration of drug entering the liver. Plasma levels of albumin, the major pro-

tein to which drugs bind, decrease in the aged, presumably the consequence of reduced synthesis, leading to lower protein binding.

In animal studies, it was repeatedly shown that the metabolism of many xenobiotics declines in old age, resulting in prolongation of the pharmacological effect of drugs ***(16,17)***. However, evidence for reduced capacity in the metabolism of drugs through cytochrome P450 catalyzed pathways is lacking ***(18)***. It is also feasible that the various cytochrome P450 proteins respond differently to the onset of old age, but this remains to be investigated. In studies carried out in male rats, aged between 1 wk and 2 yr, cytochrome P450 activity was investigated by determining the hydroxylation of testosterone at different positions and was complemented by immunological determination of the apoprotein levels ***(19)***. It was evident that age-dependent changes differed among the cytochrome P450 enzymes studied. For example, hepatic levels of CYP2C11 disappeared in old age whereas CYP2A1 levels increased and those of CYP2E1 were unaffected.

The recent availability of in vivo probes displaying selectivity for specific cytochrome P450 forms has made it possible to assess the effect of age on cytochrome P450 expression in humans. The *N*-demethylation of erythromycin, a diagnostic probe for CYP3A4, the major cytochrome P450 enzyme in the human liver, was determined by measuring the amount of carbon dioxide exhaled. No difference was detectable between healthy aged volunteers (age ranging between 70 and 88 yr) in comparison to younger adults (age ranging between 20 and 60), showing that the expression of CYP3A is not affected by age in humans ***(20)***. Similarly, the expression of CYP2E1 was constant in humans aged between 30 and 75 yr of age ***(21)***. In more recent studies, employing as probes lignocaine (CYP3A4) and coumarin (CYP2A6), a decrease was reported in the levels of these drugs with increasing age ***(22)***. In these studies the authors compared healthy young volunteers (<25 yr) with healthy elderly volunteers (>65 yr). Similarly, in recent extensive studies, the half-life of antipyrine, a drug whose metabolism involves a number of cytochrome P450 proteins, increased in the elderly whereas its clearance decreased ***(23)***. Clearly, the effect of age on individual cytochrome P450 enzymes is far from being understood, and it is only now that such studies are being undertaken. It must be emphasized that the old consume a disproportionate number of drugs compared with other subpopulations and an understanding of their ability to handle drugs will lead to more effective treatment.

1.5. Measurement of Cytochrome P450 Activities in Human Liver Using Alkoxyresorufins

In 1974, Burke and Mayer ***(24)*** demonstrated that an alkoxyphenoxazone derivative, ethoxyresorufin, could be metabolized by CYP1A1 with a high

specificity. This specificity has been demonstrated for many animals species, including humans. Furthermore, the use of methoxyresorufin and pentoxyresorufin derivatives allow the measurement of CYP1A2 and CYP2B proteins with high selectivity.

The metabolism of the alklyphenoxazone derivatives can be measured using microsomal or whole cell protein ***(26)***. Both methods are comparable except for the inclusion of dicoumarol in the whole cell protein method to prevent the cytosolic reduction of resorufin to a nonfluorescent molecule by NAD(P)H oxidoreductase.

1.6. Method for the Measurement of Ethoxy-, Methoxy-, and Pentoxyresorufin Dealkylation Using Human Liver Samples

This method can be used for measurement of CYP1A1 (ethoxyresorufin), CYP1A2 (methoxyresorufin), and CYP2B (pentoxyresorufin) activities in microsomal protein fractions or cell homogenates from primary hepatocytes or cultured cells. It should be noted that ethyoxyresorufin may be deethylated to some extent also by CYP1A2. In human liver, expression of CYP1A1 is very low and ethoxyresorufin O-deethylase activity is largely attributable to CYP1A2, although a small contribution from other subfamilies such as CYP2C cannot be excluded.

2. Materials

2.1. Preparation of Hepatic Subcellular Fractions

1. Potter–Elvehjem glass–Teflon homogenizer (BDH, Poole, Dorset).
2. 1.15% (w/v) KCl, 4°C.
3. Refrigerated centrifuge capable of producing 9000*g*, ultracentrifuge.

2.2. Measurement of Cytochrome P450 Activities Using Alkoxyresorufins

For the direct measurement of alkoxyresorufin *O*-dealkylase activity the method of Burke and Mayer ***(24)*** can be used.

1. Pentoxy-, ethoxy- and methoxyresorufin as well as resorufin can be obtained from Molecular Probes, Eugene, OR, USA. Alkoxyresorufins are dissolved in dimethylformamide (Sigma Chemical, Dorset, UK) to provide stock concentrations of 0.53 m*M* ethoxyresorufin, 1 m*M* pentoxyresorufin, and 0.53 m*M* methoxyresorufin. These solutions can be stored at –20°C until required and should be maintained in the dark at all times. Resorufin is also dissolved in dimethylformamide to produce a 0.1 m*M* stock solution. This fluorescent compound can be stored at –20°C in the dark until required.
2. Tris-HCl buffer (0.1 *M*, pH 7.8) prepared by dissolving 0.1 moles of Tris base (Sigma Chemical, Dorset, UK) in 850 mL of distilled water. Using a calibrated

pH meter the pH of the buffer is adjusted to 7.8 using 3 *M* HCl. The buffer is transferred to a 1-L volumetric flask and made up to the 1-L mark with distilled water. The pH of the buffer solution is confirmed at pH 7.8 using a pH meter.

3. NADPH (50 m*M*, Sigma Chemical, Dorset, UK) is dissolved in 1% (w/v) sodium hydrogen carbonate and kept at 4°C until required. This solution is made fresh prior to performing the assays.
4. Dicoumarol (20 m*M*, Sigma Chemical, Dorset, UK) is prepared by dissolving dicoumarol in 0.1 *M* Tris-HCl buffer, pH 7.8.
5. Spectrofluorometer with excitation wavelength of 510nm and emission wavelength of 586 nm with excitation and emission slit widths of 10nm and 2.5nm, respectively.
6. Positive controls. Samples of rodent liver microsomes that have high activity for ethoxyresorufin, methoxyresorufin, or pentoxyresorufin can be obtained from Xentox Limited, Northern Ireland, UK.

3. Methods

3.1. Preparation of Hepatic Subcellular Fractions

Microsomal fractions are prepared according to the method of Ioannides and Parke ***(26)***.

1. Liver sample is weighed and and transferred to a glass beaker with volume capacity at least 5× that of the weight of the liver sample, for example, 10 g of liver in a 50-mL beaker.
2. The sample is scissor-minced and transferred to the Potter–Elvehjem homogenizer together with 3× the liver weight of 1.15% KCl (4°C).
3. Homogenize the sample using several up-and-down strokes of the homogenizer.
4. The homogenate should be maintained at 4°C during the homogenization process using an ice jacket (metal can filled with ice surrounding the glass homogenizer).
5. The homogenate is transferred to a measuring cylinder and made up to 4× the initial sample weight with 1.15% (w/v) KCl, for example, 10 g of liver sample made up to 40 mL of final homogenate volume with 1.15% (w/v) KCl. This is a 25% w/v liver homogenate.
6. The homogenate is transferred to centrifuge tubes and the tubes balanced for centrifugation at 9000*g* for 20 min.
7. Following centrifugation at 9000*g* for 20 min in a refrigerated (4°C) centrifuge the supernatant (S9) is decanted and may be stored at –70°C for up to 6 mo.
8. For microsomal preparation the S9 is transferred to ultracentrifuge tubes and balanced for ultracentrifugation at 105,000*g* for 60 min at 4°C.
9. The supernatant (cytosolic fraction) is discarded and the pellet resuspendend in a volume of 1.15% w/v KCl equal to the volume of S9 initially placed into the ultracentrifugation tube.
10. The microsomal suspension should be kept on ice and used the same day.

3.2. Measurement of Alkoxyresorufin Metabolism

1. The reaction is carried out at 37°C. To a 3-mL fluorimetric cuvet (a 1.5-mL microfluorimetric cuvet may be used with appropriate adjustment of volumes given below) add the following reagents:
   1.935 mL of 0.1 *M* Tris-HCl buffer, pH 7.8, prewarmed to 37°C
   50 µL of microsomal suspension/cell homogenate*
   3 µL of 0.53 m*M* ethoxyresorufin
   or
   5 µL of 0.53 methoxyresorufin
   or
   5 µL of 1 m*M* pentoxyresorufin
   *If using cell homogenate (S9) then dicourmarol should be added to give a final concentration of 10 µ*M* (substitute 10 µL of Tris buffer for 10 µL of dicoumarol stock solution).
2. The cuvet is introduced into the spectrofluorometer and a baseline recorded prior to initiation of the reaction with 10 µL of NADPH solution.
3. The reaction is monitored continuously until a measurable gradient is obtained and an initial rate of reaction can be determined.
4. Resorufin production from the alkoxyresorufin substrate can be calculated using the standard resorufin solution.
5. A blank is prepared by replacing the microsomes or cell homogenate with 50 µL of Tris-buffer.
6. Following the establishment of baseline fluorescence, at least three 10-µL samples of the standard resorufin are introduced into the cuvet, noting the increase in fluorescence after each addition.

3.3. Example Calculation

1. Ten microliters of 0.1 m*M* resorufin caused an increase of 15.5 fluorescence units.
2. Fifty microliters of sample A caused an increase of 1.2 fluorescence units per minute.
3. Therefore 1 mL of sample A would cause $1000/50 \times 1.2$ unit increase per minute or 24 units per minute.
4. Ten microliters of 0.1 m*M* resorufin is equal to 1nmole of resorufin, therefore 1 nmol of resorufin will cause a 15.5 unit increase in fluorescence.
5. As such 1 mL of sample A produced 24/15.5 nmol resorufin per minute = 1.5 nmol/min/mL.
6. Having established the protein concentration in the microsomal suspension/cell homogenate, the activity can be expressed as nmol/min/mg of protein.

Many spectrofluorometers will perform these calculations directly following the calibration step with the resorufin standard.

4. Notes

1. A baseline cannot be established as the fluorescence is increasing at a steady rate. The alkoxyresorufin substrate may have become contaminated with NADPH or S9. Make up fresh substrate and ensure that a separate pipet is used for each addition.

2. No reaction appears to be occurring. Check reaction system using positive controls. Check fluorimeter settings. Ensure that buffer is warmed to 37°C.
3. No reaction seems to be occurring. Increase amount of microsomal or S9 suspension added and reassay.

References

1. Ioannides, C., ed. (1998) *Nutrition and Chemical Toxicity*. John Wiley & Sons, Chichester.
2. Hinson, J. A., Pumford, N. R., and Nelson, S. D. (1994) The role of metabolic activation in drug toxicity. *Drug Metab. Rev.* **26,** 395–412.
3. Vermeulen, N. P. E. (1996) Role of metabolism in chemical toxicity, in *Cytochromes P450: Metabolic and Toxicological Aspects* (Ioannides, C., ed.), CRC Press, Boca Raton, FL, pp. 29–53.
4. Pessayre, D., Dolder, A., Arigou, J. Y., Wandscheer, J.-C., Descatoire, V., Degott, C., and Benhamou, J. P. (1979) Effect of fasting on metabolite-mediated hepatotoxicity in the rat. *Gastroenterology* **77,** 264–271.
5. Kawajiri, K., Yonekawa, H., Hara, T., and Tagashira, Y. (1978) Biochemical basis for the resistance of guinea pigs to carcinogenesis by 2-acetylaminofluorene. *Biochem. Biophys. Res. Commun.* **85,** 959–965.
6. Maddrey, W. C. (1987) Hepatic effects of acetaminophen. Enhanced toxicity in alcoholics. *J. Clin. Gastroenterol.* **9,** 180–185.
7. Guengerich, F. P. (1993) Cytochrome P-450 enzymes. *Am. Scientist* **81,** 440–447.
8. Ioannides, C. and Parke, D. V. (1990) The cytochrome P450 I gene family of microsomal haemoproteins and their role in their metabolic activation of chemicals. *Drug Metab. Rev.* **22,** 1–85.
9. Gonzalez, F. J. and Gelboin H. V. (1994) Role of human cytochromes P450 in the metabolic activation of chemical carcinogens and toxins. *Drug Metab. Rev.* **26,** 165–183.
10. Meyer, U. A., Skoda, R. C., and Zanger, U. M. (1990) The genetic polymorphism of debrisoquine/sparteine metabolism — molecular mechanisms. *Pharmacol. Ther.* **46,** 297–308.
11. Westin, S., Tollet, P., Ström, A., Mode, A., and Gustafsson, J. Å. (1992) The role and mechanism of growth hormone in the regulation of sexually dimorphic P450 enzymes in rat liver. *J. Steroid Biochem. Molec. Biol.* **43,** 1045–1053.
12. Ioannides, C., Barnett, C. R., Irizar, A., and Flatt, P. R. (1996) Expression of cytochrome P450 proteins in disease, in *Cytochromes P450: Metabolic and Toxicological Aspects* (Ioannides, C., ed.), CRC Press, Boca Raton, FL, pp. 301–327.
13. Ameer, B. and Weintraub, R. A., 1997, Drug interactions with grapefruit juice. *Clin. Pharmacol.* **33,** 103–121.
14. Dragnev, K. H., Nims, R. W., and Lubet, R. A. (1995) The chemopreventive agent diallyl sulfide. A structurally atypical phenobarbital-type inducer. *Biochem. Pharmacol.* **50,** 2099–2104.
15. Guengerich, F. P. and Turvy, C. G. (1991) Comparison of levels of several human cytochrome P-450 enzymes and epoxide hydrolase in normal and disease states

using immunochemical analysis of surgical liver samples. *J. Pharmacol. Exp. Ther.* **256,** 1189–1191.
16. Schmucker, D. L. (1985) Aging and drug disposition in the elderly: an update. *Pharmacol. Rev.* **37,** 133–148.
17. Durnas, C., Loi, C.-M., and Cusack, B. J. (1990) Hepatic drug metabolism and aging. *Clin. Pharmacokinet.* **19,** 359–389.
18. Wynne, H. A., Mutch, E., James, O. F. W., Rawlins, M. D., and Woodhouse, K. W. (1988) The effect of age upon the affinity of microsomal monooxygenase enzymes for substrate in human liver. *Age Ageing* **17,** 401–405.
19. Imaoka, S., Fujita, S., and Funae, Y. (1991) Age-dependent expression of cytochromes P-450s in rat liver. *Biochim. Biophys. Acta* **1097,** 187–192.
20. Hunt, C. M., Westerkam, W. R., Stave, G. M., and Wilson, J. A. P. (1992) Hepatic cytochrome P-4503A (CYP3A) activity in the elderly. *Mech. Ageing Dev.* **64,** 189–499.
21. Hunt, C. M., Strater, S., and Stave, G. M. (1990) Effect of normal aging on the activity of human hepatic cytochrome P-450IIE1. *Biochem. Pharmacol.* **40,** 1666–1669.
22. Sotaniemi, E. A., Rautio, A., Lumme, P., Arvela, P., and Rautio, A. (1996) Age and CYP3A4 and CYP2A6 activities marked by the metabolism of lignocaine and coumarin in man. *Therapie* **51,** 363–366.
23. Sotaniemi, E. A., Arranto, A. J., Pelkonen, O., and Pasanen, M. (1997) Age and cytochrome P450-linked drug metabolism in humans: an analysis of 226 subjects with equal histopathologic conditions. *Clin. Pharmacol. Ther.* **61,** 331–339.
24. Burke, M. D. and Mayer, R. T. (1974) Ethoxyresorufin: Direct fluorometric assay of microsomal *O*-dealkylation which is preferentially induced by 3-methylcholanthrene. *Drug Metab. Disp.* **2,** 583–588.
25. Rodrigues, A. D. and Prough, R. A. (1991) Induction of cytochromes P450IA1 and P450IA2 and measurement of catalytic activities. *Methods Enzymol.* **206,** 423–431.
26. Ioannides, C. and Parke, D. V. (1975) Mechanism of induction of hepatic microsomal drug metabolising enzymes by a series of barbiturates. *J. Pharm. Pharmacol.* **27,** 739–746.

9

Assessing Age-Related Changes in Antioxidant Status

The FRASC Assay for Total Antioxidant Power and Ascorbic Acid Concentration in Biological Fluids

Iris F. F. Benzie and John J. Strain

1. Introduction

There is accumulating evidence that oxidative damage to protein, lipid, carbohydrate and DNA is an important cause and/or effect of cellular and subcellular changes associated with disease, and is responsible for at least some of the physiological, but ultimately fatal, changes that accompany aging ***(1–8)***. Advancing age brings increasing risk of chronic degenerative disease including cancer, cardiovascular disease, cataracts, and dementia ***(1–6,8)***. Immune status declines, with consequent increased risk of infection and, owing to a combination of physical and socioeconomic factors, nutritional status is often poor in the elderly, increasing the likelihood of poor antioxidant status ***(9)***.

Improved antioxidant status helps minimize oxidative damage, and this may delay or prevent pathological change ***(8–22)***. This suggests the possible utility of antioxidant-based dietary strategies for lowering risk of chronic, age-related disease ***(20–26)***. Vitamin C (ascorbic acid) and vitamin E (mainly α-tocopherol) are dietary derived antioxidants of major physiological importance ***(25,27–31)***, but many other exogenous and endogenous antioxidants contribute to the overall antioxidant status of the body ***(20,23,26,31,32)***. It is not yet possible to say that benefit to health is attributable to specific antioxidants at specific intake or plasma levels. Indeed it is likely that an optimal level of each antioxidant is required for maintenance of optimal health, that is, that an optimal "total" antioxidant status is desirable ***(23,27,33,34)***. In addition, the vitamin C to vitamin E ratio may be important, with risk of oxidative stress related

From: *Methods in Molecular Medicine*, Vol. 38: *Aging Methods and Protocols*
Edited by: Y. A. Barnett and C. R. Barnett

disease increasing at ratios below 1.0 ***(34)***. What constitutes optimal antioxidant status is not yet clear, however, and further study of the role of antioxidant status, and of individual antioxidants and their interrelationships, in aging and age-related disease is needed.

The ferric reducing (antioxidant) power (FRAP) assay,[1] and its modified version, the simultaneous ferric reducing (antioxidant) power and ascorbic acid (FRASC) assay, is a technically simple, inexpensive, fast, sensitive, and robust biochemical test useful for the assessment of antioxidant status of biological fluids ***(35–37)***. FRASC can be performed using routinely available laboratory equipment, and permits the direct measurement of biological fluids such as blood plasma, cerebrospinal fluid, and urine. The antioxidant and ascorbic acid content of these fluids, and of extracts of various drugs and dietary agents, can be measured objectively and reproducibly using FRASC, allowing their potential for improving the antioxidant status of the body to be assessed and compared ***(37–42)***. The assay is also analytically sensitive and precise enough to assess postingestion response to dietary antioxidants. FRASC, therefore, offers a practical analytical tool to help assess diet-, disease-, or age-related changes in antioxidant status.

1.1. Rationale of the FRASC Assay for Total Antioxidant Power and Ascorbic Acid Concentration in Biological Fluids (36,37)

In this assay, a ferric-tripyridyltriazine (Fe^{III}–TPTZ) complex is reduced to its ferrous form, which is blue colored and absorbs light of 593 nm. The ferric to ferrous reaction is driven by the reductive action of electron donating antioxidants in the test sample, and the change in absorbance at 593 nm is directly proportional to the combined, or "total," reducing (antioxidant) power of these antioxidants ***(35)***. In FRASC, ascorbic acid in the sample is selectively and specifically destroyed by ascorbate oxidase. The change in absorbance in this case is attributable to the remaining antioxidants, that is, the "total" less the contribution of ascorbic acid. The difference in antioxidant power between two paired samples, one treated with ascorbic oxidase and one untreated (and therefore still containing ascorbic acid) is equal to the contribution of ascorbic acid in the untreated sample (*see* **Fig. 1**). It is then a simple matter to calculate the molar concentration of ascorbic acid in the test sample, and to obtain three indices of antioxidant status: (1) the total antioxidant power, (2) the ascorbic acid concentration, and (3) the "non-ascorbic acid" antioxidant power of the sample.

2. Materials

1. 0.3 *M* Acetate buffer, pH 3.6; dissolve 3.1 g of sodium acetate trihydrate (Riedel-de Haen, Germany) in approx 500 mL of distilled and deionized water; add 16

[1] U.S. patent pending.

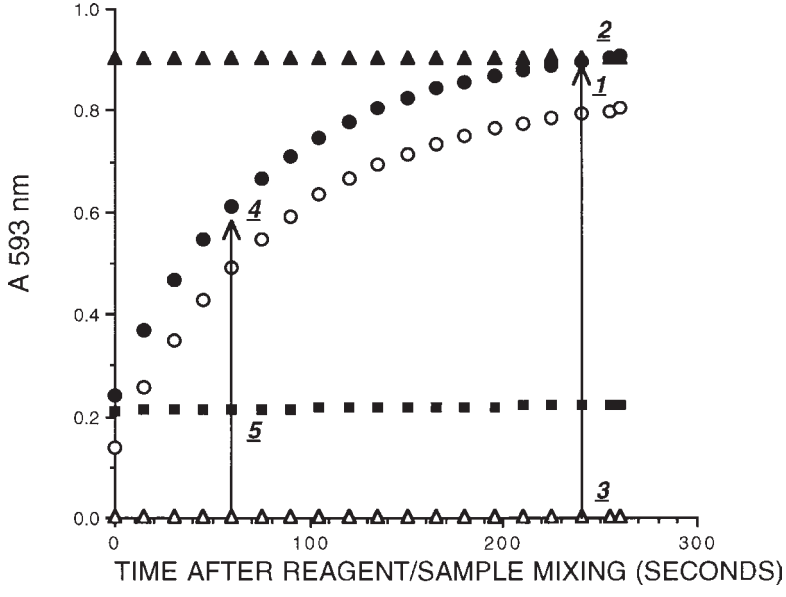

Fig. 1. Measuring concept of FRASC. This figure shows the absorbance change owing to Fe^{III} reduction by antioxidants in the sample. Calculation of FRAP value is by taking the 0–4-min change in absorbance at 593 nm for test sample (*closed circles*, *1*) and relating it to the 0–4-min absorbance change for the Fe^{II} standard (*closed triangles*, *2*), with a reagent blank correction (*open triangles*, *3*) for both. Calculation of ascorbic acid results is by subtracting the 0–1-min absorbance reading of the ascorbate oxidase-treated test sample (*open circles*) from the matching water-treated sample (*closed circles*, *4*); this signal is then related to that given by a standard solution of Fe^{II} (*closed triangles*) (or ascorbic acid, *closed squares*, *5*) of appropriate concentration. (Reproduced with permission from Benzie, I. F. F. and Strain, J. J. (1997) *Redox Report* **3,** 233–238.)

mL of glacial acetic acid (BDH Laboratory Supplies, England), and make up to a final volume of 1 L with distilled and deionized water. This solution can be stored at room temperature for up to 1 mo.

2. 0.01 *M* TPTZ (2,4,6 tripyridyl-*s*-triazine, Fluka Chemicals, Switzerland) in 0.04 *M* HCl (BDH). This solution can be stored at room temperature for up to 2 wk (*see* **Note 1**).
3. 0.02 *M* $FeCl_3 \cdot 6H_2O$ (BDH). This solution can be stored at room temperature for up to 2 wk.
4. 4000 U/L of ascorbate oxidase (EC 1.10.3.3) (Sigma Chemical, St. Louis, MO, USA) in distilled water. Aliquots of this solution should be stored at –70°C and thawed when required.
5. To prepare working FRASC reagent, mix 20.0 mL of 0.3 *M* acetate buffer, pH 3.6, 2.0 mL of 0.01 *M* TPTZ solution in 0.04 *M* HCl; and 2.0 mL of 0.02 *M* $FeCl_3 \cdot 6H_2O$ solution just before use.

6. For calibration, standard solutions of $FeSO_4 \cdot 7H_2O$ (Riedel de Haen, Germany) made up in water to a known concentration; for example, 100 µ*M*, 500 µ*M*, and 1000 µ*M* are recommended (*see* **Note 2**). Reaction of Fe^{II} represents a one-electron exchange reaction and is taken as unity, that is, the blank corrected signal given by 1000 µ*M* solution of Fe^{II} is equivalent to a ferric reducing/antioxidant power (FRAP) value of 1000 µM. As ascorbic acid has a stoichiometric factor of 2.0 in this assay ***(35–37)***, reaction of ascorbic acid gives a change in absorbance double that of an equivalent molar concentration of Fe^{II}, that is, a Fe^{II} standard of 100 µ*M* is equivalent to 50 µ*M* ascorbic acid, and a 100 µ*M* solution of ascorbic acid has a FRAP value of 200 µM.

   Freshly prepared aqueous ascorbic acid solutions (ascorbic acid extra pure crystals, Sigma Chemical, St. Louis, MO, USA) can also be used as calibrators ***(36,37,42)*** (*see* **Note 3**). Refer to **Note 4** for guidelines on quality control samples and expected linearity and precision.

3. Methods

1. Samples: Serum, plasma, urine, saliva, tears, other biological fluids, and aqueous and ethanolic extracts of drugs and foodstuffs can be used directly in FRASC. However, as some antioxidants are unstable, samples should be kept chilled and in the dark until testing, and should be tested with as little delay as possible. Hemolyzed plasma or serum samples should be avoided. Heparinized plasma is preferable to EDTA plasma and serum for FRAP and FRASC measurements, as ascorbic acid is more stable in heparinized plasma ***(39)***.
2. To measure the total antioxidant power, as FRAP, and ascorbic acid in one test (FRASC), ascorbic acid in one of a matching pair of sample aliquots is destroyed by the addition of ascorbate oxidase. Ascorbic acid reacts very quickly with the working reagent, and the 0–1-min reaction time window is used for calculation of ascorbic acid results; the 0–4-min window is used for calculation of "total" antioxidant power (FRAP) results, that is, absorbance readings are taken at 0, 1, and 4 min after reagent/sample mixing (37°C incubation).
3. To prepare samples:
   a. Add 40 µL of a 4000 U/L solution of ascorbic oxidase to 100 µL of test sample.
   b. Add 40 µL of distilled water to the paired 100-µL sample aliquot.
   c. Calibrators and QC samples are treated similarly in pairs (*see* **Note 5**). This predilution of samples, calibrators and QC samples can be performed in the analyzer sample cups.
4. The paired ascorbate oxidase diluted ("+ao") and water-diluted ("–ao") samples are then immediately loaded onto the analyzer for automated measurement (*see* **Note 6**).

3.2. Data Collection and Calculation of Results

1. The FRASC assay can be performed using any type of automated analyzer that permits blank corrected readings at 593 nm to be taken at selected intervals after

Table 1
Cobas Fara Test Program for FRASC Assay

Measurement code	Abs
Reaction mode	R1-I-S-A
Reagent blank	reag/dil
Wavelength	593 nm
Temperature	37°C
R1	300 µL
M1	1.0 s
Sample volume	10 µL
Diluent name	H_2O
Volume	30 µL
Readings	
First	0.5 s
Number	17
Interval	15 s
Reaction direction	Increase
Number of steps	1
Calculation	Endpoint
First	M1
Last	17 (i.e., 0–4 min) for FRAP; reading 5 (i.e., 0–1 min reading) is retrieved for calculation of ascorbic acid

Modified from Benzie, I. F. F. and Strain, J. J. (1997) *Redox Report* **3,** 233–238.

sample-reagent mixing. In our laboratories the Cobas Fara centrifugal analyzer (Roche Diagnostics Ltd., Basel, Switzerland) is used, and the user-defined test program is presented in **Table 1**.

2. The 0–4-min reaction time window is used for data capture for the FRAP value. The absorbance change is translated into a FRAP value by relating the change of absorbance at 593 nm of test sample to that of a standard solution of known FRAP value, for example, 1000 µ*M* Fe^{II}, as described in **Eq. 1**.
3. To obtain ascorbic acid results, the 0–1-min absorbance at 593 nm readings are retrieved, and calculation of results is performed as described in **Eqs. 2** and **3**.
4. The nonascorbic acid antioxidant power (*see* **Note 7**) is calculated according to **Eq. 4**.
5. Calculation of results is as follows:
   Using the water-diluted samples, the FRAP (µ*M*) value =

$$[\text{FRAP}]_{\text{std}}\ (\mu M) \times \frac{0\text{–}4\ \text{minute}\ A_{593\ \text{nm}}\ \text{test sample}}{0\text{–}4\ \text{minute}\ A_{593\ \text{nm}}\ \text{standard}} \quad (1)$$

(*see* **Note 6**).

Table 2
FRAP Values and Ascorbic Acid Concentrations (Mean; Median; SD; μmol/L), Using FRASC, of Fresh Fasting EDTA Plasma from Healthy Subjects

	All (n = 130)	Men (n = 66)	Women (n = 64)
Age (years)	43; 43; 16.4	42; 42; 16.3	43; 44; 16.6
FRAP	1018; 1004; 198	1086; 1077; 189	948; 927; 183
Ascorbic acid	51; 48; 17.9	49; 48; 13.8	52; 50; 21.3

Reproduced with permission from Benzie, I. F. F. and Strain, J. J. (1997) *Redox Report* **3,** 233–238.

Using the paired water (–ao) and ascorbate oxidase diluted (+ao) samples, the ascorbic acid concentration is calculated as follows:

$$\text{0–1 min ascorbic acid related change in } A_{593\text{ nm}} = (\text{0–1 min } A_{593\text{ nm}} \text{ sample –ao}) - (\text{0–1 min } A_{593\text{ nm}} \text{ sample +ao}) \quad (2)$$

$$\text{ascorbic acid concentration } (\mu M) = [\text{ascorbic acid}]_{\text{std}}\ (\mu M) \times \text{0–1 min ascorbic acid related } A_{593\text{ nm}} \text{ of test sample} / \text{0–1 min ascorbic acid related } A_{593\text{ nm}} \text{ of standard} \quad (3)$$

(*see* **Note 8**).

$$\text{nonascorbic acid antioxidant power} = \text{FRAP value } (\mu M) - 2 \times \text{ascorbic acid concentration } (\mu M) \quad (4)$$

Table 2 gives typical values obtained on fasting plasma samples from healthy adults.

4. Notes

1. The TPTZ powder, as purchased, is normally white. However, in some bottles, when opened, the contents have been found to be gray or yellow in color. The reason for this coloration is not clear, but it does not appear to affect results. The working FRASC reagent should be a pale yellow/orange color. Any visible blue color indicates contamination by either ferrous iron or a reducing agent. Visible blue color in the working reagent will give a high blank reading and decrease sensitivity: do not use.
2. Do not attempt to use Fe^{II} standards >1500 μ*M*, as there will be precipitation of iron salts. Aqueous ferrous sulfate solutions of up to 1500 μ*M* appear to be stable for at least 1 mo at 4°C. These solutions should be clear and colorless.
3. It is important that ALL samples, calibrators, and QC samples be treated identically and in matching ascorbate oxidase diluted and water diluted pairs. The same absorbance reading should be obtained for the paired Fe^{II} solutions, that is, the

addition of ascorbate oxidase should not result in any difference in the absorbance given as there is no ascorbic acid to destroy in these solutions.

4. Guidelines on quality control samples and expected performance:

   For ease of use and reliability, aqueous ascorbic acid solutions at 100, 250, 500, and 1000 μ*M* (equivalent to 200, 500, 1000, and 2000 μ*M* FRAP, prepared fresh daily) and aged QC serum freshly spiked with ascorbic acid are recommended as quality control samples. These should be run in parallel with test samples to actively monitor the performance of the test and to ensure comparability with previous results.

   Expected precision and sensitivity of the FRASC assay:

   Precision is high in FRASC: typical within- and between- run CVs obtained in our laboratories are, respectively, <1% and <3% at 900 and 1800 μ*M* for FRAP values. For ascorbic acid, typical within- and between-run CVs are <5% at 25, 50, 100, and 440 μM. Sensitivity is also high, and the limit of detection of the FRAP assay is <2 μ*M* reducing/antioxidant power.

   Expected linearity:

   The test as described will give a linear dose–response up to a FRAP value of 2000 μ*M*. If samples with FRAP values of >2000 μ*M* are to be tested, prior dilution of the test sample in water is recommended. As stoichiometric factors are constant in the FRASC assay ***(35)***, simple correction for the additional dilution is the only extra calculation required to obtain the FRAP value of the sample. Linearity of ascorbic acid dose–response of the test as described is up to at least 1000 μ*M*.
5. The enzyme-linked destruction of ascorbic acid is very fast, even at room temperature, and additional incubation time with ascorbate oxidase is not needed.
6. The "nonascorbic acid antioxidant power" is the combined antioxidant power of the other, similarly acting antioxidants such as uric acid and bilirubin (*see* **refs. *35*** and ***37***). There is also some contribution (approx 10% of the total) by the thiol groups of plasma proteins.
7. This additional step can easily be added to the test program if desired, and a direct printout of FRAP values in micromolarity obtained. Raw data are then retrieved, with capture of the 0–1-min change in absorbance at 593 nm (i.e., reading number 5 on test as programmed) for calculation of the ascorbic acid concentration.
8. The value of the standards used for calculation of micromolar ascorbic acid and for FRAP values must be expressed in micromolar ascorbic acid or FRAP value "equivalents" as appropriate. Note that each molecule of ascorbic acid has the ability to reduce two ferric ions, and therefore has a FRAP value of 2 μmol. Aqueous ascorbic acid standards are stable for 24 h at 4°C. Ferrous sulfate solutions are stable for at least 1 mo at 4°C.

References

1. Ames, B. N., Shigenaga, M. K., and Hagen, T. M. (1993) Oxidants, antioxidants and the degenerative disease of aging. *Proc. Nat. Acad. Sci. USA* **90,** 7915–7922.

2. Benzie, I. F. F. (1996) Lipid peroxidation: a review of causes, consequences, measurement and dietary influences. *Int. J. Food Sci. Nutr.* **47,** 233–262.
3. Maxwell, S. R. J. and Lip, G. Y. H. (1997) Free radicals and antioxidants in cardiovascular disease. *Br. J. Clin. Pharmacol.* **44,** 307–317.
4. Emerit, I. (1994) Reactive oxygen species, chromosome mutation and cancer: possible role of clastogenic factors in carcinogenesis. *Free Radic. Biol. Med.* **16,** 99–109.
5. Yu, B. P. (1996) Aging and oxidative stress: modulation by dietary restriction. *Free Radic. Biol. Med.* **21,** 651–668.
6. Harman, D. (1996) Aging and disease: extending functional lifespan. *Ann. NY Acad. Sci.* **786,** 321–336.
7. Harman, D. (1956) Aging: a theory based on free radical and radiation chemistry. *J. Gerontol.* **2,** 298–300.
8. Beckman, K. B. and Ames, B. N. (1998) The free radical theory of aging matures. *Physiol. Rev.* **78,** 547–581.
9. Gariballa, S. E. and Sinclair, A. J. (1998) Nutrition, ageing and ill health. *Br. J. Nutr.* **80,** 7–23.
10. Loft, S. and Poulson, H. E. (1996) Cancer risk and oxidative DNA damage in man. *J. Mol. Med.* **74,** 297–312.
11. Duthie, S. J., Ma, A., Ross, M. A., and Collins, A. R. (1996) Antioxidant supplementation decreases oxidative damage in human lymphocytes. *Cancer Res.* **56,** 1291–1295.
12. Heitzer, T., Just, H., and Munzel, T. (1996) Antioxidant vitamin C improves endothelial dysfunction in chronic smokers. *Circulation* **94,** 6–9.
13. Levine, G. N., Frei, B., Koulouris, S. N., Gerhard, M. D., Keaney, J. F., and Vita, J. A. (1996) Ascorbic acid reverses endothelial vasomotor dysfunction in patients with coronary artery disease. *Circulation* **93,** 1107–1113.
14. Ness, A. R., Chee, D., and Elliot, P. (1997) Vitamin C and blood pressure—an overview. *J. Hum. Hyperten.* **11,** 343–350.
15. Diplock, A. T. (1994) Antioxidants and disease prevention. *Mol. Aspects Med.* **15,** 293–376.
16. Frei, B., Keaney, J. F., Retsky, K. L., and Chen, K. (1996) Vitamin C and E and LDL oxidation. *Vitam. Horm.* **54,** 1–34.
17. Samman, S., Brown, A. J., Beltran, C., and Singh, S. (1997) The effect of ascorbic acid on plasma lipids and oxidisability of LDL in male smokers. *Eur. J. Clin. Nutr.* **51,** 472–477.
18. Sweetman, S. F., Strain, J. J., and McKelvey, V. J. (1997) Effect of antioxidant vitamin supplementation on DNA damage and repair in human lymphoblastoid cell. *Nutr. Cancer* **27,** 122–130.
19. Wen, Y., Cooke, T., and Feely, J. (1997) The effect of pharmacological supplementation with vitamin C on low-density lipoprotein oxidation. *Br. J. Clin. Pharmacol.* **44,** 94–99.
20. Diplock, A. T., Charleux, J. L., Crozer-Willi, G., Kok, F. J., Rice-Evans, C., Roberfroid, M., Stahl, W. and Vina-Ribes, J. (1998) Functional food science and defence against reactive oxidative species. *Br. J. Nutr.* **80,** S77–S112.

21. Bendich, A. and Langseth, L. (1995) The health effects of vitamin C supplementation. *J. Am. Coll. Nutr.* **14,** 124–136.
22. Benzie, I. F. F. (1998) Antioxidants: observational epidemiology, in *The Encyclopedia of Nutrition* (Sadler, M., Cabellero, B., and Strain, J. J., eds.), Academic Press, London, pp. 106–115.
23. Halliwell, B. (1996) Oxidative stress, nutrition and health. Experimental strategies for optimization of nutritional antioxidant intake in humans. *Free Radic. Res.* **25,** 57–74.
24. Machlin, L. J. (1995) Critical assessment of the epidemiological data concerning the impact of antioxidant nutrients on cancer and cardiovascular disease. *Crit. Rev. Food Sci. Nutr.* **35,** 41–50.
25. Strain, J. J. and Benzie, I. F. F. (1998) Antioxidant nutrients, in *Functional Foods; the Consumer, the Products and the Evidence* (Sadler, M. J. and Saltmarsh, M., eds.), Royal Society of Chemistry, Cambridge, pp. 74–79.
26. Weisburger, J. H. (1996) Tea antioxidants and health, in *Handbook of Antioxidants* (Cadenas, E. and Packer, L., eds.), Marcel Dekker, New York, pp. 469–486.
27. Benzie, I. F. F. (1999) Vitamin C: prospective functional markers for defining optimal nutritional status. *Proc. Nutr. Soc.*, **58,** 1–8.
28. Frei, B., England, L., and Ames, B. N. (1989) Ascorbate is an outstanding antioxidant in human blood plasma. *Proc. Natl. Acad. Sci. USA* **86,** 6377–6381.
29. Rose, R. C. and Bode, A. M. (1993) Biology of free radical scavengers: an evaluation of ascorbate. *FASEB J.* **7,** 1135–1142.
30. Traber, M. G. and Seis, H. (1996) Vitamin E in humans: demand and delivery. *Annu. Rev. Nutr.* **16,** 321–347.
31. Strain, J. J. and Benzie, I. F. F. (1998) Diet and antioxidant defence, in *The Encyclopedia of Nutrition* (Sadler, M., Cabellero, B., and Strain, J. J., eds.), Academic Press, London, pp. 95–105.
32. Sies, H. and Stahl, W. (1995) Vitamins E and C, B-carotene, and other carotenoids as antioxidants. *Am. J. Clin. Nutr.* **62,** 1315S–1321S.
33. Graumlich, J. F., Ludden, T. M., Conry-Cantilena, C., Cantlena, L. R., Jr., Wang, Y., and Levine, M. (1997) Pharmacokinetic model of ascorbic acid in healthy male volunteers during depletion and repletion. *Pharmacol. Res.* **14,** 1133–1139.
34. Gey, K. F. (1998) Vitamins E plus C and interacting conutrients required for optimal health. A critical and constructive review of epidemiology and supplementation data regarding cardiovascular disease and cancer. *Biofactors* **7,** 113–174.
35. Benzie I. F. F. and Strain, J. J. (1996) The reducing ability of plasma as a measure of "antioxidant power" — the FRAP assay. *Anal. Biochem.* **239,** 70–76.
36. Benzie, I. F. F. and Strain, J. J. (1997) Simultaneous automated measurement of total antioxidant (reducing) capacity and ascorbic acid concentration. *Redox Report* **3,** 233–238.
37. Benzie, I. F. F. and Strain, J. J. (1999) Ferric reducing (antioxidant) power as a measure of antioxidant capacity: the FRAP assay, in *Methods in Enzymology*, vol. 299: *Oxidants and Antioxidants* (Packer, L., ed.), Academic Press, Orlando, pp. 15–27.

38. Benzie, I. F. F., Janus, E. D., and Strain, J. J. (1998) Plasma ascorbate and vitamin E levels in Hong Kong Chinese. *Eur. J. Clin. Nutr.* **52,** 447–451.
39. Benzie, I. F. F. and Chung, W. Y. (1999) Total antioxidant power of plasma: male–female differences and effect of anticoagulant used. *Ann. Clin. Biochem.*, **36,** 104–106.
40. Benzie, I. F. F. and Szeto Y,T. (1999) Antioxidant power of teas. *J. Agric. Food Chem.*, **47,** 633–637.
41. Benzie, I. F. F. and Tomlinson, B. (1998) Antioxidant power of angiotensin-converting enzyme inhibitors in vitro. *Br. J. Clin. Pharmacol.* **45,** 168–169.
42. Benzie, I. F. F., Chung, W. Y., and Strain, J. J. (1999) Antioxidant activity of ascorbic acid is independent of concentration. *J. Nutr. Biochem.*, **10,** 146–150.

10

Measurement of DNA Damage and Repair Capacity as a Function of Age Using the Comet Assay

Peter H. Clingen, Jillian E. Lowe, and Michael H. L. Green

1. Introduction

A large number of studies indicate that DNA damage and mutation increase with age in human cells and tissues ***(1)***. Age-related degenerative disorders in which DNA damage has been invoked include heart disease and neurodegenerative conditions such as Alzheimer's disease, amyotrophic lateral sclerosis, or Parkinson's disease ***(2,3)***. Patients with deficiencies in DNA repair, including xeroderma pigmentosum (XP) ***(4)*** and ataxia–telangiectasia (A–T) ***(5)*** show characteristic patterns of neurodegeneration (as opposed to a failure of normal development). The implication is that failure of repair can lead to accumulation of damage and degenerative disease. XPs and A–Ts are hypersensitive to specific types of DNA damage, and the degenerative damage in patients is tissue specific. DNA in every tissue, however, is under attack from a range of endogenously formed mutagens, including reactive oxygen species, nitric oxide, reactive metabolites, and breakdown products such as malondialdehyde. A series of repair enzymes recognize and remove these types of DNA damage from the genome. Failure to repair DNA may cause the synthesis of defective proteins, which will repair DNA less efficiently, and in turn lead to propagation of further errors (6). Alternatively, oxidative damage to mitochondrial proteins might cause less efficient processing of oxygen, release of higher levels of reactive oxygen species and increased levels of background DNA damage.

In this chapter, we describe protocols based on modifications of the alkali Comet assay (single-cell gel electrophoresis) and describe how they may be applied to the measurement of DNA damage and repair as a function of age. The Comet assay is a simple, rapid, and inexpensive method for detecting DNA

From: *Methods in Molecular Medicine*, Vol. 38: *Aging Methods and Protocols*
Edited by: Y. A. Barnett and C. R. Barnett

strand breaks in individual eukaryotic cells. It has been used in vivo and in vitro to assess DNA damage and repair induced by various physical factors such as ultraviolet (UV) radiation ***(7,8)***, ionizing radiation ***(9,10)***, chemical agents ***(11)*** as well as physiological factors such as diet ***(10)***, cytokines ***(12)***, exercise ***(13)***, smoking, and aging ***(14,15)***. A range of applications will be addressed including:

- Detecting frank DNA strand breaks
- Investigating endogenous levels of damage
- Formation and repair of oxidative DNA damage using specific DNA repair enzymes
- Measuring intrinsic rates of cellular excision repair

Consideration is also given to experimental design and interpretation of data so that meaningful results may be obtained.

1.1. Principle of Assay

The Comet assay is a flexible and sensitive procedure for measuring DNA damage in a range of tissues and cell types. The methods described here have been largely based on the protocols of Singh et al. ***(16)*** and Collins et al. ***(17)***. Methods and applications of the assay have been extensively reviewed ***(18–22)***.

In the assay, a single-cell suspension of the cells or tissue under study are embedded in low melting point agarose on a frosted microscope slide. The slide is placed in a high salt lysis mixture that strips away cell membranes and removes most proteins from chromatin to leave behind supercoiled DNA in structures known as nucleoids ***(23)***. When placed in alkaline buffer the supercoiled DNA starts to unwind. During electrophoresis, DNA containing strand breaks is pulled toward the anode to form a Comet tail while undamaged DNA remains trapped within the nucleus. Comet tail length or tail moment are then determined by image analysis. Within a defined dose range there appears to be a linear relationship between the number of strand breaks and measures of Comet length and/or tail moment. The assay specifically measures DNA strand breaks and normally can detect less than one strand break per 10^7 basepairs. These may represent:

- Direct single-stranded breaks produced by exogenous or endogenous mutagens such as reactive oxygen species
- Alkali labile sites
- Breaks formed during the excision step of repair of damaged bases from cellular DNA

Direct single-stranded breaks are detected using the standard form of the assay. Although it has been postulated that these include alkali-labile sites, it is

controversial whether the conditions of the assay are sufficiently alkaline to generate these sites. As a means to study overall levels of DNA excision repair it is possible to incubate cells, damaged with genotoxic chemical or physical agents, with inhibitors of DNA strand resynthesis such as aphidicolin, cytosine arabinoside, or hydroxyurea. These inhibitors allow the accumulation of strand breaks formed during DNA excision repair. Although this assay is nonspecific in that it does not discriminate between the types of damage that are being repaired it may be used to compare overall rates of excision repair. A more exact approach is to use purified DNA repair enzymes. Cells embedded in agarose are treated with a damaging agent and lysed immediately or at various times after treatment. Exposed nucleoids are then washed and incubated with a repair enzyme that recognizes and cleaves DNA at the sites of specific DNA lesions. Suitable enzymes include (1) T4 endonuclease V, which recognizes ultraviolet radiation induced cyclobutane pyrimidine dimers ***(24)***; (2) endonuclease III (Endo III), which recognizes oxidized pyrimidines ***(17)***; (3) formamidopyrimidine glycosylase (FPG), which recognizes oxidized purines ***(25,26)***; and (4) uracil glycosylase, which recognizes uracil in DNA ***(27)***.

1.2. Practical Considerations

In theory, any cell type from any tissue is suitable for use in the Comet assay provided that it can be made into a single-cell suspension without introducing significant amounts of DNA damage. In practice and particularly for age-related studies, the choice of cell type may be limited. Samples from a large number of individuals should be available as should routine methods for culture of the cell type. Age groups of donors should be wide enough apart to maximize the opportunity for seeing any differences in the levels of DNA damage or repair (e.g., age groups of 25–30, 45–50, and 65–75). Caution must be taken when averaging levels of DNA damage or repair and sufficient samples need to be analyzed to take into account interindividual variation. Because both physical and physiological factors can affect levels of background DNA damage ***(7–15)*** these should be defined and controlled for as carefully as possible. Details of medical history and lifestyle factors such as recent exercise or smoking habits, alcohol consumption, and diet should be obtained where possible.

The cells that lend themselves most readily to these studies are freshly isolated peripheral blood mononuclear cells, most of which are in a nondividing (G_0) state. Details of how to handle cultured human fibroblasts in the Comet assay are also described. Although it would be possible to grow primary cultures of fibroblasts from small skin biopsies for a number of individuals of different ages, the resources and time required to do so for a significant number of donors would be considerable. Cultured fibroblasts would lend themselves

more readily to in vitro studies of aging, and to studies of genotypes that might influence the aging process.

In addition to interindividual variation, intraexperimental variation should be considered. It is essential to repeat experiments several times, to confirm consistency of effects. A minimum of duplicate slides in three independent experiments is recommended. This is particularly important in monitoring populations for evidence of preexisting or endogenous DNA damage. Age-related differences may be small and experiments may not have built-in controls for damage arising from poor experimental technique. As a guide to what can be achieved within a given study, one worker can readily perform and score one experiment of eight sets of duplicate slides per day.

2. Materials

2.1. Cells and Tissues

We will describe the use of the assay with (1) freshly isolated human mononuclear cells, and (2) cultured normal human fibroblasts

2.2. Slides, Agarose, and Chemicals

1. Slides. Fully frosted (on one surface) glass microscope slides 76 × 26 mm (Chance Propper, Smethwick, West Midlands, UK) (*see* **Note 1**). Coverslips, 22 × 22 mm, thickness no. 1.5 (Merck, Leicester, UK).
2. Agarose. Sigma type I (Sigma, Poole, Dorset, UK); NuSieve GTG low melting point agarose (FMC BioProducts, Rockland, ME, USA).
3. Culture medium, as appropriate for each cell type. We incubate freshly isolated mononuclear cells in RPMI 1640 with phenol red (Life Sciences, Paisley, UK), supplemented with 10% pooled human AB serum, 200 IU/mL of Penicillin, 200 µg/mL of streptomycin, 2 m*M* L-glutamine (Gibco-BRL, Paisley, UK), and 200 µg/mL of sodium pyruvate (Sigma, Poole, Dorset, UK). For fibroblasts, we use minimum essential medium (MEM) containing 15% fetal calf serum (FCS), 100 IU/mL of penicillin, 100 µg/mL of streptomycin, and 2 m*M* L-glutamic acid. Histopaque is from Sigma (Poole, Dorset, UK), human AB serum pools from Colindale Blood Transfusion Centre (London, UK) and FCS from PAA Laboratories GmbH (Linz, Austria). Where indicated, RPMI 1640 without phenol red is used.
4. Dulbecco's "A" phosphate-buffered saline (PBS, tablets from Oxoid, Basingstoke, UK). Bacto trypsin is from Difco Laboratories (Detroit, MI, USA). The contents of one vial are dissolved in 200 mL of PBS. Trypsin-EDTA contains 40% v/v trypsin solution and 0.4% EDTA in PBS. Other chemicals are from Sigma (Poole, Dorset, UK).
5. All solutions are made up in double-deionized water (ddH_2O).

6. Lysis mixture: 10 m*M* Tris base, 2.5 *M* NaCl, 200 m*M* NaOH, 100 m*M* EDTA-Na_2, pH 10. Store at room temperature for up to 1 wk. One hour before use, place at 4°C. Just before use add 1% v/v Triton X-100 and 10% v/v dimethyl sulfoxide (DMSO).
7. Enzyme buffer. Use the recommended buffer for the enzyme. For T4 Endonuclease V: 10 m*M* Tris-HCl, 10 m*M* EDTA-Na_2, 75 m*M* NaCl, pH 8.0. For Endo III and FPG: 40 m*M* *N*-[2-hydroxyethyl]piperazine-*N*'-[2-ethanesulfonic acid] (HEPES), 100 m*M* KCl, 0.5 m*M* EDTA-Na_2, 200 µg/mL of bovine serum albumin (BSA), pH 8.0. Enzyme buffers may be made as 10 × stock solutions and stored at –20°C. T4 Endo V was a gift from Dr. D. Yarosh, Applied Genetics (NY, USA). Endo III and FPG were a gift from Dr. A. Collins (Rowett Institute, Aberdeen, UK). Commercial sources of the enzymes are available (Trevigen, Whitney, Oxford, UK).
8. Electrophoresis buffer: 300 m*M* NaOH, 1 m*M* EDTA-Na_2, made up on day of use. The buffer must be at a defined temperature (we typically use 15°C).
9. Neutralization buffer: 400 m*M* Tris base, adjusted to pH 7.5 with concentrated HCl. This can be stored at room temperature if filter sterilized.
10. Staining solution: 20 µg/mL of ethidium bromide in ddH_2O. This can be stored indefinitely at 4°C (*see* **Note 2**).
11. Two small water baths, one at 37°C and one at 45°C. Standard histology staining troughs and racks (cover with black electrical tape to exclude light). Trays and source of ice.

2.3. Electrophoresis

1. Gel electrophoresis boxes. Commercial or custom-made boxes can be used. We use purpose built Perspex boxes, 24 × 28 × 7.5 cm, covered in black electrical tape to exclude light. These hold 16–18 slides in two rows and use 1.5 L of electrophoresis buffer.
2. Power pack. Delivering at least 400 mA at 20 V.
3. Refrigerator. The lysis stage of the assay is carried out at 4°C. Solutions must be prepared and electrophoresis must be carried out at a defined temperature. An air-conditioned room or cooled incubator are also advantageous for maintaining constant temperatures throughout the assay.

2.4. Microscopy

1. Fluorescence microscope, with an ethidium bromide filter (*see* **Note 2**). We use a 10× objective with a video camera for scoring. An integrating monochrome CCD video camera is required for sensitivity.
2. Image analysis system. We currently use the Casys system (Synoptics, Cambridge, UK) or the Komet system (Kinetic Imaging, Liverpool, UK). Although computerized software is desirable for objective scoring, it is possible to analyze Comets without it (*see* **Note 3**).

3. Methods

3.1. Preparation of Cellular Material

Results in the Comet assay are critically dependent on gentle handling of the test material. We have obtained acceptable results with the procedures outlined in the following list. Where possible all procedures should be performed under subdued lighting. Cultured cells are maintained at 37°C in a humidified atmosphere containing 5% CO_2. Typically 1–2 × 10^4 cells are required per slide when using 22 × 22 mm coverslips. Standard experiments of 16–18 slides require a total of approx 2.5–5 × 10^5 cells.

1. Whole blood samples may be obtained using a Soft Touch (Boehringer, Lewes, UK) or similar finger-pricking device and taken up using a Gilson-type disposable tip pipet (*see* **Note 4**). Blood (40 µL) is suspended in an Eppendorf tube with 160 µL of clear RPMI 1640 containing four heparin-coated beads (taken from the barrel of a blood sampling syringe). This yields sufficient cells for eight slides when diluted with 200 µL of 1.4% LMP agarose. Samples are held at room temperature and slides made as quickly as possible.
2. Mononuclear cell fractions (MNCs) from individual donors can be isolated from larger blood samples (5–50 mL) (*see* **Notes 5** and **6**). Blood is diluted 1:1 with RPMI 1640 and 10–15 mL carefully layered onto 10 mL Histopaque in centrifuge tubes. These are centrifuged at 700*g* for 20 min at room temperature. The MNCs are removed from the Histopaque/plasma interface with a sterile plastic Pasteur pipet and approx 5 mL transferred into individual centrifuge tubes. These are made up to 20 mL with RPMI 1640 and centrifuged for 10 min at 700*g*. The pellets are resuspended with 25 mL of RPMI 1640 containing 10% human AB serum and centrifuged for 10 min at 700*g*. The pellets are resuspended with 25 mL of RPMI containing 10% human AB serum and the number of cells counted. The cells are centrifuged for 10 min at 700*g*, resuspended at approx 3 × 10^6 cells/mL in 10% DMSO/90% FCS and cryopreserved in 1-mL aliquots. Typically, 1 mL of blood should yield approx 1 × 10^6 mononuclear cells. Prior to use for DNA damage or repair experiments, cryopreserved mononuclear cells should be rapidly thawed, washed with 5 mL of complete RPMI culture medium, centrifuged at 250*g* for 5 min, resuspended at 10^6 cells/mL in complete RPMI culture medium, and incubated at 37°C overnight (*see* **Note 7**).
3. Primary human fibroblasts may be obtained from small skin biopsies and maintained in tissue culture flasks in MEM culture medium ***(28)***. Cells are washed with PBS and trypsinized with fresh trypsin-EDTA. It is essential to trypsinize for a minimum period (typically less than 5 min at 37°C is sufficient). Two volumes of MEM culture medium are added to inactivate the trypsin, and cells are centrifuged at 250*g* for 5 min and resuspended in PBS at approx 10^6 cells/mL. For repair kinetic experiments on fibroblasts lasting more than 8 h it is necessary to preincubate cells for at least 72 h in MEM containing 0.5% FCS to inhibit cell division (*see* **Note 8**). Typically, 3 × 10^5 cells per dish can be maintained in a number of 5 cm diameter tissue culture grade Petri dishes.

4. Generation of single-cell suspensions from a variety of human and rodent tissues has been reviewed *(18)*.

3.2. Slide Preparation

1. Prepare 3 mL of 1% type I agarose and 2 mL of 1.4% NuSieve LMP agarose (*see* **Note 9**), made up in clear RPMI 1640 or PBS (*see* **Note 10**). Microwave for the minimum time necessary to melt the agarose.
2. Place the type I agarose in a 45°C water bath and the LMP agarose in a 37°C water bath.
3. Use a pencil to label the slides for each treatment. Warm the slides to at least 40°C, on a metal tray. Add 80 µL of type I agarose while the slide is still warm. Immediately lower a 22 × 22 mm coverslip over the agarose, avoiding incorporation of air bubbles. When all the slides have been treated, place the tray over ice and leave for at least 10 min (*see* **Note 11**).
4. Prepare the cell suspension for the second layer. For whole blood samples this is described in **Subheading 3.1.1**. For single-cell suspensions, resuspend cells in medium (37°C) at 1×10^6 cells/mL (for 16 slides 500 µL is required). Add an equal volume of 1.4% LMP agarose (i.e., 500 µL) and mix gently. From the 1-mL cell suspension place 45 µL (containing approx 2×10^4 cells) onto the 1% agarose base layer of each slide and add a 22 × 22 mm coverslip. Slides do not need to be prewarmed for this step (*see* **Note 12**). Allow to set over ice for at least 5 min.

3.3. Treatment of Material with a DNA-Damaging Agent

In a number of aging studies, no specific DNA-damaging treatment is applied, and the assay is used to detect levels of preexisting damage in blood and other tissues. Special consideration must be given to the design of such studies, if they are to have a chance of yielding useful data (*see* **Note 13**).

A wide variety of potential DNA damaging agents have been tested using the Comet assay *(18)*. **Note 14** gives experimental conditions for a number of common DNA damaging agents used in the Comet assay (H_2O_2, nitric oxide donors, xanthine/xanthine oxidase, ionizing radiation, and UV-C radiation). Depending on the nature of the experiment, treatment may be at any temperature between 0 and 37°C. Treatment on ice or at 4°C is a convenient temperature to minimize cellular DNA repair. For all treatments, preliminary time course and dose–response experiments are required to establish the optimum reaction conditions and to ensure Comet measurements are in the linear range.

1. Single-cell suspensions or monolayers of cultured cells may be incubated with the damaging agent added directly to the growth medium or appropriate buffer. This is suitable if extended treatment times are required. The disadvantage of this method is that it takes up to 20 min for the slides to be prepared, during which repair or further strand breakage can occur, before the slides can be placed in lysis mixture.

2. Cells may be treated after they have been embedded in the agarose on the slide. Slides without coverslips may be submerged in buffer containing the test agent. Alternatively, 100 µL of buffer with the damaging agent may be overlaid on the agarose, left for 10–15 s to permeate, and a coverslip added. We calculate the concentration of damaging agent, assuming a total volume of 225 µL taking into account the volume of the agarose layers (100 µL + 45 µL + 80 µL). Caution must be taken to ensure that the agarose does not dry out. All incubations should be performed in a humidified atmosphere (we typically use a black box with slides suspended on racks over moistened tissue) or sufficient buffer applied throughout the treatment. The advantage of treating cells on the slides is that it is possible to obtain time courses for rapid processes, such as repair of ionizing radiation-induced or oxidative DNA damage.

3.4. Standard assay for single strand breaks

This method is suitable for investigating the induction and repair of single strand breaks following treatment with a DNA damaging agent, or for detecting endogenous levels of strand breakage (*see* **Note 15**).

Damaging agents such as ionizing radiation, H_2O_2, xanthine/xanthine oxidase, and nitric oxide donors are capable of producing DNA strand breaks directly. Initial levels of damage are detected immediately after treatment. Repair is typically rapid and completed within 15–60 min. For these reasons cells embedded in agarose should be treated on the slide with the damaging agent suspended in suitable medium or buffer.

A typical assay of 16 slides will consist of 8 different treatments (including controls) performed in duplicate.

1. For detecting initial levels of damage, after treatment, coverslips are removed and one set of control and treated slides lysed immediately by gently lowering a staining rack into a trough containing 150 mL of lysis mixture (4°C). For lysis, slides are held for at least 1 h at 4°C. Although slides may tolerate lysis at 4°C overnight we would recommend a minimum of 1 h and a maximum of 6 h. This facilitates rapid repair studies, as cells incubated for 0–4 h may be lysed and analyzed in a single experiment.
2. For repair, slides are washed 3× by gently lowering a staining rack into a trough containing 150 mL of medium at 4°C (without damaging agent). Slides are over laid with 100 mL of medium, a coverslip added, and incubated for 0–4 h as required in a dark, humidified atmosphere at 37°C.
3. At the specified time, coverslips are removed from duplicate slides containing cells that have undergone repair and the slides placed in the same lysis mixture as described in **Subheading 3.4.1**. After the last slides have been placed in lysis incubate at 4°C for a further 1 h.
4. Slides are drained by carefully blotting their sides on tissue and placed on the gel shelf in the electrophoresis box so that the agarose layer is positioned toward the

anode (we use two rows of eight slides). Slides should be placed close together and all spaces filled with blanks to prevent any movement.
5. A volume of electrophoresis buffer at the correct temperature (*see* **Note 16**) is gently added to just cover the slides (*see* **Note 17**). The slides are incubated for a fixed period for unwinding (we use typically 40 min; *see* **Note 16**).
6. Electrophoresis. An electric current is applied (we use 20 V/24 min).
7. Remove some electrophoresis buffer by suction. Gently remove the slides and place them on a staining tray. Gently rinse with neutralizing buffer, stand for 5 min, drain, and repeat twice.
8. Place 35 µL of ethidium bromide solution on the surface of the agarose of each slide and add a coverslip.
9. Score slides as soon as possible. For storage, place slides at 4°C in the dark over moist tissue in a closed box (*see* **Note 18**).

3.5. Comet Assay for Detecting Endogenous Levels of Oxidative DNA Damage

Freshly isolated mononuclear cells exhibit little or no single strand breakage in the standard Comet assay as described in **Subheading 3.4**. However, low steady-state levels of oxidized purines and pyrimidine bases can be detected using Endo III and FPG repair enzymes.

A typical assay will consist of samples from four donors. Each sample must be incubated both with and without enzyme, giving two sets of duplicate slides for each donor.

1. Slides are prepared as outlined in **Subheading 3.2.** and lysed immediately.
2. After lysis the slides are drained by carefully blotting their sides on tissue and washed by placing in a fresh staining trough containing 150 mL of enzyme buffer at 4°C for 5 min. Replace the buffer and repeat twice.
3. Slides are drained and placed on a tray. Add 50 µL of diluted enzyme (*see* **Note 19**) to the surface of the agarose and add a coverslip to spread the enzyme solution uniformly. Each set of duplicate slides treated with enzyme must have as a control, duplicate slides treated with buffer minus enzyme. Incubate for 1 h at 37°C in a dark humidified atmosphere.
4. Place the slides in the gel box and add electrophoresis buffer to stop enzyme activity. For detection of enzyme-sensitive sites, we normally omit the unwinding step and apply electrophoresis immediately. However, for detecting low levels of endogenous oxidative damage it may be advantageous to retain an unwinding step to increase the sensitivity of the assay.
5. Electrophoresis and subsequent steps are as described in **Subheading 3.4.6**.

3.6. Repair of Oxidative Base Damage

The rate of repair of oxidative base damage can also be determined using either Endo III or FPG. In this protocol sufficient controls are required to take into account levels of endogenous damage (untreated cells with enzyme) and

the formation of single-stranded breaks (treated cells without enzyme). Consequently, untreated and damaged cells incubated with or without enzyme are required for each time point. The yield of enzyme sensitive sites (ESS) is calculated from increase in Comet length as follows:

$$\text{ESS} = [(\text{treated cells with enzyme}) - (\text{treated cells without enzyme})] - [(\text{untreated cells with enzyme}) - (\text{untreated cells without enzyme})]. \quad (1)$$

A typical assay will consist of 16 slides from a single donor, duplicate control slides incubated with and without enzyme, and three sets of duplicate slides treated with the same concentration or dose of damaging agent and incubated with and without enzyme for defined times.

1. Prepare slides as outlined in **Subheading 3.2**.
2. Treat with DNA damaging agent on the slide over ice to minimize cellular repair of damage.
3. To establish initial levels of damage immediately place duplicate control and treated slides into lysis mixture.
4. For repair, wash remaining slides 3× with 150 mL of medium (without damaging agent), and add 100 µL of medium and a coverslip to the agarose layer.
5. Incubate and at defined time intervals place in same lysis mixture as described in **Subheading 3.6.3**.
6. After the last slides have been placed in lysis, incubate at 4°C for a further 1 h.
7. Subsequent steps are as described in **Subheading 3.5.2**.

3.7. Measuring Rates of Overall Excision Repair

This assay makes use of the cell's own DNA repair capacity to reveal DNA damage. Rates of excision repair can be established by incubating cells with inhibitors of DNA resynthesis either immediately or at later times after treatment with a DNA damaging agent. It is particularly suitable for studies using agents such UV-C radiation which, at the doses used in the Comet assay, do not produce detectable levels of direct strand breaks.

A typical assay will consist of 16 slides from a single donor, duplicate control slides, and seven sets of duplicate slides treated with the same concentration or dose of damaging agent and incubated at defined time periods for repair.

1. Prepare slides as outlined in **Subheading 3.2**.
2. Remove coverslip and UV-irradiate cells embedded in agarose (*see* **Note 12**).
3. For initial rate of excision repair overlay duplicate control and treated slides with 100 µL of medium containing 100 µ*M* cytosine arabinoside and 10 m*M* hydroxyurea. Incubate for 1 h in a humidified atmosphere at 37°C and transfer to lysis mixture at 4°C (*see* **Note 20**).
4. To follow the progress of repair overlay remaining slides with 100 µL of medium without cytosine arabinoside and hydroxyurea and incubate at 37°C for various times up to 4 h.

5. As required, carefully drain duplicate slides and overlay agarose with 100 µL containing 100 µ*M* cytosine arabinoside and 10 m*M* hydroxyurea. Incubate for a further 1 h in a humidified atmosphere at 37°C.
6. After 1 h, transfer slides treated with inhibitor to the same lysis mixture as described in **Subheading 3.7.3**.
7. After the last slides have been placed in lysis mixture incubate at 4°C for a further 1 h.
8. Subsequent steps are as described in **Subheading 3.4.4**.

3.8. Scoring

1. Remove the slides from the storage box, wipe dry and allow to warm to room temperature to avoid condensation.
2. Identify fields containing Comets under the microscope and score, either using an image analysis system, or assigning Comets to arbitrary categories (*see* **Note 21**).

3.9. Interpretation and Analysis

1. There is extensive discussion over the most appropriate parameter to score in the Comet assay, whether tail length is adequate, or whether tail moment or a related function is more appropriate. In our experience, and in most cases, the parameter chosen makes almost no difference.
2. There has also been debate on the statistical distribution of tail moment and other parameters. It is not difficult to show that Comet parameters are not normally distributed, but statistical analysis should be based on the consistency of repeat determinations and experiments, where distribution of individual Comet measurements will be far less critical.
3. Nevertheless, variation in levels of damage between Comets on the same slide may be a useful indicator of the nature of the damaging event and it is desirable to keep a record of this information.
4. Results are typically expressed as mean Comet length (or tail moment) or increase or decrease in this parameter over untreated controls. These are arbitrary units of DNA damage or repair. It is possible, with caution, to calibrate the number of strand breaks against a known damaging agent, such as ionizing radiation
5. In our view the important issues are (1) design of a study with an adequate number of subjects or observations; (2) repetition of experiments; (3) preparation and disaggregation of the cells; and (4) consistency in scoring procedures.

4. Notes

1. A procedure for using standard clear slides and precoating them with agarose is available ***(29)***.
2. Other DNA stains can be used, for instance DAPI ***(17)*** or YOYO-1 ***(30)***. Ethidium bromide or propidium iodide are bright and show good stability.
3. Other systems include Perceptive Instruments (Little Yeldham, Essex, UK). It is possible to obtain reasonably good quantitation without image analysis, by placing nuclei into categories according to the extent of damage ***(31)***.

4. The predominant nucleated cells in whole blood are likely to be polymorphonuclear leukocytes, especially neutrophils. We have found that these give informative results in the Comet assay and have not found undue difficulties arising from the presence of red blood cells in the preparation ***(10)***.
5. The predominant cells in the mononuclear fraction are T cells (about 70%), with about 10% B cells and the remainder mainly monocytes.
6. This procedure can be scaled down using Eppendorf tubes to provide MNCs from 50–100 µL blood samples obtained from finger pricks.
7. After cryopreservation, mononuclear cells should be incubated at least overnight but not longer than 48 h before use.
8. It is necessary to limit division; otherwise cell growth will dilute out unrepaired damage and give the appearance of repair. A similar difficulty would arise with activated lymphocytes.
9. Although other concentrations of agarose may be used, those specified are firm enough to withstand multiple application and removal of coverslips.
10. If cells are suspended in LMP agarose that was made up in their normal culture medium, they can be treated and incubated for at least several hours. Agarose made up in PBS is satisfactory if cells are to be used immediately, but damage accumulates if the cells are incubated on the slide. It is possible to make up both agarose layers with medium.
11. A common difficulty is detachment of the bottom agarose layer from the slide. The most important precaution to avoid this is to ensure that the agarose is added to a warm slide, so that it spreads completely before it sets. It is also necessary to be sure to leave the slides long enough over ice for the agarose to set. A final remedy is to increase the concentration of agarose in the bottom layer (we now use 1% and 0.7% agarose concentrations, whereas we originally used 0.5% in both layers).
12. In warm humid weather we have found a problem with damage in controls that we attribute to condensation on the surface of the agarose. We normally obtain acceptable results by minimizing the time that the coverslip is removed from the slide.
13. In monitoring human populations for levels of background damage, results may influenced by such factors as the time of day that the sample is taken, or what the subject has recently eaten ***(10)***, exercise ***(13)***, smoking ***(14)***, and medication. Such factors must be defined as carefully as possible. It is strongly recommended that any study should include taking repeat samples from each subject.
14. Example treatments: 0.25–10 Gy of ionizing radiation, cells irradiated on slides without coverslips; 0.1–2.5 J/m^2 UV-C (254 nm) radiation, coverslips need to be removed and care must be taken to ensure that there are no photosensitisers or UV-absorbent compounds in the medium (e.g., phenol red); 10–300 m*M* H_2O_2, added in solution with a coverslip on ice for 0–10 min; 50 µ*M*–0.1 U/mL xanthine–xanthine oxidase, added as a solution with a coverslip and incubated at 37°C for 1 h. 1 m*M* *S*-Nitrosoglutathione is added as a solution with a coverslip to cells embedded in agarose or added to medium of cultured cells and incubated for 30 min to 24 h.

15. In addition to single-stranded breaks, the alkaline Comet assay may also detect alkali-labile sites. The nature of these sites has not been well defined and there is some controversy whether the conditions used are sufficiently alkaline for their detection.
16. We use electrophoresis buffer at 15°C, but any temperature between 4°C and room temperature is feasible, provided that the same temperature is used in each experiment. Again, another "unwinding time" can be chosen, provided that the same time is used throughout. We find that 40 min gives greatest sensitivity, without undue damage in controls. The time should be shortened if it is necessary to make the assay more robust.
17. Make sure that the shelf of the gel box is completely horizontal, otherwise migration of DNA will be affected by the position of the slide within the gel box.
18. Slides can also be dried and stored indefinitely. Omit the staining step. Remove the coverslip and leave on the bench overnight. To score the slides, add 100 µL of PBS and a coverslip. Leave for 2 h at room temperature. Remove the coverslip, add 35 µL ethidium bromide staining solution, replace the coverslip, and score.
19. Optimum concentration of each enzyme will need to be determined in trials to ensure that saturating conditions are applied.
20. Addition of inhibitor is essential to *see* excision breaks with normal human fibroblasts following treatments such as ultraviolet irradiation. We have not found it necessary to *see* strand breakage by reactive oxygen species in human islets of Langerhans. Freshly isolated human lymphocytes have extremely low deoxyribonucleotide pools and show delayed strand rejoining without the need to add any inhibitor. In this case, breaks represent transient repair intermediates ***(32)***.
21. To avoid bias, it is essential to set out in advance rules for accepting or rejecting Comets for scoring. Our strategy is to accept unless there are specific grounds for rejection. We reject Comets close to the edge of the slide, Comets grossly out of focus, and overlapping Comets that cannot readily be separated.

Acknowledgments

The work on which these protocols have been based was funded in part by the EC (ENV4-CT95-0174).

References

1. Vijg, J., Mullaart, E., and Boerrigter, M. E. T. I. (1990) Changes in DNA repair and its influence on genotoxicity, in *Basic Science in Toxicology* (Volans, G. N. [J. S.], Sullivan, F. M., and Turner, P., eds.), Taylor and Francis, London, pp. 390–403.
2. Davies, K. J. A. (1995) Oxidative stress — the paradox of aerobic life. *Biochem. Soc. Symp.* **61,** 1–31.
3. Halliwell, B. and Aruoma, O. I. (1993) *DNA and Free Radicals*. Ellis Horwood, Chichester, England.
4. Robbins, J. H., Polinsky, R. J., and Moshell, A. N. (1983) Evidence that lack of deoxyribonucleic acid repair causes death of neurons in xeroderma pigmentosum. *Ann. Neurol.* **13,** 682–684.

5. Gatti, R. A. and Swift, M. (1985) *Ataxia–Telangiectasia. Genetics, Neuropathology, and Immunology of a Degenerative Disease of Childhood*, Alan R. Liss, New York.
6. Orgel, L. E. (1963) The maintenance of the accuracy of protein synthesis and its relevance to ageing. *Proc. Natl. Acad. Sci. USA* **49,** 517–521.
7. Arlett, C. F., Lowe, J. E., Harcourt, S. A., Waugh, A. P. W., Cole, J., Roza, L., Diffey, B. L., Mori, T., Nikaido, O., and Green, M. H. L. (1993) Hypersensitivity of human lymphocytes to UV-B and solar irradiation. *Cancer Res.* **53,** 609–614.
8. Clingen, P. H., Arlett, C. F., Harcourt, S. A., Waugh, A. P. W., Lowe, J. E., Hermanova, N., Cole, J., Green, M. H. L., Roza, L., Mori, T., and Nikaido, O. (1995) Correlation of UVC and UVB cytotoxicity with the induction of specific photoproducts in T-lymphocytes and fibroblasts from normal human donors. *Photochem. Photobiol.* **61,** 163–170.
9. Tice, R. R. and Strauss, G. H. S. (1995) The single-cell gel-electrophoresis comet assay — a potential tool for detecting radiation-induced DNA-damage in humans. *Stem Cells* **13,** 207–214.
10. Green, M. H. L., Lowe, J. E., Waugh, A. P. W., Aldridge, K. E., Cole, J., and Arlett, C. F. (1994) Effect of diet and vitamin C on DNA strand breakage in freshly isolated human white blood cells. *Mutat. Res.* **316,** 91–102.
11. Henderson, L., Wolfreys, A., Fedyk, J., Bourner, G., and Windebank, S. (1998) The ability of the Comet assay to discriminate between genotoxins and cytotoxins. *Mutagenesis* **13,** 89–94.
12. Delaney, C. A., Green, M. H. L., Lowe, J. E., and Green, I. C. (1993) Endogenous nitric oxide induced by interleukin-1β in rat islets of Langerhans and HIT-T15 cells causes significant DNA damage as measured by the "comet" assay. *FEBS Lett.* **333,** 291–295.
13. Hartmann, A., Plappert, U., Raddatz, K., Grünert-Fuchs, M., and Speit, G. (1994) Does physical activity induce DNA damage? *Mutagenesis* **9,** 269–272.
14. Betti, C., Davini, T., Gianessi, L., Loprieno, N., and Barale, R. (1994) Microgel electrophoresis assay (comet test) and SCE analysis in human lymphocytes from 100 normal subjects. *Mutat. Res.* **307,** 323–334.
15. Piperakis, S. M., Visvardis, E. E., Sagnou, M., and Tassiou, A. M. (1998) Effects of smoking and aging on oxidative DNA damage of human lymphocytes. *Carcinogenesis* **19,** 695–698.
16. Singh, N. P., McCoy, M. T., Tice, R. R., and Schneider, E. L. (1988) A simple technique for quantitation of low level of DNA damage in individual cells. *Exp. Cell Res.* **175,** 184–191.
17. Collins, A. R., Duthie, S. J., and Dobson, V. L. (1993) Direct enzymatic detection of endogenous oxidative base damage in human lymphocyte DNA. *Carcinogenesis* **14,** 1733–1735.
18. McKelvey-Martin, V. J., Green, M. H. L., Schmezer, P., Pool-Zobel, B. L., De Meo, M. P., and Collins, A. (1993) The single cell gel electrophoresis (SCGE) assay (Comet assay): a European review. *Mutat. Res.* **288,** 47–63.
19. Fairbairn, D. W., Olive, P. L., and O'Neill, K. L. (1995) The comet assay: a comprehensive review. *Mutat. Res.* **339,** 37–59.

20. Collins, A., Dusinska, M., Franklin, M., Somorovska, M., Petrovska, H., Duthie, S., Fillion, L., Panayiotidis, M., Raslova, K., and Vaughan, N. (1997) Comet assay in human biomonitoring studies: reliability, validation, and applications. *Env. Molec. Mutagenesis* **30,** 139–146.
21. Green, M. H. L., Lowe, J. E., Delaney, C. A., and Green, I. C. (1996) Comet assay to detect nitric oxide-dependent DNA damage in mammalian cells. *Methods Enzymol.* **269,** 243–266.
22. Thomas, S., Green, M. H. L., Lowe, J. E., and Green, I. C. (1997) Measurement of DNA damage using the Comet assay (Chapter 29), in *Nitric Oxide Protocols* (Titheradge, M., ed.), Humana Press, Totowa, NJ, pp. 301–309.
23. Collins, A. R., Dobson, V. L., Dusinska, M., Kennedy, G., and Stetina, R. (1997) The comet assay: what can it really tell us? *Mutat. Res.* **375,** 183–193.
24. Woollons, A., Clingen, P. H., Price, M. L., Arlett, C. F., and Green, M. H. L. (1997) Induction of mutagenic DNA damage in human fibroblasts after exposure to artificial tanning lamps. *Br. J. Dermatol.* **137,** 687–692.
25. Boiteux, S., O'Connor, T. R., and Laval, J. (1987) Formamidopyrimidine-DNA glycosylase of *Escherichia coli*: cloning and sequencing of the *fpg* structural gene and overproduction of the protein. *EMBO J.* **6,** 3177–3183.
26. Dusinska, M. and Collins, A. (1996) Detection of oxidized purines and UV-induced photoproducts in DNA of single cells by inclusion of lesion-specific enzymes in the comet assay. *ATLA* **24,** 405–411.
27. Duthie, S. J. and McMillan, P. (1997) Uracil misincorporation in human DNA detected using single cell gel electrophoresis. *Carcinogenesis* **18,** 1709–1714.
28. Cole, J. and Arlett, C. F. (1984) The detection of gene mutations in cultured mammalian cells, in *Mutagenicity Testing — A Practical Approach* (Titheradge, M., Venitt, S., and Parry, J. M., eds.), IRL Press, Oxford, pp. 233–273.
29. Klaude, M., Eriksson, S., Nygren, J., and Ahnstrom, G. (1996) The Comet assay—mechanisms and technical considerations. *Mutat. Res.* **363,** 89–96.
30. Singh, N. P., Graham, M. M., Singh, V., and Khan A. (1995) Induction of DNA single-strand breaks in human-lymphocytes by low-doses of γ-rays. *Int. J. Radiat. Biol.* **68,** 563–569.
31. Collins, A. R., Fleming, I. A., and Gedik, C. M. (1994) In vitro repair of oxidative and ultraviolet-induced DNA damage in supercoiled nucleoid DNA by human cell extract. *Biochim. Biophys. Acta* **1219,** 724–727.
32. Green, M. H. L., Waugh, A. P. W., Lowe, J. E., Harcourt, S. A., Cole, J., and Arlett, C. F. (1994) Effect of deoxyribonucleosides on the hypersensitivity of human peripheral blood lymphocytes to UV-B and UV-C irradiation. *Mutat. Res.* **315,** 25–32.

11

Measurement of DNA Damage and Repair in Human White Blood Cells by an Immunochemical Assay

Govert P. van der Schans

1. Introduction

DNA is the most important target molecule for cell killing or the induction of cellular damage by chemical or physical agents. Cell killing depends on the type and amount of damage induced. Exposure to physical or chemical agents can induce a large variety of lesions in DNA: single- and double-stranded breaks, as well as damage to the bases and sugar residues (not leading to a break). It is important to be able to quantify the different types of DNA damage to obtain information about their persistence. The latter may attribute to our understanding of how the various lesions are involved in cell death and/or mutation induction.

Several methods are currently used to quantify single-stranded breaks in cellular DNA. The immunochemical assay, introduced by us ***(1,2)*** for the determination of single-stranded breaks, is based on the application of monoclonal antibodies directed against single-stranded DNA. In fact it is a combination of the so-called unwinding assay with an immunochemical quantification of the single-stranded DNA formed upon unwinding. The principle of the method is that DNA starts to unwind—under strictly controlled alkaline conditions—at each (double- and single-) strand break (and at each lesion converted into such breaks in alkaline medium), resulting in a long stretch of single-stranded DNA (ssDNA) to which the antibody can bind. The amount of single-stranded DNA is a measure for the amount of breaks. With this method the amount of damage induced by ionizing radiation in DNA in cells of human blood can be detected

This chapter represents Part of a European patent request, No. 93201672. 8 (10 June 1993) entitled: "Method for detecting single-strand breaks in DNA," by G. P. van der Schans.

From: *Methods in Molecular Medicine*, Vol. 38: *Aging Methods and Protocols*
Edited by: Y. A. Barnett and C. R. Barnett

within 1 h, after doses as low as 0.2 Gy. The precoating of microtiter plates with anti-ssDNA antibody enables the detection of ssDNA fragments directly in alkali-treated blood samples. Prelabeling and isolation of the nucleated cells from the blood is not necessary. Only a few microliters of blood is required and the assay can be applied simultaneously on a large number of samples.

The method is also applicable to other cell types that can be obtained in suspension and can be applied in a large variety of studies on induction and repair of damage, including that on aging ***(3)***.

A special application is that on sperm cells ***(4)***. Because in these cells the DNA is rather tightly packed the alkaline treatment conditions have to be modified to release the DNA. Owing to the absence of any repair in these cells an accumulation of (oxidative) damage occurs, resulting in a background level of single-stranded breaks corresponding to that induced by 50–200 Gy γ-rays.

2. Materials

2.1. Preparation of DNA Samples (Somatic Cells)

1. Blood collected in evacuated glass tubes containing EDTA.
2. RPMI 1640 culture medium containing 10% fetal calf serum.
3. Cultured mammalian cells.
4. MQ-water: Demineralized water purified further by filtration through a Milli-Q filter (class 1 according to ISO 3696).
5. 1 *M* NaOH solution: Dissolve 3.93 g of NaOH (in tablet form) in (by weighing) 98 g of MQ-water (or proportionally other amounts) in a 100-mL medium flask. Close with two tissues of parafilm covered with a loosely tightened screwcap. Can be stored at room temperature for 2 mo.
6. 1.3 *M* NaCl solution: Dissolve 38.0 g of NaCl in MQ-water and fill up to 500 mL. Can be stored at room temperature for 2 mo.
7. Alkali solution: Add 2.00 mL of 1 *M* NaOH or 2.50 mL of 1 *M* NaOH to 103 g of a 1.3 *M* NaCl solution (calculated pH 12.3 or 12.4, respectively). Prepare on the day of use.
8. 0.25 *M* NaH_2PO_4 solution: Dissolve 8.63 g of $NaH_2PO_4 \cdot H_2O$ in MQ-water and fill up to 250 mL.
9. Polystyrene cluster tubes, Costar, cat. no. 4408.
10. Polystyrene tubes with cap, 12.4/75 mm, Greiner, no. 120161.
11. 1.5-mL Eppendorf tubes.
12. Pipet tips (white opaque), 1–200 µL, Costar, no. 4862 (*see* **Note 2**).
13. Pipet tips (blue), 100–1000 µL, Eppendorf, no. 0030 015.002.
14. Pipets, P100, P200 and P1000, Gilson.
15. 12-Channel pipet, 25–200 µL; Micronic (Macap) cat. no. 200–12.
16. Sonicator/cell disruptor, Ultrasonics, W370 with microtip.
17. Humidified incubator of 37°C.
18. Reaction tube mixers, Vibrofix, IKA, model VF1.

2.2. Preparation of DNA Samples (Spermatozoa)

1. Spermatozoa, diluted ejaculates delivered in straws containing 5–25 × 10^6 sperm cells in 200-µL aliquots, fresh or frozen in liquid nitrogen.
2. 10× Phosphate-buffered saline (PBS) solution: 81.8 g of NaCl, 14.4 g of $Na_2HPO_4 \cdot 2H_2O$, 2.0 g of KH_2PO_4, and 1.9 g of KCl in 1 L MQ-water. Check the pH; it should be between 7.0 and 7.4. Can be stored at room temperature for 2 mo.
3. PBS solution: Add to a 10-L polythene vial, with valve, 9 L of MQ-water and 1 L of 10× PBS, and mix thoroughly.
4. Solution A: 732 µL of 10% Triton X-100 in MQ-water, 879 µL of dithiothreitol of 200 mg/mL MQ-water (freshly prepared), 2.77 mL of 1 *M* NaOH, and 65.4 mL of 2 *M* urea (freshly prepared).
5. 0.25 *M* NaH_2PO_4 solution: Dissolve 8.63 g of $NaH_2PO_4 \cdot H_2O$ in MQ-water and fill up to 250 mL.
6. 1.5-mL Eppendorf tubes.
7. Polystyrene round-bottom tubes, 6.5 mL, Greiner, no. 151101.
8. Pipet tips (white opaque), 1–200 µL, Costar, no. 4862 (*see* **Note 2**).
9. Pipet tips (blue), 100–1000 µL, Eppendorf, no. 0030 015.002.
10. Pipets, P100, P200, and P1000, Gilson.
11. Sonicator/cell disruptor, Ultrasonics, W370 with microtip.
12. Humidified incubator of 37°C.

2.3. Coating of the Microtiter Plates

1. Tween-20 (polyoxyethylenesorbitan): Sigma cat. no. P-1379.
2. 10× PBS solution: 81.8 g of NaCl, 14.4 g of $Na_2HPO_4.2H_2O$, 2.0 g of KH_2PO_4, and 1.9 g of KCl in 1 L of MQ-water. Check the pH, which should be between 7.0 and 7.4. Can be stored at room temperature for 2 mo.
3. PBS solution: Add to a 10-L polyethylene vial, with valve, 9 L of MQ-water and 1 L of 10× PBS, and mix thoroughly.
4. Na-PBS: Buffered NaCl solution (NPBI bv, Emmer-Compascuum, The Netherlands, 8.2 g of NaCl, 1.9 g of $Na_2HPO_4, 2H_2O$, and 0.3 g of $NaH_2PO_4 \cdot 2H_2O$ per liter, pH 7.4, 500 mL, sterile).
5. D1B monoclonal antibodies: Dilute D1B monoclonal antibodies prepared and purified as described elsewhere ***(1,2)***, to a concentration of 10 µg/mL in Na-PBS (*see* **Note 10**). Prepare this solution no sooner than 1 h before use.
6. PT: Add to a 25-L polyethylene flask, with valve, 18 L of MQ-water, 2 L of 10× PBS, and 10 g of Tween-20, and mix thoroughly.
7. Fetal calf serum (FCS): Gibco-BRL, cat. no. 10106–110, stored at –20°C in 500-mL flasks.
8. Heat-inactivated FCS (hiFCS): Thaw a 500-mL flask with FCS in a 37°C water bath. Divide under sterile conditions (in a laminar flow cabinet) in 30-mL flasks and/or 50 10-mL polystyrene tubes with cap. Incubate all flasks and tubes for 0.5 h in a 56°C water bath. Place in refrigerator. Can be stored for 2 mo (2–8°C).
9. PT + 5% hiFCS: Dilute hiFCS with PT in a ratio of 1 mL of hiFCS and 19 mL PT. Prepare this solution no sooner than 1 h before use.

10. High-binding polystyrene microtiter plates, Costar, 96-well, cat. no. 3590/9018.
11. Pipet tips (white opaque), 1–200 µL, Costar, no. 4862.
12. Pipet tips (blue), 100–1000 µL, Eppendorf, no. 0030 015.002.
13. Pipets, P100, P200, and P1000, Gilson.
14. 12-Channel pipet, 25–200 µL; Micronic (Macap) cat. no. 200–12.
15. 96-Well dispenser, Transtar 96, adjustable volume, cat. no. 7605 and Transtar elevator cat. no. 7606, Costar.
16. Plate washer, Skanwasher 300, Skatron.
17. 12-Channel handplate washer, with tube connected to a polypropylene flask with PT.
18. Plate vibrators, Titertek (Flow) and IKA (model MTS4).

2.4. Sandwich Enzyme-Linked Immunosorbent Assay (ELISA)

1. 1 *M* NaOH solution: Dissolve 3.93 g of NaOH (in tablet form) in (by weighing) 98 g MQ-water (or proportionally other amounts) in a 100-mL medium flask. Close with two tissues of parafilm covered with a loosely tightened screwcap. Can be stored at room temperature for 2 mo.
2. 1.3 *M* NaCl solution: Dissolve 38.0 g of NaCl in MQ-water and fill up to 500 mL. Can be stored at room temperature for 2 mo.
3. Alkali-solution: Add 2.00 mL of 1 *M* NaOH to 103 g of a 1.3 *M* NaCl solution (calculated pH 12.3).
4. Tween-20 (polyoxyethylenesorbitan): Sigma cat. no. P-1379.
5. 10× PBS solution: 81.8 g of NaCl, 14.4 g of $Na_2HPO_4.2H_2O$, 2.0 g of KH_2PO_4, and 1.9 g of KCl in 1 L of MQ-water. Check the pH, which should be between 7.0 and 7.4. Can be stored at room temperature for 2 mo.
6. PBS solution: Add to a 10-L polyethylene vial, with valve, 9 L of MQ-water and 1 L of 10× PBS, and mix thoroughly.
7. PT: Add to a 25-L polyethylene flask, with valve, 18 L of MQ-water, 2 L of 10× PBS, and 10 g of Tween-20, and mix thoroughly.
8. FCS: Gibco-BRL, cat. no. 10106–110, stored at –20°C in 500-mL flasks.
9. hiFCS: Thaw a 500-mL flask with FCS in a 37°C water bath. Divide under sterile conditions (in a laminar flow cabinet) in 30-mL flasks and/or 50 10-mL polystyrene tubes with cap. Incubate all flasks and tubes for 0.5 h in a 56°C water bath. Place in refrigerator. Can be stored for 2 mo (2–8°C).
10. Sodium dodecyl sulfate (SDS): Sigma, cat. no. L-4509.
11. 10% SDS solution: Dissolve 10 g of SDS in 100 mL of MQ-water. Can be stored at room temperature for 2 mo.
12. PT + 0.05% SDS + 5% hiFCS: Make up solution of PT, hiFCS, and 10% SDS in the ratio of 1 mL of hiFCS, 19 mL of PT, and 100 µL of 10% SDS. Prepare this solution no sooner than 1 h before use.
13. D1B-AP conjugate: Dilute D1B-AP conjugate, prepared as described elsewhere ***(2)***, to the optimal prescribed dilution (1000–40,000×; *see* **Notes 4** and **10**) in PT + 0.05% SDS + 5% hiFCS. Prepare this solution no sooner than 1 h before use.

14. 0.1 *M* $MgCl_2$ solution: Dissolve 2.03 g of $MgCl_2 \cdot 6H_2O$ in 100 mL of MQ-water.
15. Reaction buffer: Dissolve 5.26 g of diethylamine (DEA) in 5 L of MQ-water and add 50 mL of 0.1 *M* $MgCl_2$, adjust pH to 9.8, and divide over ten 500-mL flasks. Can be stored for 6 mo in the cold room. Before use, raise the temperature to room temperature. Check the pH (at room temperature) and, if needed, adjust the pH to 9.8. After use place the flask back in the refrigerator.
16. 4-methylumbelliferyl phosphate (MUP) dilithium salt·$3H_2O$: Boehringer, cat. no. 405 663, check expiration date. Mol wt: 322.1. Store in the dark at –20°C.
17. MUP stock solution: Dissolve the whole contents of a flask of MUP (approx 250 mg net weight by back weighing) in reaction buffer, pH 9.8, in **clean glassware** at a concentration of 20 m*M* (6.44 mg/mL), and divide into 1-mL portions in 1.5-mL Eppendorf tubes (with cap) and store at –20°C. Can be stored for 6 mo (in the dark).
18. MUP solution: Thaw the required amount of MUP stock solution and dilute 1:100 in reaction buffer, pH 9.8. The remaining MUP stock solution can be placed back in the freezer, marked with ink pen. Prepare this solution no sooner than 2 h before use.
19. Pipet tips (white opaque), 1–200 µL, Costar, no. 4862 (*see* **Note 2**).
20. Pipet tips (blue), 100–1000 µL, Eppendorf, no. 0030 015.002.
21. Pipets, P100, P200, and P1000, Gilson.
22. 12-Channel pipet, 25–200 µL; Micronic (Macap) cat. no. 200-12.
23. 96-Well dispenser, Transtar 96, adjustable volume, cat. no. 7605 and Transtar elevator cat. no. 7606, Costar.
24. Plate washer, Skanwasher 300, Skatron.
25. 12-Channel handplate washer, with tube connected to a polypropylene flask with PT.
26. Sonicator/cell disruptor, Ultrasonics, W370 with microtip.
27. Humidified incubator of 37°C.
28. Fluorescence microtiterplate reader, Cytofluor II (Perseptive Biosystems, Framingham, MA, USA).
29. Plate vibrators, Titertek (Flow) and IKA (model MTS4).
30. Reaction tube mixers, Vibrofix, IKA, model VF1.

3. Methods

3.1. Preparation of DNA Samples (Somatic Cells)

1. Cells (e.g., human total WBC) in 1 mL of blood are irradiated with 0, 1, 2 or 5 Gy ^{60}Co-rays at 0°C. (**Note:** Blood may contain infectious particles; wear appropriate protective devices.)
2. At yellow light, at 20 + 1°C (*see* **Note 1**): 200 µL of alkaline solution of pH 12.3 or 12.4 is added quickly, but avoiding shaking afterwards, to 30 µL of 10× diluted blood (diluted in RPMI 1640 + 10% FCS, or in PBS) on the bottom in a cluster tube (in 96-wells tray; *see* **Note 3**). The pH chosen depends on the extent of unwinding that is required.

3. Neutralize after 6 min with 35 µL of 250 m*M* NaH_2PO_4, added to the bottom of the tube.
4. Immediately after neutralization the solution is sonicated at 20°C (set at 2.5, duration 1 s).
5. The samples are used immediately for the ELISA, or stored at 4°C (approx 1 wk) or frozen (–20°C). Standing in cluster tubes at 4°C results in slow disappearance of ssDNA from the solution (adsorption to the wall?). Therefore, at later use, warm first to room temperature and sonicate before dilution.
6. The DNA samples (blood, other body cells, cultured cells) as such can be used in the sandwich ELISA. When samples are to be analyzed on the same day then store in the refrigerator (at 4°C) up to approx 1 h before use; otherwise, store samples at –20°C.

3.2. Preparation of DNA Samples (Spermatozoa)

1. Straws with frozen sperm are thawed at 37°C and sperm are pressed out in a 1.5-mL Eppendorf tube.
2. Immediately thereafter the cell suspension is mixed by pipetting and 20-µL aliquots are pipeted in triplicate into 1.5-mL Eppendorf tubes and placed on ice.
3. Within 2.5 h these samples are diluted 40× with PBS at 20°C.
4. In yellow light, at 20 ± 1°C, immediately after mixing by pipetting, 60-µL aliquots of the diluted samples are transferred in duplicate to 6.5-mL polystyrene round-bottom tubes.
5. 415 µL of solution A is added by running it along the wall of the tube and after 7 min (yellow light, 20°C) neutralized with 150 µL of 250 m*M* NaH_2PO_4, immediately followed by a brief sonication.
6. The samples are used immediately in the ELISA, or stored at 4°C (approx 1 wk). Standing in cluster tubes at 4°C results in slow disappearance of ssDNA from the solution (adsorption to the wall?). Therefore, at later use, warm first to room temperature and sonicate before dilution.

3.3. Coating of the Microtiter Plates

1. Add, to the 96-wells dispenser, 100 µL of the D1B-solution (10 µg of D1B/mL of Na-PBS) to a high-binding polystyrene microtiter plate.
2. Vibrate the plate for 10 min at room temperature (maximal 2 × 8 plates/vibrator).
3. Wash the plate 3× with PT buffer with a plate washer (as indicated in the "Wash Program Sheet") or with a hand plate washer.
4. Add with the 96-well dispenser 100 µL PT + 5% hiFCS per well.
5. Vibrate the plate for 10 min at room temperature (maximal 2 × 8 plates/vibrator).
6. Wash the plate once with PT buffer with the hand plate washer.
7. Stack the plates in groups of 10. Pack in aluminum foil and store at –20°C. (Write date on aluminum foil.) Coated plates can be stored 2 mo.
8. Before use place plates beside each other open on the table to equilibrate to room temperature (this equilibration process normally takes 10–60 min).

3.4. Sandwich ELISA

1. Make 100% ssDNA samples from an aliquot of the DNA samples to be assayed: Add, at room temperature, 25 µL of DNA sample to a cluster tube, and add 200 µL of a solution of 1.3 *M* NaCl + 0.02 *M* NaOH, pH 12.3. Shake for 1 s on a reaction tube mixer or sonicate (set at 2.5, duration 1 s), and neutralize with 25 µL of 0.25 *M* NaH_2PO_4. In the case of 100% ssDNA samples of sperm, these are always sonicated before neutralization.
2. Add to the first row of a D1B-coated "high-binding" polystyrene plate (with a 12-channel pipet) 120 µL PT and in all other rows 70 µL.
3. Place the samples in rows of 12, including the 100% ssDNA samples, according to the scheme prepared in advance.
4. Add of each sample (with a 12-channel pipet) 20 µL in a well of the first row of the plate. In the case of sperm DNA samples add the 20-µL aliquots with a single pipet.
5. Make 1:1 serial dilutions until the last row.
6. Add to wells 5–8 of the last row of each plate 140 pg of single-stranded DNA (intended to correct for plate-to-plate variations).
7. Incubate at room temperature under continuous vibration for at least 5 min (*see* **Note 7**, 2 × 8 plates/vibrator).
8. Wash 3× with PT buffer (hand wash apparatus or plate washer).
9. Add 100 µL of D1B-AP solution/well (with dispenser, use filter plate up to 200×, or with 12-channel pipet; *see* **Note 5**).
10. Incubate again at room temperature under continuous vibration for at least 5 min (up to 2 × 8 plates/vibrator).
11. Wash 3× with PT buffer (hand wash apparatus or plate washer). The last wash should be extensive and done using the hand wash apparatus (*see* **Notes 8** and **9**).
12. Add 100 µL of MUP solution/well (with dispenser or with 12-channel pipet).
13. Incubate for 1 h at 37°C in a humidified incubator (cover on plate, do not stack plates).
14. Read fluorescence in all wells (Cytofluore II, gain 45) and transfer data to a PC with lotus or excel spreadsheet (*see* **Note 6**).

3.5. Calculation of ssDNA Percentage

Provided limited amounts of DNA are used a linear relationship is obtained between the input amount of DNA and the level of fluorescence, both for completely and for partially single-stranded DNA. To calculate the fraction of single-strandedness in a particular sample, the ratio of the fluorescence of the DNA dilutions to that of the corresponding completely single-stranded DNA dilutions, both corrected for background fluorescence (fluorescence in wells without DNA), is divided by a factor of 10 (because of the predilution of the completely single-stranded DNA sample) according to the following formula:

$$\% \text{ single-strandedness} = \frac{(fl_{sample} - fl_{background})}{10 \times (fl_{100\%\ ss} - fl_{background})} \times 100\%$$

The calculations are carried out *only* for those dilutions for which a linear relationship is observed between the amount of DNA in the wells and the level of fluorescence. In daily practice, this holds for fluorescence values <1500. On the other hand values below 500 fluorescence units become less accurate. Therefore, the percentage of single-strandedness calculated for the highest amounts of DNA in the well with a fluorescence <1500 and for the lowest amounts of DNA in the well with a fluorescence >500. The average of the two data is considered as the most realistic one.

If none of the fluorescence values in a serial dilution falls within the required range then the computer program takes the value of the second dilution in the case of low fluorescence values and that of the sixth dilution in the case of high fluorescence values.

4. Notes

1. The use of an air-conditioned room at 20°C with yellow light is recommended for the alkaline treatment of the samples.
2. Use of pipet tips is recommended because of high precision in pipetting slightly viscous solutions.
3. If the use of cluster tubes causes difficulties (bad mixing), then, as an alternative, polystyrene round-bottom tubes (volume 6.5 mL) should be used. In that case 200 μL alkaline solution is added on top along the wall, to each tube separately).
4. The optimal dilution of a new batch of D1B-AP conjugate is assessed by comparing the optimal dilution with that of an old batch. The optimal dilution is the one that results in an almost equal fluorescence as obtained with the optimal dilution of the old batch. The optimal dilution is a compromise between an optimal fluorescence with respect to the range of the microtiter plate reader and the costs of the D1B-AP conjugate.
5. Owing to the fact that only a small part of the ssDNA fragment binds to the walls of the immobilized anti-ssDNA antibodies, enough antibody binding sites remain available to bind the same antibodies conjugated with alkaline phosphatase.
6. The computer program to be used depends on the purpose of the experiment. When samples are tested with a variable number of cells then it is preferred to have the 100% ssDNA samples on the same plate. The computer program directly calculates the % ssDNA of these samples.

   When the 100% ssDNA samples are not present on the same plate, then the corresponding computer program uses a fixed value for the 100% ssDNA samples, corrected only for possible plate-to-plate variations. The resulting percentages of ssDNA should be corrected for the real fluorescence values of the 100% ssDNA samples.
7. The time of incubation to adsorb the ssDNA to the D1B antibody is at least 5 min. The incubation period can be extended up to half an hour, but longer periods should not be used.

8. Sometimes the use of the plate washer, and/or the 96-well dispenser presents problems owing to (1) contamination of the washer with high amounts of D1B-AP and (2) contamination or leakage of the dispenser. In that case, the solutions should be added manually, with the 12-channel pipet, and the plates should be washed with the hand wash apparatus. The latter is preferred, at least for the last wash step before adding the reaction buffer.
9. Historically, before adding substrate in reaction buffer, the plates were washed once with 0.1 *M* diethanolamine, pH 9.8. Later on this step was omitted, as higher fluorescence values without substantial increase of the background fluorescence were obtained.
10. Both the required antibody, D1B, as well as its conjugate, D1B-AP, are made available on request to the author at a cost necessary to cover production, development, and shipment.

References

1. Van der Schans, G. P., Van Loon, A. A. W. M., Groenendijk, R. H., and Baan, R. A. (1989) Detection of DNA damage in cells exposed to ionizing radiation by use of anti-single-stranded-DNA monoclonal antibody. *Int. J. Radiat. Biol.* **55,** 747–760.
2. Timmerman, A. J., Mars-Groenendijk, R. H., Van der Schans, G. P., and Baan, R. A. (1995) A modified immunochemical assay for the detection of DNA damage in human white blood cells. *Mutat. Res.* **334,** 347–356.
3. King, C. M., Bristow-Craig, H. E., Gillespie, E. S., and Barnett, Y. A. (1995) In vivo antioxidant status, DNA damage, mutation and DNA repair capacity in cultured lymphocytes from healthy 75- to 80-year-old humans. *Mutat. Res.* **377,** 137–147.
4. Van der Schans, G. P. (1993) Method for detecting single-strand breaks in DNA. European patent request, no. 93201672.8, 10 June 1993.

12

Measurement of 8-Oxo-deoxyguanosine in Lymphocytes, Cultured Cells, and Tissue Samples by HPLC with Electrochemical Detection

Sharon G. Wood, Catherine M. Gedik, Nicholas J. Vaughan, and Andrew R. Collins

1. Introduction

8-Oxoguanine is one of the most studied base oxidation products found in DNA. It has potential biological significance, because if present in DNA that is replicating, it can lead to incorporation of adenine rather than cytosine in the daughter strand. Thus it is considered as a premutagenic lesion. It occurs as a result of attack by reactive oxygen species released during the inflammatory response, and in small but significant amounts during normal respiration. The hydroxyl ($^{\cdot}OH$) radical (arising from H_2O_2 by the transition metal ion-catalyzed Fenton reaction within the nucleus) is most likely responsible for the formation of 8-oxoguanine. Analytical methods—gas chromatography with mass spectrometric detection (GC–MS) and high-performance liquid chromatography (HPLC)—were developed for quantitation of oxidized bases produced in experimental studies of radiation and chemical damage to DNA, and these methods were naturally also applied to the measurement of *background* levels of oxidized bases in cellular DNA ***(1)***. With GC–MS, very high levels of 8-oxoguanine have been reported, typically between 10 and 100 for every 10^5 normal guanines. It has recently been recognized that spurious oxidation of DNA readily occurs during isolation and hydrolysis of DNA, and derivatization of the bases for analysis. HPLC, normally applied to measurement of the nucleoside, 8-oxo-deoxyguanosine (8-oxo-dG), has generally given values below those obtained with GC–MS; but with HPLC, too, oxidation artefacts have been identified. Currently much effort is going into reconciling the different approaches to the measurement of

From: *Methods in Molecular Medicine*, Vol. 38: *Aging Methods and Protocols*
Edited by: Y. A. Barnett and C. R. Barnett

oxidative DNA damage (GC–MS, HPLC, and various repair endonuclease-based DNA breakage assays), with some success. Most researchers in the field agree that a realistic figure for the background level of 8-oxo-dG in normal human cells is around 1 per 10^5 dGs, or even less.

One of the most popular hypotheses of aging is that oxidative damage to biomolecules accumulates, leading ultimately to dysfunction of proteins, membranes, and DNA replication and repair machinery. 8-Oxo-dG in DNA seems a reasonable and convenient biomarker for the process of aging. Here we describe the method that we have developed for the analysis of 8-oxo-dG by HPLC with electrochemical detection (HPLC–ECD) in cultured cells, lymphocytes, and tissues (though in human studies, the availability of tissue samples is obviously very limited). We have introduced modifications to limit oxidation in vitro—inclusion of various antioxidants and chelators during the preparation, storage, and hydrolysis of DNA, lowering the temperature and time of incubation with proteinase K, optimization of sample preparation for storage ***(2)***. The procedure described here gives the lowest levels of 8-oxo-dG in samples of rat liver.

2. Materials

1. Homogenization buffer: 10 m*M* Tris-HCl, 0.4 *M* NaCl, 5 m*M* deferoxamine mesylate (DF; Sigma, cat. no. D9533). Prepare in HPLC grade H_2O (Rathburn Chemicals, Walkerburn, Scotland). Adjust to pH 8.0 with dilute HCl. Make up to 1 L with water and freeze at –20°C as aliquots; cover containers in aluminum foil to protect from light (DF is unstable and light-sensitive, *see* **Note 1**). Just before use, thaw and add Triton X-100 (Sigma, cat. no. T9284) to 0.5%. Triton X-100 is viscous; to measure volume accurately, warm the Triton and use a plastic pipettor tip with the end cut off. Mix the solution very thoroughly.
2. 40 m*M* Tris-HCl buffer: Prepare in HPLC grade H_2O, adjusting to pH 8.5 with dilute HCl. Store as aliquots at –20°C.
3. Ribonuclease buffer: 10 m*M* Tris-HCl, 0.4 *M* NaCl; prepare in HPLC grade H_2O, adjusting to pH 8.0 with dilute HCl. Store at –20°C.
4. RNase T1 (ICN, cat. no. 101079) from *Aspergillus oryzae*: Powder, stored at –20°C. Add ribonuclease buffer to powder to give 10^3 U/mL. Aliquot into microcentrifuge tubes, put in 80°C water bath for 15 min (to destroy any contaminating DNases), and allow to cool slowly to room temperature. Store aliquots at –20°C (*see* **Note 2**).
5. RNase IIIA (Sigma, cat. no. R5125) from bovine pancreas: Powder, stored at –20°C. Prepare solution of 1 mg/mL in ribonuclease buffer. Aliquot into microcentrifuge tubes, put in 80°C water bath for 15 min, and allow to cool slowly to room temperature. Store at –20°C (*see* **Note 2**).
6. Proteinase K (Boehringer Mannheim, cat. no. 1373 196) from *Tritirachium album*: Supplied as solution ready for use. Store at 4°C.
7. Denley Spiramix 5 roller mixer.
8. Quartz Suprasil 150-µL microcuvet (Hellma, cat. no. 105.201-QS).

9. DNase 1 (Boehringer Mannheim, cat. no. 104132) from bovine pancreas: Store at –20°C. Supplied as a solid; dissolve 20,000 U in 4 mL of 40 m*M* Tris-HCl, pH 8.5 (i.e., 5 U/µL) and store as aliquots at –20°C (*see* **Note 2**).
10. Alkaline phosphatase from calf intestine (Boehringer Mannheim, cat. no. 1097075). Supplied at about 20 U/µL (varies between batches) in triethanolamine buffer. This stock should be kept at 4°C. Dilute to 0.25 U/µL with 40 m*M* Tris-HCl, pH 8.5, and store aliquots at –20°C. **Do not use the dephosphorylation buffer supplied because it contains EDTA which would remove the Mg^{2+} ions required for DNA hydrolysis** (*see* **Note 2**).
11. Phosphodiesterase II from calf spleen (Boehringer Mannheim, cat. no. 108251), supplied as 2 mg/mL suspension in ammonium sulfate solution. This stock should be stored at 4°C. Its activity is about 2 U/mg, that is, 4 U/mL; however, there is a 20% loss of activity in 6 mo. Dilute to 0.25 U/mL with 40 m*M* Tris-HCl, pH 8.5, and store aliquots at –20°C (*see* **Note 2**).
12. Phosphodiesterase I from *Crotalus durissus* (Boehringer Mannheim, cat. no. 108260), supplied in 50% glycerol, 1 mg in 0.5 mL, approx 1.5 U/mg or 3 U/mL. Store at 4°C. For use, dilute 3× in 40 m*M* Tris-HCl, pH 8.5 (dispense from the stock solution using sterile conditions).
13. Syringe filters with 0.2 mm pore size (Whatman, cat. no. 6777-0402).
14. HPLC hardware (isocratic system): We use Gilson 306 pump 10 washed self centering (wsc) pump head; Gilson 805 manometric module; Gynkotek GINA 50 cooling autosampler at 5°C.
15. HPLC columns: Guard column, Supelco pellicular 5 µm, 2 cm; analytical column, Capital Analytical ODS Apex 3 µm, 4.6 × 150 mm.
16. HPLC mobile phase: 50 m*M* Potassium phosphate, 8% methanol, pH 5.5. Mix 96 mL of 1 *M* KH_2PO_4 (HiPerSolv grade for HPLC; BDH, cat. no. 153184 U) and 4 mL of 1 *M* K_2HPO_4 (Aristar grade; BDH, cat. no. 45233) with HPLC grade H_2O to 1.84 L. Fine adjust pH with dilute orthophosphoric acid and add 160 mL of HPLC grade methanol to 2 L final volume (Rathburn Chemicals). Filter through a 0.45 mm nylon filter under vacuum, to remove any particulate material and to degas. Store at 4°C. Replace weekly to avoid bacterial growth.
17. Gilson Holochrome UV detector for measuring dG.
18. ESA Coulochem II electrochemical coulometric detector with a 5021 conditioning cell and a high sensitivity 5011 analytical cell. **The measurement of the low levels of background 8-oxo-dG requires the use of coulometric detection as opposed to the less sensitive amperometric method.**
19. Data collection and analysis is by Gynkotek Chromeleon software.

Note: Mention of brand names does not imply endorsement of these products in preference to other similar materials.

3. Methods

Total DNA isolated from eukaryotic cells includes mitochondrial DNA. Although this is a minor component compared with the nuclear DNA, it may

have a much higher content of oxidized bases (since the mitochondria are the site of production of reactive oxygen species), and so might lead to a significant overestimation of nuclear DNA damage. The best course, therefore, is to isolate nuclei first. This, in addition, avoids the possibility of DNA oxidation arising from cytoplasmic contamination with peroxisomes, or with free iron or copper ions, that can catalyze the Fenton reaction. Liver cytoplasm is particularly likely to provide an oxidative environment.

3.1. Isolation of DNA

1a. Isolation of nuclei from cultured cells: Suspend 20×10^6 cells in 3 mL of homogenization buffer with Triton X-100 in a 15-mL centrifuge tube, leave for 5 min on ice, and centrifuge 10 min at 1200*g*, 4°C. Wash with 5 mL of Triton-free homogenization buffer, centrifuge for 5 min at 1200*g*, 4°C, and disperse the pellet well in 1 mL of Triton-free buffer. Measure volume and make up to 4.7 mL with buffer.

1b. Isolation of nuclei from human lymphocytes: Suspend 18×10^6 lymphocytes (expected yield from 30 mL of blood, isolated by standard density gradient sedimentation method) in 5 mL of homogenization buffer with Triton X-100 and continue as described in **step 1a** above.

1c. Isolation of nuclei from tissue samples (e.g., liver): Weigh out approx 150 mg of liver (fresh, or frozen under liquid N_2) as quickly as possible to avoid exposure to air. Add to 4 mL of ice-cold homogenization buffer (with Triton X-100). Transfer to a glass homogenizer tube (Potter–Elvehjen) on ice, and break up the tissue with about six strokes of the homogenizer over 1 min. Start at slow speed, turn up to full speed, and slow down before removing pestle from tube. Place homogenate in a 15-mL tube and centrifuge for 10 min at 1200*g*, 4°C. Discard supernatant, agitate pellet by shaking, add 5 mL of Triton-free homogenization buffer to wash the pellet, and centrifuge for 5 min at 1200*g*, 4°C. Discard supernatant, and resuspend the pellet well in 1 mL of Triton-free homogenization buffer by shaking. Measure volume and make up to 4.7 mL with buffer.

2. Add 10% sodium dodecyl sulfate (SDS) in HPLC grade H_2O to the nuclear suspension to give a final concentration of 0.6%. **The pellet must be well dispersed at this stage; otherwise SDS will not lyse all the nuclei.** Gently invert tube several times to mix. Incubate for 10 min at 37°C. Add 200 µL of RNase IIIA and 10 µL of RNase T_1. Gently invert 20× to mix, and with a wide-opening pipet aspirate up and down twice. Incubate for 30 min at 37°C. Add 1 mg of proteinase K (usually about 70 µL but varies from batch to batch). Mix by aspirating gently twice up and down with a pipet. Incubate for 30 min at 37°C. Cool to room temperature.

3. Transfer the reaction mix to a stoppered glass tube (i.e., resistant to chloroform). Add an equal volume of chloroform/isoamyl alcohol (24:1). Shake vigorously for about 15 s to mix. Centrifuge in a glass centrifuge tube for 10 min at 2400*g*, room temperature, with no brake. Collect the upper aqueous layer, taking care not to disturb the cloudy interface between the two phases. **If the interface is solid then carefully pour off the top layer; however, if interface is not com-**

pacted then it is best to slowly pipet off the upper phase. The condition of the interface varies with the type of cells used.

4. Repeat **step 3** with the aqueous layer.
5. Transfer aqueous layer to a 15-mL centrifuge tube and measure volume. Add *Y* mL of 6 *M* NaCl where $Y = 0.311 \times$ measured volume. Vortex-mix immediately for 10 sec. Centrifuge for 10 min at 2000*g*, room temperature.
6. Carefully decant supernatant into a 50-mL tube, discarding the pellet. Cool the supernatant on ice for 15 min. Add 2 vol of ethanol (at –20°C). Invert gently to mix. Leave on ice for 10 min to aid precipitation of DNA. At this stage some of the DNA may be clear and gelatinous, occupying a substantial volume at the bottom of the tube. The rest of the DNA may appear white and floating in the solution.
7. Remove as much ethanol as possible. Wash with 20 mL of ice-cold 70% ethanol 3×, removing the ethanol by aspiration. The DNA will become more compact and white in color after the first wash.
8. Pick up the DNA pellet on a plastic pipettor tip and transfer to a microcentrifuge tube. Remove as much ethanol as possible with the pipettor tip. Dry DNA under a stream of N_2; this will take about 5 min. If several samples are processed together, it is useful to have a manifold outlet for the N_2 supply.
9. Add 800 µL of 40 m*M* Tris-HCl, pH 8.5. Pass N_2 over the sample for 1 min and then seal the top with Nesco Film (Para Film). Slowly turn on a roller mixer at 4°C overnight in the dark. Then leave for 2 h at 37°C to ensure that the DNA is completely dissolved. Dilute a 10 µL sample to 150 µL and read optical absorbance at 260 nm and 280 nm in a microcuvet; the ratio of absorbance 260/280 nm is a measure of purity of DNA and should be around 1.8–1.9 (pure DNA is 1.9–2.0). A more extensive purification would give even cleaner DNA but at the risk of further oxidation. Absorbance at 260 nm is used to calculate the approximate yield of DNA; 1 AU is equivalent to 50 µg/mL of double strand DNA. Generally 150–250 µg of DNA are obtained by our purification procedure.
10. Store the DNA solution at –80°C under N_2 gas until required.

3.2. Hydrolysis of DNA

Our method is based on that of Richter et al. ***(3)*** with the exception that we find 10× lower amount of phosphodiesterase I to be just as effective. DNA is hydrolyzed to its constituent nucleosides.

1. The volume containing 75 µg of DNA is calculated for the solution prepared in **Subheading 3.1.**, **step 9** above. Allowing for enzymes and $MgCl_2$, calculate the volume of buffer required for a final volume of 500 µL and place this amount in a microcentrifuge tube on ice. Add the following:
   a. 3 µL of DNase (5 U/µL)
   b. 3 µL of alkaline phosphatase (0.25 U/µL)
   c. 3 µL of phosphodiesterase II (0.25 U/mL)
   d. 3.8 µL of phosphodiesterase I (1 U/mL)
   e. 10 µL of 0.5 *M* $MgCl_2$

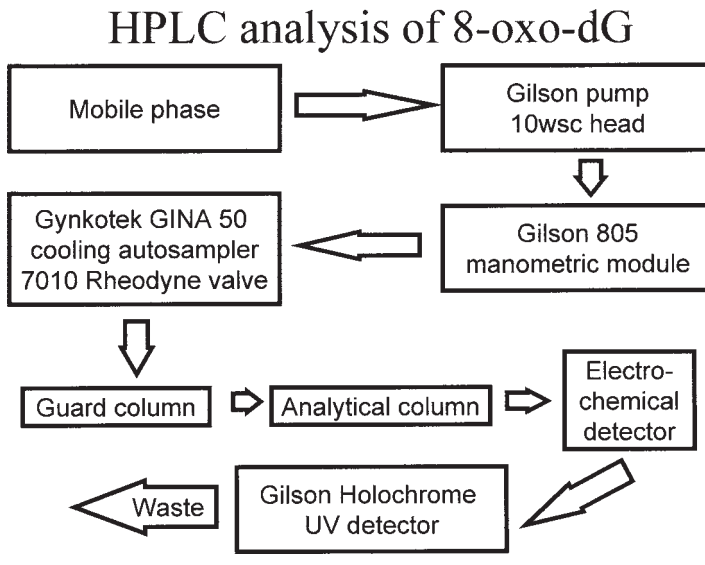

Fig. 1. A schematic diagram of the HPLC system.

Add the DNA sample and vortex-mix briefly. Incubate for 2 h at 37°C.

2. Filter through a 0.2 µm syringe-filter. Dispense the filtrate into three vials (120 µL each). In a fourth vial, place 108 µL of filtrate and 12 µL of standard 10 n*M* 8-oxo-dG and mix.

3.3. HPLC Analysis

A schematic diagram of the HPLC system is shown in **Fig. 1**.

1. Isocratic system; mobile phase 50 m*M* potassium phosphate, 8% methanol, pH 5.5; flow rate 0.5 mL/min; injection volume 100 µL.

   Electrochemical detection; 5021 conditioning cell set at 100 mV, 5011 analytical channel 1 set at 150 mV, 5 s filter time, 5 nA full scale (range), 0.1 V output, 0% offset. 8-Oxo-dG is detected by channel 2 which is set at 400 mV, 5 s filter time, 1 nA full scale (range), 0.1 V output, 0% offset.

   UV detection of dG at 254 nm, with sensitivity set at 0.2 AU.
2. Detection of the very low levels of 8-oxo-dG in normal samples (**Fig. 2**) requires certain precautions to reduce background noise to a minimum.
   - Prepare new mobile phase buffer weekly.
   - Wash out the reservoir weekly with methanol.
   - When not in use, purge the mobile phase with helium.
3. Standards: standards of dG and 8-oxo-dG are run separately. This is important because dG inevitably contains a low level of 8-oxo-dG. **When making up standard solutions, do not rely on weighing, or on the information on the label. Calculate the concentration from the extinction coefficients.** At 1 m*M*, dG

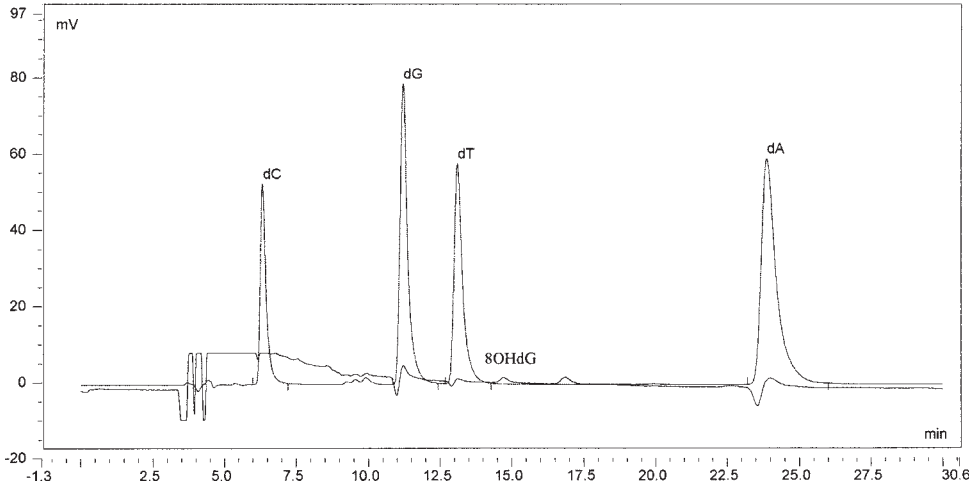

Fig. 2. ECD and UV traces for rat liver nuclear DNA with a typically low background level of 8-oxo-dG.

and 8-oxo-dG have an absorbance of 13AU (254 nm) and 12.3AU (245 nm), respectively. Standard curves are run on each day, with dG at 50, 100, and 150 m*M* and 8-oxo-dG at 0.25, 0.5, 1, and 2 n*M*.

4. Do not leave samples for longer than 12 h at 5°C in the autosampler; there is some evidence of oxidation after this time.
5. Check for carryover of 8-oxo-dG by inserting a 0.25 n*M* 8-oxo-dG standard after each set of quadruplicate samples. Check that the peak area is constant throughout the run.
6. The concentration of dG is estimated from the UV peak; 8-oxo-dG from the electrochemical signal at 400 mV. Results are usually expressed as the number of residues of 8-oxo-dG per 10^5 dG.

4. Notes

1. As DF is light sensitive, cover tubes with foil, keep lid on water bath, etc. Also DF is unstable at room temperature and 4°C, so the solid and buffers containing DF should be stored at –20°C. The buffers should be freshly thawed before use and surplus discarded.
2. Do not attempt to economize by refreezing working solutions of enzymes and saving them for use at a later date. Be ruthless and discard unused solutions.

Acknowledgments

We are grateful for financial support from the Ministry of Agriculture, Fisheries and Food and the Scottish Office Agriculture, Environment and Fisheries Department.

References

1. Collins, A., Cadet, J., Epe, B., and Gedik, C. (1997) Problems in the measurement of 8-oxoguanine in human DNA. *Carcinogenesis* **18,** 1833–1386.
2. Gedik, C. M., Wood, S. G., and Collins, A. R. (1998) Measuring oxidative damage to DNA; HPLC and the comet assay compared. *Free Radic. Res.*, **29,** 609–615.
3. Richter, C., Park, J.-W., and Ames, B. N. (1988) Normal oxidative damage to mitochondrial and nuclear DNA is extensive. *Proc. Natl. Acad. Sci. USA* **85,** 6465–6467.

13

Mutation and the Aging Process

Mutant Frequency at the HPRT *Gene Locus as a Function of Age in Humans*

Yvonne A. Barnett and Christopher R. Barnett

1. Introduction

Aging is a complex, biological process that is contributed to by intrinsic (genetic) and extrinsic (nutrition, infectious agents, xenobiotic exposure, etc.) factors ***(1)***. Several decades ago it was first proposed that instabilities in the organization and expression of the genetic material was likely to be involved in the aging process (reviewed in **ref.** ***2***). Indeed, since that time much experimental evidence has been published that details increases in DNA damage ***(3–8)*** and mutation ***(8,9–15)*** in various cells and tissues with age in humans.

Organisms are continuously exposed to a variety of extrinsic biological, chemical, and physical factors that may alter the structure and therefore have the potential to modify in vivo the function of a wide range of biomolecules, including DNA ***(16–20)***. If modifications to the structure of DNA are not recognized and removed/repaired, then mutations may result. Mutations in essential genes, in association with the age-related alterations in proteins and lipids, may result in the degradation of structural elements within the cells, tissues, and organs of the body, leading to a decline in biological function and eventually to disease and death ***(1,20,21)***. There has been a large numerical growth in the number of older people around the world, due in large part to improvements in environmental conditions such as nutrition, housing, sanitation, and medical and social services. In industrialized countries with low fertility levels this has resulted in large gains in median population ages. In the 1900s the maximum life expectancy was around 47 yr, but now this has risen to a mean of approx 75 yr ***(22)***. Further, due in large part to improvements in environmental

From: *Methods in Molecular Medicine*, Vol. 38: *Aging Methods and Protocols*
Edited by: Y. A. Barnett and C. R. Barnett

conditions such as nutrition, housing, sanitation, and medical and social services, attempts at increasing the average life expectancy and the quality of life in the elderly can be achieved only by slowing down the molecular processes underlying aging. To facilitate such intervention, the factors that cause aging at the cellular level must be identified and understood, including presumably those agents that lead to DNA damage and increase the likelihood of mutation.

The detection of in vivo somatic mutations has enhanced our knowledge of the causes and mechanisms of mutagenesis in somatic cells ***(23)***. The ease of collection of peripheral blood cells together with the presence of intact phase I and phase II xenobiotic metabolizing enzyme systems within these cells has led to the development of a number of bioassays for the detection and quantitation of mutant frequency including the determination of hemoglobin variants or glycophorin A variants in erythrocytes and the hypoxanthine phosphoribosyl transferase (HPRT) clonal assay in lymphocytes (these and others are reviewed in **ref. *24***).

HPRT is encoded by a gene that spans 44 kb containing 9 exons and is located on the long arm of the X chromosome (Xq26). It is a constitutively expressed, nonessential enzyme that functions in the purine salvage pathway to convert hypoxanthine and guanine to their respective 5' monophosphate nucleosides. In addition, HPRT can utilize a number of base analogs such as 6-thioguanine (6–TG) to produce the corresponding ribonucleoside monophosphates. Cells harboring mutation in the *HPRT* gene are able to survive in the presence of 6-TG, whereas wild-type cells will accumulate the highly cytotoxic 6-TG-monophosphate and die. This differential sensitivity to the cytotoxic potential of 6-TG between $HPRT^+$ and $HPRT^-$ cells forms the basis of assays that determine the frequency of $HPRT^-$ cells (6-TG resistant) within a mixed $HPRT^+$/$HPRT^-$ cell population.

The most frequently used method to quantitate background mutant frequency at the *HPRT* gene locus is a clonal assay. Essentially, lymphocytes are incubated in the absence (non-selective conditions) or presence (selective conditions) of 6-TG in 96-well microtiter plates for approx 14 d, after which time wells are scored according to the presence (positive) or absence (negative) of clones. The zero form of the Poisson distribution (P_0) is then used to determine the cloning efficiency (CE) in the absence and presence of the selection agent, and the mutant frequency (MF/10^6 cells) calculated. Although the clonal assay can be demanding of time, finances, and resources it has the advantage that the clones can be expanded for determination of mutant status and the mutational spectrum analyzed ***(25,26)***. The remainder of this chapter provides a thorough description of the clonal assay to quantitate HPRT mutant frequency within cultured peripheral blood derived human lymphocytes.

Other methods can be used to detect $HPRT^-$ lymphocytes. An autoradiograhic technique, based on the ability of lymphocytes to incorporate [^{3}H]thy-

midine into their DNA, following a short period of stimulation with phytohemagglutinin (PHA), in the presence or absence of the selective agent 6-TG, can be used to determine frequency of 6-TG-resistant T lymphocytes in samples of peripheral blood ***(27)***. Recently a variation of the autoradiographic assay has been reported, an immunohistochemical method that enables variant frequency to be calculated ***(28)***. Using this technique lymphocytes are cultured in the presence of 5'-bromodeoxyuridine (BrdU), in the presence or absence of the selective agent 6-TG. The frequency of viable cells in selective and nonselective conditions can then be determined by fluorescence microscopy following labeling of the cells with a suitably tagged anti-BrdU antibody. The variant frequency is then calculated, although it is found to be higher than mutant frequency determined using the clonal assay, because of the detection of a high frequency of phenocopies in this assay (due to the detection of cycling $HPRT^-$ lymphocytes). Both of these nonclonal techniques have the advantage of being relatively simple, rapid, and inexpensive. However, they may overestimate mutant frequency and have the ability to verify phenotype, genotype, or clonal relationships.

2. Materials

1. Lymphocyte separation medium (LSM, ICN Flow,Wycombe, Buckingham, England).
2. 25-mL Sterile universal containers (Sterilin, Stone, Staffordshire, England).
3. Graduated, sterile tissue culture pipets (Sterilin, Stone, Staffordshire, England).
4. Autoclaved glass Pasteur pipets.
5. RPMI 1640 — Dutch Modification (Imperial Laboratories, Smeaton Rd., West Portway, Andover, Hampshire, England).
6. Foetal calf serum (FCS; Gibco-BRL, Life Technologies, Renfrew Rd., Paisley, Scotland), heat-inactivated (56°C/30 min).
7. Hybridoma medium, serum-free medium (HL-1, BioWhittaker UK, Ashville Way, Wokingham, Berkshire, England).
8. Phytohemagglutinin, HA15 (Murex Diagnostics, Murex Biothech Ltd., Centra Rd., Dartford, England). Reconstitute each bottle of freeze-dried PHA by adding 5 mL of sterile distilled water using a sterile disposable hypodermic syringe. Wipe cap with alcohol, then pierce the center of the rubber plug, holding the syringe in a vertical position.Transfer the reconstituted PHA to a sterile universal and store at 4°C for a maximum of 1 mo.
9. 6-TG (available as 2-amino-6-mercaptopurine, Sigma). Dissolve 3.34 mg of 6-TG in 0.5% sodium carbonate (0.5g/100 mL). Cover the container with tin foil (6-TG is photosensitive) and store at 4°C for a maximum of 1 mo.
10. Human recombinant interleukin-2 (rIL-2), (Chiron UK, Salamander Quay West, Hareford, Middlesex). rIL-2 is delivered from the supplier in a vial containing 1.2 mg of freeze-dried powder. Reconstitute the contents of the vial with 1.2 mL of sterile distilled water to give 1 mg/mL containing 1.8×10^7 U/mL of rIL-2. Stock rIL-2 should be stored frozen at a concentration of 1×10^5 U/mL (add 1.2 mL

of reconstituted rIL-2 to 214.8 mL of RPMI + 10% FCS), aliquot into 1.5-mL volumes in sterile Eppendorf tubes, and store at –20°C until required. Each batch of rIL-2 must be tested to establish the most suitable concentration for use in the cloning assay (*see* **Note 1**).

11. Feeder cells, RJK (Epstein–Barr virus [EBV]-transformed B-lymphoblastoid) cells that carry complete *HPRT* deletion are used as feeder cells in the cloning assay. RJK cells should be cultured in RPMI 1640 (Gibco-BRL), 10% heat-inactivated FCS, 100 U/mL of penicillin, 100 mg/mL streptomycin, and 0.2 mg/mL of sodium pyruvate. Irradiate (40 Gy) exponentially growing RJK cells prior to their use in a cloning assay.
12. Plastic reagent reservoirs for multipipets (Sigma, Fancy Rd., Poole, Dorset, England).
13. 96-well, flat-bottomed microtiter plates (Nunc, Rosklide, Denmark).
14. Pyruvic acid — sodium salt (Sigma, Fancy Rd., Poole, Dorset, England).
15. Penicillin/streptomycin (1000 U/mL and 1000 mg/mL) (Gibco-BRL, Life Technologies, Renfrew Rd., Paisley, Scotland).
16. L-Glutamine (200 m*M*) (Gibco-BRL, Life Technologies, Renfrew Rd., Paisley, Scotland).
17. RPMI 1640 with L-glutamine (Gibco-BRL, Life Technologies, Renfrew Rd., Paisley, Scotland).
18. Lithium-Heparin Vacutainers, 10 mL (Becton-Dickinson, Cowely, Oxfordshire, England).
19. 3-mL Cryotubes (Nunc, Roskilde, Denmark).
20. Lymphocyte culture medium (LCM) should be prepared in advance and stored at 4°C: 435.9 mL of RPMI 1640, Dutch modification; 50.0 mL of 10% heat-inactivated FCS; 100 U/mL of penicillin, 5.0 mL of 100 mg/mL of streptomycin; and 9.1 mL of 0.2 mg/mL of sodium pyruvate.
21. 4+ should be made up in advance and stored in 9 mL aliquots in sterile containers at –20°C until required: 50.0 mL of 20 m*M* L-glutamine; 100 mL of 100 U/mL penicillin and 100 µg/mL streptomycin; 50.0 mL of 20 mg/mL sodium pyruvate.
22. Cloning medium should be made up just before use: 46.0 mL RPMI (Dutch modification); 10.0 mL heat-inactivated FCS; 20.0 mL hybridoma medium; 1.0 mL PHA; 2.0 mL rIL-2; 8.0 mL 4+; 1×10^7 feeder cells resuspended in a volume of 3.0 mL.

3. Methods

3.1. Isolation of Lymphocytes from Peripheral Blood Samples

1. Peripheral blood samples should be collected into lithium–heparin-coated blood tubes (*see* **Note 2**).
2. Following collection, gently dilute whole blood 1:1 with RPMI 1640 (Gibco-BRL) at room temperature. Carefully layer 15 mL of diluted blood onto 10 mL of LSM at room temperature. Centrifuge at 400*g* for 30 min at room temperature (switch

brake off on centrifuge). Following centrifugation gently aspirate (*see* **Note 3**) the upper layer using a sterile glass Pasteur pipet, to within 0.5 cm of the opaque interface containing the mononuclear cells (MNCs). Discard the aspirate.

3. Gently aspirate the opaque layer containing the MNCs and transfer to a sterile universal containing 15 mL of RPMI 1640 (Gibco-BRL). Mix MNC suspension gently by aspiration and then centrifuge at 250*g* for 10 min. Remove supernatant by aspiration and discard.
4. Pool each MNC pellet (for each subject blood sample) and wash 1× with RPMI 1640 (Gibco-BRL) at room temperature. Remove an aliquot, add trypan blue, and count viable cells using a hemocytometer. Recovery is generally in the region of 2.5 million MNC/mL of whole blood.
5. Resuspend MNCs in LCM at a concentration of 1×10^6 cells/mL and incubate overnight at 37°C, in a 5% CO_2/air, humidified atmosphere. Monocytes will adhere to the surface of the flask while lymphocytes remain in suspension in the culture medium.

3.2. Cryopreservation of MNCs

It may not always be possible to perform the cloning assay on the same day as the blood is collected. In such circumstances the MNC fraction can be cryopreserved until required.

1. Prepare freeze down medium (FDM): 90% FCS (not heat inactivated) and 10% glycerol.
2. When the MNC fractions from one blood sample have been prepared (**Subheading 3.2.**, **step 4**) add FDM to achieve a final concentration of 3×10^6 MNCs/mL.
3. Transfer the resultant cell suspension into 3-mL cryotubes and then place the tubes into a polystyrene box. Put the box in a freezer at –70°C overnight, then transfer to liquid nitrogen for long-term storage.

3.3. Thawing of Previously Cryopreserved Lymphocytes

If cryopreserved, lymphocytes have to be gently thawed 24 h prior to cloning.

1. Thaw the required number of vials rapidly in a 37°C water bath.
2. Transfer the contents of the vials to a universal and dilute dropwise, slowly with cold RPMI 1640 (Dutch Modification) to a volume of 20 mL. Agitate the universal container during addition of the RPMI.
3. Centrifuge at 440*g* for 10 min. Remove supernatant and resuspend in warm RPMI 1640 containing 5% FCS (heat-inactivated).
4. Centrifuge at 440*g* for 10 min.
5. Discard supernatant and resuspend pellet in warm culture medium at a concentration of 1×10^6 cells/mL.
6. Incubate overnight at 37°C in a 5% CO_2/air, humidified atmosphere. After overnight incubation count lymphocytes using a hemocytometer. The number of lymphocytes per milliliter is usually less than 1×10^6. A successful thaw will yield $7–9 \times 10^5$ cells/mL. A count of less than 4×10^5 cells/mL should not be used for cloning.

Table 1
Preparation of a 30 Lymphocyte/mL Suspension

Serial dilution step	Volume (mL) of lymphocyte suspension from 2×10^5 cells/mL initial suspension	Volume of warm (37°C) culture medium	Resultant concentration of lymphocytes/mL
A	1.0	1.0	1×10^5
B	0.5 of suspension A	4.5	1×10^4
C	0.5 of suspension B	4.5	1×10^3
D	0.5 of suspension C	4.5	1×10^2
E	3.75 of suspension D	8.75	30

7. Dilute lymphocyte suspension to 2×10^5 cells/mL using warm culture medium (RPMI 1640 (Dutch modification), 10% heat-inactivated FCS, 100 U/mL of penicillin, 100 mg/mL of streptomycin and 0.2 mg/mL of sodium pyruvate.

3.4. Determination of Cloning Efficiency in Non-Selective Medium

1. Take 1 mL of lymphocytes at 2×10^5 cells/mL and carry out the serial dilutions in duplicate (A–E) (*see* **Table 1**).
2. Add 10 mL of cloning medium to 10 mL of E in a sterile universal container. Keep universal in 37°C water bath until ready to plate out.
3. Decant cloning mixture into a sterile plastic reagent reservoir (*see* **Note 4**).
4. Using an eight-channel multipipet and sterile tips, transfer 200 µL of the mixture into each well of a 96-well microtiter plate. Set up two such 96-well plates. Clearly code each plate.

3.5. Determination of Cloning Efficiency in Selective Medium

1. For each selective plate to be made up (5–8 in total should be set up) mix together in a universal container 10 mL of lymphocytes at 2×10^5 cells/mL, 9 mL of cloning medium, and 1 mL of 6-TG.
2. Decant cloning mixture from the universal container into the reagent reservoir.
3. Using an eight-channel multipipet and sterile tips, transfer 200 µL of cloning mixture into each well of a 96-well microtiter plate. Clearly code each plate.

3.6. Incubation and Scoring of Cloning Efficiency Plates

1. Stack all nonselective and selective plates for each blood sample and tape together (*see* **Note 5**). Incubate plates on a sloped shelf at 37°C in a 5% CO_2/air humidified atmosphere for 14–15 d.
2. At 1–2 d before the end of the plate incubation period, reverse the slope of the plates by turning through 180°. The live cells present in each well should move toward the top of the well and form a crescent.

3. To score the plates, place each plate on the stage of an inverted microscope and commence scoring from top left hand well down the remaining wells. Move across and score upwards. Exclude all wells in which evaporation has taken place.
4. A well should be scored positive if more than 50 viable lymphocytes are present (*see* **Note 6**).

3.7. Calculation of MF/10^6 cells

Using the figures obtained (number of positive or number of negative wells and total number of wells counted per plate) from the scoring of the CE plates in selective and nonselective conditions the following equations are used to calculate MF/10^6 cells.

$$\text{CE in nonselective plates or selective plates} = -\ln (P_0)\ \text{CE plate / no. of cells per well}$$

Where:

$$P_0 = \text{no. of negative wells / total no. of wells}$$

Then,

$$\text{MF/}10^6\ \text{cells} = \text{CE in selective plates / CE in nonselective plates}$$

4. Notes

1. For each new batch of IL-2 purchased it is necessary to establish the optimal amount of IL-2 to support lymphocyte culture. To do this, a number of cloning efficiency plates (non-selective conditions) are set up using a range of IL-2 concentrations, for example, 50, 100, 150, 200, 250, 300, 350, 400, and 450 U/mL. The concentration at which optimum growth conditions (highest cloning efficiencies in nonselective plates) are achieved is then chosen for use in all subsequent cloning assays until that batch of IL-2 runs out.
2. Following collection, blood tubes, if they require transportation, should be protected from sudden temperature changes and vibration, as these factors contribute to low lymphocyte cloning efficiencies.
3. An aspiration pump creates a vacuum to remove all unwanted layers from the separation process. A vacuum pump is attached to a Buchner flask, creating a vacuum that extracts all unwanted materials through a glass Pasteur pipet.
4. The same reagent reservoir can be used per sample for nonselective and selective plates provided that the nonselective plates are plated first, so as not be to contaminated with 6-TG.
5. To reduce evaporation from the 96-well plates, place the plates inside a plastic storage container with small holes to permit gaseous exchange.
6. Viable cells are pleomorphic with regular borders and bright, nongranular centers. They form tightly packed, regular shaped clumps. Dead feeder cells and lymphocytes (various sizes with irregular borders and dark granular centres) also form clumps but these clumps are loosely packed.

Acknowledgment

Dr. Yvonne Barnett is grateful for the support of Dr. Jane Cole, MRC Cell Mutation Unit, University of Sussex for help with the establishment of the cloning assay within the Cancer and Aging Research Laboratories at the University of Ulster. The authors acknowledge the assistance of Ms. Caroline Warnock in the preparation of this manuscript.

References

1. Barnett, Y. A. (1995) How and why do we age? in *Celebrating Age* (Allen, J. M., Barnett, Y. A., Gibson, F., and McKenna, P. G., eds.), Avebury Press, Aldershot, pp. 78–92.
2. Slagbroom, P. E. and Vijg, J. (1989) Genetic instability and aging: theories, facts and future perspectives. *Genome* **31,** 373–385.
3. Ono, T. and Okada, S. (1976) Comparative studies of DNA size in various tissues of mice during the aging process. *Exp. Gerontol.* **11,** 127–132.
4. Chetsanga, C. J., Tuttle, J. Jacoboni, A., and Johnson, C. (1977) Age-associated structural alterations in senescent mouse brain DNA. *Biochim. Biophys. Acta* **474,** 180–187.
5. Mullaart, E., Lohman, P. H. M., Berends, F., and Vijg, J. (1990) DNA damage metabolism and aging. *Mutat. Res.* **237,** 189–210.
6. Singh, N. P., Danner, D. B., Tice, R. R., Pearson, J. D., Brant, L. J., Morrell, C. H., and Schneider, E. L. (1991) Basal DNA damage in individual human lymphocytes with age. *Mutat. Res.* **256,** 1–6.
7. Barnett, Y. A. and King, C. M. (1995) An investigation of antioxidant status, DNA repair capacity and mutation as a function of age in humans. *Mutat. Res.* **338,** 115–128.
8. King, C. M., Bristow-Craig, H. E., Gillespie, E. S., and Barnett, Y. A. (1997) In vivo antioxidant status, DNA damage, mutation and DNA repair capacity in cultured lymphocytes from healthy 75–80-year-old humans. *Mutat. Res.* **377,** 137–147.
9. Fenech, M. and Morley, A. A. (1985) The effect of donor age on spontaneous and induced micronuclei. *Mutat. Res.* **148,** 99–105.
10. Branda, R. F., Sullivan, L. M., O'Neill, J. P., Falta, M. T., Nicklas, J. A., Hirsch, B., Vacek, P. M., and Albertini, R. J. (1993) Measurement of HPRT mutant frequencies in T-lymphocytes from healthy human populations. *Mutat. Res.* **285,** 267–279.
11. Tates, A. D., Van Dam, F. J., Van Mossel, H., Schoemaker, H., Thijssen, J. C. P., Woldring, V. M., Zwinderman, A. H., and Natarjan, A. T. (1991) Use of the clonal assay for the measurement of frequencies of HPRT mutants in T-lymphocytes from five control populations. *Mutat. Res.* **253,** 199–213.
12. Cole, J., Waugh, A. P. W., Beare, D. M., Sala-Trepat, M., Stephens, G., and Green, M. H. L. (1991) HPRT mutant frequencies in circulating lymphocytes: population studies using normal donors, exposed groups and cancer prone syndromes, in *New Horizons in Biological Dosimetry* (Gledhill, B. L. and Mauro, F., eds.), Wiley-Liss, New York, pp. 319–328.

13. Trainor, K. J., Wigmore, D. J., Chrysostomou, A., Dempsey, J., Seshadr, R., and Morley, A. A. (1984) Mutation frequency in human lymphocytes increases with age. *Mech. Aging Dev.* **27,** 83–86.
14. Vijayalaxmi and Evans, H. J. (1984) Measurement of spontaneous and X-irradiation induced 6-thioguanine resistant human blood lymphocytes using a T-cell cloning technique. *Mutat. Res.* **125,** 87–94.
15. King, C. M., Gillespie, E. S., McKenna, P. G., and Barnett, Y. A. (1994) An investigation of mutation as a function of age in humans. *Mutat. Res.* **316,** 79–90.
16. Sugimura, T. (1988) Successful use of short-term tests for academic purposes: their use in identification of new environmental carcinogens with possible risk for humans. *Mutat. Res.* **205,** 33–39.
17. Takayama, S., Nakatsura, Y., and Sato, S. (1987) Carcinogenic effect of the simultaneous administration of five heterocyclic amines to F344 rats. *Jpn. J. Cancer Res.* (Gann) **78,** 1068–1072.
18. Hayatsu, H. (1991) in *Mutagens in Food: Detection and Prevention*. CRC Press, Boca Raton, FL.
19. Freeman, B. A. and Crapo, J. D. (1982) Biology of disease, free radicals and tissue injury. *Lab. Invest.* **47,** 412–426.
20. Pacifici, R. E. and Davies, K. J. A. (1991) Protein, lipid and DNA repair systems in oxidative stress; the free radical theory revisited. *Gerontology* **37,** 166–180.
21. Mera, S. L. (1992) Senescence and pathology in ageing. *Med. Lab. Sci.* **49,** 271–282.
22. Andrews, K. and Brocklehurst, J. C. (1985) The implications of demographic changes on resource allocation. *J. R. Coll. Phys.* (Lond.) **19,** 109–111.
23. Albertini, R. J. (1985) Somatic gene mutations *in vivo* as indicated by the 6-thioguanine-resistant T-lymphocytes in human blood. *Mutat. Res.* **150,** 411–422.
24. Cole, J. and Skopek, T. R. (1994) Somatic mutant frequency, mutation rates and mutational spectra in the human population *in vivo*. *Mutat. Res.* **304,** 33–105.
25. Edwards, A., Voss, H., Rice, P., Civitello, A., Stegeman, J., Schwager, C., Zimmerman, J., Erfle, H., Caskey, C. T., and Ansorge, W. (1990) Automated DNA sequencing at the human *hprt* locus. *Genomics* **6,** 593–608.
26. Hou, S.-M. Steen, A.-M., Falt, S., and Andersson, B. (1993) Molecular spectrum of background mutation at the hprt locus in human T-lymphocytes. *Mutagenesis* **8,** 43–49.
27. Strauss, G. H. and Albertini, R. J. (1979) Enumeration of 6-thioguanine-resistant peripheral blood lymphocytes in man as a potential test for somatic cell mutations arising *in vivo*. *Mutat. Res.* **61,** 353–379.
28. Montero, R., Norppa, H., Autio, K., Lindholm, C., Ostrosky-Wegman, P., and Sorsa, M. (1991) Determination of 6-thioguanine resistant lymphocytes in human blood by immunohistochemical antibromodeoxyuridine staining. *Mutagenesis* **6,** 169–170.

14

Somatic Mutations and Aging

Methods for Molecular Analysis of HPRT *Mutations*

Sai-Mei Hou

1. Introduction

The increasing information on the specific DNA sequence alterations that occur in mutated genes of human somatic cells has allowed the establishment of mutational spectra. Endogenous and exogenous exposures as well as individual susceptibility factors seem to contribute to the complexity of mutational spectra. The X-linked *HPRT* (*hypoxanthine phosphoribosyl transferase*) gene in human T lymphocytes has been considered as a suitable target for studying somatic in vivo mutations ***(1)***, including those related to aging. The mutant frequency in adults is 10-fold higher than that in newborns and the proportion of point mutations is also considerably higher in adults (90% vs 20%), possibly as results of accumulation of point mutations induced later in life and dilution of the V(D)J-recombinase-mediated spontaneous deletions observed in newborns ***(2)***. A significant age-related increase of *HPRT* mutant frequency (1–3%/yr) has been reported in most studies, with a more rapid increase in smokers compared to nonsmokers (reviewed in **ref. *1***).

Knowledge of the whole *HPRT* gene sequence ***(3)*** and the polymerase chain reaction (PCR) techniques have made the molecular characterizations of all types of mutations possible. More than 2000 mutants have been characterized and included in the *HPRT* mutation database ***(4)***. The wide spectrum of mutations in this reporter gene resembles very much that in the p53 tumor suppressor gene, sharing many common features, such as heterogeneity, fingerprints, and strand specificity of carcinogenic agents. It would be of great interest if mutations related to aging-specific damages could be recovered from the *HPRT* mutational spectrum in human populations.

From: *Methods in Molecular Medicine*, Vol. 38: *Aging Methods and Protocols*
Edited by: Y. A. Barnett and C. R. Barnett

The *HPRT* mutational spectrum consists mainly of point mutations (missense, nonsense, frameshift), splice mutations, and larger deletions. Multiplex PCR (MP-PCR, ***5***) has replaced the Southern blotting technique used earlier for detection of mutants with larger genomic arrangements ***(6)***. The reverse transcription PCR (RT-PCR) and subsequent sequencing enables the identification of point mutations in the coding region such as base substitutions and small deletions/insertions. By this technique, splice errors (exon skippings) and larger genomic alterations can also be recognized as aberrant mRNA/cDNA products, but can be truly distinguished only by the genomic PCR and sequencing which enables the identification of the splicing mutations (mainly in the splice sequences at the exon/intron boundaries) and the intronic deletion break points.

The primary strategy for mutational screening has been to first distinguish large genomic alterations from point mutations by MP-PCR ***(7)***. The point mutations are then further subdivided into splicing and coding errors by RT-PCR. A partial gene deletion is defined by an abnormal MP-PCR pattern and a shorter cDNA band, and a total gene deletion by an absence of *HPRT* DNA from both MP-PCR and RT-PCR. A normal MP-PCR but an abnormal cDNA product (shorter or longer) is classified as a "splice error." Finally, a "coding error" is characterized by normal products from both MP-PCR and RT-PCR.

However, larger deletions in normal individuals detectable by multiplex PCR seem to be much less frequent ***(7)*** than previously reported from Southern analysis ***(6)***. This could be related partly to mutations affecting intronic restriction sites, and partly to limitations of PCR in amplifying larger deletions involving several exons and larger insertions (> 1 kb). Mutations affecting primer annealing would result in an overestimate of deletion frequency, but seemed to be a rare event. The multiplex PCR requires optimal priming conditions for exon fragments, both within, across, and together. The reactions often need to be repeated or verified by exon-specific PCR, not only for the "negative" exons, but probably also for the "positive" exons.

Furthermore, genomic alterations can be detected only in cells from male donors owing to the masking effect of the inactive X-chromosome in females, although PCR across common breakpoints may be applied to screen for specific types of larger rearrangements regardless of gender, such as the V(D)J-recombinase-mediated deletions of exons 2 and 3 ***(2)***. A screening strategy starting with cDNA analysis followed by confirmation at the genomic level should thus be considered as the most convenient way of screening, as it minimizes the total number of PCR reactions and facilitates the spectrum establishment of point mutations in both males and females (**Fig. 1**).

The methods described below (published in **refs. *7–9***) are modified from the original techniques developed for molecular analysis of unexpanded mutant

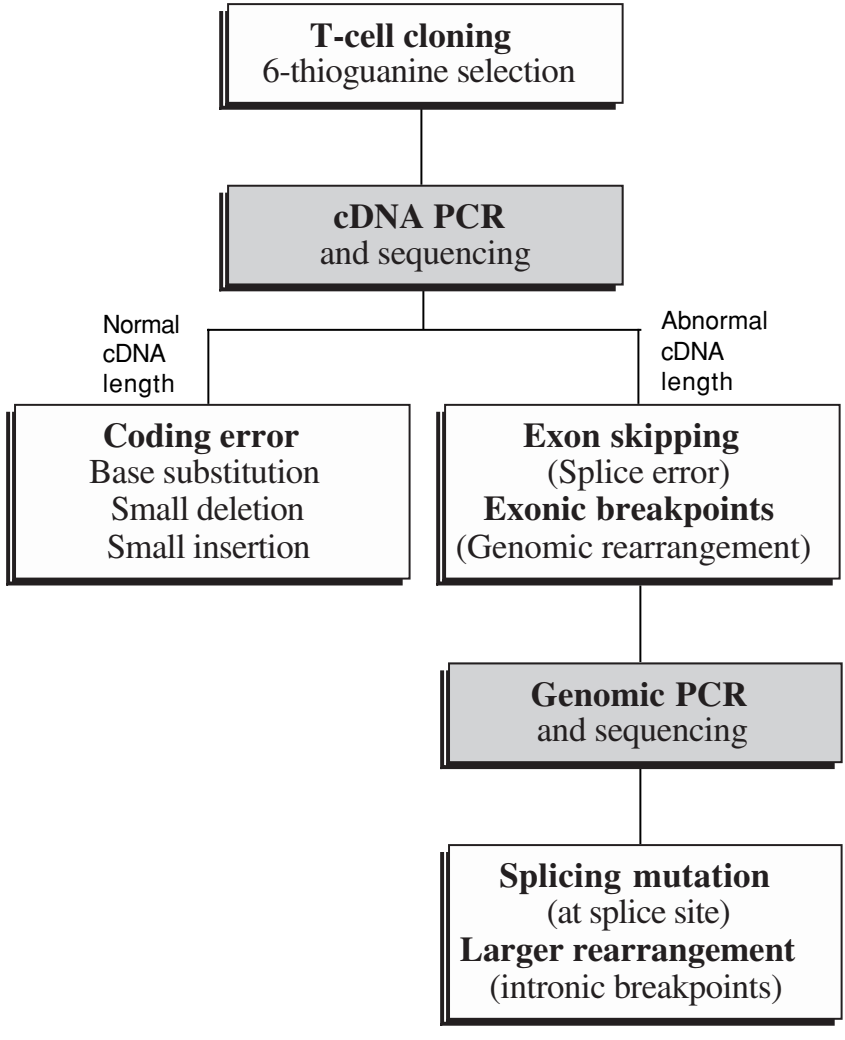

Fig. 1. An optimal strategy for screening and identification of *HPRT* mutations.

clones without RNA and DNA preparation, as they directly utilize lysates prepared from small numbers of cells for the cDNA synthesis ***(10)*** and the MP-PCR ***(11)***.

In the RT-PCR, cDNA was synthesized by reverse transcription of *HPRT* mRNA and amplified by a two-step (nested) PCR amplification. In the MP-PCR, all exons of the gene can be amplified at the same time in one reaction ***(5)***. Each fragment is of different size, and loss of fragment or change in its size can easily be detected after electrophoresis. For easier optimization, however, the

amplifications are carried out in two separate reactions. The short fragments corresponding to exons 1, 2, 4, and 6 are amplified in one reaction, and the long fragments containing exons 3, 5, 7 + 8, and 9 in a second reaction.

2. Materials

2.1. Equipments and Enzymes

1. PCR: All PCR reactions are performed in DNA-Engine™ (MJ Research, PTC-200) or GeneAmp 2400® (Perkin Elmer, Foster City, CA, USA) thermal cyclers. All enzymes and dNTPs originate from Promega (Madison, WI, USA) or Pharmacia Biotech (Uppsala, Sweden).
2. Sequencing: Magnetic beads and concentrator used for strand separation are purchased from Dynal (Oslo, Norway). Sequencing kit and equipment are obtained from Applied Biosystems (Foster City, CA, USA).

2.2. RT-PCR Primers and Buffers

1. RT-PCR primers (20 µ*M* stocks, f = forward, r = reverse):
   RT1f; $_{(-50)}$ 5'-ACC GGC TTC CTC CTC CTG AG-3' $_{(-31)}$
   RT2r; $_{(721)}$ 5'-GAT AAT TTT ACT GGC GAT GT-3' $_{(702)}$
   RT3f; $_{(-19)}$ 5'-TAC GCC GGA CGG ATC CGT T-3' $_{(-1)}$ (+/– biotinylation)
   RT4r; $_{(697)}$ 5'-AGG ACT CCA GAT GTT TCC AA-3' $_{(678)}$ (–/+ biotinylation)
2. cDNA internal sequencing primers (Cy–5 labeled, 20 m*M* stocks):
   RT5f: $_{(124)}$ 5'-ATT ATG GAC AGG ACT GAA-3'$_{(141)}$
   RT6f: $_{(166)}$ 5'-GAG ATG GGA GGC CAT CAC AT-3'$_{(185)}$
   RT7r: $_{(302)}$ 5'-CTG ATA AAA TCT ACA GTC AT-3'$_{(283)}$
   RT8r: $_{(373)}$ 5'-AAG TTG AGA GAT CTT CTC CAC-3'$_{(353)}$
3. cDNA cocktail: 50 m*M* Tris-HCl, pH 8.5; 75 m*M* KCl; 3 m*M* $MgCl_2$; 2.5% Nonidet P-40 (NP-40); 10 m*M* dithiothreitol (DTT); 500 µ*M* of each dNTP; 1.6 µ*M* of primer RT2r; 1 U/µL of RNase inhibitor; and 2.5 U/µL of M-MLV reverse transcriptase.
4. 10× cDNA PCR buffer: 150 m*M* Tris-HCl, pH 8.5; 600 m*M* KCl; and 15 m*M* $MgCl_2$.

2.3. MP-PCR Primers and Buffers

1. 10× buffer T (sterile filtered): 670 m*M* Tris-HCl, pH 8.8, 67 m*M* $MgCl_2$, 166 m*M* $(NH_4)_2SO_4$, 50 m*M* β-mercaptoethanol, and 68 m*M* EDTA.
2. Lysis buffer (master mix, 150 µL/sample): 15 µL of 10× buffer T, 7 µL NP-40 (10%), 7 µL of Tween-20 (10%), 15 µL of proteinase K (1 mg/mL) and 106 µL of H_20.
3. 2× MP-PCR buffer: 134 m*M* Tris-HCl, pH 8.8, 13.4 m*M* $MgCl_2$, 33.2 m*M* $(NH_4)_2SO_4$, 10 m*M* β-mercaptoethanol, and 13.6 µ*M* EDTA.
4. 10× primer mix (for primer sequences *see* **Table 1**):
   a. Long fragments (exons 3, 5, 7–8, and 9, forward and reverse): 1.6 µ*M* MP3, 2.4 µ*M* MP5, 2.4 µ*M* MP78, and 2 µ*M* MP9.
   b. Short fragments (exons 1, 2, 4, and 6, forward and reverse): 5 µ*M* MP1, 1 µ*M* MP2, 1 µ*M* MP4, and 1.6 µ*M* MP6.

Table 1
HPRT Primers Used in the Multiplex PCR *(5)*

Exon[a]	Primer sequences[b]
Long fragments	
3 (1059)	MP3F: (16252) 5'-CCT TAT GAA ACT TGA GGG CAA AGG-3' (16275) MP3R: (17310) 5'-TGT GAC ACA GGC AGA CTG TGG ATC-3' (17287)
5 (708)	MP5F: (31442) 5'-CAG GCT TCC AAA TCC CAG CAG ATG-3' (31465) MP5R: (32149) 5'-GGG AAC CAC ATT TTG AGA ACC ACT-3' (32126)
7+8 (1533)	MP78F: (38667) 5'-GAT CGC TAG AGC CCA AGA AGT CAA G-3' (38691) MP78R: (40199) 5'-TAT GAG GTG CTG GAA GGA GAA AAC-3' (40176)
9 (1278)	MP9F: (40443) 5'-GAG GCA GAA GTC CCA TGG ATG TGT-3' (40466) MP9R: (41720) 5'-CCG CCC AAA GGG AAC TGA TAG TC-3' (41698)
Short fragments	
1 (626)	MP1F: (1205) 5'-TGG GAC GTC TGG TCC AAG GAT TCA-3' (1228) MP1R: (1831) 5'-CCG AAC CCG GGA AAC TGG CCG CCC-3' (1808)
2 (572)	MP2F: (14678) 5'-TGG GAT TAC ACG TGT GAA CCA ACC-3' (14701) MP2R: (15249) 5'-GAC TCT GGC TAG AGT TCC TTC TTC-3' (15226)
4 (334)	MP4F: (27765) 5'-TAG CTA GCT AAC TTC TCA AAT CTT CTA G-3' (27792) MP4R: (28098) 5'-ATT AAC CTA GAC TGC TTC CAA GGG-3' (28075)
6 (441)	MP6F: (34850) 5'-GAC AGT ATT GCA GTT ATA CAT GGG G-3' (34874) MP6R: (35290) 5'-CCA AAA TCC TCT GCC ATG CTA TTC-3' (35267)

[a]Number within parentheses indicates the length of exon fragment amplified.
[b]Genomic positions for the first and last base indicated within parentheses.

3. Methods

3.1. RT-PCR

1. cDNA synthesis: Collect 6000 cells (preferably fresh) in an Eppendorf tube with 1 mL of ice-cold phosphate-buffered saline (PBS). Centrifuge 5 min at 13,000 rpm (4°C). Resuspend the cells in 20 µL of cDNA cocktail. Incubate for 1 h at 37°C (run a control tube with cDNA cocktail only).
2. cDNA PCR: Use 5 µL of the cDNA reaction in a PCR (50 µL) with 0.2 µ*M* of primer RT1f and 0.1 µ*M* of primer RT2r, 200 µ*M* of each dNTP, PCR buffer, 10% dimethyl sulfoxide (DMSO), and 1 U of *Taq* polymerase. After an initial denaturation for 4 min at 94°C, run 30 cycles of 94°C (30 s), 50°C (30 s), and 72°C (1 min), followed by a 7-min polymerization at 72°C.
3. Nested PCR: Use 2 µL of the PCR reaction as template in a nested PCR (50 µL) with 0.4 µ*M* of both RT3f primer and RT4r primer (one of them biotinylated) under the same conditions as described previously.

4. Reading: Load 10 µL of the reaction on a 3.75% polyacrylamide gel. Save the remaining sample for magnetic bead (Dynal) separation and single-stranded DNA sequencing.

3.2. MP-PCR

1. MP-lysate: Pellet 30,000 cells and wash with PBS. Resuspend the cells, add 150 µL of lysis buffer, and mix carefully. Incubate 56°C for at least 1 h. Heat inactivate the proteinase K at 96°C for 10 min. Store at –20°C (–80°C for longer storage).
2. MP-PCR: Mix the following for a 50-µL PCR: 25 µL 2× MP-PCR buffer (preheated at 37°C for 10 min), 5 µL of DMSO, 3 µL of dNTP mix (25 m*M*), 5 µL of 10× primer mix, and 3.7 µL of H_2O. Overlay the reaction with mineral oil and run a hot start (80–94°C, 5 min) in a thermocycler. Add 4 U of *Taq* polymerase and 8 µL of the template. Heat up the reaction to 94°C (4.5 min) and run 33 cycles of 94°C (30 s), 61°C (2 min), and 68°C (2 min), followed by a 7 min prolonged polymerization (68°C).
3. Reading: Load 25 µL of the PCR product on a 1.4% agarose gel.

3.3. Exon-Specific PCR

For identification of splicing mutations, exon-specific primers closer to the splice sites are used at different annealing temperatures (**Table 2**). Run a hot start and 30 PCR cycles (30 s each segment) in the cDNA PCR buffer but with 5 µL of MP-lysate, 0.5 µ*M* of each primer, 200 µ*M* of each dNTP, 10% of DMSO, and 1 U of *Taq* polymerase.

3.4. Direct Sequencing

1. Strand separation: Immobilize biotinylated PCR product (45 µL) on streptavidin-coated magnetic beads. Separate DNA strands in alkali (1 *M* NaOH, 0.075% Tween-20) with the help of a magnetic concentrator. Precipitate nonbiotinylated DNA strand with 1/10 volume of 3 *M* sodium acetate, pH 5.2, and 2 vol of ice-cold 95% ethanol. Wash twice with 70% ethanol. Vacuum dry and dissolve in water.
2. Sequencing reactions: Use the biotinylated or nonbiotinylated strand, 0.2 µ*M* of a Cy–5 labeled sequencing primer, and PRISM Sequenase® Terminator single-stranded DNA sequencing kit according to the manufacturer's instructions.
3. Run the reactions on a 373A or 377A Automated Sequencer.

4. Notes

4.1. RT-PCR

The main problem in the RT-PCR has been failure in obtaining PCR products from all MP-PCR-positive mutants, especially when using frozen pellets after long-term storage. This may be explained partly by difficulties in handling small frozen cell pellets, and partly by limited quality and quantity of templates in the beginning. The latter may partly be related to growth arrested

Table 2
HPRT* Exon-Specific Primers Used for Genomic PCR and Sequencing *(8)

Exon	Primer sequence
1	E1F[b]: (1599) 5'-GCG CCT CCG CCT CCT CCT CTG-3' (1619)
(65°C)[a]	E1R[c]: (1801) 5'-CCG CCC GAG CCC GCA CTG-3' (1784)
2	E2F[c]: (14678) 5'-TGG GAT TAC ACG TGT GAA CCA ACC-3' (14701)
(61°C)	E2R[b]: (15249) 5'-GAC TCT GGC TAG AGT TCC TTC TTC-3' (15226)
3	E3F[c]: (16519) 5'-TCC TGA TTT TAT TTC TGT AG-3' (16538)
(55°C)	E3R[b]: (16973 5'-ATA TCC TCC AAG GTG ACT AG-3' (169549)
4	E4F[c]: (27765) 5'-TAG CTA GCT AAC TTC TCA AAT CTT CTA G-3' (27792)
(57°C)	E4R[b]: (28098) 5'-ATT AAC CTA GAC TGC TTC CAA GGG-3' (28075)
5	E5F[c]: (31440) 5'-TAC AGG CTT CCA AAT CCC AG-3' (31459)
(57°C)	E5R[b]: (31707) 5'-GCT TAC CTT TAG GAT GGT GC-3' (31688)
6	E6F[c]: (34728) 5'-CCT GCA CCT ACA AAA TCC AG-3' (34347)
(57°C)	E6R[b]: (35781) 5'-TCT GCC ATG CTA TTC AGG AC-3' (35762)
7+8	E78F[b]: (39768) 5'-CCC TGT AGT CTC TCT GTA TG-3' (39887)
(50°C)	E78R[c]: (40200) 5'-TTA TGA GGT GCT GGA AGG AG-3' (40181)
9	E9F[c]: (41353) 5'-AAC CCT GAC AAC TAA TAG TG-3' (41372)
(57°C)	E9R[b]: (41551) 5'-AGG ACT CCA GAT GTT TCC AA-3' (41532)

[a]Annealing temperature within parentheses.
[b]After primer name indicates that the primer is biotinylated.
[c]After primer name indicates that the primer is Cy-5 labeled.

clones, which may be comparable to the unsuccessfully expanded clones. The mutation itself, such as nonsense, frameshift, deletion, and splice mutation, may also result in low copy number of mRNA ***(12)***.

Make at least two pellets for both RT- and MP-PCR, and save the remaining of the clone as "rest pellet." Store all pellets at –80°C. Use pellets (preferably fresh) from nonselected (wild-type) clones or previously successfully amplified lysates as positive controls. The possibility of using another gene (expressed at a comparable level) as an internal control for cDNA synthesis/PCR may also be considered. For RT-PCR-negative mutants, the "rest pellets" can be subjected to isolation of RNAs using commercially available kits. When necessary, the individual exons may be amplified and screened for mutation by SSCP (single-strand conformation polymorphism) before sequencing of the mutated exon.

4.2. MP-PCR

Use preferably DNA or lysates from nonselected (wild-type) clones as positive controls, and DNA from the RJK853 cells with a total *HPRT*-gene deletion ***(13)*** as a negative control. To confirm partial deletions, amplify single *HPRT* exons using conditions for MP- or exon-specific PCR (**Tables 1** and **2**), but with a primer concentration of 0.5 μ*M*, 200 μ*M* of each dNTP and 1 U of *Taq* polymerase.

To distinguish methodological failure from total deletion, include a primer pair for another gene as an internal DNA/PCR control in an exon-specific PCR. The intronless coding region of the *N*-acetyltransferase 2 gene can be amplified by using forward primer $_{(1)}$5'-GTC ACA CGA GGA AAT CAA ATG-3'$_{(21)}$ and reverse primer $_{(1002)}$5'-GAG AGG ATA TCT GAT AGC AC-3'$_{(1022)}$ at an annealing temperature of 58°C ***(14)***.

4.3. Siblings and Spectrum

For establishing a more reliable spectrum, the clonality should be checked for clones with identical mutations from same individual, especially when the individual in vivo mutant frequency is extremely high. The method for analysis of T-cell receptor (TCR) γ-gene rearrangement have been described by de Boer et al. ***(15)***. Clonal MP-lysate can be used in a two-step PCR with primers (annealing at 60 and 63°C) originally described by Bourguin et al. ***(16)***:

Outer forward: 5'-GAA GCT TCT AGC TTT CCT GTC TC-3' (Var)
Outer reverse: 5'-CGT CGA CAA CAA GTG TTG TTC CAC-3' (J)
Inner forward: 5'-CTC GAG TGC GCT GCC TAC AGA GAG G-3' (Var)
Inner reverse: 5'-GGA TCC ACT GCC AAA GAG TTT CTT-3' (J)

The nested PCR product is subjected to an analysis of restriction fragment length polymorphisms (RFLPs) with restriction digestions (*Bst*O1 and *Rsa*I) followed by electrophoresis in a 15% polyacrylamide gel ***(17)***.

Finally, to avoid artifacts in comparing mutational spectra between groups of individuals with different ages and/or exposures, the number of clones collected from each subject for molecular analysis should be kept as even as possible. A large collection of mutations identified from many different subjects would probably be more suitable than that from few individuals.

References

1. Cole, J., and Skopek, T. (1994) Somatic mutant frequency, mutation rates and mutational spectra in the human population *in vivo*. *Mutat. Res.* **304,** 33–106.
2. Fuscoe, J. C., Zimmerman, L. J., Lippert, M. J., Nicklas, J. A., O'Neill, J. P., and Albertini, R. J. (1991) V(D)J recombinase-like activity mediates *hprt* gene deletion in human fetal T-lymphocytes. *Cancer Res.* **51,** 6001–6005.

3. Edwards, A., Voss, H., Rice, P., Civitello, A., Stegeman, J., Schwager, C., Zimmerman, J., Erfle, H., Caskey, C. T., and Ansorge, W. (1990) Automated DNA sequencing of the human *hprt* locus. *Genomics* **6,** 593–608.
4. Cariello, N. F. (1994) Software for the analysis of mutations at the human *hprt* gene. *Mutat. Res.* **312,** 173–185 (database updated 1996)
5. Gibbs, R. A., Nguyen, P. N., Edwards, A., Civitello, A. B., and Caskey, C. T. (1990) Multiplex DNA deletion detection and exon sequencing of the hypoxanthine phosphoribosyltransferase gene in Lesch-Nyhan families. *Genomics* **7,** 235–244.
6. Albertini, R. J., O'Neill, J. P., Nicklas, J. A., Heintz, N. H., and Kelleher, P. C. (1985) Alterations of the *hprt* gene in human *in vivo*-derived 6-thioguanine-resistant T lymphocytes. *Nature* **316,** 369–271.
7. Österholm, A.-M., Fält, S., Lambert, B., and Hou, S.-M. (1995) Classification of mutations at the human *hprt*-locus in T-lymphocytes of bus maintenance workers by multiplex-PCR and reverse transcriptase-PCR analysis. *Carcinogenesis* **16,** 1909–1912.
8. Österholm, A.-M. and Hou, S.-M. (1998) Splicing mutations at the *hprt* locus in human T-lymphocytes *in vivo*. *Environ. Mol. Mutagenesis* **32,** 25–32.
9. Podlutsky, A., Österholm, A.-M., Hou, S.-M., Hofmaier, A., and Lambert, B. (1997) Spectrum of point mutations in the coding region of the hypoxantine phosphoribosyl transferase (*hprt*) gene in human T-lymphocytes *in vivo*. *Carcinogenesis* **19,** 557–566.
10. Yang, J. L, Maher, V. M., and McCormick, J. J. (1989) Amplification and direct nucleotide sequencing of cDNA from the lysate of low numbers of diploid human cells. *Gene* **83,** 347–354.
11. Fuscoe, J. C., Zimmerman, L. J., Harrington-Brock, K., and Moore, M. M. (1992) Large deletions are tolerated at the *hprt* locus of *in vivo* derived human T-lymphocytes. *Mutat. Res.* **283,** 255–262.
12. Steen, A.-M., Sahlén, S., Hou, S.-M., and Lambert, B. (1993) *Hprt*-activities and RNA phenotypes in 6-thioguanine resistant human T-lymphocytes. *Mutat. Res.* **286,** 209–215.
13. Yang, T. P., Patel, P. I., Chinault, A. C., Stout, J. T., Jackson, L. G., Hildebrand, B. M., and Caskey, C. T. (1984) Molecular evidence for new mutation at the *hprt* locus in Lesch–Nyhan patients. *Nature* **310,** 412–414.
14. Hou, S.-M., Lambert, B., and Hemminki, K. (1995) Relationship between hprt mutant frequency, aromatic DNA adducts and genotypes for GSTM1 and NAT2 in bus maintenance workers. *Carcinogenesis* **16,** 1913–1917.
15. de Boer, J. G., Curry, J. D., and Glickman, B. W. (1993) A fast and simple method to determine the clonal relationship among human T-cell lymphocytes. *Mutat. Res.* **288,** 173–180.
16. Bourguin, A., Tung, R., Galili, N., and Sklar, J. (1990) Rapid, nonradioactive detection of clonal T-cell receptor gene rearrangements in lymphoid neoplasms. *Proc. Natl. Acad. Sci. USA* **87,** 8536–8540.
17. Bastlova, T. and Podlutsky, A. (1996) Molecular analysis of styrene oxide-induced hprt mutation in human T-lymphocytes. *Mutagenesis* **11,** 581–591.

15

Assessment of Susceptibility of Low-Density Lipoprotein to Oxidation

Jane McEneny and Ian S. Young

1. Introduction

It is now recognized that oxidation of low-density lipoprotein (LDL) is a key event in the development of atherosclerosis ***(1)***. In vivo, oxidation is believed to occur primarily in the arterial wall. In early atherosclerotic lesions oxidation may be initiated by enzymes, including myeloperoxidase and 15-lipoxygenase, or by reactive nitrogen species, while in more advanced lesions transition metals including copper play a role ***(2)***. Oxidized LDL has a number of atherogenic properties ***(3)***. It is taken up via the macrophage scavenger receptor and promotes the formation of foam cells. It is chemotatic for circulating monocytes and inhibits the migration of tissue macrophages out of the arterial wall. In addition, oxidized LDL promotes platelet aggregation, is directly toxic to cells in the arterial wall, promotes the synthesis of a range of cytokines and growth factors, and inhibits nitric oxide mediated arterial dilation.

The assessment of the susceptibility of LDL to oxidation in vitro has become a widely used technique since it was introduced by Esterbauer ***(4)***. The assay is based on the assumption that LDL, which is easily oxidized in vitro, will also be readily oxidized in vivo. Following isolation, the oxidation of LDL is monitored by continuously measuring absorbance at 234 nm, which reflects the formation of conjugated dienes. The period of time prior to an increase in absorbance is referred to as the lag time, and is the period during which endogenous antioxidants within the LDL particle protect it from oxidation. A prolonged lag time implies increased resistance to oxidation. There then follows a period of rapid increase in absorbance referred to as the propagation phase, during which a free radical mediated chain reaction results in peroxidation of polyunsaturated fatty acids within the LDL particle. When all polyunsaturated fatty acids have become

From: *Methods in Molecular Medicine*, Vol. 38: *Aging Methods and Protocols*
Edited by: Y. A. Barnett and C. R. Barnett

oxidized, there is a second plateau period, which may be followed by a slight decrease in absorption due to decomposition of lipid hydroperoxides.

Because this technique involves isolation of LDL from aqueous phase chain breaking antioxidants such as urate and ascorbate, the susceptibility of LDL to oxidation is influenced mainly by its composition and size ***(5)***. Increased antioxidant content, particularly of α-tocopherol and ubiquinol, favors increased resistance to oxidation. The fatty acid composition is also important, with an increased percentage content of monounsaturated fatty acids protecting against oxidation and an increased content of polyunsaturated fatty acids decreasing resistance to oxidation. An increase in the cholesteryl ester to cholesterol ratio also results in increased susceptibility to oxidation, as does a preponderance of small dense LDL particles.

Increased susceptibility of LDL to oxidation is a feature of many of the degenerative diseases associated with aging. In healthy elderly men lag times are reduced in comparison with younger subjects ***(6)***. Increased LDL oxidation is also a feature of established coronary artery disease, peripheral vascular disease, diabetes mellitus, and stroke ***(7–10)***. Oxidation of LDL may contribute to impaired vascular endothelial reactivity in old age ***(11)***, and hence contribute to the development of both myocardial ischemia and cerebrovascular disease. Various interventions have been shown to improve the resistance of LDL to oxidation, including antioxidant supplements and change to a diet rich in monounsaturated fatty acids ***(12,13)***. However, as yet there are no prospective studies showing that a reduced lag time is an independent risk factor for the development of vascular disease.

The assay as originally described by Esterbauer involved a prolonged ultracentrifugation step (up to 24 h) to isolate LDL from EDTA plasma, followed by dialysis to remove potassium bromide, EDTA, and small chain breaking antioxidants such as urate and ascorbate. In total, the procedure required approx 48 h, and artifactual oxidation and loss of endogenous antioxidants from LDL was therefore a problem ***(14)***. The modified procedure as described here has a number of significant advantages. First, a rapid ultracentrifugation protocol using a bench top ultracentrifuge allows the isolation of LDL in 1 h. Second, LDL is purified by size-exclusion chromatography on a Sephadex column, obviating the need for prolonged dialysis. Third, the measurement of the lag time prior to the onset of oxidation and the calculation of rate of propagation has been automated, removing any possibility of subjective bias in determining results.

2. Materials

Metal ion contamination in buffers and solutions used in the extraction and purification of LDL can initiate oxidation prematurely. To minimize their presence all solutions are made using Millipore quality water.

1. Fasting peripheral venous blood is taken into 10-mL glass tubes containing lithium heparin (50 kU/L). Plasma is isolated by centrifugation (1500*g* for 10 min) and stored in 1-mL aliquots at –70°C until required. These samples are stable for up to 6 mo (*see* **Note 1**).
2. Polyallomer belltop centrifuge tubes (3 mL; 13 × 32 mm; Beckman cat. no. 349621).
3. Potassium bromide; 0.4451 g (Sigma cat. no. P5912) is placed directly into the ultracentrifuge tube. This is performed by means of a small homemade funnel made from a small sheet of flexible plastic, containing an opening small enough to fit into the neck of the ultracentrifuge tube.
4. Sodium chloride solution (d = 1.006g/mL: 0.196 molal — made by adding 11.42 g to 1 L deionized water). This solution is stored at 4°C and is stable for up to 1 *mo*.
5. Phosphate-buffered saline (PBS), pH 7.4, 0.01 *M*. This solution is stored at 4°C and is stable for up to 1 mo.
6. Peristaltic pump for overlaying NaCl solution onto density adjusted plasma. We use a Gilson Miniplus 2 (Gilson Medical Electronics, France, cat. no. 50482) at a setting of 400 for this procedure. The pump is fitted with narrow-bore Auto Analyser tubing (Bran and Luebbe, Germany, cat. no. 116-0549-08) or similar, connected to a 21 gauge needle (21G) attached using parafilm.
7. Beckman tabletop ultracentrifuge (TL100), together with a Beckman fixed-angle rotor 30° (TL100.3). The advantage of using a benchtop ultracentrifuge of this type is that it allows rapid isolation of LDL, greatly shortening the overall length of the procedure and allowing the isolation to be carried out in the absence of EDTA.
8. Beckman Tube Topper Sealer, which includes tube topper, stand, seal cap, seal guide, heat sink, and removal tool (Beckman cat. no. 348137) together with tube spacers (Beckman cat. no. 355937). The latter are required to prevent distortion or movement of the ultracentrifuge tubes within the rotor.
9. 21G needle, 2-mL syringe (clean needle and syringe for each LDL sample to be isolated, plus two extra needles per ultracentrifugation run).
10. 2-mL O-ring tubes for collection of crude LDL (Sarstedt cat. no. 72.694), 10-mL tubes for collection of desalted PD10-treated LDL (Sarstedt cat. no. 57.469), and 4-mL tubes for protein estimation and standard curve (Sarstedt cat. no. 55.478).
11. PD10 columns containing Sephadex G25 (Pharmacia, Milton Keynes, UK). These columns are disposable. However, they can be reused many times by ensuring they are thoroughly washed with at least 25 mL of PBS immediately prior to reuse. Columns are prepared and stored at 4°C.
12. Bovine serum albumin (BSA) solution, 25 µg/mL (Sigma cat. no. A2153) (*see* **Note 2**).
13. Bio-Rad dye reagent, 300 µL/sample (Bio-Rad 500-006, Bio-Rad Hemel, Hempstead, UK), stored at 4°C.
14. Disposable semimicro cuvets, 1 mL (Sarstedt, cat. no. 67.746).
15. Semimicro quartz cuvets (cells), 1 mL (Starna, Romford, Essex). The number of quartz cells required depends on the capacity of the spectrophotometer; in our case we require 6 cells.

16. Disposable cups, 20 mL (Sarstedt, cat. no. 73.1056).
17. Nusonics ultrasonic cleaner (Quayl Dental, Worthing, Sussex).
18. Copper chloride solution (40 µmol/L, BDH cat. no. 10088). This solution is stored at 4°C and is made in sufficient quantities for use in a series of experiments (*see* **Note 3**).
19. Saline solution (0.9% NaCl: BDH cat. no. 10241AP).
20. Decon-90 (4% solution; Decon Laboratories, E. Sussex).
21. HCl (0.5 *M* made from 37%, Janssen cat. no. 12.463.47).
22. Thermostatically controlled spectrophotometer (37°C, Hitachi U-2000-1, cat. no. HIT/121-0032), containing automatic six-cell positioner (Hitachi cat. no. HIT/121-0304) linked to a PC with software package for automatic handling of data (Hitachi, Enzyme Kinetic Data System).
23. Microsoft Excel software package for data computation utilizing a specially written macroprogram ***(15)*** (a copy of this macro is available from the authors).

3. Methods

Separation of the lipoprotein species is achieved by flotation nonequilibrium ultracentrifugation. The method described is very rapid and requires less than 2 h total preparation time (including ultracentrifugation) prior to oxidation.

1. To a Beckman 3-mL ultracentrifuge tube containing 0.4451 g of KBr is added 0.9 mL of heparinized plasma. This plasma is added from a pipet connected to fine-bore tubing (approx 2.5 cm in length and a diameter small enough to enter the neck of the ultracentrifuge tube). The ultracentrifugation tube is temporarily sealed with parafilm, allowing gentle inversion to dissolve the salt. This solution has a resultant density of 1.30 g/mL.
2. To this density-adjusted plasma, NaCl (d = 1.006 g/mL) is added, using the tubing and 21G needle connected to the peristaltic pump. The needle requires shaping to enable it to rest on the inside of the ultracentrifuge tube. Allow the solution to gently run down the side onto the top of the density adjusted plasma (ensure no mixing or distortion of the layers occurs during this procedure).
3. The ultracentrifugation tubes are sealed using the Beckman Tube Topper Sealer. They are gently placed in the Beckman rotor together with the Beckman spacers. Ultracentrifugation is performed using the following settings: 4°C, 100,000 rpm (541,000*g*) for 1 h. An acceleration and deceleration setting of 6 is chosen; total ultracentrifugation run time is 1 h and 6 min. The acceleration and deceleration parameters prevent disturbance of the density gradient created during ultracentrifugation.

   Note: During ultracentrifugation the following steps are performed.

   a. Preparation of columns: one column per sample is prepared (at 4°C) by washing through with 25 mL of PBS prior to use. These columns are designed to retain a reservoir of buffer within the gel bed. They do not run dry and may be left unattended for short periods of time.

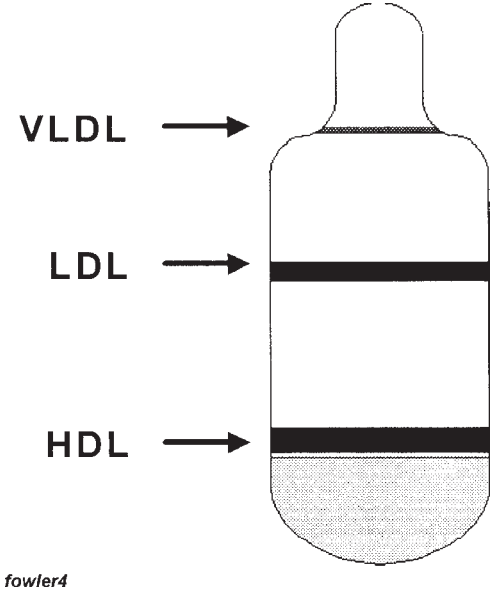

Fig. 1. Positions of VLDL, LDL, and HDL after ultracentrifugation.

b. Preparation of quartz cells (*see* **Note 4**).
c. Preparation of protein standard curve (*see* **Note 2**).

4. On completion of ultracentrifugation, the ultracentrifuge tubes are gently removed from the rotor and placed in the rack holder. The LDL band is visible in all cases, and in most is a distinct orange band located approximately one third distance from the top of the tube. It is distinctly separate from other lipoprotein species, that is, very-low-density lipoprotein (VLDL) and high-density lipoprotein (HDL) (the former being found at the top of the tube and the latter below the level of LDL) (*see* **Fig. 1**). The sample within the ultracentrifuge tube is contained within a vacuum that has to be broken to remove the sample without distortion of the layers. This is achieved by first inserting a needle (21G) at least twice at the top of the tube, leaving it in place on the second puncture; this allows the entry of air into the tube. At the position of the LDL layer puncture the side of the tube with a second needle to remove a plug of polyallomer that would otherwise prevent the removal of sample. The LDL layer is then removed through this opening by a third needle attached to a 2-mL syringe in a volume of 0.9 mL (ensure the needle remains within the LDL band). A new needle and syringe is used for the collection of each LDL sample. (Removal of the LDL by aspiration minimizes contamination with other lipoproteins and plasma proteins which can occur if the sample is collected by downward fractionation). The LDL sample is placed in a 2-mL O-ring tube and placed on ice for immediate use. This sample equates to “crude” LDL.

5. Size-exclusion chromatography for desalting crude LDL using the PD10 column. Crude LDL is contaminated with KBr. The sample also contains small molecules such as urate that can alter its susceptibility to oxidation. Desalting is performed as follows: 0.5 mL of crude LDL is added to the prewashed PD10 columns; this is allowed to enter the gel bed. Two milliliters of PBS is then added and also allowed to enter the gel bed. Both these eluants are discarded. The LDL is then obtained by adding a second 2-mL aliquot of PBS and this eluant is collected into a 10-mL tube. The LDL sample is now termed "desalted" (PD10) LDL and is placed on ice until the sample is ready to be oxidized after protein determination. (After collection of the LDL sample start preparing the columns for reuse by washing with PBS before sealing).

   Note: Subjecting LDL to column chromatography renders it less stable. Crude LDL can be stored at 4°C for up to 2.5 h with little deterioration of lag time. However, PD10-treated LDL must be used as rapidly as possible. It is therefore important to prepare all stages post PD10 treatment in advance while ultracentrifugation is being performed (e.g., quartz cells and protein assay).
6. Protein determination and standardization of PD10 LDL: LDL protein is read against the prepared BSA standard curve. The dilution of LDL is taken into account by multiplying the figure obtained by a factor of 15, as 100 µL of PD10 LDL is added to 1100 µL of water plus 300 µL of Bio-Rad dye reagent, giving a final volume of 1500 µL and thus a dilution of 15. The LDL is then standardized to 50 µg/mL of protein with PBS, taking into account the volume of copper solution added. The final volume of each cuvet is 1000 µL.

   The volume of LDL (Y) and PBS (Z) required can be obtained using the following formula:

$$Y\ \mu\text{L of LDL} = 50/X\ \mu\text{g/mL LDL} \times 1000$$
$$Z = 1000\ \mu\text{L} - (Y\ \mu\text{L of LDL} + 50\ \mu\text{L Cu}^{2+})$$

   where X is the concentration of protein determined from the standard curve × 15, Y is the volume of LDL required in the cell to give a final concentration of 50 µg/mL when the volume is made up to 1000 µL, and Z is the volume of PBS required to dilute the LDL to the required concentration (*see* **Note 5**).

   Dilution of the LDL sample is performed in the quartz cuvet. The copper chloride solution is added after LDL and PBS. (The action of the pipet is used to mix the copper solution with the LDL/PBS mixture by expelling and drawing the copper solution back and forth several times. In our experience this procedure is more effective than cell inversion). The samples are then placed into the spectrophotometer and data collection initiated.
7. Oxidation of the sample is followed in the thermostatically controlled spectrophotometer. Change in absorbance is followed at 234 nm and recorded every 2 min. The change in absorbance is recorded on a Nimbus PC-386 utilizing the Enzyme Kinetic Data System software package. This automated system removes the need for lengthy manual recording.
8. Oxidation profile: A typical profile is shown in **Fig. 2A**, and has two distinct phases:

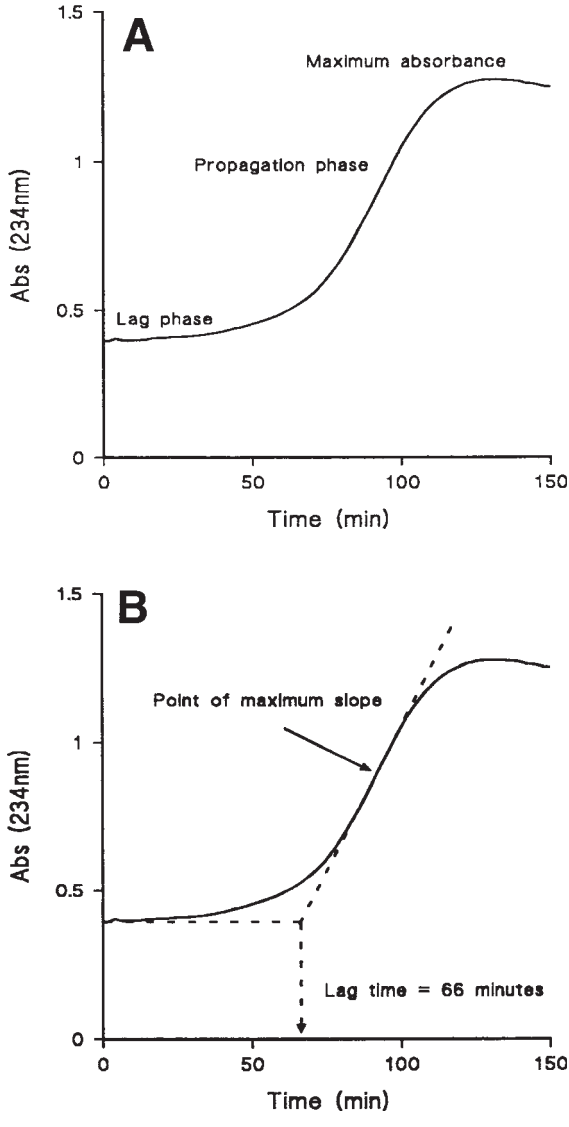

Fig. 2. Typical curve obtained by monitoring oxidation of LDL with copper at 234 nm.

a. Initial or lag phase: This is a slope with a slow increase in absorbance. The duration of this phase is indicative of the inherent resistance to oxidation of the LDL sample being examined.
b. Propagation phase: The lag phase is followed by a steep increase in absorbance due to the rapid formation of conjugated dienes. This occurs only when all the endogenous antioxidants within the LDL molecule and their protective

effect have been utilized. When the propagation phase is complete a plateau of maximum absorbance is reached.

9. Data analysis: *See* **Fig. 2B**. Determination of lag time using the mathematical program removes subjective error which may occur if determined manually. This is calculated using a specially written macroprogram after the results obtained on the PC are converted into ASCII file format and imported into the spreadsheet program Excel. The lag time is calculated as the intercept between the line of maximum slope of the propagation phase and the baseline where absorbance was at time = zero (*see* **Note 6**).

4. Notes

1. Heparinized plasma is used in preference to serum purely for logistic reasons, as serum collection lengthens total preparation time. However, this technique may be applied equally well to serum samples with no detectable difference in lag time when compared to heparinized plasma.
2. Protein standards and protein estimation: Stock BSA (25 µg/mL) is prepared by placing 12.5 mg of BSA into a 500-mL beaker. Add approx 300 mL of deionized water and gently stir (care is required as vigorous mixing can cause BSA to foam and make it difficult to bring to the correct volume). Add this solution to a 500-mL volumetric flask and rinse the beaker with remaining water to bring to correct volume. Aliquot 7 mL of this solution into 10-mL tubes, cap, and freeze at –20°C. This solution is stable for up to 6 mo.

   Working standard solutions (0, 2.5, 10, 15, 20 µg/mL) are prepared from the stock BSA. These together with the samples are diluted with distilled water to a final volume of 1.2 mL and prepared in duplicate in the 4-mL tubes. Three hundred microliters of Bio-Rad dye reagent is then added, making a final volume 1.5 mL. The standards and samples are then gently inverted and absorbance at 595 nm recorded within 5–60 min. The PD10 LDL is made up to 1.2 mL using 0.1 mL of sample and 1.1 mL of distilled water. If the protein concentration of crude LDL is required use only 10 µL and dilute to 1.2 mL with water (dilution factor for crude LDL is 150).
3. Copper chloride solution: The working solution of copper chloride is 40 µ*M*. This solution is made by serial dilution of a 33.2 m*M* stock solution.
   a. Solution A: 33.2 m*M* — 0.567 g of $CuCl_2 \cdot 2H_2O$ made in a 100-mL volumetric flask using deionized water.
   b. Solution B: 332 µ*M* — 1 mL of solution A is added to a 100-mL volumetric flask and the volume is made up using saline solution.
   c. Solution C: 40 µ*M* working solution — 6.024 mL of solution B is added to a 50-mL volumetric flask and the volume made up using either PBS or saline solution (addition of PBS in the earlier solutions causes precipitation).
4. Preparation of quartz cells: New or used cells must undergo the following procedure before use.

   Each cell is rinsed at least 10× with distilled water. They are then placed into a separate disposable cup containing sufficient 4% Decon–90 to cover them. The

cups are placed in the sonic bath and sonicated for 5 min. The cells are then inverted (not the cups), while trying to retain as much solution as possible within the cells. They are then sonicated again for 5 min, removed, rinsed with distilled water (10×), and placed in 0.5 *M* HCl for at least 1 h prior to use/reuse.

Before use in the oxidation experiment the acid-soaked cells must be thoroughly cleaned. The cells are rinsed with distilled water (10×), placed into clean cups containing water, and sonicated for 5 min, before again inverting and sonicating for a further 5 min. The cells are then allowed to drain on absorbent paper and are now ready for use.

The reason for this rigorous cleaning regime is because oxidation of LDL produces lipoperoxides which may adhere to the side of the cells. These seed the oxidation reaction and would artefactually increase the rate of oxidation in the sample being examined. In our hands this rigorous cleaning procedure is essential if reproducible results are to be obtained.

5. A worked example of the formula is shown here. If the concentration of LDL protein is 157 mg/mL, determined from the standard curve X dilution factor, the volumes of LDL (*Y*) and PBS (*Z*) are as follows:

$$Y = 50/157 \times 1000 = 318\ \mu\text{L of LDL}$$

As the LDL is made up to a final volume of 1000 µL the volume of PBS required, taking into account the 50 µL of copper to be added, is

$$Z = 1000 - (318\ \mu\text{L of LDL} + 50\ \mu\text{L of Cu}) = 632\ \mu\text{L of PBS}$$

Therefore to the cell is added 318 µL of LDL + 50 µL of Cu + 632 µL of PBS. The final volume is 1000 µL.

6. The lag time is determined by taking the point of maximum slope over an interval of 20 min and fitting a line by the least squares method. The point of maximum slope was found by repeated computation of the average slope for 11 consecutive points moving along 1 point at a time, enabling deviations due to random noise from the spectrophotometer to be removed.

References

1. Witztum, J. L. (1993) Susceptibility of low-density lipoprotein to oxidative modification. *Am. J. Med.* **94,** 347–356.
2. Heinecke, J. W. (1997) Mechanisms of oxidative damage of low density lipoprotein in human atherosclerosis. *Curr. Opin. Lipidol.* **8,** 268–274.
3. Westhuyzen, J. (1997) The oxidation hypothesis of atherosclerosis: an update. *Ann. Clin. Lab. Sci.* **27,** 1–10.
4. Esterbauer, H., Striegl, G., Puhl, H., and Rotheneder, M. (1989) Continuous monitoring of *in vitro* oxidation of human low-density lipoprotein. *Free Radic. Res. Commun.* **6(1),** 67–75.
5. Esterbauer, H., Gebicki, J., Puhl, H., and Jurgens, G. (1992) The role of lipid-peroxidation and antioxidants in oxidative modification of LDL. *Free Radic. Biol. Med.* **13(4),** 341–390.

6. Napoli, C., Abete, P., Corso, G., Malorni, A., Postiglione, A., Ambrosio, G., Cacciatore, F., Rengo, F., and Palumbo, G. (1997) Increased low-density lipoprotein peroxidation in elderly men. *Coron. Art. Dis.* **8,** 129–136.
7. Karmansky, I., Shnaider, H., Palant, A., and Greuner, N. (1996) Plasma lipid oxidation and susceptibility of low density lipoproteins to oxidation in male patients with stable coronary artery disease. *Clin. Biochem.* **29,** 573–579.
8. Iribarren, C., Folsom, A. R., Jacobs, D. R., Gross, M. D., Belcher, J. D., Eckfeldt, J. H. (1997) Association of serum vitamin levels, LDL susceptibility to oxidation, and autoantibodies against MDA-LDL with carotid atherosclerosis — a case-control study. *Arterioscler. Thromb. Vasc. Biol.* **17,** 1171–1177.
9. Yoshida, H., Ishikawa, T., and Nakamura, H. (1997) Vitamin E lipid peroxide ratio and susceptibility of LDL to oxidative modification in non-insulin-dependent diabetes mellitus. *Arterioscler. Thromb. Vasc. Biol.* **17,** 1438–1446.
10. Palinski, W. and Horkko, S. (1997) Biological consequences of oxidation in atherosclerosis and other pathologies. Lipoprotein oxidation in brain arteries. *Nutr. Metab. Cardiovasc. Dis.* **7,** 237–247.
11. Khder, Y., Bray, L., Boscs, D., Aliot, E., and Zannad, F. (1996) Endothelial, viscoelastic and sympathetic factors contributing to the arterial wall changes during ageing. *Cardiol. Elderly* **4,** 161–165.
12. deWaart, F. G., Moser, U., and Kok, F. J. (1997) Vitamin E supplementation in elderly lowers the oxidation rate of linoleic acid in LDL. *Atherosclerosis* **133,** 255–263.
13. Parthasarathy, S., Grasse, B. J., Miller, E., Almazan, F., Khoo, J. C., Steinberg, D., and Witztum, J. L. (1991) Using an oleate-rich diet to reduce susceptibility of low-density lipoprotein modification in humans. *Am. J. Clin. Nutr.* **54,** 701–706.
14. Scheek, L. M., Wiseman, S. A., Tijburg, L. M., and Vantol, A. (1995) Dialysis of isolated low density lipoprotein induces a loss of lipophilic antioxidants and increases the susceptibility to oxidation *in vitro*. *Atherosclerosis* **117,** 139–144.
15. McDowell, I. F., McEneny, J., Trimble, E. R. (1995) A rapid method for measurement of the susceptibility to oxidation of low-density-lipoprotein. *Ann. Clin. Biochem.* **32,** 167–174.

16

Measurement of Pentosidine in Biological Samples

Jesus R. Requena, David L. Price, Suzanne R. Thorpe, and John W. Baynes

1. Introduction

Pentosidine is a highly fluorescent advanced glycation end product (AGE) and crosslink derived from one molecule of arginine and one of lysine bridged in an imidazo-pyridinium structure (**Fig. 1**). It was first isolated from articular cartilage by Sell and Monnier ***(1)***, and has now been detected and quantified in a variety of human and animal tissues, including skin and kidney collagen ***(2–5)***, lens crystallins ***(6,7)***, plasma ***(8,9)***, serum ***(10)***, urine ***(11)***, and synovial fluid ***(12,13)***. Pentosidine is readily prepared from arginine, lysine, and a pentose (hence its name). Dyer et al. ***(14)*** have also described its formation from glucose, albeit at a slower rate and probably through oxidation of glucose to arabinose ***(15)***. Because its formation from either glucose or ribose requires oxidation, pentosidine is both an AGE and a "glycoxidation" product ***(16)***.

Pentosidine accumulates in long-lived tissue proteins with age (**Fig. 2**). The kinetics of its accumulation in human skin collagen have been fitted to a linear regression by Dyer et al. (μmol pentosidine/mol of lysine = $0.41 \times \text{age} - 0.48$ [$r = 0.78$, $p < 0.001$]) ***(3)*** and to an exponential one by Sell et al. (pmol pentosidine/mg collagen = $0.008 \times \text{age}^2 + 0.325 \times \text{age} + 3.45$ [$r = 0.927$, $p < 0.0001$]) ***(5)***. The rate of accumulation of pentosidine in skin collagen is inversely proportional to species life-span ***(5)***. Because it is a crosslink, it was hypothesized that pentosidine might contribute to the age-related increase in collagen stiffness. However, the trace concentration of pentosidine in tissues, in the range of a few millimoles per mole of triple helical collagen (**Fig. 2**), makes it unlikely

From: *Methods in Molecular Medicine*, Vol. 38: *Aging Methods and Protocols*
Edited by: Y. A. Barnett and C. R. Barnett

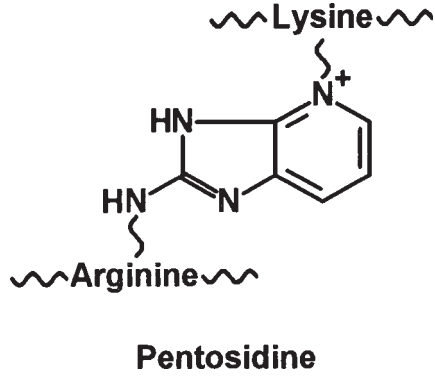

Fig. 1. Structure of pentosidine.

that pentosidine would have a significant effect on collagen structure. Pentosidine is, however, an excellent biomarker for nonenzymatic modification of long-lived proteins by the Maillard reaction, providing insight into overall role of the Maillard reaction in aging and disease. Concentrations of pentosidine in plasma protein and collagen are elevated in several pathological conditions, especially in end-stage renal disease ***(2,8,10)***, and, to a lesser extent, in diabetes ***(2–4,6,8,11,16,17)***, rheumatoid arthritis ***(12,13,18)***, atherosclerosis, and neurodegenerative diseases ***(19)***. The elevation in pentosidine concentration in these diseases is attributed to increased precursor concentrations, resulting from either increased oxidative stress and/or decreased detoxification of reactive carbonyl intermediates in the Maillard reaction.

This chapter describes a procedure for the preparation, purification, and calibration of a pentosidine standard, followed by a general method for measuring pentosidine by reverse-phase high-performance liquid chromatography (RP-HPLC) with fluorescence detection. This method is suitable for collagen samples, which produce clean chromatograms. In these cases, pentosidine is normalized to the hydroxyproline ***(20)*** or lysine content of the sample, or to the amount of protein. More complex samples, such as tissue extracts, plasma, and serum, yield noisy chromatograms in which pentosidine cannot always be resolved from other components. In these cases, the basic procedure is modified to include a simple clean-up procedure using sulfopropyl–Sephadex (SP-Sephadex) solid-phase extraction columns, based on a modification of the method of Takahashi et al. ***(10)***. In these cases, pentosidine concentration is expressed per mole of lysine, per milligram of protein, or per milliliter of serum or plasma. In general, to facilitate comparisons between proteins, it is more convenient to express the data as moles of pentosidine per mole of lysine.

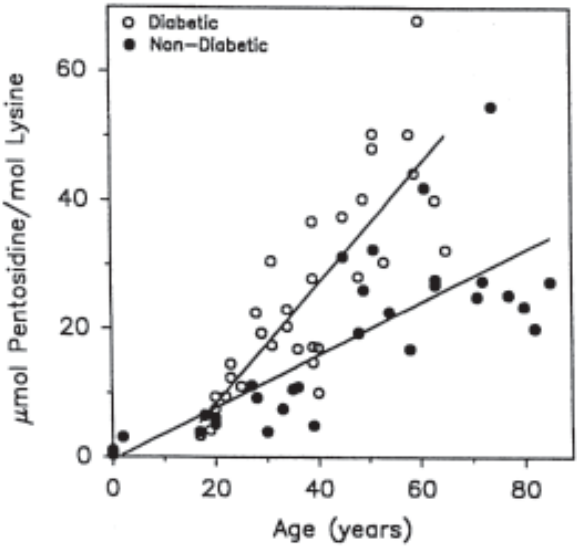

Fig. 2. Effects of age and diabetes on concentration of pentosidine in human skin collagen ***(3)***.

2. Materials

1. N^a-Acetyl-lysine, N^a-acetyl-arginine, D-ribose, trifluoroacetic acid (TFA) and heptafluorobutyric acid (HFBA) are available from Aldrich (St. Louis, MO, USA); SP-Sephadex C-25 from Pharmacia (Bromma, Sweden); C-18 solid phase extraction columns (Sep-Paks) from Waters (Milford, MA, USA); and 0.22 μ*M* luer-adaptable filters from Millipore (Bedford, MA, USA).
2. HPLC system: Two-solvent gradient system, equipped with fluorescence and diode array detectors. Reverse-phase, C-18 column, 15 × 0.46 cm, Vydac 218TP, 300A Pore Size; HPLC grade acetonitrile (CH_3CN).
3. Speed-Vac Centrifugal evaporator system (Savant Instruments, Farmingdale, NY, USA).
4. Heating block for heating 13 × 100 mm screw-cap test tubes at 65°C and 110°C.
5. Source of nitrogen gas (10 psi pressure).

3. Methods

3.1. Preparation of Pentosidine Standard

1. Dissolve N^a-acetyl-lysine (18.8 mg, 0.1 mmol), N^a-acetyl-arginine (21.6 mg, 0.1 mmol), and D-ribose (15 mg, 0.15 mmol) in 1 mL of 0.2 *M* sodium phosphate buffer, pH 9.0, in a 13 × 100 mm screw-cap tube with Teflon-lined cap. Adjust to pH 9 with 0.1 *M* NaOH.
2. Place in heating block at 65°C. Monitor pH, initially at hourly intervals, readjusting to pH 9.0, as needed.

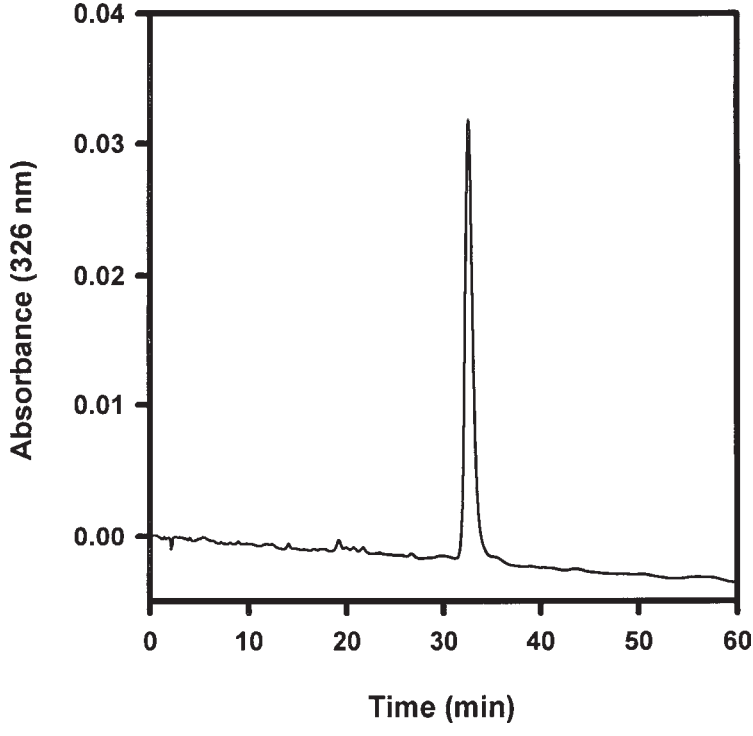

Fig. 3. RP-HPLC analysis of *N*,*N*'-diacetyl-pentosidine, the precursor of the pentosidine standard. Hydrolysis of this compound yields pure pentosidine, or a slightly contaminated product that can be further purified by analytical RP-HPLC.

3. After 48 h, dilute 300 µL of the resulting light brown solution to 3 mL with 1% TFA and apply to a 3-mL C-18 solid-phase extraction minicolumn previously equilibrated with 1% TFA.
4. Wash the column with 1% TFA. Collect fractions (2 mL) and monitor absorbance at 226 and 326 nm. After the initially high absorbance at 226 nm decreases to ~0.2 and stabilizes (~25 fractions), elute the column with 5% CH_3CN containing 1% TFA. Collect and pool fractions, with peak absorbance at 326 nm, corresponding to elution of *N*,*N*'-diacetyl-pentosidine, and dry *in vacuo* (*see* **Note 1**).
5. Redissolve sample in 500 µL of deionized water and purify *N*,*N*'-diacetyl-pentosidine by RP-HPLC (**Fig. 3**). Apply to 15 × 0.46 cm C-18 column, equilibrated with CH_3CN:0.1% HFBA in H_2O (1:6), and elute isocratically at a flow rate of 1 mL/min. Monitor absorbance at 326 nm. A single major peak corresponding to *N*,*N*'-diacetyl-pentosidine should appear. Collect and pool peak fractions; dry *in vacuo*.
6. Prepare pentosidine standard by hydrolysis of *N*,*N*'-diacetyl-pentosidine in 2 *M* HCl for 4 h at 110°C. Dry the hydrolysate and redissolve in 1 mL of deionized

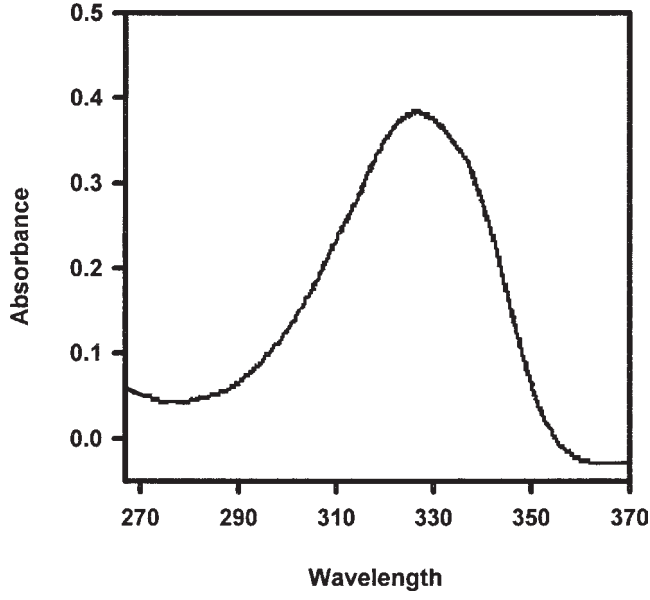

Fig. 4. Absorbance spectrum of pentosidine in 0.1 M HCl.

water. Check purity of pentosidine by RP-HPLC analysis, as described in **Subheading 3.2., step 4**. If fluorescent contaminants are present, repurify pentosidine by RP-HPLC using analytical conditions, then pool pentosidine fractions. For calibration, dissolve an aliquot of the pooled pentosidine in 0.1 *M* HCl, measure absorbance at 326 nm, and calculate pentosidine concentration using a molar extinction coefficient of 14,200 at 326 nm (**Fig. 4**; *see* **Note 2**). A convenient concentration for a working standard is 0.5 pmol/µL. Store dilute, working standards frozen at –20°C in 0.1% HFBA.

3.2. General Method for Measuring Pentosidine in Collagen

1. Place weighed sample of collagen (1–5 mg) in 13 × 100 mm screw-cap test tube. Reduce by addition of 1 mL of 0.2 *M* sodium borate buffer, pH 9.2, followed by 100 µL of 1 *M* $NaBH_4$ dissolved in 0.1 *M* NaOH. Reduction can be carried out for 4 h at room temperature or overnight at 4°C (*see* **Note 3**).
2. Recover collagen by centrifugation or decanting, discard supernatant, and wash with deionized water.
3. Hydrolyze collagen in 5 mL of 6 *M* HCl at 110°C for 24 h in screw-cap tubes flushed with N_2 (*see* **Note 3**).
4. Dry hydrolysates *in vacuo*. Redissolve samples in 500 µL of 0.1 *M* HFBA using vortex mixing or sonication, as required, and inject a 200-µL aliquot onto an RP-HPLC column for analysis. HPLC solvents: A, 0.1% HFBA in H_2O; B, CH_3CN. Gradient: 5 min in 10% B, followed by linear gradient of 10 to 22% B

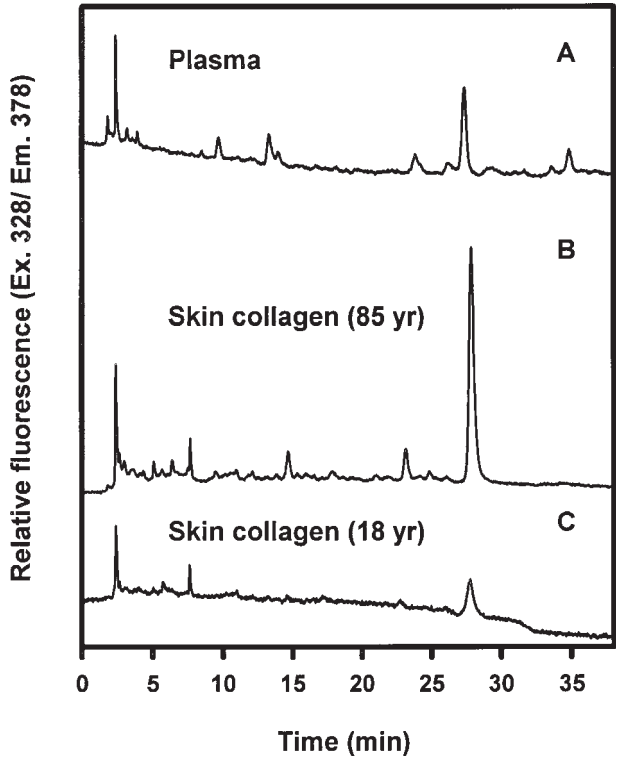

Fig. 5. RP-HPLC chromatograms of analysis of **(A)** normal human plasma and **(B**,**C)** human skin collagen from 85- and 18-yr-old donors, respectively.

over 35 min, followed by 15-min wash with 95% CH_3CN (*see* **Note 4**). Monitor fluorescence at excitation $\lambda = 328$, emission $\lambda = 378$. Typical chromatograms are shown in **Fig. 5B**,**C**. The limit of detection of pentosidine on our HPLC system is approx 0.2 pmol, but will vary with instrumentation.

5. The concentration of pentosidine in the sample is determined using a standard curve prepared with authentic pentosidine. A separate analysis of the hydrolysate is required to measure hydroxyproline or lysine, depending on the method of expressing the data. The intraassay coefficient of variation is typically 6–8% for middle-aged human skin collagen.

3.3. Method for Measuring Pentosidine in Plasma Proteins (see Note 5)

3.3.1. Sample Preparation

1. Mix 200 µL of plasma with an equal volume of 0.2 *M* borate buffer, pH 9.2, in a 13 × 100 mm screw-cap test tube. Add 40 µL of a freshly prepared 1 *M* solution of $NaBH_4$ in 0.1 *M* NaOH, and let the sample reduce at room temperature for 4 h.

2. Precipitate protein by addition of 440 mL of 20% trichloroacetic acid (TCA) while vortex-mixing. Centrifuge the sample at 1000*g* for 5 min (tabletop, clinical centrifuge) and discard the supernatant. Wash pellet once by suspension in 10% TCA and recentrifugation.
3. Hydrolyze protein in 5 mL of 6 *M* HCl for 24 h at 110°C in screw cap tube under N_2.
4. Dry hydrolysate *in vacuo* and redissolve sample in 10 mL of deionized water and filter through 0.22 µm luer-adaptable filters. Wash the filter with 1 mL of deionized water and pool with the filtrate.

3.3.2. Solid-Phase Extraction with SP-Sephadex Minicolumns

1. Swell SP-Sephadex overnight in deionized water at 4°C, according to the manufacturer's instructions.
2. Prepare minicolumns by filling small plastic columns with 3 mL of swollen gel.
3. Wash minicolumns with 15 mL of deionized water, apply filtered samples, and wash with 20 mL of 0.1 *M* HCl. Elute with 7 mL of 1 *M* HCl. Pool and dry eluate (*see* **Note 6**).
4. Redissolve eluate in 500 mL of 0.1% HFBA. Analyze a 200-µL aliquot by RP-HPLC, as described in **Subheading 3.2**. A typical chromatogram of a human plasma sample is shown in **Fig. 5A**. Pentosidine may be expressed as µmoles of pentosidine per milliliter plasma or per mole of lysine, measured separately by analysis of the plasma sample or hydrolysate. The intraassay coefficient of variation is typically 8–10%.

4. Notes

1. The yield of pentosidine is typically ~1%, so the HPLC column could be overloaded by impurities during purification. The preliminary clean-up step is designed to eliminate excess reactants and salts that are not retarded by the column, and brown products that are retained on the column after elution of pentosidine. Column washing with 1% TFA is stopped when absorbance at ~226 nm is less than 0.2 or has ceased to decrease. Switch to eluting solvent (1% TFA in 5% CH_3CN) if absorbance at 326 nm begins to increase. Collected fractions should be transparent or pale yellow. Brown color indicates overloading of the minicolumn and calls for a decrease in the amount of sample applied. At this stage, sacrifice yield for purity.
2. Dyer et al. ***(14)*** used radioactive lysine to calibrate their pentosidine standard. Sell and Monnier ***(1)*** used a gravimetrically calibrated standard (Monnier, *personal communication*). They reported a molar extinction coefficient of 4195 at 326 nm in 0.1 *M* HCl. For determination of the extinction coefficient in the present study, we prepared a sample of pure *N*-acetyl,*N*'- hippuryl-pentosidine (hippuryl = benzoyl-glycine) from N^a-hippuryl-lysine and N^a-acetyl-arginine. The product was purified by C-18 solid extraction and RP-HPLC using procedures similar to those described previously. Analysis by HPLC using a diode-array detector yielded a single peak with an absorbance maximum at 326 nm (pentosidine) and secondary maxima at 226 nm (amide carbonyl and carboxyl groups) and 278 nm (benzoyl

group). Following hydrolysis in 6 *M* HCl for 4 h at 110°C, RP-HPLC yielded two well-resolved absorbance peaks, with maxima at 226 nm (benzoic acid) and 326 nm (pentosidine). The extinction coefficient for pentosidine was calculated from the yield of glycine determined by amino acid analysis. The molar extinction coefficient of 14,200 at 326 nm, measured in 0.1 *M* HCl, was in good agreement with that for our previous pentosidine standard, based on the use of radioactive lysine ***(14)***, but was 3.4 times higher than that reported by Sell and Monnier ***(1)***.

3. Reduction with $NaBH_4$ prevents the interference from products of decomposition of Amadori compounds and reactive AGEs on protein. This step, together with hydrolysis under nitrogen, generally reduces the complexity of chromatograms.
4. The washing step is helpful for removing both fluorescent and nonfluorescent impurities that may interfere with resolution of the pentosidine peak.
5. The method described is for analysis of human plasma proteins, but can be adapted to analysis of other types of complex matrices.
6. Some pressure from a rubber bulb may be needed to start flow, but once started, the minicolumns operate under gravity. Sample pH is ~2, and pentosidine is retained on the column during the washing step. The gel collapses 10–20% during elution of pentosidine in 1 *M* HCl and should be discarded after use.

Acknowledgments

This work was supported by Research Grant DK–19971 to J. W. B. from the National Institutes of Diabetes, Digestive and Kidney Diseases. J. R. R. is the recipient of a postdoctoral fellowship from the Juvenile Diabetes Foundation International.

References

1. Sell, D. R. and Monnier, V. M. (1989) Structure elucidation of a senescence crosslink from human extracellular matrix. *J. Biol. Chem.* **264,** 21,597–21,602.
2. Sell, D. R. and Monnier, V. M. (1990) End-stage renal disease and diabetes catalyze the formation of a pentose-derived crosslink from aging human collagen. *J. Clin. Invest.* **85,** 380–384.
3. Dyer, D. G., Dunn, J. A., Thorpe, S. R., Bailie, K. E., Lyons, T. J., McCance, D. R., and Baynes, J. W. (1993) Accumulation of Maillard reaction products in skin collagen in diabetes and aging. *J. Clin. Invest.* **91,** 2463–2469.
4. Sell, D. R., Lapolla, A., Odetti, P., Fogarty, J., and Monnier, V. M. (1992) Pentosidine formation in skin correlates with severity of complications in individuals with longstanding IDDM. *Diabetes* **41,** 1286–1292.
5. Sell, D. R., Lane, M. A., Johnson, W. A., Masoro, E. J., Mock, O. B., Reiser, K. M., Fogarty, J. F., Cutler, R. G., Ingram, D. K., Roth, G. S., and Monnier, V. M. (1996) Longevity and the genetic determination of collagen glycoxidation kinetics in mammalian senescence. *Proc. Natl. Acad. Sci. USA* **93,** 485–490.
6. Lyons, T. J., Silvestri, G., Dunn, J. A., Dyer, D. G., and Baynes, J. W. (1991) Role of glycation in modification of lens crystallins in diabetic and non-diabetic senile cataracts. *Diabetes* **40,** 1010–1015.

7. Nagaraj, R. H., Sell, D. R., Prabhakaram, M., Ortwerth, B. J., and Monnier, V. M. (1991) High correlation between pentosidine protein crosslinks and pigmentation implicates ascorbate oxidation in human lens senescence and cataractogenesis. *Proc. Natl. Acad. Sci. USA*. **88,** 10,257–10,261.
8. Odetti, P. O., Fogarty, J., Sell, D. R., and Monnier, V. M. (1992) Chromatographic quantitation of plasma and erythrocyte pentosidine in diabetic and uremic subjects. *Diabetes* **41,** 153–159.
9. Taneda, S. and Monnier, V. M. (1994) ELISA of pentosidine, an advanced glycation end product, in biological specimens. *Clin. Chem.* **40,** 1766–1773.
10. Takahashi, M., Kushida, K., Kawana, K., Ishihara, C., Denda, M., Inoue, T., and Horiuchi, K. (1993) Quantification of the cross-link pentosidine in serum from normal and uremic subjects. *Clin. Chem.* **39,** 2162–2165.
11. Takahashi, M., Ohishi, T., Aoshima, H., Kawana, K., Kushida, K., Inoue, T., and Horiuchi, K. (1993) The Maillard protein cross-link pentosidine in urine from diabetic patients. *Diabetologia* **36,** 664–667.
12. Rodriguez-Garcia, J., Requena, J. R., and Rodriguez-Segade, S. (1998) Increased concentrations of serum pentosidine in rheumatoid arthritis. *Clin. Chem.* **44,** 250–255.
13. Miyata, T., Ishiguro, N., Yasuda, Y., Ito, T., Nangaku, M., Iwata, H., and Kurokawa, K. (1998) Increased pentosidine and advanced glycation end product, in plasma and synovial fluid from patients with rheumatoid arthritis and its relation with inflammatory markers. *Biochem. Biophys. Res. Commun.* **244,** 45–49.
14. Dyer, D. G., Blackledge, J. A., Thorpe, S. R., and Baynes, J. W. (1991) Formation of pentosidine during nonenzymatic browning of proteins by glucose. *J. Biol. Chem.* **266,** 11,654–11,660.
15. Wells-Knecht, K. J., Zyzak, D. V., Litchfield, J. E., Thorpe, S. R., and Baynes, J. W. (1995) Mechanism of autoxidative glycosylation: identification of glyoxal and arabinose as intermediates in the autoxidative modification of proteins by glucose. *Biochemistry* **34,** 3702–3709.
16. Baynes, J. W. (1991) Role of oxidative stress in development of complications in diabetes. *Diabetes* **40,** 405–412.
17. McCance, D. R., Dyer, D. G., Dunn, J. A., Bailie, K. E., Thorpe, S. R., Baynes, J. W., and Lyons, T. J. (1993) Maillard reaction products and their relation to complications in insulin-dependent diabetes mellitus. *J. Clin. Invest.* **91,** 2470–2478.
18. Takahashi, M., Suzuki, M., Kushida, K., Miyamoto, S., and Inoue, T. (1997) Relationship between pentosidine levels in serum and urine and activity in rheumatoid arthritis. *Br. J. Rheumatol.* **36,** 637–642.
19. Thorpe, S. R. and Baynes, J. W. (1996) Role of the Maillard Reaction in diabetes and diseases of aging. *Drugs Aging* **9,** 69–77.
20. Stegemann, H. and Stalder, K. (1967) Determination of hydroxyproline. *Clin. Chim. Acta* **18,** 267–273.

17

Causes and Consequences of Damage to Mitochondria

Morphological Aspects

Jaime Miquel and Carlo Bertoni-Freddari

1. Introduction

In recent years the role played by mitochondria in cellular aging has become the focus of intensive research. The concept that these energy-producing organelles are involved in aging derives from the views of Harman ***(1)*** and Gerschman ***(2)*** linking senescence to the damaging effects of free radicals, especially those released in the mitochondrial respiratory chain.

However, most gerontologists held the opinion that, because mitochondria are self-replicating organelles, they should be able to counteract any age-related loss. Our own electron microscopic studies have provided data in contradiction with that former view. Thus, in our study of *Drosophila* aging we were the first to demonstrate that the fixed-postmitotic cells of insects accumulate an age pigment structurally similar to the lipofuscin present in mammalian cells and that many of the pigment granules derive from degenerating mitochondria ***(3,4)***. Further, our investigation of the testis of aged mice showed a striking mitochondrial degeneration and loss in the fixed-postmitotic Sertoli and Leydig cells, while the mitochondria of the fast-replicating spermatogonia (also present in that organ) did not show any age-related change. This led us to propose the *mitochondrial theory of aging* ***(5–7)***, according to which senescence is linked to the injurious effects of oxy-radicals on the mitochondrial genome of neurons and other types of differentiated cells. This extranuclear somatic mutation concept of aging is supported by the finding that mitochondrial DNA (mtDNA) synthesis takes place at the inner mitochondrial membrane near the sites of formation of highly reactive oxygen radicals and their products such as

From: *Methods in Molecular Medicine*, Vol. 38: *Aging Methods and Protocols*
Edited by: Y. A. Barnett and C. R. Barnett

lipoperoxides and malonaldehyde. Further, mtDNA may be unable to counteract the chronic oxygen stress because, in contrast to the nuclear genome, it lacks histone protection and excision repair.

If oxidative injury is not limited to organellar membranes (as proposed by early free radical theory advocates) but also occurs in mtDNA, the organelles that have suffered oxidation-related genome mutation, inactivation, or loss will be unable to rejuvenate themselves by normal replication. Further, there will be an impaired renewal of the macromolecules coded by that genome, namely the 13 hydrophobic polypeptides of the electron transport chain and of ATP synthase as well as the mitochondrial rRNAs and tRNAs. This may lead to a progressive decline in mitochondrial function with decrease in ATP production and ATP-dependent protein synthesis.

It is very important from a clinical viewpoint that, because most cellular energy is produced in mitochondria through the process of oxidative phosphorylation, the age-related dysfunction and loss of these organelles must result in bioenergetic decline. This may trigger apoptotic death ***(8)*** and play a key role in the senescent decrease of physiological performance and in the pathogenesis of some age-related degenerative diseases of the somatic tissues mainly composed of fixed-postmitotic cells such as the cardiac and skeletal muscle and the central nervous system (CNS).

In our opinion, the preceding summary on the causes and effects of mitochondrial aging justifies the present compilation of very detailed and practical instructions for the electron microscopic study of mitochondria regarding tissue fixation, sectioning, staining, and quantitative morphological observation of the organelles. We hope that this information will be especially useful to researchers interested in furthering the understanding of the role of mitochondria as promoters or targets in the senescence of diverse cellular types and animal models. The techniques described may also interest the workers exploring the modulation of the rate of animal aging by genetic manipulation, underfeeding, and pharmacological and antioxidant treatments.

2. Materials

1. Anesthetic solution: 2,2,2-Tribromoethanol (200 mg/kg body weight) in 10% ethanol solution.
2. Perfusion solution: Prepare 0.1 *M* sodium cacodylate buffer at pH 7.4. If necessary, adjust the solution at the desired pH value by adding some drops of 0.1 *N* HCl (*see* **Note 1**). Dissolve 2% paraformaldehyde in cacodylate (**Note 2**). The weighed amount of paraformaldehyde is warmed in about half the final volume of cacodylate buffer at a temperature of 55–60°C. This solution is then cooled under running tap water before addition of glutaraldehyde. Add 5% glutaraldehyde (**Note 3**) and bring the fixation solution to the final volume. As shown in

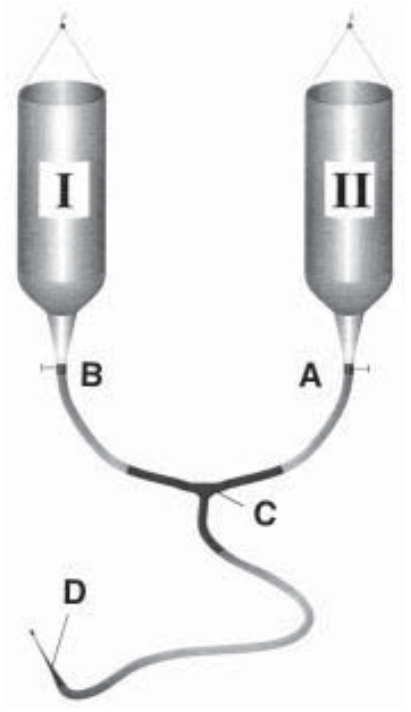

Fig. 1. This simple apparatus for vascular perfusion can be easily assembled using inexpensive materials. Plastic flasks can be adapted to contain saline (I) and fixation solution (II). **(A**,**B)** Clamps to stop either the saline or the fixative flow. **(C)** Y-Shaped tube to regulate both flows. **(D)** Infusion needle with rounded tip.

Fig. 1, a simple apparatus to carry out fixation by perfusion can be easily assembled. In essence, it consists of an infusion set with two plastic flasks, 4 m of small-sized plastic, transparent tubes, one Y-shaped tube, two clamps, and one perfusion needle.

3. Osmium tetroxide preparation (*see* **Note 4**): Remove the label from the ampoule containing the osmium tetroxide crystals, clean the ampoule carefully with ethanol to erase debris of any kind due to the label, and wash with twice-distilled water. A glass-stopped bottle, a glass tube, and a heavy glass rod must be cleaned with concentrated nitric acid to remove the organic matter. Twice-distilled water should be used to wash out traces of the acid. Never wipe with paper or cloth towel, as they can let loose particles that reduce the solution to hydrated dioxide. Add to the bottle a measured amount of twice-distilled water; place the ampoule containing osmium tetroxide crystals gently in the bottle; use the glass tube and the heavy glass rod to break the osmium ampoule and then quickly stop and shake the bottle vigorously. Complete dissolution of osmium crystals in the water takes at least half an hour. Wrap the bottle with aluminum foil and store in refrigerator

at 4°C. Protect this solution from exposure to light. Because of the high volatility of osmium tetroxide, there is a rapid decrease in the concentration of its solutions. Therefore, they should be prepared in small quantities and stored in flasks fitted with a glass stopper and Teflon sleeve (**Note 5**). We dissolve 1 g of osmium tetroxide in 33 mL of twice-distilled water, and then this solution is diluted (usually to 1%) and used according to our needs within a couple of weeks (**Note 6**).

4. Ethanol as a dehydrating agent for electron microscopy: The solutions with different concentrations of ethanol (at 70% and 80%) should be freshly prepared before their use by adding the proper volume of twice-distilled water. Ethanol at 95% for electron microscopy is commercially available at a reasonable price and good purity. Therefore, it is advantageous to buy it instead of preparing a solution starting from ethanol at 100%.
5. Propylene oxide: Used as transitional solvent from ethanol to the embedding resin.
6. Epoxy resin (Araldite) preparation (**Note 7**): Araldite, a yellowish, transparent epoxy resin, is prepared by mixing the following amounts of four components (**Note 8**):

Araldite (**Note 9**)	10 mL
Dodecenyl succinic anhydride (DDSA)	10 mL
Dimetilaminometil-fenol (DMP-30)	0.5 mL
Dibutil-ftalate (**Note 10**)	1 mL

7. Embedding molds.
8. Laboratory oven with facilities to program times and temperatures.
9. Knifemaker, glass strips, electric tape, copper grids, tweezers for electron microscopy, Petri dishes, filter paper, twice-distilled water, dental wax.
10. Preparation of glass knives (**Note 11**): Glass knives are made from glass strips (thickness, 0.5 mm). They are prepared (just prior to usage) by means of a knifemaker, a mechanical device that allows to obtain clean breaks, provided that the glass strip is firmly blocked, First, the glass strip must be broken into several squares, which, in turn, are scored and broken into two knives (**Fig. 2**) (**Note 12**).
11. Preparation of troughs: Choose a glass knife of good quality and wrap a piece of adhesive electrical tape (**Note 13**) from one side to the other of the cutting edge of the glass knife (**Fig. 2**) (**Note 14**). Seal the heel of the trough with melted paraffin to make it waterproof. The trough is then mounted on the proper holder of the ultramicrotome and it is filled up with distilled water, as flotation fluid (**Note 15**).
12. Ultramicrotome(s).
13. Uranyl acetate preparation: This chemical is supplied as a powder and it is used as 3% aqueous or ethanol solution. It takes about 20 min to dissolve it completely in water on an automatic shaker (**Note 16**).
14. Lead citrate preparation: This staining solution is prepared as follows in a 50-mL volumetric flask: lead nitrate (1.33 g), sodium citrate (1.76 g), and twice-distilled water (30 mL).

    This mixture must be shaken vigorously several times for at least 30 min until a milky solution is obtained. Add to this suspension 8 mL of 1 *N* NaOH previ-

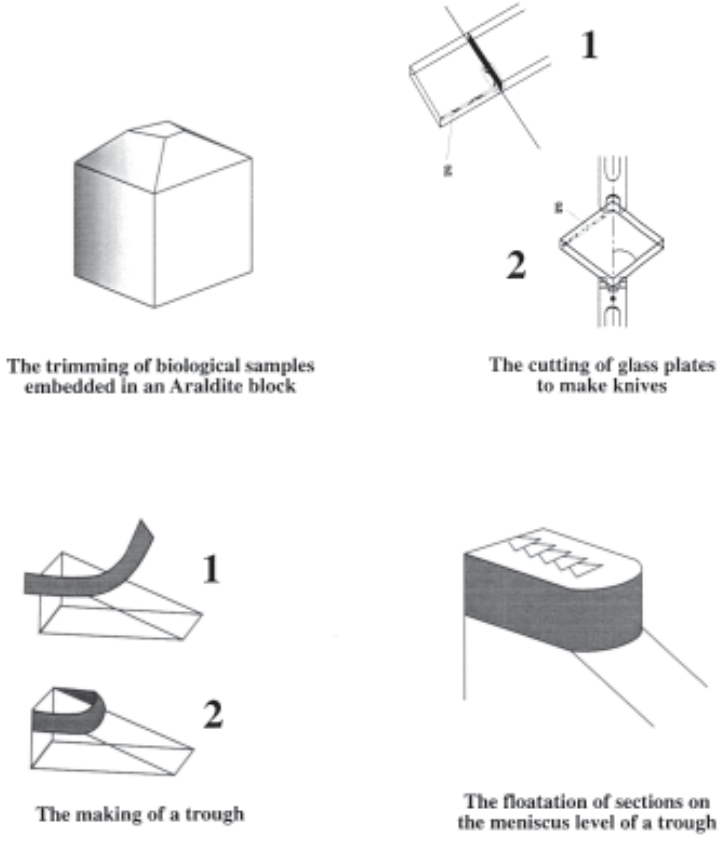

Fig. 2. *Upper left*: A trimmed Araldite block ready to be sectioned at 0.06 µm thickness. The tissue specimen at the tip of the block can be clearly seen in osmium-treated samples. *Upper right*: (1) Squares are obtained by scoring and breaking a glass strip perpendicularly to its longitudinal axis. (2) Squares are scored and broken to obtain knives (g: *see* **Note 43**). *Lower left*: a trough is made with a piece of electrical tape wrapped around the cutting edge and sealed at the through heel. *Lower right*: A section ribbon floating at the center of the trough provides evidence that the entire sectioning procedure has been properly accomplished.

ously diluted with twice-distilled water to 50 mL and mix until the suspension clears up completely (**Note 17**).

15. Transmission electron microscope.

3. Methods

Routine preparation of biological samples to be studied by electron microscopy is carried out through the following steps: animal anesthesia, perfusion–fixation, embedding, sectioning, and staining of the tissue samples.

3.1. Animal Anesthesia

Medium-sized laboratory animals (adult Wistar rats, average weight 250 g) are easily anesthesized by injection with 200 mg/kg body weight of 2,2,2-tribromoethanol dissolved in 10% ethanol, which induces sleep within 5–7 min.

3.2. Perfusion

The thorax of the anesthesized animal is opened and the heart and major blood vessels are exposed. A small incision is made in the left ventricle to guide the perfusion needle to the aorta. As soon as the saline (to prevent clotting, a heparinized solution should be used) starts to flow (**Note 18**), a second incision is made in the auricle to allow the blood to escape (**Note 19**). The saline must flow up to a complete washout of the blood and should be followed immediately by perfusion of the fixation solution (**Note 20**). The selected tissue samples are dissected out and a further fixation of the material is performed by immersion in the same solution used to perfuse the animal (**Note 21**).

3.3. Embedding

Following fixation, to minimize any reaction between the fixative and the dehydration agent, the excess fixative must be washed off (*see* **Note 22**). Washing should be carried out in the same buffer as that used to prepare the fixative mixture (*see* **Note 23**). For most tissues, two or three rinses in the buffer, for a total period of 15 min, are needed (*see* **Note 24**). If fixation has been carried out in a refrigerator at 4°C, wash the tissue samples at the same temperature. Wide-mouth vials are suitable to process the tiny samples, which should not be transferred from one vial to another. Each solution must be withdrawn with a micropipet and immediately replaced with the other solution (**Note 25**). The 3% aqueous solution of osmium tetroxide is diluted to 1% with cacodylate buffer. This fresh-made reagent is poured into the vials containing the tissue samples (**Note 26**). Immersion in osmium tetroxide lasts 2 h and is carried out in a refrigerator at 4°C to reduce autolytic activity (**Note 27**). Dehydration by ethanol follows osmium tetroxide postfixation (**Note 28**) according to the following procedure:

1. Rapid wash in cacodylate buffer.
2. 70% Ethanol (**Note 29**): 10 min.
3. 80% Ethanol: 10 min.
4. 95% Ethanol: 10 min.
5. 100% Ethanol: 15 min (two changes).

Because most resins are not readily miscible with ethanol, tisssue samples must be immersed in a transitional solvent that is completely miscible with both ethanol and embedding resins, according to the following procedure:

1. 100% propylene oxide: 20 min (three changes).
2. Propylene oxide and embedding resin (3:1): 30 min.
3. Propylene oxide and embedding resin (1:1): 30 min.
4. Propylene oxide and embedding resin (1:3): overnight (**Note 30**).
5. Embedding resin 100% (**Note 31**): 30 min.

Final embedding is carried out in rubber molds of different size which allow an easy orientation of the tissue samples. Polymerization of the epoxy resin is completed within 48 h at 60°C. Polymerized blocks can be sectioned best after 2 d.

3.4. Sectioning (Fig. 2)

Because sections are cut from a very small portion of the tissue specimens, trimming of the blocks must be carried out. The block is mounted on the blockholder which is placed in the microtome (**Note 32**). Rough trimming of the block must be performed with a sharp razor blade to remove the excess of embedding medium around the tissue sample. Too large tissue samples should be also reduced in size to obtain a block face of suitable size. Afterwards, fine trimming is carried out with the aim of obtaining a block tip with smooth and clean sides. In our experience, when making sections from a brain sample, it is usually necessary to examine a semithin section (thickness: 1.5 μm) at the optical microscope to select the area to be viewed at the electron microscope. When the area of interest in the tissue sample is identified, the block is retrimmed to obtain a trapezoid face with parallel lower and upper sides and two sloped sides (**Note 33**). Because the shortest of the two parallel edges is mounted up, each section will move the previous one from the cutting edge and a straight ribbon of sections will be formed (**Fig. 2**; **Note 15**). Section collection (**Note 34**) is accomplished by the following steps:

1. Hold the edge of a grid with a pair of curved tweezers.
2. Bend the edge of the grid by about 100°.
3. Lower the grid onto the upper face of the ribbon (**Note 35**).
4. Dry the grid with the sections by placing it on filter paper which absorbs the water (of course the side of the grid without sections is to be brought into contact with the filter paper!) (**Note 36**).

3.5. Staining

To obtain a better contrast and resolution, the sections mounted on a grid are stained by the deposition of heavy metal ions, such as uranium and lead (*see* **Note 37**). The simplest method to stain sections is to let the grid (with section side down) float on a drop of a staining solution in a Petri dish. The staining surface is constituted by the lid of a glass Petri dish partially filled with melted paraffin which is allowed to cool. This surface must be kept very clean and should be protected from dust by keeping it covered during staining. The basic

steps to carry out a conventional double staining with uranyl acetate (ethanol solution) and lead citrate are:

1. An ethanol atmosphere is produced within the Petri dish by placing a piece of filter paper wetted with ethanol 50% at one side of the staining surface.
2. A small volume of uranyl acetate is drawn up from below the surface of the staining solution with the aid of a clean pipet and a small drop is placed on the paraffin surface (**Note 38**).
3. The grid to be stained is wetted in distilled water (**Note 39**) and then floated on the drop of uranyl acetate, where it should be left from 30 s to a few minutes depending on whether or not it must undergo multiple staining.
4. The stained grid is then thoroughly washed by immersion in a small beaker containing a 50% aqueous solution of ethanol for at least 5 min. Washing can also be carried out by holding the grid with tweezers and dipping and shaking it in the solution, in the beaker (**Note 40**).
5. The washed grid is then dried by placing it on a filter paper, taking care that the section side does not touch the paper.
6. **Steps 1–5** can be repeated to stain the same grid with lead citrate. However, as regards **step 1**, a carbon dioxide free atmosphere must be generated within the Petri dish by placing a small amount of NaOH pellets at one side of the staining surface. Washing should be carried out using twice-distilled water. Usually, the duration of the lead staining (5–15 min) is longer than that with uranyl acetate (**Note 41**).

3.6. Quantitative Mitochondrial Study

A mere qualitative evaluation by electron microscopy of tissue samples is not enough to document reliably the age-related changes. Therefore, quantitative fine-structural determinations must be performed. With the introduction of the dissector procedure ***(8–10)***, the methods of estimating subcellular particle and organelle number and size have been changed, with a considerable improvement of the reliability of the findings by moving from assumption-dependent to assumption-free methods (**Note 4**2). Thus, suppositions about particle size, shape, and orientation have been replaced by design-based random sampling, which is a well grounded and reliable procedure to carry out quantitations. It must be pointed out that, because these unbiased stereological techniques have entered into common usage during the last decade, most published morphometric data have been obtained without the use of the dissector. This does not mean that useful information was not obtained. Thus, to cite an example, in our previous studies on the ultrastructure of nerve cell terminals in aged rats, the morphometric techniques in use prior to the dissector method enabled us to measure closely related structural parameters of functional significance. Thus, an estimation of the remodelling process taking place in the synaptic regions of the aged CNS was obtained. Namely we found that, while the numerical den-

sity (no. of particles/μm^3 of tissue) of synaptic mitochondria decreases significantly with aging, their average size (average mitochondrial volume) increases to reach a complete recovery of the total volume in a μm^3 of tissue (volume density) ***(8–10)***. These findings appear to be significant if referred to the limited specific volume where sampling has been carried out. In conclusion, it seems reasonable to assume that the data obtained by many laboratories prior to the introduction of the dissector procedure may still be trusted when the conclusions drawn refer not to quantitation of the total number of structures but to the relationships present among the structures (e.g., number of mitochondria found in a synapse cross-section).

4. Notes

1. The buffer solutions should be prepared the day before their use. Freshly prepared solutions are stable for a week if stored at 4°C.
2. To prevent spontaneous polymerization during storage, commercial formalin contains more than 10% methanol. Thus, to yield a high-purity solution, it is preferred to prepare the fixative for electron microscopy by depolymerizing powdered paraformaldehyde.
3. The commercially available glutaraldehydes have varying amounts of impurities which can affect tissue fixation to a high extent. Although it is more expensive, the use of glutaraldehyde of optimal purity is more advantageous to obtain a good preservation of biological samples. Glutaraldehyde is supplied as a 50% or 25% solution that stays relatively stable for long periods of time if stored in the cold. If the solution turns yellow, some polymerization has occurred and the chemical should not be used unless it is purified with charcoal. However, the purification procedure implies that the concentration of the final clear, oily solution must be checked with a recording spectrometer. Therefore, we recommend purchasing the right amount of glutaraldehyde to be used in a reasonably short period of time.
4. Osmium tetroxide is volatile, and its fumes are very toxic and able to fix biological tissues. Thus, any manipulation involving this chemical should be performed in a fume cupboard. Exposure to the vapor should be kept to an absolute minimum and contact with hands and face should be avoided. Great care should be taken to avoid any contamination by dust particles or light, which would result in a striking decrease in the fixing capacity of the solution.
5. Osmium vapors readily leak out of many containers, and in many electron microscopy laboratories a typical sign of this contamination is the black precipitate found on the inside of refrigerator walls. To prevent this leakage, osmium solutions should be stored in glass vacuum-type blood collection tubes. Plugging them with rubber stoppers prevents contamination of the surrounding environment.
6. Before disposing of the used solutions of osmium tetroxide, neutralize them by twice the volume of corn oil, a product that has a high percentage of unsaturated bonds. Confirmation that the toxic osmium tetroxide has been completely inactivated can be obtained by soaking a piece of filter paper in corn oil and then

suspending it over the solution. Blackening indicates that osmium tetroxide is present.

7. Araldite (as all epoxy resins) and propylene oxide are toxic. Therefore, any manipulation involving these chemicals should be carried out under a fume cupboard and wearing lattice gloves.
8. To facilitate the preparation of Araldite, the needed amount of the different components can be measured in grams instead of milliliters. Large amounts of Araldite can be prepared to save time and disposable laboratory ware as well as to minimize any mistake in the weighing of the chemicals. Routinely, we prepare 500 g of Araldite, storing the unused quantity in syringes (of 5, 10, and 20 mL) at –20°C. Great care must be taken in filling each syringe with resin: remove the tip cover, slowly draw in the resin, hold the syringe with the tip in an upward position, and remove eventual air bubbles by pulling the plunger slowly; push the plunger upward until the resin appears at the end of the tip, cover the tip with parafilm, and store in a refrigerator at –20°C. Thirty minutes before its use, the required amount of Araldite must be warmed up to room temperature.
9. After pouring Araldite and DDSA, the mouth of their bottles must be carefully wiped with filter paper, because with time, even at room temperature, small residual amounts of these reagents can polymerize and cause a strong bonding between the screw plug and the neck of the bottle.
10. The hardness of the blocks to be sectioned can be varied by changing the amount of dibutyl phthalate (plasticizer); however, a low amount of this reagent will result in brittle blocks.
11. Diamond knives can be used instead of glass knives. Diamond knives are commercially available at a rather high cost, but they are convenient as they are supplied already sealed to a stainless steel or aluminum alloy trough. The shape and color (usually black) of this trough make it possible to obtain an optimal meniscus level (in relation to the cutting edge).
12. The quality of each glass knife must be checked according to the instructions for using the knifemaker. The most useful (and sharpest) part of the knife is represented by the left third of the whole cutting edge.
13. The fingers should not come into contact with the adhesive side of the tape, as grease will be transferred to the flotation water. The black (or silver) color of the tape will facilitate the viewing of the sections on the water surface, as these colors can prevent interference due to reflection.
14. The lower edge of the tape must be parallel to the lower edge of the knife and the upper edge of the tape must be precisely attached to the tip of the cutting edge. These steps should be carried out with special care, as the resulting trough should not be tilted toward or away from the cutting edge. The optimal trough will make it possible to obtain a good meniscus level of the flotation water. As a consequence, the sections will glide smoothly away from the cutting edge and thickness can be easily checked on the basis of their interference color.
15. A straight ribbon of sections is easily obtained if the flotation water in the trough is wetting the cutting edge of the knife to its very end. The shape of the meniscus

of the flotation water is primarily responsible for the wetting of the knife facet. The optimal wetting of the knife is obtained when the meniscus is flat (with a knife angle of about 90°). To obtain the most advantageous meniscus level, first a convex meniscus is developed and then, by withdrawing the water with a micropipet up to an initial drying of the cutting edge, the meniscus becomes concave.

16. A freshly prepared solution of uranyl acetate should be used, as the recommended 3% solution is close to saturation and gradually a precipitate forms with time. However, in our experience, the solution can be used at least for a couple of weeks, until it looks slightly cloudy.
17. The lead citrate solution can be used concentrated or diluted up to 5× with 0.01 *N* NaOH according to the contrast to be obtained. To prepare lead citrate, the NaOH solution should be fresh and carbonate free. If it is tightly stopped, the solution will stay stable enough for 6–8 wk. When precipitates appear, the solution must be discarded.
18. The blood washout by saline should be carried out in a short period of time (2–4 min) to minimize any tissue deterioration and ensure the best fixative preservation.
19. The temperature of the perfusion solution should be kept as close to body temperature as possible to prevent vasoconstriction. The pressure head of the solutions (saline and the aldehyde-containing fixative), especially for fixation of CNS structures, must be equivalent to 130–140 cm of water. This can be easily set up by positioning the perfusion bottles shown in **Fig. 1** about 130 cm higher than the body of the animal to be perfused.
20. A fixation solution containing the right amounts of glutaraldehyde and paraformaldehyde is more adequate than a solution containing just one of these aldehydes. This is due to the complementary effects of the two chemicals: formaldehyde diffuses rapidly and fixes slowly, whereas the glutaraldehyde action is characterized by a slow penetration and a rapid fixation of tissues, due to the crosslinking effects on the adjacent protein molecules.
21. The uniformity of fixation throughout the tissue sample is a good criterion for adequate fixation. The size of the specimen exerts an important influence on the homogeneity of fixation. As a general rule, the smaller the size of the biological sample, the more complete and uniform will be the quality of fixation. With the above described perfusion procedure, a nearly uniform fixation is obtained. However, the size of the samples should not exceed 0.5 mm^3, as osmium tetroxide penetrates little in most tissues. Perfused tissues can be easily cut into thin strips of about 0.5 mm thickness and then sectioned into smaller pieces before osmium postfixation.
22. If washing of the tissue samples is improperly carried out, residual glutaraldehyde will react with osmium tetroxide and produce a fine, dense precipitate of reduced osmium.
23. If tissues fixed in buffered solutions are washed with water, dissolution and progressive disintegration of some unfixed cellular structures takes place when the added electrolytes (or nonelectrolytes) are removed by washing with water. By

contrast, washing with buffer avoids a sudden, drastic change in the environment of the tissue specimens. Because cellular membranes of aldehyde-fixed samples maintain in part their selective permeability, a significant decrease in the osmolarity of the washing solution would result in a marked ballooning of cellular organelles, particularly mitochondria.

24. Washing should not be longer than necessary, as the crosslinks caused by glutaraldehyde are potentially reversible and therefore long washings may affect the final appearance of the fine structure.
25. Solution changes (during fixation, washing, dehydration, and infiltration) should be carried out with speed to avoid drying of the samples. The original vial serves to perform fixation up to the transfer of the specimens to rubber molds, for embedding.
26. Because of the hypotonicity of the water in which osmium tetroxide is dissolved, animal tissues exhibit a marked and rapid swelling when they are immersed in the final buffer-diluted 1% solution of this reagent. However, this swelling is neutralized by the shrinkage occurring during dehydration.
27. Rapid osmium tetroxide penetration lasts up to 1 h and reaches a depth of about 0.6 mm. After this period, the fixed outer layers of the tissue samples resist deeper penetration of the fixative and the concentration of osmium tetroxide in solution decreases. Consequently, the rate of penetration of the fixative slows down and it takes 2 h to fix throughout a tissue sample of 1 mm thickness. Osmium tetroxide is unable to make all cellular components insoluble in water and extraction of cellular products (proteins) may occur during prolonged fixation. Thus, short fixation times are more suitable, considering that the fixation time can be increased when osmium tetroxide is used in postfixation.
28. Provided that the duration of each step is long enough to accomplish a gradual replacement of water by the solvent, dehydration should be as short as possible to minimize shrinkage and extraction of cellular constituents. A rapid dehydration causes striking osmotic changes resulting in distortion of the structures. The dehydration time required will depend on the size and type of the tissue specimen.
29. Even in fixed tissue samples, the possible presence of soluble proteins is to be taken into account and the concentration of ethanol at the start of dehydration should be high enough to denature (and insolubilize) these proteins.
30. Because of the high volatility of propylene oxide, the vials containing the third mixture (1:3, overnight) must be sealed carefully with a stopper and parafilm.
31. Residual propylene oxide can be completely eliminated from tissue samples by storing for 2–4 min the open vials with 100% embedding medium into an oven prewarmed at 60°C for subsequent polymerization.
32. To keep the trimmed block firmly attached to its holder, the block should not extend more than 2–3 mm from the front edges of the holder jaws. The evident results of a loose block are sections of uneven thickness, alternation of thick and thin sections, or even total failure of sectioning.
33. Trimming of the block should be performed avoiding sharp, deep cuts. To obtain the form of a short pyramid, the block should be trimmed by short cuts and its tip

should not be too thin nor too long. Otherwise, it will vibrate at high frequency when hitting the cutting edge.

34. Before collecting the sections, the compression due to the impact of the block with the cutting edge of the knife can be relieved by exposing the sections very briefly to the vapors of a strong solvent such as chloroform.
35. The grid should be pressed gently over the floating sections with the aim of depressing (not breaking) the water surface. As soon as the grid reaches across a ribbon, the sections stick firmly to the grid along with a drop of water. Because the electrostatic charges on the grid surface are responsible for the attraction of the ribbon, rinse the grid with acetone just prior to use, to reduce the charge and get a better control in orienting and centering the ribbon.
36. The most frequent mistake in making sections for electron microscopy is represented by periodic variations in the contrast of a section (commonly termed "chatter"). Usually, this failure is not detected during sectioning, but only while viewing the section at the electron microscope when it is too late to correct the mistake. Usually, "chatter" is due to vibrations of microtome parts that include the cutting edge, the specimen block, and the microtome arm. However, some other causes may be involved, for example, too fast cutting speed, too large and/or irregular block face, specimen or knife loosely held, too hard or too soft specimen block, dull knife, and incomplete polymerization of the epoxy resin.
37. Contrast in an electron micrograph depends essentially on the density and thickness of the different parts of the section. By combination with elements of higher atomic weight (osmium, uranium, and lead), some cellular structures are made denser than their surroundings.
38. The first one or two drops of stain from the pipet are discarded to avoid any contamination. The drop used should be small enough to allow the grid to float on it instead of sliding down to its sides.
39. Wetting of the sections decreases the risk of contamination due to extensive stain–air contact.
40. To remove any excess of uranyl acetate, a quick rinse in 0.5% tartaric acid can be performed after washing in a 50% aqueous solution of ethanol. This step must be carried out very rapidly (2–3 s!) and it must be followed by repeated washings in distilled water.
41. Keep the staining time as short as possible because there is a risk of overstaining, which results in an overall increase in contrast with poor differentiation of cellular structures.
42. The dissector method is designed to identify particles seen in one section ("look-up section") but not in a following one ("reference section"), and serves to evaluate the number of particles per unit volume (numerical density: Nv). Serial sections are needed to perform counting of particles or organelles. For instance, the mitochondria present in a discrete area of the reference section, but not in the look-up section are counted (**Fig. 3**, arrows) and referred to the height of each dissector which takes into account the section thickness (further details in **refs. *11–13***).

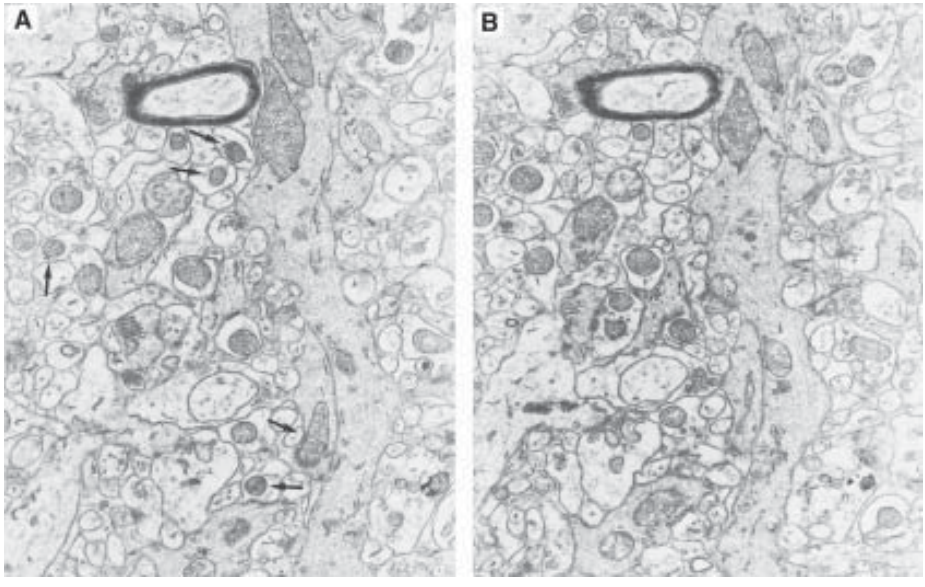

Fig. 3. Electron microscopy pictures of rat cerebellar cortex processed according to the procedure described in the text. These photos constitute a dissector, that is, **A** is the "look-up" section, while **B** is the "reference" section. *Arrows* indicate the mitochondria which are present in **A** but not in **B** and therefore those to be counted. ×22,000.

43. When preparing knives, do not touch their sides with the fingers. When making squares from the glass strip with the diamond-tipped shaft of the knifemaker, check that the rough end of the strip (g) is positioned upward, whereas when making knives it should be turned downward.

Acknowledgment

Dr. J. Miguel acknowledges the support of FIS-Grant 99/1264.r. The skillful help of Mr. M. Solazzi and Mrs. F. Trucchia is greatly acknowledged by Dr. C. Bertoni-Freddari.

References

1. Harman, D. (1956) Aging: a theory based on free radical and radiation chemistry. *J. Gerontol.* **11,** 298–300.
2. Gerschman, R. (1962) Man's dependence on the earthly atmosphere, in *Proceedings of the 1st Symposium on Submarine and Space Medicine* (Schaeffer, K. S., ed.), MacMillan, New York, pp. 475.
3. Miquel, J. (1971) Aging of male *Drosophila melanogaster*: histological, histochemical and ultrastructural observations, in *Advances in Gerontological Research*, vol. 3 (Strehler, B. L., ed.), Academic Press, London, New York, pp. 39–71.

4. Miquel, J., Lundgren, P. R., and Johnson, J. E., Jr. (1978) Spectrophotometric and electron microscopic study of lipofuscin accumulation in the testis of aging mice. *J. Gerontol.* **33,** 5–19.
5. Miquel, J. and Fleming, J. E. (1986) Theoretical end experimental support for an "oxygen radical-mitochondrial injury" hypothesis of cell aging, in *Free Radicals, Aging and Degenerative Diseases* (Johnson, J. E., Jr., Walford, R., Harman, D., and Miquel, J., eds.), Alan R. Liss, New York, pp. 51–74.
6. Miquel, J., editor-in-chief (1989) *CRC Handbook of Free Radicals and Antioxidants in Biomedicine* (3 vols.), CRC Press, Boca Raton, FL.
7. Miquel, J. (1998) An update on the oxygen stress-mitochondrial mutation theory of aging: genetic and evolutionary implications. *Exp. Gerontol.* **33,** 113–126.
8. Bertoni-Freddari, C., Fattoretti, P., Casoli, T., Spagna, C., Meier-Ruge, W., and Ulrich, J. (1993) Morphological plasticity of synaptic mitochondria during aging. *Brain Res.* **628,** 193–200.
9. Bertoni-Freddari, C., Fattoretti, P., Caselli, U., Paoloni, R., and Meier-Ruge, W. (1996) Age-dependent decrease in the activity of succinic dehydrogenase in rat CA1 pyramidal cells: a quantitative cytochemical study. *Mech. Ageing Dev.* **90,** 53–62.
10. Fattoretti, P., Bertoni-Fredari, C., Caselli, U., Paoloni, R., and Meier-Ruge, W. (1998) Impaired succinic dehydrogenase activity of rat Purkinje cell mitochondria during aging. *Mech. Ageing Dev.*, **101,** 175–182.
11. Sterio, D. C. (1984) The unbiased estimation of number and sizes of arbitrary particles using the dissector. *J. Microsc.* **134,** 127–136.
12. Mayew, T. M. and Gundersen, H. J. G. (1996) "If you assume, you can make an ass out of you and me": a decade of the dissector for stereological counting of particles in 3D space. *J. Anat.* **188,** 1–15.
13. Coggeshall, R. E. (1992) A consideration of neural counting methods. *Trends Neurol. Sci.* **15,** 9–13.

18

Causes and Consequences of Damage to Mitochondria

Study of Functional Aspects by Flow Cytometry

Federico V. Pallardo, Juan Sastre, Jaime Miquel, and José Viña

1. Introduction

A rapidly increasing amount of data supports the view that progressive bioenergetic loss caused by injury of the main energy-producing subcellular organelles, that is, the mitochondria, plays a key role in aging. A link between senescence and energy loss is already implied in Harman's ***(1)*** free radical theory of aging, according to which oxygen-derived free radicals injure the cells, with concomitant impairment of performance at the cellular and physiological levels. Further, Miquel and co-workers ***(2,3)*** have proposed a *mitochondrial theory of aging*, according to which aging results from oxygen stress damage to the mitochondrial genome, with concomitant bioenergetic decline. More recently, a number of laboratories, including our own ***(4–6)***, have provided biochemical data in agreement with the above views. Thus, we have shown that, as the result of age-related oxygen stress, mitochondrial glutathione is oxidized in direct relation to injury of the mitochondrial DNA ***(5)***. Further, our studies suggest that an antioxidant product extracted from *Ginkgo biloba* may counteract in part the damaging effects of free radicals on mitochondrial and cellular aging ***(7)***.

As reviewed elsewhere ***(6)***, age-related functional changes in mitochondrial respiration and in transport systems have been reported. Nevertheless, because of differences in the techniques and biological aging models used, the literature on mitochondrial aging abounds in conflicting reports. Further, it is often difficult to assess the functional significance of the mitochondrial changes shown by standard biochemical techniques. This makes it advisable to study the effects of

From: *Methods in Molecular Medicine*, Vol. 38: *Aging Methods and Protocols*
Edited by: Y. A. Barnett and C. R. Barnett

age on mitochondria by flow cytometry methods which allow a direct measurement of the organellar function as shown by its membrane potential value. This value can be determined both on mitochondria isolated using standard techniques and on those that remain in their normal environment inside the cells. Our own mitochondrial flow cytometry studies ***(6)*** on isolated rat hepatocytes have shown, for the first time in intact cells, a correlation between age-related changes in cell size and impaired mitochondrial function (**Fig. 1**). Specifically, we have observed that age is accompanied by a decrease in mitochondrial membrane potential (MMP), an increase in mitochondrial size, and a loss of organellar homeostasis (resulting in raised levels of peroxide generation). The pathogenetic mechanisms responsible for these changes are not well understood, although as pointed out by Hagen et al. ***(8)***, loss of the membrane phospholipid cardiolipin (which is essential for respiratory chain work) may play a role in the age-related MMP decrease. Because MMP supports mitochondrial protein synthesis ***(9)***, its decrease with age may be linked to a general decline in the biochemical and functional competence of mitochondria ***(2)***.

It is well known that aging results in mitochondrial membrane changes that increase the vulnerability of these organelles to the stress caused by the isolation procedure. Therefore, during isolation a considerable number of organelles (precisely those most altered by aging) may be lost, and therefore the data obtained will not provide an accurate measurement of the functional state of the whole mitochondrial population. Nevertheless, because useful information can be obtained on isolated mitochondria, we will describe the methods used in our laboratory for flow cytometry study of isolated mitochondria and of mitochondria present in their normal environment in cells previously isolated from their tissue. A detailed presentation of these methods may be of interest to workers interested in the mechanisms of senescence of mitochondria of different cell types, changes in the rate of aging caused by genetic or environmental modulation of mitochondrial development and function, and protection of the mitochondrial membranes and DNA by dietary antioxidants and free radical scavengers.

The procedures presented here for the study of key parameters of mitochondrial membrane function that change with age are as follows: (1) preparation of the respiration buffer for suspension of isolated mitochondria or cells and (2) determination of mitochondrial membrane mass, membrane potential, membrane lipid composition, and peroxide production.

Of course, a more complete understanding of the causes and effects of mitochondrial aging will require determination of many other parameters, such as fine structural changes (*see* Chapter 17), NADH/NAD redox state, reduced and oxidized thiol contents, activity of the inner membrane respiratory enzymes, state 3/state 4 respiratory control ratios (which indicate

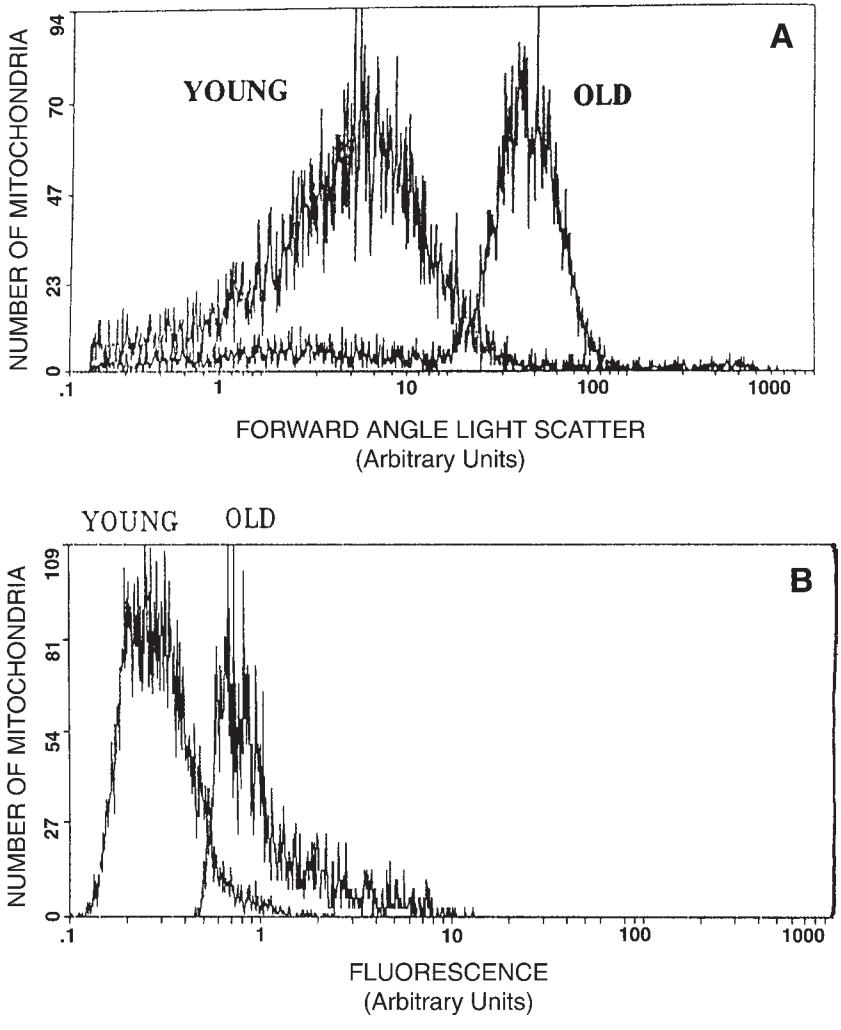

Fig. 1. Examples of application of flow cytometric methods to study mitochondrial function in isolated whole cells (hepatocytes) of young (aged 3–4 mo) and old (aged 22–36 mo) male Wistar rats. **(A)** Distribution of mitochondrial size obtained using the forward-angle light scatter. (The arbitrary units correlate positively with size.) **(B)** Peroxide generation in mitochondria (isolated from the above young and old rats) measured with the DhRh123 technique. (Reproduced from **ref. *6***).

the level of coupling of mitochondrial electron transport to ATP production), and oxidative damage and deletions of mtDNA. A number of recent publications (including **refs. *5–8*** and ***10–12***) provide examples of methods and age-related research on these parameters.

2. Materials

1. Buffer for mitochondria or cell suspensions ("buffer," pH 7.4): Solution in twice-distilled water of 5 mmol of KH_2PO_4, 0.3 mol of sucrose, 1 mmol of ethylene glycol bis(β-aminoethyl ether)-*N*,*N*,*N*′,*N*′,-tetraacetic acid (EGTA), 5 mmol of morpholinopropanesulfonic acid (MOPS), and 0.1% bovine serum albumin.
2. Stock solution of nonyl-acridine orange (NAO) (high purity, from Molecular Probes) at 10 mg/mL of dimethylformamide. (Store at –20°C, protected from light.) ***(13)***.
3. Stock solution of rhodamine 123 (Rh123) (from SIGMA) at 5 mg/mL of dimethylformamide. (Store at –20°C in 20 µL aliquots, using Eppendorf tubes protected from light) ***(14)***.
4. Stock solution of nile red (from Molecular Probes) at 2 mg/10 mL of ethanol. (Store at –20°C in 20-µL aliquots, using Eppendorf tubes protected from light.) ***(15)***.
5. Stock solution of dihydrorhodamine 123 (DhRh123) (from Sigma) at 10 mg/mL of dimethylformamide. (Store at –20°C, protected from light.) ***(16)***.
6. EPICS ELITE cell sorter (Coulter Electronics, Hialeah, FL, USA).

3. Methods

3.1. Flow Cytometry

1. Flow cytometry tubes: Polypropylene tubes (3 mL).
2. Flow cytometry parameters: Sample volume = 50 µL; sample flow rate = 25 µL/min; sheath pressure = 7.50 psi; laser power = 400 mW; parameter voltages: SS = 711 V; FL1 = 1750 V; FL2 = 0 V; FL3 = 0 V; color compensation: FL1 = 5% of FL2; FL2 = 50% of FL3; FL2 = 70% of FL1; FL2 = 0% of FL3; FL3 = 43% of FL1; FL3 = 1% of FL2.
3. Windows: For all parameters used (LFS, FSL, FL1, and LSS), the maximal window was 1023.
4. General fluorimetric procedure: The stained cells or mitochondria pass through the flow chamber, where the fluorochromes are excited with an argon laser tuned at 488 nm. Forward-angle and right-angle light scatter are measured and fluorescence is detected through a 488 nm blocking filter, a 550 nm long-pass dichroic, and a 525 nm band pass or a 575 nm long pass.

3.2. Sampling of Isolated Cells (see Note 1)

1. Prepare cellular suspensions containing approx 300,000 cells/mL. (Cell viability is determined by the fluorescent dye propidium iodide at a final concentration of 5 µg/mL, at 630 nm fluorescence emission, by light-scatter properties. All studies should be performed on viable cells.)
2. Place 50 µL of the suspension in the flow cytometry tube and mix with "buffer" and reagents needed for each specific determination, as indicated below (**Subheadings 3.4.** and **3.5.**).

3.3. Sampling of Isolated Mitochondria (see Note 1).

1. Suspend gently in 2 mL of "buffer" a sample of the mitochondrial pellet containing 1 mg of mitochondrial protein.

2. To obtain the "working suspension," mix 100 µL of the above suspension with 1900 µL of "buffer."
3. Place 50 µL of the "working suspension" in the flow cytometry tubes and mix with "buffer" and reagents needed for each specific determination, as indicated below (**Subheadings 3.4.–3.7.**).

3.4. Mitochondrial Membrane Mass

This is measured with NAO at 525 ± 5 nm fluorescence emission (*see* **Notes 2** and **3**).

1. Dilute the NAO stock solution with "buffer" to a final concentration of 1 mg/mL ("working solution").
2. Place 10 µL of "working solution" in a flow cytometry tube.
3. Add 940 µL of "buffer."
4. Add 50 µL of cell or mitochondria suspension.
5. Incubate in a water bath at 37°C for 20 min, protecting from light.
6. Assay in a flow cytometer.

3.5. Mitochondrial Membrane Potential

This is determined measuring Rh123 fluorescent emission at 525 ± 5 nm (*see* **Notes 4–7**).

1. Mix 10 µL of Rh123 stock solution with 990 µL of "buffer" to obtain the "diluted solution."
2. Add 10 µL of "diluted solution" to 90 µL of "buffer," to prepare the "working solution."
3. Place 10 µL of "working solution" in a flow cytometry tube.
4. Add 940 µL of "buffer."
5. Add 50 µL of cell or mitochondria suspension.
6. Incubate at 37°C for 20 min, protecting from light.
7. Assay in a flow cytometer.

3.6. Mitochondrial Membrane Lipid Composition

Composition of polar and apolar lipids in the mitochondrial membranes is assessed by fluorescence emission of nile red.

1. Place 10 µL of stock Nile solution in a flow cytometry tube.
2. Add 940 µL of "buffer."
3. Add 50 µL of mitochondrial suspension.
4. Incubate at 37°C for 30 min, protecting from light.
5. Assay in a flow cytometer at 525 (green), 575 (orange), and 675 (red) nm.

3.7. Peroxide Production by Mitochondria (see Note 8)

For this determination, the fluorochrome DhRh123 is excited at 488 nm. This fluorophore is oxidized by H_2O_2-dependent reactions involving oxygen species ***(16)*** (*see* **Note 5**).

1. Mix 5 µL of DhRh123 stock solution with 495 µL of "buffer," to prepare the "diluted solution."
2. Mix 5 µL of "diluted solution" with 95 µL of "buffer," to prepare the "working solution."
3. Place in a flow cytometry tube 10 µL of "working solution," 940 µL of "buffer," and 50 µL of mitochondrial suspension.
4. Incubate at 37°C for 30 min, protecting from light.
5. Assay in a flow cytometer.

4. Notes

1. Cell and mitochondria isolation procedures are not presented here, because the methods vary according to the organ used. For a wealth of information on standard mitochondria techniques, we recommend the monograph *Mitochondria, a Practical Approach* ***(10)***.
2. The fluorochrome NAO binds to all protein membranes regardless of their membrane potential ***(13)*** and, hence, the mitochondrial uptake of this metachromatic dye does not depend on the mitochondrial energy status.
3. The forward angle light scatter represents the mitochondrial size, which contributes to the refraction of light as it travels through the organelle. As an example of age-related changes, we showed that the forward angle scatter for mitochondria isolated from old rats (aged 22–36 mo) was about 140% of that of young rats (aged 3–4 mo). Therefore, we concluded that the isolated organelles from old rats were larger than those from young rats. In agreement with the mitochondrial theory of aging (which assumes an impairment in mitochondrial division), a senescent enlargement of the mitochondria of hepatocytes has been also shown, using electron microscopy, by Miquel et al. ***(17)*** in hepatocytes, and by Bertoni-Freddari on nerve cells (*see* Chapter 17). As pointed out by Sastre et al. ***(6)***, the increase in mitochondrial size with age probably affects mitochondrial function, as volume-dependent regulation of matrix protein packing influences metabolite diffusion and therefore mitochondrial metabolism.
4. The fluorescent dye DhRh123 is uncharged but it is oxidized to positively charged Rh123 in the extramitochondrial space and then it is taken up by mitochondria, where it accumulates. The MMP is the driving force for Rh123 uptake.
5. The MMP is monitored by fluorescence quenching of Rh123 in isolated mitochondria under respiratory state 4. Under these conditions, the MMP is an index of mitochondrial energy status. To induce state 4, mitochondria are incubated with 5 m*M* sodium succinate.
6. As an example of gerontological application of the DHR123-flow cytometry method to isolated cells, our work ***(6)*** on rat hepatocytes has shown that the MMP of old rats (aged 22–36 mo) is 70% of that found in the hepatocytes of young rats (aged 3–4 mo).
7. Hagen et al. ***(9)*** have also demonstrated an age-associated decline in the MMP of hepatocyte mitochondria. Thus, evidence is building up in support of the view that senescence is associated with an impairment of the mechanisms involved with ATP

synthesis, that is, with the main function of mitochondria. In our opinion, this justifies further application of the above techniques to elucidate the specific role played by mitochondria in cellular aging under normal and experimentally altered conditions.

8. Another proof of the usefulness of flow cytometry study of mitochondrial aging is provided by our finding of an increased DhRh oxidation in mitochondria isolated from the liver of old rats as compared to those isolated from young animals, which suggests that senescence is accompanied by an increased oxygen stress.

References

1. Harman, D. (1956) Aging: a theory based on free radical and radiation chemistry. *J. Gerontol.* **11,** 298–300.
2. Miquel, J. and Fleming, J. (1986) Theoretical and experimental support for an "oxygen radical-mitochondrial injury hypothesis of cell aging, in *Free Radicals, Aging and Degenerative Diseases* (Johnson, J. E., Jr., Walford, R., Harman, D., and Miquel, J., eds.) Alan R. Liss, New York, pp. 51–74.
3. Miquel, J. (l998) An update on the oxygen stress-mitochondrial mutation theory of aging: genetic and evolutionary implications. *Exp. Gerontol.* **33,** 113–126.
4. Yen, T. C., Chen, Y. S., King, K. L., Yeh, S. H., and Wei, Y. H. (1989) Liver mitochondrial respiratory functions decline with age. *Biochem. Biophys. Res. Commun.* **165,** 994–1003.
5. García de la Asunción, J., Millán, A., Pla, R., Bruseghini, L., Esteras, A., Pallardo, F. V., Sastre, J., and Viña, J. (1996) Aging of the liver: age associated oxidative damage to mitochondrial DNA. *FASEB J.* **10,** 333–338.
6. Sastre, J., Pallardo, F. V., Pla, R., Pellin, A., Juan, G., O'Connor, E., Estrela, J. M., Miquel, J., and Viña, J. (1996) Aging of the liver: age associated mitochondrial damage in intact hepatocytes. *Hepatology* **24,** 1199–1205.
7. Sastre, J., Millan, A., García de la Asunción, J., Pla, R., Juan, G., Pallardó, F. V., O'Connor, E., Martin, J. A., Droix-Lefaix, M. T., and Viña, J. (1998) A *Ginkgo biloba* extract (Egb 761) prevents mitochondrial aging by protecting against oxidative stress. *Free Radic. Biol. Med.* **24,** 298–304.
8. Hagen, T. M., Yowe, D. L., Bartholomew, J. C., Wehr, C. M., Do, K. L., Park, J.-Y., and Ames, B. N. (1997) Mitochondrial decay in hepatocytes from old rats: membrane potential declines, heterogeneity and oxidants increase. *Proc. Natl. Acad. Sci. USA* **94,** 3064–3069.
9. Chen, L. B. (1989) Mitochondrial membrane potential in living cells. *Ann. Rev. Cell Biol.* **4,** 155–181.
10. Darley-Usmar, V. M., Rickwood, D., and Wilson, M. T., eds. (1987) *Mitochondria: a Practical Approach*, IRL, Oxford, pp. 1–16.
11. Ferrandiz, M. L., Martínez, M., De Juan, E., Díez, A., Bustos, G. and Miquel, J. (1994) Impairment of mitochondrial oxidative phosphorylation in the brain of aged mice. Brain Res. **644,** 335–338.
12. Martínez, M., Ferrándiz, M. L., Díez, A., and Miquel, J. (1995) Depletion of cytosolic GSH decreases the ATP levels and viability of synaptosomes from aged mice but not from young mice. *Mech. Ageing Dev.* **84,** 77–81.

13. Maftah, A., Petit, J. M., Ratinaud, M. H., and Julien, R. (1989) 10-*N* nonyl-acridine orange: a fluorescent probe which stains mitochondria independently of their energetic state. *Biochem. Biophys. Res.* **164,** 185–190.
14. Petit, P. X., O'Connor, J. E., Grunawald, D., and Brown, S. C. (1990) Analysis of the membrane potential of rat- and mouse-liver mitochondria by flow cytometry and possible implications. *Eur. J. Biochem.* **194,** 389–397.
15. Greenspan, P., Mayer, E. P., and Fowler, S. D. (1985) Nile red: a selective fluorescent stain for intracellular lipid droplets. J. Cell Biol. **100,** 965–973.
16. Royal, J. A. and Ischiripoulos, H. (1993) Evaluation of 2'-7'-dichloro intracellular H_2O_2 in cultured endothelial cells. *Arch. Biochem. Biophys.* **302,** 348–355, 1993.
17. Miquel, J., Economos, A. C., and Bensch, K. G. (1981) Insect vs. mammalian aging, in *Aging and Cell Structure* (Johnson, J. E. Jr., ed.), Plenum Press, New York, pp. 347–379.

19

Analysis of Mitochondrial DNA Mutations

Deletions

Robert W. Taylor, Theresa M. Wardell, Emma L. Blakely, Gillian M. Borthwick, Elizabeth J. Brierley, and Douglass M. Turnbull

1. Introduction

Although the precise mechanisms of the aging process remain poorly understood, a plausible theory for cellular dysfunction and deterioration during aging involves mitochondria ***(1,2)***. The major function of mitochondria is to generate energy for cellular processes in the form of ATP by oxidative phosphorylation. Mitochondria contain their own DNA (mtDNA), a small 16.5 kb circular molecule that encodes 13 essential polypeptides of the mitochondrial respiratory chain, as well as 2 rRNAs and 22 tRNAs required for intramitochondrial protein synthesis ***(3)***. The mitochondrial respiratory chain is a series of five, multisubunit protein complexes located within the inner mitochondrial membrane. The first four of these (complexes I–IV) reoxidize reduced cofactors (NADH and $FADH_2$) generated by the oxidation of foodstuffs, thereby generating an electrochemical gradient across the inner mitochondrial membrane which is harnessed by the fifth complex, the ATP synthetase, to drive the formation of ATP.

The mitochondrial aging hypothesis proposes that aging results from the accumulation of detrimental mtDNA mutations during life, compromising the cellular production of ATP to such a degree that it results in cellular dysfunction and death. A number of features help to explain why mtDNA is particularly vulnerable to deleterious mutational events. The mitochondrial genome has a mutation rate some 10-fold greater than that of nuclear DNA, lacks protective histones, and possesses few and inefficient DNA repair mechanisms. It

From: *Methods in Molecular Medicine*, Vol. 38: *Aging Methods and Protocols*
Edited by: Y. A. Barnett and C. R. Barnett

is also highly vulnerable to nucleolytic attack by free radicals, a natural byproduct of oxidative phosphorylation. Moreover, because mtDNA has no introns and little redundancy, any mutational event within the genome is likely to affect a coding sequence, and therefore biochemical function.

An increasing body of scientific evidence has arisen supporting a mitochondrial involvement in the aging process, in particular the finding of pathogenic mtDNA mutations in healthy, elderly subjects. Numerous mtDNA deletions ***(4–15)*** have been shown to appear and accumulate with age in a variety of human tissues. Point mutations have also been detected ***(16)***, although whether they increase with age is debatable ***(17)***. The accumulation of age-related mtDNA deletions has also been shown to correlate with increased cellular levels of 8-hydroxy-2-deoxyguanosine, an indicator of free radical induced mtDNA damage. Furthermore, cytochrome c oxidase (COX)-deficient muscle fibers, a pathological hallmark of mitochondrial disease, have also been shown to accumulate in an age-related manner ***(18,19)***. Although an apparent decline in the activity of several respiratory chain enzymes has been reported with age, these changes (as much as a 50% decline in activity in a tissue homogenate) are hard to equate with the low levels of mtDNA mutations (<0.1% of the total mtDNA) observed in tissues of elderly individuals. The mitochondrial genome is present in multiple copies in individual mitochondria, and depending upon the oxidative demand of the tissue in question, there may be up to several thousand genomes within individual cells. Because mtDNA mutations have been shown to be incredibly recessive, with high levels (often >85% mutant mtDNA) required before any biochemical dysfunction is apparent ***(20,21)***, a more subtle molecular mechanism must exist to enable the low levels of mutations reported in various tissues to impair biochemical function.

Recent studies in single muscle fibers from patients with autosomal dominant progressive external ophthalmoplegia (adPEO) ***(22)*** and healthy elderly individuals ***(23)*** have shown that the clonal expansion of somatic mtDNA deletions in individual cells occurs to the extent that it results in a biochemical (COX activity) defect. It has been proposed that a replicative advantage (either at the level of the genome or for the mitochondria itself) allows mutant mtDNA to accumulate within a cell over time to such a level that it surpasses the critical threshold required to express a biochemical defect. Because somatic mtDNA mutations may occur anywhere within the genome, one would expect to find individual COX-deficient fibers harboring high levels of different deleted mtDNA species, which has been shown to be the case ***(22,23)***.

In view of these findings, the molecular genetic techniques that are applied to the study of somatic mtDNA mutations in aging must allow either the accurate quantification of these mutations at very low levels within tissue homogenates, or be applicable to single-cell studies in which the level of mutant

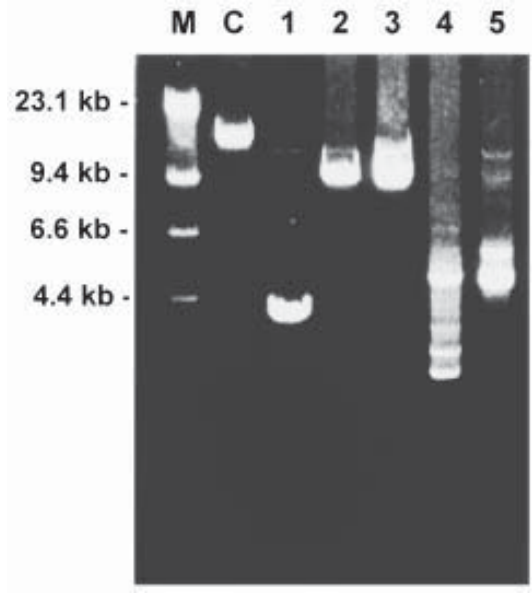

Fig. 1. 13 kb long-range PCR of mtDNA using primers L3200 and H16215. **M**, λ-*Hind*III DNA markers; **C**, control subject showing a single wild-type band; lanes **1–5**, subjects demonstrating different mtDNA rearrangements.

mtDNA is high compared to wild-type. Because of the number of polymerase chain reaction (PCR)-based techniques available, we describe these protocols in two chapters. In this, the first chapter, we discuss the methods used to investigate mtDNA deletions, whereas the second chapter (Chapter 20) focuses on the analysis of mtDNA nucleotide substitutions.

1.1. Long-Range PCR of mtDNA

Long-range PCR is now commonly used as an initial screen for the presence of large-scale rearrangements (deletions or duplications) of mtDNA ***(24)***. In this respect, it has many advantages over Southern Blotting. Low levels of rearranged mtDNA species can be detected from small amounts of DNA template within one day, whereas Southern blotting requires 2–3 μg of total DNA, takes a number of days to complete, and has a detection threshold of about 5% mutant mtDNA. For these reasons long-range PCR has been used to study the accumulation of age-related deletions in muscle and other tissues ***(25,26)*** as well as characterizing pathogenic rearrangements in blood ***(27)*** and muscle (**Fig. 1**).

Although there are a number of commercially available kits for long-range PCR, we and others favor the Expand™ Long Template PCR system produced by Boehringer Mannheim. This uses a mixture of thermostable *Taq* and *Pwo*

(with a 3'→5' exonuclease proofreading activity) DNA polymerases to enable the accurate and efficient amplification of PCR products up to 40 kb in size.

1.2. Single-Cell PCR

The clonal expansion of mtDNA deletions within individual cells calls for sensitive PCR-based techniques to enable the identification and characterization of these mtDNA mutations. Single-cell PCR on COX-deficient (biochemically compromised) cells highlights the focal nature of these mutational events, otherwise masked if analyzing DNA from tissue homogenates, and permits the comparative study of mtDNA rearrangements in different cell types within the same organ.

This section describes both the histochemical analyzes required to identify those cells that are biochemically affected as demonstrated by COX activity, and protocols for isolating total DNA from these single cells.

1.3. Quantitative analysis of the 4977 Basepair Common Deletion in Single Cells

The PCR-based techniques described in the preceding section will detect any rearrangement between nt 8355 and nt 13832, but will not quantify the absolute levels of mutant mtDNA (deletion). When searching for high levels of deleted mtDNA due to clonal expansion, competitive PCR (using three oligonucleotide primers to simultaneously amplify both wild-type and mutant mtDNA) is a useful method for detecting and quantifying the common 4977-basepair deletion ($mtDNA^{4977}$) in single cells *(23)*. The method described below is essentially that of Sciacco and colleagues *(21)*.

1.4. Semiquantitative PCR of the 4977 Basepair Common Deletion in Tissue Homogenates

Although the age-related accumulation of mtDNA deletions in various tissues has been demonstrated, the absolute levels of rearrangement in total cellular DNA extracted from tissue homogenates are very low. Consequently, semiquantitative PCR-based methods have been described to permit the investigation of these accumulating mutations in different cell types. The protocol we describe is based extensively on the method of Corral-Debrinski and colleagues *(7,8)*, in which the PCR amplification of wild-type mtDNA and $mtDNA^{4977}$ from serially diluted DNA samples allows the estimation of the amount of deletion in a tissue.

1.5. Primer-Shift PCR

Primer-shift PCR was first described by Ozawa et al. *(28)* as a means to fine map differentially deleted mtDNA species from total cellular DNA isolated from tissue homogenates. The rationale is straightforward; using pairs of primers

designed to amplify both (H) and (L) strands and relatively short extension times, PCR products are obtained only if a deletion is present, thereby shifting the PCR primers closer together, facilitating amplification. These PCR products will contain the specific deletion breakpoint, and as such can either be cloned or sequenced directly to map the precise location. Furthermore, because this technique excludes nonspecific PCR amplification due to the misannealing of PCR primers, it amplifies only deleted mtDNA species. Consequently, primer-shift PCR has been used to characterize the multiple mtDNA associations observed in patients with inclusion body myositis ***(29,30)*** and demonstrate the clonal expansion of mtDNA deletions in COX-deficient skeletal muscle fibers of patients with adPEO ***(22)***. This study highlights the power of this technique to screen for mtDNA deletions associated with disease or the aging process in DNA isolated from a single cell. The protocol described in the following sections describes the use of primer-shift PCR to investigate the presence of mtDNA deletions in DNA isolated from single muscle fibers or individual neurons. The same method is easily applied to the characterization of deleted mtDNA species in total cellular DNA isolated from a tissue homogenate.

2. Materials

2.1. Long-range PCR of mtDNA

1. Expand™ Long Template PCR system (Boehringer Mannheim): This is supplied with the enzyme mix and three buffers. Reaction buffer 3 is suitable for most applications as it contains dimethyl sulfoxide (DMSO) (20% [v/v]) which prevents DNA depurination and intrastrand secondary structure formation. The enzyme can be stored at –20°C for approx 3 mo. Reaction buffer 3 should be checked for the appearance of crystals that may have precipitated before use.
2. Deoxynucleoside triphosphates (dNTPs): Separate 10 m*M* working solutions of dATP, dCTP, dGTP, and dTTP are recommended. These are made from 100 m*M* lithium salt dNTP stocks purchased from Boehringer Mannheim. Store at –20°C.
3. Bovine serum albumin (BSA): Although not essential for the reaction, the addition of BSA (200 µg/mL final concentration) may increase the efficiency of the long template amplification. A 10 mg/mL stock solution of BSA that is often supplied with restriction endonucleases can be diluted to a 1 mg/mL working solution for this purpose, and stored at –20°C.
4. Oligonucleotide primers: Any primers designed to amplify mtDNA may be used; however, successful amplification may require testing various combinations of primers and annealing temperatures. Increasing the annealing temperature and reducing primer concentrations may help to reduce any non-specific PCR amplification. We find that short primers (20–24 bases long) give good results, whereas longer primers (>30 bases) do not. Interestingly, this inefficiency of amplification may be overcome by using a short primer in combination with a long primer. For much of our routine screening, we amplify a 13-kb fragment of the mitochon-

drial genome using a forward primer L3200 (nt 3200–3219) and a reverse primer H16215 (nt 16215–16196), numbered according to the Cambridge sequence ***(3)***. For whole genome amplification, a number of articles have been published with primer sequences; we have successfully used those described by Kovalenko and colleagues ***(26)***. Stock solutions (10 μ*M*) of primers are stored at –20°C (*see* **Note 1**).

5. DNA template: Only 10–50 ng of total DNA is required for amplification of the genome in part or whole. The quality of the DNA template is crucial for successful amplification, and protein contamination (determined by measuring the A_{260}/A_{280} ratio should be no less than 1.8. We recommend that solutions of DNA (10–50 ng/μL) be made fresh from concentrated DNA stocks, although these may be stored for 3–4 d at 4°C and for 1–2 wk at –20°C (*see* **Note 2**).
6. Sterile water.
7. Ice: The reaction should always be set up on ice to avoid hot start.
8. Mineral oil if required to overlay the reaction.
9. Thin-walled PCR tubes: These permit a more efficient transfer of heat, and as such are crucial for amplifying long templates. Use 0.2- or 0.5-mL thermotubes (Applied Biosystems) depending upon thermal cycler used.
10. Thermal cycler: Both the Hybaid Omnigene and Perkin–Elmer GeneAmp® PCR System 2400 thermal cyclers give good, reproducible results.
11. Horizontal gel electrophoresis equipment.
12. Agarose gel containing ethidium bromide; 1× TAE (40 m*M* Tris-acetate, 1 m*M* EDTA, pH 8.0) running buffer.
13. UV transilluminator.

2.2. Single-Cell PCR

1. Tissue sections: Fresh muscle and neuronal tissue are frozen in liquid nitrogen cooled isopentane and stored at –85°C. Fresh frozen sections (30 μm) are cut using a Brights OTF cryostat and air-dried at room temperature for 30 min. These sections can be used immediately or stored at –80°C in air-tight slide containers.
2. Histochemical staining: The assay of COX activity requires stock solutions of 5 m*M* 3,3'-diaminobenzidine tetrahydrochloride (light sensitive) (DAKO) in 0.1 *M* phosphate, pH 7.0, and 500 μ*M* cytochrome *c* (light sensitive) (Sigma) in 0.1 *M* phosphate, pH 7.0. The assay of succinate dehydrogenase (SDH) activity requires stock solutions of 1.875 m*M* nitroblue tetrazolium (Sigma), 1.30 *M* sodium succinate (Sigma), 2 m*M* phenazine methosulfate (light sensitive) (Sigma), and 100 m*M* sodium azide (BDH) all in 0.1 *M* phosphate, pH 7.0. Toluidine blue staining is performed with a 1% solution of toluidine blue (light sensitive) (Sigma) in 1% sodium borate (Sigma).
3. Capillaries: Standard wall borosilicate glass capillaries without filament, 1.0 mm outer diameter × 0.58 mm inner diameter (GC100–15 Clark Electromedical Instruments) are used for muscle dissection. Standard wall borosilicate glass capillaries without filament, 1.5 mm outer diameter × 0.86 mm inner diameter (GC150–10 Clark Electromedical Instruments) are used for neuronal dissection. Micropipets are produced using a Narishige PC-10 micropipet puller.

4. Micromanipulation: An inverted microscope (Zeiss Axiovert 25) fitted with 10× and 20× objectives is used for muscle dissection. A Leica inverted microscope (DMIRB/E) fitted with 4×, 10×, 20×, and 40× long-distance working objectives and a Leica mechanical micromanipulator fitted with a Narishige injection holder (HI–6) is used for neuronal dissection. A stock solution of 10 m*M* Tris-HCl, 1 m*M* EDTA, pH 7.4 (TE buffer) is required.
5. Cell lysis: Stock solutions of 1% Tween-20 (Sigma); 100 m*M* EDTA, pH 8.0; 0.5 *M* Tris-HCl, pH 8.5; and 50 mg/mL of proteinase K (NBL Gene Sciences).
6. PCR amplification: The following stock solutions are required: 2 m*M* (10×) dNTPs (Boehringer Mannheim), 10× GeneAmp® PCR buffer containing 100 m*M* Tris-HCl, pH 8.3; 500 m*M* KCl and 15 m*M* $MgCl_2$ (Perkin–Elmer); 20 μ*M* stock solution of each forward and reverse oligonucleotide primer, and 5 U/μL of AmpliTaq® DNA polymerase (Perkin–Elmer). Each PCR amplification is performed in a 0.5-mL thin-walled thermo-tube (Applied Biosystems).
7. Ice: All PCR reactions are set up on ice.
8. Thermal cycler.
9. Horizontal gel electrophoresis equipment.
10. UV transilluminator.

2.3. Quantitative Analysis of the 4977 Basepair Common Deletion in Single Cells

1. Sterile water.
2. Sterile 500-μL Eppendorf tubes for PCR.
3. Ice: All PCR reactions are set up on ice.
4. Lysis solution: 200 m*M* KOH, 50 m*M* dithiothreitol (DTT). Combine 200 μL of 1 *M* KOH (make fresh weekly and store at 4°C), 100 μL of 500 m*M* DTT (store aliquots at –20°C), and 700 μL of water.
5. Neutralization solution (900 m*M* Tris-HCl, pH 8.3; 200 m*M* HCl). Combine 900 μL of 1 *M* Tris-HCl (store at 4°C), 40 μL of 5 *M* HCl (room temp), and 60 μL of sterile water just before use.
6. Heat block.
7. Oligonucleotide primers: A set of three primers are used to amplify both wild-type and deleted mtDNA simultaneously. These are L8273 (nt 8273–8289), H9028 (nt 9028–9008), and H13720 (nt 13720–13705). The primers L8273 and H9028 amplify 755 basepairs corresponding to wild type mtDNA and the primers L8273 and H13720 amplify a 470-basepair fragment corresponding to $mtDNA^{4977}$. Stock solutions (20 μ*M*) are stored at –20°C.
8. PCR amplification: 2 m*M* (10×) dNTPs are from Boehringer Mannheim. Thermostable DNA polymerase and the associated 10× reaction buffer (containing $MgCl_2$) are from Advanced Biotechnologies.
9. [α-^{32}P] dATP (3000 Ci/mmol) (Amersham Life Science Products).
10. Mineral oil.
11. PCR thermal cycler.
12. Vertical polyacrylamide gel electrophoresis system (SE 600, Hoefer)

13. 5% nondenaturing polyacrylamide gel.
14. Whatman 3MM filter paper.
15. Saran Wrap®.
16. Running buffer (1× TBE): 90 m*M* Tris-borate, 2 m*M* EDTA, pH 8.0.
17. Gel dryer (Model 543, Bio-Rad Laboratories).
18. PhosphorImager and ImageQuant software (Molecular Dynamics).

2.4. Semiquantitative PCR of the 4977-Basepair Common Deletion in Tissue Homogenates

1. Template DNA.
2. *Bam*HI restriction endonuclease (10 U/µL) and SuRE/Cut Buffer B for restriction (10×) (Boehringer Mannheim).
3. PCR amplification: The following stock solutions are required: 2 m*M* (10×) dNTPs (Boehringer Mannheim), 10× GeneAmp® PCR buffer containing 100 m*M* Tris-HCl, pH 8.3; 500 m*M* KCl and 15 m*M* $MgCl_2$ (Perkin–Elmer), AmpliTaq® DNA polymerase (Perkin–Elmer). Each PCR amplification is performed in a 0.5-mL thin-walled thermo-tube (Applied Biosystems).
4. Oligonucleotide primers: Two pairs of primers are used to amplify a rarely deleted region of mtDNA (wtDNA) and mtDNA containing the common deletion ($mtDNA^{4977}$). The primers L3108 (nt 3108–3127) and H3717 (nt 3717–3701) amplify a 610-basepair fragment corresponding to wtDNA, whereas L8282 (nt 8282–8305) and H13851 (nt 13851–13832) amplify a 593-basepair fragment corresponding to $mtDNA^{4977}$. Stock solutions (20 µ*M*) are stored at –20°C.
5. Thin-walled PCR tubes: 0.5-mL thermotubes (Applied Biosystems) are recommended.
6. Ice: All PCR reactions are set up on ice.
7. PCR thermal cycler.
8. Large horizontal gel electrophoresis unit (Maxi unit, Scotlab) with well-forming combs to produce wells of 50 µL volume.
9. 1.5% Agarose gel containing ethidium bromide, 1× TAE running buffer.
10. UV transilluminator.
11. Digital imaging system and imaging software for PCR quantitation (AlphaImager and AlphaEase, Flowgen).

2.5. Primer-Shift PCR

1. Template DNA: The isolation of total DNA from single muscle fibers and individual neurons is described in detail in **Subheading 3.2.**
2. PCR reagents: Primer-shift PCR is performed on a Perkin–Elmer GeneAmp® PCR System 2400 thermal cycler using AmpliTaq® DNA polymerase (Perkin–Elmer) and the 10× reaction buffer supplied. dNTPs are made as a 2 m*M* (10×) stock. Thin-walled PCR tubes (0.2 mL) are also from Perkin–Elmer.
3. Oligonucleotide primers: Although any combinations of mtDNA-specific PCR primers can be used to map mtDNA deletions, we have essentially used those described by Moslemi et al. ***(22)***, in the combinations shown in **Fig. 2**. The sequences of these primers are as follows: L1 (nt 1–20), L7901 (nt 7901–7920),

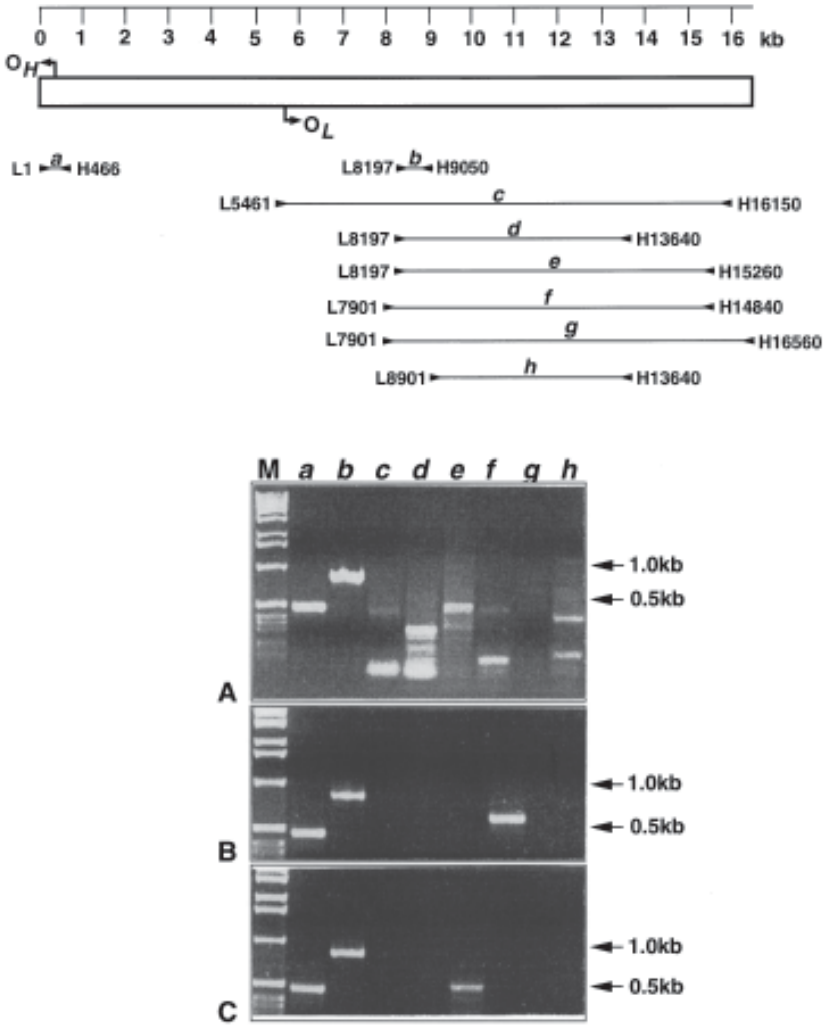

Fig. 2. Primer-shift PCR from single muscle fibers showing the combination of PCR primers (pairs *a–h*) used to screen the mtDNA genome. **A** shows the products generated from total DNA isolated from skeletal muscle of a patient with multiple mtDNA deletions. **B** and **C** represent the products generated from the DNA isolated from two individual COX-deficient muscle fibers, highlighting the presence of different deleted mtDNA species in each fiber.

L8197 (nt 8197–8216), H466 (nt 466–447), H9050 (nt 9050–9031), H13640 (nt 13640–13621), H14840 (nt 14840–14821), H15260 (nt 15260–15241), H16150 (nt 16150–16131), and H16560 (nt 16560–16541). Stock solutions (20 μ*M*) are stored at –20°C.

4. Sterile water.
5. Ice: All reactions are set up on ice.
6. Horizontal gel electrophoresis equipment.
7. 1.5% Agarose gel containing ethidium bromide; 1× TAE running buffer.

3. Methods

3.1. Long-Range PCR of mtDNA

1. Thaw all components stored at –20°C and bring reaction buffer 3 to room temperature. Vortex well to mix, checking the reaction buffer for crystals. If crystals are present leave at room temperature overnight and mix well again. Place all the components on ice.
2. Label two, sterile 1.5-mL Eppendorf tubes A and B; the master mix is made up as two separate mixes to avoid degradation of the primers or template due to the 3'→5' exonuclease activity of the *Pwo* enzyme.
3. Combine the following components to form mix A for each 50 µL PCR:

2.5 µL	10 m*M* dATP
2.5 µL	10 m*M* dCTP
2.5 µL	10 m*M* dGTP
2.5 µL	10 m*M* dTTP
1.5 µL	10 µ*M* Forward primer
1.5 µL	10 µ*M* Reverse primer
12 µL	Sterile water

4. Vortex-mix briefly, centrifuge the mix, and aliquot 25 µL into each thin-walled tube on ice.
5. Add 1 µL of DNA template to each separate tube.
6. Prepare master mix B; for each 50-µL reaction combine the following:

5 µL	10× Reaction buffer 3
10 µL	1 mg/mL of BSA
8.65 µL	Sterile water
*0.35 µL	Expand™ enzyme

*While the kit recommends using 0.7 µL of enzyme per 50 µL of PCR reaction, we find that the same efficiency of amplification is achieved using only 0.35 µL.

Vortex-mix and briefly centrifuge the mix, aliquoting 24 µL into each thin-walled tube, mixing gently to avoid introducing air bubbles.

7. If necessary overlay the reactions with 30 µL of mineral oil.
8. Centrifuge the samples briefly, and place back on ice.
9. Begin the following PCR program to heat the block to 92–94°C:

Initial denaturation	92–94°C*	3 min
10 Cycles	92–94°C*	10–30 s
	55–68°C**	30 s

	68°C†	*x* min
20 cycles	92–94°C*	10–30 s
	55–68°C**	30 s
	68°C†	*x* min + 5 s per cycle
Final extension	68°C	15–20 min

*Use lower denaturing temperatures and shorter times for longer products to avoid damaging the template.

**Annealing temperature is dependent upon the oligonucleotide primers used in the PCR reaction. For the amplification of a 13-kb product using L3200 and H16215, we use an annealing temperature of 58°C.

†*x* depends on the length of product to be amplified; generally allow 1 min for every 1 kb to be amplified.

10. Place tubes in thermal cycler when there is 90 s remaining of the initial denaturation step.
11. When the program is complete, electrophorese 15–20 µL of the PCR products through a 0.7% agarose gel at 65 V for 2–4 h (*see* **Notes 3–5**). The remaining product may be used for further analysis such as restriction enzyme digest or primer-shift PCR to map the rearrangement ***(31)***.

3.2. Single Cell PCR

1. Histochemical staining: Tissue sections that have been stored at –85°C should be equilibrated at room temperature for 30 min, then removed from the air-tight container and air-dried for a further 30 min prior to histochemical analysis. COX activity is detected using incubation medium containing 4 m*M* 3,3'-diaminobenzidine tetrahydochloride and 100 µ*M* cytochrome *c*. Each section is incubated with 100–200 µL of incubation medium at 37°C for up to 60 min in a humid chamber. Any excess medium is rinsed using distilled water. The activity of SDH in the sections is detected using incubation medium containing 1.5 m*M* nitroblue tetrazolium, 130 m*M* sodium succinate, 0.2 m*M* phenazine methosulfate and 1 m*M* sodium azide. Each section is incubated at 37°C with 100–200 µL of incubation medium, in a humid chamber for 30 min. Sections are rinsed in distilled water to remove excess medium. COX-deficient cells are detected by a double activity assay; sections are initially assayed for COX activity, as measured by the production of a brown end product. After removal of the excess medium, the sections are subsequently assayed for SDH activity. COX-deficient cells are easily identified as they do not produce the brown reaction product associated with COX activity, but do react for SDH activity, which gives a characteristic blue appearance ***(32)***. The neuronal cell harvesting is performed immediately after histochemistry; however, muscle sections can be stored in 50% alcohol at 4°C for several months.
2. Micropipets: Micropipets of a specific diameter are produced from heat-sterilized glass capillaries, using a micropipet puller in the double pull mode. A range of tip diameters (1–50 µm) can be made, depending on the size of the cells to be

harvested. The diameter of the micropipet is determined using a light microscope fitted with a graticule. Crude micropipets for muscle fiber work can be prepared by heating and pulling glass capillaries in a Bunsen burner flame. These micropipets can then be heat sterilized. Prior to using these crude micropipets the tip is gently broken against the microscope slide to yield a tip of appropriate diameter (*see* **Note 6**).

3. Dissection of single muscle fibers: Single muscle fibers can be picked from appropriately stained sections (30 µm) by hand, using a standard inverted microscope. The muscle section is kept under 50% alcohol during this procedure. The micropipet is held by hand, and the tip is used to tease around the edge of an individual muscle fiber and pick up the fiber. The presence of a cell on the capillary is determined visually with a hand held eyepiece.
4. Dissection of neuronal cells: An inverted microscope with long-distance working objective lenses is used in conjunction with a micromanipulator. The micropipets are held in position with an injection holder attached to an instrument holder on the micromanipulator. Stained sections (30 µm) of the neuronal tissue under investigation are moistened prior to micromanipulation with TE buffer. Single neurons are then picked up on the end of a micropipet. Visual confirmation of the presence of a cell is obtained by focusing on the micropipet while it is still held in the injection holder (**Fig. 3**) (*see* **Note 7**)
5. Cell lysis: The tip of the micropipet containing the single cell is broken off into sterile microfuge tubes, containing 20 µL of TE buffer. At this point the cells can be stored at 4°C for several weeks, prior to lysis. The microfuge tubes containing the individual cells are centrifuged at 7000*g* for 10 min. The supernatant is removed and the cells are lysed with 10 µL of 50 m*M* Tris-HCl, pH 8.5; 1 m*M* EDTA, pH 8.0; 0.5% Tween-20, and 200 µg/mL of proteinase K ***(33)***. The cells are incubated for 2 h at 55°C, with agitation every 30 min. This is followed by heat inactivation of the proteinase K at 95°C for 10 min (*see* **Note 8**).
6. PCR amplification of single cells: PCR amplification of a rarely deleted region of mtDNA (ND1 and 16S rRNA genes) is performed to demonstrate the presence of template DNA (wtDNA) within the single cell lysate. The primers are L3108 (nt 3108–3127) and H3717 (nt 3717–3701) which amplify a 610-basepair product. The common deletion ($mtDNA^{4977}$) is amplified using the primers L8282 (nt 8282–8305) and H13851 (nt 13851–13832) which yield a 593-basepair product. The cell lysate is used as the template in a single PCR reaction. A standard PCR procedure is performed using AmpliTaq® (1 U/reaction), PCR buffer, 0.6 µ*M* forward and reverse primer, and 200 µ*M* dNTPs in a 50-µL reaction volume. PCR amplification is performed under the following conditions: initial denaturation at 94°C for 2 min, denaturation at 94°C for 45 s, annealing at 51°C (wtDNA) or 56°C ($mtDNA^{4977}$) for 45 s, and extension at 72°C for 1 min for 34 cycles followed by a final extension at 72°C for 8 min ***(7)***. PCR products (40 µL) are electrophoresed through a 1.5% agarose gel in 1× TAE buffer containing ethidium bromide, and visualized by UV transillumination.

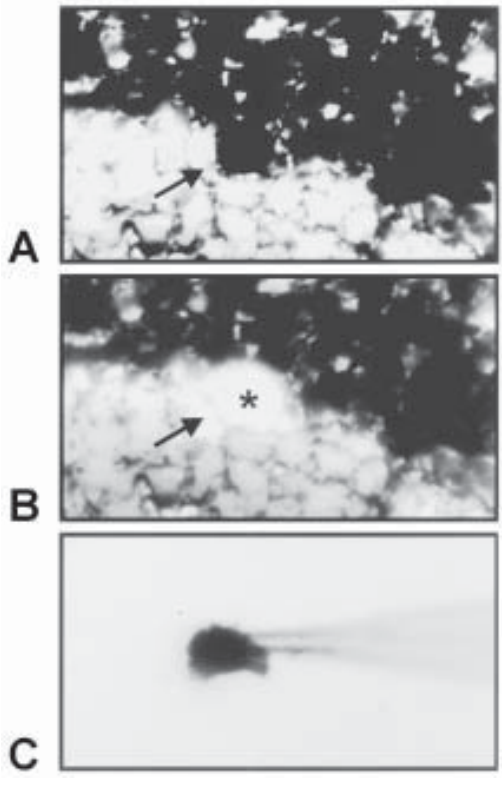

Fig. 3. Microdissection of an individual Purkinje cell for PCR analysis. The neuronal tissue section is stained with 1% toluidine blue, a single cell targeted (**A**, *arrow*) and removed by micromanipulation **(B)** onto the end of a micropipet **(C)**. The asterisk (*) highlights the position from where the single cell was removed.

7. Seminested PCR: The PCR products from the PCR reactions described in the previous section can be amplified by performing a semi-nested PCR using 1 µL of the primary PCR product as template and one internalized primer. The PCR is performed as described in **step 6** using the primers L3275 (nt 3275–3306) and H3717, and an annealing temperature of 56°C for wtDNA. The primers L8333 (nt 8333–8355) and H13851 to13832 are used to amplify deleted mtDNA in the mtDNA^{4977} PCR, annealing at a temperature of 56°C.

3.3. Quantitative Analysis of the 4977 bp Common Deletion in Single Cells

1. Isolate cells as described in the previous section and then place in a sterile 500 µL Eppendorf containing 20 µL water. Centrifuge tube for 10 min, remove the water carefully then add 5 µL of the lysis solution. Place tubes into the heat block at

65°C for 1 h, add 5 µL of the neutralising solution to each tube and remove from heat.

2. Prepare a PCR mastermix by combining, for 10 tubes, the following:

582.5 µL	Sterile water
100 µL	10× Reaction buffer
100 µL	2 mM (10×) dNTPs
50 µL	20 µM L8273
50 µL	20 µM H13720
12.5 µL	20 µM H9028
5 µL	Thermostable DNA polymerase
5 µL	[α-^{32}P] dATP (3000 Ci/mmol)

3. Add 90 µL of the PCR master mix to each tube containing 10 µL of single cell lysis and overlay with mineral oil.
4. Place tubes into thermal cycler and begin the following PCR program:

Initial denaturation	94°C	1 min
25 Cycles	94°C	1 min
	55°C	1 min
	72°C	2 min
Final extension	72°C	15 min

5. Electrophorese samples through a 5% nondenaturing polyacrylamide gel in 1× TBE.
6. Place polyacrylamide gel on filter paper, cover with cling film, and dry on gel dryer. When dry, lay gel on PhosphorImager cassette overnight, and analyze and quantitate the radioactive fragments using a PhosphorImager and ImageQuant software (*see* **Notes 9–11**).

3.4. Semiquantitative PCR of the 4977-Basepair Common Deletion in Tissue Homogenates

1. Linearization of DNA: A 125 ng/µL solution of the DNA sample under investigation is digested with the restriction endonuclease *Bam*HI at 37°C for 90 min (*see* **Notes 12** and **13**). Set up the following reaction:

   8 µL DNA
   1 µL *Bam*HI (Boehringer Mannheim)
   1 µL SuRE/Cut Buffer B (10×) (Boehringer Mannheim)

2. Serial dilution of DNA: A serial dilution (1:2) of DNA is prepared for each PCR (wild-type and common deletion). The range for the wild-type PCR is 10–3.81 × 10^{-5} ng/µL, comprising a total of 19 concentrations. The common deletion PCR has a range of DNA concentrations from 100 to 0.003 ng/µL, comprising a total of 16 dilutions (*see* **Note 14**).

3. PCR amplification: For each concentration of serially diluted DNA (1 µL), set up the following reaction:

35.8 µL	Sterile water
5 µL	10× GeneAmp® reaction buffer
5 µL	2 mM dNTPs
1.5 µL	L3108 or L8282
1.5 µL	H3717 or H13832
1 µL	Template DNA
0.2 µL	AmpliTaq® DNA polymerase (see Note 15)

When setting up a number of PCR reactions to investigate a number of concentrations, make an appropriate volume of a PCR master mix for each primer pair containing all the components except template DNA. Aliquot these into the respective tube, and add 1 µL of the appropriate serially diluted DNA.

4. Perform 34 cycles of amplification as follows:

Initial denaturation	94°C	2 min
34 Cycles	94°C	45 s
	51°C for 30 s (wtDNA) **or**	
	56°C for 30 s ($mtDNA^{4977}$)	
	72°C	1 min
Final extension	72°C	8 min

5. Electrophorese the PCR products (40 µL) through a 1.5% agarose gel in 1× TAE buffer using a large horizontal electrophoresis unit.
6. Visualize bands by UV transillumination.
7. Quantitation of PCR: The gel image is stored using a digital imaging system, and the optical densities of the PCR products are quantified using image analysis software. An integrated density value (IDV) for a set area is obtained for each PCR product. The DNA concentration at which the IDV is zero is obtained for the wtDNA and $mtDNA^{4977}$, respectively. The percentage of $mtDNA^{4977}$ deletion in the DNA sample is calculated by dividing the DNA concentration at which the wtDNA IDV is zero by the DNA concentration at which the $mtDNA^{4977}$ IDV is zero (*see* **Note 16**).

3.5. Primer-Shift PCR

1. PCR amplification: Prepare a master mix containing all the components of the PCR reactions with the exception of oligonucleotide primers. For eight reactions (final volume of 50 µL) you will need the following:

282.8 µL	Sterile water
40 µL	10× Reaction buffer
40 µL	2 mM dNTPs
10 µL	Template DNA (single cell lysis)
3.2 µL	AmpliTaq® DNA polymerase

2. Vortex-mix briefly, centrifuge, and aliquot 47 µL into each of eight tubes labeled *a–h*.
3. Add 1.5 µL of each of the appropriate forward and reverse primer.
4. Centrifuge briefly and place in PCR thermal cycler
5. Perform 35 cycles of amplification as follows:

Initial denaturation	94°C	2 min
35 cycles	94°C	30 s
	53°C	30 s
	72°C	30 s
Final extension	72°C	8 min

6. Electrophorese samples (30–40 µL) through a 1.5% agarose gel for 1 h, and visualize by UV transillumination (*see* **Notes 17–19**).

4. Notes

1. Ensure working solutions of oligonucleotide primers are prepared regularly, as they are prone to degrade more rapidly at lower concentrations and after repeated cycles of freeze–thawing.
2. Identify a DNA sample that can be used as a control for each reaction; this will allow identification of nonspecific products.
3. Nonspecific products can be avoided by raising annealing temperatures or decreasing primer concentrations.
4. If no product is amplified from a particular DNA sample, raise the concentration of DNA added to the reaction up to 100 ng. If there is still no visible product check protein contamination and treat the sample with phenol/chloroform if necessary (this may also be required for DNA samples extracted more than a year prior to amplification).
5. If smearing occurs reduce the number of cycles or the amount of DNA added.
6. The tips of the micropipets are very fragile and can be damaged during autoclaving; therefore it is important to sterilize the capillaries prior to pulling. The procedure then needs to be performed maintaining the sterility of the micropipets. During the production of micropipets it is essential to check while measuring the diameter of the tips that a smooth edge has been produced.
7. Initially using this single cell method it is recommended that a number of cells are pooled and lysed as the template to establish the technique.
8. There are several alternatives to this lysis method. Individual cells can be lysed by adding 10 µL of 200 m*M* KOH, 50 m*M* DTT, and incubated at 65°C for 1 h ***(21,23)***. Samples are neutralized by the addition of 10 µL 900 m*M* Tris-HCl, pH 8.3, and 200 m*M* HCl, and the DNA phenol/chloroform extracted and precipitated at –85°C in 2 vol of 100% ethanol, 1/10 vol of 3 *M* sodium acetate, pH 5.2, and 5 µL of 0.3 mg/mL glycogen (Boehringer Mannheim). The resulting pellet is centrifuged, air-dried, and resuspended in a volume of sterile water. Alternatively, cell lysis can be performed in the PCR mix by the addition of 5 µL of 10% Triton

X-100. This mix is then heated at 94°C for 5 min prior to adding 0.2 µL of AmpliTaq® DNA polymerase and commencing the PCR amplification as described in **Subheading 3.2.**, **step 6**.

9. It is essential that preliminary control studies are done using samples containing a varying proportion of wild-type mtDNA and mtDNA^{4977}, proportions determined by Southern blotting. This ensures that the PCR reflects the two populations of mtDNA in the original sample.
10. The concentration of the template DNA affects the ratios of wild-type to mtDNA^{4977} especially at very low concentrations ***(21)***.
11. A control sample containing wild-type mtDNA and mtDNA^{4977} of known proportion must be run and quantitated on each PCR run.
12. The template DNA must be of good quality, with an A_{260}/A_{280} ratio of no less than 1.8.
13. Other restriction enzymes that linearize the mitochondrial genome (e.g., *Pvu*II) can be used as an alternative to *Bam*HI. Linearized DNA samples can be stored successfully at –20°C for 2–3 d. Over longer periods of time, degradation of the DNA sample will lead to the appearance of additional, nonspecific bands following PCR amplification.
14. Serial dilution of DNA: It is essential that great care is taken at this stage to obtain an accurate dilution. This requires accurate pipetting and thorough mixing of each sample.
15. DNA polymerase: We strongly recommend that AmpliTaq® DNA polymerase (Perkin–Elmer) is used. Cheaper alternatives do not give reliable amplification in our hands.
16. Quantitation of PCR: When analyzing the gels of the PCR products, it is important to link the IDV values to a local background setting.
17. Primer pairs *a* and *b* are designed to amplify normal mtDNA from regions of the genome that are rarely (primer pair *a*) and often (primer pair *b*) deleted (**Fig. 3**). They serve as good controls for effective cell lysis.
18. PCR products generated by amplification with primer pairs *c–h* are specific to the deletion found in that particular cell. **Figure 2** shows the amplification of two different deletions from individual COX-deficient muscle fibers, and highlights the presence of a single mutation at high levels in these fibers. These PCR products encompass the deletion breakpoint, the sequence of which can be determined by directly sequencing the primer-shift PCR product.
19. If no visible products are amplified using any of the primer pairs, a secondary PCR can be performed exactly as described using 1 µL of the initial PCR reaction as template.

Acknowledgments

The financial support of the Northern Regional Health Authority, Research into Ageing, the Muscular Dystrophy Group of Great Britain, and the Wellcome Trust is acknowledged.

References

1. Harman, D. (1972) The biologic clock: the mitochondria? *J. Am. Geriatr. Soc.* **20,** 145–147.
2. Fleming, J. E., Miquel, J., Cottrell, S. F., Yengoyan, L. S., and Economos, A. S. (1982) Is cell aging caused by respiration-dependent injury to the mitochondrial genome? *Gerontology* **28,** 44–53.
3. Anderson, S., Bankier, A. T., Barrell B. G., de Bruijn, M. H., Coulson, A. R., Drouin, J., Eperon, I. C., Nierlich, D. P., Roe, B. A., Sanger, F., Schreier, P. H., Smith, A. J., Staden, R., and Young, I. G. (1981) Sequence and organisation of the human mitochondrial genome. *Nature* **290,** 457–465.
4. Cortopassi, G. A. and Arnheim, N. (1990) Detection of a specific mitochondrial DNA deletion in tissues of older humans. *Nucleic Acids Res.* **18,** 6927–6933.
5. Ozawa, T., Tanaka, M., Ikebe, S., Ohno, K., Kondo, T., and Mizuno, Y. (1990) Quantitative determination of deleted mitochondrial DNA relative to normal DNA in parkinsonian striatum by a kinetic PCR analysis. *Biochem. Biophys Res. Commun.* **172,** 483–489.
6. Hattori, K., Tanaka, M., Sugiyama, S., Obayashi, T., Ito, T., Satake, T., Hanaki, Y., Assai, J., Nagano, M., and Ozawa, T. (1991) Age-dependent increase in deleted mitochondrial DNA in the human heart: possible contribution factor in presbycardia. *Am. Heart J.* **121,** 1735–1742.
7. Corral-Debrinski, M., Stepien, G., Shoffner, J. M., Lott, M. T., Kanter, K., and Wallace, D. C. (1991) Hypoxemia is associated with mitochondrial DNA damage and gene induction: implications for cardiac disease. *JAMA* **266,** 1812–1816.
8. Corral-Debrinski, M., Shoffner, J. M., Lott, M. T., and Wallace, D. C. (1992) Association of mitochondrial DNA damage with aging and coronary atherosclerotic heart disease. *Mutat. Res.* **275,** 169–180.
9. Corral-Debrinski, M., Horton, T., Lott., M. T., Shoffner, J. M., Beal, M. F., and Wallace, D. C. (1992) Mitochondrial DNA deletions in human brain: regional variability and increase with advanced age. *Nature Genet.* **2,** 324–329.
10. Zhang, C., Baumer, A., Maxwell, R. J., Linnane, A. W., and Nagley, P. (1992) Multiple mitochondrial DNA deletions in an elderly human individual. *FEBS Lett.* **297,** 34–38.
11. Simonetti, S., Chen, X., DiMauro, S., and Schon, E. A. (1992) Accumulation of deletions in human mitochondrial DNA during normal aging: analysis by quantitative PCR. *Biochim. Biophys. Acta* **1180,** 113–122.
12. Cooper, J. M., Mann, V. M., and Schapira, A. H. (1992) Analyses of mitochondrial respiratory chain function and mitochondrial DNA deletion in human skeletal muscle: effect of ageing. *J. Neurol. Sci.* **113,** 91–98.
13. Baumer, A., Zhang, C., Linnane, A. W., and Nagley, P. (1994) Age-related human mtDNA deletions: a heterogeneous set of deletions arising at a single pair of directly repeated sequences. *Am. J. Hum. Genet.* **54,** 618–630.
14. Lee, H. C., Pang, C. Y., Hsu, H. S., and Wei, Y. H. (1994) Differential accumulations of 4,977 bp deletion in mitochondrial DNA of various tissues in human ageing. *Biochim. Biophys. Acta* **1226,** 37–43.

15. Melov, S., Shoffner, J. M., Kaufman, A., and Wallace, D. C. (1995) Marked increase in the number and variety of mitochondrial DNA rearrangements in aging human skeletal muscle. *Nucleic Acids Res.* **23,** 4122–4126.
16. Munscher, C., Rieger, T., Muller-Hocker, J., and Kadenbach, B. (1993) The point mutation of mitochondrial DNA characteristic for MERRF disease is found also in healthy people of different ages. *FEBS Lett.* **317,** 27–30.
17. Palotti, F., Chen, X., Bonilla, E., and Schon, E. A. (1996) Evidence that specific mtDNA point mutations may not accumulate in skeletal muscle during normal human aging. *Am. J. Hum. Genet.* **59,** 591–602.
18. Muller-Hocker, J. (1990) Cytochrome *c* oxidase deficient fibres in the limb muscle and diaphragm of man without muscular disease: an age-related alteration. *J. Neurol. Sci.* **100,** 14–21.
19. Brierley, E. J., Johnson, M. A., James, O. F. W., and Turnbull, D. M. (1996) Effects of physical activity and age on mitochondrial function. *Q. J. Med.* **89,** 251–258.
20. Boulet, L., Karpati, G., and Shoubridge, E. A. (1992) Distribution and threshold expression of the $tRNA^{(Lys)}$ mutation in skeletal muscle of patients with myoclonic epilepsy and ragged-red fibers (MERRF) *Am. J. Hum. Genet.* **51,** 1187–1200.
21. Sciacco, M., Bonilla, E., Schon, E. A., DiMauro, S., and Moraes, C. T. (1994) Distribution of wild-type and common deletion forms of mtDNA in normal and respiration-deficient muscle fibers from pateints with mitochondrial myopathy. *Hum. Mol. Genet.* **3,** 13–19.
22. Moslemi, A.-R., Melberg, A., Holme, E., and Oldfors, A. (1996) Clonal expansion of mitochondrial DNA with multiple deletions in autosomal dominant progressive external ophthalmoplegia. *Ann. Neurol.* **40,** 707–713.
23. Brierley, E. J., Johnson, M. A., Lightowlers, R. N., James, O. F. W., and Turnbull, D. M. (1998) Role of mitochondrial DNA mutations in human aging: implications for the central nervous system and muscle. *Ann. Neurol.* **43,** 217–223.
24. Fromenty, B., Manfredi, G., Sadlock, J., Zhang, L., King, M. P., and Schon, E. (1996) Rapid mapping of identified partial duplications of human mitochondrial DNA by long PCR. *Biochem. Biophys. Acta* **1308,** 222–230.
25. Reynier, P. and Malthiery, Y. (1995) Accumulation of deletions in mtDNA during tissue aging: analysis by long PCR. *Biochem. Biophys. Res. Commun.* **217,** 59–67.
26. Kovalenko, S. A., Kopsidas, G., Kelso, J. M., and Linnane, A. W. (1997) Deltoid human muscle is extensively rearranged in old age subjects. *Biochem. Biophys. Res. Commun.* **232,** 147–152.
27. De Coo, J. F. M., Gussinklo, T., Arts, P. J. W., Van Oost, B. A., and Smeets, H. J. M. (1997) A PCR test for progressive external ophthalmoplegia and Kearne–Sayre syndrome on DNA from blood samples. *J. Neurol. Sci.* **149,** 37–40.
28. Paul, R., Santucci, S., Sauntieres, A., Desnuelle, C., and Paquis-Flucklinger, V. (1996) Rapid mapping of mitochondrial DNA deletions by large fragment PCR. *Trends Genet.* **12,** 131–132.
29. Johnson, M. A., Bindoff, L. A., and Turnbull, D. M. (1993) Cytochrome *c* oxidase activity in single muscle fibers: assay techniques and diagnostic applications. *Ann. Neurol.* **33,** 28–35.

30. Zhou, L. A., Chomyn, A., Attardi, G., and Miller, C. A. (1997) Myoclonic epilepsy and ragged red fibers (MERRF) syndrome: selective vulnerability of CNS neurons does not correlate with the level of mitochondrial $tRNA^{lys}$ mutation in individual neuronal isolates. *J. Neurosci.* **17,** 7746–7753.
31. Ozawa, T., Tanaka, M., Sugiyama, S., Hattori, K., Ito, T., Ohno, K., Takahashi, A., Sato, W., Takada, G., Mayumi, B., Yamamoto, K., Adachi, K., Koga, Y., and Toshima, H. (1990) Multiple mitochondrial DNA deletions exist in cardiomyocytes of patients with hypertrophic or dilated cardiomyopathy. *Biochem. Biophys. Res. Commun.* **170,** 830–836.
32. Oldfors, A., Moslemi, A.-R., Fyhr, I.-M., Holme, E., Larsson, N.-G., and Lindberg, C. (1995) Mitochondrial DNA deletions in muscle fibres in inclusion body myositis. *J. Neuropathol. Exp. Neurol.* **54,** 581–587.
33. Santorelli, F. M., Sciacco, M., Tanji, K., Shanske, S., Vu, T. H., Golzi, V., Griggs, R. C., Mendell, J. R., Hays, A. P., Bertorini, T. E., Pestronk, A., Bonilla, E., and DiMauro, S. (1996) Multiple mitochondrial DNA deletions in sporadic inclusion body myositis: a study in 56 patients. *Ann. Neurol.* **39,** 789–795.

20

Analysis of Mitochondrial DNA Mutations

Point Mutations

Robert W. Taylor, Richard M. Andrews, Patrick F. Chinnery, and Douglass M. Turnbull

1. Introduction

Since the first demonstration that mutations of the mitochondrial genome were associated with human disease, more than 100 pathological mitochondrial DNA (mtDNA) defects have been characterized in patients with a broad spectrum of clinical manifestations ***(1)***. Single-point mutations, involving either protein-encoding genes or more commonly RNA (rRNA and tRNA) genes, represent a substantial proportion (more than one third) of the pathogenic mtDNA mutations described in the literature, and this number is steadily increasing ***(2,3)***. Although some of the more common mtDNA point mutations can be screened using simple polymerase chain reaction (PCR)-based techniques (e.g., restriction digest analysis), an increasing number of pathological point mutations are identified only when large-scale sequencing of either all 22 tRNA genes or the whole mitochondrial genome is performed ***(4–7)***.

Any point mutation that is identified by sequence analysis must fulfil a number of accepted criteria before pathogenicity is ascribed, particularly as the mitochondrial genome is highly polymorphic, with any two individuals differing by as much as 40–50 basepairs from the reference Cambridge sequence ***(8)***. The majority of pathogenic mtDNA mutations are heteroplasmic, that is, both mutant and wild type mtDNA are present within the same cell and tissue. Because the proportion of mutant to wild-type mtDNA can vary between different tissues, this can cause problems when sequencing if the level of mutant mtDNA is particularly low, and as such these studies are performed using DNA extracted from postmitotic tissues such as skeletal muscle in which the level of

From: *Methods in Molecular Medicine*, Vol. 38: *Aging Methods and Protocols*
Edited by: Y. A. Barnett and C. R. Barnett

mutant mtDNA is often high. However, the demonstration of heteroplasmy is only one of a number of accepted criteria for a pathogenic role, particularly as mtDNA heteroplasmy in both coding and noncoding regions of mtDNA is increasingly being found in nondisease subjects ***(9)***. The mutation can be shown to be disease specific by demonstrating high levels of mutated mtDNA segregating with a biochemical defect (e.g., cytochrome *c* oxidase [COX] deficiency) in single cells ***(5–7)***.

This chapter describes the strategies developed in our laboratory to amplify and sequence the entire mitochondrial genome, and the methods with which we confirm and quantify the level of mtDNA heteroplasmy in a DNA sample.

1.1. Automated Sequencing of mtDNA

The automation of DNA sequencing makes it possible to undertake large-scale sequencing projects to detect mtDNA mutations involved in disease and the aging process. Although a number of protocols exist in the literature that differ in both the method of template preparation and sequencing chemistries used ***(10)***, any strategy adopted must be capable of detecting mtDNA heteroplasmy. We have therefore chosen to amplify segments of the genome by PCR using forward and reverse mtDNA primers that have 18 bases of universal M13 primer sequence at their 5' ends (**Tables 1** and **2**). Dye primer cycle sequencing with universal M13 primers using ABI PRISM Ready Reaction kits is subsequently performed, and samples separated electrophoretically on an ABI 373 DNA sequencer (Appled Biosystems). This approach is efficient in both labor and time while providing high-quality sequence data for the whole mitochondrial genome including the noncoding region from 28 primary PCR amplifications.

Two methods of cycle sequencing are currently available. Dye terminator sequencing involves using unlabeled sequencing primers with fluorescently labeled dideoxynucleotides. Although this is the most rapid and convenient approach, individual peak heights are typically variable which can make the interpretation of base calling difficult. Dye primer cycle sequencing utilizes fluorescently tagged primers, while the dideoxynucleotides are unlabeled. Although this method requires four separate extension reactions that are subsequently pooled, dye primer sequencing has the advantage that it provides a cleaner signal with more even peak heights which facilitates the identification of heteroplasmic bases changes (*see* **Note 1**).

To generate sufficient mtDNA template for sequencing, we have chosen to use PCR amplification rather than bacterial cloning on account of both ease of use and speed, while still giving comparable results. The purity of the prepared template is extremely important in determining the quality of the final sequence data, and each PCR amplification will require optimization (i.e., a single product of the correct size in appropriate amounts). We have found that the main

Table 1
L-strand PCR Primers Used for Amplification of mtDNA for Dye Primer Sequencing

Primer	Position	Sequence (5'-3')
01F	516–534	TGTAAAACGACGGCCAGTCACACACACCGCTGCTAAC
02F	1138–1156	TGTAAAACGACGGCCAGTGAACACTACGAGCCACAGC
03F	1756–1776	TGTAAAACGACGGCCAGTAATTGAAACCTGGCGCAATAG
04F	2395–2415	TGTAAAACGACGGCCAGTACCAACAAGTCATTATTACCC
05F	2992–3010	TGTAAAACGACGGCCAGTGTTGGATCAGGACATCCCG
06F	3536–3553	TGTAAAACGACGGCCAGTTAGCTCTCACCATCGCTC
07F	4184–4202	TGTAAAACGACGGCCAGTTCCTACCACTCACCCTAGC
08F	4832–4849	TGTAAAACGACGGCCAGTCACCCCTCTGACATCCGG
09F	5526–5545	TGTAAAACGACGGCCAGTAATACAGACCAAGAGCCTTC
10F	6115–6144	TGTAAAACGACGGCCAGTTACCCATCATAATCGGAGGC
11F	6730–6750	TGTAAAACGACGGCCAGTCTATGATATCAATTGGCTTCC
12F	7349–7369	TGTAAAACGACGGCCAGTCCTAATAGTAGAAGAACCCTC
13F	7960–7979	TGTAAAACGACGGCCAGTATTATTCCTAGAACCAGGCG
14F	8563–8581	TGTAAAACGACGGCCAGTACAATCCTAGGCCTACCCG
15F	9181–9198	TGTAAAACGACGGCCAGTAGCCTCTACCTGCACGAC
16F	9821–9841	TGTAAAACGACGGCCAGTACTTCACGTCATTATTGGCTC
17F	10394–10414	TGTAAAACGACGGCCAGTCTGAACCGAATTGGTATATAG
18F	10985–11004	TGTAAAACGACGGCCAGTACAATCATGGCAAGCCAACG
19F	11633–11651	TGTAAAACGACGGCCAGTAGCCACATAGCCCTCGTAG
20F	12284–12302	TGTAAAACGACGGCCAGTCTTCCATTGGTCTTAGGC
21F	12951–12969	TGTAAAACGACGGCCAGTCGCTAATCCAAGCCTCACC
22F	13568–13587	TGTAAAACGACGGCCAGTTTACTCTCATCGCTACCTCC
23F	14227–14246	TGTAAAACGACGGCCAGTCCCATAATCATACAAAGCCC
24F	14732–14752	TGTAAAACGACGGCCAGTACTACAAGAACACCAATGACC
25F	15372–15391	TGTAAAACGACGGCCAGTTAGGAATCACCTCCCATTCC
D01F	15879–15897	TGTAAAACGACGGCCAGTAATGGGCCTGTCCTTGTAG
D02F	16495–16514	TGTAAAACGACGGCCAGTCGACATCTGGTTCCTACTTC
D03F	315–332	TGTAAAACGACGGCCAGTCGCTTCTGGCCACAGCAC

problem is the formation of PCR artefacts, particularly "primer–dimers." If carried through to the sequencing reaction, dye primer labeling of these artefacts will result in an increase in the background noise and the formation of "stop peaks" at the start of the sequence, rendering some of the data unreadable. Such artefacts are reduced by performing a "hot start" in the PCR. We therefore use AmpliTaq Gold™ (Perkin–Elmer), which requires a pre-PCR heat activation at 94°C for 12 min to provide a "hot start."

Although it is possible to cycle sequence PCR products directly, we have found both quantification and purification of the amplified products necessary

Table 2
H-strand PCR Primers Used for Amplification of mtDNA for Dye Primer Sequencing

Primer	Position	Sequence (5'-3')
01R	1190–1172	CAGGAAACAGCTATGACCGATATGAAGCACCGCCAGG
02R	1801–1782	CAGGAAACAGCTATGACCTCATCTTTCCCTTGCGGTAC
03R	2444–2426	CAGGAAACAGCTATGACCTGAGCATGCCTGTGTTGGG
04R	3074–3054	CAGGAAACAGCTATGACCTGAACTCAGATCACGTAGGAC
05R	3640–3622	CAGGAAACAGCTATGACCCTAGGCTAGAGGTGGCTAG
06R	4239–4219	CAGGAAACAGCTATGACCGATTGTAATGGGTATGGAGAC
07R	4866–4848	CAGGAAACAGCTATGACCATGTGAGAAGAAGCAGGCC
08R	5570–5551	CAGGAAACAGCTATGACCAGTATTGCAACTTACTGAGG
09R	6188–6171	CAGGAAACAGCTATGACCGGGAAACGCCATATCGGG
10R	6781–6761	CAGGAAACAGCTATGACCAATATATGGTGTGCTCACACG
11R	7398–7379	CAGGAAACAGCTATGACCGGCATCCATATAGTCACTCC
12R	8009–7990	CAGGAAACAGCTATGACCCTCGATTGTCAACGTCAAGG
13R	8641–8621	CAGGAAACAGCTATGACCTGATGAGATATTTGGAGGTGG
14R	9231–9212	CAGGAAACAGCTATGACCGATAGGCATGTGATTGGTGG
15R	9867–9848	CAGGAAACAGCTATGACCGGATGAAGCAGATAGTGAGG
16R	10516–10497	CAGGAAACAGCTATGACCAGTGAGATGGTAAATGCTAG
17R	11032–11013	CAGGAAACAGCTATGACCTCGTGATAGTGGTTCACTGG
18R	11708–11689	CAGGAAACAGCTATGACCTTATGAGAATGACTGCGCCG
19R	12361–12341	CAGGAAACAGCTATGACCTGGTTATAGTAGTGTGCATGG
20R	13005–12987	CAGGAAACAGCTATGACCTTTGCCTGCTGCTGCTAGG
21R	13614–13595	CAGGAAACAGCTATGACCTATTCGAGTGCTATAGGCGC
22R	14276–14258	CAGGAAACAGCTATGACCGGTTGATTCGGGAGGATCC
23R	14928–14911	CAGGAAACAGCTATGACCGTTGAGGCGTCTGGTGAG
24R	15419–15400	CAGGAAACAGCTATGACCTGTAGTAAGGGTGGAAGGTG
25R	16067–16048	CAGGAAACAGCTATGACCGTCAATACTTGGGTGGTACC
D01R	16545–16526	CAGGAAACAGCTATGACCAACGTGTGGGCTATTTAGGC
D02R	559–542	CAGGAAACAGCTATGACCGGGTTTGGTTGGTTCGGG
D03R	803–786	CAGGAAACAGCTATGACCGGTGTGGCTAGGCTAAGC

to give consistently high quality sequence data. QIAquick PCR Purification columns (Qiagen) are both quick and easy to use and have the advantage that the final elution volume can be varied to give a template concentration appropriate for the length of fragment to be sequenced.

1.2. Last Hot Cycle PCR

The demonstration of mtDNA heteroplasmy associated with a biochemical defect remains the most compelling piece of evidence of pathogenicity for any mutation as it implies a recent mutational event. In view of the high levels of

mutant mtDNA required for the expression of a biochemical defect (often >85% for point mutations), a number of different methods have been developed to accurately measure the level of mtDNA heteroplasmy, thus providing more clues about the molecular basis of their pathogenesis. These include PCR-single-strand conformation polymorphism (PCR-SSCP) analysis, multiple clonal analysis, allele-specific oligonucleotide hybridization, and more recently a fluorescence-based primer extension method ***(11–14)***. However, for many laboratories, the method of choice remains PCR-restriction fragment length polymorphism (RFLP) analysis, especially as this is readily applicable to the study of mtDNA heteroplasmy in single cells. Essentially, the region of mtDNA containing the point mutation under investigation is amplified by PCR, radiolabeled, and digested by a restriction endonuclease that can discriminate between wild-type and mutant mtDNA molecules at the site of the point mutation. Digestion products are electrophoresed through either agarose or nondenaturing polyacrylamide gels and the level of heteroplasmy calculated by determining the incorporation of radiolabel into each of the restriction products. The formation of heteroduplex molecules during the PCR reaction can make quantitation difficult because these are not digested by restriction endonucleases. However, the addition of radiolabel to the last cycle of amplification (hence "last hot cycle PCR") avoids the detection of these heteroduplexes, allowing an accurate determination of heteroplasmy ***(15,16)***.

We describe in the following section the methodology associated with determining the level of mtDNA heteroplasmy in both tissue homogenates and single cells. As an example, we describe the strategy used to investigate a patient previously described as heteroplasmic for a T10010C transition in the *tRNA*^{Gly} gene ***(17)***.

2. Materials

2.1. Automated Sequencing of mtDNA

1. 2 m*M* (10×) dNTP mix for PCR. Store at –20°C
2. 10× GeneAmp PCR buffer: 100 m*M* Tris-HCl, pH 8.3, 500 m*M* KCl, 15 m*M* $MgCl_2$, 0.01% (w/v) gelatin (Perkin–Elmer). Store at –20°C.
3. AmpliTaq Gold™ DNA polymerase (5 U/µL) (Perkin–Elmer). Store at –20°C.
4. Template DNA: Dilute to 200 ng/µL for PCR amplification.
5. Oligonucleotide primers for PCR: Owing to the length of read that is now possible using automated DNA sequencers, the mitochondrial genome is amplified in fragments of between 650 and 750 basepairs using a set of forward (L) and reverse (H) primer pairs (e.g., 01F and 01R) that have been designed to anneal at 58°C. Both sets of primers have 18 bases of M13 sequence at their 5' end, allowing the products to be cycle sequenced. The M13 sequences used are: forward (L) primers are prefixed by 5' TGTAAAACGACGGCCAGT 3'; reverse (H) primers

are prefixed by 5' CAGGAAACAGCTATGACC 3' (*see* **Tables 1** and **2**). Owing to the length of these PCR primers (35–40 basepairs), we recommend that they are *hplc* purified following synthesis. Stocks for PCR amplification (20 μ*M*) are stored at –20°C (*see* **Note 2**).

6. DNA thermal cycler: This is required for the initial PCR amplifications and the subsequent cycle sequencing. To achieve a high throughput of samples, a thermal cycler capable of running 96 samples is desirable. We use the GeneAmp® PCR System 9700 (Perkin–Elmer) which has a heated lid facility, thereby negating the need for mineral oil overlay for either the PCR amplification or cycle sequencing reactions.
7. Sterile water.
8. 0.2 mL—MicroAmp® Reaction tubes (Perkin–Elmer).
9. Horizontal gel electrophoresis equipment for running 1% agarose gels; 1× TAE (40 m*M* Tris-acetate, 1 m*M* EDTA, pH 8.0) running buffer containing ethidium bromide.
10. UV transilluminator.
11. QIAquick PCR Purification Columns (Qiagen).
12. Microfuge capable of holding 1.5-mL Eppendorf tubes.
13. Dye primer cycle sequencing ready reaction kits, –21 M13 and M13Rev (Perkin–Elmer). Because both of the primers used in the PCR amplification of the fragment of interest have M13 tails, the product can be sequenced in both (forward and reverse) directions. Store these kits at –20°C.
14. Bucket microfuge capable of spinning a 96-well PCR tray.
15. Ethanol, 95% (v/v).
16. Glycogen, 0.3 mg/mL solution. Store at –20°C.
17. Sample buffer: A 5:1 (v/v) mixture of deionized formamide and 25 m*M* EDTA, pH 8.0, containing blue dextran (50 mg/mL).

2.2. Last Hot Cycle PCR

1. Template DNA: Although initial studies are likely to be performed on total DNA extracted from a tissue homogenate, this technique is perfectly suited to the investigation of mtDNA mutations in single cells. Methods describing the isolation of DNA from single cells are found in the preceding chapter.
2. PCR amplification: The following stock solutions are required: 2 m*M* (10×) dNTPs (Boehringer Mannheim), GeneAmp® PCR buffer containing 100 m*M* Tris-HCl, pH 8.3; 500 m*M* KCl; and 15 m*M* $MgCl_2$ (Perkin–Elmer), AmpliTaq® DNA polymerase (Perkin–Elmer).
3. Oligonucleotide primers: These will amplify a region of the mitochondrial genome containing the mutation of interest. In this case, a 350-basepair fragment is amplified using L9695 (nt 9695–9717) and H10044 (nt 10044–10022). Stock solutions (20 μ*M*) are stored at –20°C.
4. Sterile water.
5. PCR tubes: 0.5-mL Thermotubes (Applied Biosystems) are recommended.
6. Ice: All PCR reactions are set up on ice.

7. PCR thermal cycler.
8. Horizontal gel electrophoresis equipment.
9. 1% Agarose gels containing ethidium bromide, 1× TAE running buffer.
10. UV transilluminator
11. [α-^{32}P] dCTP (3000 Ci/mmol) (Amersham Life Science Products).
12. Phenol (Molecular Biology grade).
13. Chloroform:isoamyl alcohol (24:1 [v/v]).
14. 7.5 *M* Ammonium acetate, sterile.
15. Ethanol, 100%.
16. Ethanol, 70% (v/v).
17. Cerenkov counter.
18. Appropriate restriction enzyme supplied with 10× reaction buffer: For the investigation of the T10010C mutation, the restriction endonuclease *Rsa*I (Boehringer Mannheim) is required.
19. Heat block with variable temperature setting.
20. Vertical electrophoresis system: We regularly use a 16 cm unit (SE 600) manufactured by Hoefer (Pharmacia Biotech).
21. 5% Nondenaturing polyacrylamide gel: This is made using a 30% polyacrylamide stock solution (29:1 acrylamide/bisacrylamide [w/w]) and contains 1× TBE (45 m*M* Tris-borate, 1 m*M* EDTA, pH 8.0) as the buffering component.
22. 1× TBE (45 m*M* Tris-borate, 1 m*M* EDTA, pH 8.0) running buffer.
23. Gel drying equipment (Bio-Rad Laboratories).
24. Phosphorimage cassette and imaging system, including ImageQuant software (Molecular Dynamics).

3. Methods

3.1. Automated Sequencing of mtDNA

1. For each PCR amplification, prepare the following reaction at room temperature:

35.75 µL	Sterile water
5 µL	10× PCR reaction buffer
5 µL	10× (2 m*M*) dNTPs
1.5 µL	20 µ*M* forward primer
1.5 µL	20 µ*M* reverse primer
1 µL	Template DNA (200 ng/µL stock)
0.25 µL	AmpliTaq Gold™

2. Centrifuge briefly and place in PCR thermal cycler.
3. Perform 30 cycles of amplification as follows:

Initial denaturation	94°C	12 min
30 cycles	94°C	30 s
	58°C	30 s
	72°C	30 s
Final extension	72°C	8 min

4. Electrophorese samples (5 µL) through a 1% agarose gel containing 0.4 µg/mL of ethidium bromide for about 1 h, and visualize by UV transillumination.
5. Purify the remaining sample using a QIaquick PCR purification column according to the manufacturer's instructions. At the last step, elute the DNA into a volume of water to give a DNA concentration appropriate for the length of fragment to be sequenced (e.g., a sample of 500 basepairs will need to be at a concentration of about 7 ng/µL). Once purified, these samples can be stored at –20°C prior to cycle sequencing.
6. When sequencing, thaw the dye primer cycle sequencing ready reaction mixes slowly on ice, and vortex to mix well.
7. Combine the following into four separate PCR tubes:

Reagent	**Reaction:**	**A** (µL)	**C** (µL)	**G** (µL)	**T** (µL)
Ready Reaction Premix		4	4	8	8
PCR product		1	1	2	2

8. Vortex briefly to mix, and centrifuge to bring the sample to the bottom of the tube.
9. Place the tubes in a thermal cycler, set the reaction volume to "10 µL," and cycle sequence using the following linked cycles:

15 Cycles	96°C	10 s
	55°C	5 s
	70°C	60 s
linked to		
15 Cycles	96°C	10 s
	70°C	60 s

10. Aliquot 80 µL of 95% ethanol and 5 µL of glycogen into a fresh sterile PCR tube.
11. Add the four extension reactions (**A**, **C**, **G**, and **T**) into the ethanol/glycogen mix, cover the tubes with aluminum foil, and vortex-mix briefly.
12. Place the tubes on ice and leave for 15 min to precipitate the extension products.
13. Centrifuge in the bucket centrifuge for 15 min ($1800g_{av}$).
14. Discard the foil and decant the supernatant by inverting the tubes over a paper towel and centrifuging for a further minute at $100g_{av}$.
15. Air-dry the resulting pellets at room temperature for 5 min and replace on ice. These can be stored at –20°C for several months prior to resuspension and electrophoresis.
16. Just prior to electrophoresis, the pellet is dissolved in 3 µL of sample buffer (*see* **Subheading 2.1.**). The DNA sample is heated at 90°C for 2 min, placed on ice immediately and loaded onto a 6% polyacrylamide gel (29:1 [w/w] acrylamide/bisacrylamide, Bio-Rad Laboratories) containing 8 *M* urea that has been preelectrophoresed for 15 min in 1× TBE buffer. Samples are electrophoresed at 39 W for 14 h, and sequence data collected on an ABI Model 373A automated DNA sequencer (Applied Biosystems). Factura and Navigator sequence analysis software (Perkin–Elmer, Applied Biosystems Division) are used to compare and align sequence files (*see* **Note 3**).

3.2. Last Hot Cycle PCR

1. For each PCR amplification, prepare the following reaction:

35.75 µL	Sterile water
5 µL	10× PCR reaction buffer
5 µL	10× (2 mM) dNTPs
1.5 µL	20 µ*M* forward (L9695) primer
1.5 µL	20 µ*M* reverse (H10044) primer
1 µL	Template DNA (200 ng/µL stock)*
0.25 µL	AmpliTaq® DNA polymerase

   *If template DNA is from a single cell lysis, reduce the volume of water accordingly. A master mix of these components without the template DNA can be made if multiple samples are being investigated. Overlay with mineral oil if required.
2. Centrifuge briefly and place in PCR thermal cycler
3. Perform 30 cycles of amplification as follows:

Initial denaturation	94°C	8 min
30 Cycles	94°C	1 min
	56°C	1 min
	72°C	1 min
Final extension	72°C	8 min

4. Electrophorese samples (5 µL) through a 1% agarose gel containing 0.4 µg/mL of ethidium bromide and visualize by UV transillumination.
5. If the amplification is successful, add another 1.5 µL of each primer, 0.25 µL AmpliTaq® DNA polymerase, and 0.5 µL of [α-^{32}P] dCTP (3000 Ci/mmol) to each reaction, and perform the following cycle:

Denaturation	94°C	8 min
Annealing	56°C	1 min
Final extension	72°C	12 min

6. Extract the products with 50 µL of phenol, followed by 50 µL of phenol:chloroform:isoamyl alcohol (25:24:1).
7. Precipitate the labeled products by the addition of 25 µL of 7.5 *M* ammonium acetate (½ volume) and 100 µL of 100% ethanol (2 vol) and place at –80°C for 1 h.
8. Centrifuge the precipitated products, wash with 70% ethanol, and air-dry.
9. Count the pellets using the Cerenkov counter, and resuspend in sterile water so that equal amounts (2000–8000 cpm) are digested.
10. Set up the restriction digest in a final volume of 20 µL using the appropriate restriction endonuclease (5–10 U) and 10× reaction buffer as recommended by the manufacturer.
11. Separate the digested products through a 5% nondenaturing polyacrylamide gel, dry the gel, and expose to a PhosphorImage cassette (*see* **Note 4**).
12. Using the available software, determine the level of heteroplasmy in the sample by calculating the amount of radiolabel in each restriction fragment, ensuring

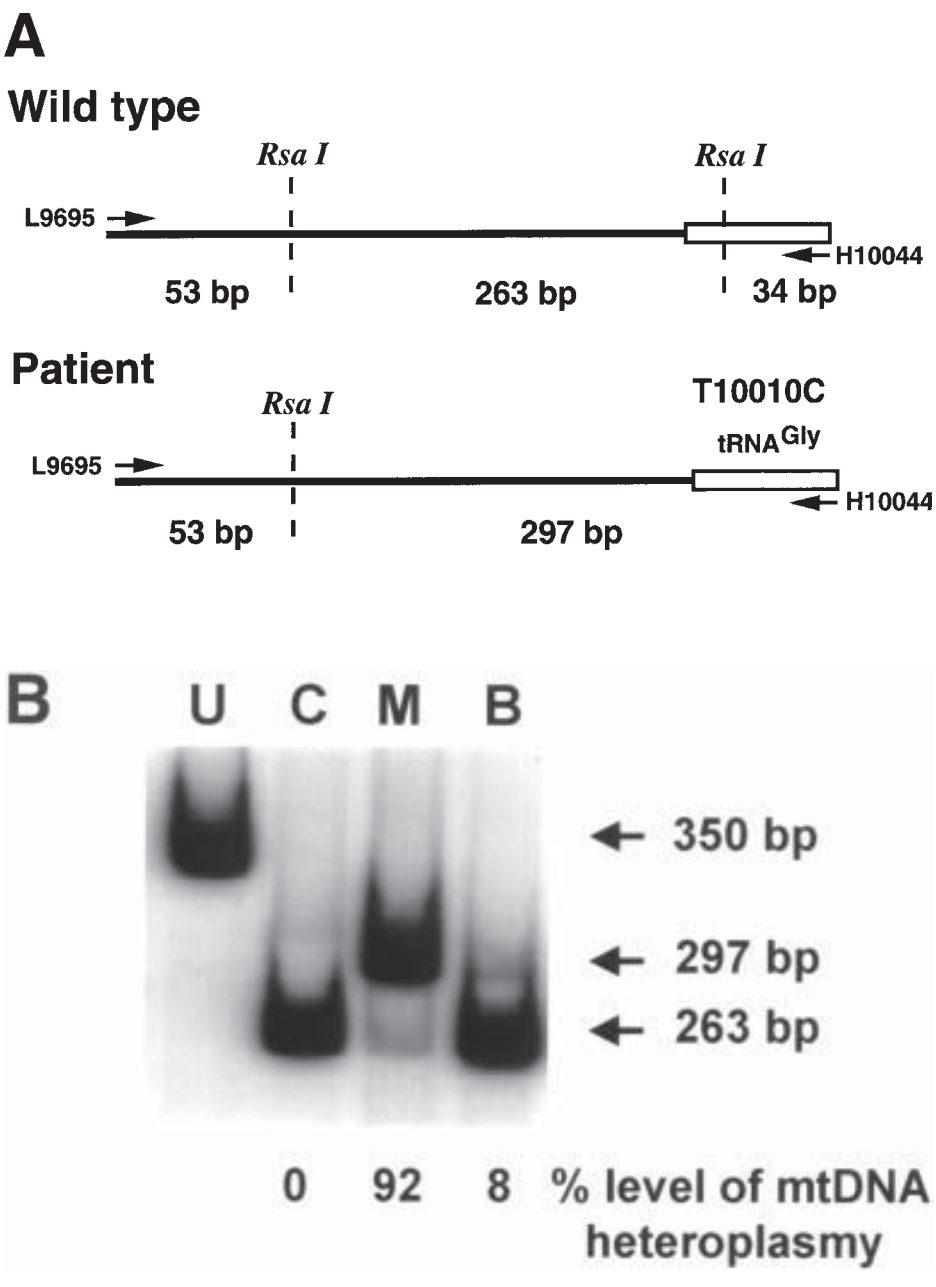

Fig. 1. PCR-RFLP analysis of mtDNA heteroplasmy in a patient with a pathogenic T10010C mutation. **U**, uncut PCR product; **C**, control subject; **M**, skeletal muscle showing a high level of mutant mtDNA; **B**, blood that has a much lower level of heteroplasmy. In the presence of the mutation, the 297-basepair fragment remains uncut.

that the digestion has gone to completion. For the T10010C mutation analysis, there are two *Rsa*I recognition sites in the wild type product, which generate fragments of 263, 53, and 34 basepairs. In the presence of the mutation, a site is lost, leaving two fragments of 297 and 53 basepairs. For quantitation, the 263-basepair fragment is normalized to the 297-basepair fragment for deoxycytosine content, and the level of heteroplasmy calculated as a percentage of the amount of radiolabel in the 263-basepair fragment relative to the combined amount in the 263 and 297-basepair fragments (**Fig. 1**) (*see* also **Notes 5–7**).

4. Notes

1. Although dye primer cycle sequencing typically provides an even peak height making it easier to detect heteroplasmic base changes, peak height is not directly proportional to the level of mtDNA heteroplasmy within a sample. Consequently, proportions of mutant or wild-type mtDNA below 30% are unlikely to be detected. If a novel change from the Cambridge sequence ***(8)*** is detected that does not appear to be a recognized polymorphism, last hot cycle PCR-RFLP analysis should be performed to exclude or confirm the presence of heteroplasmy and its level within the DNA sample.
2. As previously mentioned, we recommend that both PCR primers are synthesized with the universal sequencing primer sequences at their 5' ends, thus allowing each PCR product to be sequenced bidirectionally and any base substitutions confirmed. Moreover, there are occasionally small lengths of sequence (usually less than 5 basepairs) that cannot be read in one direction, presumably due to the nature of the DNA secondary structure. Sequencing of these samples in the opposite direction resolves this problem.
3. The complementary DNA strands of the mitochondrial genome have an asymmetric distribution of G's and C's, generating a heavy purine-rich H-strand, and a light pyrimidine-rich L-strand. Sequence data from the H-strand typically show higher levels of background noise and poorer base-calling than that obtained from sequencing the L-strand.
4. A sample of the undigested, labeled PCR product must always be run on the gel to ensure that the restriction digest is 100% efficient.
5. The most critical part of this method is the design of the RFLP to analyze the mutation. Ideally, the PCR-generated fragment should have two restriction sites for the enzyme used, one of which is unique to the mutation. This can be either gain or loss of a site. If the putative mutation does not create or destroy a naturally occurring restriction site, it is possible to engineer a site that is specific for the mutation into the PCR fragment using a mismatch primer ***(7,18)***.
6. Instead of performing a last hot cycle, the use of radioactivity can be avoided by the addition of fluorescent-labeled deoxyuridinetriphosphates (dUTPs) to the final cycle of PCR, separating the restriction products by nondenaturing polyacrylamide gel electrophoresis (PAGE) (ABI Model 373A automated DNA sequencer [Applied Biosystems]), and quantitating the level of heteroplasmy using Genescan software (Applied Biosystems) ***(19)***.

8. Quantitating the level of heteroplasmy in single cells (e.g., individual muscle fibers) will confirm whether high levels of the mutation above the required threshold for disease expression precipitate an observable biochemical defect. In this case, single-fiber PCR analysis will reveal significantly higher levels of mutant mtDNA in COX-deficient fibers than in COX-positive fibers. The protocols describing the isolation of template DNA from single cells are described in detail in the preceding chapter.

Acknowledgments

The financial support of the Muscular Dystrophy Group of Great Britain, the Medical Research Council, and the Wellcome Trust is gratefully acknowledged.

References

1. Chinnery, P. F. and Turnbull, D. M. (1997) Clinical features, investigation, and management of patients with defects of mitochondrial DNA. *J. Neurol. Neurosurg. Psychiatr.* **63,** 559–563.
2. Shoffner, J. M. (1996) Maternal inheritance and the evaluation of oxidative phosphorylation diseases. *Lancet* **348,** 1283–1288.
3. Schon, E. A., Bonilla, E., and DiMauro, S. (1997) Mitochondrial DNA mutations and pathogenesis. *J. Bioenerg. Biomembr.* **29,** 131–149.
4. Taylor, R. W., Chinnery, P. F., Haldane, F., Morris, A. A. M., Bindoff, L. A., Wilson, J., and Turnbull, D. M. (1996) MELAS associated with a mutation in the valine transfer RNA gene of mitochondrial DNA. *Ann. Neurol.* **40,** 459–462.
5. Chinnery, P. F., Johnson, M. A., Taylor, R. W., Lightowlers, R. N., and Turnbull, D. M. (1997) A novel mitochondrial tRNA phenylalanine mutation presenting with acute rhabdomyolysis. *Ann. Neurol.* **41,** 408–410.
6. Chinnery, P. F., Johnson, M. A., Taylor, R. W., Durward, W. F., and Turnbull, D. M. (1997) A novel mitochondrial tRNA isoleucine mutation causing chronic progressive external ophthalmoplegia. *Neurology* **49,** 1166–1168.
7. Taylor, R. W., Chinnery, P. F., Bates, M. J. D., Jackson, M. J., Johnson, M. A., Andrews, R. M., and Turnbull, D. M. (1998) A novel mitochondrial DNA point mutation in the $tRNA^{Ile}$ gene: studies in a patient presenting with chronic progressive external ophthalmoplegia and multiple sclerosis. *Biochem. Biophys. Res. Commun.* **243,** 47–51.
8. Anderson, S., Bankier, A. T., Barrell, B. G., de Bruijn, M. H., Coulson, A. R., Drouin, J., Eperon, I. C., Nierlich, D. P., Roe, B. A., Sanger, F., Schreier, P. H., Smith, A. J., Staden, R., and Young, I. G. (1981) Sequence and organisation of the human mitochondrial genome. *Nature* **290,** 457–465.
9. Lightowlers, R. N., Chinnery, P. F., Turnbull, D. M., and Howell, N. (1997) Mammalian mitochondrial genetics: heredity, heteroplasmy and disease. *Trends Genet*. **13,** 450–455.
10. Tanaka, M., Hayakawa, M., and Ozawa, T. (1996) Automated sequencing of Mitochondrial DNA. *Methods Enzymol.* **264,** 407–421.

11. Tanno, Y., Yoneda, M., Tanaka, K., Tanaka, H., Yamazaki, M., Nishizawa, M., Wakabayashi, K., Ohama, E., and Tsuji, S. (1995) Quantitation of heteroplasmy of mitochondrial $tRNA^{Leu(UUR)}$ gene using PCR-SSCP. *Muscle Nerve* **18,** 1390–1397.
12. Howell, N., Halvorson, S., Kubacka, I., Mccullough, D. A., Bindoff, L. A., and Turnbull, D. M. (1992) Mitochondrial gene segregation in mammals: is the bottleneck always narrow? *Hum. Genet.* **90,** 117–120.
13. Ghosh, S. S., Fahy, E., Bodis-Wollner, I., Sherman, J., and Howell, N. (1996) Longitudinal study of a heteroplasmic 3460 Leber hereditary optic neuropathy family by multiplexed primer-extension analysis and nucleotide sequencing. *Am. J. Hum. Genet.* **58,** 325–334.
14. Fahy, E., Nazarbaghi, R., Zomorrodi, M., Herrnstadt, C., Parker, W. D., Davis, R. E., and Ghosh, S. S. (1997) Multiple fluorescence-based primer extension method for quantitative mutation analysis of mitochondrial DNA and its diagnostic application to Alzheimer's disease. *Nucleic Acids Res.* **25,** 3102–3109.
15. Tanno, Y., Yoneda, M., Nonaka, I., Tanaka, K., Miyatake, T., and Tsuji, S. (1991) Quantitation of mitochondrial DNA carrying $tRNA^{Lys}$ mutation in MERRF patients. *Biochem. Biophys. Res. Commun.* **179,** 880–885.
16. Moraes, C. T., Ricci, E., Bonilla, E., DiMauro, S., and Schon, E. A. (1992) The mitochondrial $tRNA^{Leu(UUR)}$ mutation in mitochondrial encephalomyopathy, lactic acidosis, and stroke-like episodes (MELAS): genetic, biochemical, and morphological correlations in skeletal muscle. *Am. J. Hum. Genet.* **50,** 934–939.
17. Bidooki, S. K., Johnson, M. A., Chrzanowska-Lightowlers, Z., Bindoff, L. A., and Lightowlers, R. N. (1997) Intracellular mitochondrial triplasmy in a patient with two heteroplasmic base changes. *Am. J. Hum. Genet.* **60,** 1430–1438.
18. Yoneda, M., Tanno, Y., Tsuji, S., and Attardi, G. (1996) Detection and quantification of point mutations in mitochondrial DNA by PCR. *Methods Enzymol.* **264,** 432–441.
19. Chalmers, R. M., Lamont, P. J., Nelson, I., Ellison, D. W., Thomas, N. H., Harding, A. E., and Hammans, S. R. (1997) A mitochondrial DNA $tRNA^{Val}$ point mutation associated with adult-onset Leigh syndrome. *Neurology* **49,** 589–592.

21

Assessment of T-Cell Function in the Aged

T-Cell Proliferative and T-Cell Adherence Assays

Ian Beckman

1. Introduction

Certain immunological activities, particularly cell-mediated immunity, decline with advancing age. Gaining insight into the underlying mechanism(s) is complicated by the fact that human T-cells comprise several functionally and phenotypically distinct populations and subpopulations. Proliferative studies designed to identify differences between old and young subjects that are based entirely on unfractionated peripheral blood lymphocytes (PBLs) or pan T-cell responses run the risk, therefore, of missing subtle but perhaps crucial changes in a particular T-cell type.

Although it is outside the scope of this chapter to describe T-cell purification procedures, it is important to emphasize several key considerations before venturing down this road.

First, choose several different procedures that operate sequentially rather than one method repeated several times over. For example, my laboratory employs simple nylon wool columns to obtain an initial 90–95% purity (nylon wool-adherent cells also make an excellent source of blood monocytes if required in subsequent cell mixing experiments). The partially purified T-cells are then further depleted of residual monocytes by layering over plastic Petri dishes before being divided into various subpopulations (e.g., $CD4^+CD45RO^+$ or $CD8^+CD28^+$) either by negative selection, using two rounds of antibody panning with an appropriate cocktail of monoclonal antibodies (MAbs), or by positive selection, via flow microfluorimetry sorting ***(1,2)***. Magnetic beads are, of course, another option.

From: *Methods in Molecular Medicine*, Vol. 38: *Aging Methods and Protocols*
Edited by: Y. A. Barnett and C. R. Barnett

Whatever the mechanism employed, it is important that the final T-cell fraction is free of B cells (and other T-cell subpopulations if desired), monocytes, and natural killer (NK) cells. For example, "young" T-cells in particular can respond well to a single mitogenic signal such as phytohemagglutinin (PHA) with < 1% contaminating monocytes. NK cells, on the other hand, are often overrepresented in the circulation of aged individuals and because NK cells can be purified along with T-cells, they not only may skew the final "T" cell count but also are a potent source of interferon-γ when activated.

Some of the advantages of working with purified populations of T-cells are that functional changes can be related to a specific cell type(s), and most importantly, when comparing young and aged subjects, the actual number of T-cells (and indeed, accessory cells) seeded into a given well can be controlled in all experiments.

The disadvantages of multiple purification procedures are low cell yields (despite relatively large volumes of blood) and increased risk of contamination. It is also important that the purification process *per se* does not preactivate the cells. For example, avoid using strongly mitogenic MAbs or sheep red blood cells (SRBCs) during positive selection. Although T-cell binding to SRBCs (E-rosettes) is a well-known means of enriching for T-cells, very low numbers of SRBCs provide sufficient stimulus to activate purified T-cells in the presence of PHA.

Human peripheral T-cells are normally quiescent. They can be activated to secrete interleukin-2 (IL-2) and proliferate by a variety of stimuli. In general, complete T-cell activation requires two signals. The first is delivered through the T-cell receptor (TCR)–CD3 complex by small antigenic peptides in association with HLA molecules. This is best achieved in the laboratory using reagents such as superantigens or MAbs directed against TCR or CD3. The first signal can also be triggered by ligands that bind the surface receptor CD2. Second signals follow engagement of ligands on the surface of antigen presenting cells (APCs) with T-cell surface receptors (TCRs) such as CD28. However, a variety of molecules and in vitro systems can bypass the need for APCs or other accessory cells (ACs), making it possible to dissect specific T-cell–AC interactions and identify actual sites of dysfunction.

Two potent pan T-cell mitogens, namely MAb OKT3 (anti-CD3) and the superantigen, staphylococcal enterotoxin B (SEB), have an obligatory requirement for ACs. However, OKT3-induced activation can be achieved in the absence of ACs either using wells precoated with anti-mouse IgG, which promotes crosslinking of the TCR–CD3 complex, or using plate-bound OKT3 and fibronectin. The latter combination is a particularly strong T-cell stimulus.

Alternatively, plate-bound 64.1 (an IgM anti-CD3 MAb) alone can induce proliferation in highly purified T-cells.

With respect to CD2-induced stimulation, mitogens such as PHA and several anti-CD2 MAbs that trigger the CD2 receptor are powerful activators. Interestingly, CD2-induced activation is markedly diminished in the elderly and because PHA is relatively nonspecific, CD2 activation is probably best observed using the anti-CD2 MAb pair T112 and T113. Together they are strongly mitogenic for T-cells in the presence of ACs. More importantly, when used with purified T-cells at relatively low concentrations, this pair of MAbs provides a potent signal 1 without causing IL-2 secretion. Full activation is achieved, however, when used in combination with any one of a number of different costimulatory factors or cells. To this end, various cofactors can easily be tested for their ability to provide an effective signal 2.

Proliferation or activation can be determined in a number of ways. Clearly, the choice of the primary readout system is best governed by the type of information required. Other factors, including the availability of technical expertise, the sensitivity and specificity of the assay, cost, and time are also important considerations.

The simplest approach is to measure tritiated thymidine incorporation. Probably the best marker of T-cell activation, however, is the production of IL-2 and other T-cell-derived cytokines. Resting unstimulated human T-cells remain transcriptionally silent even after several days of in vitro culture. Cytokines can be detected at the mRNA level by reverse transcriptase-polymerase chain reaction (RT-PCR), *in situ* hybridization using labeled probes, or by *in situ* PCR. The RT-PCR method (described in detail below) is relatively simple to perform; it is also fast, sensitive and semiquantitative (if required). Moreover, it allows the expression of a large range of activation-associated genes to be examined simultaneously using very small cell numbers, for example, cytokines and their receptors, other immune function genes (e.g., HLA DR, LFA–1, transferrin receptor, adhesion receptors, CD80, CD86, CD40), cell-cycle-associated genes, proto-oncogenes etc.

At the protein level, cytokines are readily detected by enzyme-linked immunosorbent assay (ELISA) (using cell supernatants) and *in situ* immunohistochemistry. The latter technique is very impressive (particularly when coupled to double or triple labeling and flow cytometry allowing the accurate enumeration of specific cell types, e.g., IL-4 producing $CD4^+CD45RO^+$ T-cells) but the trick to getting it to work consistently is obtaining the right MAbs (e.g., *see* **refs. *3–5***). It is definitely a procedure worthwhile pursuing in the aging area.

Immunophenotyping and cell-cycle analysis using BrdU or propidium iodide could also be used to complement the above readouts. Wherever possible, utilize a number of different detection systems when comparing T-cell proliferation in aged and young subjects. Finally on the subject of read-out, if "old" T-cells do not appear to respond to a particular stimulus, check if they have actually apoptosed.

T-cell adherence to vascular endothelium is, I believe, an important issue in immunogerontological studies. To egress the circulation and enter tissues, T-cells must interact with, and adhere to, endothelial cells. Changes in T-cell–endothelium interactions may well have implications for atherogenesis and the observed age-related decline in cell-mediated immunity, particularly delayed type hypersensitivity (DTH). For example, activated "old" T-cells may display an increased propensity to "stick" to endothelial cells (EC) and facilitate inflammation, or conversely, they may exhibit a diminished ability to bind and transmigrate through the endothelium. To this end, I have included in this chapter a simple assay that provides a measure of the capacity of various T-cells to bind human umbilical vein endothelial cells.

2. Materials

1. Complete culture medium (CC*M*); RPMI-1640 (Flow Labs) supplemented with 10% heat-inactivated fetal calf serum (FCS), 2 m*M* glutamine (added just prior to culture) and penicillin/streptomycin (10,000 U/mL) (*see* **Note 1**).
2. Sterile flat, 96-well microtiter (Linbro) and 24-well tissue culture (Costar) plates with lids (*see* **Note 2**).
3. Phosphate buffered saline (PBS).
4. 50 m*M* Tris-HCl, pH 9.5.
5. Tritiated thymidine ([^{3}H]-TdR) (Amersham).
6. Exogenous activators: MAbs (OKT3 [anti-CD3] [from American Type Culture Collection], 64.1[anti-CD3] and 9.3 [anti-CD28] [from Bristol–Myers–Squibb, Seattle], T112 and T113 [anti-CD2] [from E. Reinherz, MIT, Boston MA, USA]); PHA (Sigma), phorbol 12-myristate 13-acetate (PMA) (Sigma), SEB (SEB) (from Sigma), fibronectin (Collaborative Research Incorporated, or Integrated Sciences), and various cytokines (Boehringer Mannheim and Genzyme).
7. Goat anti-mouse IgG (GAM) (Dakopatts).
8. Mitomycin C (Sigma).
9. Collagenase (Sigma).
10. Fluorescein-labeled (FITC-) goat or sheep anti-mouse IgG (Becton-Dickinson).
11. Vanyl ribonucleoside complexes (Gibco-BRL).
12. 123-basepair DNA ladder (Gibco-BRL).
13. Endothelial cell growth factor supplement (Integrated Sciences).
14. ECV304: Transformed immortal human endothelial cell line from umbilical cord (ATCC CRL-1998).
15. Trypsin/EDTA solution (1×) in PBS (Boehringer Mannheim).

3. Methods

3.1. T-Cell Activation Using Unfractionated PBL

1. Add 20 µL or 100 µL of MAb OKT3, at a single predefined optimal concentration (e.g., 50 ng/mL; note the final concentration in each well is 5 ng/mL) or use

a range of concentrations, to triplicate wells of a 96- or 24-well plate, respectively (*see* **Note 3**).

2. Alternatively or in parallel experiments, add titrated amounts of SEB (a final concentration of 10 ng/mL is optimal in my laboratory) or MAbs T112 and T113 for anti-CD2 stimulation (as a guide we use a final dilution each of 1:500 ascites fluid).
3. Dispense 180 µL or 900 µL of PBL (prewashed twice in PBS and resuspended in CCM at 5.5×10^5/mL) to each 96- or 24-well plate, respectively, and incubate at 37°C in a 5% CO_2 controlled atmosphere for 3–4 d. Try a range of cell concentrations ranging from 2×10^5/mL to 1×10^6/mL (*see* **Note 4**).
4. At the designated time(s), appropiate cultures are spiked with 0.5 µCi [^{3}H]TdR for 4 h before harvesting the cells using a semiautomated sample harvester. The amount of [^{3}H]TdR incorporation is measured in a beta scintillation counter (subtract the cpm recorded in negative control wells, i.e., wells containing nonactivated cells).

   Cells are also harvested from parallel cultures at identical times for other analyses, for example, RT-PCR, cell cycle, and/or immunohistochemical analysis (*see* **Note 5**). Remember to store the centrifuged culture supernatants at –80°C for cytokine ELISAs, if required.

   Alternatively, T-cell responses generated in one-way mixed lymphocyte reactions (MLR) using PBLs are analyzed by coculturing 1×10^5 cells (responder cells) from one individual with an equal number of irradiated (2000 rads) or mitomycin C-treated cells (stimulator cells) from one or more unrelated individuals in triplicate round-bottom 96-well plates in a final volume of 200 µL (*see* **Note 6**). Incubate for 7 d and spike with 0.5 µCi [^{3}H]TdR per well for 16–18 h before harvesting as described previously.

3.2. T cell Activation Using Purified T Cells and AC

1. Cultures are basically set up as described previously except purified T-cells are employed (*see* **Note 7**); however, in these experiments the proportion of ACs or monocytes to T-cells is controlled for each subject.
2. We usually add 10% irradiated (2000 rads) AC-enriched cells (i.e., nylon wool-adherent and plastic-adherent peripheral blood mononuclear cells) to each well containing 1×10^5 or 1×10^6 T-cells (*see* **Note 8**).

Again, it is often informative to try a range of AC concentrations (i.e., 5% to 30%).

Furthermore, these experiments provide a degree of flexibility. That is, the ACs can be either (1) irradiated autologous ACs (2) irradiated heterologous ACs (a MLR is avoided here by culturing for 3 d) (3) transformed cell lines such as K562 or U937 (irradiated with 4000 rads to prevent outgrowth) (4) irradiated CHO transfectants expressing specific human ligands singularly or in combination, for example, HLA DR, CD80, CD86, LFA-3, CD40, Fas, etc., or (5), irradiated OKT3–hybridoma cells. Interestingly, the OKT3 expressing

T3 hybridoma cells satisfy the dual requirements for full activation by providing both first and second signals.

Judicious use of transfectants can help accurately dissect specific T-cell–AC interactions and thus provide real insight into potential age-related deficiencies.

3.3. AC-Independent T-Cell Activation

3.3.1 Anti-Mouse IgG-Coated Plates

1. Precoat wells with 750 ng/well goat anti-mouse IgG (GAM) prepared in 50 m*M* Tris-HCl, pH 9.5.
2. Leave overnight at 4°C, then wash the plates 3× with PBS and store at –20°C until required.
3. Incubate T cells at 1×10^6/mL with OKT3 (100 ng/mL) for 1 h at 4°C.
4. Wash once in PBS, resuspend in CCM at 5×10^5/mL, and dispense 200 µL per GAM-coated well. Culture for 3–4 d.

3.3.2. Plate-bound OKT3 + Fibronectin (FN)

1. Precoat wells with 100 ng/well OKT3 in 50 m*M* Tris-HCl, pH 9.5, and leave overnight at 4°C.
2. Flick off the supernatant and without washing the plates, add a freshly prepared solution of F*N* (1 µg/50 µL/well, diluted in PBS).
3. Incubate at room temperature for 2 h, wash 3× in PBS, and store at 4°C until required.
4. Dispense 200 µL of T cells at 5×10^5/mL to each well. Culture for 3–4 d.

3.3.3. Immobilized 64.1

MAb 64.1 is diluted in PBS to 1 mg/mL (aliquot and store at –20°C).

1. Add titrated amounts of 64.1 (1000 ng–20 ng/50 µL/well) to flat-well plates and leave at room temperature for 5 h.
2. Wash 3× in PBS and leave the plates wrapped in alfoil at 4°C (long-term storage at –20°C).
3. Start the experiment by adding 200 µL of T cells at 5×10^5/mL and culture for 3–4 d (*see* **Note 9**).

3.3.4. Anti-CD_2-Induced T-Cell Activation in the Presence of Cofactors

1. Titrate both T112 and T113 together to determine a concentration that does not induce activation in pure T-cell preparations, that is, a submitogenic dose (in our hands this is usually a 1:1000 or 1:2000 dilution of each ascites fluid).
2. Full activation, including IL-2 secretion, requires a second costimulatory stimulus. To this end, we have used a variety of cofactors including cytokines IL-2 (20 U/mL), IL-1β (20 U/mL), IL-6 (200 U/mL), and IL-7 (100 U/mL); PMA (1 ng/mL); MAb anti-CD44 (1:1000 ascites); and the anti-CD28 MAb 9.3 (1:1000 ascites) (*see* **Note 10**). The above concentrations are a guide only.

3. Dispense the anti-CD2 MAbs and graded amounts of cofactor(s) to microtiter wells, add 2×10^5 T-cells per well, and culture for 3–4 d. Thus the capacity of each cofactor to induce activation is easily tested. Anti-CD28 MAbs are excellent costimulatory reagents, presumably because they mimic the key CD28–CD80 signal transduction pathway.

3.4. RT/PCR Analysis

We have established a reliable and semiquantitative RT-PCR technique that is based on taking several 5-µL aliquots during the linear phase of the PCR and relating the amount of target product to two control genes, actin and CD3 δ, for a given starting cell number. However, good commercial kits are now available for quantitative RT-PCR that are designed for a number of cytokines.

1. After 4–48 h of culture, harvest as few as 2×10^5 and up to 1×10^6 stimulated and nonstimulated (control) T cells from 24-well Costar plates and wash twice in PBS-containing 0.01% diethylpyrocarbonate (DEPC) (an RNase inhibitor) (*see* **Note 11**).
2. To extract cytoplasmic RNA, pellet the cells in Eppendorf tubes and remove as much PBS as possible. Lyse the cell pellets in 0.1 mL of solution A (10 m*M* Tris, pH 7.5; 150 m*M* NaCl; 0.65% NP-40; and 10 m*M* vanyl ribonucleoside complexes). After about 10 s, centrifuge the tubes at 12,000*g* for 1 min and transfer the supernatant containing the cytoplasmic fraction (be careful not to disturb the pellet) to a new tube containing 0.3 mL of solution B (10 m*M* sodium acetate, pH 5.0; 50 m*M* NaCl; 5 m*M* EDTA; and 0.5% sodium dodecyl sulfate [SDS]).
3. Vortex-mix the mixture and then extract twice with 800 µL phenol/chloroform (1:1) and finally once more with chloroform alone.
4. Remove about 40 µL of the aqueous phase and use an aliquot for the cDNA reaction. Store the remainder at –80°C as 1250 or 2500 cell equivalents per microliter of supernatant. The RNA is stable for at least 12 mo.
5. First-strand cDNA is synthesized from 5 to 10 µL of RNA supernatant, using M-MLV reverse transcriptase (BRL) and oligo dT priming according to the manufacturer's directions, in a final volume of 40 µL. The reaction is carried out at 37°C for 1 h.
6. One eighth of the cDNA is then added to 45 µL of PCR mix and the tubes subjected to 27–34 cycles of PCR amplification using a thermal cycler with a 1 min/95°C denaturation, 2 min/60°C annealing, and 3 min/72°C extension profile.
7. A 5 µL aliquot is taken at the end of several cycles (e.g., 27, 29, and 31), mixed with loading buffer, and then analyzed by electrophoresis on 2% agarose gels and subsequently stained with ethidium bromide (Et Br). A 123-basepair DNA ladder (Gibco-BRL) is used as a marker. Compare and contrast each gene product with the actin and CD3 δ product. Thus its possible to screen about 30–40 different genes from a single cell preparation. For relevant primer sequences *see* ***(1)***.

Having identified a candidate gene(s) it is important, however, to examine not just message but where possible, protein levels (ELISA) and functional integrity (bioassay).

3.5. T-Cell Adherence to Endothelial Cells (ECs)

This simple assay measures the capacity of resting and activated T-cells to adhere to activated or resting endothelium (*see* **Note 12**).

3.5.1. Preparation of Human EC

1. Human ECs are prepared by washing intact human umbilical veins, one end closed with a sterile stopcock and valve, with 20 mL of Hanks' balanced salt solution (HBSS) containing 0.08% collagenase.
2. After 10 min at 37°C, 20 mL of medium 199 is injected into the vein and the collagenase solution washed out. The vein is massaged with fresh medium and the stripped EC collected by centrifugation.
3. ECs are cultured in medium 199 supplemented with 20% FCS and 20 µg/mL Endothelial Cell Growth Factor Supplement (Integrated Sciences) in flasks (Costar) precoated with 2.5 mL of gelatin (a 2% solution in HBSS).
4. To remove the ECs from a flask, treat with 5 mL of trypsin/EDTA solution for 5 min, then wash twice and resuspend the cells in 3 mL of the above medium.
5. Add 1 mL per well to a 24-well culture plate containing a sterile round glass coverslip (sterilized by soaking in ethanol, flaming, and washing in sterile PBS). After 2 d the cells form a new monolayer.
6. Alternatively, monolayers can be derived from the spontaneously transformed immortal human endothelial cell line, namely ECV304, by culturing cells at 2×10^5/mL in 24-well plates in medium 199 plus 10% FCS.
7. To prepare activated EC monolayers, incubate with 5 ng/mL of tumor necrosis factor-α (TNF-α) for 4 h and then wash the cells three times with PBS.

3.5.2 Adherence Assay

1. Dispense half a million resting or activated pan T cells (e.g., activation can achieved by incubating the cells with plate-bound MAb 64.1 for 4 h) to the EC-coated glass coverslips.
2. After 90 min at 37°C wash the coverslips twice in PBS and incubate with 200 µL of MAb; for example, anti-CD3, anti-CD4 (helper T cells), anti-CD8 (supressor/cytotoxic T cells), anti-CD45RA (naive T cells), anti-CD45RO (memory T cells), or irrelevant MAbs (negative controls).
3. Incubate for 20 min at 4°C and then wash the coverslips twice with PBS.
4. Add 200 µL of pretitrated FITC-labeled goat anti-mouse IgG per well for 20 min at 4°C.
5. Wash the coverslips thrice and remove them from the wells using a needle with a bent tip and place on a glass slide for subsequent examination by UV microscopy. T-cells bound to the EC monolayers are easily identified by their staining pattern with the appropriate MAb.

4. Notes

1. Test several different FCS batches and select one that is neither inhibitory in the presence of known activators nor mitogenic in the absence of activators. It should also be relatively cheap and available in sufficient quantity to complete all experiments. FCS can be replaced with pooled human AB sera, however, varying amounts of platelet-derived growth factor (PDGF) in human sera may alter T-cell activity, particularly cytokine production. "Old" T-cells are reported to be sensitive to PDGF. If possible, therefore, use a proven serum-free medium or supplement, such as Stratagenes Cell/Perfect PBL serum-free media supplement, that consistently supports T-cell proliferation in your hands.
2. I recommend flat 96-well microtiter plates (Linbro) or 24-well plates (Costar) with lids but different types and brands should be compared. Some plates are clearly better at supporting cellular proliferation than others. (Note that round-bottom plates are optimal for MLR).
3. Identify the optimal and suboptimal concentrations of all exogenous stimuli by running dose–response curves and kinetic studies over several days. The importance of these experiments cannot be overstated, and they should be performed on cells from both aged and young control subjects. Such experiments also help to define the experimental conditions, and indeed help exploit the differences that may exist between age groups. For example, "old" T-cells that do not respond to a particular stimulus at one concentration may respond well at a higher concentration or a day later, when compared to "young" cells.
4. Determine cell viabilities (should be >95%). If <90%, either abort the experiment (and potentially save on time and money in the long term) or try to remove the damaged cells (e.g., by Percoll gradient centrifugation or flow cytometry). Dead or dying cells can influence the final outcome of cultures significantly.
5. In my experience, some of the different readout systems do not always correlate with each other and vital information may be lost if just one or two systems are used to measure the proliferative response. For example, I have observed activated T-cells from aged subjects that produced very low levels of IL-2 but still displayed normal levels of tritiated thymidine incorporation, and vice versa.
6. Prepare a solution of mitomycin C in PBS at 0.5 mg/mL, filter sterilize, and store the bottle in the dark (mitomycin C is light sensitive). Incubate PBL at 1×10^6/mL in PBS with 50 µg/mL of mitomycin C for 20 min at 37 C. Wash the cells twice with large volumes of CCM and resuspend the pellet in CCM at 1×10^6/mL.
7. To ascertain that accessory cells or monocytes have been removed, albeit functionally, culture the T-cell preparations alone with PHA (5 µg/mL) for 3–4 d and measure the amount of tritiated thymidine uptake. Residual NK cells, B cells, and monocytes can also be checked by immunophenotyping and flow cytometry using appropriate MAbs.
8. AC-enriched populations are obtained from spent nylon-wool columns (i.e., after the T-cells have been eluted) by loading the column with warm medium and vigorously and continously proding the nylon-wool with a sterile 10-mL pipet. Collect the adherent cell eluate and plate out on plastic Petri dishes for 1–2 h. Wash

the plates vigorously with medium and harvest the plastic-adherent cells by gently scraping with the rubber end of a 10-mL syringe plunger.

9. Proliferative T-cell responses to immobilized 64.1 are significantly enhanced by the addition of IL-1β (20 U/mL), but only at the relatively lower antibody concentrations of 100 ng–20 ng/well. In our hands this is a simple but very effective bioassay for IL-1β.
10. It is advisable to use well-defined reagents (e.g., antibodies, cytokines, etc.) that can be purchased or prepared in purified form. Dialyze extensively against PBS to remove preservatives and other potentially inhibitory factors and then filter sterilize. Check for endotoxin activity and confirm, where possible, the specificity of the reagents before aliquoting and placing in long-term storage.
11. IL-2 (and other cytokine transcripts) may be detected in unstimulated or control T-cells by RT-PCR if the medium contains even trace amounts of mycoplasma or nonspecific serum-derived mitogenic factors. This is another good reason to use serum-free medium.
12. We have tried several methods based on differential prestaining of T-cells and ECs with a number of dyes to detect T-cells bound to EC monolayers but with mixed success, largely due to background staining from the ECs. However, an indirect immunofluorescence method proved to be fast and effective, and allowed identification of specific T-cell subtypes without the need to first purify these cells before addition to the EC monolayers. If background staining is a problem, block with normal goat serum or try other second antibodies.

References

1. Beckman, I., Shepherd, K., Dimopolous, K., Ahern, M., Firgaira, F., and Bradley, J. (1994) Differential regulation and expression of cytokine mRNA's in human CD45R T cell subsets. *Cytokine* **6,** 116–123.
2. Beckman, I., Shepard, K., Ahern, M., and Firgaira, F. (1995) Age-related defects in CD2-receptor induced activation in human T cell subsets. *Immunology* **86,** 533–536.
3. Sewell, W. A., North, M. E., Webster, A. D., and Farrant, J. (1997) Determination of intracellular cytokines by flow-cytometry following whole blood culture. *J. Immunol. Methods* **10,** 67–74.
4. Morita, Y., Yamamura, M., Kawashima, M., Harada, S., Tsuji, K., Shiuya, K., Maruyama, K., and Makino, H. (1998) Flow cytometric single cell analysis of cytokine production by $CD4^+$ T cells in synovial tissue and peripheral blood from patients with rheumatoid arthritis. *Arthritis Rheum.* **41,** 1669–1676.
5. Collins, D. P., Luebering, B. J., and Shaut, D. M. (1998) T-lymphocyte functionally assessed by analysis of cytokine receptor expression, intracellular cytokine expression, and femtomolar detection of cytokine secretion by quantitative flow cytometry. *Cytometry* **33,** 249–255.

22

Dendritic Cells in Old Age

Beatrix Grubeck-Loebenstein, Maria Saurwein-Teissl, and Nikolaus Romani

1. Introduction

1.1. General Background

Dendritic cells (DCs) are powerful antigen-presenting cells that have the unique capacity to stimulate naive T-cells ***(1,2)***. DCs are identified by a triad of criteria: *Morphologically*, they exhibit pronounced cytoplasmic veils that are mobile and can easily be observed under a phase-contrast microscope. These veils become apparent only in the mature state. *Phenotypically*, they express high levels of major histocompatibility class (MHC) (class I and II), adhesion (CD11c, CD54, CD58), and costimulatory (CD80, CD86, CD40) molecules on their cell surfaces. They also express CD1a and CD83, but lack CD14. On cytocentrifuge smears stained with anti-CD68, a marker of the endocytic system that is abundant in macrophages, DCs display spotlike staining whereas typical macrophages are strongly positive all over the cytoplasm. When looking at forward/side scatter profiles in the fluorescence-activated cell sorter (FACS), DCs show high light scattering and are outside the typical lymphocyte gate. *Functionally*, they are potent stimulators of resting T lymphocytes in the allogeneic mixed leukocyte reaction. DCs derived from various tissues have been shown to undergo a complex maturation process during which their morphology, phenotype, and function change. DCs are derived from bone marrow progenitors and circulate in the blood as immature precursors before they migrate into peripheral tissues, such as the epidermis, heart, lung, liver, gut, thymus, spleen, and lymph nodes. DCs of myeloid as well as of lymphoid origin have been described ***(3–5)***. Within tissues DCs take up and process antigen which is then presented in the context of MHC molecules. Upon appropriate stimulation they undergo further maturation and migrate to secondary lymphoid tissue where they present antigens to

From: *Methods in Molecular Medicine*, Vol. 38: *Aging Methods and Protocols*
Edited by: Y. A. Barnett and C. R. Barnett

T-cells and induce an immune response ***(6)***. Recent knowledge on DCs and how they control immunity has been summarized in excellent reviews ***(4,6–9)***. It is the aim of the present chapter to give a brief overview on what is known on DCs in aged humans and animals. Particular emphasis is given to outline the methodology required to purify, culture, and characterize this interesting cell type.

1.2. How Studies on DCs Can Be Performed

In the past, DCs from various sources could be isolated only by using sophisticated protocols ***(10–12)***. These protocols are still being used for studies in which freshly isolated DCs have to be analyzed. Rapid progress in the characterization of DCs has, however, been made in recent years, as simple methods to generate large numbers of DCs from precursors have been developed. $CD34^+$ progenitor cells from cord blood or bone marrow or monocytes from the peripheral blood can hereby be used as starting populations ***(13–15)***. Depending on the nature of these populations and on the stimulatory agents applied, DCs with a varying degree of maturation can be propagated ***(16,17)***. Although granulocyte/macrophage colony-stimulating factor (GM-CSF) and tumor necrosis factor-α (TNF-α) have mainly been used to induce the generation of a typical DC progeny from $CD34^+$ cells, combinations of GM-CSF and interleukin (IL-4/IL-13) have been shown to trigger the differentiation of monocytes into typical DCs. Various factors, such as serum, monocyte conditioned medium ***(18,19)***, transforming growth factor-β (TGF-β) ***(20,21)***, flt-3 ***(22)***, and stem cell factor ***(23)*** have been shown to support the in vitro generation of DCs. Organ cultures to study the outgrowth of DCs from tissue samples have additionally been developed ***(18)***.

1.3. DCs in Aged Rodents

1.3.1. Murine DCs in Aging

Inbred strains of laboratory mice represent well-defined and suitable systems to study effects of aging on DCs. It is easy to obtain large numbers of animals at defined ages. There is even a special strain of mice that may be used for senescence-related work: the SAMP1 (senescence-accelerated) mouse ***(24)***. In spite of such good preconditions, little research has been done with regard to DCs and aging. Yet, some interesting data are available and are reviewed here.

1.3.2. Ontogeny of DCs

As mentioned previously, DCs arise from progenitors in the bone marrow. One study has addressed whether the capacity of the bone marrow to give rise to Langerhans cells (LCs) changes with age ***(25)***. When bone marrow cells from young and old mice were transplanted into irradiated recipients of the same age it was observed that the density of LCs was lower in those mice that

had received marrow cells from aged animals than in those mice that had been grafted with marrow from young mice. This suggests that the frequency of DC progenitors may be lower in aged mice. Alternatively, the migration of progenitors from the marrow to their target tissues or the homing of progenitors may be impaired in aged animals. These possibilities are yet to be clarified.

1.3.3. Distribution of DCs

LCs, that is, the epidermal variant of DCs, have been studied in some detail, the most obvious question being whether the numbers of LCs change with age. Immunohistochemistry (using monoclonal antibodies [MAbs] against MHC class II) and enzyme histochemistry (using ATPase staining) were generally applied to address this issue. Several authors found a decline of LC densities in the epidermis with age ***(25–27)***. The extent of LC reduction was about one third. This was also observed with LCs in the oral mucosa: a reduction by 30–60% was reported in the mouse ***(28)*** and a reduction of LC foci and interfocal LCs in the hamster cheek pouch ***(29)***. In contrast, a study in the rat reported an unchanged density of DCs (reactive with MAb OX-6) in the mucosa of the tooth pulp ***(30)***. So did another investigation of the mouse gingiva ***(31)***. No detailed studies are available concerning age-related changes in numbers and distribution of DCs from sources other than the skin (spleen, lymph nodes, thymus).

1.3.4. Function of DCs

The experiments reviewed here are too few in number to allow well-founded conclusions. Important questions have not yet been addressed. It has not been dissected which component of DC function is reduced with age. The three broad functions of DCs as delineated by Steinman (***1***; *see* **Subheading 1.1.**) are separated from each other in space and time. They are down- and up-regulated in the course of the maturation process. Therefore, the experiments discussed below also imply an analysis of the maturation process in relation to age.

1.3.5. T-Cell Stimulatory Properties of Murine DCs

Antigen processing may be affected by age. The observations by Haruna et al. ***(24)*** that the impaired T-cell stimulatory function of DCs did not correlate with the expression of such crucial molecules as the costimulators CD80 and CD86 leads one to speculate that perhaps the generation of immunogenic MHC class II/peptide complexes may be diminished as well. This aspect of immunogenicity could easily be studied by means of peptide-specific T-cell hybridomas ***(32)***. The development of T-cell-sensitizing capacity of DCs with age is another important point. Early work showed an increase of the immunostimulatory capacity of spleen DCs from C57BL/6 mice in the syngeneic mixed leukocyte reaction, but not in the allogeneic mixed leukocyte reaction or in the

polyclonal response to concanavalin A ***(33)***. A recent and detailed study utilized a substrain of SAMP1 mice. The authors investigated the allogeneic mixed leukocyte reaction as a measure for the capacity of DCs to stimulate resting T-cells. Spleen DCs from aged SAMP1 mice stimulated less well in this assay than DCs derived from age-matched BALB/c mice or from young SAMP1 mice ***(24)***. These changes correlated with the expression of MHC class II and adhesion molecules (CD54/ICAM–1) but, interestingly, not with the expression of costimulator molecules (CD80/B7–1 and CD86/B7–2) on DCs. Clearly, more studies are needed to construct a conclusive picture. Other factors contributing to the sensitizing potential of murine DCs have not been analyzed to date. Examples are the capacity to cluster T-cells in vitro ***(34)*** and in vivo ***(35)*** or the ability to secrete IL-12 ***(36)***.

1.3.6. Migratory Function

Migration of DCs from the sites of antigen uptake (e.g. the skin) to the regional lymphatic organs is essential for the successful generation of an immune response. DCs typically migrate through lymphatic vessels. Recently, a novel pathway of DC migration was identified, namely a transition of DCs from the blood into the lymph in the liver ***(37)***. It would be interesting to know whether migration is impaired in aged mice. Indirect evidence for this stems from contact hypersensitivity experiments. The induction of contact hypersensitivity correlates with an efflux of LCs from the epidermis and their entry into dermal lymphatics ***(38)***. Sprecher et al. ***(25)*** noted that the capacity of LCs to transport antigen (the contact sensitizer rhodamine) from the skin to the draining lymph nodes was not impaired in old mice. The clinical outcome of this antigen transport, that is contact hypersensitivity, was found to be reduced in one study with aged mice ***(39)***, and more variable but not reduced in another study ***(27)***. No consensus has thus yet been reached regarding DC migration during aging. Skin organ cultures ***(38,40)*** may be a suitable experimental system to directly study this issue in more depth.

1.4. DCs in Aged Humans

1.4.1. Ontogeny and Distribution of DCs

Only limited information is at present available on DCs in aged humans. It is therefore not clear whether the frequency of DCs progenitors decreases during the aging process. No studies have ever addressed the question whether the capacity of the bone marrow to generate DCs changes with age. Early studies have demonstrated a decreased density and functional activity of LCs in the aged skin ***(41,42)***. This may, however, partly be due to UV irradiation, as sig-

nificantly fewer LCs were observed in exposed vs covered skin in old individuals, while no such disparity was noted in the younger subjects.

1.4.2. Characterization of DCs Generated from Blood Monocytes

A detailed analysis of functional and phenotypic characteristics of DCs from aged humans has only recently been performed, when large numbers of DCs were generated from blood monocytes of healthy aged persons ***(43)***. After 1 wk of culture in GM-CSF and IL-4 these cells have a typical dendritic morphology, have an intact capacity of phagocytosis, and express DC surface marker molecules in the same way as corresponding populations from young persons ***(43,44)***. They represent a relatively homogeneous population of intermediate maturity, which matures further in response to stimulation with pathogens.

1.4.3. Maturation of Human DCs

Factors such as pathogens ***(45–47)*** and cytokines ***(48,49)*** have been demonstrated to stimulate the maturation of DCs in vitro and in vivo. The responsiveness of DCs from elderly humans to stimuli has been tested in a recent study, in which it has been demonstrated that inactivated influenza virus induces DC maturation ***(50)***. Whereas unstimulated blood-derived DCs from old and young healthy individuals express MHC class II, CD54, CD80, and CD86 on their surface at medium density and secrete moderate amounts of IL-12 and TNF-α, stimulation with inactivated influenza virus leads to a marked increase in the production of surface molecules and cytokines. These changes are equally pronounced in cells from old and young individuals. The results demonstrate that DC responsiveness to stimulation with certain vaccines is unimpaired in old age. DCs may therefore represent a suitable tool for immunotherapy and may increase the efficacy of vaccines in the elderly.

1.4.4. T-Cell Stimulatory Properties of DCs from Aged Humans

Monocyte-derived DCs from aged persons are equally effective as young control cells in presenting antigen to tetanus-specific T-cell clones ***(43)*** and have even been shown to rescue aged T-cells in an in vitro senescence model from terminal apoptosis ***(44)***. In this model, tetanus toxoid (TT)-specific T-cell lines are derived from young and old individuals and kept in long-term culture. T-cell proliferation in response to stimulation with antigen presented by either irradiated autologous peripheral blood mononuclear cells (PBMCs) or DCs is assessed soon after the initiation of the cultures and after 20 and 30 population doublings. At this late stage T-cell growth is characteristically slow and programmed cell death imminent. Antigen presentation by DCs enhances T-cell proliferation at each time point and reinduces proliferation in T-cell populations that have stopped dividing. Terminal apoptosis is thus prevented. DCs

from old individuals are hereby as effective as cells from young donors. The results of the study demonstrate that DCs from aged individuals may still stimulate the clonal expansion and postpone the clonal elimination of antigen-specific T-cell populations. As a consequence DCs may increase immunoreactivity, prolong immunological memory, and be of particular importance for the maintenance of the T-cell repertoire in old age.

It must, however, be pointed out that the aforementioned studies concentrated only on the stimulation of cloned T-cell lines, which usually do not return to a completely resting stage, but remain partly activated during long-term culture. The described system, therefore, rather represents a model of a secondary than of a primary immune response. No data are presently available on the capacity of DCs of aged humans to activate naive and resting T cells. In view of the increased clinical use of DCs as vaccine carriers, studies on this topic would be of utmost importance.

1.4.5. Migratory function

Interestingly, higher numbers of DCs can be derived from the blood of aged than of young individuals ***(43)***. In view of the low numbers of DCs in the aged skin ***(41,42)***, this result suggests that the migration of DCs/DC precursors from the bloodstream to peripheral organs is affected by the aging process. As the expression of surface molecules is unimpaired in DCs from elderly persons — at least following in vitro culture — it seems possible that the DCs themselves meet the necessary requirement for migration, but that their mobility is reduced owing to age-specific changes of the endothelium or the extracellular matrix.

1.5. Methods Described in this Chapter

Depending on the aim of the study, a choice has to be made of which method to use for the purification or generation of DCs. As only few studies on lymphoid DCs have so far been published ***(3–5)*** and there is virtually no information on lymphoid DCs in the aged, this chapter concentrates on DCs of the myeloid lineage and describes seven short protocols that we consider particularly suitable for the characterization of DCs from aged humans and mice. We would still like to point out that the methodologies described here represent only a very small part of the published literature. We would therefore like to refer the interested reader to some new excellent reviews and textbooks on methodological aspects of DCs ***(18,51–53)***.

2. Materials

2.1. Purification of DCs (LCs) from Murine Skin

1. Utensils: Two pairs of thin but strong forceps with rounded tips (anatomical type); two pairs of thin, curved, and pointed forceps; flat-bottom tea strainer with handle

to fit into a 100 mm Petri dish (e.g. "cell dissociation sieve" CD-1, Sigma, St. Louis, MO, USA); nylon gauze with a mesh size of about 40 mm (NITEX 3–325–44; Tetko, Elmsford, NY, USA; alternatively, nylon gauze with a wide range of mesh sizes may be obtained from suppliers for the graphic arts); tissue culture 100 mm dishes (e.g. Falcon, Oxnard, CA, USA, cat. no. 3003) and bacteriological 100 mm Petri dishes (e.g. Falcon no. 1029).

2. Culture medium: RPMI-1640 supplemented with 5% or 10% fetal calf serum (FCS), 50 m*M* 2-mercaptoethanol, 200 m*M* L-glutamine, and 20 mg/mL of gentamicin.
3. Cytotoxicity medium: For complement-mediated cytotoxicity RPMI-1640 containing 25 m*M* *N*-2-hydroxyethylpiperazine-*N*'-2-ethanesulfonic acid (HEPES) buffer and 0.3% bovine serum albumin (BSA), pH 7.2, is used.
4. Complement: Rabbit Low-Tox-M complement from Cedarlane Laboratories, Hornby, ON, Canada.
5. Salines: Phosphate-buffered saline (PBS) and Hank's balanced salt solution (HBSS), both without calcium and magnesium salts.
6. Trypsin: 2.5% commercial stock, aliquoted and frozen at –20°C.
7. Deoxyribonuclease (DNase I): (Boehringer Mannheim, Mannheim, Germany; cat. no. 104 159). Prepare a stock solution of 5 mg/mL in PBS, sterile filter, and store at 4°C for up to 3 mo.
8. Antibodies used for enrichment of LCs: Mouse IgM anti-Thy-1/CD90 (ATCC no. TIB99); rat IgG2b anti-I-$A^{b,d}$/clone B21–2 (no. TIB229), and mouse IgG2a anti-I-$E^{k,d}$/clone 14-4-4S (no. HB32) can be used as hybridoma culture supernatants. Hybridoma cells can be obtained from the American Type Culture Collection (ATCC), Rockville, MD, USA.

Although LCs can be prepared from body skin, the ears are clearly the best source for obtaining highly enriched LCs (*see* **Note 1**).

2.2. Purification of DCs (LCs) from Human Skin

One best uses split thickness skin (300–400 µm thick) that is obtained from patients undergoing reconstructive plastic surgery of breasts or abdomen, or less preferably from cadaver skin (within 24 h of death). Aged skin samples may sometimes be obtainable as a byproduct of hernia operations. Use materials, utensils, and reagents as for murine LCs.

2.3. Purification of DCs from Human Blood

This protocol works only for the purification of human DCs, as murine blood is available in too small amounts.

1. Culture medium: RPMI-1640 supplemented with 10% heat-inactivated (56°C, 30 min) human serum, 20 µg/mL of gentamicin, and 10 m*M* HEPES.
2. Chelating washing medium: HBSS without Ca^{2+} and Mg^{2+} containing 1% BSA and 1 m*M* EDTA.

3. Neuraminidase-treated sheep erythrocytes for E rosetting: Sheep red blood cells (SRBC; Cocalico, Reamstown, PA, USA) are washed 3× with RPMI-1640 at room temperature and centrifuged with 460*g*. A 5% SRBC solution is prepared. Add neuraminidase (Calbiochem, La Jolla, CA, USA; or Behring, Marburg, Germany) to give a final activity of 0.01 U/mL. Incubate for 1 h at 37°C. Centrifuge and wash two more times at 460*g* with warm PBS without Ca^{2+} and Mg^{2+}. Store on ice and use on the same day.
4. Antibodies for sorting DC: A "cocktail" of MAbs against CD3 (Becton-Dickinson Immunocytometry Systems, Mountain View, CA, USA), CD11b (OKM1, ATCC, Rockville, MD, USA), CD16 (3G8; Immunotech-Coulter, Marseille, France), and CD19 (J4.119; Immunotech) is prepared. Antibody concentrations in the cocktail should be chosen according to manufacturers' instructions. Antibodies with well-defined CD specificities from other reliable manufacturers may also be used. Furthermore, phycoerythrin (PE)-conjugated anti-HLA-DR, fluorescein isothiocyanate (FITC)-conjugated goat anti-mouse IgG + IgM (Jackson Immunoresearch, Westgrove, PA, USA), and mouse IgG (Jackson) are used to identify the HLA-DR-positive DC within the "cocktail negative" population.
5. Monocyte-conditioned medium: Fresh PBMCs are adhered to Petri dishes that have been coated with human γ-globulin. 50×10^6 PBMC are plated in 10-mL culture medium per 100 mm dish. After 30 min at 37°C, nonadherent cells are washed away and adherent cells are cultured in culture medium for 24 h. Supernatants are collected, centrifuged, tested for activity, aliquoted, and stored at –20°C until needed.
6. Coating: Bacteriological Petri dishes (e.g., Falcon no. 1029) are covered with a solution of human Ig (Calbiochem, La Jolla, CA, USA) in PBS at a concentration of 10 µg/mL and incubated at room temperature for 1 h. After four washes with PBS the dishes are ready. Dishes may be coated on the day before use; they should not be stored longer, however.

2.4. Generation of DCs from Human Blood Monocytes

1. Culture medium: RPMI-1640 supplemented with 5–10% FCS, L-glutamine, 2-mercaptoethanol, and gentamicin (all from Seromed-Biochrom, Berlin, Germany). To generate DCs for clinical use FCS must be avoided as well as any other nonhuman proteins.
2. Multiwell tissue culture plates (24-well or 6-well).
3. Cytokines: Recombinant human cytokines are used throughout. GM-CSF (Novartis, Basel, Switzerland) and IL-4 (Genzyme, Cambridge, MA, USA).

2.5. Generation of DC from Human Blood $CD34^+$ Progenitors

1. Culture medium: RPMI-1640 supplemented with 10% FCS.
2. MiniMACS Multisort kit (Miltenyi Biotech, Bergisch-Gladbach) for purification of $CD34^+$ cells.
3. Antibody for purity control: CD34 mAB (HPCA-2, PE conjugated).

4. Cytokines: Recombinant human cytokines are used: GM-CSF (Novartis, Basel, Switzerland), TNF-α (Bender, Vienna, Austria), flt-3 (Neupogen; Amgen, Thousand Oaks, CA, USA), stem cell factor (rhSCF, Amgen, Thousand Oaks, CA, USA), TGF-β (British Biotechnology, Abington, UK).

2.6. Generation of DCs from Murine Bone Marrow (53)

1. Utensils: Autoclaved strong scissors, anatomical forceps, 5- or 10-mL syringe with a 25-gauge needle.
2. Culture medium: RPMI-1640 supplemented with 10% FCS, 50 m*M* 2-mercaptoethanol, and 20 mg/mL gentamicin.
3. Cytokines: Recombinant murine cytokines are used: GM-CSF (e.g. from Immunex, Seattle, WA, USA; specific activity 4×10^7 U/mg); TNF-α (e.g. from Bender, Vienna, Austria; specific activity 2.6×10^7 U/mg)
4. Culture vessels: 24-well plates and 60 or 100 mm tissue culture dishes.
5. Cytotoxicity medium: For complement-mediated cytotoxicity RPMI-1640 containing 25 m*M* HEPES buffer and 0.3% BSA, pH 7.2, is used.
6. Complement: Rabbit Low-Tox-M complement from Cedarlane Laboratories, Hornby, ON, Canada.
7. Antibodies used for enrichment of DC: anti-B220 (RA3-3A1, no. TIB146, ATCC) for B cells, anti-CD4 (GK1.5, no. TIB207) and anti-CD8 (HO-2.2, no. TIB150) for T-cells, RB6-8C5 for granulocytes, and anti-MHC class II (e.g., B21-2, no. TIB229 for BALB/c mice).

2.7. Generation of DCs from Human Bone Marrow

1. Culture medium: RPMI-1640 supplemented with 10%FCS.
2. Cytokines: Recombinant human cytokines are used: GM-CSF (Novartis, Basel, Switzerland), TNF-α (Bender, Vienna, Austria), SCF (rhSCF, Amgen, Thousand Oaks, CA, USA).

3. Methods

3.1. Purification of DCs (LCs) from Murine Skin

1. Rinse mice ears briefly twice in 70% ethanol, place on sterile gauze in a Petri dish and allow to air-dry for approx 20–30 min. Split ears. Place the ear halves separately into two Petri dishes with dermal side down in a way that they float and do not submerge.
2. Incubate the ear halves in 1% (ventral sides) and 0.33% (dorsal sides) of trypsin in HBSS at 37°C for 30 (dorsal) to 60 (ventral) min (*see* **Note 2**).
3. Carefully aspirate the trypsin solution. Peel off the epidermal sheets from the underlying dermis. The extent of trypsinization is optimal when the sheets can be pulled off in one piece. Put the sheets dermal side down in a tissue culture dish containing a tea strainer. Shake the tea strainer for 3 min to release basal layer cells into the medium.
4. After removing the strainer, resuspend the cells using a 5- or 10-mL pipet. Filter the suspension through a nylon mesh and centrifuge it in 50-mL tubes at 300*g* for

10 min. Wash twice in culture medium afterwards. At this point the cells may either be processed further to enrich LCs (**step 5a**) or be put in culture (**step 5b**).

5a. To preenrich LCs, epidermal cells can be treated with anti-Thy-1 and complement to remove most keratinocytes and lymphocytes. In a 50-mL polypropylene tube, resuspend 100–150 × 10^6 epidermal cells (the expected yield from 60 ears) in 3 mL of hybridoma culture supernatant of MAb anti-Thy–1 (ATCC no. TIB99). Then add 10 mL of a sterile-filtered solution consisting of 8.5 mL of cytotoxicity medium, 1 mL of reconstituted complement, and 0.5 mL of DNase stock solution. After incubation for 1 h at 37°C in a shaking water bath, the resulting epidermal cell suspension (viability 10–20%) is washed twice with cold PBS. Treat cells for 10 min at 37°C with 0.125% trypsin and 80 µg/mL of DNase in PBS at a cell concentration of 1–2 × 10^6 viable cells/mL. To stop the digestion, add an equal volume of culture medium and centrifuge the cells for 10 min at 4°C, at 200*g* with brakes off. This simple procedure ("trypsin trick") removes most dead cells and results in viable (>90%) epidermal cell suspensions containing about 15% (range 10–28%) LCs, which can then be further purified by positive selection by sorting (by FACS or MACS, Miltenyi, 1990) for, for example, MHC class II (*see* **Note 3**).

5b. Untreated or anti-Thy–1/C' treated (i.e. LC preenriched) epidermal cell suspensions can be cultured for 2–4 d after which the LCs have matured and can be enriched to 60–90% by simple Ficoll–Hypaque/Lymphoprep density gradient centrifugation according to standard methodology of the nonadherent fraction and harvesting of the low-density fraction (*see* **Note 4**).

3.2. Purification of DCs (LCs) from Human Skin

1. Incubate skin for about 1 h in culture medium containing 25 m*M* HEPES and 10-fold concentrated gentamicin at room temperature (*see* **Note 5**).
2. Rinse the pieces of skin twice in PBS in 100 mm Petri dishes. Cut it into pieces (1 cm^2 if thin, 15 mm^2 if thick) and put them into another 100 mm Petri dish containing 11.25 mL of PBS. When correctly placed epidermal side up, the skin will spread on the PBS. When all pieces are floating on PBS add 1.25 mL of 2.5% trypsin.
3. Incubate with trypsin overnight at 4°C.
4. Next morning aspirate the medium from the dishes and remove epidermal sheets from the dermis with two thin forceps. Put epidermal sheets into a tea strainer placed in another 100 mm Petri dish with 30 mL of culture medium containing 80 µg/mL of DNase I and 25 m*M* HEPES buffer. The sheets should not overlap. When the strainer is filled with sheets, stir *vigorously* to release single cells, remove the strainer from the dish, filter the cell suspension through a Nitex nylon mesh (54 µm mesh size), and centrifuge it in 50-mL tubes at 300*g* for 10 min followed by two washes in culture medium. The primary epidermal cell suspension contains between 1% and 3% LCs (*see* **Note 6**).
5. Culture of LCs: Plate epidermal cells in culture medium in culture vessels of your choice.

6. Harvest of cultured LCs: After 3 d of culture nonadherent cells are rinsed off the tissue culture vessels and collected. This cell suspension has a very low viability (sometimes <20%). Under the hemocytometer one can readily identify very "hairy" LCs. Further enrichment of cultured LCs can be achieved by a variety of different methods such as fluorescent cell sorting, panning, magnetic bead techniques, and density separations (*see* **Note 7**).

3.3. Purification of DCs from Human Blood

1. PBMCs are obtained by standard Ficoll–Hypaque/Lymphoprep centrifugation (*see* **Note 8**).
2. T-cell depletion by E rosetting: PBMCs are resuspended in 10% human serum at a density of 20×10^6/mL. Add an equal volume of 5% neuraminidase-treated SRBC. Centrifuge gently at 25*g* at 4°C for 5 min and incubate on ice for 1 h. Resuspend very carefully so as not to disrupt the rosettes that have formed. Layer resuspended cells on a Ficoll–Hypaque/Lymphoprep gradient (20–30 mL of cell suspension per gradient tube). Harvest nonrosetted cells (Er^-) from the interface.
3. B, NK, and monocyte depletion by panning: Er^- cells are mixed with a cocktail of MAb's against CD11b, CD16, CD19, and CD3. Cells are incubated with the cocktail for 30 min on ice, washed with chelating medium and added to dishes coated with goat anti-mouse IgG. A maximum of 30×10^6 cells may be loaded onto one 100 mm Petri dish. Dishes are incubated on ice for 30 min. Nonadherent cells are collected in a tube and processed further for cell sorting. Instead of panning one can, of course, also use immunomagnetic depletion, for example, by the Dynabead (Dynal, Oslo, Norway) or MACS (Miltenyi Biotec GmbH, Bergisch Gladbach, Germany) technology, although this approach is more expensive.
4. Positive selection of DCs by two-color cell sorting: Nonadherent cells are incubated for 30 min on ice with a FITC-conjugated goat anti-mouse IgG + IgM antibody, to label any cells that carry a mouse monoclonal antibody but have not been depleted by the preceding panning procedure. This is followed by a quenching step of 15 min on ice with 100 µg/mL of mouse Ig (to quench free FITC-goat anti-mouse IgG + IgM binding sites) and finally PE-conjugated anti-HLA-DR (Becton Dickinson, Mountain View, CA, USA). Again, cells are washed with chelating medium and are subjected to the fluorescent cell sorting procedure. DCs are those that are FITC-cocktail negative and PE-HLA-DR positive (*see* **Notes 9** and **10**).

3.4. Generation of DCs from Human Blood Monocytes

1. PBMCs are prepared from buffy coats from the blood bank, or from freshly drawn whole blood, by standard Ficoll–Hypaque/Lymphoprep density centrifugation. PBMC are seeded into 6-well plates at a density of 10×10^6 per well in 3 mL of culture medium *without* cytokines (*see* **Note 11**).
2. Enrichment of monocytes: After 2 h the nonadherent cells (mostly lymphocytes) are aspirated and discarded. Warm medium is added back to the adherent fractions and the plates are rinsed *very gently* (*see* **Note 12**).

3. DC differentiation: Monocytes/monocyte-enriched fractions are cultured at a density of about 3–5 × 10^5/mL in GM-CSF (800 U/mL) + IL-4 (1000 U/mL) for 6–9 d. The cells have then acquired the characteristics of DCs of intermediate maturity. Cell markers of mature DCs are expressed, but at low density. Further differentiation/maturation can be achieved by a 2–3-d exposure to either monocyte-conditioned medium (*see* **Subheading 2.3.**), or, alternatively, a cocktail (TNFα ± IL-1 ± IL-6 + prostaglandin E_2) that mimics monocyte-conditioned medium ***(54,55)*** in the continued presence of GM-CSF ± IL-4. When TGF-β is added together with GM-CSF and IL-4 from the beginning of the cultures, LC development is most pronounced ***(20)***.
4. Feeding of the cultures: The cultures have to be fed every other day, starting on d 2 of culture. To this end 1 mL of culture medium is carefully aspirated from the wells. To compensate for evaporation it is replaced by 1.5 mL of fresh culture medium containing 1600 U/mL of GM-CSF and 1000 U/mL of IL-4.

3.5. Generation of DCs from Human Blood CD34+ Progenitors

1. PBMCs are obtained from buffy coat by standard Ficoll–Hypaque/Lymphoprep density centrifugation, washed twice, and centrifuged through 10% BSA to remove platelets.
2. Purification of $CD34^+$ cells: 5 × 10^8 cells are incubated for 5 min at 4°C in 500 µL of FcR blocking reagent (included in the MiniMACS multisort kit). Five hundred micoliters of CD34 Multisort microbeads are then added and the cells left to incubate at 4°C for 60 min. After this incubation period cells are centrifuged and resuspended in PBS-EDTA. Microbead-labeled cells (10^8 cells) are loaded onto each column of the kit in 500 µL and inserted into the magnetic field. Columns are washed 3× and then removed from the magnetic field. $CD34^+$ cells bound to beads are cosequently eluted with 1.5 mL buffer and then loaded onto a further column. The procedure is repeated. Finally, the microbead-labeled $CD34^+$ cell population is incubated with Multisort Release Reagent for 10 min at 4°C to release the beads from the cells and loaded onto another column in a magnetic field. The eluate which contains the unbound $CD34^+$ cells is centrifuged through 10% BSA in PBS for 10 min at 600*g* and the pellet is resuspended. Purity control by FACS analysis (*see* **Note 13**).
3. Differentiation of DCs from stem cells: $CD34^+$ cells are put into 24-well culture plates (1–10^5 cells/well) in culture medium and stimulated every 2 d with GM-CSF (400 U/mL) and TNF-α (500 U/mL). A greater yield will be achieved when flt-3 (100 ng/mL), SCF (20 ng/mL), and TGF-β (0.5 ng/mL) are additionally present. The latter cytokine works particularly well under serum-free conditions, under which it prevents apoptosis ***(21)***.
4. Harvesting of DCs: DCs are best harvested after 7–14 d of culture.

3.6. Generation of DCs from Murine Bone Marrow CD34+ Progenitors

1. Preparation of bone marrow: Remove muscles from the femurs and tibias. Immerse the bones in a Petri dish with 70% ethanol for 1 min, wash twice in

Ca^{2+}- and Mg^{2+}-free PBS, and put them into a Petri dish with RPMI-1640. Cut off both ends (epiphyses) of each bone with scissors. Make a marrow suspension by flushing out the shafts with a syringe containing about 2 mL of RPMI-1640 per bone. Larger clumps are removed by passage through nylon mesh. Red blood cells are depleted by hypotonic lysis with NH_4Cl. The marrow is then depleted of mature leukocytes by treatment with antibodies for B cells, T cells, granulocytes, and complement. For the exact procedure consult **Subheading 3.1.** (*see* **Note 14**).

2. Culturing the cells: Bring the cells to $5–6 \times 10^5$/mL in culture medium containing GM-CSF (final concentration of 200 U/mL) and plate 1–1.5-mL volumes into the wells of a 24-well plate.
3. Propagation and differentiation of DCs: The wells are washed and fed every 2 d. Early in the course of the culture (d 2–4) one rinses off the many nonadherent granulocytes that are developing. On d 4 the rinsing step with RPMI-1640 is omitted. By d 4 one begins to *see* aggregates of growing DCs attached to the adherent stroma. The aggregates are round, in contrast to macrophage colonies, which are flattened and dispersed. One can also recognize many cell processes ("veils") extending from the periphery of the aggregates, giving them a "hairy" appearance. By d 6, the wells are usually covered with many aggregates ("balls") of proliferating DCs. TNF-α (500 U/mL) when added during the last 2 d of culture significantly increases the percentage and yield of mature DCs (MHC class II^+; $CD86^+$).
4. Harvesting of DCs: Between d 6 and 8, dislodge the growing aggregates from the adherent stroma and transfer them to tissue culture dishes. Cells are pooled, centrifuged, and plated in 10 mL of fresh culture medium containing GM-CSF per 100 mm Petri dish at a maximal cell number of 10×10^6 per dish. During the 24 h following this transfer, free, nonproliferating, mature DCs are released from the aggregates. They can be collected by *gently* swirling the cells from the plate. Harvesting the mature progeny is best performed after 8 or 9 d of culture (*see* **Note 15**).

3.7. Generation of DCs from Human Bone Marrow

Sufficient amounts of bone marrow for the generation of DCs will only rarely be available from healthy aged person. Upon suspension culture in GM-CSF + TNF-α + SCF for 12–14 d an effective yield of about 1.7×10^6 mature DCs per single milliliter of adult human bone marrow can be obtained. The generation of DCs from bone marrow $CD34^+$ cells has yet to be optimized with respect to (1) increasing the low percentage of DCs in the bulk cultures and (2) avoidance of FCS.

4. Notes

4.1. Purification of DCs (LCs) from Murine Skin

1. Cell yields: Depending on the mouse strain ***(56)***, $3–5 \times 10^6$ primary epidermal cells, containing 1.4–3% LCs, can be obtained per mouse. Lower yields have to be expected in aged animals ***(25)***.

2. Reagents: Standard tissue culture reagents including FCS may be obtained from many different manufacturers with no differences in results. An exception to this is *trypsin*, where batch-to-batch variability may be of importance. It might be a good idea to use one batch for a series of experiments.
3. Pre-enriched (10–15%) fresh LCs are as good as highly enriched LCs (>90%) for many experimental purposes. For instance, the antigen-processing capacity can be measured in such populations without interference from the majority population of keratinocytes ***(57)***.
4. According to a recently published method ***(18,40)***, DCs can also be obtained from an organ culture system in which whole ear halves are cultured in one well of a 24-well plate in 2 mL of culture medium for 3 d. DCs migrate into the culture medium from where they can be harvested. This is a good test to assess the migratory capacity of DCs, and the simplest procedure to obtain highly potent mature DCs.

4.2. Purification of DCs (LCs) from Human Skin

5. Cell yields: From 1 cm^2 of "young" epidermis, one may expect up to 3×10^6 viable epidermal cells containing 1–3% LCs. This percentage may be considerably lower when skin from aged individuals is used.
6. It should be noted that, in contrast to the murine system, there is no simple way to *preenrich* human LCs by depletion of a majority of keratinocytes.
7. Organ culture: As in the mouse, DCs can also be readily obtained from the supernatants of skin explants (size 0.5×0.5 to 3×3cm) cultured for 3 d ***(58)***.

4.3. Purification of DCs from Human Blood

8. Cell yield: One obtains 1×10^6 virtually pure DCs after sorting a 500×10^6 starting population.
9. The obtained DC population contains functionally mature ($CD11c^+$, $CD83^+$, $CD86^+$) as well as functionally immature ($CD11c^-$, $CD83^-$, CD86dim) cells. The functionally immature population develops into mature DCs with typical dendritic morphology and potent T-cell stimulatory function provided that monocyte-conditioned medium is present. Otherwise the $CD11c^-$ subset dies if cultured further.
10. An alternative and rather simple method to isolate DCs from fresh blood is based on the fact that both, functionally mature as well as immature DCs, express significant levels of CD4. A blood DC isolation kit is available from Miltenyi Biotec GmbH (Bergisch Gladbach, Germany). DCs are enriched by depletion of T, B, and natural killer (NK) cells and then enriched using CD4 MicroBeads.

4.4. Generation of DCs from Human Blood Monocytes

11. Cell yields: After 1 wk of culture about $2–5 \times 10^6$ DCs can be retrieved from a starting volume of 40 mL of whole blood ***(59)***. When blood from healthy aged persons is used the yield of DCs is usually as high as $8–10 \times 10^6$ per 40 mL of blood. DC yields are generally lower when PBMCs are used following freezing and rethawing.

12. DC precursors are only weakly adherent. Therefore it is important to avoid strong washing after the initial 2 h of adherence lest the adherent fraction is depleted of DC progenitors. If done correctly, control cultures of the nonadherent fraction, which is normally discarded, should not show aggregates.

4.5. Generation of DCs from Human Blood CD34$^+$ Progenitors

13. The percentage of proliferating CD34$^+$ precursors is extremely low (0.06% in the peripheral blood of healthy adults).

4.6. Generation of DCs from Murine Bone Marrow CD34$^+$ Progenitors

14. It is essential to proceed quickly with the procedure. Avoid delays and interruptions. Initially, do not try to handle more than three mice at one time.
15. Cell yields: Generally, we obtain up to $20–30 \times 10^6$ MHC class II-negative cells from one mouse (two femurs and two tibias), of which most are washed away at d 2 of culture. By d 7, the yield of DCs is about 5×10^6 per mouse ***(60)***. Cell yields are dependent on the age of the mice. Five to six weeks is optimal. DC yields decline substantially at an age of more than 10 wk. It is preferable to use male mice. One usually obtains 30–50% more cells from male than from female mice.

References

1. Steinman, R. M. (1991) The dendritic cell system and its role in immunogenicity. *Annu. Rev. Immunol.* **9,** 271–296.
2. Hart, D. N. J. (1997) Dendritic cells: unique leukocyte populations which control the primary immune response. *Blood* **90,** 3245–3287.
3. Süss, G. and Shortman, K. (1996) A subclass of dendritic cells kills CD4 T cells via Fas/Fas-ligand-induced apoptosis. *J. Exp. Med.* **183,** 1789–1796.
4. Steinman, R. M., Pack, M., and Inaba, K. (1997) Dendritic cells in the T-cell areas of lymphoid organs. *Immunol. Rev.* **156,** 25–37.
5. Kronin, V., Vremec, D., Winkel, K., Classon, B. J., Miller, R. G., Mak, T. W., Shortman, K., and Süss, G. (1997) Are CD8$^+$ dendritic cells (DC) veto cells? The role of CD8 on DC in DC development and in the regulation of CD4 and CD8 T cell responses. *Int. Immunol.* **9,** 1061–1064.
6. Banchereau, J. and Steinman, R. M. (1998) Dendritic cells and the control of immunity. *Nature* **392,** 245–252.
7. Schuler, G., Thurner, B., and Romani, N. (1997) Dendritic cells: from ignored cells to major players in T-cell mediated immunity. *Int. Arch. Allergy Immunol.* **112,** 317–322.
8. Stingl, G. and Bergstresser, P. R. (1995) Dendritic cells: a major story unfolds. *Immunol. Today* **16,** 330–333.
9. Caux, C., Liu, Y. J., and Banchereau, J. (1995) Recent advances in the study of dendritic cells and follicular dendritic cells. *Immunol. Today* **16,** 2–4.

10. Romani, N., Lenz, A., Glassel, H., Stossel, H., Stanzl, U., Majdic, O., Fritsch, P., and Schuler, G. (1989) Cultured human Langerhans cells resemble lymphoid dendritic cells in phenotype and function. *J. Invest. Dermatol.* **93,** 600–609.
11. O'Doherty, U., Steinman, R. M., Peng, M., Cameron, P. U., Gezelter, S., Kopeloff, I., Swiggard, W. J., Pope, M., and Bhardwaj, N. (1993) Dendritic cells freshly isolated from human blood express CD4 and mature into typical immunostimulatory dendritic cells after culture in monocyte-conditioned medium. *J. Exp. Med.* **178,** 1067–1078.
12. Pavli, P., Hume, D. A., Van de Pol E., and Doe, W. F. (1993) Dendritic cells, the major antigen-presenting cells of the human colonic lamina propria. *Immunology* **78,** 132–141.
13. Caux, C., Dezutter-Dambuyant, C., Schmitt, D., and Banchereau, J. (1992) GM-CSF and TNF-α cooperate in the generation of dendritic Langerhans cells. *Nature* **360,** 258–261.
14. Romani, N., Reider, D., Heuer, M., Ebner, S., Kämpgen, E., Eibl, B., Niederwieser, D., and Schuler, G. (1996) Generation of mature dendritic cells from human blood: an improved method with special regard to clinical applicability. *J. Immunol. Methods* **196,** 137–151.
15. Bender, A., Sapp, M., Schuler, G., Steinman, R. M., and Bhardwaj, N. (1996) Improved methods for the generation of dendritic cells from nonproliferating progenitor in human blood. *J. Immunol. Methods* **196,** 121–135.
16. Cella, M., Sallusto, F., and Lanzavecchia, A. (1997) Origin, maturation and antigen presenting function of dendritic cells. *Curr. Opin. Immunol.* **9,** 10–16.
17. Robinson, S. P., Saraya, K., and Reid, C. D. (1998) Developmental aspects of dendritic cells *in vitro* and *in vivo*. *Leuk. Lymphoma* **29,** 477–490.
18. Romani, N., Bhardwaj, N., Pope, M., Koch, F., Swiggard, W. J., O'Doherty, U., Witmer-Pack, M. D., Hoffman, L., Schuler, G., Inaba, K., and Steinman, R. M. (1997) Dendritic cells, in *Weir's Handbook of Experimental Immunology* (Herzenberg, L. A., ed.), Blackwell Science Oxford, Sect. 156.1–156.14.
19. Reddy, A., Sapp, M., Feldman, M., Subklewe, M., and Bhardwaj, N. (1997) A monocyte conditioned medium is more effective than defined cytokines in mediating the terminal maturation of human dendritic cells. *Blood* **90,** 3640–3646.
20. Geissmann, F., Prost, C., Monnet, J. P., Dy, M., Brousse, N., and Hermine, O. (1998) Transforming growth factor β1, in the presence of granulocyte/macrophage colony-stimulating factor and interleukin 4, induces differentiation of human peripheral blood monocytes into dendritic Langerhans cells. *J. Exp. Med.* **187,** 961–966.
21. Riedl, E., Strobl, H., Majdic, O., and Knapp, W. (1997) TGF-β1 promotes *in vitro* generation of dendritc cells by protecting progenitor cells from apoptosis. *J. Immunol.* **158,** 1591–1597.
22. Lynch, D. H., Andreasen, A., Maraskovsky, E., Whitmore, J., Miller, R. E., and Schuh, J. C. L. (1997) Flt ligand induces tumor regression and antitumor immune responses *in vivo*. *Nat. Med.* **6,** 625–631.
23. Zhang, Y., Mukaida, N., Wang, J., Harada, A., Akiyama, M., and Matsushima, K. (1997) Induction of dendritic cell differentiation by granulocyte-macrophage colony-

stimulating factor, stem cell factor, and tumor necrosis factor alpha *in vitro* from lineage phenotypes-negative c-kit$^+$ murine hematopoietic progenitor cells. *Blood* **90,** 4842–4853.
24. Haruna, H., Inaba, M., Inaba, K., Taketani, S., Sugiura, K., Fukuba, Y., Doi, H., Toki, J., Tokunaga, R., and Ikehara, S. (1995) Abnormalities of B cells and dendritic cells in SAMP1 mice. *Eur. J. Immunol.* **25,** 1319–1325.
25. Sprecher, E., Becker, Y., Kraal, G., Hall, E., Harrison, D., and Shutz, L. D. (1990) Effect of aging on epidermal DC populations in C57BL/6J mice. *J. Invest. Dermatol.* **94,** 247–253.
26. Belsito, D. V., Epstein, S. P., Schultz, J. M., Baer, R. L., and Thorbecke, G. J. (1989) Enhancement by various cytokines or 2-β-mercaptoethanol of Ia antigen expression on Langerhans cells in skin from normal aged and young mice: effect of cyclosporine A. *J. Immunol.* **143,** 1530–1536.
27. Choi, K. L. and Sauder, D. N. (1987) Epidermal Langerhans cell density and contact sensitivity in young and aged BALB/c mice. *Mech. Ageing Dev.* **39,** 69–79.
28. Rittman, B. R., Hill, M. W., Rittman, G. A., and MacKenzie, I. C. (1987) Age-associated changes in Langerhans cells of murine oral epithelium and epidermis. *Arch. Oral. Biol.* **32,** 885–889.
29. Schwartz, J. L., Weichselbaum, R., and Frim, S. R. (1983) The effect of aging on the density and distribution of oral mucosal Langerhans cells. *Exp. Gerontol.* **18,** 65–71.
30. Okiji, T., Kosaka, T., Kamal, A. M. M., Kawashima, N., and Suda, H. (1996) Age-related changes in the immunoreactivity of the monocyte/macrophage system in rat molar pulp. *Arch. Oral Biol.* **41,** 453–460.
31. Raffaniello, R. D. and Roy, M. (1990) Immunohistological analysis of the immune cells in the normal oral mucosa of aging mice. *Gerontology* **9,** 51–57.
32. Koch, F., Trockenbacher, B., Kämpgen, E., Grauer, O., Stössel, H., Livingstone, A. M., Schuler, G., and Romani, N. (1995) Antigen processing in populations of mature murine dendritic cells is caused by subsets of incompletely matured cells. *J. Immunol.* **155,** 93–100.
33. Komatsubara, S., Cinader, B., and Muramatsu, S. (1996) Functional competence of dendritic cells of ageing C57BL/6 mice. *Scand. J. Immunol.* **24,** 517–525.
34. Inaba, K. and Steinman, R. M. (1986) Accessory cell-T lymphocyte interactions. Antigen-dependent and -independent clustering. *J. Exp. Med.* **163,** 247–261.
35. Ingulli, E., Mondino, A., Khoruts, A., and Jenkins, M. K. (1997) *In vivo* detection of dendritic cell antigen presentation to CD4$^+$ T cells. *J. Exp. Med.* **185,** 2133–2141.
36. Koch, F., Stanzl, U., Jennewein, P., Janke, K., Heufler, C., Kämpgen, E., Romani, N., and Schuler, G. (1996) High level IL-12 production by murine dendritic cells: upregulation via MHC class II and CD40 molecules and downregulation by IL-4 and IL-10. *J. Exp. Med.* **184,** 741–746.
37. Kudo, S., Matsuno, K., Ezaki, T., and Ogawa, M. (1997) A novel migration pathway for rat dendritic cells from the blood: hepatic sinusoids-lymph translocation. *J. Exp. Med.* **185,** 777–784.

38. Weinlich, G., Heine, M., Stössel, H., Zanella, M., Stoitzner, P., Ortner, U., Smolle, J., Koch, F., Sepp, N. T., Schuler, G., and Romani, N. (1998) Entry into afferent lymphatics and maturation in situ of migrating cutaneous dendritic cells. *J. Invest. Dermatol.* **110,** 441–448.
39. Villadsen, J. H., Langkjer, S. T., Ebbesen, P., and Bjerring, P. (1987) Syngrafting skin among mice of similar and different ages increases the number of Langerhans cells and decreases responsiveness to 1,4-dinitrofluorobenzene. *Compr. Gerontol.* **1,** 78–79.
40. Ortner, U., Inaba, K., Koch, F., Heine, M., Miwa, M., Schuler, G., and Romani, N. (1996) An improved isolation method for murine migratory cutaneous dendritic cells. *J. Immunol. Methods* **193,** 71–79.
41. Thiers, B. H., Maize, J. C., Spicer, S. S., and Cantor, A. B. (1984) The effect of aging and chronic sun exposure on human Langerhans cell populations. *J. Invest. Dermatol.* **82(3),** 223–226.
42. Gilchrest, B. A., Murphy, G. F., and Soter, N. A. (1982) Effect of chronological aging on Langerhans cells in the human epidermis. *J. Invest. Deramtol.* **79,** 85–88.
43. Steger, M. M., Maczek, C., and Grubeck-Loebenstein, B. (1996) Morphologically and functionally intact dendritic cells can be derived from the peripheral blood of aged individuals. *Clin. Exp. Immunol.* **105,** 544–550.
44. Steger, M. M., Maczek, C., and Grubeck-Loebenstein, B. (1997) Peripheral blood dendritic cells reinduce proliferation in *in vitro* aged T cell populations. *Mech. Ageing Dev.* **93,** 125–130.
45. Henderson, R. A., Watkins, S. C., and Flynn, J. L. (1997) Activation of human dendritic cells following infection with *Mycobacterium tuberculosis*. *J. Immunol.* **159,** 635–643.
46. Schnorr, J. J., Xanthakos, S., Keikavoussi, P., Kämpgen, E., ter Meulen, V., and Schneider-Schaulies, S. (1997) Induction of maturation of human blood dendritic cell precursors by measles virus is associated with immunosuppression. *Proc. Natl. Acad. Sci. USA* **94,** 5326–5331.
47. Thurnher, M., Ramoner, R., Gastl, G., Radmayr, C., Böck, G., Herold, M., Klocker, H., and Bartsch, G. (1997) *Bacillus Calmette-Guerin* mycobacteria stimulate human blood dendritic cells. *Int. J. Cancer* **70,** 128–134.
48. Romani, N., Heufler C., Koch, F., Kämpgen, E., and Schuler, G. (1999) Dendritic cells as donors and recipients of cytokine signals, in *Dendritic Cells: Biology and Clinical Applications* (Lotze, M. T. and Thomson, A. W., eds.), Academic Press, London, Sect. 37, 653–672.
49. Lardon, F., Snoeck, H. W., Berneman, Z. N., Van Tendeloo, V. F., Nijs, G., Lenjou, M., Henckaerts, E., Boeckxtaens, C. J., Vandenabeele, P., Kestens, L. L., Van Bockstaele, D. R., and Vanham, G. L. (1997) Generation of dendritic cells from bone marrow progenitors using GM-CSG, TNF-alpha, and additional cytokines: antagonistic effects of IL-4 and IFN-gamma and selective involvement of TNF-alpha receptor-1. *Immunology* **91,** 553–559.
50. Saurwein-Teissl, M., Schönitzer, D., and Grubeck-Loebenstein, B. (1998) Dendritic cell responsiveness to stimulation with influenza vaccine is unimpaired in old age. *Exp. Gerontol.* **33,** 625–631.

51. Schuler, G., Lutz, M. B., Bender, A., Röder, C., and Romani, N. (1999) A guide to the isolation and propagation of dendritic cells, in *Dendritic Cells: Biology and Clinical Applications* (Lotze M. T. and Thomson, A. W., eds.), Adcademic Press, London, Sect. 27, 515–533.
52. Koch, F., Kämpgen, E., Schuler, G., and Romani, N (1999) Isolation, enrichment and culture of murine epidermal Langerhans cells, in *Dendritic Cell Protocols — Methods in Molecular Medicine* (Robinson, S. and Stagg, A. J., eds.), Humana Press, Totowa, NJ, in press.
53. Inaba, K., Swiggard, W. J., Steinman, R. M., Romani, N., and Schuler, G. (1998) Isolation of dendritic cells, in *Current Protocols in Immunology* (Coligan, J. E., Kruisbeek, A. M., Margulies, D. H., Shevach, E. M., and Strober, W., eds.), John Wiley & Sons, New York, Sect. 3.7.1–3.7.15.
54. Rieser, C., Böck, G., Klocker, H., Bartsch, G., and Thurnher, M. (1997) Prostaglandin E2 and tumor necrosis factor α cooperate to activate human dendritic cells: synergistic activation of interleukin 12 production. *J. Exp. Med.* **196,** 1603–1608.
55. Jonuleit, H., Kühn, U., Müller, G., Steinbrink, K., Paragnik, L., Schmitt, E., Knop, J., and Enk, A. H. (1997) Pro-inflammatory cytokines and prostaglandins induce maturation of potent immunostimulatory dendritic cells under fetal calf serum-free conditions. *Eur. J. Immunol.* **27,** 3135–3142.
56. Schuler, G. and Steinman, R. M. (1985) Murine epidermal Langerhans cells mature into potent immunostimulatory dendritic cells *in vitro*. *J. Exp. Med.* **161,** 526–546.
57. Kämpgen, E., Koch, N., Koch, F., Stoger, P., Heufler, C., Schuler, G., and Romani, N. (1991) Class II major histocompatibility complex molecules of murine dendritic cells: synthesis, sialylation of invariant chain, and antigen processing capacity are down-regulated upon culture. *Proc. Natl. Acad. Sci. USA* **88,** 3014–3018.
58. Pope, M., Betjes, M. G. H., Hirmand, H., Hoffman, L, and Steinman, R. M. (1995) Both dendritic cells and memory T lymphocytes emigrate from organ cultures of human skin and form distinctive dendritic- T-cell conjugates. *J. Invest. Dermatol.* **104,** 11–17.
59. Romani, N., Gruner, S., and Brang, D. (1994) Proliferating dendritic cells progenitors in human blood. *J. Exp. Med.* **180,** 83–93.
60. Inaba, K., Inaba, M., Deguchi, M., Hagi, K., Yasumizu, R., Ikehara, S., Muramatsu, S., and Steinman, R. M. (1993) Granulocytes, macrophages, and dendritic cells arise from a common major histocompatibility complex class II-negative progenitor in mouse bone marrow. *Proc. Natl. Acad. Sci. USA* **90,** 3038–3042.

23

Age-Related Alterations to Natural Killer Cell Function

Erminia Mariani, Corona Alonso, and Rafael Solana

1. Introduction

Human natural killer (NK) cells represent a heterogeneous lymphoid population involved in the recognition and lysis of tumor and virally infected cells. NK cells are defined by the expression of the IgG Fc receptor CD16 (FcγRIIIA) and/or CD56. NK cells do not rearrange immunoglobulin (Ig) or T-cell receptor (TCR) genes. Therefore, neither Ig nor the TCR–CD3 complex is expressed at the cell surface, except for the zeta (ζ) chain. Both markers, CD16 and CD56, have been used to analyze age-associated changes in the number of NK cells.

The most characteristic function of NK cells is non-major histocompatibility complex (MHC) restricted cytotoxicity of tumor cell lines and killing of target cell lines, in particular the erythroleukemia cell line K562. The effect of aging on NK cytotoxicity has been extensively studied. NK cytotoxicity is based on the interaction between the NK effector cells and target cells, usually cell lines that do not express HLA class I antigens on the surface. Several steps can be differentiated in the cytotoxic assays. The first is conjugate formation, in which NK cells binds the target cell. In a second phase of NK cell triggering, activation signals are transmitted from the cell surface inside the cells. As a result perforin granules are reoriented to the effector–target contact site, and they are finally released and the target cell lysed.

The K562 cell line is the target cell most commonly used for measuring lysis by resting NK cells from elderly people, whereas the NK-resistant Daudi cell line is used for testing the cytotoxic capacity of activated NK cells. Both Daudi or P815, a mastocytoma murine cell line that is also resistant to lysis by

From: *Methods in Molecular Medicine*, Vol. 38: *Aging Methods and Protocols*
Edited by: Y. A. Barnett and C. R. Barnett

resting NK cells, are frequently used for testing the antibody-dependent cell cytotoxicity (ADCC, Fc receptor-mediated lysis by NK cells).

The results on the different phenotypic and functional analysis of NK cells have demonstrated age-associated changes both in the number and function of NK cells. Thus, although there is a general consensus that NK cytotoxicity of peripheral blood lymphocytes is well preserved not only in healthy elderly people but also in centenarians, a significant expansion in the number of NK cells is also found in healthy aging *(1)*. This indicates that NK cell killing is impaired when it is considered on a per cell basis, as it is shown when single-cell cytotoxic assays are performed *(2,3)*. The ability of interleukin-2 (IL-2)-activated NK cells to lyse the normally NK-resistant Daudi cell line is also significantly decreased in the elderly, when compared to young people *(4)*. However, ADCC- and LAK-mediated killing remain comparable between young and elderly subjects. The decreased NK cytotoxic capacity found in the elderly is associated with defective signal transduction *(5)*. On the other hand, perforins are distributed in the cytoplasm of almost all the NK cells from the elderly, as in NK cells from the young, the ability to utilize perforin in the generation of cytolytic activity against tumor target cells is maintained in NK cells from the elderly *(6)*.

Recently Ogata et al. *(7)* showed that low NK cell function relates to the development of severe infections in elderly subjects and that well preserved NK cell cytotoxicity is relevant for survival. These findings strengthen the interest in studying NK cytotoxicity in aging.

In the following sections we introduce the techniques and experimental protocols usually employed for the analysis of NK cell phenotype and function in the elderly. The standard immunofluorescence and cytotoxicity assay as well as the techniques for determining NK signal transduction are presented.

2. Materials

2.1. Analysis of NK Cell Phenotype and Perforin Content by Immunofluorescence

1. Lymphocyte separation medium (LSM), density 1.077 g/mL (e.g., Histopaque-1077, Sigma, St. Louis, MO, USA).
2. Culture medium: RPMI 1640 with *N*-2-hydroxyethylpiperazine-*N*'-2-ethanesulfonic acid (HEPES) buffer supplemented with 10% fetal calf serum (FCS), antibiotics (penicillin: 100 U/mL plus streptomycin 100 µg/mL or alternatively gentamicin 200 µg/mL) and 2–4 m*M* L-glutamine (all reagents from Gibco Life, Paisley, UK).
3. Phosphate-buffered saline (PBS) (Gibco Life).
4. Trypan blue solution: 0.2% w/v in PBS/3 m*M* sodium azide (Sigma).

5. Petri dishes (Corning Costar Europe, Bad Loevedorp, The Netherlands).
6. Nylon wool (Robbins, Sunnyvale, CA, USA).
7. Monoclonal antibodies (MAbs): anti-CD16 (3G8, Immunotech, Marseille Cedex, France; Leu11, Becton Dickinson, San Josè, CA, USA), anti-CD56 (NKH-1, Coulter Corporation, Miami, FL, USA; Leu19 Becton Dickinson, San Josè, CA, USA), anti-CD94 (HP3B1, Coulter Corporation, Miami, FL, USA). These MAbs are available as PE or FITC labeled. Double fluorescence with anti-CD3 (Anti-Leu 4, Becton Dickinson, San Josè, CA, USA) is recommended.
8. For intracellular labeling of perforins the following additional material is required:
   a. 2% Paraformaldehyde (Fluka Chemie AG, Buchs, Switzerland) solution in PBS.
   b. 0.2% Tween-20 (Sigma, St. Louis, MO, USA) solution in PBS.
   c. PBS with 2% FCS and 0.1% sodium azide (Sigma, St. Louis, MO, USA) (PBS–FCS–Az).
   d. MAb anti-human perforin and Ig isotype control (Pharmingen, San Diego, CA, USA).
   e. Fluorescein isothiocyanate (FITC)- or phycoerythrin (PE)-conjugated goat anti-mouse Ig (GAM-FITC or GAM-PE) (Pharmingen, San Diego, CA, USA).
   f. Normal mouse serum (Dako, Glostrup, Denmark).
9. Flow cytometer (FacsCount, Becton Dickinson, San Josè, CA, USA).

2.2. NK Cell Enrichment and Purification

1. LSM, density 1.077 g/mL (Histopaque–1077, Sigma, St. Louis, MO, USA).
2. Culture medium prepared as indicated in **Subheading 2.1**.
3. PBS (Gibco Life, Paisley, UK).
4. Laminar flow hoods.
5. Petri dishes (Corning Costar Europe, Bad Loevedorp, The Netherlands).
6. Nylon wool (Robbins, Sunnyvale, CA, USA).
7. MAbs: anti-CD3 (Anti-Leu 4, Becton-Dickinson, San Josè, CA, USA) anti-CD19 (J4.119, Immunotech, Marseille Cedex, France; Leu12 Becton Dickinson, San Josè, CA, USA), and anti-CD16 (3G8, Immunotech, Marseille Cedex, France; Leu11, Becton Dickinson, San Josè, CA, USA).
8. GAM coupled magnetic beads (Dynal AS, Skoyen, Norway).
9. Magnetic particle concentrator (MPC1, Dynal AS, Skoyen, Norway).
10. MACS cell separation reagents and equipment (Miltenyi Biotec GmbH, Bergisch Gladbach, Germany) can also be used to purify NK cells.
    a. Separation reagents: the NK isolation kit consists of: reagent A, a cocktail of hapten-conjugated monoclonal CD3, CD4, CD19, CD33 antibodies; reagent B, colloidal superparamagnetic MACS microbeads conjugated to an anti-hapten antibody and depletion columns.
    b. Equipment: VarioMACS magnetic cell separator.

2.3. Cytotoxic Assays: NK Cytotoxicity, Lymphokine-Activated Killing, ADCC, and Redirected Lysis

1. ^{51}Sodium chromate (^{51}Cr) solution in normal saline with a specific activity of 400–1200 Ci/g (14.8–44.4 TBq) (NEN, Bad Homburg, Germany)
2. Triton X-100 (Sigma, St. Louis, MO, USA).
3. 96-Well round- or V-bottom microtiter plates (Corning Costar Europe, Bad Loevedorp, The Netherlands).
4. γ-Counter (Ultrogamma LKB, Upsala, Sweden, or Gamma counter, Beckman, Palo Alto, CA, USA).
5. Cultured target cells: The most commonly used target cells for measuring NK lysis are K562 cells, an HLA negative erythroleukemia derived cell line. The HLA class I negative EBV transformed cells C1R or 721.221 are also extensively used at present as NK target cells. Other cell lines such as Daudi (derived of a Burkitt lymphoma) or P815 (a murine mastocytoma), that are resistant to NK killing, are used to determine LAK activity, ADCC, or redirected lysis.

2.4. Signal Transduction in Aging

1. Inositol-free RPMI 1640 (Gibco Life, Paisley, UK) supplemented with 10% FCS.
2. myo-[^{3}H]Inositol (Amersham International, Buckinghamshire, UK) (specific activity 3.15 Tbq/mmol).
3. Susceptible target cells: K562.
4. Nonsusceptible target cells: Daudi as negative control.
5. MAb anti-CD16 and irrelevant MAb (Becton Dickinson, San Josè, CA, USA) that will be used as negative control.
6. Extraction solution: methanol/chloroform/HCl 37% (80:160:1 v/v) (Fluka Chemie AG, Buchs, Switzerland).
7. Washing solution: 0.7 mL of methanol/chloroform/1 *N* HCl (235:15:245 v/v) (Fluka Chemie AG, Buchs, Switzerland).
8. 1 *M* KOH (Fluka Chemie AG, Buchs, Switzerland).
9. Bidistilled water.
10. Amprep ion-exchange minicolumns (Amersham International, Buckinghamshire, UK).
11. Elution buffers: 0.1 *M* $KHCO_3$, 0.17 *M* $KHCO_3$, 0.25 *M* $KHCO_3$ (Fluka Chemie AG, Buchs, Switzerland).
12. Solubilizing solution: chloroform/methanol (2:1) (Fluka Chemie AG, Buchs, Switzerland).
13. 1% K oxalate (Sigma, St. Louis, MO, USA).
14. Thin-layer chromatography (TLC) plates.
15. Developing solution: chloroform/methanol/water/saturated ammonia (45:35:8:2 v/v) (Fluka Chemie AG, Buchs, Switzerland).
16. Extraction solution: 0.6 *N* HCl/methanol (60:40 v/v) (Fluka Chemie AG, Buchs, Switzerland).
17. Enhancer (NEN, Bad Homburg, Germany).

18. Iodine (Sigma, St. Louis, MO, USA).
19. Pico-Fluor 40 scintillation cocktail (Packard, Meriden, CT, USA).
20. Beta-counter (Beckman, Palo Alto, CA, USA).

3. Methods

3.1. Flow Cytometric Analysis of NK Cells

1. Isolate peripheral blood mononuclear cells (PBMCs) by centrifugation (900*g*/20 min) of peripheral blood, diluted 1:1 with PBS, over the lymphocyte separation medium. Remove PBMCs from the interface, dilute with PBS, and centrifuge at 400*g*/10 min. Decant and repeat wash steps two additional times.
2. Perform white cell count. Dilute the cell suspension to a final concentration of 5×10^6 PBMCs/mL in culture medium.
3. For direct immunofluorescence 2×10^5 PBMC are incubated with each labeled MAb in the dark in V-bottom plates for 30 min at 4°C, washed twice with PBS plus 2% FCS and 0.1% sodium azide and resuspended in 1% paraformaldehyde for the analysis. Mixtures of two PE or FITC differently labeled MAbs (i.e., FITC anti-CD3 in combination to PE anti-CD56) can be incubated simultaneously with the same cells for double fluorescence. Isotype fluorescence labeled Ig control MAbs should be used as negative controls.
4. For indirect immunofluorescence (IIF) incubate 2×10^5 PBMCs as for the direct method but using unlabeled antibodies. After washing with PBS, incubate cells again with FITC- or PE-labeled goat anti-mouse Ig for 30 min at 4°C. After washing fix the cells in 1% paraformaldehyde for the analysis. For negative control, incubate cells only with the secondary labeled antibody or with a primary antibody of the same isotype but with irrelevant specificity followed by the secondary antibody (**Note 1**). When a double immunofluorescence technique is used, perform an incubation with an optimal dilution (1:10 usually) of normal mouse serum after the secondary antibody incubation, to reduce nonspecific binding before the last incubation with a directly labeled MAb. The combination of IIF with labeled anti-CD56 MAbs is useful to study the presence of other differentiation or activation antigens on NK cells (**Note 2**).
5. Techniques of IIF on permeabilized NK cells can be used to evaluate the perforin content of NK cells. Resuspend 10^6 PBMCs in 1 mL of cold 2% paraformaldehyde solution in PBS, incubate for 1 h at 4°C, and centrifuge for 10 min at 250*g* at 4°C. Resuspend the fixed cells in 1 mL of 0.2% Tween-20 in PBS at room temperature and incubate for 15 min at 37°C. Add 3 mL of PBS–FCS–Azide and centrifuge the suspension for 10 min at 250*g* at room temperature. Incubate the cell pellet with an optimal dilution of an anti-human perforin MAb for 30 min at 4°C; develop positive cells using a 1:20 diluted GAM Ig conjugated with FITC for 30 min at 4°C. The cell pellet is then washed with PBS–FCS–Azide and analyzed.
6. Flow cytometry: The simultaneous measurement of "forward scatter" that measures cell size and "side scatter" that indicates heterogeneity of the cell structure ("granularity or complexity") allows the identification and gating of the different

subpopulations of white blood cells (**Note 3**). Optimal gating for the identification of lymphocyte populations requires polygonal computer-generated windows (**Note 4**). FITC green fluorescence or PE red fluorescence can be simultaneously analyzed. For each sample, 10^4 gated cells are usually analyzed.

3.2. Cytotoxic Assays for NK Cells: Preparation of Effector Cells

Different sources of effector cells can be used as effectors of NK cell cytotoxicity. In age-related studies plastic- and nylon-wool-depleted PBMCs are commonly used to analyze NK killing of K562 target cells whereas IL-2-activated cells are used to study LAK killing of the NK-resistant Daudi cell line.

1. PBMC enriched by depletion of plastic and NW adherent cells. Incubate PBMCs at 5×10^6 PBMCs/mL in a Petri dish for 60–90 min at 37°C in 5% CO_2, for monocyte depletion. Recover nonadherent cells, wash twice with PBS, and dilute in 2 mL of medium. The cells are then incubated in prewashed nylon wool for 45–60 min at 37°C in 5% CO_2, for B cell depletion. Recover the nonadherent (T/NK cells) by washing the column with 20 mL of culture medium and resuspend. This cell population contains 20–30% of $CD56^+$ NK cells.
2. Activation of NK cells with IL-2. Culture the cells obtained as indicated in **step 1** in 5% CO_2 at 37°C for 7–10 d in the presence of 500 U/mL of IL-2, without further activation requirements. This population is considered LAK cells and is constituted by a mixture of activated NK and T-cells able to lyse NK-resistant cell lines.
3. Purification of NK cells by immunomagnetic separation. Incubate the nonadherent cells (T/NK cells) obtained as indicated in **step 1** with anti-CD3 MAb for 30 min at 4°C and add $0.7–0.9 \times 10^8$ of GAM-coupled magnetic beads. Incubate for 30 min at 4°C under gentle shaking for T-cell depletion. Remove the cells rosetting with the beads by using a magnetic particle concentrator (MPC1) and collect the supernatant with the CD3-negative cells. Alternatively, whole PBMCs (5×10^6/mL) can be directly incubated with CD3, CD4, CD19, and CD14 MAb for 30 min at 4°C, and then with GAM-beads for 45 min at 4°C. Cells and beads should be gently mixed throughout. After the incubation with beads, use a magnet to separate beads with attached CD3/CD4 T-cells, CD14 monocytes, and CD19 B cells from NK cells. Centrifuge and wash with complete medium the recovered free cells. This cell population should be 75–95% $CD56^+$ and $CD16^+$, <10% $CD3^+$ and <5% $CD14^+$, and $CD19^+$ as routinely established by flow cytometry.
4. Isolation with the MACS system. Resuspend 10^7 PBMCs in 80 µL of buffer (PBS with 2 m*M* EDTA and 0.5% bovine serum albumin [BSA]), add 20 µL of reagent A, and incubate for 15 min at 6°–12°C. Wash the cell suspension carefully, resuspend again with 80 µL of buffer, add 20 µL of reagent B, and incubate as before. Wash cell suspension and resuspend the pellet with 500 µL of buffer. Apply cell suspension to a prefilled depletion column placed in the magnetic field of the VarioMACS and collect effluent cells representing the purified NK cell fraction.

3.3. Cytotoxic Assays for NK Cells: Preparation of Target Cells

Several cell lines are used as target cells for measuring NK lysis. The most commonly used are K562 cells, as well as C1R or 721.221. Daudi cell line, an NK-resistant cell line, is used to study cytotoxicity by IL-2-activated NK cells. Furthermore, P815, an NK-resistant mastocytoma murine cell line which express high concentrations of Fc receptors, can be used to analyze redirected lysis, for example, lysis of the target in the presence of antibodies against NK triggering structures. Both Daudi and P815 cell lines can be used to analyze ADCC by using NK cells and IgG antibodies specific for the target cells. Grow these cell lines in RPMI 1640 + 10% FCS, 2 m*M* glutamine, 100 U/mL of penicillin, and 10 μg/mL of streptomycin and use them during the logarithmic growth phase (**Note 5**).

1. Radioactive labeling of target cells with ^{51}sodium chromate: Use ^{51}Cr solution in normal saline to label target cells and no later than 15 d after the reference day. For target cell labeling, wash 1–2 × 10^6 once with fresh medium, remove the supernatant, and incubate pellet with 100 μCi ^{51}Cr in differing volumes, according to the decay table (**Note 6**). Incubate the cells at 37°C in 5% CO_2 for 1 h with occasional shaking at 10–15-min intervals. During following procedures, keep the target cells on ice to reduce spontaneous isotope release. Wash the target tumor cells 3× at 4°C in cold RPMI 1640 + 10% FCS and resuspend in medium at a concentration of 5 × 10^4 cells/mL (**Note 7**).
2. NK cell cytotoxicity assays: The effector/target cell ratio will depend on the nature of the effector population and its level of cytotoxic activity. A starting effector/target ratio of 100:1 or 50:1 will be required for assaying freshly isolated NK cells, whereas for purified NK cells or activated LAK this may be at most 20:1 or 10:1. In addition to NK and LAK assays ADCC can be determined when an NK-resistant cell line is used and anti-target antibodies are added to the assay. Redirected lysis is measured when P815 are used as targets and MAbs against NK triggering structures (i.e., CD16, CD69) are added to the assay. Perform the cytotoxicity assays in V-bottom 96-well microtiter plates with a final volume of 200 μL. Seed each effector/target cell ratio (E/T) in triplicate. For spontaneous release control, samples of target cells are resuspended in medium alone. Maximum or total release of ^{51}Cr from the target cells is obtained by mixing 5 × 10^3 labeled target cells with 100 μL of 2% Triton X-100. Use at least six replicate wells to evaluate spontaneous and maximum release. Seed serial dilutions of mononuclear effector in 100 μL of culture medium and 100 μL of ^{51}Cr-labeled tumor target cells with an E/T ranging from 100:1 to 12:1 (**Note 8**). Centrifuge the plates at 4°C for 3 min and incubate at 37°C in 5% CO_2 for 4 h. Harvest and transfer to a tube 100 μL of culture supernatant at the end of the incubation time. Determine ^{51}Cr release in a γ-counter. Calculate specific ^{51}Cr release according to the formula:

[(test release — spontaneous release) /
(maximum release – spontaneous release)] × 100.

3.4. Analysis of Phosphoinositide Turnover in NK Cells from Elderly People

1. Labeling of inositol phospholipids: Resuspend purified NK lymphocytes at a concentration of 1×10^6 cells in a final volume of 1 mL of inositol-free RPMI 1640 supplemented with 10% heat-inactivated and dialyzed FCS. NK lymphocytes are metabolically labeled with *myo*-[^{3}H] inositol (5 μCi/10^6 cells/mL) for 18 h at 37°C in 5% CO_2. Wash the labeled cells 2× for 10 min at 300*g* using cold inositol-free RPMI 1640 with 10% FCS and resuspend the pellet in the same medium at 2.5×10^6 cells/mL. Stimulate the purified NK cell samples (2.5×10^5/100 μL) in Eppendorf tubes with either a similar number of target cells (E/T ratio 1:1) or with an appropriate amount of MAb for various time intervals (from 1 to 30 min) at 37°C in a water bath. Incubate control samples for the same time both in the absence of stimuli and with nonsusceptible targets and/or irrelevant MAbs. Stop incubation by adding methanol/chloroform/HCl 37% (80:160:1 v/v), keep the samples at 4°C, and extract phospholipids by vortex-mixing the cells in the above extraction solution. After centrifugation (100,000*g* for 5 min) an upper aqueous phase containing inositol phosphates and a lower chloroform phase containing phospholipids are obtained. Collect the upper phase, dry it *in vacuo*, and store at –80°C until further use. Wash the lower phase with 0.7 mL of methanol/chloroform/1 *N* HCl (235:15:245 v/v) by vigorous mixing. After centrifugation (100,000*g* for 5 min) collect the new lower phase and dry it *in vacuo*.
2. Analysis of inositol phosphate (IP) fractions (IP, IP_2, IP_3). To analyze inositol phosphates, treat the dried samples of the inorganic upper phase with 1 *M* KOH, resuspend these samples in 4 mL of bidistilled water, and load them onto Amprep ion-exchange minicolumns. IP and IP_2 are eluted together from the column with 5 mL of 0.1 *M* $KHCO_3$, while the remaining IP_3 is eluted using a gradient based on 0.17 *M* of $KHCO_3$ and 0.25 *M* $KHCO_3$ buffers at a flow rate of 1 mL/min. Collect samples in three fractions of 5 mL and measure ^{3}H-labeled inositol phosphates by liquid scintillation counting using a β-counter. Compare the eluted peaks to retention times for standards prepared from [^{3}H]PI, [^{3}H]PIP, and [^{3}H]PIP_2. The scintillation counting is set to obtain a counting error lower than 5%.
3. Analysis of phosphatidylinositol phosphate fractions (PIP, PIP_2, PIP_3). Solubilize the lower phase containing phosphatidylinositols in chloroform/methanol (2:1) and spot it onto 1% K oxalate-sprayed TLC plates to separate [3H] labeled phosphatidylinositols. Develop TLC plates with chloroform/methanol/water/saturated ammonia (45:35:8:2 v/v), spray with Enhancer, and fluorograph at –80°C. Autoradiograph TLC plates before exposure to iodine to visualize internal lipid standards obtained from Sigma (St. Louis, MO, USA). Scrape off the single "spot" of PI, PIP, and PIP_2; extract with 1.5 mL of 0.6 *N* HCl/methanol (60:40 v/v) for 48 h with gentle stirring, and count with a liquid scintillation counter using

9 mL of Pico-Fluor 40 scintillation cocktail. The scintillation counting is set to obtain a counting error lower than 5%.

4. Notes

1. The use of normal mouse serum is also recommended to reduce nonspecific binding when an indirect immunofluorescence reaction is combined with a direct immunofluorescence reaction on the same cell sample.
2. To study the expression of differentiation markers on NK cells the use of double fluorescence, using PE labeled anti-CD56 or anti CD16 MAbs, is recommended.
3. Cytofluorimeters are instruments that measure cell size and phenotype by the presence of bound fluorochrome-labeled antibodies and are widely used for analysis of cells labeled as described earlier. A single-cell suspension labeled with FITC- or PE-conjugated antibodies is forced through the nozzle of the machine under pressure. The light scattered and reflected by the cells and fluorescence emitted by excited fluorochromes bound to the cell membrane are detected, analyzed, processed, and stored by a computer. Forward light scatter or "forward scatter" (FS) measures cell size while perpendicular light scatter or "side scatter" (SS) indicates heterogeneity of the cell structure ("granularity or complexity").
4. Most NK cells show large granular lymphocyte morphology and therefore produce forward and side scatter signals higher than other lymphocyte subsets. Thus we do not have to use a too-restricted lymphocyte gate. This point should be borne in mind when setting gates for analyzing NK cells in whole PBMCs.
5. In the lysis assays the target cells should be collected in the logarithmic phase of growing, as ^{51}Cr labeling is poorer when quiescent cells are used.
6. The optimal labeling is obtained when ^{51}Cr is added to a target cell pellet as dried as possible to avoid dilution by culture medium.
7. One cpm per target cell can be considered an adequate total labeling. The spontaneous release should be as low as possible, but is considered optimal if it is less than 10% of the maximum release although about 30% can also be exceptionally accepted.
8. Assaying the lytic activity of peripheral blood lymphocytes with the standard test may present some limitations when it is possible to collect only minimal blood samples, as it occurs in elderly people. In these situations, the possibility of using a low number of effector cells would greatly facilitate the performance of cytotoxicity assays. In this microcytotoxicity assay, use a 10-fold lower number of cytolytic effector and target cells with a maintained E/T ratio ***(3)***.

Acknowledgements

R. S. and C. A. are supported by grants from Spanish Ministry of Health (FIS95/1242, FIS 98/1052) and Junta de Andalucía (Spain). E. M. is supported by grants from MURST (60% fund) and University of Bologna. This work was carried out under the aegis of the European Union Concerted Action on the Molecular Biology of Immunosenescence (EUCAMBIS; Biomed I contract CT94–1209).

References

1. Borrego, F., Alonso, C., Galiani, M., Carracedo, J., Ramirez, R., Ostos, B., Pena, J., and Solana, R. (1999) NK phenotypic markers and IL2 response in NK cells from elderly people. *Exp. Gerontol.* **34,** 253–265.
2. Mariani, E., Roda, P., Mariani, A. R., Vitale, M., Degrassi, A., Papa, S., and Facchini, A. (1990) Age-associated changes in $CD8^+$ and $CD16^+$ cell reactivity: clonal analysis. *Clin. Exp. Immunol.* **81,** 479–484.
3. Mariani, E., Monaco, M. C., Sgobbi, S., de Zwart, J. F., Mariani, A. R., and Facchini, A. (1994) Standardization of a micro-cytotoxicity assay for human natural killer cell lytic activity. *J. Immunol. Methods* **172,** 173–178.
4. Kutza, J. and Murasko, D. M. (1996) Age-associated decline in IL-2 and IL-12 induction of LAK cell activity of human PBMC samples. *Mech. Ageing Dev.* **90,** 209–222.
5. Mariani, E., Mariani, A. R., Meneghetti, A., Tarozzi, A., Cocco, L., and Facchini, A. (1998) Age-dependent decreases of NK cell phosphoinositide turnover during spontaneous but not Fc mediated cytotlytic activity. *Int. Immunol.* **10,** 981–989.
6. Mariani, E., Sgobbi, S., Meneghetti, A., Tadolini, M., Tarozzi, A., Sinoppi, M., Cattini, L., and Facchini, A. (1996) Perforins in human cytolytic cells: the effect of age. *Mech. Ageing Dev.* **92,** 195–209.
7. Ogata, K., Yokose, N., Tamura, H., An, E., Nakamura, K., Dan, K., and Nomura, T. (1997) Natural killer cells in the late decades of human life. *Clin. Immunol. Immunopathol.* **84,** 269–275.

24

Immunogenetics and Life-Span

HLA

Derek Middleton, Martin D. Curran, and Fionnuala Williams

1. Introduction

The major histocompatibility complex (MHC) is located in the region 9p21–6pter on the short arm of chromosome 6 and encompasses approx 4000 kilobases of genomic DNA. Contained within this complex are numerous genes with immune-related functions: notably the class I and class II human leukocyte antigens (HLA), tumor necrosis factor A and B, the complement genes, and genes that orchestrate the transport (*TAP*) and processing (*LMP*) of antigens for presentation. The HLA class I (HLA-A, HLA-B, HLA-C) and HLA class II (HLA-DR, HLA-DQ, HLA-DP) cell surface glycoproteins present antigenic peptides to $CD8^+$ and $CD4^+$ T cells, respectively, and play a central role in mediating the immune response. The HLA class I and class II genes display extreme degrees of polymorphism, making the MHC region the most polymorphic and densely populated area of the human genome. It is now well established that certain HLA specificities are strongly associated with numerous diseases, especially those with an autoimmune dimension, and confer resistance/susceptibility to certain infectious diseases. The possibility that HLA identity may have a genetic role in longevity in humans has long been suspected, spurred on by the importance of the HLA antigens in the immune response and data from studies in mice indicating that genes in the MHC region are associated with a significant effect on life-span. The results to date from these studies are confusing and contradictory, with no consistent association found as yet ***(1)***. Critical examination of the studies highlights the use of serology, known to lack the resolution capable of defining many HLA specificities, and the small number of cases >90 yr included in the studies. The advantages

From: *Methods in Molecular Medicine*, Vol. 38: *Aging Methods and Protocols*
Edited by: Y. A. Barnett and C. R. Barnett

(greater specificity and accuracy) of using molecular methods instead of serological typing to define the HLA system have been well shown in transplantation and disease association ***(2,3)***. Such approaches should allow future studies, examining whether certain HLA alleles influence longevity, to reach a meaningful conclusion.

Many molecular methods are available to define the HLA alleles. Described in this chapter is the sequence-specific oligonucleotide probe (SSOP) method. This method is also directly applicable to defining other polymorphic loci within the MHC or elsewhere in the genome. The basis of this method is the specific amplification of the HLA locus by the polymerase chain reaction (PCR) and the subsequent probing of this product by SSOPs. Most of the vast polymorphism of the HLA system results from conversion events whereby small nucleotide sections of one allele (usually no more than 100 bases long) are transferred to another allele. Thus many of the sequences tend to be shared by alleles and are not allele specific. Therefore probes are used that are sequence specific. To differentiate the alleles, a battery of probes is required and it is the pattern of reactivity of these probes that distinguishes the HLA alleles.

The detection system used in this laboratory consists of labeling the probes with digoxigenin (DIG) and detecting the hybridization of these probes to a complementary sequence present in the PCR-amplified HLA allele of an individual by adding an anti-DIG antibody conjugated with alkaline phosphatase (ALP). The ALP then uses disodium 3-(4-methoxyspiro {1, 2-dioxetane –3, 2'-5'-chloro tricyclo [3.3.1.1] decan}-4-yl) phenyl phosphate (CSPD) as its chemiluminescent substrate and the light emitted is detected by autoradiography.

To define all alleles at any specific locus at the same time would require a large number of probes as, although each allele group has a specific probe pattern, the combined probe pattern of two alleles present in a heterozygous individual can be identical to the combined probe pattern of another heterozygous individual with two different alleles. In addition the system would constantly need up-dating to take account of newly discovered alleles. In this laboratory we use a two-tier SSOP system. The first level of resolution is equivalent to very good serology, that is, the allele group is defined, for example, HLA-A*02. Thereafter, depending on the initial type, a second PCR specific for a group of alleles is performed and a further set of probes used to give definition to the allele level. Thus the number of probes required is kept to a minimum and, except for exceptional circumstances, only the high-resolution system needs alteration to take account of new alleles. The primers used for each locus are listed in **Table 1**. The primers for HLA-A and -B loci give a locus-specific product covering exons 2 and 3 and the primer for HLA-DR gives a product from exon 2. This product is not specific for the HLA-DRB1 locus and amplifies alleles of other HLA-DR loci (e.g., HLA-DRB3 locus).

Table 1
HLA-A, -B, -C, -DR Primers Used for SSOP Typing

	Primers	Sequence 5' → 3'	Band size
HLA-A		94 (Intron 1) → 116	
Generic	A15	GAGGGTCGGGCG(A)GGTCTCAGCCA	863
	AL#AW	TGGCCCCTGGTACCCGT	
		13 (Intron 3) → 274 (exon 3)	
HLA-B		36 (Intron 1) → 57	
Generic	5 BINI-57M	GGGAGGAGC(A)G(A)AGGGGACCGCAG	970
		68 (Intron 3) → 37	
	3 BIN3-37M	AGG(C)CCATCCCCGG(C)CGACCTAT	
		68 (Intron 3) → 37	
	3 BIN3-AC	AGGCCATCCCGGGCGATCTAT	
HLA-B27	5 BINI-57M	See above	970
	3 BIN3-37M	See above	
		42 (Intron 1) → 61	937
HLA-C	5 CIN1-61	AGCGAGGG(T)GCCCGCCCGGCGA	
Generic			
		35 (Intron 3) → 12	
	3 BCIN3-12	GGAGATGGGGAAGGCTCCCCACT	
HLA-DRB		(Intron 1) 15 (Exon 2) → 24	
Generic	AMP-A*	CCCCACAGCACGTTTCT(C)TG	274
	AMP-B	CCGCTGCACTGTGAAGCTCT	
		279 (Exon 2) → 260	
HLA-DRB		17 (Exon 2) → 38	
3/11/6 group	3/11/6 GF	GTTTCTTGGAGTACTCTACGTC	263
	AMP-B	CCGCTGCACTGTGAAGCTCT	
		279 (Exon 2) → 260	

*A ( ) in primer indicates that at this position two nucleotides are inserted when the primer is being made. The primer is referred to as being degenerate.

Thus it is necessary to include a further amplification for alleles of HLA-DRB1*03, -DRB1*11, -DRB1*13, and -DRB1*14. This is referred to as the HLA-DRB3/11/6 group. The reason for two 3' end primers for HLA-B is because HLA-B*7301 differs in intron 3 from all other known alleles at this locus and the extra primer is required to amplify this allele.

In this laboratory we do not use tetramethylammonium chloride (TMAC) owing to its toxic properties and the fact that in our experience it does not necessarily mean the use of one wash temperature. It would appear that to follow this practice a laboratory would require a large number of water baths. In this laboratory one individual normally performs 12 hybridizations at the same time. Thus if a laboratory is defining alleles at three loci (HLA-A, -B, -DR), probes can be selected for use at the same time according to their wash temperature. This eliminates the requirement for a large number of water baths.

In the methods described each probe is hybridized to two different membranes in the same hybridization bottle and the reagents are prepared accordingly. The SSOP method is thus very suitable for typing large numbers of samples — we test at the same time 192 samples (96 on each membrane) which includes controls. However, the volume of reagents can be scaled down and if a laboratory is not performing tests on large numbers of samples, only one lot of membranes need be hybridized.

2. Materials

1. Buffer 1 (4×): 0.4 *M* Maleic acid, 0.6 *M* NaCl, pH 7.5. Add 300 mL of 4 *M* NaCl and 400 mL of 2 *M* maleic acid followed by 200 mL of 4 *M* NaOH to approx 800 mL of double-distilled H_2O (ddH_2O). Add 27 g of NaOH pellets. (**Note:** A white precipitate forms when all reagents are added — this will disappear as the pH approaches 7.0.) Cool to room temperature and adjust pH to 7.5 by adding 4 *M* NaOH by drops. Adjust volume to 2 L with ddH_2O and sterilize by autoclaving.
2. Buffer 2: 2% Blocking reagent in buffer 1. Combine 768 mL of 5% blocking reagent (in buffer 1), 288 mL of 4× buffer 1, and 864 mL of ddH_2O. Leave 5% blocking reagent at room temperature for 10 min before use.
3. Buffer 3: 0.1 *M* Tris-HC1, 0.1 *M* NaCl, 0.05 *M* $MgCl_2$, pH 9.5. Add approx 1400 mL of ddH_2O to 200 mL of 1 *M* Tris-HCl, pH 9.5, and 50 mL of 4 *M* NaCl. Add 100 mL of filter sterilized 1 *M* $MgCl_2$ and mix. Adjust pH to 9.5 and make up to 2 L with ddH_2O. Do not autoclave as precipitates tend to form. Store at room temperature for up to 1 wk.
4. Buffer hybridization: 192 mL of 2% blocking reagent, 144 mL of 6× saline sodium phosphate EDTA (SSPE), 48 mL of 5× Denhardts, 48 mL of 0.1% *N*-laurylsarcosine, 0.96 mL of 0.02% sodium dodecyl sulfate (SDS) and make up to 480 mL with ddH_2O.
5. Buffer washing: 0.3% Tween-20 in buffer 1. Add 14.4 mL of Tween-20 to 1200 mL of 4× buffer 1 and make up to 4800 mL by adding ddH_2O.
6. Blocking reagent: 5% in buffer 1 (Boehringer, Lewes, England, cat. no. 1096176). Prepare 2 L of 1× buffer 1 by combining 500 mL of 4× buffer 1 with 1500 mL of ddH_2O. Add 100 g of blocking reagent in parts, with vigorous mixing using a magnetic stirrer, to approx 1600 mL of 1× buffer 1. As blocking reagent is supplied in 50 g tubs, there is no need to weigh out. Heat to 65°C until blocking

reagent is dissolved. Allow to cool to room temperature and make up to 2 L with buffer 1. Sterlize by autoclaving and store at 4°C.

7. Cresol red: 10 mg/mL, sodium salt (Sigma, St. Louis, MO, USA, cat. no. C9877). Add 200 mg to some ddH_2O taken from measured 20 mL dH_2O in a sterile bottle. Resuspend in remaining volume. Filter sterilize and dispense into 1-mL aliquots and freeze at –20°C.
8. CSPD (Boehringer, cat. no. 1655884). Vortex-mix and centrifuge CSPD in a microcentrifuge for 1 min before use. Dilute CSPD stock solution (25 m*M*, .6 mg/mL) 1:100 in buffer 3.
9. Denhardts (50×): 1% Polyvinyl pyrrolidone (PVP), 1% Ficoll, 1% bovine serum albumin (BSA). Prepare 200 mL of 2% PVP and 2% Ficoll by adding 4 g of each to 180 mL ddH_2O. (Prepare this solution in a fume cupboard. PVP is harmful if inhaled.) Dissolve with gentle mixing and make up to 200 mL with ddH_2O. Sterilize by autoclaving and cool to room temperature. Add 4 g of BSA to 200 mL of the above solution slowly with gentle mixing. When the BSA has dissolved make up to 400 mL with ddH_2O, mixing well. Filter solution through 0.45 µm filter and aliquot. Do not autoclave. Store at –20°C. Leave to thaw at +4°C the evening before it is to be used.
10. Anti-DIG–ALP conjugate (Boehringer, cat. no. 1093274). Just prior to use remove anti-DIG–ALP stock conjugate (0.75 U/µL) from the refrigerator, vortex-mix for 15 s and centrifuge for 1 min in a microcentrifuge. Make a 1:10,000 dilution of the conjugate in buffer 2 (i.e., 192 µL of anti-DIG–ALP conjugate in 1920 mL of buffer 2).
11. 0.5 *M* EDTA, pH 8.0. Add 186.1 g of EDTA Na_22H_2O in parts to 800 mL of ddH_2O. Adjust the pH to 8.0 using 4 *M* NaOH. Make up to 1 L with ddH_2O and sterilize by autoclaving.
12. Ethidium bromide (10 mg/mL, Sigma, cat. no. E-1510).
13. Gel loading buffer (GLB): Add 8 g of sucrose (slowly) to 10 mL of ddH_2O and mix by inversion until dissolved. Then add 1 mL of 1 *M* Tris, pH 7.6; 2 mL of 0.5 *M* EDTA; 1 mL of 10% SDS; 0.02 g of cresol red. Make up to 20 mL with ddH_2O. Do not autoclave.
14. ddH_2O. Double-distilled H_2O or equivalent. Note that ddH_2O used to set up PCR is of ultra-high-purity quality.
15. $MgCl_2$. Supplied with *Taq* enzyme.
16. dNTPs (Pharmacia Biotech, St. Albans, England, cat. no. 27-2094).
17. NH_4 buffer. Supplied with *Taq* enzyme.
18. *N*-Laurolysarcosine (1%). Barrier face mask should be worn when weighing *N*-laurylsarcosine. Dissolve 10 g of *N*-lauryl sarcosine in approx 800 mL of ddH_2O. Adjust volume to 1 L with ddH_2O and autoclave.
19. Nylon membrane (Boehringer, cat. no. 1417 240).
20. PCR plates, 96-well (Advanced Biotechnologies, Epsom, England, cat. no. AB-0366).
21. Size marker Φ×174/*Hae*III (0.1 mg/mL, Promega, Southampton, England, cat. no. G1761). Add 450 µL of ddH_2O to vial of the size marker. Add 20 µL of

GLB to 12 µL (1.2 µg) of the size marker and 8 µL of Tris-EDTA (TE) buffer. Store at 4°C.

22. 10% SDS. This reagent is extremely harmful if inhaled. Wear a mask when working with SDS powder. Also wear gloves. Wash skin thoroughly if in contact with SDS. Wipe down work area after use. Preferably add SDS to ddH_2O in fume cupboard. SDS sometimes comes out of solution but will go back on heating. Add 100 g of SDS in parts to approx 800 mL of ddH_2O. As SDS is supplied in 100 g tubs there is no need to measure. Apply heat (up to 68°C) if necessary to assist dissolution. Allow to cool to room temperature and adjust the volume to 1 L. Do not autoclave.
23. 20× SSPE: 3 *M* NaCl, 0.2 *M* NaH_2PO_4, 0.02 *M* EDTA, pH 7.4. Add 350.6 g of NaCl followed by 48 g of NaH_2PO4 to approx 1600 mL of ddH_2O. Then add 80 mL of 0.5 *M* EDTA, pH 8.0. Adjust the pH to 7.4 using 4 *M* NaOH. Adjust volume to 2 L and sterlize by autoclaving.
24. Saran Wrap® (Genetic Research Instrumentation, Felsted, England, SW1).
25. 2× SSPE/0.1% SDS: Combine 240 mL of 20× SSPE and 24 mL of 10% SDS. Make up to 2400 mL with ddH_2O.
26. 5× SSPE/0.1% SDS: Combine 600 mL of 20× SSPE and 24 mL of 10% SDS. Make up to 2400 mL with ddH_2O.
27. Sodium saline citrate (2×, pH 7.0) (SSC): 0.3 *M* NaCl + 0.03 *M* trisodium citrate.
28. *Taq* enzyme (Bioline, London, England, cat. no. M958013).
29. Thermofast Plate (Advanced Biotechnologies, cat. no. AB-0600).
30. 1 *M* Tris, pH 7.6. Add 242.28 g of Tris base to 1400 mL of ddH_2O. Adjust the pH to 7.6 by adding 100 mL of concentrated HCl (take care — wear a mask and goggles and where possible perform this in a fume cupboard). Allow the solution to cool to room temperature before making final adjustments to the pH. Make up to 2 L with ddH_2O and sterilize by autoclaving. If the 1 *M* solution has a yellow color, discard it and obtain better quality Tris. More than 100 mL of conc HCl may be required.
31. Tris borate EDTA (10×) (TBE): Add 216 g of Tris, 110 g of orthoboric acid, and 80 mL of 0.5 *M* EDTA to 1400 mL of ddH_2O. Adjust volume to 2 L with ddH_2O and sterilize by autoclaving.
32. TE buffer (10 m*M* Tris, 1 m*M* EDTA, pH 7.6). Combine 10 mL 1 *M* of Tris, pH 7.6, with 2 mL of 0.5 *M* EDTA and make up to 1 L with ddH_2O. Sterilize by autoclaving and aliquot.

2.1. Equipment

1. Enzyme boxes (Boehringer, cat. no. 800058).
2. Gel sealer and casting tray (Merck, Poole, England, cat. no. 306/7252/12).
3. Robbins hybridization incubator (Robbins Scientific, Sunnyvale, CA, USA, cat. no. 1040-60-2).
4. Robbins Hydra dot blotting machine (Robbins Scientific, cat. no. 1029-60-1).
5. Robbins water bath (Robbins Scientific, cat. no. 1051-20-2).

3. Methods

3.1. PCR (using 96 well plates)

1. Heat DNA samples to be tested to 60°C for 5–10 min, vortex-mix, and centrifuge for 5 s in microcentrifuge (*see* **Note 1**).
2. Prepare 10 mL of mastermix for appropriate locus (**Table 2**). Use dH_2O of ultra high purity quality. Dispense 100 µL slowly into tubes of the 96-well plate. Take care to avoid splashes and air bubbles at the bottom of the tubes. When all tubes have been filled, cover the 96-well plate with a sterile microtiter tray lid (*see* **Note 2**).
3. Add 1 µL of DNA sample to each well from position 1A→1H, 2A→2H, etc. Only one row at a time should be uncovered by the lid. Leave two wells with master mix only, to act as negative controls, and leave appropriate number of wells for control DNA (*see* **Note 11**). When a complete row of DNA samples have been added, place a strip of eight caps over these samples and press down gently. When DNA samples have been added to all tubes and caps are in place, use a cap sealing tool to ensure that all caps are pushed firmly into place.
4. Centrifuge the plate for 1 min at 500*g*, place in PCR machine, and run appropriate cycle program (**Table 3**). After amplification, if the PCR samples are not to be processed immediately, store at –20°C (*see* **Note 3**).

3.2. Electrophoresis of PCR Samples

1. Add 4.5 g of agarose to 300 mL of 1× TBE, boil, and allow solution to cool to 65°C. It is important to stir agarose while cooling to prevent "lumps" from forming.
2. While agarose is cooling prepare 96-well-gel template by placing casting tray in the gel sealer. Take care to ensure gel sealer is not over tightened; otherwise casting tray may separate when agarose is added.
3. Place sealed casting tray on top of a leveling table and adjust the feet of the leveling table until the bubble in the "spirit level" is centred.
4. Once agarose has cooled to 65°C add 15 µL of ethidium bromide (10 mg/mL) and mix gently. (Ethidium bromide is mutagenic)
5. Pour the molten agarose solution into the level casting tray. Immediately push any air bubbles to edges of the template using a pipet tip.
6. Insert four 24-slot combs into the gel, with equal spacing between combs. Allow gel to set for approx 1 h at room temperature.
7. Add 1000 mL of 1× TBE to an electrophoresis tank. Carefully remove combs from gel. Remove gel from the gel sealer. Place gel in tank containing 1× TBE buffer. Ensure gel is covered by buffer to a depth of 2–3 mm.
8. Add 4 µL of each PCR product to a 96-well Thermofast plate. Ensure product is in each well. Add 8 µL of GLB to each well. Centrifuge plate for 1 min to ensure mixing.
9. Load 10 µL of size marker into first well of each of the four rows.
10. Using an octapipet carefully load 10 µL of sample into each well of the gel. Care must be taken to ensure the octapipet is oriented properly when the samples are added to the gel.

Table 2
PCR Master Mixes

Locus	Stock conc	Master mix
HLA-A generic		
ddH_2O		8220 µL
Cresol red	10 mg/mL	100 µL
NH_4 buffer	10×	1000 µL
$MgCl_2$	50 m*M*	300 µL
dNTPs	20 m*M* each	100 µL
Each primer (×2)	25 µ*M*	120 µL
Taq	5 U/µL	40 µL
HLA-B generic		
ddH_2O		12345 µL
Cresol red	10 mg/mL	150 µL
NH_4 buffer	10×	1500 µL
$MgCl_2$	50 m*M*	450 µL
dNTPs	20 m*M* each	150 µL
Each primer (×3)	25 µ*M*	120 µL
Taq	5 U/µL	45 µL
HLA-B27		
ddH_2O		4155 µL
Cresol red	10 mg/mL	50 µL
NH_4 buffer	10×	500 µL
$MgCl_2$	50 m*M*	150 µL
dNTPs	20 m*M* each	50 µL
Each primer ×2	25 µ*M*	40 µL
Taq	5 U/µL	15 µL

(continued)

11. Place the lid of the electrophoresis system on to the electrophoresis tank, connect the electrodes to the power pack, and electrophorese the samples at 250 V, 250 mAmp for 20 min.
12. Once electrophoresis is complete, remove the gel from the tank and photograph under UV light. Check size of PCR product against size marker to ensure correct product has been amplified (**Table 1**) (*see* **Notes 4** and **5**).

3.3. Dot blotting of membranes.

We use the Robbins Hydra dot blotting machine which enables us to make as many replicate membranes as required from the PCR product. Other laboratories use other equipment and some will dot blot by hand. If the preparation of

Table 2 (cont.)

Locus	Stock conc	Master mix
HLA-C generic		
ddH_2O		8300 µL
Cresol red	10 mg/mL	100 µL
NH_4 buffer	10×	1000 µL
$MgCl_2$	50 m*M*	300 µL
dNTPs	20 m*M* each	100 µL
Each primer ×2	25 µ*M*	80 µL
Taq	5 U/µL	40 µL
HLA-DRB generic		
ddH_2O		8280 µL
Cresol red	10 mg/mL	100 µL
NH_4 buffer	10×	1000 µL
$MgCl_2$	50 m*M*	300 µL
dNTPs	20 m*M* each	100 µL
Each primer (×2)	25 µ*M*	100 µL
Taq	50 U/µL	20 µL
HLA-DR3/11/6		
ddH_2O		8300 µL
Cresol red	10 mg/mL	100 µL
NH_4 buffer	10×	1000 µL
$MgCl_2$	50 m*M*	300 µL
dNTPs	20 m*M* each	100 µL
Each primer ×2	25 µ*M*	80 µL
Taq	5 U/µL	40 µL

the required number of membranes proves difficult an alternative method is to dehybridize used membranes as follows.

1. Dehybridize a maximum of three membranes in 300 mL of each solution with shaking.
2. Rinse membranes in ddH_2O for 5 min at room temperature.
3. Wash membranes in 0.4 *M* NaOH/0.1% SDS at 45°C for 30 min.
4. Wash membranes in 2× SSC for 30 min at room temperature.
5. Check dehybridization is complete by exposing membranes overnight to X-ray film and developing in usual manner.
6. Store membrane flat at +4°C in a sealed plastic bag if not using immediately.

3.4. Denaturation and Fixing of Blots

1. After PCR product has been dispensed onto the membranes, allow to air-dry for at least 20 min.

Table 3
PCR Amplification Conditions

Locus	Hold	Cycle	No. of cycles	Hold	Hold
HLA-A generic	96°C/5 min	96°C/1 min 60°C/30 s 72°C/1 min	35	72°C/5 min	15°C/forever
HLA-B generic + HLA-B27 Testing	96°C/5 min	96°C/30 s 65°C/30 s 72°C/45 s	32	72°C/5 min	15°C/forever
HLA-C generic	96°C/5 min	96°C/1 min 66°C/30 s 72°C/1 min	30	72°C/5 min	15°C/forever
HLA-DRB generic	96°C/5 min	96°C/1 min 55°C/1 min 72°C/1 min	30	72°C/5 min	15°C/forever
HLA-DR 3/11/6	96°C/5 min	96°C/1 min 64°C/1 min 72°C/1 min then 96°C/1 min 56°C/1 min 72°C/1 min	10 20	72°C/5 min	15°C/forever

2. Carefully place membranes DNA face up onto two sheets thick (3MM) Whatman paper soaked in 0.4 *M* NaOH. Leave for 10 min. When placing membranes onto Whatman paper, take care to ensure that membrane is not dragged over denaturation pad, all of the membrane soaks up the 0.4 *M* NaOH, and there are no air bubbles beneath the membrane.
3. Transfer each membrane onto Whatman paper (3MM) soaked in 10× SSPE. Leave for 5 min.
4. Gently wash in 2× SSPE and allow to air-dry for at least 25 min.
5. Wrap membranes in Saran Wrap and place (DNA face down) on UV transilluminator for 4 min. Ensure that all the UV lights are fully on during the procedure; do not switch transilluminator off between each step. Place a glass plate on top of membranes to hold them flat during this procedure. Store membranes wrapped in tin foil at +4°C if not using immediately.

3.5. 3' End Labeling of HLA Oligonucleotides

The labeling reagents are obtained in a kit from Boehringer (cat. no. 1362372) (*see* **Notes 6** and **7**).

1. Remove all reagents from freezer (except Terminal Transferase; this should be removed just before use) and allow to thaw. Vortex-mix reagents briefly, and centrifuge in a microcentrifuge for 5 s.
2. Combine the following: 4 µL of reaction buffer (5×), 4 µL of $CoCl_2$ (25 m*M*), 1 µL of DIG–ddUTP (1 m*M*), 1 µL of Terminal Transferase (50 U), and 100 pmol of probe. Make up to 20 µL with ddH_2O. Vortex-mix samples briefly, centrifuge in a microcentrifuge for 5 s, and incubate at 37°C for 30 min in a water bath.
3. Centrifuge for 5 s in a microcentrifuge and place on ice for 5 min. Add 80 µL of ddH_2O, vortex mix briefly, and centrifuge in a microcentrifuge for 5 s. Aliquot in volumes related to the amount of probe used (**Tables 4–8**) and store at –20°C.

3.6. Prehybridization, Hybridization and SSPE Stringency Washes

Each probe is simultaneously hybridized to two different membranes each containing 96 DNA samples.

1. Hand roll membranes lengthwise to form a cylinder. Place two membranes in a hybridization bottle. One membrane should have the DNA side of the membrane facing the glass, while the second membrane should have the DNA side facing inwards in the bottle.
2. Add 20 mL of freshly prepared, hybridization buffer. Screw cap on tightly and clamp to the rotisserie of a Robbins incubator (preset at 45°C). Rotate the bottles for 1 h.
3. Just before the incubation is complete thaw appropriate aliquots of DIG-labeled oligonucleotide probe, vortex-mix briefly, and centrifuge for 5 s in a microcentrifuge.
4. Add the appropriate number of picomoles of probe (**Tables 4–8**) to 20 mL of prewarmed (45°C) hybridization buffer and mix by inversion.
5. Remove the hybridization bottle from the incubator and pour off the hybridization buffer into a disposable collection container. Add 20 mL of hybridization buffer containing DIG-labeled probe and incubate bottle for 1 h at 45°C.
6. Remove the bottle from the incubator and pour off the fluid into a disposable collection container.
7. Add 100 mL of 2× SSPE/0.1% SDS. Recap the bottle and place inside a Robbins incubator (preset to 25°C) and incubate for 10 min. Make sure temperature does not rise above this.
8. Discard the fluid and repeat **step 7**.
9. Remove the bottle from the incubator. Uncap the bottle and using forceps carefully remove the membranes from the bottle, prior to discarding fluid, directly into a small plastic tray containing 200 mL of 5× SSPE/0.1% SDS, which has been heated to the appropriate temperature (**Tables 4–8**) (*see* **Notes 8** and **9**). Place one

Table 4
Probes Used for HLA-A Typing

Probe	Sequence 5' ⟶ 3'	Wash temp (°C)	Picomoles used	Nucleotide position
				Exon 2
W (A94)	TTCTTCACATCCGTGTC	50	50	22–38
A (56R)	GAGAGGCCTGAGTAT	46	40	163–177
B (62LQ)	TGGGACCTGCAGACA	48	50	178–192
C (62G)	GACGGGGAGACACGG	52	20	181–195
O (62RN)	GACCGGAACACACGG	52	20	181–195
D (62EG)	GAGGAGACAGGGAAA	46	40	184–198
Y (A276)	GGCCCACTCACAGACT	52	50	204–219
E (731)	TCACAGATTGACCGA	45	40	211–225
X (A290)	CTGACCGAGTGGACCT	51	40	218–233
R (A26)	TGACCGAGCGAACCTG	54	40	219–234
F (77S)	GAGAGCCTGCGGATC	50	20	226–240
				Exon 3
Z (A347)	CTCACACCATCCAGA	45	70	5–19
T (95V)	CACACCGTCCAGAGG	48	40	7–21
P (114EH)	TATGAACAGCACGCC	46	30	67–81
G (131R)	CGCTCTTGGACCGCG	52	40	121–136
H (142TK)	ACCACCAAGCACAAG	46	40	154–168
I (149T)	TGGGAGACGGCCCAT	50	40	169–183
J (150V)	GAGGCGGTCCATGCG	60	20	172–186
K (151R)	GCGGCCCGTGTGGCG	60	20	175–189
1 (A525)	TGAGGCGGAGCAGTTG	54	40	183–198
N (156Q)	GAGCAGCAGAGAGCC	52	20	190–204
Q (156W)	GAGCAGTGGAGAGCC	50	10	190–204
L (161D)	CTGGATGGCACGTGC	50	20	208–222
V (A551)	TGGAGGGCACGTGCGT	56	40	209–224
M (163R)	GAGGGCCGGTGCGTG	54	20	211–225
S (A355)	GGCGAGTGCGTGGAGTGGC	68	10	214–232
U (A357)	GGCGAGTGCGTGGACGGGC	68	10	214–232

membrane DNA face down and the other membrane DNA face up into the washing solution. Incubate with shaking for 40 min. Check temperature reading and record any variation on the hybridization record sheet. If the temperature varies more than 2°C above or below the required temperature abandon this hybridization.

10. Remove the membranes from the tray, blot dry, but do not allow the membrane to dry out. Wrap the membrane in Saran Wrap, and store in tin foil at 4°C, until ready to perform chemiluminescent detection.

Table 5
Probes Used for HLA-B Typing

Probe	Sequence 5' ⟶ 3'	Wash temp (°C)	Picomoles used	Nucleotide position
				Exon 2
31 (B89)	GGTATTTCGACACCGCC	56	40	17–33
32 (B156)	GGACGGCACCCAGTT	52	40	84–98
33 (B168)	GTTCGTGCGGTTCGA	50	40	96–110
09 (BL09)	GAGTCCGAGAGAGGAGCC	57	6	123–140
01 (BL01)	GAGGAAGGAGCCGCGGGC	64	20	129–146
02 (BL02)	GAGGACGGAGCCCCGGGC	64	40	129–146
07 (BL07)	GAGGATGGCGCCCCGGGC	64	60	129–146
34 (B249)	TTGGGACGGGGAGAC	50	40	177–191
24 (BL24)	GGGAGACACAGATCTCCA	55	40	185–202
05 (BL05)	ACACAGATCTTCAAGACC	55	14	190–207
10 (BL10)	GATCTACAAGGCCCAGGC	58	10	195–212
12 (BL12)	ATCTGCAAGGCCAAGGCA	56	20	196–213
18 (BL18)	ACTGACCGAGTGAGCCTG	58	20	217–234
35 (B73)	ACTGACCGAGTGGGCCTG	63	40	217–234
20 (BL20)*	AGCGGAGCGCGGTGCGCA	64	40	233–250
21 (BL21)	CGGAACCTGCGCGGCTAC	62	40	235–252
22 (BL22)	CGGACCCTGCTCCGCTAC	61	30	235–252
23 (BL23)	CGGATCGCGCTCCGCTAC	62	40	235–252
				Exon 3
27 (BL27)	CTCACACTTGGCAGAGGA	56	20	5–22
36 (B348)	TCACACCATCCAGAGG	49	50	6–21
37 (B354)	CATCCAGGTGATGTAT	46	40	12–27
28 (BL28)	CCAGTGGATGTATGGCTG	56	40	15–32
38 (B361)	AGGATGTTTGGCTGC	48	40	19–33
26 (BL26)	CTGCGACCTGGGGCCCGA	65	40	30–47
30 (BL30)	GGCATAACCAGTTAGCCT	54	50	65–82
39 (B409)	TATGACCAGGACGCCT	55	40	67–82
40 (B427)	GACGGCAAAGATTACA	46	40	85–100
41 (B499)	ACCCAGCTCAAGTGG	47	40	157–171
42 (B505)	CGCAAGTTGGAGGC	46	40	163–176
43 (B532)	GAGCAGCTGAGAGCCT	52	40	190–205
44 (B539)	GAGAACCTACCTGGA	46	40	197–211
45 (B553a)	GAGGGCCTGTGCGT	48	40	211–224
46 (B553b)	GAGGGCACGTGCGT	48	40	211–224
47 (B566)	TGGAGTCGCTCCGC	48	40	224–237
48 (B597)	GAAGGACACGCTGGA	52	40	255–269
49 (B599)	AGGACAAGCTGGAGCG	52	40	257–272

[a]Complementary to coding sequence.

Table 6
Probes Used for HLA–C Typing

Probe	Sequence 5' ⟶ 3'	Wash temp (°C)	Picomoles used	Nucleotide position
				Exon 2
15 (C2D6)	AGCCCCGGGCGCCGT	56	35	137–151
1 (C2EALL)	GGGTGGAGCAGGAGGG	56	20	152–167
3 (C2G2)	AGTGAACCTGCGGAAACTG	59	25	225–243
2 (C2G1)	TGAGCCTGCGGAACCTG	56	30	227–243
17 (C2H303)	CCAGAGCGAGGCCAGT	54	25	258–2 (Intron 2)
				Exon 3
21 (C3A14)	CTCCAGTGGATGTTTGGC	56	25	13–30
4 (C3A1)	TCCAGTGGATGTGTGGC	54	25	14–30
19 (C3A4)	CAGAGGATGTTTGGCTGC	56	20	16–33
12 (C3A7023)	AGGATGTCTGGCTGCGA	54	25	19–35
7 (C3A212)	TGTACGGCTGCGACCTG	56	20	23–39
22 (C3C15)	GGCATGACCAGTTAGCC	54	25	65–81
18 (C3CA)	GTATGACCAGTCCGCCT	54	25	66–82
20 (C3D58)	GCCCTGAATGAGGACCT	55	30	103–119
6 (C3E1203)	TCCTGGACTGCCGCGG	56	25	124–139
5 (C3E12)	GGACCGCTGCGGACAC	56	25	128–143
11 (C3G17712)	CGCAAGTTGGAGGCGG	54	25	163–178
13 (C3G716)	GGCCCGTGCGGCGGA	56	25	177–191
23 (C3G8013)	GCCCGTACGGCGGAG	54	25	178–192
8 (C3G2612)	TGAGGCGGAGCAGTGGA	57	25	183–199
14 (C3G16)	GCGGCGGAGCAGCAGA	57	25	184–199
9 (C3H2)	GGAGGGCGAGTGCGTG	57	25	210–225
16 (C3H3)	GGAGGGCCTGTGCGTG	56	25	210–225
10 (C3J17)	GCTCCGCGGATACCTG	54	25	231–246

3.7. Chemiluminescence

All steps are performed at room temperature with shaking using a platform shaker. Use separate enzyme storage boxes for different buffer solutions and keep light-tight. Use one enzyme box for a maximum of three membranes at the same time (*see* **Note 10**).

1. Add 240 mL of anti-DIG–ALP conjugate in buffer 2 to the enzyme box. Place membranes into the boxes DNA side down. Incubate for 15 min on shaker.

Table 7
Probes Used for HLA-DR Typing

Probe	Sequence 5' ⟶ 3'	Wash temp (°C)	Picomoles used	Nucleotide position
				Exon 2
09 (1007)	GAAGCAGGATAAGTTTGA	50	10	24–41
03 (1008N)	GAGGAGGTTAAGTTTGAG	54	2	25–42
07 (1004)	GAGCAGGTTAAACATGAG	56	4	25–42
08 (1006)	TGGCAGGGTAAGTATAAG	50	10	25–42
06 (1003)	GTACTCTACGTCTGAGTG	56	4	27–44
02 (1002)	AGCCTAAGAGGGAGTGTC	56	30	29–46
18 (DR18)	CTACGGGTGAGTGTTAT	48	40	32–48
10 (2810)	GCGAGTGTGGAACCTGAT	56	10	66–83
01 (2801)	CGGTTGCTGGAAAGATGC	60	6	73–90
25 (DR25)	CGGTTCCTGGACAGATA	52	40	73–89
11 (DRB12)	CAGGAGGAGCTCCTGCGC	58	4	100–117
13 (DRB6)	CAGGAGGAGAACGTGCGC	62	7	100–117
22 (DR22)	CGGCCTAGCGCCGAGTA	58	50	163–179
05 (5703)	GCCTGATGAGGAGTACTG	54	20	165–182
15 (DRB14/1)	GGCCTGCTGCGGAGCACT	64	4	164–181
26 (DRB ALL)	TGGAACAGCCAGAAGGAC	56	40	181–198
14 (7031)	CTGGAAGACAAGCGGGCCG	60	30	202–220
16 (DRB13)	TGGAAGACGAGCGGGCCG	64	3	203–220
24 (DR24)	AGCGGAGGCGGGCCGAG	62	40	206–222
17 (7012)*	ACCGCGGCCCGCCTCTGC	66	30	207–224
23 (7005)*	ACCGCGGCCCGCTTCTGC	66	40	207–224
12 (DRB8)	GCGGGCCCTGGTGGACAC	64	20	213–230
04 (7004)	GGCCGGGTGGACAACTAC	62	1	217–234

[a]Complementary to coding sequence.

2. Transfer membranes to 300 mL of washing buffer and incubate for 15 min on shaker. Discard washing buffer and replace with fresh washing buffer and incubate for a further 15 min.
3. Transfer membrane to 300 mL of buffer 3 and incubate for 5 min on shaker.
4. Remove from buffer 3, and place two membranes back to back in a plastic bag. Add 20 mL of CSPD (1:100 dilution) and reseal the bag. Place the bag on a platform shaker, cover with tin foil, and shake for 5 min at room temperature.
5. Pour off CSPD fluid into a 20-mL plastic tube for reuse (up to 5×). Store at –20°C if using on more than 1 d, but note that CSPD should only be frozen once. Carefully remove the membrane from the bag, blot off excess liquid, and wrap in Saran Wrap.

Table 8
Probes Used for HLA-DR 3/11/6 Group

Probe	Sequence 5' ⟶ 3'	Wash temp (°C)	Picomoles used	Nucleotide position
				Exon 2
1 (DR19)	CGGTACCTGGACAGAT	50	40	73–88
2 (5703)	GCCTGATGAGGAGTACTG	54	20	165–182
3 (DRB14/1)	GGCCTGCTGCGGAGCACT	64	4	164–181
4 (7031)	CTGGAAGACAAGCGGGCCG	60	30	202–220
5 (DRB13)	TGGAAGACGAGCGGGCCG	64	3	203–220
6 (DR24)	AGCGGAGGCGGGCCGAG	62	40	206–222
7 (7012)	ACCGCGGCCCGCCTCTGC	66	30	207–224
8 (7005)	ACCGCGGCCCGCTTCTGC	65	40	207–224
9 (DRB8)	GCGGGCCCTGGTGGACAC	64	20	213–230
10 (7004)	GGCCGGGTGGACAACTAC	62	1	217–234
11 (5701)	GCCTGATGCCGAGTACTG	58	40	165–182

6. Tape two membranes to the one X-ray film and place a second film on top. Expose the top film for 5 min and check the intensity of the dots. Depending on these results process the second film accordingly. It may be necessary to reexpose the membrane to a third or fourth film for a further period of time, depending on dot intensity.
7. Record the probe reaction for each sample and analyze according to the known patterns (**Tables 9–13**) using a computer programme (*see* **Notes 11** and **12**).

4. Notes

1. We do not routinely determine the concentration of DNA in each isolation. When isolating DNA the amount of TE buffer added to the pellet of DNA is judged by eye. However, we assess approx 10% of samples to ensure that the DNA is at an appropriate concentration. For our methods we normally have the DNA concentration at approx 0.5 µg/µL.
2. When setting up a PCR wear a separate laboratory coat, wear gloves and change them frequently, and perform all work in pre-PCR room using dedicated equipment. Pipettes should not be removed from the pre-PCR room. Pipets are labeled according to reagents and must be used only for these reagents. The use of tips with filters is advisable. When preparing the master mix thaw out following reagents ($MgCl_2$, dNTPs, PCR buffer, and appropriate primers). Vortex-mix each reagent briefly and centrifuge in a microcentrifuge for 5 s and place in an ice bucket (PCR buffer and $MgCl_2$ should be centrifuged for 2 min). *Taq* polymerase should always be added last, after vortex-mixing and centrifuging, and just prior to dispensing the master mix. The aliquoted master mixes should not be left on

Table 9
HLA-A SSOP Patterns

Probes	A	B	C	D	E	F	G	H	I	J	K	L	M	N	O	P	Q	R	S	T	U	V	W	X	Y	Z	1
HLA-A alleles																											
0101							+			+			+					+					+		+	+	
0102							+			+			+					+							+	+	
2.1[a]		+					+	+												+		+	+		+		
0202		+					+	+									+					+	+		+		
0203		+					+	+	+								+			+		+	+		+		
0204/17		+					+	+														+	+		+		
0205/08		+					+	+									+					+			+		
0206/10/21		+					+	+												+		+			+		
0211		+		+			+	+												+		+	+	(+)			
0212/13		+					+	+						+						+		+	+		+		
0214		+					+	+														+			+		
0216		+					+	+											+	+			+		+		
0219		+					+							+						+		+	+		+		
0222		+					+	+									+			+		+	+		+		
0301/03N							+					+											+	+		+	+
0302							+					+		+									+	+		+	
1101/02/03							+						+	+										+		+	
1104							+							+								+		+		+	
2301			+				+				+											+			+		
2402/03/05			+				+							+								+			+		
2404			+				+							+				+				+			+		
2406			+				+										+					+			+		
2407			+				+							+								+					
2408		+					+							+								+			+		
2409N			+				+							+								+			+		
2410			+				+						+	+											+		
2413			+				+															+			+		
2414			+				+							+						+		+			+		
2501					+	+	+		+				+		+		+								+	+	
2502					+	+	+		+				+		+		+									+	

(continued)

the bench too long (max 15 min — *Taq* loses activity once diluted in buffer). Switch on the PCR machine for at least 10 min prior to use to allow the machine to heat up. PCR machine should be situated in the post-PCR room.

3. After setting up a PCR, wash work areas with sodium hypochlorite (containing 2% chlorine). Soak all racks used to hold samples in sodium hypochlorite for approx 30 min, and rinse thoroughly in water. Pipets should be wiped with sodium hypochlorite, followed by ddH_2O. Wipe microcentrifuge, vortex-mix, freezer

Table 9 (cont.)

Probes	A	B	C	D	E	F	G	H	I	J	K	L	M	N	O	P	Q	R	S	T	U	V	W	X	Y	Z	1
2601/02							+		+				+		+		+	+							+	+	
2603/05/06							+		+				+		+		+								+	+	
2604							+		+						+		+	+							+	+	
2607			+				+		+				+				+	+							+	+	
2608							+		+				+	+	+			+							+	+	
68011/012/02							+	+							+		+					+		+		+	
6803							+	+							+		+					+		+	+	+	
6804					+		+	+							+		+					+		(+)		+	
6805							+	+							+		+					+			+	+	
6901							+	+							+					+		+		+			
2901/02/03		+					+				+							+				+				+	
3001	+						+									+						+		+		+	
3002	+						+									+						+			+	+	
3003							+									+						+			+	+	
3004	+						+									+	+					+			+	+	
31012	+				+		+				+											+		(+)		+	
3201						+	+				+											+	+		+	+	
3202						+	+							+								+	+		+	+	
3301/03					+		+				+				+							+		(+)		+	
3401							+		+						+		+					+		+		+	
3402							+		+						+							+		+		+	+
3601							+			+								+				+	+		+	+	
4301		+					+		+				+				+	+							+	+	
6601							+		+				+		+		+							+		+	
6602							+		+						+		+		+					+		+	
6603							+		+						+		+		+					+	+	+	
7401/02/03							+				+											+	+	+	+	+	
8001							+											(+)			+		+		+	+	

The alleles listed are those identified in HLA-A sequences from ASHI, April 1997.

[a]2.1 represents the alleles 0201, 0207, 0215 N, 0218, 0220.

A (+) indicates probe is positive in practice but would not appear to be from sequence.

handle, etc., with sodium hypochlorite. Expose the working area, including pipets etc., to UV light for 60 min.

4. When performing a PCR on 96 samples there may be one or two samples that are not amplified. Therefore we always run a gel to ensure that we have product. This enables the SSOP method to be well controlled. (If an amplification fails in the Sequence Specific Primer method this would lead to an incorrect result.) On some occasions the product is deemed weak and this sample will always be repeated. Good amplification always gives a clean and clear-cut SSOP hybridization whereas almost all the problematic typing results we have encountered were due

Table 10
HLA-B SSOP Patterns

HLA-B allele	7.2	0703	0708	0801	0802	0803	0804	1301/02	1303	1401	1801	2701	2702	2722	2708	3503	3508/18	3514	3515	3519	3520	3701	3702	3801	3802	3902	3903	4001	4002	4005
Probe																														
01																				+							+	+	+
02											+					+	+	+	+		+	+	+							
05			+	+	+	+										+	+	+	+	+										
07								+	+																					
09		+	+	+	+	+	+	+		+		+	+	+	+									+	+	+	+			
10		+																												
12												+	+	+	+															
18																														
20					+			+	+			+													+					
21		+	+	+	+		+			+	+				+	+	+	+	+	+	+					+	+	+	+	+
22														+								+	+							
23						+							+											+						
24								+	+													+	+			+	+	+	+	
26																+	+		+	+	+									
27																														
28										+																				
30								+	+																					
31				+	+	+	+																							
32											+																			
33																														
34																														
35																														
36																						+								
37																														
38																														
39																														
40																														
41								+																						
42																												+		
43								+	+	+	+	+	+	+	+	+		+	+	+	+		+					+	+	+
44																								+	+	+	+			
45									+							+	+	+		+	+									+
46				+	+	+	+			+	+											+		+	+	+	+			
47																														
48				+	+	+	+																							
49		+	+	+																								+		

(continued)

Table 10 (cont.)

HLA-B allele / Probe	4007	4008	4101	4102	4201	4402	4401	4404	4405	4406	4408	4410	4501	4601	4701	4702	4801/03	4802	4901	5001	5101	5102	5107	5201	5301	5401	5501	5503	5504	5506
01	+	+	+	+		+	+	+	+			+	+		+	+			+	+											
02										+											+	+	+	+	+					
05	+	+								+											+	+				+				
07											+			+																
09					+												+	+									+	+	+	+
10					+																					+	+	+	+	
12																														
18														+														+		
20						+	+	+	+		+	+																		
21	+	+	+	+	+								+	+		+	+	+		+						+	+	+	+	+
22															+															
23										+									+		+	+	+	+	+					
24			+	+		+	+	+	+		+	+	+		+	+	+	+	+	+				+						
26												+	+					+	+	+					+					
27			+										+						+	+										
28																														
30												+														+	+	+		
31																														
32																														
33																										+				
34																														
35																														
36																														
37																														
38												+			+	+														
39						+	+	+		+	+																			
40																					+	+	+	+						
41																														
42	+																+													
43	+	+				+						+			+	+	+	+	+	+	+		+	+	+	+	+	+	+	+
44																														
45						+	+		+	+	+	+	+	+				+	+	+	+	+	+	+	+					
46			+	+	+			+																		+	+	+	+	+
47						+	+	+	+	+	+	+	+																	
48			+	+	+																									
49	+																+													

(continued)

Table 10 (cont.)

HLA-B allele	5601	5603	5701/03	5702	5704	5801	5802	5901	6701	7301	7801	8101	8201	1503	15021/21	1503	15025/25	1506	1508	1509	1515	1514	15137/17	1514	1516	1520	1522	1523	1524	1527
Probe																														
01																														
02						+	+				+															+				
05								+			+								+							+				
07			+	+	+									+	+		+	+	+			+	+	+	+	+			+	+
09		+	+					+	+	+		+	+			+				+	+						+			
10		+	+						+			+	+																	
12										+																				
18																														
20																														
21		+	+						+	+	+	+	+	+	+	+	+	+	+	+	+	+	+		+		+	+			+
22																														
23				+	+	+	+	+	+															+		+			+	+	
24														+		+	+	+					+		+				+	+
26						+	+						+													+				
27																									+					
28							+																							
30		+						+					+																	
31																														
32																														
33																														
34			+	+	+	+	+																							
35										+																				
36																														
37			+	+	+																									
38													+					+												+
39					+																									
40											+									+										
41																														
42												+																		
43		+		+		+	+	+		+	+	+			+	+	+	+		+	+		+		+	+		+		
44									+																					
45		+	+	+	+	+	+	+			+			+	+	+	+	+	+	+	+	+	+	+	+	+	+	+	+	+
46								+	+																					
47													+											+						
48																														
49												+																		

(continued)

Table 10 (cont.)

HLA-B allele 1 5 2 9 Probe		Designation of groups	
01		7.2	0702 0704 0705 0706 0707
02		14	1401 1402
05	+	18	1801 1802 1803
07		4001	40011 40012
09	+	40.2	4002 4003 4004 4006 4009
10		44.1	44031 44032 4407
12		51.1	51011 51012 51021 51022 5103 5104 5106
18		39.2	39011 39013 3903 3904 3905 39061 39062 3907 3909 3910 3911 3912
20		39.3	39021 39022 3908
21	+	35.3	3501 3502 3503 3504 3505 3506 3507 35091 35092 3510 3511 3513 3521
22		35.4	3512 3516 3517
23		27.2	2703 2704 27052 27053 2706 2707 2709 2710 2711
24		15.3	1501 1504 1507 1512 1519 1526 N 1530 1532 1533 1534 1535
26		15.4	1511 1515 1528 1531*
27		15.5	1510 1518 1537
28		55.1	5501 5502 5505
30		56.1	5601 5602
31		67	67011 67012
32		78	7801 78021 78022
33		52	52011 52012
34			
35			
36			
37			
38			
39			
40			
41			
42			
43	+		
44			
45	+		
46			
47			
48			
49			

The alleles listed are those identified in HLA-B sequences from ASHI, April 1997.
[a]NB 1531 full sequence data not available for probes B532 and B553A.

Table 11
HLA-C SSOP Patterns

Probes	1	2	3	4	5	6	7	8	9	10	11	12	13	14	15	16	17	18	19	20	21	22	23
HLA-Cw																							
01	+	+		+																			
02021	+						+	+	+									+					
02022/024	+		+				+	+	+									+					
02023	+		+					+	+									+					
0302	+	+														+		+					
0303	+	+														+	+						
0304	+	+														+							
04	+		+																+				
0501	+		+																	+			
0602	+		+					+							+			+					
7.1[a]	+	+									+		+					+					
0702	+	+									+	+	+					+					
0703	+	+										+	+					+					
0704	+	+									+		+		+								
0707	+		+								+		+					+					
0801/03	+	+																		+			+
0802	+	+																		+			
1202	+	+			+		+	+										+					
1203	+	+				+		+										+					
1204	+		+					+										+					
1301	+	+			+		+	+							+			+					
14	+	+																+			+		
1502/03	+		+																			+	
1504	+		+															+					
1505	+		+																				
1601	+	+											+	+				+					
1602	+		+										+	+				+					
17	+		+						+	+	+												
18	+		+												+				+				

The alleles listed are those identified in HLA-C sequences from ASHI, April 1997.
[a]7.1 represents 0701, 0705, 0706.

to poor amplification. Interpretation of weak hybridization signals can give an incorrect result.

5. When determining the conditions necessary for this technique one important aspect is to ensure that the amplification works for both alleles. On some occasions when we were determining the amplification conditions we found that a product could be obtained whereby only one allele could be detected. Therefore,

Table 12
HLA-DR SSOP Patterns

Probe		01	02	03	04	05	06	07	08	09	10	11	12	13	14	15	16	17	18	22	23	24	25	26
HLA-DR	allele																							
1	1.1	+																+						+
	01022	+																						+
	0103	+															+							+
2	15.2		+																				+	+
	1503/1607		+																					+
	16.1		+																				+	+
	1604		+										+										+	+
	1608		+											+									+	+
3	3.1				+		+							+										+
	3.2						+							+										+
	0304				+		+																	+
	0308				+	+	+							+										+
4	4.2							+			+						+					+	+	+
	4.3							+			+										+	+	+	+
	4.5							+			+											+	+	+
	4.6							+			+									+		+	+	+
	4.7							+			+							+				+	+	+
	4.8							+			+							+		+		+	+	+
	0409							+			+									+	+	+	+	+
	0412							+			+		+							+		+	+	+
	0415					+		+			+											+	+	+
	0418							+			+		+									+	+	+
	0422				+			+			+											+	+	+
11	11.2					+	+										+						+	+
	11.4					+	+																+	+
	11.16					+	+							+			+						+	+
	1105/30					+																	+	+
	1107				+	+	+																+	+
	1109					+	+							+									+	+
	1117					+	+															+	+	+
	1122					+		+															+	+
	1123/25					+	+						+										+	+
	1126					+	+											+					+	+
12	12.1											+							+					+
	1204					+						+							+					+
	1205																		+					+

(continued)

Table 12 (cont.)

Probe		01	02	03	04	05	06	07	08	09	10	11	12	13	14	15	16	17	18	22	23	24	25	26
HLA-DR	allele																							
13	13.2						+							+			+						+	+
	13.3						+																+	+
	13.5						+							+									+	+
	13.6						+													+			+	+
	13.8						+										+						+	+
	13031/32						+								+					+			+	+
	1304						+										+			+			+	+
	1310						+							+	+								+	+
	1313						+						+							+			+	+
	1315/27						+							+			+							+
	1317																+		+				+	+
	1318						+						+	+									+	+
	1319						+										+							+
	1326						+							+										+
14	14.1						+									+						+	+	+
	14.3						+						+	+										+
	14.4						+							+				+						+
	14.5						+															+	+	+
	14.7						+							+				+					+	+
	1404/28															+			+			+	+	+
	1410							+								+						+	+	+
	1411					+													+			+	+	+
	1413						+							+				+		+				+
	1415												+						+				+	+
	1416						+									+	+						+	+
	1418						+							+								+		+
	1419						+							+							+			+
	1420						+											+						+
	1421						+							+							+		+	+
	1422/25						+									+							+	+
	1423						+															+	+	+
	1424						+							+										+
	1426						+									+						+		+
7	0701								+		+											+		+
8	8.2												+						+	+			+	+
	8.3												+						+				+	+
	0808												+			+			+				+	+
9	09012									+	+											+		+
10	1001			+																				+

The alleles listed are those identified in HLA-DR sequences from ASHI, April 1997.

Table 12 (cont.)

Designation of groups:	
1.1	0101 01021 0104
15.2	15011 15012 15021 15022 1504 1505 1506
16.1	16011 16012 16021 16022 1603 1605
3.1	03011 03021 0303 0305 0306 0307
3.2	03012 03022 0311
4.2	0402 0414
4.3	04011 04012 0413 0416 0421
4.5	0403 0406 0407 0420
4.6	0411 0417 0424
4.7	0404 0408 0419 0423
4.8	04051 04052 0410
11.2	1102 1103 1111 1114 1121
11.4	11011 11012 11013 11041 11042 1106 11081 11082 1110 1112 1113 1115 1118 1119 1124 1127 1129
11.16	1116 1120
12.1	1201 12021 12022 12031 12032
13.2	1301 1302 1316 1320 1328 1329
13.3	1307 1311 1314 1325
13.5	1305 1306 1309
13.6	1312 1321 1330
13.8	1308 1322 1323 1324
14.1	1401 1407
14.3	1403 1412 1427
14.4	1402 1406 1429
14.5	1405 1408 1414
14.7	1409 1417
8.2	0801 08031 08032 0805 0806 0810 0812 0814 0816
8.3	08021 08022 08041 08042 0807 0809 0811 0813 0815

if a laboratory is setting up a technique from scratch it should ensure that there is no differential amplification by testing various combinations of alleles.

6. Many of the probes used in this laboratory are DIG-labeled during their manufacture, adding the DIG moiety to 5' amino oligonucleotides by incubating with a DIG ester under mild alkali conditions.
7. A commercial method similar to that described is now available (Lifecodes Corporation, Stamford, CT, USA) whereby probes are supplied already labeled with alkaline phosphatase. This removes the DIG labeling of probes and the use of anti-DIG antibody.
8. When we implement new probes to the system we will initially use a wash temperature that is equivalent to the melting temperature of the probes. This is equal

Table 13
HLA-DR 3/11/6 Subgroup SSOP Patterns

		1	2	3	4	5	6	7	8	9	10	11
DR3	3.1	+									+	+
	3.2	+										+
	3.3										+	+
	0308	+	+								+	
DR11	11.1		+									
	11.2		+			+						
	11.3		+							+		
	1107		+								+	
	1117		+				+					
	1126		+					+				
DR13	13.1					+						+
	13.2/1424											+
	1303				+							
	1304					+						
	1310				+							+
	1313									+		
	1318/14.3									+		+
	1327	+				+						+
	13.4											
DR14	14.1			+			+					
	14.2							+				+
	14.4						+					
	14.5						+					+
	14.6								+			+
	14.7			+								
	1413							+				
	1416			+		+						

(continued)

in °C to 2× (number of A + T bases) +4 × (number of G + C bases). Thereafter we adjust the wash temperature by 1°C either up or down according to the probe reaction at the melting temperature. We also start with 20 pmol of probe and adjust accordingly.

9. When the probe conditions, that is, number of picomoles and wash temperature have been determined it is worthwhile to keep a record on the performance of the probes, that is, whether the probe is not giving an adequate signal with its positive control or whether it is crossreacting with controls with which it should be negative. On occasions the conditions for the probes need to be altered. This in a way is similar to HLA sera whereby after long-term storage the specificities iden-

Table 13 (cont.)

Designation of groups:	
3.1	03011 0304 0305 0306
3.2	03012 0311
3.3	03021 03022 0303 0307
11.1	11011 11012 11013 11041 11042 1106 11081 11082 1109 1110 1112 1113 1115 1118 1119 1124 1127 1129
11.2	1102 1103 1111 1114 1116 1120 1121
11.3	1123 1125
13.1	1301 1302 1308 1315 1316 1319 1320 1322 1323 1324 1328 1329
13.2	1305 1306 1307 1309 1311 1314 1325
1303	13031 13032
13.4	1312 1321 1326 1330
14.1	1401 1407
14.2	1402 1406 1409 1417 1420 1429
14.3	1403 1412 1427
14.4	1405 1408 1418
14.5	1414 1423
14.6	1419 1421
14.7	1422 1425 1426
Alleles not amplified by this system:	1105 1122 1130 1317 1404 1410 1411 1415 1428

tified can change. If a probe appears to be giving strong false-positive reactions we will initially increase the wash temperature by 1°C, or if giving weak false-positive reactions we will decrease the probe concentration by approx 20%. If a probe appears to be giving false-negative results we will decrease the wash temperature by 1°C. If a probe is giving weak reactions we will initially increase the probe concentration by approx 20%. One way to monitor the performance of the probes is to record the length of time needed for autoradiography exposure. If this varies to such an extent that it takes more than 30 min to achieve a good signal the conditions of the probe should be altered.

10. It is normal practice in this laboratory for chemiluminescent detection to be performed on 24 membranes at the same time. All membranes are processed up to the end of **step 2**. Thereafter membranes are processed in groups of six simultaneously, leaving the remaining membranes in the washing buffer.
11. Enough controls should be included so that each probe will have two positive reactions. In addition control DNA should be included as negative controls. These contain alleles with sequences that are closely related to the sequence that the probe detects and with which the probe might cross-hybridize. This is especially important when initally determining the optimum conditions for the probe

to work. To maintain consistency between membranes we try to use the same controls. If a laboratory finds it difficult to have a large enough supply of the same control DNA it may consider cloning control DNA by long-range amplification ***(4)***. (Owing to lack of sequence information this is practical only for HLA-A and -B at present). This gives material to use in as many tests as needed. This is especially important when the control DNA has been obtained from an outside source.

12. In this laboratory we always have two independent readings of the membrane. We do not believe in recording a result according to the strength of the reaction (e.g., 1, 2, 4, 6, 8, as in serology). The result should be positive or negative. If in doubt it should be repeated. In the future it would be beneficial to all laboratories if a scanning mechanism was available for reading the membranes as mistakes are possible in the transmissions of results. We believe it is important that the probe patterns are not analyzed by eye. It would be far too easy to *see* the obvious allele(s) when examining the probe patterns rather than those that are obscure. To overcome this laboratories should have a computer program.

References

1. Rea, I. M. and Middleton, D. (1994) Is the phenotypic combination A1 B8 Cw7 DR3 a marker for male longevity? *J. Am. Geriatr. Soc.* **42,** 978–983.
2. Opelz, G., Mytilineos, J., Scherer, S., Dunckley, H., Trejaut, J., Chapman, J., Middleton, D., Savage, D., Fischer, O., Bignon, J., Bensa, J., Albert, W., and Noreen, H. (1991) Survival of DNA HLA-DR typed and matched cadaver kidney transplants. *Lancet* **338,** 461–463.
3. Charron, D. and Fauchet, R., eds (1997) *HLA. Genetic Diversity of HLA Functional and Medical Applications*. Vol. 1 Workshop, EDK, Paris, France.
4. Curran, M. D., Williams, F., Earle, J. A. P., Rima, B. K., Van Dam, M. G., Bunce, M., and Middleton, D. (1996) Long range PCR amplification as an alternative strategy for characterizing novel HLA-B alleles. *Eur. J. Immunogenetics* **23,** 297–309.

25

Dietary Restriction and Life-Span Extension

Byung Pal Yu

1. Introduction

The popularity of the dietary restriction (DR) paradigm (often used interchangeably with calorie restriction) among gerontologists is primarily based on the research finding of the last two decades. Originally discovered by McCay's group in the 1930s, this paradigm showed that animals placed on the DR regimen, meaning reduced nutrition without malnutrition, had robust life extensions ***(1)***. This scientific breakthrough showed that nutritional status can bring about distinctive metabolic adjustments.

Among the most obvious phenotypic changes seen with the implementation of DR are reduced body weight or size, slow growth, leanness due to reduced adipose mass, young appearance, and agility. The hallmark of these age-related changes, however, is a robustly extended life-span, accompanied by low morbidity and mortality rates ***(2)***. The life prolonging action of DR is unparalleled with any other laboratory paradigm in its ability to induce such a broad spectrum of physiological and pathological anti-aging effects ***(3)***. The unequivocal experimental data confirmed by many laboratories around the world have established dietary intervention as the most effective and dependable tool or procedure available tool today for gerontologists in their exploration of the aging process.

As an experimental tool, DR has at least three important characteristics that make it the gold standard of aging research ***(1,4,5)***. They are as follows:

1. *Simplicity of execution*: Studies using this paradigm are simple to execute and the procedures are easy to implement. Unlike other nutritional manipulations in which either individual dietary components or ingredients are adjusted either quantitatively or qualitatively, DR can be administered by simply reducing the amount of the food given, thereby resulting in the calorie restriction. This simple-

From: *Methods in Molecular Medicine*, Vol. 38: *Aging Methods and Protocols*
Edited by: Y. A. Barnett and C. R. Barnett

to-implement intervention and calorie reduction (not anything else) are the most important assets of the DR paradigm.
2. *Reproducibility*: Good laboratory procedures must effectively reproduce consistent results, regardless of the location of the experiment or the responsible investigator. To date, no reproducibility failure has been reported in the ability of DR to extend life in laboratory animals, when conducted under proper experimental conditions and conscientiously followed procedures.
3. *Diverse effect*: The DR paradigm has a broad application. Not only has it been used in the study of laboratory rats and mice, but it also has been proven effective when applied to the study of lower organisms, such as in studies using fruit flies and nematodes. In addition, several investigators have shown DR to work equally well using both sexes of rodents, allowing DR to manipulate physiological systems without concern regarding their differences. Another factor that often raises questions relating to the use of DR is age at implementation. Studies indicate that timing is not a problem with the DR paradigm. DR shows effective results when imposed at any point during the life cycle, whether pre- or postpuberty, maturity, or even during early senescence ***(1,4,6,7)***.

2. Materials

DR, as a dietary manipulation, requires no special tools or instrumentation. However, for a more appropriate discussion, in lieu of the chemical reagents and instruments normally found in the laboratory, descriptions of desirable (if not required) facilities and features are needed, which researchers should consider to obtain optimal results. The main reason for these considerations is that DR work requires the use of a long-term, chronic feeding paradigm. Readers interested in understanding the various forms of the DR paradigm in detail should consult the recent publication of Bertrand et al. ***(5)***.

1. *The barrier facility*: It should be stated at the onset of this discussion that DR studies do not require specific barrier conditions. In fact, many aging studies claim that experiments can be carried out successfully using conventional animal facilities without the use of a specific pathogen-free facility ***(4–6,8,9)***. Researchers should be aware, however, that aging studies using the DR paradigm often involve life-span measurements, pathological monitoring, and survival analysis. It is therefore this author's view and recommendation that if only a conventional facility is available, a separate location for long-term housing of animals is essential, one that is as far as possible from other animal facilities. If logistically possible, investigators should conduct long-term, chronic studies under specific pathogen-free conditions, or at least in a self-contained facility that is isolated from the institution's usual animal facility. This precaution aids in the prevention of cross-contamination by minimizing the heavy trafficking that results in mixed gender, rodent species, etc. These protective measures cannot be overemphasized for the assurance of high-quality animals and successful experimentation outcomes.

Table 1
Dietary Composition[a]

Component	Percentage
Dextrin	45.99
RP 101 soy protein	21.00
Sucrose	15.00
Corn meal	6.00
Mineral mix	5.00
Vitamin mix	3.30
Fiber	3.00
DL-Methionine	.35
Choline chloride	.35

[a]This semisynthetic diet mixture is available from Purina Test Diets (Richmond, IN, USA).

2. *Specific pathogen-free animals*: A discussion similar to that of animal facility conditions required to guard against possible infections can be extended to the health status of the animals used in studies, particularly when employing long-term, chronic DR. Although the beneficial effects of DR are known to occur in almost all laboratory rodents, even when housed in conventional, nonbarrier facilities, researchers would be better served to use animals having specific pathogen-free status ***(1,9)***. Experience has taught that prudent animal selection should be made from strains having well-documented records that show the animal's growth patterns, metabolic responses, and pathologic status. This precautionary measure gives an added advantage when used in combination with a specific pathogen-free barrier. This is especially true when holding and maintaining animals for a lifelong study to investigate aging processes or survival effects, during which time the animals have an increased susceptibility to infection.
3. *Selection of animal cages*: Although not essential, shoebox type, plastic-bottom cages that are fitted with a wire rack are recommended. The reason for choosing this type of cage over wire-bottom cages relates to food spillage, among other considerations. Food spillage is common to the use of wire-bottom cages and can create inaccurate food consumption data. On the other hand, plastic-bottom cages with raised wire-meshed floor racks allow food spillage recovery, which would result in more accurate data.
4. *Requirements for a balanced diet*: A word of caution is need for the selection of the chow used in DR studies. As practiced in the laboratory, DR is imposed on test animals by a reduction of daily food allotments (usually 40%). It is therefore of prime importance that the reduced amounts of diet contain all the required nutrients, particularly those given during the growth period, to avoid any deficiencies. To ensure nutritional sufficiency, it is prudent to choose a well-defined, semisynthetic diet (*see* **Table 1**) from a reputable test chow manufacturer. As part

of their quality control procedures, investigators should periodically send sample chows to independent laboratories for complete analysis. In some cases, researchers carrying out DR studies should use chows fortified with additional vitamins proportional to the reduced food amounts, which would ensure that the DR animals receive a vitamin intake equal to that of the nonrestricted, control animals.

One other important practical matter concerning chow selection is the choice of using powder or pellet form. Although more time consuming to use, the powder form is usually preferred because it permits more accurate weight measurements and less spillage. Pellet form, on the other hand, is likely to be spilled by the animals because they tend to grab the pellets outside the food cup, which results in even more food spillage.

3. Methods

3.1. Preparatory Procedures

1. Acclimatize animals to their new environment by caging them singly for 2 wk. Although age of animals depends on the study design, shipped animals are typically 1 mo old. Note that the younger the animal, the more robust the DR effect. Also, specifying a body weight range is advantageous.
2. Initiate collection of animal body weights 2 d after arrival.
3. Allow all animals free access to water and choice of chow during the 2-wk acclimatization period.
4. Monitor and record food consumption during the 2-wk acclimatization period to determine DR food allotments.
5. Select animals randomly to initiate DR regimen.
6. If periodic sacrifices for cross-sectional studies are planned, it is wise to place more rats in the nonrestricted (i.e., *ad libitum* group) owing to the required shorter life-span of these animals. This will ensure sufficient rats are available at senescence, a prudent measure to compensate for the higher mortality from *ad libitum* feeding. A guideline for choosing the number of animals needed for survival and longevity studies is given in **Subheading 3.4.**, **step 1**.
7. For DR animals, initiate the regimen at the end of the 2-wk acclimatization period with the set amounts of reduced chow. For the *ad libitum* fed, control animals, continue to monitor and record food consumption twice weekly. The amount of food consumed will serve as the basis for the next dietary allotment.

3.2. Optimal DR Levels

1. Because the DR paradigm can be executed in varying degrees (i.e., 10–40%), researchers should first decide on the extent of restriction, as dictated by the study design. A common observation is that the efficacy of DR is inversely related to the extent of DR; that is, the greater the restriction, the more robust the DR effect and the longer the life extension ***(10)***. The common practice is to implement 40% DR ***(1)***.
2. As explained in **Subheading 3.1.**, **step 7**, the chow consumption of the *ad libitum* group is used as the basis to allot daily food amounts for the DR group. Thus, it is

important to allow true *ad libitum* feeding. However, one word of caution is needed: Ensure the chow in food cups is fresh, as rodents tend to consume less if the food is stale, which would preclude accurate food consumption measurements, especially for small rodents.
3. Continually collect, usually twice weekly, the average amount of food consumed from the *ad libitum*, control animals.
4. During the animal's rapid growth phase, adjust food allotment for the DR animals, twice weekly if necessary.

3.3. Animal Monitoring

An animal's morbidity and mortality are profoundly influenced by its nutritional status. It is therefore imperative that the colony of experimental animals be closely monitored as follows:

1. Check animal behavior and health conditions daily, paying close attention to spontaneous movements and eating and drinking habits.
2. Inspect animals with increased frequency as they age (more than twice daily, if possible).
3. Perform necropsy on all animals killed, fixing tissue specimens in a formulin solution for a histological evaluation for the probable cause of death.

3.4. Longevity Studies: Survival Data and Analysis

The hallmark of DR is life extension. It is therefore important to carefully collect and analyze survival data based on animal mortality.

1. Prior to the start of the study, consider the number of animals needed to meet the statistical requirements of your study based on power function analysis.
2. If possible, allow animals to die naturally, using death as the endpoint for data collection criterion.
3. To construct survival data, register each death, noting age in days.
4. Use data collected to calculate median life-span, 10% survival, and maximum life-span.
5. Another method used to analyze longevity data is to measure mortality rate doubling time (MRDT) base on the Gompertzian equation. Some investigators consider MRDT a more reliable expression of the rate of aging or "biomarker" of aging ***(11)***. Although DR intervention has been show to increase MRDT, this method has some inherent shortcomings as the Gompertzian derivation is based on mortality rate (i.e., death) as an index of the rate of aging, which it is not in actuality.

4. Notes

4.1. Extent and Time of DR Intervention

Today, the DR paradigm is the most powerful and reproducible intervention available to gerontologists to retard aging processes and suppress the patho-

genesis of major diseases ***(1–4,9)***. When considering DR implementation, investigators face the following three practical questions in evaluating its maximum effect: How much (or little) restriction is need to show a discernible life-span extension? When is the best time to initiate DR? How long should an animal remain on the restricted diet? Brief comments regarding these important questions are listed below:

1. *Extent of DR*: Consider these facts when deciding the extent of the DR to be imposed.
   a. The effectiveness of DR is inversely related to the amount of caloric intake (i.e., the greater the DR, the stonger the DR effect, the longer the life-span).
   b. Beyond 40% restriction, which has become a routine procedure for some studies, increases the risk of premature death among young animals.
2. *The optimal timing for DR implementation*: Based on the results of all studies using DR, it is safe to say that the younger the animal when DR is imposed, the more robust the outcome. In one of our studies ***(2)*** we began DR at 6 mo of age (i.e., after sexual maturity). A reanalysis of the survival data from this study by Neafsey ***(7)*** concluded that, although to varying degrees, DR exerts a life-prolonging action irrespective of its initiation time. Another study ***(6)*** showed that mice benefited from the effects of DR by a substantial life extension (~15%), even when DR was initiated at 12 mo of age. The consensus is that, for many reasons, the earlier DR is implemented, the more marked the results.
3. *Length of DR*: The rule of thumb is that the longer DR is imposed, the longer the life-span extension. The success of DR is also dependent on time of initiation (e.g., at young age or in adulthood). To date, all indications are that DR is more effective when initiated during an animal's youth or growth phase and continued through adulthood than when simply carried out over the same length of time and initiated during adulthood.

4.2. DR as a Mechanistic Probe

Because DR is the subject of widespread scientific inquiry ***(9,10)***, even outside the field of gerontology, some comments are merited for those who are not familiar with the DR paradigm. Below are some of its advantages as well as limitations.

1. *Advantages*: DR is shown to extend life-span by preventing most physiological dysfunction and pathological changes. This ability provides researchers with an important tool by which to uncover the mechanisms that underlie age-related deterioration at various biological system levels, including the molecular events involved in gene activity. This amazing aspect of the effectiveness of DR is highlighted by the evidence showing its ability to modulate almost all the age-related changes observed in *ad libitum* fed animals.

   DR has also been used successfully to test several theories and hypothesis of aging ***(3)***. One interesting recent test using the DR paradigm to substantiate the "oxidative stress theory of aging" demonstrated its ability to attenuate oxidative

damage and enhance antioxidant defense systems. If DR turned out not to have the ability to modulate oxidative stress, then the basis as a *bona fide* theory of aging would be weakened.

2. *Limitations*: A caveat should be added that the DR paradigm has a limitation that critics refer to as its nonspecificity (i.e., lacking a specific action), because of the broad modulation spectrum of DR in almost all biological systems. The broad efficacy of DR should be expected, however, because the aging process itself is broad and multifaceted. This limitation is therefore clearly outweighed by its advantages, especially as studies move toward more molecular approaches and the DR paradigm shows its usefulness in its ability to modulate genomic activity.

Acknowledgments

This work was supported, in part, by a grant from the National Institute on Aging (AGA–01188). The author thanks Ms. Corinne Price for manuscript preparation.

References

1. Yu, B. P., ed. (1994) *Modulation of Aging Processes by Dietary Restriction*. CRC Press, Boca Raton, FL.
2. Yu, B. P., Masoro, E. J., and McMahan, C. A. (1985) Nutritional influences on aging Fischer 344 rats: 1. Physical, metabolic and longevity characteristics. *J. Gerontol.* **40,** 657–670.
3. Yu, B. P. (1996) Aging and oxidative stress: modulation by dietary restriction. *Free Radic. Biol. Med.* **21,** 651–668.
4. Weindruch, R. and Walford, R. L. (1988) *The Retardation of Aging and Disease by Dietary Restriction*. Charles C Thomas, Springfield, IL.
5. Bertrand, H. A., Herlihy, J. T., Ikeno, Y., and Yu, B. P. (1999) Methods of assessing aging processes: dietary restriction, in *Methods in Aging Research* (Yu, B. P., ed.), CRC Press, Boca Raton, FL.
6. Weindruch, R. and Walford, R. L. (1982) Dietary restriction in mice beginning at 1 year of age: effect of life span and spontaneous cancer incidence. *Science* **215,** 1415–1418.
7. Neafsey, P. J. (1990) Longevity hormesis: a review. *Mech. Ageing Dev.* **51,** 1–31.
8. Lane, M. A., Baer, D. J., Rumpler, W. V., Weindruch, R, Ingram. D. K., Tilmont, E. M., Culter, R. G., and Roth, G. (1996) Calorie restriction lowers body temperature in rhesus monkeys, consistent with postulated anti-aging mechanisms in rodents. *Proc. Natl. Acad. Sci. USA* **93,** 4159–4164.
9. Lewis, S. M., Leard, B. L., Turturro, A., and Hart, L. W. (1999) Long-term housing of rodents under specific-pathogen free barrier conditions, in *Methods in Aging Research* (Yu, B. P., ed.), CRC Press, Boca Raton, FL.
10. Weindruch, R., Walford, R. L., Fligiel, S., and Guthrie, D. (1986) The retardation of aging in mice by dietary restriction: longevity, cancer, immunity, and lifetime energy intake. *J. Nutr.* **116,** 641–654.
11. Finch, C. E. Pike, M. C., and Witten, M. (1990) Slow mortality rate accelerations during aging in some animals approximate that of humans. *Science* **249,** 902–905.

26

The Use of Genetically Engineered Mice in Aging Research

Julie K. Andersen

1. Introduction

The primary model systems used for studying the role of regulated gene expression in senescence and the effects that genetic variations have on this process have been to date either mammalian cells in vitro or invertebrate systems such as yeast, *C. elegans*, and *Drosophila*. Both types of model systems have been very useful in elucidating potential genetic pathways involved in the aging process and are appealing owing to a variety of factors, not the least of which is the ease of genetic manipulation. As such, they constitute a good starting point for understanding the phenomenon of aging. However, such models have their limitations; no tissue culture system can yet approach the subtleties of complex cell–cell interactions existing in the whole, intact animal, and although significant evolutionary conservation has been found between many genes in invertebrates and humans, they are still farther removed from humans than available vertebrate model systems.

In the last 20 yr, rapid advances have been made in techniques allowing the introduction of selected mutations into mammalian systems in vivo. The ability to create laboratory mouse strains containing targeted mutations has allowed the creation of vertebrate models to study the aging process and has extended our understanding of many age-related diseases in humans.

2. Making a Transgenic Mouse: The Basics

In the mouse, transgenic technology is a process by which genetic engineering at the embryonic stage is performed to allow elevated expression of existing genes or ectopic expression of novel genes in the adult animal. This process involves microinjection of a cloned gene of interest into the pronuclei of a

From: *Methods in Molecular Medicine*, Vol. 38: *Aging Methods and Protocols*
Edited by: Y. A. Barnett and C. R. Barnett

mouse embryo at the one-cell stage ***(1)***. The transgenic DNA thus introduced will randomly integrate into the genomic DNA of the embryo, where it can be transcribed and translated into functional protein. Following injection of the foreign DNA, the embryos are implanted into pseudopregnant recipient females. Because the transgenic DNA integrates into the mouse's genomic DNA at the one-cell stage, the integrated DNA will be contained in the DNA of all cells of the mouse's body including its germ line cells and will therefore become a heritable component of its genetic make-up. Following their birth, founder animals are tested for presence of the transgene via the polymerase chain reaction (PCR) or Southern blot analysis, and positive founders bred out to create transgenic lines in which patterns and levels of expression of the gene can be observed as well as its physiological consequences. The extent of expression of the transgene appears to be more related to its site of genomic integration as opposed to copy number. Many independent lines must be examined to separate out the effects that the integration site vs the transgene itself have on the observed phenotype.

3. Further Considerations in Transgene Design

Normally, the injected foreign DNA used for transgenic production is designed to contain the gene of interest expressed under the control of a regulatory promoter element that designates at what time and in what cell types the expression of the transgene will occur. The injected DNA can be either the entire gene itself including its native promoter element and all of its introns and exons and 5' and 3' regulatory DNA sequences, or it may consist of a heterologous promoter driving expression of the cDNA that is missing the introns and regulatory sequences. It has been demonstrated in previous studies that genomic constructs are expressed more efficiently than cDNAs. However, owing to the large size of some genes, it is not always possible to use the entire gene although there have now been several reports of successful integration of transgenic yeast artificial chromosome (YAC) DNAs of several hundred kilobases in size into the mouse genome ***(2–7)***. It has been suggested that the presence of the first intron is necessary for high levels of expression of a cDNA even if the intron is a heterologous one ***(8)***. The choice of the promoter (native vs heterologous) is normally dependent on when, where, and to what extent expression of the gene product is desired.

4. Making a "Knockout" Mouse: The Basics

Although expression of an antisense mRNA in a transgenic construct has been used in a few instances to reduce levels of a desired gene product ***(9–14)***, the success of antisense RNA expression is dependent on several factors including the level of expression of the endogenous RNA and its turnover rate as well

as the rate of turnover of the protein product produced from it. However, in the last decade a second type of genetic engineering called gene targeting or gene "knockout" has been developed that allows the elimination of expression of an endogenous gene of interest by producing an insertional mutation in the endogenous gene. Here, a cloned fragment from the gene (a minimum of 2 kb in size) is altered in vitro usually via insertion of a neomycin resistance (*neoR*) gene into a region of the gene vital for its expression, for example, an exon ***(15,16)***. Thymidine kinase sequences from the herpes simplex virus (HSV-tk) are next introduced at both ends of the linearized gene fragment and the altered gene (termed the "targeting vector") is introduced into pluripotent embryo-derived stem (ES) cells either via either direct injection or electroporation (for a review of ES culture conditions, *see* **ref.** ***17***). The most well-studied and commonly used ES cells are derived from the inbred 1295v mouse strain, although the use of ES cells from both inbred C57B1/6 and hybrid C57B1/6 × CBA/JNCrj backgrounds has also been described ***(18–20)***.

Following introduction of the altered gene fragment into the ES cell, homologous recombination occurs between it and the endogenous gene in the ES cell DNA at the ends of the region of homology between the transgene and genomic target sequence so that the copy of the gene containing the *neoR* insertional mutation replaces the normal copy of the endogenous gene ***(14,15)***. Use of DNA in the targeting vector that is derived from the same background strain as the ES cells used may improve the frequency of homologous recombination, that is, syngeneic or isogenic DNA ***(21)***.

During homologous recombination, the distal HSV-tk sequences are eliminated. When the transgene is inserted into the ES cell DNA via random integration (a more frequent event than homologous recombination in mammalian cells unlike in yeast), the HSV-tk sequences are retained. Cells containing the homologously integrated copy of the gene can therefore then be selected by growth in media containing both neomycin and gancyclovir to select for cells containing the *neoR* insertion but not the HSV-tk sequences ("positive–negative selection"). Other methods to distinguish homologous recombination from random integration include using targeting vectors containing a positive selection marker lacking either its own promoter or polyadenylation site ***(22)***.

ES cells containing the *neoR* gene insertion in the gene of interest are next introduced into mouse blastocysts by either injection into the cavity of a host blastocyst (a 3.5-d embryo at the 32-cell stage, ***23***) or aggregation with a host embryo at the morula stage (2.5-d embryo at the 8–16-cell stage, ***23–26***). Because they remain pluripotent even following long periods of growth in tissue culture, the ES cells will contribute to all tissues of the developing animal including cells of the germ line. ES cells derived from mice with one coat color may be introduced into a host embryo of a different coat color to distinguish

which resulting animals are chimeras, that is, made up of tissues from both ES and host cells. Following implantation into foster mothers, the resulting chimeric offspring are bred, producing mice that, if the ES cells have become part of the germ line, are heterozygous for the introduced mutation. Heterozygous animals are bred to obtain homozygous mutant mice.

5. Generation of a Particular Genetic Mutation via Gene Targeting

Sometimes, a specific subtle mutation in the endogenous gene is desired rather than generation of a *neoR* insertional mutation. This requires a two-step double gene replacement. First the mutant is made containing the *neoR* marker, and then the *neoR* marker is replaced with another targeting vector containing the desired mutation. Following selection, the ES cell clones can be checked by PCR or Southern blot analysis to ascertain that they contain the correct mutation.

6. Special Factors to Consider When Making Genetically Engineered Mice for Aging Studies

6.1. Adult-Specific Expression

In aging studies, the researcher is generally interested in the effects of alterations in a particular gene product in a particular tissue in the adult animal. Many cell-type specific promoters are available that will allow the researcher to target the particular tissue of interest; however, they often allow expression prior to adulthood in a manner that may confound the researcher's analysis of aging effects related to changes in the activity of the gene product. To eliminate any developmental effects of gene alteration, inducible systems can be used.

Previously, the only types of inducible systems available were those that involved the use of inducing agents that themselves could be toxic to cells or elicit pleiotrophic changes that could confound the analysis of any resulting phenotype, for example, heat shock, heavy metals, glucocorticoids, and interferon ***(27–29)***. These systems were also plagued by low levels of inducibility, leakiness in the noninduced state, and the inability to achieve effective induction in vivo. In the last few years, new inducible systems have been developed that overcome many, if not all, of the drawbacks of the earlier systems and allow both temporal and cell specificity of gene expression.

The tetracycline (Tet) system allows inducible expression of transgenes without the requirement of agents that might themselves cause cellular stress ***(30)***. In this system, a Tet-inducible reverse transcriptional transactivator (rTta) protein consisting of a "reverse" Tet repressor (rTetR) fused to the herpes simplex virus VP16 transcription activation domain is constitutively expressed via a cytomegalovirus immediate early promoter (pCMV) from what has been termed the "regulatory" transgene. Expression of this transgene can be limited

in both cell lines and transgenic animals by replacing the CMV promoter normally used with one that is cell specific. The gene of interest is placed into a second vector called the "response" transgene at a multiple cloning site located downstream of a Tet response element (TRE) consisting of seven tandem Tet operator sequences fused to a minimal CMV promoter (pminCMV). The components of this system are now commercially available from Clontech. The rTta protein will bind and activate the gene of interest only in the presence of Tet or its more lipophilic derivatives such as doxycyclin (dox). Both highly inducible and tightly controlled levels of transgene expression are observed upon treatment with inducing agent with little basal expression. The Tet inducible system has been recently used to generate transgenic mice containing tetracycline-inducible transgenes in a cell-type specific manner including under the control of neuronal-specific promoters indicating that dox administered orally crosses the blood–brain barrier ***(31,32)***. In addition, oral dox treatment seems to have no detrimental effects on body tissues or general toxicity for the animals ***(33)***. The Tet system can be used to drive expression of antisense RNAs to control the activity of endogenous gene expression ***(34)***. Like with other transgenic systems, the site of integration of both activator and response transgenes may have an effect of their levels of expression.

In addition to the Tet system, other systems are also available that appear to be effective in inducing both cell-specific and inducible transgene expression. The recently described ecydysone system, for example, also boasts high levels of inducibility, low basal expression, rapid kinetics, a minimum of confounding inducing agent-elicited effects, no apparently toxicity to mammalian cells in vitro or in vivo, and the components are also now commercially available from Invitrogen ***(35)***. This system requires the expression of two separate components of a modified nuclear *Drosophila* ecdysone receptor (the *Drosophila* ecdysone receptor itself and a mammalian retinoic X receptor both can be expressed from cell-specific promoters); these receptors bind to one another and activate expression of the transgene of interest from an ecdysone responsive promoter upon administration of the steroid compound, muristerone. Induction of transgene expression using this system was reported by the authors to be greater than that obtained with the Tet system and to have lower levels of basal expression; however, there has been only one publication to date in which the system has been demonstrated to work in vivo ***(35)***.

Besides the availiability of systems for tissue-specific and inducible expression of transgenes, systems have also been developed for the inducible inactivation of gene expression only in certain organs or cell types. Such systems overcome the problems associated with the possible lethality associated with disrupting genes during the embryonic period so that the effects of gene loss can be analyzed at later stages in the life of the organism. One such system is

based on the Cre–lox recombinase system in bacteriophage P1 ***(29,36,37)***. The Cre recombinase protein will catalyze site-specific recombination between two short segments of phage recombinase recognition sequence DNA within the genome called loxP sites, removing any intervening sequences between them. The targeting vector can therefore be designed to contain lox sites flanking a portion of the endogenous gene that the researcher wishes to delete. The lox sequence-containing mice can then be mated with transgenic mice containing the cre recombinase gene behind a particular cell-specific promoter resulting in an animal in which the fragment of the gene of interest is excised only in the tissues in which the cre recombinase is expressed. The sites of the original lox insertions in the targeting vector must be carefully chosen as to not disrupt normal endogenous gene function. A second similar system involves the use of a recombinase from yeast called flp that can remove DNA flanked by 34-basepair sequences called frt ***(38,39)***.

These systems can also be used to incorporate subtle alterations into a gene of interest by introducing a targeting vector containing both the mutation and at a separate location the *neoR* gene flanked by lox sequences into ES cells. Cre recombinase can then be transfected into selected drug-resistant cells to remove the selectable marker leaving only the mutation within the ES cell genome ***(40)***.

The cre recombinase protein can be expressed in a tissue-specific and inducible fashion by use of the Tet system. In this way, the researcher is able to produce mice that when bred with *lox* sequence-containing lines produce progeny in which loss of function of the gene of interest is both inducible and cell-specific ***(41)***.

6.2. Genetic Background

Another important factor to consider in the construction of genetically engineered mice for aging studies is the choice of genetic background. Genetic background may have a significant effect on the expression phenotype of a particular gene as there may be allelic modifiers in one genetic background vs another that alter the phenotype of the modified gene's expression, for example, by suppressing or enhancing activity of another related gene with redundant function ***(42)***.

Life-span studies done by crossing various inbred strains of mice have determined that genetic background has a significant effect on longevity ***(43–45)***. A current problem in the aging field as well as many others is that many people perform their phenotypic analyses in hybrid rather than inbred or outbred strains so it is unclear whether observed phenotypic effects can be attributed to the specific genetic modification or are due to background effects ***(46)***. A com mon solution to this problem is to measure the phenotypic effect in a large

number of animals, thereby increasing the probability that the difference between the phenotype in the genetically altered mice vs control animals is statistically significant and decreasing sampling error. Another solution is to backcross into an inbred strain prior to phenotypic analysis. The most commonly used inbred strain in aging studies is C57B1, which is often the background of choice for many studies owing to its extensive characterization; the 129 strain from which the original ES cells are often derived have unique behavioral and neuroanatomical anomalies, are difficult to breed, and are prone to a number of diseases ***(46,47)***. However, if an allelic modifier gene is linked, that is, in close physical proximity to the genetically altered gene, then backcrossing into the desired strain will not be sufficient to alleviate the effects of the modifier unless it is done numerous times, which can be both incredibly time consuming and expensive. In terms of phenotype in knockout mouse strains, one possible solution is to see if transgenic gene replacement negates the effects of loss of gene function ***(47)***.

Lastly, it is also important to be aware that genetic alteration, such as administration of pharmacological agents, can have pleiotropic effects leading to a plethora of compensatory changes that result in secondary phenotypical alterations unrelated to the effects of alteration of expression in the original gene product. Therefore, whatever gene is altered or background strain is used, it is important to be aware that considerable care must be taken in intepreting the results of genetic manipulation experiments in mice.

7. Examples of Genetically Engineered Mice Constructed to Test Molecular Theories of Aging

Transgenic mouse lines with extended lifespans have not yet been reported. However, likely candidates for such analyses based on studies in lower organisms such as *Drosophila* would include such genetically engineered models as superoxide/catalase double transgenic lines and those containing metabolic genes found to be important in dietary restriction paradigms in rodents ***(48)***.

Although the use of genetic engineering has yet to produce any longer-lived mouse strains, engineered lines have been used to assess the validity of some current popular molecular theories of aging including the roles of replicative senescence and DNA damage and repair on longevity, examples of which are described in the following subheadings.

7.1. Replicative Senescence

Fibroblasts cultured in vivo undergo a limited number of cell divisions before they enter a senescent phase where they can remain for long periods of time without undergoing further rounds of mitosis. This phenomenon is known as replicative senescence ***(49)***. It has been suggested that the loss of proliferative

capacity of cells is due either to random accumulation of cellular damage or to a genetic preprogrammed process or innate "biological clock."

Replicative senescence of fibroblasts can be prevented by expression of large T antigen (T Ag) which allows proliferation to continue indefinitely as long as T Ag is expressed. If it is removed, cells enter a postmitotic state. To test at what point fibroblasts become dependent on T Ag for continued cell division, embryonic fibroblasts were prepared from transgenic mice expressing a temperature-sensitive form of T Ag under the control of the interferon promoter ***(50)***. When grown in the presence of interferon at 33°C, fibroblasts derived from these animals become immortal. Removal of interferon or switching cultures to 39°C resulted in reduction of functional T Ag and cessation of cell division. When T Ag levels were reduced while the cells were still dividing, they did not lose proliferative potential. T Ag appeared to be required to maintain cell division only once the normal mitotic life-span had elapsed. In addition, when cells that were immortalized by switching them to growth in the presence of T Ag were switched back to conditions of no T Ag, they underwent only the exact number of cell divisions that would have been remaining if they had not ever been exposed to T Ag. This suggests that fibroblast replication is a regulated phenomenon and that the biological clock that limits mitotic life-span continues to operate in the presence of functional T Ag.

7.2. DNA Damage and Repair

Mice containing a targeted deletion of the *Pms2* DNA mismatch repair gene show a 1000-fold elevation in mutation frequency in all tissues examined compared to control animals; however, the presence of increased rates of mutagenesis did not affect life-span ***(51)***. This suggests that DNA damage and repair is not a limiting factor in longevity.

8. Examples of Genetically Engineered Mice Constructed to Dissect Cellular Events Involved in Age-Related Diseases

The use of genetically engineered mice has been invaluable in aiding in the understanding of a myriad of age-related diseases. Transgenics and knockouts have provided us with several valuable animal models that have not only allowed the analysis of disease progression but also the testing of new drug therapies for various disorders associated with aging in the human population. Some selected examples are described briefly in the following sections.

8.1. Alzheimer's Disease

In the case of Alzheimer's disease, several recent transgenic studies have contributed greatly to our knowledge of how mutations in both the amyloid precursor protein (APP) and the presenilin genes may contribute to the accu-

mulation of amyloid plaques and neuritic tangles in the cerebral cortex and the hippocampus that eventually leads to the neurodegeneration and resulting cognitive decline associated with this disorder.

APP overexpressing transgenic lines have been constructed in which either a shorter form of the human APP cDNA containing the same mutation found in a familial Swedish Alzheimer's pedigree was expressed behind the prion protein promoter (PrP) or a longer form of the cDNA containing a separate mutation was expressed from the platelet-derived growth factor (PDGF) promoter ***(52,53)***. In both cases, mice were found to develop the selective amyloid plaques and gliosis in the hippocampus and cortex characteristic of the disease by 6 to 12 mo of age. Plaque development appeared to be dependent on which background strain the APP cDNA was expressed in, suggesting the presence of allelic modifier genes ***(52)***. In the Hsiao line, a loss in cognitive ability as exemplified by a deficit in various learning and memory tests was also reported, although the loss was somewhat variable ***(52)***.

Transgenic mice expressing mutant human presenilin-1 (PS-l) cDNA under control of the PDGF promoter exhibited an increase in β-amyloid (Aβ) deposition, a product of abberrant APP processing that is found to be elevated in the brains of Alzheimer's disease patients and is considered a hallmark of the disease ***(54)***. Amyloid deposits or behavioral deficits have yet to be reported in these animals. Double transgenics expressing both mutant APP and PS-i cDNA have an accelerated rate of amyloid deposition ***(55)***.

An important issue to be addressed with the lines described above is the temporal relationship between the formation of amyloid deposits and the onset of memory deficits in these animals ***(56)***. If cognitive effects occur prior to Aj3 deposition, this would imply that it is the soluble form of Aβ as opposed to the fibrillary form that is responsible for disease pathology and that amyloid plaques may occur coincidentally along with cognitive decline. Interestingly, there appears to be no correlation between the amount of Aβ deposition and degree of dementia in humans with the disease, and in addition transgenic mice expressing the Swedish APP mutation in the FVB background show cognitive effects in the absence of plaque formation ***(52,57)***.

8.2. Immunosenescence

Genetically engineered mice have also been used to study the phenomenon of immunosenescence. Older people have an increased susceptibility to infection as a result of an age-related decrease in the responsiveness of the immune system to attack by foreign antigens such as bacteria and viruses. This immunodeficiency appears to be primarily due to a decline in the response of T cells to receptor stimulation which in turn can result in a decline in both T-cell proliferation and alterations in cytokine secretion ***(58)***. There appears to be an

age-related shift in T-cell populations so that the number of T cells that express a naive phenotype, that is, those T cells that have never encountered an antigen, decreases while the number of memory T cells that have specificity toward a particular antigen with age increases. It has been suggested that it is this decline in the proportion of naive T cells that can respond to novel antigen that may account for the age-related decrease in immune function or immunosenescence. To test this hypothesis, the function of T cells from a transgenic mouse line expressing naive T cell receptor (TCR) were examined in both young and aged animals ***(58)***. T cells expressing the naive TCR had decreased proliferative and secretion capacities in the older animals compared to those in younger mice, suggesting that age-related deficiencies in immune function may not be solely attributable to the switch in the proportion of naive vs memory T cells but may also include a decrease in the response of naive T cells in older individuals.

8.3. Atherosclerosis

Atherosclerosis is the major cause of mortality among elderly populations in most highly developed nations. Genetically engineered mouse models developed in the last several years which mimic this condition have contributed much toward our understanding of the genetic and environmental factors involved in susceptibility to this disease. For example, mice have been generated that are deficient in apolipoprotein E (apoE), the surface component of lipoprotein particles that is necessary for their recognition by lipoprotein receptors and therefore their clearance from the bloodstream. These mice demonstrate delayed clearance of lipoproteins and develop pathology characteristic of atherosclerosis in an age-dependent manner including fatty deposits in the blood vessels and plaque formation at the same types of vascular sites (i.e., arterial branch points) seen in humans with this disorder. This condition was exacerbated by feeding the mice a high-cholesterol, high-fat "Western" style diet ***(59,60)***. Replacement of apoE in these mice specifically in macrophages and blood vessels, however, appeared to be sufficient to decrease at least some of the disease pathology ***(61)***.

Other atherosclerotic models have been generated in mice via transdominant expression of mutant forms of the apoE protein such as the Leiden and R142C mutations which have been demonstrated to cause altered clearance of lipoproteins in humans ***(62,63)***. When fed a high-cholesterol diet, animals from both these transgenic lines developed cardiovascular lesions including fatty deposits and formation of fibrous plaques. Transgenic mice containing the human apolipoprotein E*2(Arg-158 → Cys) mutation on an apoE null background develop an even more severe hyperlipoproteinemia than the apolipoprotein E*3–Leiden transgenic mice ***(64)***.

Other atherosclerotic models developed to date include mice deficient in low-density lipid (LDL) receptors ***(65)***. In LDL-deficient animals, a high-fat diet was found to have a greater effect on lesion size in male vs female animals, suggesting a role for hormones in the initiation or progression of the disease. Transgenic mice expressing the human apoB protein, the only protein component of LDL and a ligand for removal of this type of lipoprotein from the circulation, develop fatty lesions but only when fed a high-fat diet ***(66)***.

All of these models have provided insight into genetic modifiers and particular environmental elements involved in lesion formation and disease progression and are allowing this phenomenon to be teased out at the molecular level. They should be extremely valuable in the testing of various candidate drugs to combat the disease whose effects would be more expensive to investigate in currently more widely used rabbit or primate model systems.

8.4. Adult-Onset Diabetes

Adult-onset or type II diabetes is yet another age-related disorder in which the advent of genetically engineered mice as models of the disease has been extremely informative in understanding the molecular process involved in its development. A major target of alterations in such experiments has been the glucose transporters, a family of molecules involved in mediating the uptake of glucose into cells with various tissue-specific expressions, glucose affinities, and insulin sensitivities.

Glucose transporter 4 (glut 4) is the major molecule involved in insulin-induced transport of glucose into skeletal muscle and fat tissue when blood glucose levels are high, for both use it as a primary energy source via glycolysis by these tissues and store it in the form of glycogen for leaner times ***(67)***. Both glut 4 transgenics in which glut 4 levels were increased in relevant tissues, for example, muscle and glut 4 knockout mice have been generated to examine what effects alterations in the levels of this molecule have on insulin sensitivity and whole body metabolism. In one line of transgenics expressing glut 4 specifically in muscle under the control of the myosin light chain enhancer and promoter, fast-twitch muscle tissue was found to have increased basal and insulin-stimulated glucose uptake ***(68)***. These animals also displayed more rapid clearance of glucose from the bloodstream, decreased glucose levels after an oral glucose feeding, and increased basal and insulin-stimulated whole body glucose utilization. Mice in which muscle-specific expression of glut 4 was driven by the aldolase A promoter made diabetic by streptozotocin adminstration were found to clear blood glucose more rapidly after insulin injection than controls, which suggests that in the presence of elevated glut 4 levels, insulin resistance may be overcome even under diabetic conditions ***(69)***. However, in these studies the mice were unable to significantly decrease levels

of glucose after a high glucose load, which suggests that although elevation of glut 4 in muscle cells reverses insulin resistance it is not sufficient to maintain homeostatic blood glucose levels. Mice deficient in the glut 4 locus suprisingly were able to maintain normal glycemic control and therefore appear to be able to compensate for the loss of the glut 4 in some manner, perhaps via elevation of other glucose transporters ***(70)***. However, these animals do develop a reduction in adipose tissue and an enlargement of the heart muscle and die at 5–7 mo of age. These animals will doubtless be valuable in studying the role of glut 4 in various tissues by replacing the molecule selectively in the knockout lines with cell-specific promoters to see if this prevents the observed loss in these animals. It would also be interesting to examine the effects of deletion of glut 4 later in life by making a conditional knockout animal; in the current knockout, glut 4 expression was eliminated prior to birth during late embryogenesis.

9. Summary

In conclusion, genetically engineered animal models have been and will continue to be invaluable for exploring the various factors involved in the basic aging process as well as extending our understanding of many of the diseases found to be more prevalent in the older human population. Further development of such in vivo systems will allow scientists to dissect further the role genetic and environmental factors play in aging and in age-related disease states and to enhance our understanding of these processes.

References

1. Palmiter, R. D. and Brinster, R. (1985) Transgenic mice. *Cell* **41,** 343–345.
2. Schedl, A., Montoliu, L., Kelsey, G., and Schutz, G. (1993) A yeast artificial chromosome covering the tryosine gene confers copy number dependent expression in transgenic mice. *Nature* **6417,** 258–261.
3. Pearson, B. E. and Choi, T. K. (1993) Expression of the human beta-amyloid precursor gene from a yeast artificial chromosome in transgenic mice. *Proc. Natl. Acad. Sci. USA* **22,** 10,578–10,582.
4. Montoliu, L., Schedl, A., Kelsey, G., Zentgraf, H., Lichter, P., and Schutz, G. (1994) Germ line transmission of yeast artificial chromosomes in transgenic mice. *Reprod. Fertil. Dev.* **5,** 577–584.
5. Peterson, K. R., Clegg, C. H., Huxley, C., Josephson, B. M., Haugen, H. S., Furukawa, T., and Stamatoyannopoulos, G. (1993) Transgenic mice containing a 248-kb yeast artificial chromosome carrying the human beta-globin locus display proper developmental control of humanglobin genes. *Proc. Natl. Acad. Sci. USA* **90,** 7593–7597.
6. Peterson, K. R., Li, Q. L., Clegg, C. H., Furukawa, T., Navas, P. A., Norton, E. J., Kimbrough, T. G., and Stamatoyannopoulos, G. (1995) Use of yeast artificial chromosomes (YACs) in studies of mammalian development: production of beta-globin

locus YAC mice carrying human globin developmental genes. *Proc. Natl. Acad. Sci. USA* **12,** 5655–5659.
7. Lamb, B. T., Call, L. M., Slunt, H. H., Bardel, K. A., Lawler, A. M., Eckman, C. B., Younkin, S. G., Holtz, G., Wagner, S. L., Price, D. L., Sisodia, S. S., and Gearhart, J. D. (1997) Altered metabolism of familial Alzheimer's disease-linked amyl oid precursor protein variants in yeast artificial chromosome transgenic mice. *Hum. Mol. Genet.* **9,** 1535–1541.
8. Palmiter, R. D., Sandgren, E. P., Avarbock, M. R., Allen, D. D., and Brinster, R. L. (1991) Heterologous introns can enhance expression of transgenes in mice. *Proc. Natl. Acad. Sci. USA* **2,** 478–482.
9. Valera, A., Solanes, G., Fernandez-Alvarez, J., Pujol, A., Ferrer, J., Asins, G., Gomis, R., and Bosch, F. (1994) Expression of GLUT-2 antisense RNA in beta cells of transgenic mice leads to diabetes. *J. Biol. Chem.* **269,** 28,543–28,546.
10. Prockop, D. J., Kuivaniemi, H., and Tromp, G. (1994) Molecular basis of osteogenesis imprefecta and related bone disorders. *Clin. Plast. Surg.* **21,** 7–13.
11. Cockayne, D. A., Bodine, D. M., Cline, A., Nienhuis, A. W., and Dunbar, C. E. (1994) Transgenic mice expressing anti-sense interleukin-3 develop a B-cell lymphoproliferative syndrome or neurologic disfunction. *Blood* **84,** 2699–2710.
12. Stec, I., Barden, N., Reul, J. M., and Holsboer, F. (1994) Dexamethosone nonsuppression in transgenic mice expressing antisense RNA to the glucocorticoid receptor. *J. Psychiatr. Res.* **28,** 1–5.
13. Davis, B. M., Lewin, G. R., Mendell, L. M., and Jones, M. E. (1993) Altered expression of nerve growth factor in the skin of transgenic mice leads to changes in response to mechanical stimuli. *Neuroscience* **56,** 789–792.
14. Matsumoto, K., Kakidani, H., Takahashi, A., Nakagata, N., Anzai, M., Matsuzaki, Y., Takahashi, Y., Miyata, K., Utsumi, K., and Iritani, A. (1993) Growth retardation in rats whose growth hormone gene expression was suppressed by antisense RNA transgene. *Mol. Repro. Dev.* **36,** 53–58.
15. Capecchi, M. R. (1989a) The new mouse genetics: altering the genome by gene targeting. *Trends Genet.* **5,** 70–76.
16. Capecchi, M. R. (1989b) Altering the genome by homologous recombination. *Science* **244,** 1288–1292.
17. Abbondanzo, S. J., Gadi, I., and Stewart, C. L. (1993) Derivation of embryonic stem cell lines, in *Methods in Enzymology* (Wasserman, P. M. and DePamphilis, M. L., eds.), Academic Press, New York, pp. 803–823.
18. Kagi, D., Ledermann, B., Burki, K. Seiler, P., Odermatt, B., Olsen, K. J., Podack, E. R. Zinkernagel, R. M., and Hengartner, H. (1994) Cytotoxicity mediated by T cells and natural killer cells is greatly impaired in perform-deficient mice. *Nature* **369,** 31–37.
19. Kontgen, F., Suss, G., Stewart, C. L., Steinmetz, M., and Bluthman, H. (1993) Targeted disruption of the MIIIC class II Aa gene in C57BL/6 mice. *Int. Immunol.* **5,** 957–964.
20. Nada, S., Yagi, T., Takeda, H., Tokunaga, T., Nakagawa, H., Ikawa, Y., Okada, M., and Aizawa, S. (1993) Constitutive activity of src family kinases in mouse embryos that lack Csk. *Cell* **73,** 1125–1135.

21. te Riele, H., Maandag, E. R., and Berns, A. (1992) Highly efficient gene targeting in embryonic stem cells. *Proc. Natl. Acad. Sci. USA* **11,** 5128–5132.
22. Fassler, R., Martin, K., Forsberg, E., Litzenburger, T., and Iglesias, A. (1995) Knockout mice: how to make them and why. An immunological approach. *Int. Arch. Allergy Immunol.* **106,** 323–334.
23. Bradley, A. (1987) Production and analysis of chimeric mice, in *Tetracarcinomas and Embryonic Stem Cells: A Practical Approach* (Robertson, E. J., ed.), IRL Press, Oxford, pp. 113–123.
24. Wood, S. A., Allen, N. D., Rossant, J., Auerbach, A., and Nagy, A. (1993a) Non-injection methods for the production of embryonic stem cell-embryo chimerics. *Nature* **365,** 87–89.
25. Wood, S. A., Pascoe, W. S., Schmidt, C., Kemler, R., Evans, M. J., and Allen, N. D. (1993b) Simple and efficient production of embryonic stem cell-embryo chimerics by co-culture. *Proc. Natl. Acad. Sci. USA* **90,** 4582–4587.
26. Nagy, A., Rossant, J., Nagy, R., Abramov-Newerly, W., and Roder, J. C. (1993) Derivation of completely cell culture-derived mice from early passage embryonic stage stem cells. *Proc. Natl. Acad. Sci. USA* **90,** 8424–8429.
27. Kothary, R., Clapoff, S., Darling, S., Perry, M. D., Moran, L. A., and Rossant, J. (1989) Inducible expression of an hsp6o-lacZ hybrid gene in transgenic mice. *Development* **105,** 707–714.
28. Filmus, J., Remani, J., and Klein, M. H. (1992) Synergistic induction of promoters containing metal and glucocorticoid-response elements. *Nucleic Acid Res.* **20,** 2755–2760.
29. Kuhn, R., Schwenk, F., Aguet, M., and Rajewsky, K. (1995) Inducible gene targeting in mice. *Science* **269,** 1427–1429.
30. Gossen, M., Freundlieb, S., Bender, G., Muller, G., Hillen, W., and Bujard, H. (1995) Transcriptional activation by tetracyclines in mammalian cells. *Science* **268,** 1766–1769.
31. Furth, P. A., St Onge, L., Boger, H., Gruss, P., Gossen, M., Kistner, A., Bujard, H., and Hennighausen, L. (1994) Temporal control of gene expression in transgenic mice by the tetracycline-responsive promoter. *Proc. Natl. Acad. Sci. USA* **91,** 9302–9306.
32 Mayford, M., Bach, M. E., Huang, Y. Y., Wang, L., Hawkins, D., and Kandel, E. R. (1996) Control of memory formation through regulated expression of a CaMKII transgene. *Science* **274,** 1678–1683.
33. Kistner, A., Gossen, M., Zimmermann, F., Jerecic, J. UlImer, C., Lubbert, H., and Bujard, H. (1996) Doxycyclin-mediated quantitative and tissue-specific control of gene expression in transgenic mice. *Proc. Natl. Acad. Sci. USA* **93,** 10,933–10,938.
34. Gingrich, J. R. and Roder, J. (1998) Inducible gene expression in the nervous system of transgenic mice. *Annu. Rev. Neurosci.* **21,** 377–405.
35. No, D., Yao, T. P., and Evans, R. M. (1996) Ecdysone-inducible expression in mammalian cells and transgenic mice. *Proc. Natl. Acad. Sci. USA* **93,** 3346–3351.
36. Gu, H., Zou, Y. R., and Rajewsky, K. (1993) Independent control of immunoglobulin switch recombination at individual regions evidenced through Cre-loxP-mediated gene targeting. *Cell* **73,** 1155–1164.

37. Gu, H., Marth, J. D., Orban, P. C., Mossmann, H., and Rajewsky, K. (1994) Deletion of a DNA polymerase beta gene segment in T cells using cell type-specific targeting. *Science* **265,** 103–106.
38. Dymecki, S. (1996) A modular set of FIp, FRT, and lacZ fusion vectors for manipulating genes by site-specific recombination. *Gene* **171,** 197–201.
39. Dymecki, S. (1996) Flp recombinase promotes site-specific DNA recombination in embryonic stem cells and transgenic mice. *Proc. Natl. Acad. Sci. USA* **93,** 6191–6196.
40. Rossant, J. and Nagy, A. (1995) Genome engineering: the new mouse genetics. *Nature Med.* **1,** 592–594.
41. St-Onge, L., Furth, P. A., and Gruss, P. (1996) Temporal control of the Cre recombinase in transgenic mice by a tetracycline responsive promoter. *Nucleic Acid Res.* **24,** 3875–3877.
42. Erickson, R. P. (1996) Mouse models of human genetic disease: which mouse is more like a man? *BioEssays* **18,** 993–998.
43. Yunis, E. J., Watson, A. L., Gelman, R. S., Sylvia, S. J., Bronson, R., and Dorf, M. E. (1984) Traits that influence longevity in mice. *Genetics* **108,** 999–101.
44. Gelman, R., Watson, A., Bronson, R., and Yunis, E. (1988) Murine chromosomal regions correlated with longevity. *Genetics* **118,** 693–704.
45. Dear, K. B., Salazar, M., Watson, A. L., Gelman, R. S., Bronson, R., and Yunis, E. J. (1992) Traits that influence longevity in mice: a second look. *Genetics* **132,** 229–239.
46. Gerlai, R. (1996) Gene-targeting studies of mammalian behavior: is it the mutation or the background phenotype? *Trends Neurosci.* **19,** 177–180.
47. Crawley, J. N. (1996) Unusual behavior phenotypes of inbred mouse strains. *Trends Neurosci.* **19,** 181–182.
48. Orr, W. C. and Sohal, R. S. (1994) Extension of life-span by overexpression of superoxide dismutase and catalase in *Drosophila melanogaster*. *Science* **263,** 1128–1130.
49. Goldstein, S. (1990) Replicative senescence: the human fibroblast comes of age. *Science* **249,** 1129–1133.
50. Ikram, Z., Norton, T., and Jat, P. S. (1994) The biological clock that measures the mitotic lifespan of mouse embryonic fibroblasts continues to function in the presence of simian virus 40 large tumor antigen. *Proc. Natl. Acad. Sci. USA* **91,** 6448–6452.
51. Narayanan, L., Fritzell, J. A., Baker, S. M., Liskay, R. M., and Glazer, P. M. (1997) Elevated levels of mutation in multiple tissues of mice deficient in the DNA mismatch repair gene Pms2. *Proc. Natl. Acad. Sci. USA* **94,** 3122–3127.
52. Hsaio, K., Chapman, P., Nilsen, S., Eckman, C., Harigaya, Y., Younkin, S., Yang, F., and Cole, G. (1996) Correlative memory deficits, beta-amyloid elevation, and amyloid plaques in transgenic mice. *Science* **274,** 99–103.
53. Games, D., Adams, A., Alessandrini, R., Barbour, R., Berthelette, P., Blackwell, C., Carr, T., Clemens, J., Donaldson, T., Gillespie, F., Guido, T., Hagopian, S., Wood-Johnson, K., Khan, K., Lee, M., Liebowitz, P., Leiberburg, I., Little, S., Masliah, E., McConlogue, L., Montoya-Zavala, M., Mucke, L., Paganini, L., Penniman, E.,

Power, M., Schenk, D., Seubert, P., Snyder, B., Soriano, F., Tan, H., Vitale, J., Wadsworth, S., Wolozin, B., and Zhao, J. (1995) Alzheimer-type neuropathology in transgenic mice overexpressing V717F beta-amyloid precursor protein. *Nature* **373,** 523–527.

54. Duff, K., Eckman, C., Zehr, C., Yu, X., Prada, C. M., Perez-tur, J., Hutton, M., Buee, L., Harigaya, Y., Yager, D., Morgan, D., Gordon, M. N., Holcomb, L., Refolo, L., Zenk, B., Hardy, J., and Younkin, S. (1996) Increased amyloid-beta42(43) in brains of mice expressing mutant presenilin 1. *Nature* **383,** 710–713.
55. Holcomb, L., Gordon, M. N., McGowan, E., Yu, X., Benkovic, S., Jantzen, P., Wright, K., Saad, I., Mueller, R., Morgan, D., Sanders, S., Zehr, C., O'Campo, K., Hardy, J., Prada, C. M., Eckman, C., Younkin, S., Hsiao, K., and Duff, K. (1998) Accelerated Alzheimer-type phenotype in transgenic mice carrying both mutant amyloid precursor protein and presenilin I transgenes. *Nat. Med.* **4,** 97–100.
56. Duff, K. (1997) Alzheimertransgenic mouse models come of age. *Trends Neurosci.* **20,** 279–280.
57. Hsiao, K. K., Borchelt, D. R., Olson, K., Johannsdottir, R., Kitt, C., Yunis, W., Xu, S., Eckman, C., Younkin, S., and Price, D. (1995) Age-related CNS disorder and early death in transgenic FVB/N mice overexpressing Alzheimer amyloid precursor proteins. *Neuron* **15,** 1203–1218.
58. Haynes, L., Linton, P. J., and Swain, S. L. (1997) Age-related changes in CDC4 T cells of T cell receptor transgenic mice. *Mech. Ageing Dev.* **93,** 95–105.
59. Nakashima, Y., Plump, A. S., Raines, E. W., Breslow, J. L., and Ross, R. (1994) ApoE-deficient mice develop lesions of all phases of atherosclerosis throughout the arterial tree. *Arteriosclerosis Thromb.* **14,** 133–140.
60. Palinski, W., Ord, V. A., Plump, A. S., Breslow, J. L., Steinberg, D., and Witztum, J. L. (1994) ApoE-deficient mice are a model of lipoprotein oxidation in atherogenesis. Demonstration of oxidation-specific epitopes in lesions and high titers of autoantibodies to malondialdehyde-lysine in serum. *Arteriosclerosis Thromb.* **14,** 605–616.
61. Bellosta, S., Mahley, R. W., Sanan, D. A., Murata, J., Newland, D. L., Taylor, J. M., and Pitas, R. E. (1995) Macrophage-specific expression of human apolipoprotein E reduces atherosclerosis in hypercholesterol emi c apolipoprotei n E-null mice. *J. Clin. Invest.* **96,** 2170–2179.
62. van Vlijmen, B. J., van den Maagdenberg, A. M., Gijbels, M. J., van der Boom, H., HogenEsch, H., Frants, R. R., Hofker, M. H., and Havekes, L. M. (1994) Diet-induced hyperlipoproteinemi a and atherosclerosis in apolipoprotein E3*-Leiden transgenic mice. *J. Clin. Invest.* **93,** 4 1403–41410.
63. Fazio, S., Horie, Y., Simonet, W. S., Weisgraber, K. H., Taylor, J. M., and Rall, S. C., Jr. (1994) Altered lipoprotein metabolism in transgenic mice expressing low levels of a human receptor-binding-defective apolipoprotein E. *J. Lipid Res.* **35,** 408–416.
64. van Vlijmen, B. J., van Dijk, K. W., van't Hof, H. B., van Gorp, P. J., van der Zee, A., van der Boom, H., Breuer, M. L., Hofker, M. H., and Havekes, L. M. (1996) hr the absence of endogenous mouse apolipoprotein E, apolipoprotein E*2(Arg-l58

→ Cys) transgenic mice develop more severe hyperlipoproteinemia than apolipoprotein E*3-Leiden transgenic mice. *J. Biol. Chem.* **271,** 30,595–30,602.
65. Ishibashi, S., Goldstein, J. L., Brown, M. S., Herz, J., and Burns, D. K. (1994) Massive xanthomatosis and atherosclerosis in cholesterol-fed low density lipoprotein receptor-negative mice. *Clin. Invest.* **93,** 1885–1893.
66. Purcell-Huynh, D. A., Farese, R. V. Jr., Johnson, D. F., Flynn, L. M., Pierotti, V., Newland, D. L., Linton, M. F., Sanan, D. A., and Young, S. G. (1995) Transgenic mice expressing high levels of human apolipoprotein B develop severe atherosclerotic lesions in response to a high-fat diet. *J. Clin. Invest.* **95,** 2246–2257.
67. Katz, E. B., Burcelin, R., Tsao, T. S., Stenbit, A. E., and Charron, M. J. (1996) The metabolic consequences of altered glucose transporter expression in transgenic mice. *J. Mol. Med.* **74,** 639–652.
68. Tsao, T. S., Burcelin, R., Katz, E. B., Huang, L., and Charron, M. J. (1996) Enhanced insulin action due to targeted GLUT4 overexpression exclusively in muscle. *Diabetes* **45,** 28–36.
69. Leturque, A., Loizeau, M., Vaulont, S., Salminen, M., and Girard, J. (1996) Improvement of insulin action in diabetic transgenic mice selectively overexpressing GLUT4 in skeletal muscle. *Diabetes* **45,** 23–27.
70. Katz, E. B., Stenbit, A. E., Hatton, K., DePinho, R., and Charron, M. J. (1995) Cardiac and adipose abnormalities but not diabetes in mice deficient in GLUT4. *Nature* **377,** 151–155.